

# JET PUMPS: MOVING AIR WITH MOVING AIR

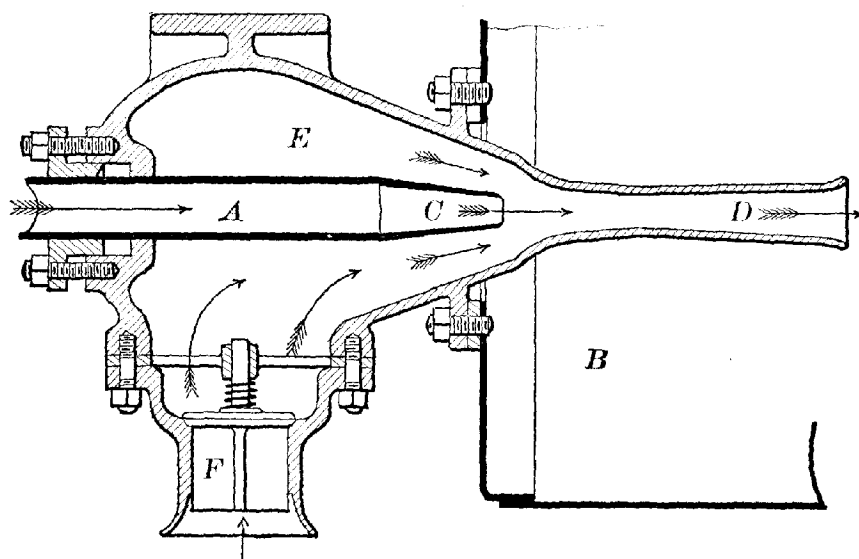


FIG. 448. —THE COMPRESSED-AIR INJECTOR.

## CONTENTS

1.	Jet Pump Engineering .....	1
2.	Pulsed-Drive Jet Pumps Entrain More Air .....	65
3.	The Dynamics of Pulsating Flow .....	144
4.	Sample Applications of Jet Pump Technology .....	243
5.	Patents on Jet Pump Technology .....	252
6.	Steam Boiler Injectors: cold water into hot boiler with no moving parts, proven technology since 1858: Why not air? .....	262
7.	<i>Steam Injectors: Their Theory &amp; Use</i> , M. Leon Pochet (1890) .....	301

## CHAPTER V

## AIR AT PRESSURES BELOW THE ATMOSPHERE

A study of the properties of air, and of its applications would not be complete without reference to at least a few of the uses of air at pressures below the atmosphere.

For purposes of experiment and for laboratory uses, these low pressures are usually obtained by means of the familiar air pump.

**Venturi Vacuum Pump.**—Another method of securing these low pressures is by means of a very simple hydraulic air ejector or “venturi vacuum pump” as it is sometimes called.

This convenient instrument for quickly obtaining an approximate vacuum depends on the principle that a fluid passing at a high velocity through a converging and diverging nozzle in which the curves

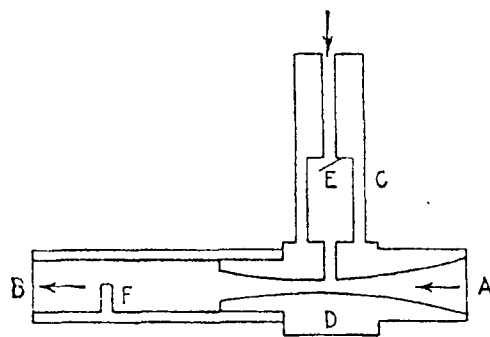


FIG. 13.—Hydraulic air pumps.

conform to the shape of the “vena contracta” of a jet from an orifice, will produce an approximate vacuum at a point nearest its greatest contraction and if an air chamber is connected through an orifice at this point the air will be drawn into the jet and a very good vacuum formed in the chamber.

In the sketch shown in Fig. 13, tube *A* may be connected by a rubber hose to a faucet. The converging-diverging tube through which the water is forced is shown at *D*. Tube *C*, which is connected with the chamber from which the air is to be exhausted, has a check valve *E* and is connected to the smallest diameter of the nozzle. It has been found that better results are secured when a baffle *F* is introduced into the discharge pipe *B*, as shown.

# An Investigation of the Performance and Design of the Air Ejector Employing Low-pressure Air as the Driving Fluid

By Professor L. J. Kastner, M.A., M.Sc., M.I.Mech.E.\* and J. R. Spooner, M.Sc. Tech., Wh.Sc., A.M.I.Mech.E.†

The air ejector, in its various forms, is a device which has many applications in engineering practice, and several attempts have been made to analyse its mode of action, some of these having been supported by experimental work. Most of the experimental results available are related to ejectors in which relatively high-pressure steam is utilized as the driving fluid, but even in these cases the information provided is restricted to a narrow field.

The investigation described relates to an air ejector employing as the driving fluid air at a relatively low pressure, not exceeding 40 lb. per sq. in. (abs.), and covering a wide range of operating conditions by means of interchangeable nozzles. Two distinct experimental arrangements were built—one for the set of conditions in which the ejector draws in a relatively small quantity of suction fluid and pumps it through a relatively high pressure-ratio, and the other covering conditions in which the quantity of suction fluid is much larger, but the pressure ratio is quite small. For a given initial pressure and quantity of driving fluid, the rate of mass flow of suction fluid depends chiefly on the diameter of the combining tube, in which the driving and suction fluids mix; in the experiments, the ratio of combining-tube area to driving-nozzle area was varied in twelve steps, covering a range of area ratios from 1.44 to 1,110.0, and compression ratios ranging from about 3 to about 1.001.

Efforts were made to find the best proportions of those parts of the ejector which exert a major influence on performance, and certain conclusions are drawn from the results of the experiments. Theoretical aspects of the problem are briefly discussed.

## INTRODUCTION

The air ejector is a simple form of vacuum pump which has many possible applications in engineering practice, and although its efficiency, in terms of pumping work at output divided by available energy at input, is low compared with that of reciprocating or rotary compressors, its convenience, its simplicity, and the absence of moving parts make it admirably adapted for many applications where low initial and maintenance costs, small size, and freedom from mechanical breakdown are more important than the absolute amount of energy input required to perform a given amount of compression work. Although the efficiency of the ejector as a pump is low, its performance can be regarded as good since almost the whole amount of energy supplied to it re-appears in the delivery stream, mostly as heat.

Wherever a supply of vapour or gas is available at a pressure above atmospheric, the ejector should give useful service, since the experiments described indicate that a good performance can be obtained with very moderate pressures, and this suggests that the ejector principle may, in addition to its obvious applications in ventilating plants, condensers, boiler draught inducers, vacuum brake systems, and for the carriage of granular material, prove worthy of future study and development.

Most of the early applications of the ejector were concerned with the maintenance of a high vacuum in steam condensers, and the devices of Parsons, Le Blanc, and Körting are familiar to most engineers. The quantity of published information is fairly considerable and almost all of it refers to ejectors which employ steam as the driving fluid, but the experimental results available are somewhat restricted in utility since they apply, mostly, to a rather narrow range of working conditions. Previous investigations may be roughly divided into two classes—the first comprising the results of those workers who appear to have

been chiefly interested in the performance of the ejector as a whole, and the second the work of those who have studied the processes occurring in free jets and the mixing of one gaseous stream with another. In the first class one may mention the papers of Watson (1933)‡, Bailey and Wood (1933 and 1939), Bosnjakovic (1936), Royds and Johnson (1941), and Keenan and Neumann (1942 and 1948), whilst in the second, the work of Prandtl (1925), Tollmien (1926), Kuether (1935), Busemann (1931), Goff and Coogan (1942), and Hawthorne and Cohen (1944) is noteworthy.

The mixing of two streams of gaseous fluid is a problem of great interest but of very considerable complexity, and difficulty arises when an attempt is made to generalize from the results of individual analyses. A theoretical approach to the solution of the ejector problem must necessarily be concerned with conditions arising when two jets of fluid, whose initial pressure and specific volume are known, unite, but a solution, when achieved, should be in such a form as to enable the performance of a complete ejector to be predicted, and to be compared with the results of experiment, when the inlet and outlet conditions vary widely. The solution thus demands that attention be given not only to the mixing process, but also to the processes of expansion and recompression which occur in the practical form of the instrument, and requires that the results of the theoretical treatment are of sufficiently broad application. Although the investigation described below was mainly experimental in character, efforts were made to develop a straightforward mathematical analysis, and Appendix I gives the outline of a theoretical treatment enabling the performance of an idealized ejector to be compared with the results of practice.

## APPARATUS

In view of the number of variables involved, it was decided to confine the experiments to single-stage compression, and to cover a range of pressure ratios from about 3.0 to about 1.001,

The MS. of this paper was originally received at the Institution on 17th September 1948, and in its revised form, as accepted by the Council for publication, on 2nd May 1949.

\* Engineering Department, University College of Swansea.

† Engineering Department, University of Manchester.

‡ An alphabetical list of references is given in Appendix III, p. 159.

the delivery pressure usually being atmospheric. Preliminary trials established the importance of the ratio of combining-tube throat area to forcing-nozzle throat area in governing the suction pressure and the amount of air induced, and provision was made for varying this area ratio over a wide range of values, from a smallest value of 1.44 to a largest value of 1,110.0. To cover this range, two experimental arrangements were constructed: the first, termed the "small-area-ratio apparatus", covered area ratios between 1.44 and 40.7 in seven steps, and the second, or "large-area-ratio apparatus", covered area ratios between 76.0 and 1,110.0 in five steps. The actual area ratios employed were: 1.44, 2.25, 5.06, 10.07, 14.06, 25, 40.7, 76, 161, 334, 683, and 1,110.

*Small-area-ratio Apparatus.* The small-area-ratio apparatus is shown in Fig. 1a. The forcing air entered the apparatus

The suction air was drawn in through a 4-inch pipe, 10 feet long, acting as a flow straightener. At the end of this pipe farthest from the intake an airflow meter was fitted, consisting of a plate orifice gripped between two flanges, the pressure difference across the orifice being obtained by "corner-taps" and being measured by an inclined water gauge giving a moderate degree of magnification—about 4 to 1. A series of eight brass plate orifices enabled a convenient head of water to be obtained. The suction vacuum was measured by a mercury or water gauge according to its magnitude, and was governed by a valve fitted between the suction airflow meter and the suction-air reservoir. The delivery air from the ejector was led to a reservoir, the pressure in which could be measured by a water gauge and could be varied by a valve fitted to the discharge pipe.

The small-area-ratio ejector consisted of a cast-iron body, as

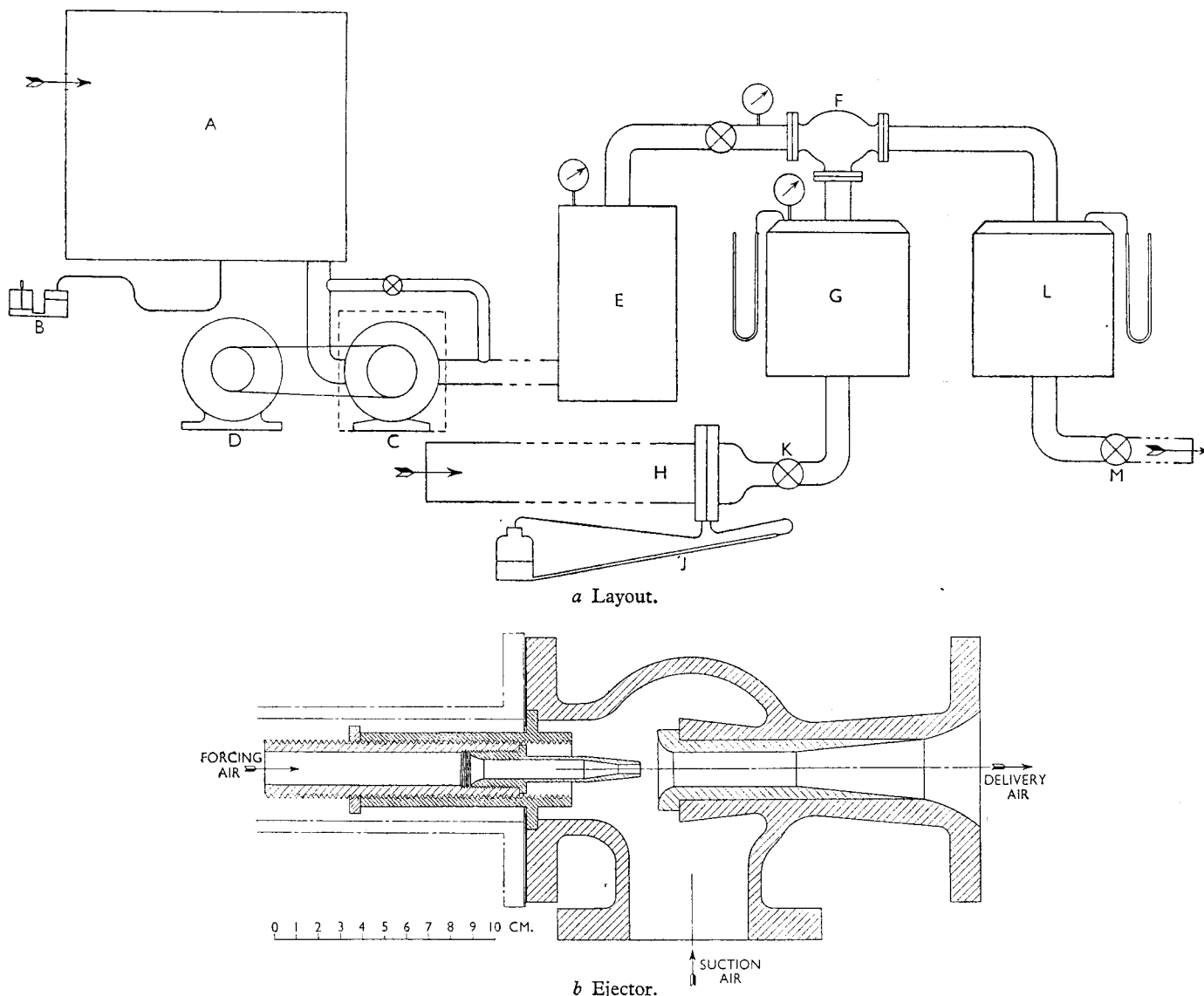


Fig. 1. Small-air-ratio Apparatus

- A Forcing-air measuring tank.
- B Forcing-air measuring gauge.
- C Air compressor.
- D Electric driving motor.

- E Forcing-air reservoir.
- F Ejector.
- G Suction-air reservoir.
- H Suction-air-flow straightener and orifice meter.

- J Inclined water gauge.
- K Suction-air pressure regulator.
- L Delivery-air reservoir.
- M Delivery-air regulator.

through a large tank (160 cu. ft. capacity), equipped with measuring orifices, on its way to the air compressor, which was of the rolling-drum, rotating-vane type, and was immersed in a water bath. By suitably adjusting the flow of water to the bath, the temperature in the forcing-air reservoir could be held at  $70 \pm 3$  deg. F.

shown in Fig. 1b. The combining nozzle and diffuser nozzle were made either of brass or of phosphor bronze and formed a unit which was made a push fit in the body and secured by a set screw. The forcing nozzle was fitted to a long brass bush, which could be screwed up and down in an outer sleeve and secured in any desired position by a locking ring.



**Large-area-ratio Apparatus.** Preliminary trials showed that it was necessary to provide a considerable range of movement for the forcing nozzle of the large-area-ratio ejector, and if the same construction as employed for the small-area-ratio ejector had been adopted the ejector body would have been unnecessarily large and weighty. Experiment had shown that the small-area-ratio ejector would cover a range of pressure ratios from about 3 to about 1.01, and it was not anticipated that the large-area-ratio apparatus would be employed for pressure ratios greater than, say, 1.015. Accordingly, it was decided to design the latter apparatus in such a way that the suction pressure would always be atmospheric, the discharge pressure consequently being somewhat higher. By this means a considerable simplification in design became possible, and it was considered safe to assume that the performance of the ejector would not vary appreciably when sucking air from a space at a pressure a few inches of water below atmosphere and delivering to atmosphere, or when pumping air initially at atmospheric pressure to a pressure a few inches of water above this.

The final form of the large-area-ratio apparatus is shown in Fig. 2; both the forcing nozzle and the combining-and-discharge nozzle are adjustable longitudinally. A total range of movement of about 16½ inches was provided but for some of the later trials this range was much exceeded by detaching the forcing-nozzle

of the work, it was decided that the forcing-nozzle throat area should be kept constant throughout the experiments, and a throat diameter of 4 mm. was adopted, but, towards the end of the trials, it was desired to undertake a few experiments with an area ratio less than the minimum value then available, which was 2.25. Consequently a forcing nozzle having a 5 mm. throat was made, which gave an area ratio of 1.44 with a combining-and-discharge nozzle already existing.

In designing the ejector the main objects were to vary over a considerable range (1) the area ratio, (2) the length ratio, or length of combining-tube throat divided by its diameter, (3) the inlet angle, or flare radius, at entrance to the combining tube, (4) the projection ratio, or distance from the discharge end of the forcing nozzle to the commencement of the parallel throat of the combining tube divided by the diameter of the combining tube throat, and (5) the angle of the diffuser. The diffuser profiles near the delivery end of nozzles Nos. 12 and 13 are somewhat irregular, but the shape at this point was imposed by the existing dimensions of the ejector body.

#### EXPERIMENTAL RESULTS

**Preliminary Trials.** Early experiments showed that ejector characteristics could most easily be demonstrated by plotting

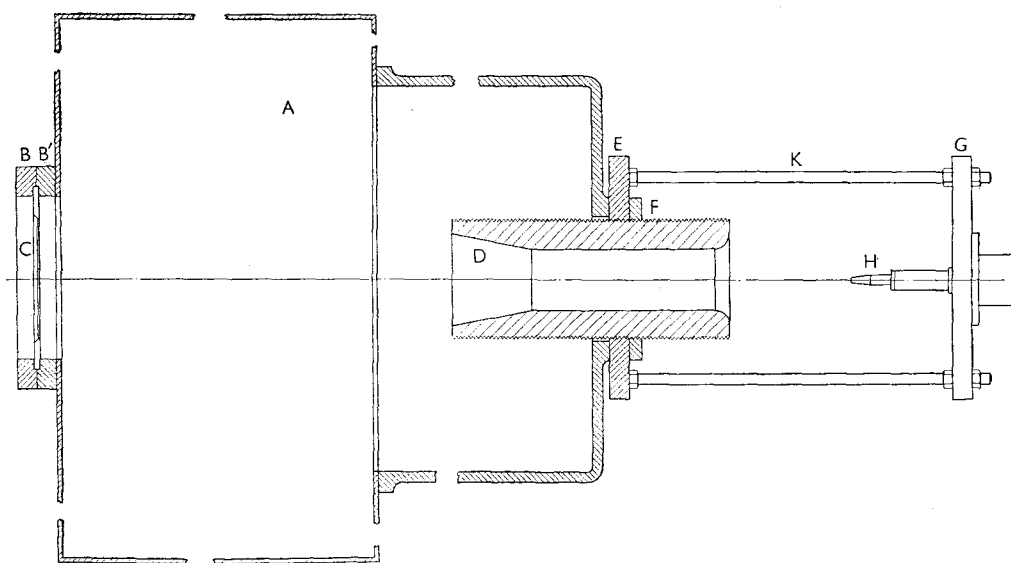


Fig. 2. Large Area-ratio Apparatus

A Tank.  
B, B' Orifice plate flanges.  
C Orifice plate.  
D Combining-and-discharge nozzle.

E Back plate.  
F Locking ring.  
G Nozzle plate.  
H Forcing nozzle.  
J Forcing-air pipe.  
K Distance bolt.

plate from the distance bolts and using sights to ensure that the forcing jet was truly axial. The combining-and-discharge nozzle exhausted into a tank, fitted with baffles to destroy the kinetic energy of the delivery stream, and equipped with measuring orifices to enable the rate of mass flow to be determined. The measuring orifices were calibrated by removing the combining tube and the forcing nozzle, and bolting together the two retaining flanges, the forcing-air pipe being suitably lengthened. The whole of the air which passed through the delivery orifice had then passed through the blower, and if the latter was set to deliver roughly the same quantity of air as would be handled (as the sum total of forcing air plus suction air) by a large-area-ratio ejector, it became possible to calibrate the measuring orifices of the tank on the delivery side of the ejector, using the orifices in the forcing-air measuring tank as standards. The pressure difference across the delivery orifice was measured by a micrometer water gauge, reading to 0.001 inch.

**Nozzles.** The nozzle profiles used in the experiments are shown in Fig. 3. In all cases, the entrance cross-section of both forcing nozzles and combining-and-discharge nozzles is on the left, the exit cross-section on the right. At the commencement

curves of vacuum, or pressure ratio, against mass ratio (suction mass-flow divided by forcing mass-flow). Typical examples of such curves, relating to the small-area-ratio apparatus, are shown in Fig. 4. The point corresponding to zero mass ratio was obtained by measuring the suction vacuum after keeping the suction-air regulating valve fully closed for a standard period of 5 minutes, this vacuum being designated the "terminal vacuum". The regulating valve was then opened slightly, the vacuum was reduced, and the suction airflow through the orifice meter was measured. This procedure was repeated, with different openings of the regulating valve, until the desired range of pressure ratios had been covered.

Three standard forcing pressures, namely, 20, 14, and 7 lb. per sq. in. (gauge) were employed throughout the majority of the trials. It is believed that the forcing pressures adopted are considerably lower than those used by previous experimenters, but, nevertheless, by proper attention to design it was found possible to obtain good ejector performance. A characteristic feature of ejector behaviour is demonstrated by the curves of Fig. 4; the use of a relatively high forcing pressure will, generally, result in a higher terminal vacuum than would be obtained with a lower forcing pressure, but, as the vacuum decreases and the

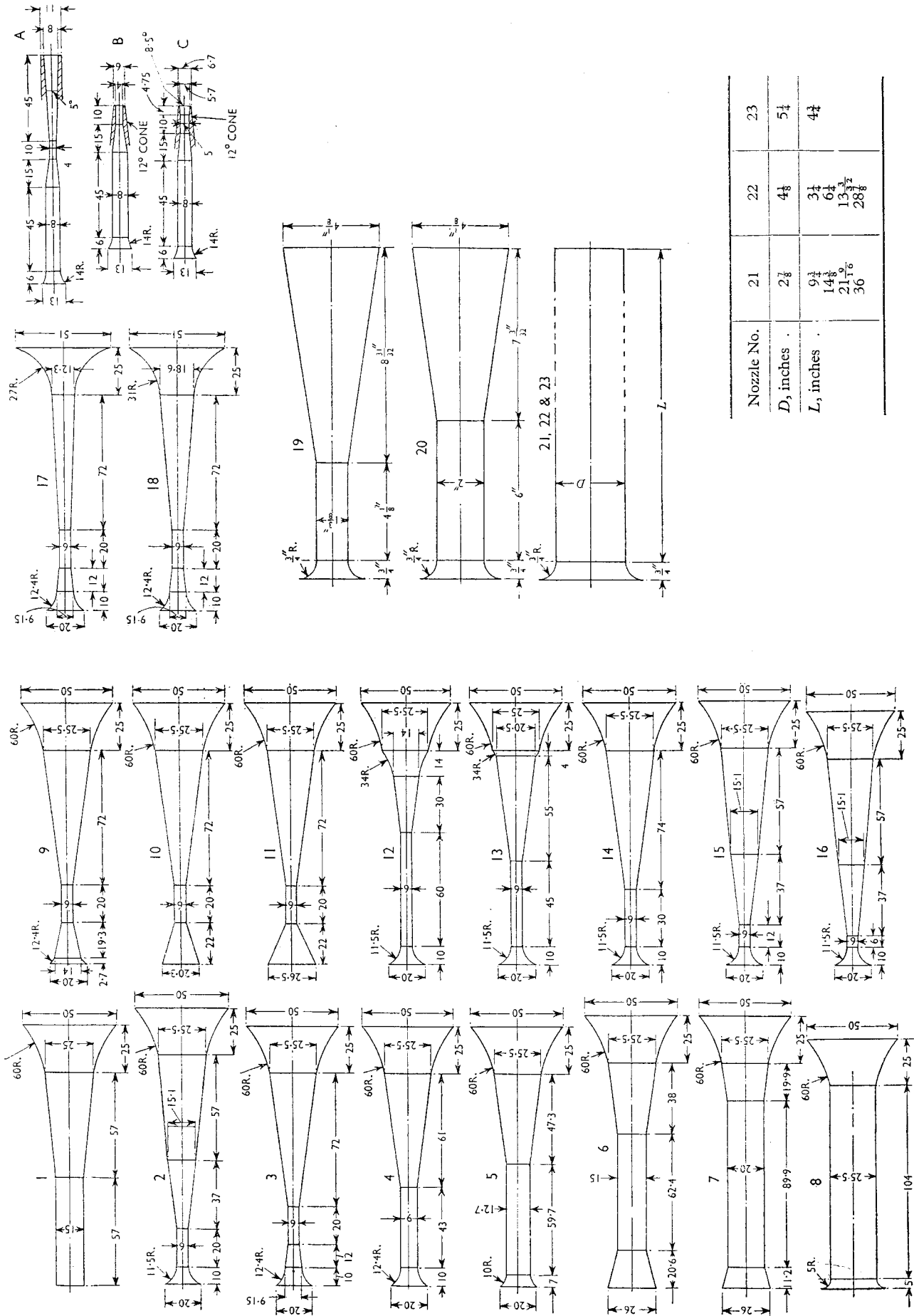


Fig. 3. Nozzle Dimensions  
All dimensions in millimetres except for nozzles 19-23.

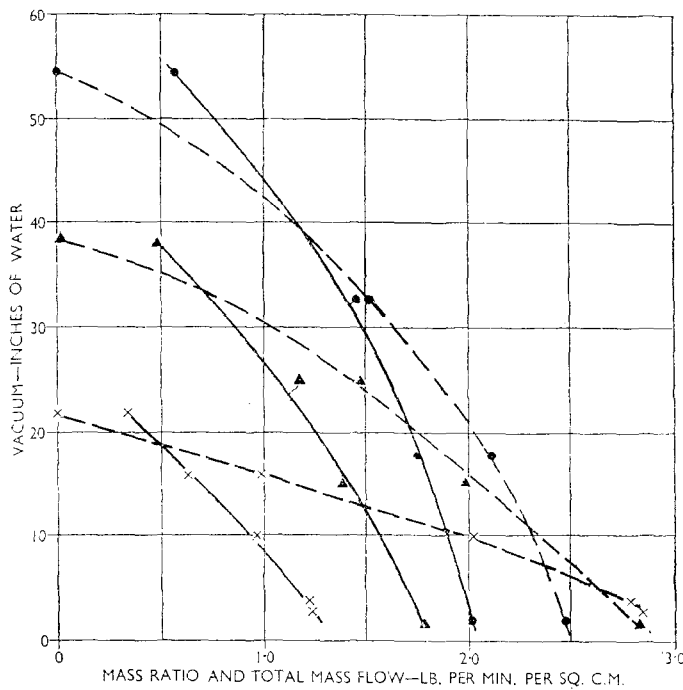


Fig. 4. Characteristic Curves

Area ratio = 14.06; forcing nozzle B; combining nozzle 1; dotted lines represent curves of mass ratio; full lines represent curves of total mass flow.

- 20 lb. per sq. in. (gauge) forcing pressure.
- ▲ 14 " " " " " "
- × 7 " " " " " "

mass ratio increases the mass ratios for the two cases become more nearly equal, and, for small vacua, the mass ratio may actually be greater with the lower forcing pressure than with the higher. If, however, total mass flow—forcing mass plus suction mass—be plotted against vacuum, it becomes clear that the total mass passing per unit area of combining-tube throat is greater for a higher forcing pressure than for a lower one.

**Forcing Nozzle Design.** Although it was not anticipated that any difficulties would arise in designing a suitable forcing nozzle for the range of pressures to be employed, some trouble was

experienced in the early stages because an attempt was made to use an "over-expanding" forcing nozzle. It has been stated (Watson 1933) that over-expansion is advantageous and results in a very steady vacuum, but the authors' experiences with an over-expanding nozzle (A in Fig. 3) were discouraging, and it is suggested that good results under such conditions may, perhaps, be related to the use of higher initial pressures, or to the use of steam as a forcing fluid.

The ratio of exit area to throat area for nozzle A is much greater than the theoretical ideal, being 4 instead of a "correct" value of rather less than 2 for the pressure ratios involved, but a progressive shortening of the nozzle resulting in a reduction of exit area (the position of the nozzle outlet relative to the combining tube being, of course, kept constant) indicated that over-expansion had no advantages, and forcing nozzle B, which was used for nearly all subsequent experiments, was designed to give no expansion in the nozzle beyond the throat, and proved very successful. The results of a large number of measurements showed the mean coefficient of discharge of this nozzle to be 0.975 over the working range, but no allowance is made for this when area ratios are quoted, the measured value of area ratio being always employed.

**Optimum Performance of the Ejector.** Performance curves, similar to those of Fig. 4, were drawn for the whole range of area ratios from 2.25 up to 1,110.0 for each of a series of forcing-nozzle positions, and it thus became possible to determine the best performance of which the ejector was capable. In general, the form of the curve relating pressure ratio of compression to mass ratio was the same for all area ratios, the effect of increasing the area ratio being to increase the suction flow and to decrease the pressure ratio; but for area ratios greater than 161 and small degrees of compression, the greatest mass flow did not occur at the smallest compression ratio, as had been expected, but showed a maximum when the compression ratio was somewhat greater than unity, and thereafter decreased if the pressure difference between the suction and outlet ends of the mixing tube was still further lowered, as exemplified by the curves of Figs. 5c and 12. This effect may not be a property of the larger area ratios only—it was not observed to occur when the pressure difference across the mixing tube was greater than about 0.5 inch of water, and so small a pressure rise is quite outside the working range of ejectors for which the area ratio is less than about 100, and it was therefore not investigated in such cases.

When the optimum nozzle positions and dimensions had been determined, the highest mass ratio measured at any compression ratio for all the area ratios investigated was plotted, the result being a series of overlapping curves showing the range of compression ratios which could be covered by an ejector of any

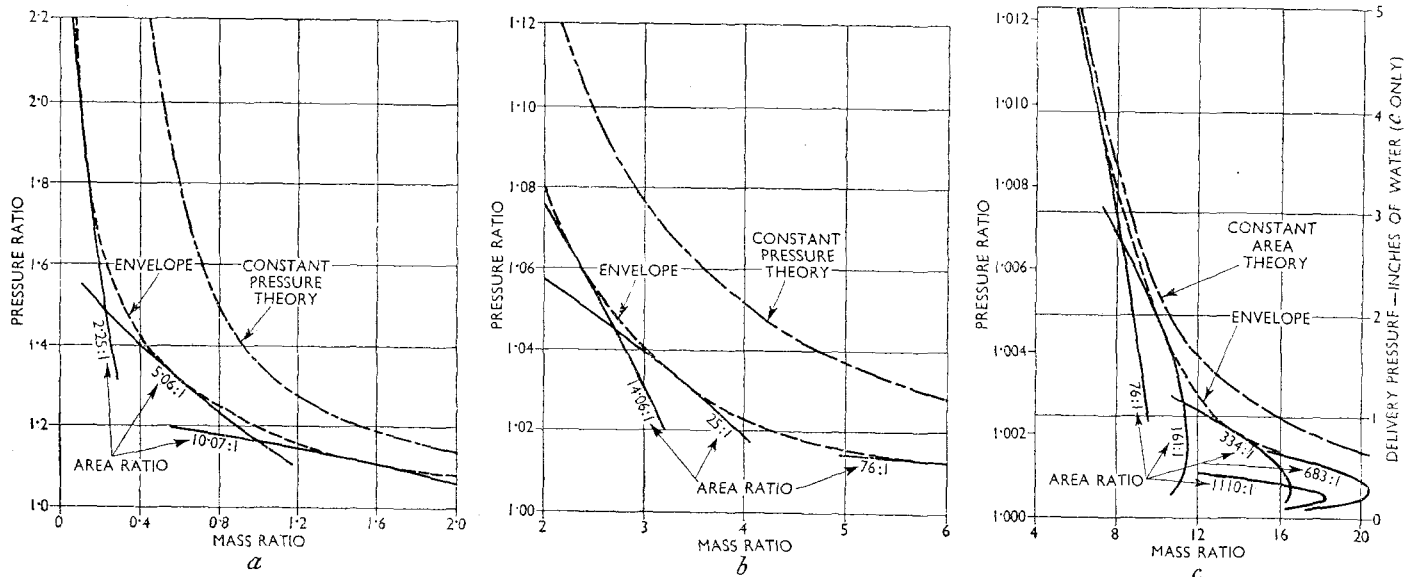


Fig. 5. Optimum Performance Curves  
Forcing pressure = 20 lb. per sq. in. (gauge).

known area ratio. The optimum mass ratio obtainable experimentally for any assigned pressure ratio could be obtained from the envelope of these curves. Three such diagrams, for a forcing pressure of 20 lb. per sq. in. (gauge) are shown in Fig. 5. For the total range of mass ratios, the pressure ratio varied between unity and about 3, whilst the area ratio varied between 2.25 and 683. When the area ratio is increased to 1,110, the best mass ratio for a forcing pressure of 20 lb. per sq. in. (gauge) showed a reduction as compared with that obtained at an area ratio of 683, but the length ratio of the combining and discharge nozzle No. 23, corresponding to an area ratio of 1,110, was too small to give the best performance and could not be increased. A greater length ratio would be expected to give a larger mass ratio by analogy with the results of Fig. 12, but the advantage of increasing the area ratio beyond 700 or so is still doubtful for ejectors employing low-pressure forcing air.

The chain-dotted curves of Fig. 5 refer to results calculated from the theories outlined in Appendix I. For large area-ratios the assumption of constant-area mixing agrees reasonably well with the experimental results; for small area-ratios, the assumption of constant-pressure mixing is preferred, but the dimensions of the small-area-ratio ejector were not great enough to enable pressure and temperature measurements to be made in the mixing tube.

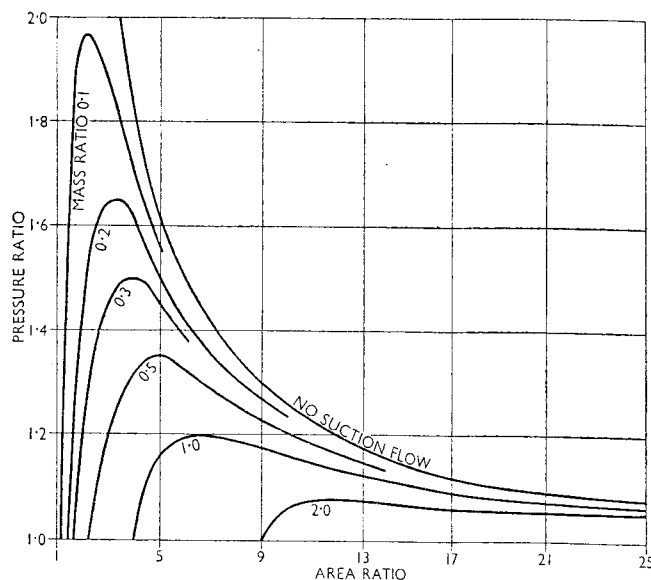


Fig. 6. Relationships Between Area Ratio and Pressure Ratio for Various Mass Ratios

Forcing pressure = 20 lb. per sq. in. (gauge).

On the assumptions that mixing occurs at constant pressure and constant density in a free space, the equations of momentum and continuity indicate that the greatest mass ratio  $m$  obtainable with any area ratio  $a$  is given by the equation  $m = \sqrt{a-1}$ . Experimental results agree well with this equation over a wide range, but for very large area-ratios the agreement breaks down.

Area ratio, pressure ratio, and mass ratio may be related by families of curves of the type given in Fig. 6. This diagram applies only to a limited range of area ratios, between 1 and 25, but within this range it shows the possible variations in pressure ratio and mass ratio, including the case of no suction flow.

**Ultimate Pressure Ratio, or Maximum Vacuum.** The experimental relationship between the ultimate pressure ratio  $r$  (corresponding to the terminal vacuum under "no flow" conditions) and the area ratio  $a$  for area ratios from 1.44 upwards is given by Fig. 7, in which the quantities  $\log_{10}(a-1)$  and  $\log_{10}(r-1)$  are related. It appears that an approximate straight-line relationship holds until a critical area ratio is reached, and for area ratios less than this the ultimate pressure ratio (or maximum vacuum) decreases.

Further, the results demonstrate that the ultimate compression ratio is dependent upon the forcing pressure and, in general,

increases as this pressure rises, but it is noticeable that the critical area ratio becomes greater with an increase of forcing pressure.

A theoretical analysis (Appendix II) confirms these general conclusions with a reasonable degree of accuracy. Fig. 8 shows

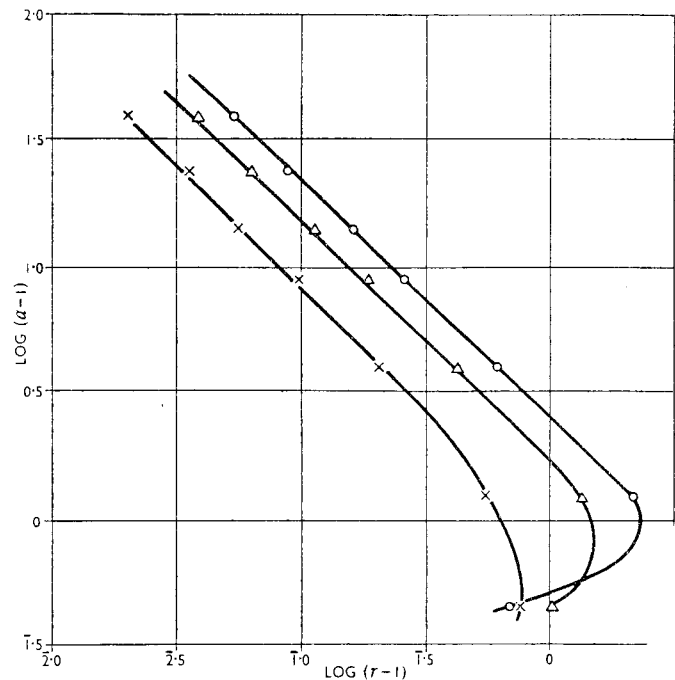


Fig. 7. Relationship between Area Ratio and Terminal Ratio of Compression

$r$  is pressure ratio of compression.

Projection ratio chosen to give maximum compression ratio.

- 20 lb. per sq. in. (gauge) forcing pressure.
- △ 14 " " " " " "
- × 7 " " " " " "

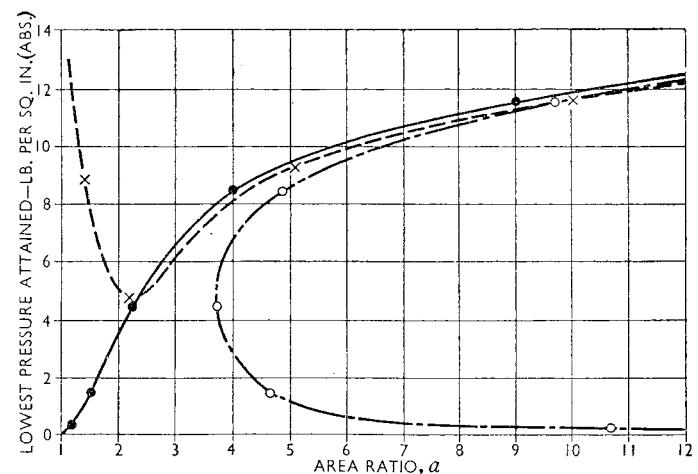


Fig. 8. Comparison of Computed and Experimental Values of Lowest Pressure Attained

Forcing pressure = 20 lb. per sq. in. (gauge).

- × Experimental values.
- Calculated values from  $a = \text{mixing-tube throat area/forcing-nozzle exit area}$ .
- Calculated values from  $a = \text{mixing-tube throat area/forcing-nozzle throat area}$ .

the lowest pressure ratio attained versus area ratio for a forcing pressure of 20 lb. per sq. in. (gauge), and also two theoretical curves; the full line curve refers to the case in which the exit area of the forcing nozzle is the same as its throat area (this applies to forcing nozzle No. 2 which was used throughout the experiments described in the present section), and the chain-

dotted curve refers to the case in which the exit area of the forcing nozzle is correctly proportioned to give the greatest velocity at exit. The agreement between the practical and theoretical cases breaks down for very small area-ratios but holds above an area ratio of about 5.

If the area ratio is made too small, the ejector tends to choke itself and part of the jet may blow back into the suction space, raising the pressure there and even, in an extreme case, causing it to exceed that of the atmosphere. Conditions of this kind occurred with the 1.44 area-ratio ejector, the pressure in the closed suction vessel at first falling as the forcing pressure was increased, then rising, and finally becoming greater than atmospheric as the choking effect grew more pronounced. Forcing nozzle C, Fig. 3, was used to obtain the desired area ratio.

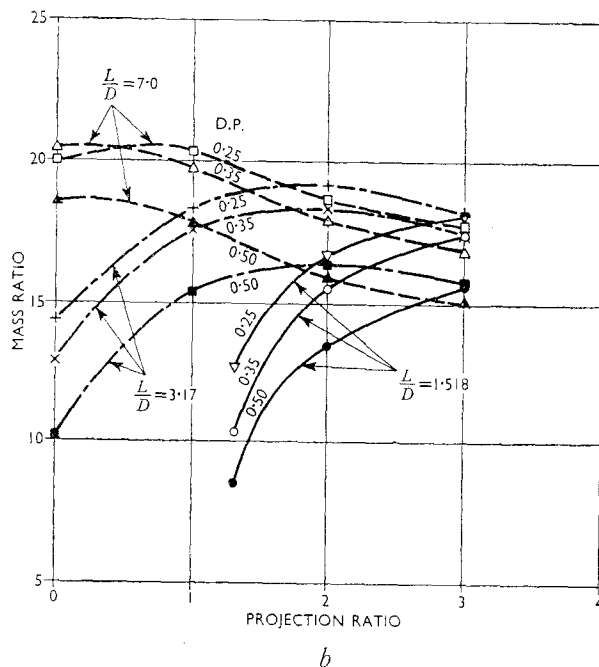
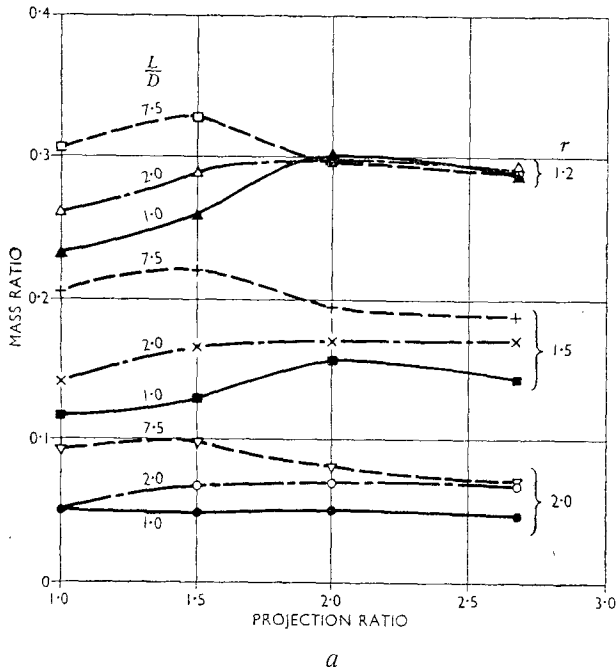


Fig. 9. Influence of Projection Ratio

a Area ratio = 2.25. b Area ratio = 683.0.

Forcing pressure = 20 lb. per sq. in. (gauge).

$L/D$  = combining tube length/diameter;  $r$  = pressure ratio; D.P. = delivery pressure, inches water.

For ejectors in which the mixing pressure is less than about half the delivery pressure, analysis suggests that the minimum area-ratio should be about equal to the ratio of the forcing pressure to the delivery pressure.

**Projection Ratio.** Fig. 9 shows the effects of changes in projection ratio for ejectors having area ratios of 2.25 and 683. For the small-area-ratio ejector, three sets of three curves each are plotted, each set applying to a different pressure ratio, and containing information relating to combining tubes of varied length of parallel, the values of  $L/D$  being 1.0, 2.0, and 7.5 respectively. For the large area-ratio, pressure ratios are not given, as they are nearly equal to unity, but the degree of compression is indicated by quoting the pressure rise above atmosphere. (Suction occurs at atmospheric pressure in the large area ratio apparatus.) The values of  $L/D$  applying in this latter case are 1.518, 3.17, and 7.0.

The curves applying to the small area-ratio suggest that the optimum projection ratio, for that value of  $L/D$  which gives the best performance, is about 1.5, but if the value of  $L/D$  is too small the optimum projection ratio becomes larger than 1.5. For the ejector having an area ratio of 683.0, the optimum projection

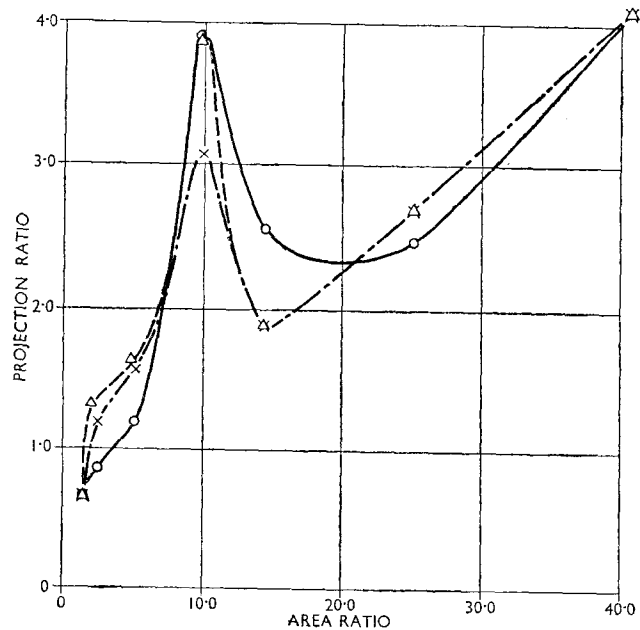


Fig. 10. Projection Ratio for Maximum Compression

○ 20 lb. per sq. in. (gauge) forcing pressure.  
△ 14 " " " " " "  
× 7 " " " " " "

ratio falls between zero and 1.0 when the value of  $L/D$  is chosen correctly, but when the value of  $L/D$  is too small the projection ratio must be increased. It is concluded that, if the mixing tube is too short, the forcing nozzle exit must be moved away from the combining tube entrance to enable some mixing to take place before the streams enter the tube proper; Fig. 9b indicates strong evidence of this. Even with large area-ratios, however, it would be too much to expect the total mixing length, for a given area ratio, to remain constant, since the character of the mixing process will probably be different in the free space between forcing nozzle and combining tube from what it would be in a single, parallel mixing chamber. The fact that the projection ratio should be somewhat greater for small area-ratios than for large ones may be accounted for by supposing that, in the former case, pure constant-area mixing is not satisfactory, a region of converging flow preceding the constant-area region. A convergent passage at entry to the parallel mixing tube would appear to be necessary for area ratios less than about 40.

Fig. 10 shows the projection ratio which was found by experiment to give the highest terminal vacuum with no secondary air flow for area ratios up to 40.7. Terminal vacua were not measured for the larger area-ratios. Over the range

covered, it appears that the projection ratio for maximum vacuum increases as the area ratio becomes larger, unlike the projection ratio for maximum secondary flow, which remains substantially constant, but the causes of the peak in the region of an area ratio of 10 are not evident. Previous experimenters (Watson 1933 and Mellanby 1928) have discussed the influence of shock waves in ejectors, but since these waves can only arise when the mean velocity of the jet exceeds the acoustic, it would seem unlikely that they can account for the phenomena demonstrated in Fig. 10, since for a forcing pressure of 7 lb. per sq. in. (gauge) the pressure ratio across the forcing nozzle is always greater than 0.528, the critical pressure ratio for air.

**Combining Nozzle Design.** The correct design of the parallel mixing chamber for small-area-ratio ejectors was investigated with the help of nozzles Nos. 16, 15, 14, 13, and 12, Fig. 3, and forcing nozzle No. 2. By the use, in every case, of a 6 mm. bore parallel tube, the area ratio was kept constant at 2.25, and a standard type of convergent entry, consisting of a smooth flare of 11.5 cm. radius, was adopted. The diffuser angle was 15 deg., but, owing to limitations imposed by the ejector body, it was not possible to maintain the diffuser design precisely constant throughout the tests. However, such differences as existed were confined to the delivery end of the diffuser, and it is considered

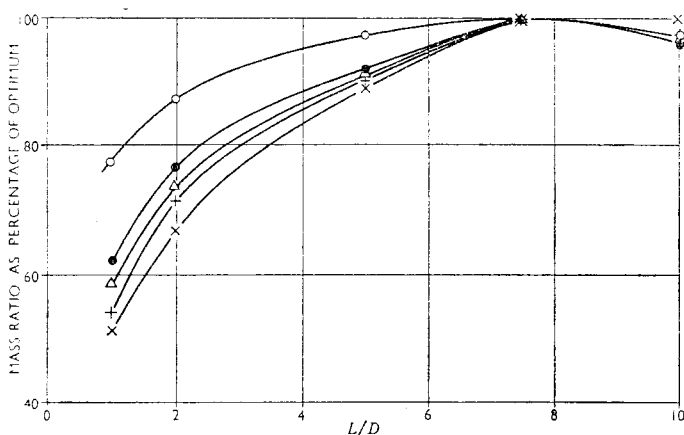


Fig. 11. Influence of Length/Diameter Ratio

Area ratio = 2.25; projection ratio = 1.5; forcing pressure = 20 lb. per sq. in. (gauge).

- Pressure ratio = 1.2.
- " " = 1.4.
- △ " " = 1.6.
- + " " = 1.8.
- × " " = 2.0.

that their influence was slight. It will be shown later that a 15 deg. diffuser is not the most efficient type, and the best results obtained here are therefore inferior to some quoted later, but the 15 deg. angle was adopted to avoid difficulties which would have arisen if an attempt had been made to employ in the existing ejector body a smaller angle of divergence together with a parallel mixing chamber more than about 6 diameters long.

The nozzles available enabled the length/diameter ratio of the mixing tube to be varied in five steps to cover a range between 1 and 10, and it was found that the optimum ratio is in the neighbourhood of 7.5 for forcing pressures of 20 and 14 lb. per sq. in. (gauge) and is about 5 when the forcing pressure falls to 7 lb. per sq. in. (gauge). The curves of Fig. 11 refer only to a forcing pressure of 20 lb. per sq. in. (gauge) and show that the reduction in performance resulting from an incorrect choice of parallel mixing tube length is more serious for a high-pressure ratio than for a low one—indeed, the mass of suction air which can be pumped through a pressure ratio of 2.0 is reduced by half if the mixing tube throat length is reduced from 7.5 diameters to 1 diameter.

Results obtained with the large-area-ratio apparatus generally confirm these findings; Fig. 12 relates to an area ratio of 683 and four different length/diameter ratios, the combining tube varying

in length from 0.759 to 7.0 diameters. There is again a serious loss of performance if the parallel tube is too short, and this cannot be recovered by increasing the projection ratio, although the optimum projection ratio increases if the combining nozzle is shortened below its best length.

**Influence of Entry Angle.** A simple conical tube forms a convenient entrance to the parallel combining nozzle for small area ratios and a series of experiments was carried out to determine the best angle of convergence of the cone. For the purpose of these experiments, four combining tubes of diameter 6 mm., corresponding to an area ratio of 2.25, were designed, having a conical entry of total included angle 15, 24, 36, or 50 deg. respectively.

It was found that the angle of the entrance cone was of negligible importance as far as the maximum vacuum obtainable under "no flow" conditions was concerned, provided the projection ratio was suitably adjusted; for a given projection ratio,

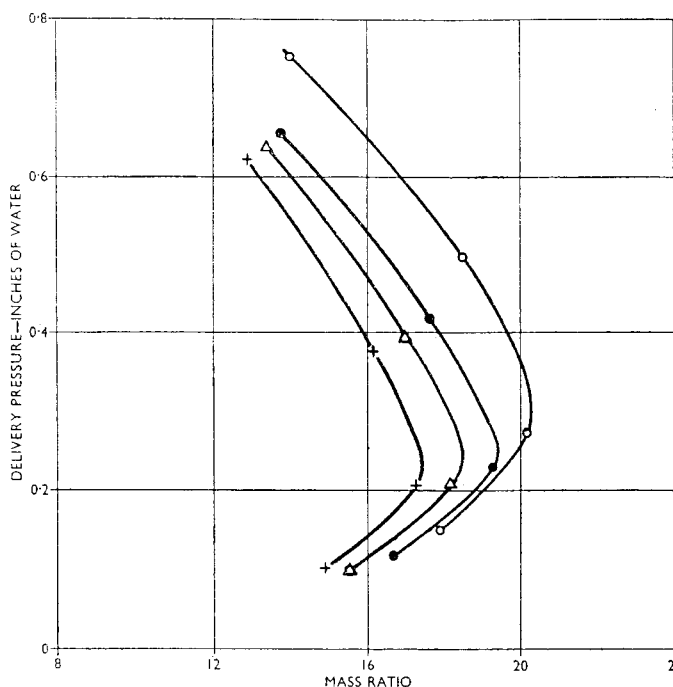


Fig. 12. Influence of Length/Diameter Ratio of Parallel Mixing Tube

Area ratio = 683.0; forcing pressure = 20 lb. per sq. in. (gauge); suction pressure is atmospheric; the projection ratio is the optimum for each length/diameter ratio.

- Length/diameter = 7. Projection ratio = 0.
- " " = 3.17. " " = 2.0.
- △ " " = 1.518. " " = 3.0.
- + " " = 0.759. " " = 3.66.

however, the mass of air drawn in at any compression ratio below that corresponding to the "no flow" condition was in some degree dependent on entry angle, the optimum angle falling within the range 24–36 deg. and the performance becoming distinctly less good if the angle was increased to 50 deg. A smaller angle than 24 deg. caused some reduction in performance but an entry angle of 15 deg. was better than one of 50 deg. For pressure ratios smaller than about 1.10 the influence of entry angle was uncertain but such low pressure-ratios are outside the ordinary working range for the area ratio of 2.25 to which the above trials refer.

Several of the combining tubes employed, shown in Fig. 3, were preceded by a flare of known radius, instead of by a straight cone; experiments indicated that such a flare could give a performance equal to that of a cone but the cone would, presumably, be preferred in most cases because of the greater ease of manufacture. The combining tubes employed to give area ratios

greater than 25 were all preceded by a flare, and, when a detachable cone of 36 deg. included-angle was substituted for this flare during experiments with an ejector of 1,110 area ratio, the quantity of air drawn in was reduced if the length of the cone was greater than about half its smallest diameter. This result should not, however, be expected to hold good for small-area-ratio ejectors.

**Influence of Diffuser Angle.** The optimum rate of divergence of the diffuser was investigated with nozzles Nos. 3, 17, and 18, and forcing nozzle No. 2 (Fig. 3). The area ratio was 2.25 throughout, the length/diameter ratio of the parallel throat was 3.33, and the length of the diffuser cone was 12 throat diameters. The conical diffuser was followed by a smooth bellmouth, terminating at the outlet flange.

The curves of Fig. 13 show results obtained with 5, 10, and 15 deg. diffusers, and forcing pressures of 7, 14, and 20 lb. per sq. in. (gauge), the projection ratio being set to the value which gave the best performance over the widest possible range of compression ratios. The inset diagram shows results extracted for two fixed pressure-ratios, namely, 1.4 and 2.0. The pressure ratios quoted represent the delivery pressure expressed as the quotient of suction pressure, so that, if the pressure in the mixing

extend any inferences drawn from the present series of experiments to cases where widely differing conditions apply.

### CONCLUSIONS

(1) Single-stage ejectors, in which air is both the suction and the forcing fluid, can be designed to pump through pressure ratios of compression between 1.0 and 3.0, if the forcing pressure is 20 lb. per sq. in. above atmospheric, and if the delivery pressure is equal to atmospheric. Under such circumstances the ratio of suction mass-flow to forcing mass-flow will vary between 0 and 20, the higher value corresponding to the lower pressure ratio.

(2) The range of area ratio  $a$ , defined as combining-tube throat area divided by forcing-nozzle throat area, to cover the above range of performance is from about 2.25 to about 700. It seems doubtful if area ratios above 700, for forcing pressures not exceeding 20 lb. per sq. in. (gauge), confer an appreciable gain, but the area ratio corresponding to the greatest induced flow may depend on the scale of the apparatus and to some extent on suction conditions.

(3) The optimum projection ratio, defined as distance from end of forcing nozzle to commencement of parallel mixing tube divided by mixing tube diameter, should be about 1.5 for ejectors

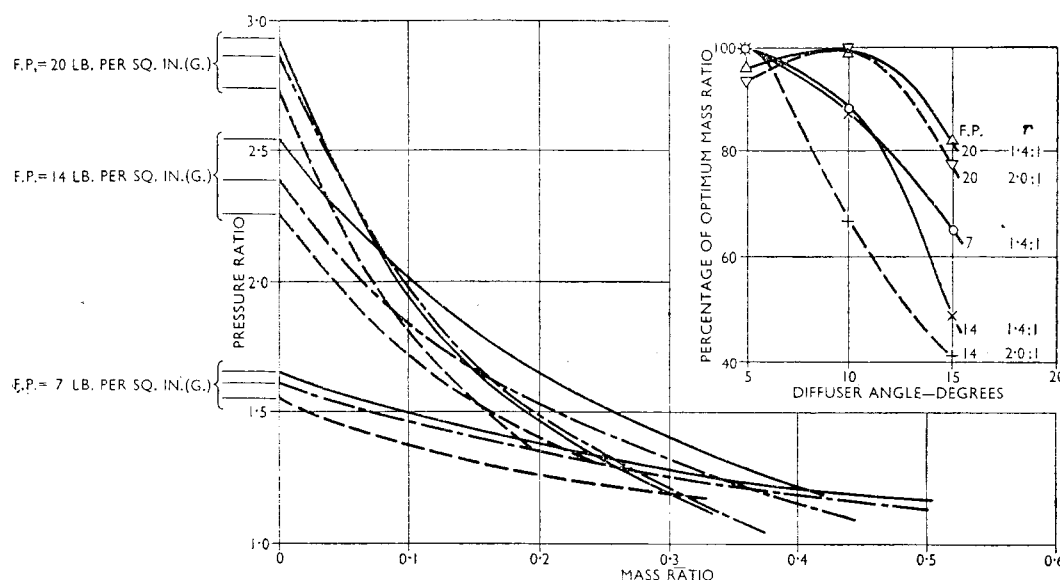


Fig. 13. Influence of Diffuser Angle

Area ratio = 2.25; projection ratio = 1.67 for 5 and 10 deg. diffusers, and 1.5 for 15 deg. diffuser; F.P. = forcing pressure;  $r$  = pressure ratio.

Key to larger figure: ————— 5 deg. diffuser.      - - - - - 10 deg. diffuser.      - . - . - 15 deg. diffuser.

tube falls appreciably below the pressure measured in the suction space, the true pressure ratios across the diffuser will be larger than those quoted, and may be greater than the value corresponding to the sonic ratio (roughly 1.9 for air). Whilst the experimental results do not enable an estimate of diffuser efficiency to be made, it is apparent that the correct choice of diffuser angle is of considerable importance, especially with the lower forcing pressures: for instance, when working with an overall pressure-ratio of 1.4 and a forcing pressure of 14 lb. per sq. in. (gauge), the substitution of a 15 deg. diffuser for a 5 deg. one results in a 35 per cent reduction in air quantity entrained, and even more with a forcing pressure of 7 lb. per sq. in. Under "no flow" conditions the lower efficiency of the 15 deg. diffuser is shown by a reduction in the ultimate pressure-ratio of compression; at the other end of the range, when the ejector is pumping a relatively large mass of air through a small pressure-range, there is still some indication that it is inadvisable to exceed a 10 deg. angle.

The results suggest that, as the forcing pressure rises, the optimum diffuser angle increases, but the data are insufficient to enable definite conclusions to be drawn. The problem of diffuser design is a difficult one, and it is probably unwise to

of small area-ratio. For larger-area-ratio ejectors the optimum projection ratio falls between zero and 1.0. These values refer to cases where the maximum suction air-flow is desired at a given degree of compression, and, if the requirement is merely the largest pressure ratio with zero mass flow, no simple relation can be given. Variations met with in practice are exhibited in Fig. 12.

(4) The length/diameter ratio of the parallel mixing tube is important and should be between 7.0 and 8.0. If this ratio is too small, some compensation can be obtained by increasing the projection ratio but the performance cannot then be made equal to the optimum.

(5) For cases where the combining-nozzle entrance is conical, experiments indicate that the cone angle should be between 24 and 36 deg. An increase to 50 deg. causes a considerable reduction in performance, and, if the angle is made less than 24 deg., the performance again falls off somewhat, though not so seriously.

(6) The diffuser angle is important in small-area-ratio ejectors (say, less than 25) and a value of about 5–10 deg. is indicated. It is suggested that no diffuser is necessary when the area ratio exceeds about 75.

## APPENDIX I

## List of Symbols.

$A$	Area of cross-section.
$c_p$	Specific heat at constant pressure.
$g$	Acceleration due to gravity.
$I$	Total heat (enthalpy).
$J$	Mechanical equivalent of heat.
$m$	Mass ratio, suction flow to forcing flow.
$p$	Pressure.
$R$	Gas constant.
$T$	Absolute temperature.
$u$	Velocity.
$\rho$	Density.
$\gamma$	Ratio of specific heats.
$\eta_{N_1}, \eta_{N_2}, \eta_D$	Forcing nozzle, suction passage and diffuser efficiencies, respectively.
$\phi$	Entropy.

**Constant-pressure Mixing.** If it is assumed (see Fig. 14a and b) that mixing occurs at constant pressure  $p_4$  and that there

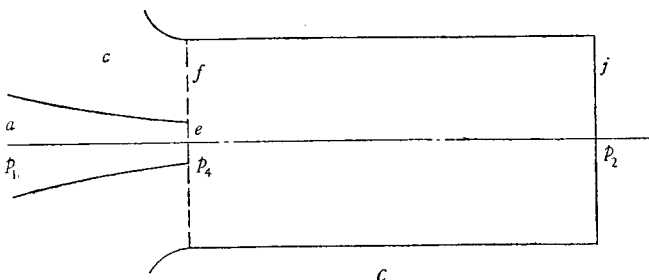
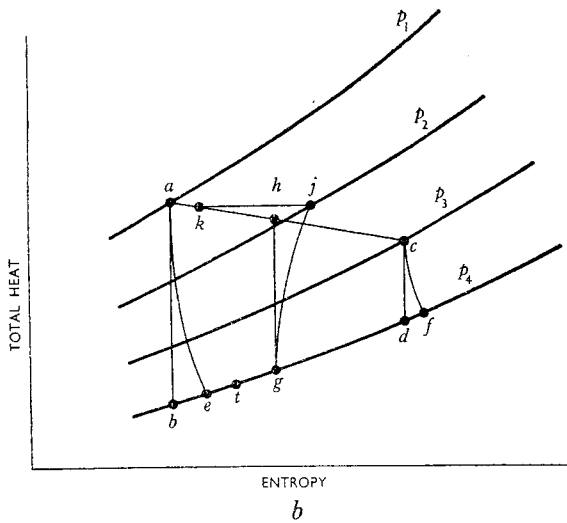
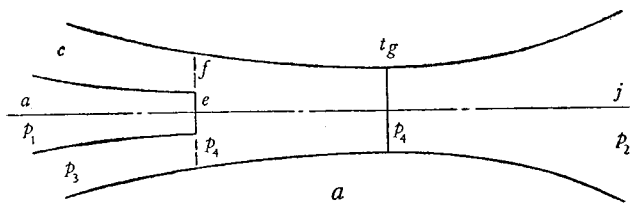


Fig. 14. The Mixing Process

a and b Constant-pressure mixing. c Constant-area mixing.

is no appreciable kinetic energy at delivery, the following equations apply:—

the energy equation,

$$T_a + mT_c = (1+m)T$$

the entropy equations, if  $\Delta\phi$  is the gain in entropy on mixing,

$$\phi_e + m\phi_f + (1+m)\Delta\phi = (1+m)\phi_g = (1+m)\phi_h$$

$$\phi_e = \phi_a + c_p \log_e \frac{T_e}{T_b}$$

$$\phi_f = \phi_c + c_p \log_e \frac{T_f}{T_d}$$

$$\phi_g = \phi_h = \phi_j - c_p \log_e \frac{T_j}{T_h}$$

the temperature equations,

$$T_e = T_a - \eta_{N_1}(T_a - T_b), \quad T_b = T_a \left( \frac{p_4}{p_1} \right)^{\frac{\gamma-1}{\gamma}}$$

$$T_f = T_c - \eta_{N_2}(T_c - T_d), \quad T_d = T_c \left( \frac{p_4}{p_3} \right)^{\frac{\gamma-1}{\gamma}}$$

$$T_j = T_g + \frac{T_h - T_g}{\eta_D}, \quad T_h = T_g \left( \frac{p_2}{p_4} \right)^{\frac{\gamma-1}{\gamma}}$$

and the momentum equation,

$$u_e + mu_f = (1+m)u_g$$

The reheat on mixing, for  $1+m$  lb. of gas, is

$$\begin{aligned} \Delta I &= \frac{1}{2gJ} \frac{m}{(1+m)} (u_e - u_f)^2 \\ &= c_{p1} \frac{m}{1+m} (\sqrt{\eta_{N_1}(T_a - T_b)} - \sqrt{\eta_{N_2}(T_c - T_d)})^2 \end{aligned}$$

and this raises the temperature of  $1+m$  lb. of gas from  $T_i$  to  $T_g$ .

$$\text{But} \quad T_i = \frac{T_e + mT_f}{1+m}$$

$$\Delta\phi = c_p \log_e \frac{T_g}{T_i}$$

$$T_g = T_i + \frac{\Delta I}{(1+m)c_p}$$

and a solution may be found for  $m$ . A graphical solution for constant-pressure mixing was developed, which required the use of  $H-\phi$  charts with lines of constant pressure at very close intervals. For accuracy, such charts have to be drawn to a large scale, and space was saved by an artifice which allowed the "forcing" region of the chart to be drawn to one-quarter of the scale of the "suction" and "delivery" regions.

**Constant-area Mixing.** For constant area mixing the momentum equation is, referring to Fig. 14c,

$$u_e + mu_f + gp_4 A_m = (1+m)u_j + gp_2 A_m$$

The area equations, if  $v = \frac{1}{\rho}$ , are

$$A_f = \frac{mv_f}{u_f} = \frac{m}{u_f} v_c \left( \frac{p_3}{p_4} \right)^{\frac{1}{\gamma}}$$

$$A_e = \frac{v_e}{u_e} = \frac{v_a}{u_e} \left( \frac{p_1}{p_4} \right)^{\frac{1}{\gamma}}$$

$$A_m - A_e = A_f$$

If the pressure ratio across the forcing nozzle is such that the nozzle should have a throat area  $A_t < A_e$ , then, calling  $\frac{A_m}{A_t} = a$  and making  $T_a = T_j$ , which was nearly true for the experiments described, the equation for  $m$  becomes for large area ratios

$$m = \frac{a}{0.259} \frac{p_3}{p_1} \sqrt{\left( \frac{p_4}{p_1} \right)^{\frac{2}{\gamma}} - \left( \frac{p_4}{p_3} \right)^{\frac{\gamma+1}{\gamma}}}$$

and for a given area ratio the mass ratio may be calculated for a selected value of  $p_4$ .



As a check, the momentum equation is solved by writing

$$u_j = \frac{(1+m)v_j}{A_m} = \frac{(1+m)v_j}{aA_t},$$

$v_j$  being found by substitution in the energy equation which becomes

$$T_a + mT_c = (1+m)\left[T_j + \frac{u_j^2}{2gJ}\right]$$

## APPENDIX II

**Calculation of Terminal Vacuum.** If it is assumed that there is no suction flow, and that the forcing jet suffers a sudden enlargement in cross-section as it passes from the forcing nozzle into the combining tube, and if, referring to Fig. 15

$$\rho_B = \rho_0 \text{ and } \frac{p_B}{\rho_B^\gamma} = \frac{p_C}{\rho_C^\gamma}$$

Then

$$\frac{p_B - p_0}{\rho_0} = \frac{u_0^2 - u_B^2}{2g} - \frac{(u_0 - u_B)^2}{2g}$$

and

$$\frac{u_B^2}{2g} = \frac{\gamma}{\gamma-1} RT_C \left\{ 1 - \left( \frac{p_B}{p_C} \right)^{\frac{\gamma-1}{\gamma}} \right\}$$

if the jet velocity is negligible at C.

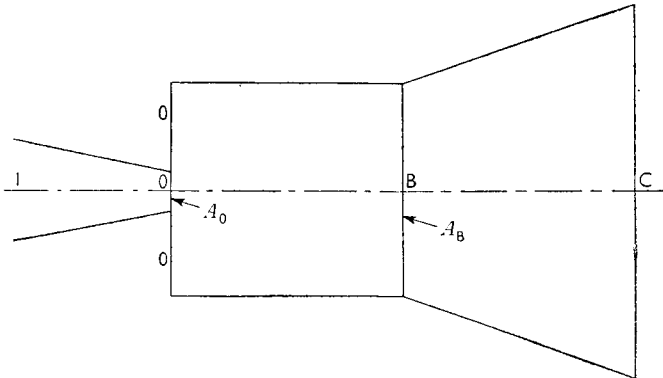


Fig. 15. Sudden Enlargement of Forcing Jet

These give, if  $\frac{p_C}{p_0} = r$ ,  $\frac{A_B}{A_0} = a$ ,  $T_1 = T_c$

$$r = \frac{1 + 7\left(\frac{a-1}{a^2}\right) \frac{1 - \left(\frac{p_0}{p_1}\right)^{\frac{\gamma-1}{\gamma}}}{\left(\frac{p_0}{p_1}\right)^{\frac{\gamma-1}{\gamma}}}}{\left[1 - \frac{1}{a^2} \left(1 - \left(\frac{p_0}{p_1}\right)^{\frac{\gamma-1}{\gamma}}\right)\right]^{\frac{\gamma}{\gamma-1}}}$$

If  $a$  is large the denominator  $\doteq 1$ .

For known values of  $p_C$ ,  $p_1$ , and  $a$ ,  $p_0$  is guessed and the equation solved by trial to give  $\frac{p_C}{p_0}$ , the terminal compression ratio.

If the exit area of the forcing nozzle is the same as the throat area and if  $\frac{p_0}{p_1}$  is less than the critical ratio, the maximum velocity attained by the jet within the forcing nozzle is less than the ideal value. Nevertheless, the above equation gives a result closer to the experimental value of  $r$  if the measured area ratio is substituted for  $a$  rather than an area ratio obtained by assuming the correct degree of divergence. This is illustrated by Fig. 8.

## APPENDIX III

### BIBLIOGRAPHY

- BAILEY, A., and WOOD, S. A. 1933-34 Technical Report of the Aeronautical Research Committee, vol. 2, p. 875.
- BOSNJAKOVIC, F. 1936 Zeitschrift für die Gesamte Kälte-Industrie, vol. 43, p. 229.
- BUSEMANN, A. 1931 Handbuch der Experimental Physik, vol. 4, p. 403.
- DOWSON, R. 1937 *The Engineer*, vol. 164, pp. 650 and 680.
- ELROD, H. G. 1945 Trans. A.S.M.E., vol. 67, p. A-170.
- EWALD, P. P., PÖSCHL, T. H., and PRANDTL, L. 1930 "The Physics of Solids and Fluids with Recent Developments" (Blackie and Son, Ltd., London).
- GOFF, J. A., and COOGAN, C. H. 1942 Trans. A.S.M.E., vol. 64, p. A-151.
- HARTMAN, J., and LAZARUS, F. 1940 *Philosophical Magazine*, 7th series, vol. 29, p. 140.
- 1941 *Philosophical Magazine*, 7th series, vol. 31, p. 35.
- HAWTHORNE, W. R., and COHEN, H. 1944 Royal Aircraft Establishment Report, E. 3997.
- KEENAN, J. H., and NEUMANN, E. P. 1942 Trans. A.S.M.E., vol. 64, p. A-75.
- KEENAN, J. H., NEUMANN, E. P., and LUSTWERK, F. 1948 Massachusetts Institute of Technology Meteor Report No. 18.
- KUETHE, A. M. 1935 Trans. A.S.M.E., vol. 57, p. A-87.
- MCCLINTOCK, F. A., and HOOD, J. H. 1946 *Jl. Aeronautical Sciences*, p. 559.
- MELLANBY, A. L. 1928 Trans. Inst. Chemical Eng., vol. 6, p. 66.
- NIKURADSE, J. 1929 Z.V.D.I., vol. 289.
- PRANDTL, L. 1925 Zeitschrift für Angewandte Mathematik und Mechanik, vol. 5, p. 136.
- ROYDS, R., and JOHNSON, E. 1941 Proc. I.Mech.E., vol. 145, p. 193.
- STODOLA, A. 1927 "Steam and Gas Turbines", vol. 2, p. 927 (McGraw-Hill Publishing Company, New York and London).
- THIRD, A. D. 1927 *Jl. Roy. Tech. College of Glasgow*, vol. 1, p. 84.
- THOMAS, J. S. G. 1922 *Philosophical Magazine*, 6th series, vol. 44, p. 969.
- 1924 *Philosophical Magazine*, 6th series, vol. 47, p. 1048.
- THOMAS, J. S. G., and EVANS, E. V. 1924 *Philosophical Magazine*, 6th series, vol. 46, p. 785.
- TOLLMEIN, W. 1926 Zeitschrift für Angewandte Mathematik und Mechanik, vol. 6, p. 476.
- WATSON, F. R. B. 1933 Proc. I.Mech.E., vol. 124, p. 231.
- WOOD, S. A., and BAILEY, A. 1939 Proc. I.Mech.E., vol. 142, p. 149.

Graham Manufacturing Co., Batavia, New York

## Can Air-Operated Ejectors Solve Your Problem?

*Improved vacuum engineering techniques have advanced performance of air-operated ejectors; modern units can be made to function over wide ranges of loads and pressures. Here are some details*

BY C.G. LINCK

For many years manufacturers have been marketing air-operated ejector. These ejectors have by and large been of the "garden variety" type involving the more simple applications and without too much stress placed on the efficiency of the apparatus. We are speaking particularly of purge ejectors, liquid-moving ejectors, low-vacuum evacuation ejectors, and similar applications.

Today, however, the air-operated ejector is being considered for many applications and the efficiency of the unit has assumed prime importance. The aircraft industries, as well as several process industries, have begun to recognize the value of air-operated ejectors, and in some instances, future installations will be made using air or a combination of air and steam as the motive fluid.

This article will concern itself with one such installation as well as some general data on air-operated ejectors.

To permit the reader to understand the function of an ejector, the principle of operation is given. See Fig. 2; the motive fluid,  $P_1$ , at a relatively high pressure is expanded through a nozzle to a lower pressure,  $P_2$ , thereby converting its energy to velocity, and, in turn, entrains the load fluid from the lower pressure,  $P_3$  and compresses both fluids to an intermediate or discharge pressure,  $P_5$ .

An air-steam operated injector has recently been designed, built and successfully performance-tested for installation in the altitude study facilities at a large eastern university.

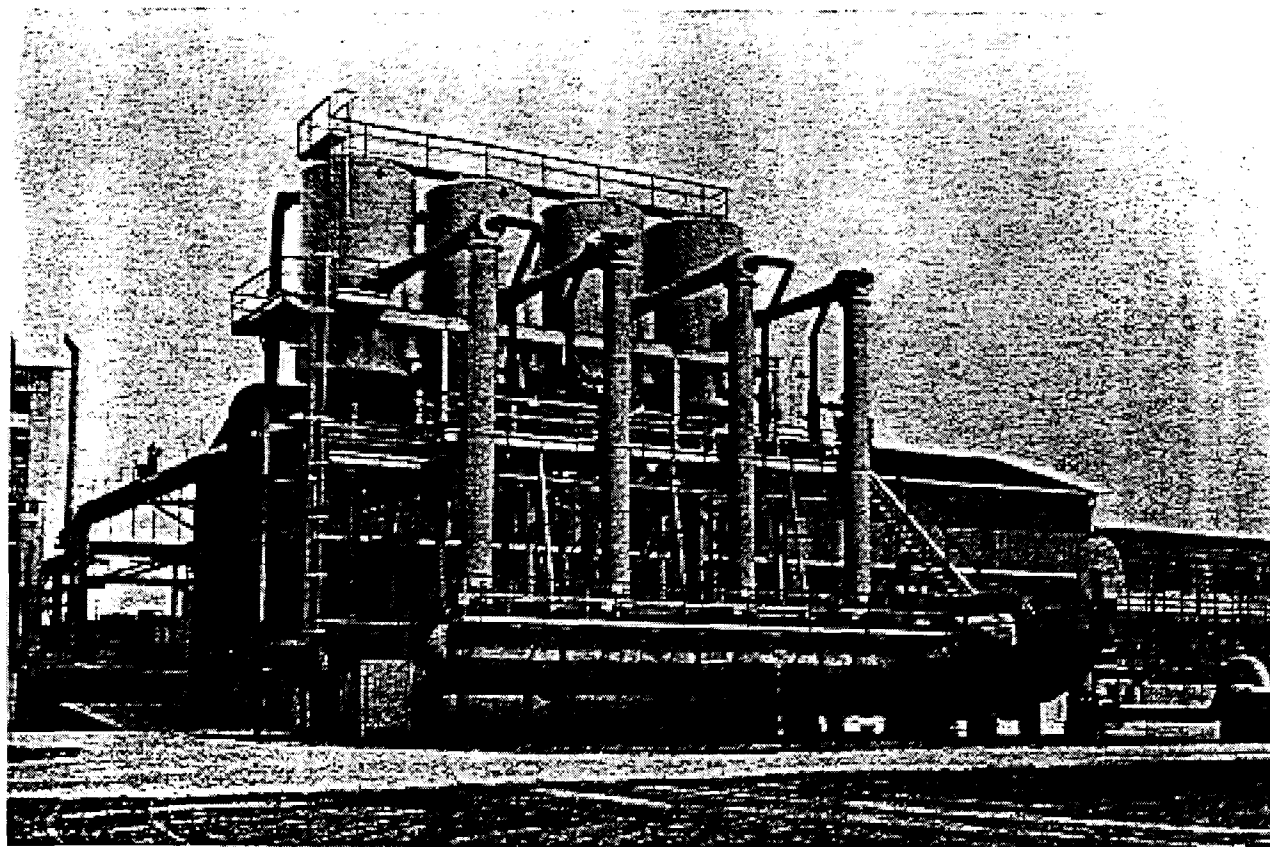


Fig. 1. One of the largest, this first-stage ejector in combination with two-stage barometric condenser handles test job

This ejector is being used to evacuate air and/or combustion products in aerodynamic and combustion experiments. The installation is believed to be the first of its size and type in the United States.

The motive fluid consists of 13,500 lb per hr of water vapor plus 24,950 lb per hr of air and combustion products. The mixture is at a temperature of 1000 F, and at a pressure of 90 psia.

## TEMPERATURE RAISED

To attain the high temperature mixture, the university takes air from mechanical compressors at 200 F, injects and burns hydrocarbon fuel in a specially designed burner, and raises the temperature of the gas mixture to approximately 3500 F. Water is then injected into the stream to cool the mixture to 1000 F, thereby producing the motive fluid specified in the previous paragraph.

Usually an ejector, regardless of its type of motive, is designed for one condition or for compressing over one range, such as from 24 in. Hg vacuum to atmospheric pressure. In the apparatus under discussion, however, the ejector is required to function over many compression ranges. Note curve in Fig. 3 which pictures the ranges covered. The manufacturer in this case guaranteed the entire curve yet maintained high ejector efficiency.

## PRESSURE CONVERTED TO VELOCITY

The design of the ejector is such that pressure energy is converted to velocity as previously stated. The first portion of the ejector is supersonic flow, the middle is sonic, and the latter part of the unit is subsonic. For the design under discussion, Fig. 4 shows Mach number encountered at three points of the unit. The Mach numbers are indicative only, since these will change for each particular range of compression.

Figure 5 shows the principal dimensions of the air-steam ejector as it left the manufacturer's plant ready for installation at the University's altitude test facilities. All dimensions are critical in nature and the shop or manufacturing technique must be of the highest standard in order not to sacrifice efficiency.

The materials of construction are listed below:

- Motive Air Inlet - Forged Steel, ASTM — A181
- Suction Chamber — Flanged Quality Steel, ASTM — A-285, Gr. C
- Air Nozzle — Stainless Steel
- Diffuser — Flanged Quality Steel, ASTM — A-285, Gr. C.

A liberal allowance for corrosion is added to the thickness required for pressure and vacuum service.

Referring to Fig. 2, a few general remarks will be of assistance to the engineer who is considering the use of air-operated ejectors for his facility.

## POINTS TO CONSIDER

1. As  $P_1$  increases in pressure, the amount required to perform a specified duty is decreased.
2. As  $P_5/P_3$  increases, the amount of  $P_1$  fluid increases. There is, however, no direct relationship between increasing  $P_5/P_3$  and the extra motive required. For example, if we consider compressing from 8 in. Hg abs to 30 in. Hg abs,  $P_5/P_3 = 30/8 = 3.75$ . From Fig. 3 we note that the amount of motive required for each pound of load =  $38400/11000 = 3.49/1$ . Then if we compress from 4 in. Hg abs to 30 in. Hg abs,  $P_5/P_3 = 30/4 = 7.5$ , so one might conclude the ratio would be  $7.5/3.75 = 2 \times 3.49 = 6.98$ . However, from Fig. 3 we can readily see the ratio is  $38400/4300 = 9.0/1$ . In other words, increasing the compression ratio merely indicates that the amount of propellant required will also increase, the extent of which can only be determined by detailed calculations or by actual test.
3.  $P_2$  and  $P_4$ , the nozzle mouth or outlet and the diffuser throat are of first importance to performance. While the theory necessary for calculating the ejector is reasonably well-known by some manufacturers, the actual ejector deviates considerably from the theoretical. There is no mathematical answer for the deviation and therefore engineers interested in air- or gas-operated ejectors should refer their problems to experienced manufacturers of this type of equipment.

Referring to Fig. 6, it will be noted that air ratios for various vacua at various temperatures are plotted to picture the decrease in motive required as the temperature of the motive increases. The pressure of the motive air remains the same for all temperatures listed.

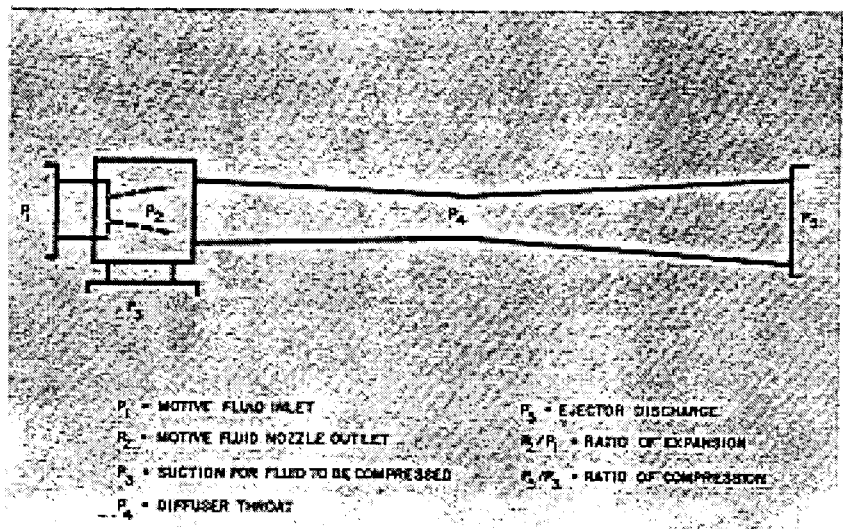


Fig. 2. Diagram of ejector; motive fluid at high pressure expands from  $P_1$  to  $P_2$ , converting energy to velocity and entraining load fluid from low-pressure  $P_3$ .

The reader will note that Fig. 6 does not show air temperatures beyond 800 F. This is because any further increase in air temperature (using 100 psig) will not decrease the amount of motive or propellant required.

This is caused by the fact that as the temperature of motive fluid is increased, two things occur. First, the velocity of expansion increases, but at the same time the duty required for compression increases. When the increase in compression duty offsets the advantages of the higher temperature motive, the "point of no return" has been reached.

### FOR EACH PRESSURE, A TEMPERATURE

This means that for each air pressure there is one temperature which will yield maximum results. Some variation in best temperature for a particular motive pressure will exist since the compression ratio also plays a part in determining the most efficient temperature for any selected motive pressure.

It is further true that the load temperature will influence the selection of the most efficient motive pressure for any given motive pressure.

Figure 7 shows the ratios obtained for various air pressures when the propellant temperature is held constant. The effect of this curve is to point up the importance of the motive pressure as well as the motive temperature and other points that have been discussed.

Naturally, high-pressure air is extremely desirable, but it is many times possible to increase the air temperature and achieve the desired results even though the air pressure is moderately low.

### INFORMATION NEEDED

In considering air, air-steam, or gas-operated ejectors, the engineer needs to know the following properties and conditions:

- Motive pressure
- Motive temperature
- Motive molecular weight
- Motive specific heat
- Motive specific gravity
- Load suction pressure
- Load suction temperature
- Load molecular
- Weight
- Load specific heat
- Load specific gravity

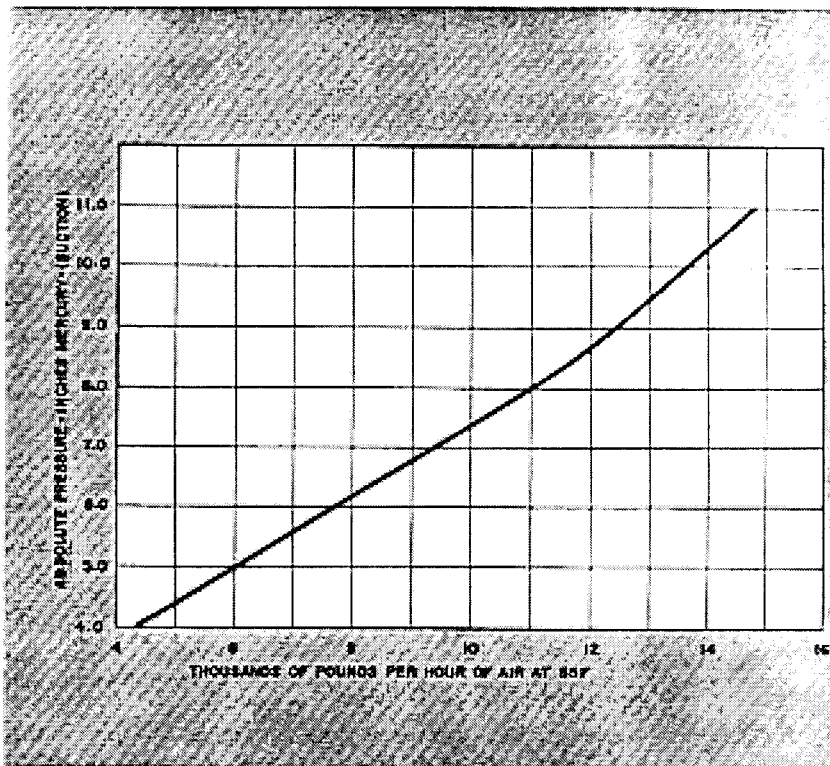


Fig. 3. Curve shows range of compression produced by an air ejector at a large eastern university. Most ejectors are designed to operate at one condition, and over relatively narrow range of compression; this unit functions over range above

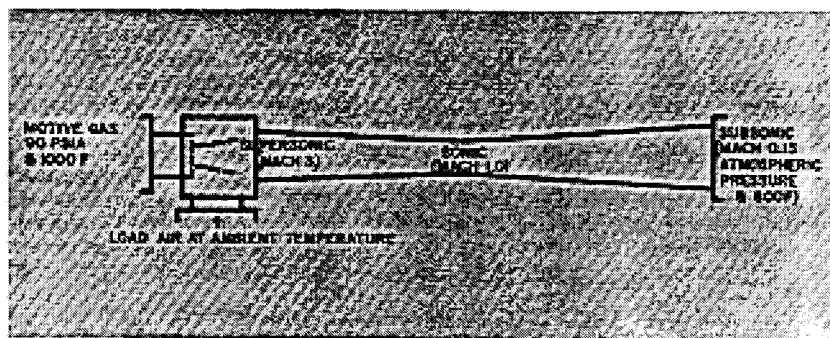


Fig. 4. Conditions existing in air ejector that has performance characteristics shown in Fig. 3. Motive fluid at inlet is supersonic, drops to sonic in throat, and to subsonic at outlet. Mach numbers typical of only one set of conditions

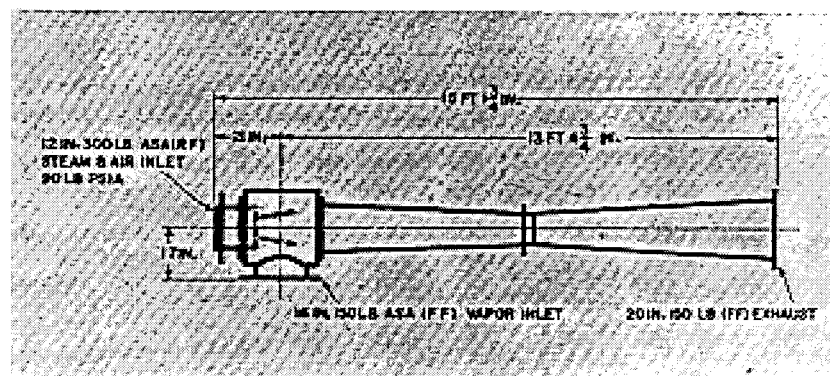


Fig. 5. Physical dimensions of ejector from Figs. 3 and 4. Dimensions are very critical, but performance is not matter of simple geometry; while theory is well known, actual design of this equipment requires experience with its intricacies

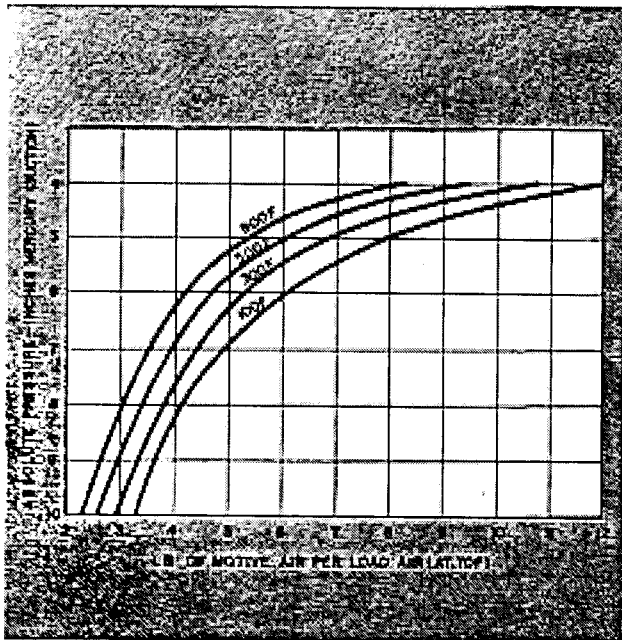


Fig. 6. Air ratios; various vacua at various temperatures; note decrease in motive required as temperature increases

Ejector discharge pressure. (Particular care should be taken to add to the discharge pressure any pressure losses anticipated from the ejector proper outlet to the final point of discharge.

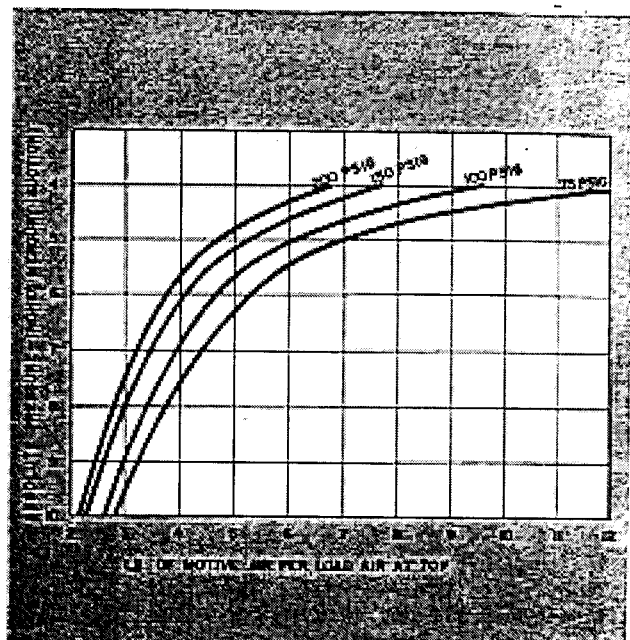
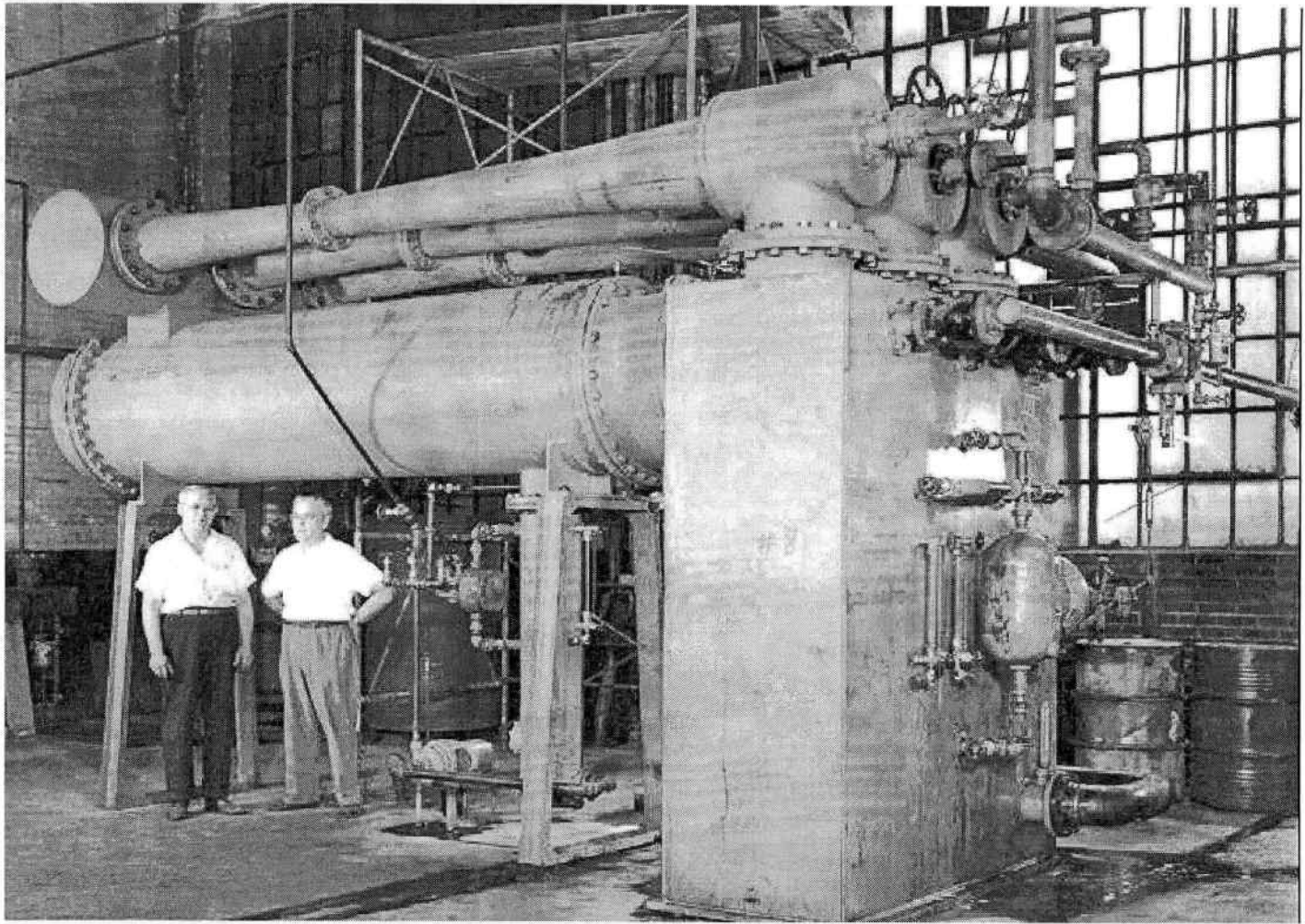


Fig. 7. Ratios obtained for various air pressures when the propellant temperature is constant; note motive pressure

In the months and years ahead, the engineer will see more and more use of the highly efficient and economical air- or gas-operated ejector. The initial cost is frequently lower than other types of vacuum producing apparatus, and the cost of obtaining high temperature motive is usually incidental to the project. Also, the operation of an air operated ejector is much quieter than ejectors motivated by steam. Like steam-operated ejectors, there are no moving parts, hence maintenance costs are negligible and operation is trouble free.





## Air Ejectors Cheaper Than Steam

When all the cost factors are considered, the air-operated ejector often proves to be the superior method for producing vacuum. Here are figures you can use.

### F. Duncan Berkeley

For many years the air-operated ejector has been a neglected child in the field of vacuum producing apparatus. It has been greatly overshadowed by its highly successful, fully reliable and popular kin, the steam ejector. The popularity of the steam ejector has been somewhat justified because air-operated ejectors have been limited in their use by a relatively expensive and somewhat scarce supply of high-pressure motive air. Major reasons for selecting steam rather than air to operate ejectors have

been the unavailability of air compressors and the relatively high cost of compressed air in most localities.

Improvements in air compressors have greatly reduced the cost of compressed air as compared to 20 years ago; and the greater availability of compressed air in process plants today makes the air ejector a reasonable and in some instances a preferred means of producing a vacuum.

The fact that air is a non-condensable gas under common conditions of temperature and pressure, limits its use as a propelling material for ejectors to two or three stages. In a steam ejector the steam from each stage of multistage units can usually be condensed in an intercondenser and the successive stage need handle only the non-condensable gases plus a relatively small saturation component from all previous stages. By condensing the

*Graham Mfg. Co., Batavia, NY*

motive steam from previous stages, it is both economical and practical to use as many as five or more stages.

### CONSIDER ALL THE FACTORS

Recent tests and studies on air-operated ejectors have brought to light some rather interesting and useful facts concerning these units. The results, although neither highly revolutionary nor startling, prove that the air jet has the same desirable feature as the steam jet; and in some instances can prove to be very economical and more desirable than the steam jet.

All factors of cost should be carefully considered for a specific application. They are:

- Initial cost of the equipment used to produce the compressed air or steam.
- Versatility of employing steam or air generating equipment for other uses in a plant or process.
- Relative costs of compressed air and steam for a particular locality.
- Operating requirements for the ejector, both vacuum and load. With all of these factors in mind, using the air-operated ejector often proves to be quite superior to other methods of producing vacuum.

### HOW THEY WORK

All ejectors operate on a common principle. They entrain air or other fluids in a high velocity jet of propelling air, steam, water or other fluid. And they use the kinetic energy in the high velocity stream of that fluid to push back the atmosphere from the discharge of the ejector.

This would suggest that the higher the velocity of the jet from the nozzle of the ejector, the greater the pressure against which the ejector can exhaust. Or if the exhaust pressure remains constant, the higher the vacuum produced by the ejector. This is true and for any particular velocity of the jet there is, of course, a limit to the vacuum that can be produced.

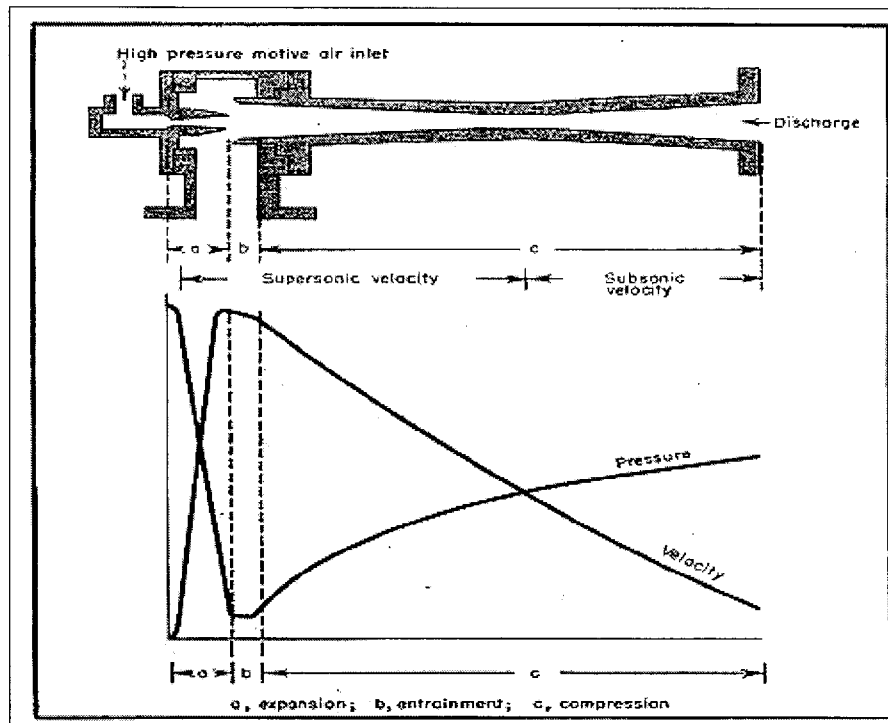


Fig. 1 - Ejector nozzle converts air pressure into velocity and the diffuser converts velocity back into pressure.

Fig. 1 illustrates approximately the conversion of air pressure into velocity in the nozzle of the ejector and the conversion of velocity into pressure in the diffuser.

Air, under the same conditions of temperature and pressure, has less internal energy in its molecules than steam. And theoretically air cannot produce as high a vacuum as can steam. However, the inefficiencies of the expansion and compression processes in an ejector when the ejector is operating over its maximum range of compression obscure the differences in ultimate vacuum produced.

For most practical purposes a one or two stage air ejector will produce as high an ultimate vacuum as will a one or two stage steam ejector. The steam jet, however, requires fewer lbs. of motive fluid to evacuate a closed vessel than the air jet and fewer lb./hr. of motive fluid to exhaust a constant load at a particular vacuum as compared to an air jet. Therefore we need to know some additional comparative characteristics to base our cost estimates on.

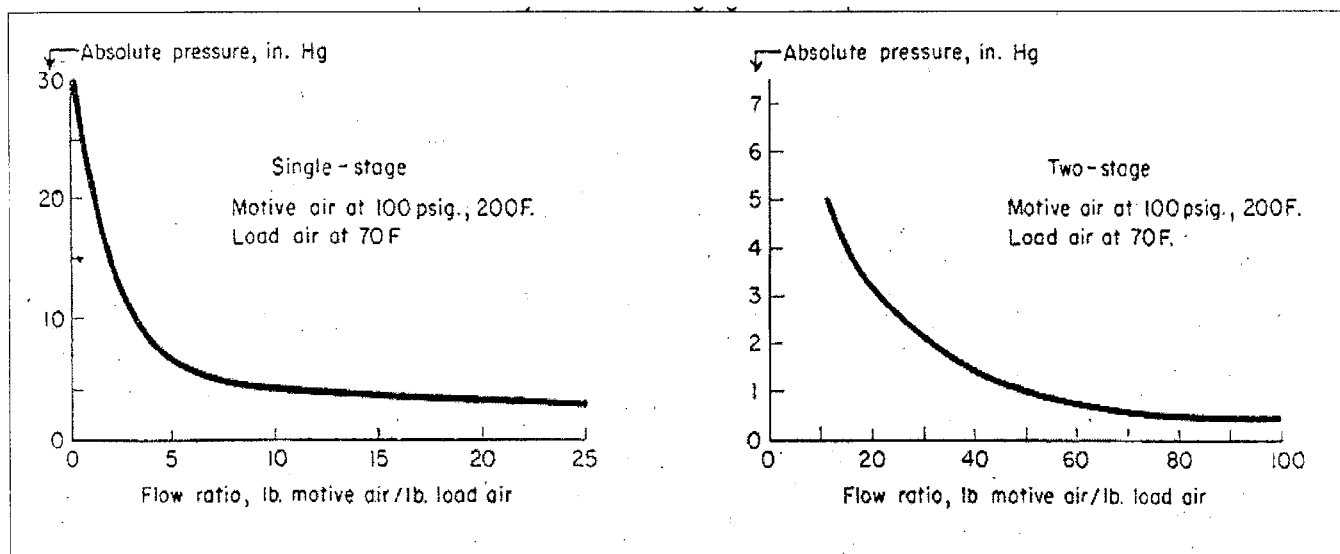
### BASIS OF COMPARISON

Because 100 psig. is a very common pressure for both compressed air and steam in industrial plants, it is a good pressure on which to base a comparison between air-operated and steam operated ejectors.

200 F. is approximately the maximum air temperature at which 100 psig. single stage air compressors will deliver air without requiring the compressor to run excessively hot. The hotter the air to the ejector, the less air is required by the ejector for any particular condition of vacuum and load.

If the air aftercooler of a compressor is bypassed or if the cooling water to the aftercooler is shut off, relatively hot air can be obtained for use in an ejector. But by doing so the air storage tank capacity is reduced and condensate will collect in the storage tank and air lines.

This might be undesirable for some compressed air installations. It is more desirable to heat the air by means of an electric heater or with a steam to air heat exchanger. Only a very small amount of electricity or low pressure steam is required to reach 200 °F.



Figs. 2 and 3 - Air consumption for single-stage and two-stage air-operated ejectors.

(or hotter), and in most cases the reduced air requirements of the ejector are well worth the additional expense.

By heating motive air to 200 F., the air required to operate an ejector can be reduced to as little as 70% of the air requirements for 70 F. air. Sometimes air ejectors are selected to keep the temperature of the load fluid low. This rules out steam ejectors. And to remove the load fluid in condensers most efficiently it would then be necessary to operate the ejector with cold air.

## TEST RESULTS

Data from our test runs on one and two stage air ejectors (of optimum design) correlate very well with data on steam ejectors. We used air at 100 psig. and 200 F. in our tests and compared the results with steam ejectors operating on 100 psig. dry saturated steam.

Single stage air ejectors require 1.4 - 1.5 lb. of air to handle the same condition of vacuum and load that 1.0 lb. of steam will when it is supplied to a single stage steam ejector.

In a two stage air ejector, 2.5-2.7 lb. of air will be needed to do the same job that 1.0 lb. of steam will do in a two stage non-condensing steam ejector.

These ratios change somewhat when the pressure of the motive air is changed. A typical figure for single stage might be 1.7 lb. of 200 psig air per

lb. of dry saturated steam at 200 psig. Or 1.4 lb. of 60 psig. air per lb. of dry saturated steam at 60 psig.

Fig. 2 shows the ratio of motive air to load air required for one stage ejectors. The absolute pressure scale covers the operating vacuum range of one stage units. Fig. 3 shows the ratio of motive air to load air required for typical two stage ejectors designed for any particular vacuum in the operating range for two stage ejectors. The ratios are based on supplying motive air at 100 psig. and 200 F. to remove load air at 70 F.

These ratios will be higher for load air above 70 F. and lower for load air below 70 F. But the corrections are small between 50-90 F. If the ejector is to handle a fluid other than air, the flow ratio must be corrected for the difference in the thermodynamic properties of the load fluid and those of air. This correction factor is usually considered a function of the relative molecular weights of the load fluid and air.

Fig. 2 shows that for pressure above 3.2 in. Hg abs., a single stage air-operated ejector is more economical to operate than a two stage ejector (when the motive air pressure is 100 psig.). The exact pressure at which two stages of compression become more economical depends on the pressure of the motive air supply. Absolute pressures as low as 0.394 in. Hg abs. (10 mm.) are practical with a two stage air-operated ejector.

## WHAT IT COSTS

Figs. 4, 5 and 6 show the operating costs of one and two stage air ejectors when the cost of the compressed air is known.

Compressor manufacturers have organized and published much useful data which permit an analysis of compressed air costs. These costs are made up of:

- Operating costs including power, labor, repairs, maintenance, lubricants, etc.
- Depreciation of equipment.
- Interest on the investment made for the equipment.

Power is the largest portion of total cost. And in many cases the cost of power need be the one consideration necessary for a study of compressed air costs.

We have used the tables in "Compressed Air Data," Ingersoll-Rand Co., Phillipsburg, N.J. (1939) to compute the cost of power required for compressed air. The other costs, being unique to each application, should be studied to determine their relative importance and effect on the overall cost.

To use the "Compressed Air Data" tables it is necessary to know the brake horsepower required to compress and deliver 100-cfm. of air and the local cost of the various fuels under consideration.



Since the brake horsepower will vary considerably with the size and type of compressor, you should obtain exact data on brake horsepower requirements from the manufacturer after the air requirements are known. However, typical figures are shown in a table of the reference we mentioned above. And the use of these figures will permit an approximate cost analysis.

### SAMPLE PROBLEM

Let's assume that an air-operated ejector is required to maintain an absolute pressure of 5 in. Hg in a system that has an air leakage of 25 lb/hr. The costs of various fuels available are:

Electricity	1.5 c./kwh
Fuel oil	9.5 c./gal
Gas	63.7 c./M cu. ft.
Gasoline	22.0 c./gal.
Coal	\$9.79/ton

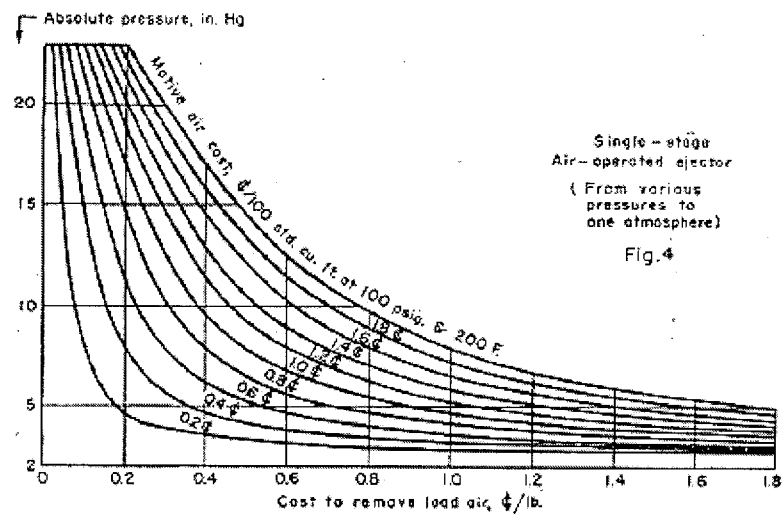
Fig. 2 shows that a one stage ejector will do the job and that 6.7 lb of 100 psig., 200 F. motive air are required for every lb. of air to be evacuated. Therefore, the total motive air required to operate the ejector would be:

$$\frac{6.7 \text{ lb.}}{\text{lb. load air}} \times \frac{25 \text{ lb. load air}}{\text{hr.}} = 167.5 \text{ lb. motive air/hr.}$$

We can now use Fig. 7 to find that 167.5 lb./hr. of air is equivalent to 37.5 standard cu. ft. of air per min.

From our reference, the brake horsepower requirements of a typical single

### Cost to Compress Dry Air



stage 100 psig. air compressor with a capacity of slightly more than 37.5 scfm. is found to be approximately 22 bhp./100 scfm. delivered. With this value and the fuel costs listed above we can enter the other tables of the "Compressed Air Data" book and find the power costs for running the compressor on the various fuels:

Electricity	0.412c. 100 cu.ft. 9.27 c./hr.	(37.5) (60)=
Fuel Oil	0.218 c. 100 cu. ft. 4.91 c./hr.	(37.5) (60)=
Gasoline	0.962 c. 100 cu. ft. 21.65 c./hr.	(37.5) (60)=
Gas	0.242 c. 100 cu. ft. 5.45 c./hr.	(37.5) (60)=

In order to determine the cost of air compressed by a steam turbine or steam engine driven compressor, we would have to know the steam rate of the turbine engine in lb. of steam per bhp.-hr. A typical figure might be 28 lb. of steam per bhp.-hr. Then the power cost for the ejector might be:

$$\frac{\$9.79}{\text{ton}} \times \frac{0.0733 \text{ c.-ton}}{100 \text{ cu.ft. \$}} \times (37.5) (60) = 16.15 \text{ c./hr.}$$

The reference table we have used is based on evaporation rate of 7 lb. of water per lb. of coal burned. It will be necessary to correct this for the actual evaporation rate.

Our calculations show that for our assumed conditions a compressor driven by an engine burning fuel oil would be the

cheapest way of producing the air necessary to operate the ejector (when only power costs are considered).

### AIR COSTS ARE REASONABLE

When making cost analyses of air requirements from the reference tables, the various assumptions upon which each table is based should be checked against the actual conditions of operation. It is likely that some particular fuel will be outstandingly cheap due to local conditions. In such cases these approximate calculations will show conclusively which fuel is most economical.

Although the data above are limited to ejectors operating on 100 psig., 200 F. air, we can see that power costs of air-operated ejectors can be quite reasonable.

### AIR vs STEAM

Under most circumstances where steam is already available, a steam ejector would be used in preference to an air-operated ejector. Economics would dictate the choice. If steam is not available, air might well be the cheaper motive fluid.

There are also cases where air-operated ejectors are selected for other than economic reasons. In general, air-operated ejectors are most desirable where the heating or diluting features of the steam ejector are objectionable; where compressed air is more readily available than steam; where the properties of air are desirable as the motivating fluid.

### SOME APPLICATIONS

There are many services for which an air-operated ejector is ideally suited. Pump priming is readily done by means of an air or steam operated ejector which operates only long enough to exhaust the air from the pump casing and piping. This permits the system to become fined with the liquid to be pumped. The ejector is then isolated from the system by means of a valve. The pump is turned on. And the ejector air supply is turned off. This leaves the pump primed and ready for operation.

A siphon pipe system which uses gravity to draw water or some other liquid over a high elevation without the use of

expensive pumps requires some initial priming to start-up. It can be primed by using an air-operated ejector operating on air from a portable or stationary compressor.

The pumping of corrosive, tarry or sludge liquids can be done without the use of special pumps by means of an air-operated ejector.

Frequently we want to recover vapor in an intercondenser in its pure state, undiluted and unheated. To accomplish this we can use an air-operated ejector for the initial stage of compression to compress the vapor to a pressure where it can be easily condensed. Either a steam ejector or an air-operated ejector can be used to maintain the required intercondenser vacuum.

### THE THERMOCOMPRESSOR

Many applications require compressed air at a pressure below the available air pressure. This makes it necessary to throttle the air through an orifice or valve to reduce its pressure. The cost of compressing air to a high pressure and then throttling to a lower pressure for a particular application can be reduced by installing an air operated thermocompressor.

Working on the same principle as a vacuum producing ejector, the thermocompressor picks up air at atmospheric pressure (or higher) and by means of a high velocity air jet compresses the atmospheric air to the required pressure. The savings accomplished by the thermocompressor are derived from reducing the consumption of high pressure air by the amount of atmospheric air that the thermocompressor will entrain.

Thermocompressors operating on air, steam and many other fluids have found a wide and useful field of application in industry.

The rugged and simple construction of ejectors along with the fact that they can handle large volumes of fluids (without the relatively enormous proportions of other types of vacuum pumps) often determines when and where an ejector should be used. Other considerations may, of course, outweigh the size and simplicity factors. An overall picture of requirements is necessary to select the best suited vacuum pump for your needs.

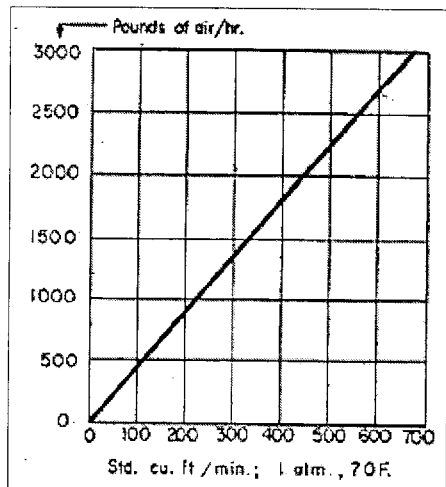


Fig. 7 - Volume-weight conversion chart

# DESIGN AND PERFORMANCE OF A VARIETY OF INJECTOR SYSTEMS

M. L. Hoggarth\* D. A. Jones\*

A study of the design of injectors or ejectors as used in the gas industry has led to the identification of three principal methods of entrainment of the induced gas by the driving gas. The performances of injectors using these methods have been compared both theoretically and experimentally using the criterion of pressure efficiency. From the results obtained it was found that in practice the highest pressure efficiencies were obtained by jet entrainment injectors. This method of injection was used in an examination of the consistency of the injection ratio over the operating range with respect to variations in gas supply, governor and downstream pressures and changes in specific gravity and discharge losses.

## 1 INTRODUCTION

AN IMPORTANT APPLICATION of injectors or ejectors is in the utilization of gaseous fuels; they are used both as a device that can produce sufficient pressure to drive the fuel-air mixture through the burner port on which the flame is stabilized and as a means to control fuel/air proportioning over the range of operation required. The most familiar use is in the bunsen burner, where a stream of gas entrains part of the air for combustion, the remainder being supplied as secondary air from the atmosphere around the flame. In the context of industrial gas utilization, it is advantageous to use low-pressure air from a fan to induce gas because more favourable mass entrainment ratios (i.e. mass of induced gas/mass of driving gas), ranging from  $\frac{1}{8}$  for town gas to  $\frac{1}{17}$  for natural gas, can be employed. As a result, greater mixture pressures can be used to force the fuel-air mixture through small burner ports to give high combustion intensities, high exit velocities and improved plant efficiency.

Commercially available injectors vary greatly in construction, operation and performance. Consequently it is desirable to investigate their performance so as to establish the most effective design and method of operation. Inspection indicates that there are three distinct categories of proprietary injector in regular use differing in the method of entrainment employed:

(1) *Jet entrainment.* In this method (Fig. 1) the driving gas (air) is accelerated through a nozzle forming a high-velocity jet in which the entrained fuel gas mixes. There is a large velocity gradient at the edge of the driving gas stream that draws in the almost stationary surrounding fuel gas and carries it forward into a cylindrical mixing tube or throat. The jet of mixed gas continues to expand to fill the throat by entrainment of recirculated mixture. Momentum is lost in the process and some static pressure is recovered. Further recovery may be obtained by decelerating the mixture in a gradual diffuser following the throat. Perhaps the most important features of this method are that there is a high shearing force between the two gas streams and that the induced gas contributes little axial momentum.

(2) *Entrainment at equal velocities.* The driving gas (air) is again accelerated through a nozzle, but in this

instance the induced fuel gas is entrained coaxially by the creation of a substantial pressure reduction at the outlet of the driving gas nozzle. If the discharge area of the driving and induced gas streams are correctly selected, equal driving and induced gas velocities result and shearing forces are eliminated. Mixing is achieved by eddy diffusion between the two gas streams.

(3) *Entrainment into a venturi tube.* Venturi tubes, in which gas is induced through orifices at a position corresponding to the vena contracta, are sometimes used as injectors, presumably because the venturi tube has been recognized as a good pressure recovery device in flow metering. When a venturi is used as an injector, entrainment takes place, which reduces this pressure recovery.

A useful concept for the assessment of effectiveness of injector performance at a specified injection ratio is the pressure efficiency  $\eta_p$ , the fraction of the driving static pressure that appears as mixture pressure at the outlet of the injector.

The key to the calculation of performance for all these different injector configurations is the application of a force-momentum balance to the mixing process in the throat to find the static pressure rise. The purpose of this paper is to compare the theoretical and measured performance of the injector types discussed and to identify

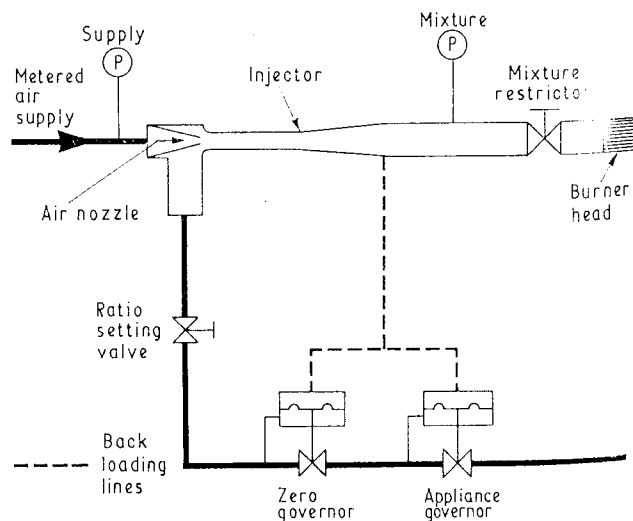


Fig. 1. Arrangement of apparatus.

The MS. of this paper was received at the Institution on 24th January 1972 and accepted for publication on 9th August 1973. 34

\* British Gas Corporation, Midlands Research Station, Wharf Lane, Solihull, Warwickshire.

the most effective and economic design for producing pressure rise and maintaining a consistent control of fuel/air proportioning.

The injector is particularly useful in air/fuel ratio control, because it inherently exercises a self-proportioning action; that is, it has the ability to maintain a substantially constant air/fuel ratio over a wide range of throughputs, providing the induced gas is supplied at a pressure substantially equal to that into which the exit orifice from the injector vents and variations in flow characteristics of components and gas quality are small. Both theoretical and experimental studies have been made on the possible variation in air/fuel ratio over the operating range with realistic changes in induced gas supply pressure, friction and discharge losses through valves and the injector body, downstream pressure changes and gas quality (i.e. density) variations.

### 1.1 Notation

$A$	Cross-sectional area.
$C$	Discharge coefficient.
$C_{cj}$	Contraction coefficient.
$C_{dp}$	Flame port discharge coefficient.
$C_{vj}$	Velocity coefficient.
$C_{wj}$	Mass flow coefficient.
$g$	Gravitational acceleration.
$f$	Gauge pressure (because the driving pressures available for combustion systems are small, it is convenient to express all the equations in terms of gauge pressures).
$\dot{Q}$	Volume flow rate.
$R_a$	Air/fuel ratio (in an air blast system the reciprocal of injection ratio).
$R_v$	S.t.p. volume ratio, injected/jet fluid (injection ratio).
$S$	Total friction loss coefficient.
$S_{12}$	Mixture-tube friction loss coefficient.
$S_d$	Diffuser friction loss coefficient.
$s$	Specific gravity (air = 1).
$\dot{W}$	Mass flow rate.
$\eta$	Pressure efficiency.
$\rho$	Density.

#### Subscripts

$g$	Gas.
$i$	Injected fluid inlet.
$j$	Jet supply.
$n$	Mixture-tube or throat.
$1$	Jet nozzle exit.
$2$	End of mixture tube or throat.

## 2 THE DESIGN OF AIR BLAST INJECTORS

The three main methods of entrainment used in air blast injectors have been introduced in the previous section. More detailed consideration of their design and operation is given below.

### 2.1 Jet entrainment injectors

The design of jet entrainment injectors has been considered in some detail by Francis (1)\*. In designing the injector it is usual for the mass or volume ratio of entrained to jet fluid and the quantity of jet fluid or the jet supply pressure to be specified. It is then necessary to calculate

\* Reference is given in the Appendix.

the pressure rise from the inlet of the entrained fluid to the outlet of the diffuser. For a given injection ratio, there is one ratio of throat to jet nozzle cross-sections that makes this outlet mixture pressure a maximum and gives the optimum performance of the injector. The basis of the calculations is the application of the force-momentum equation to the mixing and pressure-recovery processes taking place in the parallel throat or mixture-tube. The assumptions that are made are:

- (1) Turbulent conditions prevail in the jet and at the end of the mixing tube or throat, implying that velocity, composition and temperature are reasonably uniform over a cross-section at these two positions.
- (2) No phase changes take place.
- (3) The flow between nozzle exit and diffuser exit is incompressible, i.e. density changes due to absolute pressure changes are negligible. This does not rule out density changes due to change of temperature.
- (4) Buoyancy effects are unimportant.

Denoting the planes at the exits of the nozzle and throat by subscripts 1 and 2 respectively, application of the momentum theorem to the mixing-process between planes 1 and 2 leads to

$$\left[ p_2 - p_1 + S_{12} \frac{W_m Q_m}{2g A_m^2} \right] A_m = \frac{W_j Q_j}{g A_j C_{cj}} - \frac{W_m Q_m}{g A_m} \quad (1)$$

where  $S_{12}$  is the wall friction pressure loss in the throat expressed in velocity heads of mixed fluid at the end of the throat. If the diffuser loss  $S_d$  is expressed in the same terms, then the final pressure at the end of the diffuser will be

$$p_m = p_2 + (1 - S_d) \frac{W_m Q_m}{2g A_m^2} \quad (2)$$

The performance of the injector may be expressed in terms of pressure efficiency for an injector consisting of a parallel throat and gradual diffuser:

$$\eta = \frac{(p_m - p_1)}{\frac{W_j Q_j}{2g A_j^2 C_{cj}^2}} = \frac{2A_j C_{cj} - (1 + S_{12} + S_d)(1 + R_m)^2 \left( \frac{\rho_1}{\rho_2} \right) \frac{A_j^2 C_{cj}^2}{A_m^2}}{A_m} \quad (3)$$

For a given mass ratio of  $R_m$  the injector or pressure efficiency can easily be shown to be equal to a maximum when:

$$\eta = \frac{A_j C_{cj}}{A_m} = \frac{1}{(1 + S_{12} + S_d)(1 + R_m)^2} \frac{\rho_2}{\rho_1} \quad (4)$$

If entrainment is assumed to take place isothermally from atmospheric pressure, equation (4) can be rewritten with due allowance for frictional and discharge losses as:

$$\eta = \frac{p_m}{p_j} = \frac{A_j C_{vj}^2}{A_m} = \frac{R_a^2 C_{vj}^2}{(1 + S)(1 + R_a)(s + R_a)} \quad (5)$$

and similar calculations for an injector without a diffuser give:

$$\eta = \frac{p_m}{p_j} = \frac{A_j C_{vj}^2}{A_m} = \frac{R_a^2 C_{vj}^2}{(2 + S_{12})(1 + R_a)(s + R_a)} \quad (6)$$

The predicted variation in pressure efficiency with changes in the area ratio and air/fuel ratio is given in Fig. 2, both for a simple parallel throat injector and for an injector consisting of a parallel throat followed by a diverging cone acting as a diffuser.

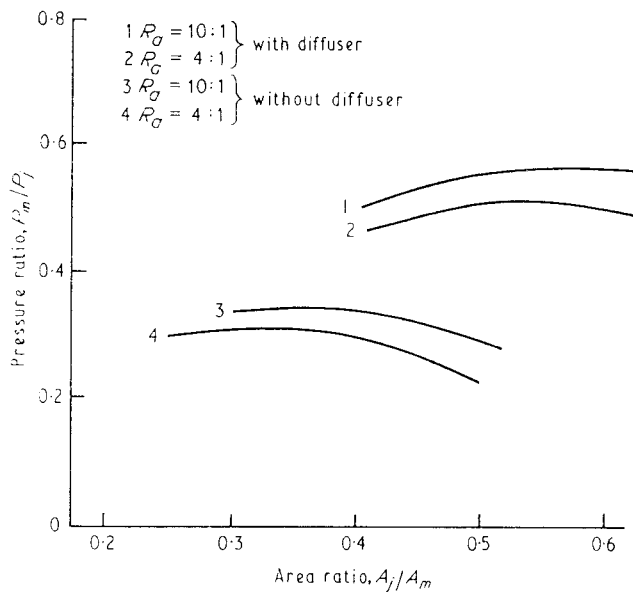


Fig. 2. Variation of pressure ratio with area ratio for an injector with and without a diffuser

The efficiency and the relative areas of the jet and throat obtained from equation (5) depend on the air/fuel ratio, the specific gravity of the gas and the friction loss and discharge coefficients. The values of the discharge and the total friction loss coefficients have been assumed to be 0.95 and 0.3, and 0.95 and 0.4 respectively.

The effects of variation in frictional and discharge coefficients on the optimum design of the injector are shown in Fig. 3. This plot has been calculated from

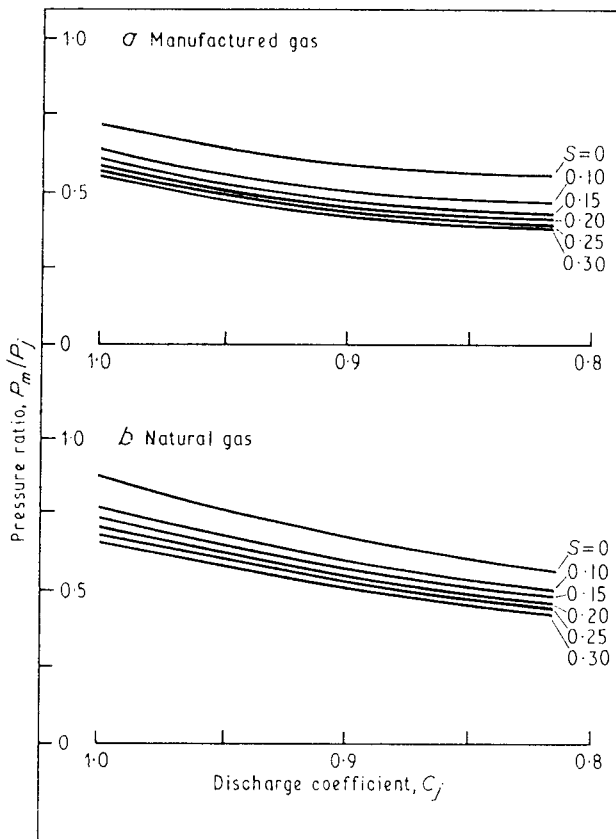


Fig. 3. Variation of pressure ratio with air nozzle discharge coefficient for various friction loss coefficients (jet entrainment)

equation (5) for a specific gravity of 0.5 (relative to air) and air/fuel ratios ( $R_a$ ) of 4:1 and 10:1. It is clear that there is only a gradual reduction in the efficiency as the discharge coefficient is reduced. Over a practical region of operation, with a discharge coefficient of 0.9 to 1.0, the reduction is about 7 per cent. Similarly, as the friction loss coefficient is increased, there is only a relatively small reduction in the pressure efficiency.

Experimental confirmation of these theoretical predictions was obtained using the injector illustrated in Fig. 4 installed in the system shown in Fig. 1. In these investigations, the effect of changes in area ratio,  $A_j/A_m$ , was explored using a series of different air nozzle sizes. The comparison between prediction and experiment for an air/fuel ratio of 4:1 is given in Fig. 5. Similar agreement between theory and experiment was obtained for a simple parallel injector without a diffuser.

From a consideration of the predictions of Figs 2 and 3

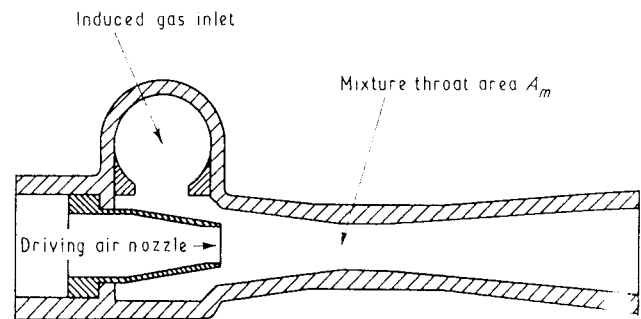


Fig. 4. Section of proprietary jet-entrainment air-blast injector

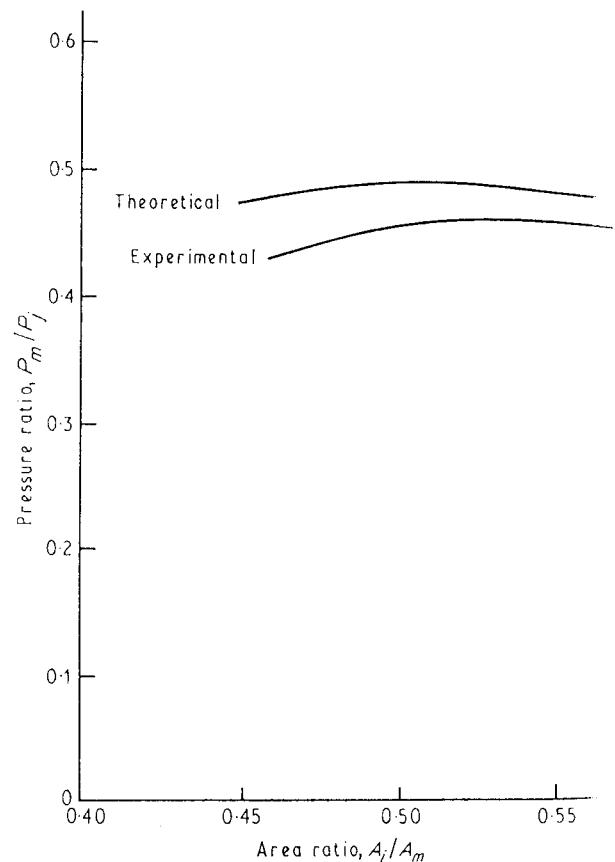


Fig. 5. Variation of ratio of mixture pressure to air supply pressure with nozzle to throat area ratio (jet entrainment)

and the experimental results shown in Fig. 5, it is clear that high injection or pressure efficiencies can be obtained using jet entrainment without the need for excessively strict manufacturing tolerances. In cases where proprietary injectors working on the jet entrainment method did not achieve the maximum efficiency predicted, it was found that the area ratios  $A_j/A_m$  seriously deviated from those required for optimum performance. Measured efficiencies were, however, generally in agreement with the values expected from the dimensions as found. It is clear that effective but simple and inexpensive injectors can be made if the jet entrainment method is used.

## 2.2 Equal velocity injectors

In this type of injector, entrainment is not produced by shearing between the driving and entrained streams, but as a result of the creation of a negative pressure around the outlet of the driving nozzle, which encourages the induction of the secondary flow. It has been assumed in this paper that a condition for the optimum performance exists when the shearing action between the jet and entrained streams is a minimum, thus leading to equal velocities between these two streams.

In predicting the performance of equal velocity entrainment injectors, the momentum of the entrained fluid, which flows parallel to the jet fluid, must be considered. To achieve equal velocities it is important to manufacture the driving air and inducing fuel gas nozzles accurately. This is most easily achieved if the air nozzle forms an annulus around the gas nozzle so that clearance for the annular gap can be as large as possible. A typical construction is shown in Fig. 6.

The analysis that follows is a development of the well known equations of continuity, momentum and energy, incorporating the following simplifying assumptions:

- (1) The injecting and injected fluids enter axially.
- (2) The flow is incompressible throughout.
- (3) Buoyancy effects are unimportant.
- (4) The driving nozzle wall thickness is negligible.

Denoting the planes at the exit of the jet and throat by 1 and 2, application of the momentum theory to the mixing process leads to:

Force = final momentum—original momentum

$$(p_1 - p_2)A_m = \frac{\rho_m Q_m^2}{2A_m} + S_{12} \frac{\rho_m Q_m^2}{2A_m} - \frac{\rho_j Q_j^2}{A_j} - \frac{\rho_i Q_i^2}{A_i} \quad (7)$$

The final pressure rise at the end of the diffuser will be:

$$p_2 - p_m = -(1 - S_d) \frac{\rho_m Q_m^2}{2A_m^2} \quad (8)$$

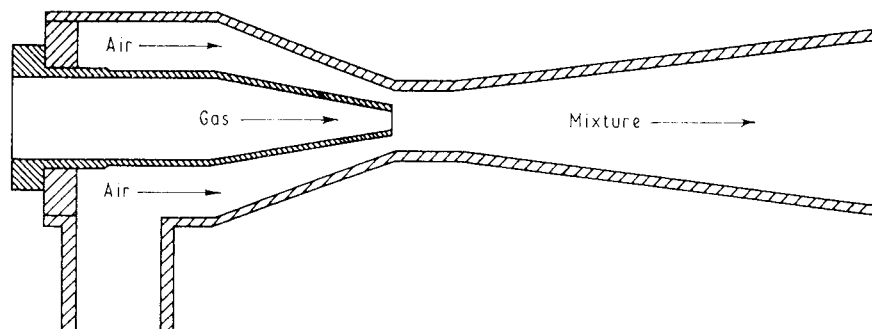


Fig. 6. Section of an equal velocity injector (annular air nozzle type)

Combining equations (4) and (5) leads to the mixture pressure recovery:

$$p_m - p_1 = \frac{\rho_j Q_j^2}{A_m A_j} + \frac{\rho_i Q_i^2}{A_m A_i} - (1 + S_d + S_{12}) \frac{\rho_m Q_m^2}{2A_m^2} \quad (9)$$

Also

$$p_j - p_1 = \frac{\rho_j Q_j^2}{2A_j C_j^2} \quad (10)$$

By applying the conditions for equal velocities and assuming the nozzle wall thickness to be negligible, the pressure efficiency of the injector may be obtained by dividing the pressure lift by the pressure drop across the air nozzle.

Two distinct efficiencies can be defined depending on whether the lift is taken from the position of plane 1 or at the inlet to the nozzle. These are:

Recovery pressure efficiency =  $\eta_1$

$$= \frac{p_m - p_1}{p_j - p_1} = \frac{\text{Mixture pressure recovery}}{\text{Differential air supply pressure}}$$

Injection or pressure efficiency =  $\eta_{gs}$

$$= \frac{p_m}{p_j} = \frac{\text{Mixture pressure}}{\text{Air supply pressure}}$$

which are expressed as:

$$\eta_1 = \frac{p_m - p_1}{p_j - p_1} = C_j^2 \frac{R_a + s}{R_a + 1} [1 - S_d - S_{12}] \quad (11)$$

Now assuming  $p_i \rightarrow 0$ , which is usually the case with air blast injectors, it can be shown that:

$$\eta_{gs} = \frac{p_m - p_i}{p_j - p_i} = \frac{p_m}{p_j} = \frac{(R_a + s)C_j^2(1 - S_d - S_{12}) - (R_a + 1)s}{(R_a + 1)[(C_j/C_i)^2 - s]} \quad (12)$$

In practice, the injection or pressure efficiency is the most useful definition to apply since it gives a measure of performance in terms of the available driving pressure above atmospheric pressure.

Results of the predictions are summarized in Fig. 7. It is noticeable from these results that, although the theoretical maximum efficiency is high when it is assumed that there are no frictional losses and that the discharge coefficient is unity, the efficiency falls off rapidly as the friction losses are increased and the discharge coefficients decreased.

In theory  $\eta_1 = 90$  per cent and  $\eta_{gs} = 80$  per cent for  $R_a = 4$  and  $\eta_1 = 96$  per cent and  $\eta_{gs} = 91$  per cent for  $R_a = 10$  when there are assumed to be no frictional losses and the discharge coefficients are unity. For practical values  $S_{12} = 0.10$ ,  $S_d = 0.15$  and  $C_j = 0.95$ ,  $\eta_1$  and  $\eta_{gs}$

26

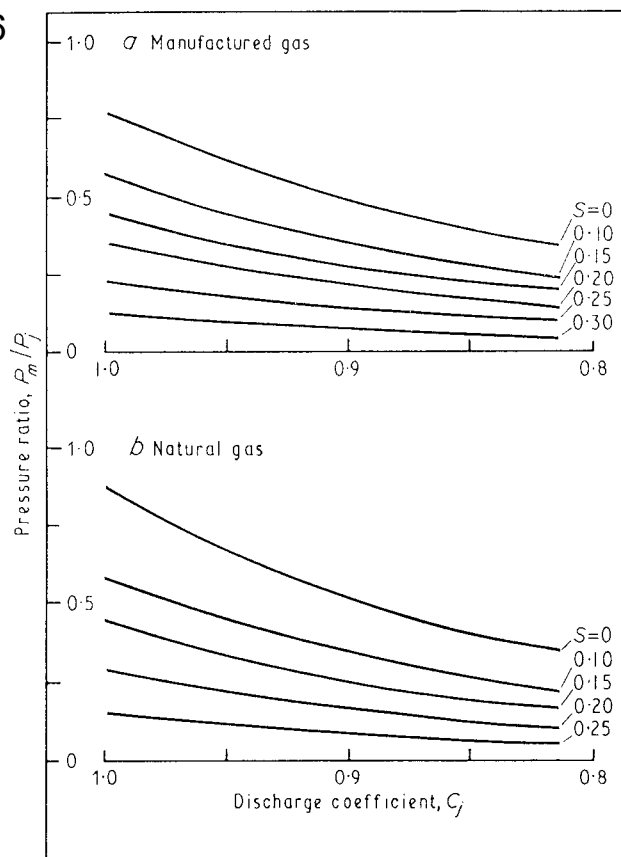


Fig. 7. Variation of pressure ratio with air nozzle discharge coefficient for various friction loss coefficients (equal velocity)

are 61 per cent and 18 per cent for  $R_a = 4$  and 65 per cent and 11 per cent for  $R_a = 10$ . Since there is little shearing action between the two streams, mixing can only result from molecular and eddy diffusion and is therefore unlikely to be as good as in the jet entrainment injector. The lengths of the throat and diffuser may however be sufficient to rectify this.

From a series of experimental investigations it was found that the discharge coefficient for the jet and injected nozzle were 0.97 and 0.94 respectively. Their areas were accurately matched by electroplating the outside of the central nozzle until the required dimensions were achieved. The smooth surface in the injector body was assumed to

give a friction loss coefficient of 0.2, resulting in the maximum injector efficiency of 25 per cent at a fuel/air ratio of  $R_a = 4$ .

The experimental results obtained were for the most favourable configuration where the discharge coefficients were as close to unity and the friction losses were as small as possible. It seems then that although this method has a high efficiency for a frictionless system, in practice, when friction losses are appreciable, the efficiency is very low.

### 2.3 Entrainment into a venturi tube

In a venturi tube, Fig. 8, there is a considerable reduction in pressure at the throat, but the overall loss in static pressure across the device is only about 15 per cent. Consequently it might be expected that an efficient injector would be produced if a series of holes were drilled in the throat. It should, however, be realized that, as soon as the secondary fluid is entrained, work is done by the entraining fluid and less pressure is recovered than when the venturi tube is used as a metering device.

The pressure efficiency and dimensions of a venturi injector are again calculated by applying a force momentum balance across the mixing zone and applying the assumptions given in 2.1 and 2.2 previously. The resulting equation is:

$$\eta = 2 \frac{A_j C_{vj}}{A_m} = \frac{(R_a + 1)(R_a + s)}{R_a^2} (1 + S) \left( \frac{A_j C_{vj}}{A_m} \right)^2 \quad (13)$$

Since there is no separate driving nozzle in a venturi injector,  $A_j C_{vj}$  is considered to be equal to  $A_m$  thus resulting in:

$$\eta = 2 - \frac{(R_a + s)(R_a + 1)}{R_a^2} (1 + S) \quad (14)$$

The pressure lift and pressure efficiency of this device depend both on the air/fuel ratio  $R_a$  and the friction loss.

Experimental results using a proprietary injector (Fig. 8) of this type gave a pressure efficiency of 26 per cent for a value of  $R_a = 4$ . For this to be achieved, the friction loss coefficient  $S$  for the throat and diffuser had to be about 0.25, a value compatible with smooth surfaces. It should, however, be pointed out that a friction loss coefficient of about 0.4, which is frequently encountered, would result in a pressure efficiency of only 4 per cent. Consequently, the performance of this type of injector is very sensitive to the quality of finish of the product. Predicted pressure

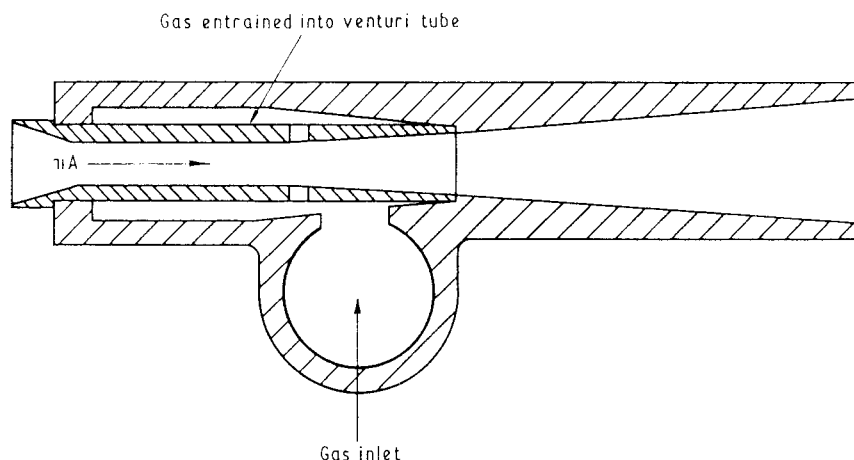


Fig. 8. Section of a proprietary venturi injector

efficiencies for  $R_a = 10$  (i.e. equivalent to use with natural gas) for friction loss coefficients of 0.25 and 0.4 result in values of 55 per cent and 38 per cent respectively. While these values do not quite match those for jet entrainment systems, they are much improved over the previous values. In this context it is perhaps interesting to note that this type of injector originates from the U.S.A. where natural gas has been widely used for some time.

### 3 AIR/FUEL RATIO CONTROL

#### 3.1 The effect of variation in governor outlet pressure and air/fuel ratio

One of the most important functions of an injector fitted to a burner is to control the injection ratio so that satisfactory flame stabilization and an acceptable combustion quality can be realized. If the air entrains the gas from a supply that is controlled to the pressure into which the injector discharges, there is then an inherent self-proportioning action which maintains the injection ratio substantially constant, thus enabling the throughput to be controlled by the operation of one valve on the air supply line. The precision with which the air/fuel ratio is maintained depends on many factors, including the consistency of the specific gravity of the gas, the friction losses throughout the system, the governor outlet pressure and the pressure downstream of the injector.

Although in practice the relative changes in these variables are generally small, it is desirable to be able to assess the possible variation that they can produce and to minimize any undesirable deviations.

To illustrate the steps involved, an air blast system as shown in Fig. 1 is considered. Here air from a low-pressure supply is driven through a convergent nozzle and entrains gas from a controlled pressure supply.

To obtain accurate control of the injection ratio, the pressure into which the burner fires must be substantially atmospheric or the inlet pressure must be controlled to be the same as the outlet pressure. The air/gas ratio is set at the low flow rate by adjusting the zero governor spring (see Fig. 1). At the high flow rate, the injection ratio must be set by a ratio setting valve, which may be either an integral part of the injector or a separate external valve. The accuracy of the self-proportioning action over the flow range can be affected both by changes in the outlet pressure of the zero governor and by the type and size of ratio setting valve chosen. If the variations in governor outlet pressure and the flow characteristics of the ratio setting valve and burner orifice are known, as a function of throughput, then the theoretical variation in injection ratio can be calculated. For an injector using jet entrainment the relationship is:

$$\frac{p_m - p_i}{p_j - p_i} = \frac{2A_j C_j^2}{A_m} \frac{(R_a + 1)(R_a + s)(1 + S_{12} + S_u)}{R_a^2} \left( \frac{A_j}{A_m} \right)^2 C_j^2 - \frac{s}{R_a^2} \left( \frac{A_j}{A_i} \right)^2 \left( \frac{C_j}{C_i} \right)^2 \quad (15)$$

The effect of the ratio setting valve characteristics and the variation in governor outlet pressure is quantitatively expressed in Fig. 9, where a comparison is made between the measured air/fuel ratio and the predicted ratio using the values of discharge coefficient and outlet pressure shown. The discharge coefficient was obtained by making rough assessment of the flow area of the valve  $A_i$  at a

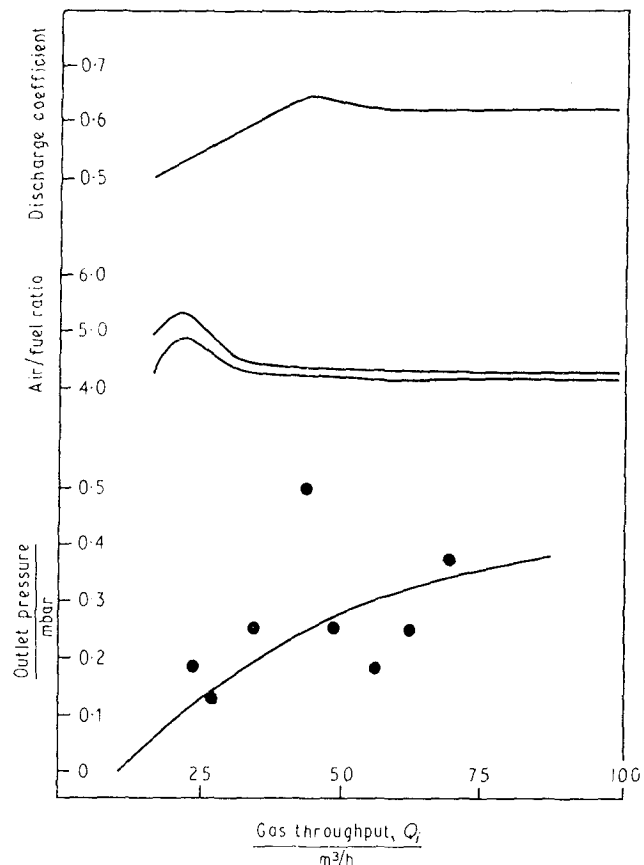


Fig. 9. Composite diagram showing: (1) comparison between the variation of measured and predicted air/gas ratio with flow rate, (2) variation of the discharge coefficient of the ratio setting valve with fluid rate, and (3) variation in zero governor outlet pressure with fluid rate

particular setting and measuring the pressure differential across the valve at each throughput. This means that although the absolute value of the discharge coefficient may be incorrect, the relative values at each flow rate will be reasonably accurate. Even closer agreement between theory and experiment can be achieved if the friction loss characteristics through the body of the injector are taken into account, although this is generally considered an unnecessary refinement. The choice of type and size of ratio setting valve is important, however, and experiments have shown that full bore straight through valves provide the greatest accuracy of air/gas ratio control.

#### 3.2 Operation against a variable back pressure

If the pressure into which the burner fires is other than atmospheric or if there are changes in the burner head orifices or the gas itself brought about for example by temperature changes, then, to maintain the self-proportioning action, the reference pressure for the appliance and zero governors should be altered from atmospheric pressure. To compensate for changes in heating chamber pressure, the tops of both the appliance and zero governors are loaded with the chamber pressure. For complete compensation for any pressure changes downstream of the injector the mixture pressure is back loaded to both the appliance and zero governors. A considerable proportion of the back loaded pressure is dropped across the ratio setting valve, so giving more precise control of the air/fuel ratio.



Experiments to test the effectiveness of mixture pressure back loading in maintaining a constant air/fuel ratio against varying downstream pressures have been carried out using a proprietary injector. The system illustrated in Fig. 1 was used with the addition of back loading lines from the outlet of the injector to the appliance and zero governors. Variations in mixture pressure were produced by an adjustable valve at the outlet of the injector. Particular attention was paid to sealing the back loading lines into the injector and into the zero and appliance governors. From Fig. 10 it can be seen that a consistent injection ratio was obtained despite severe changes in mixture pressure.

Further measurements verified the theoretical predictions for back loaded injector systems made by Francis (1), who showed that the consistency of injection ratio control was related to the pressure drops across the effective gas and air orifices and the pressure rise in the injector after mixing.

The predictions were that:

$$P_{r1} = \frac{p_j - p_i}{p_i - p_m} = \frac{(1+S)(R_a+1)(R_a+s)}{(1+S)(R_a+1)(R_a+s) - R_a^2 C_j^2} \quad (16)$$

$$P_{r2} = \frac{p_m - p_i}{p_j - p_m} = \frac{R_a^2 C_j^2}{(1+S)(R_a+1)(R_a+s) - R_a^2 C_j^2} \quad (17)$$

Comparisons between the predicted pressure ratios ( $P_{r1} = 1.96$  and  $P_{r2} = 0.84$ ) and the measured values, for an injector ratio of 4:1 and a specific gravity of 0.5 (relative to air), show close agreement (Table 1).

### 3.3 Variation of the air/fuel ratio with specific gravity of the fuel gas

In the previous discussions, the specific gravity of the fuel gas has been assumed to be constant. In practice, changes in the specific gravity do occasionally occur and their effect on the air/fuel ratio must be considered. The effect is most pronounced in an air blast system where a stoichiometric mixture is supplied by the injector and secondary air is not entrained. In these circumstances it is important that the air/fuel ratio of the mixture supplied is as close to the stoichiometric value as possible.

To calculate the rate of change of air/fuel ratio with specific gravity it is firstly necessary to consider the pressure changes throughout the combined injector and burner head system. The mixture pressure delivered by the injector must be accurately matched to the flow resistance of the burner ports. The resulting equations must then be implicitly differentiated with respect to  $dR_a/ds$ .

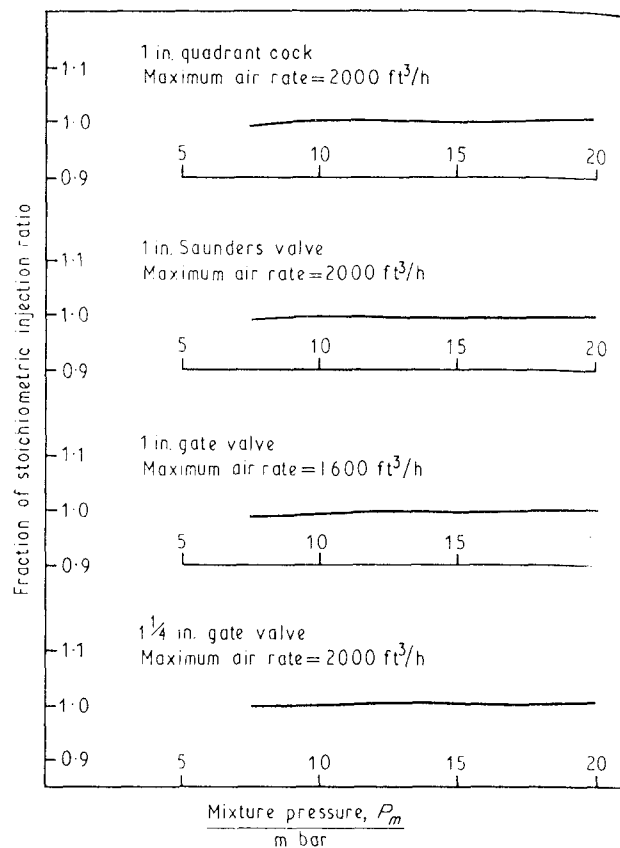


Fig. 10. Variation of injection ratio with change in mixture back pressure

The mixture pressure delivered by the injector is calculated from the well known continuity, momentum and energy equations:

$$\text{Continuity:} \quad (R_a + s)Q_i = Q_m(R_m + s) \quad (18)$$

$$\text{Momentum:} \quad p_m = \frac{\rho_j Q_j^2}{g A_j A_2} - \frac{\rho_2 A_2^2}{g A_j^2} \quad (19)$$

$$\text{Energy:} \quad p_m = p_2 + (1 - S_d) \frac{\rho_2 Q_2^2}{2g A_2^2} \quad (20)$$

to give

$$p_m = \frac{\rho_j Q_j^2}{g A_j A_2} - \frac{\rho_2 Q_2^2}{g A_2^2} - \frac{S_g \rho_g Q_g^2}{A_g^2 2g} - S_{12} \frac{\rho_2 Q_2^2}{2g A_2^2} + (1 - S_d) \frac{\rho_2 Q_2^2}{2g A_2^2} \quad (21)$$

Table 1

Air flow rate, m³/h	Gas flow rate, m³/h	Air/gas ratio	Air pressure $P_j$ , mbar	Mixture pressure $P_m$ , mbar	Gas inlet pressure $P_i$ , mbar	Measured pressure ratio	
						$P_{r1}$	$P_{r2}$
45.9	10.50	4.37	28.75	4.50	-17.00	1.89	0.89
45.4	10.40	4.36	31.50	8.00	-12.50	1.88	0.89
45.1	10.31	4.37	34.00	11.00	-9.50	1.89	0.89
44.8	10.22	4.38	36.25	13.50	-6.25	1.87	0.89
44.6	10.20	4.38	38.40	14.75	-4.00	1.88	0.89
44.3	10.13	4.38	41.00	18.25	-0.50	1.87	0.89
43.9	10.10	4.38	43.00	21.50	+2.25	1.90	0.90
43.6	9.94	4.39	45.00	24.75	+6.25	1.87	0.87
43.1	9.80	4.41	49.00	29.00	+11.00	1.90	0.90
42.5	9.67	4.41	51.50	31.75	+14.25	1.85	0.89
42.3	9.10	4.65	54.00	35.25	+17.50	1.95	0.92

This is matched to the pressure drop across the burner port of

$$p_m = \frac{\rho_2 Q_2^2}{2gA_p^2 C_{dp}^2} \quad \dots \quad (22)$$

which, after simplification, gives

$$\frac{2A_j R_a^2}{m(R_a + s)(R_a + 1)} - \left(\frac{A_j}{A_g}\right)^2 \left(\frac{S_g s}{(R_a + 1)(R_a + s)}\right) = (1 + S_a + S_{12}) \left(\frac{A_j}{A_m}\right)^2 + \left(\frac{A_j}{C_{dp} A_p}\right)^2 \quad (23)$$

This latter expression is differentiated implicitly to give:

$$\frac{dR_a}{ds} = \frac{\frac{S_g}{A_g^2} + \left[(1 + S) \frac{1}{A_m^2} + \frac{1}{C_{dp}^2 A_p^2}\right] (R_a + 1)}{\left[2R_a \left\{2 \frac{1}{A_m A_j} - \left[(1 + S) \frac{1}{A_m^2} + \frac{1}{C_{dp}^2 A_p^2}\right]\right\} - (1 + S) \left[(1 + S) \frac{1}{A_m^2} + \frac{1}{C_{dp}^2 A_p^2}\right]\right]} \quad \dots \quad (24)$$

Experimental verification of the above theoretical predictions has been made using a proprietary injector and burner head operating at an air/fuel ratio of 4:1. In calculating the change in air/fuel ratio the following values have been used in the equation:

$$A_j/A_m = 0.5, A_p = 477.4 \text{ mm}^2, A_j = 141.9 \text{ mm}^2$$

$$\text{Total frictional losses} = 0.4$$

$$\text{Burner port discharge coefficient} = 0.84$$

The only unknowns in equation (24) are the area of the gas valve opening and the corresponding friction losses through the valve, which are found from equation (21) by substituting the above values at an air/fuel ratio of 4:1. Subsequent changes in the specific gravity will not affect the ratio  $S_g/A_g^2$ .

Evaluating equation (24) gives  $dR_a/ds = 3.14$ . Experimental confirmation was obtained by introducing known proportions of nitrogen into the gas mixture, thus creating variations in specific gravity. The variation of air/fuel ratio with specific gravity ( $dR_a/ds = 3.52$ ) was in close agreement with the predicted value (Fig. 11).

#### 4 CONCLUSIONS

From the results of the theoretical and experimental investigation of the three methods of injection described it is clear that the simplest, most economic and effective design is that which employs jet entrainment. Although, in theory, under ideal conditions, the efficiency of the equal velocity injector was greater than that of the jet entrainment system, in practice very marked reductions in efficiency occurred when realistic values were taken for the friction losses and discharge coefficients. Furthermore the need for extreme accuracy in manufacturing makes this an unattractive design. Similar objections have been raised to the use of a venturi tube as an injector and here again realistic efficiencies are lower than for conventional jet entrainment systems.

The investigations into the accuracy of control of the air/fuel or injection ratio over the range of operation have shown that the possible variation in air/fuel ratio due to

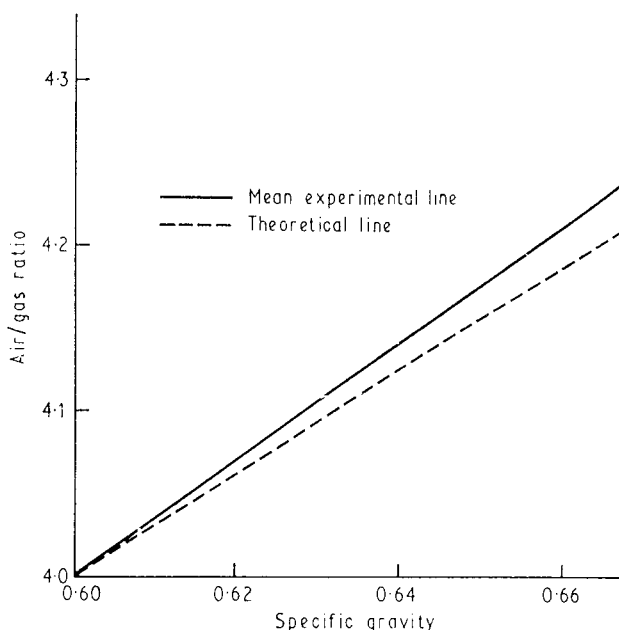


Fig. 11. Variation of air/gas ratio with specific gravity of entrained gas

the effect of the flow characteristics of the ratio setting valve, the governor outlet pressure, the effect of varying mixture back pressure and specific gravity variations, can be confidently predicted. By carefully selecting the ratio setting valve type and size and taking variation in mixture pressures into account, consistent injection ratios over turndown ratios of 5:1 can be achieved.

#### 5 ACKNOWLEDGEMENTS

This work is published by permission of the British Gas Corporation. We would like to thank Mr W. E. Francis, Assistant Director (Research), for his advice in preparing this paper and Dr L. A. Moignard, Assistant Director (Administration), for his help in editing the final text.

#### APPENDIX

##### REFERENCE

- (1) FRANCIS, W. E. 'A generalised procedure for optimum design of injectors, ejectors and jet pumps', *Inst. Gas Engrs* 1964 **4**, 373-8.

##### BIBLIOGRAPHY

- BAILEY, A. and WOOD, S. A. 'Principles of the air injector', *Aeronaut. Res. Comm. Rep. Memo. No. 1545*, 1933.
- FRANCIS, W. E. and JACKSON, B. 'Jet burner design for pressure efficiency using air blast injection', *Trans. Inst. Gas Engrs* 1957-58 **107**, 555-615.
- GOSLINE, J. E. and O'BRIEN, M. F. 'The water jet pump', *Univ. Calif. Pub. Engng* 1934 **3**, 167.
- KASTNER, L. J. and SPOONER, J. R. 'The low-pressure air driven air ejector', *Proc. Instn mech. Engrs* 1950 **162**, 149-66.
- KEENAN, J. H. and NEUMANN, E. P. 'A simple air ejector', *Appl. Mech.* 1942 **64**, 75-81.
- SILVER, R. S. 'The calculation of air entrainment in gas burners', *Gas Research Board Pub. GRB/39/23/1948*.
- SIMMONDS, W. A. 'Primary air entrainment in gas burners', *Trans. Inst. Gas Engrs* 1954-55 **104**, 557.
- WRIGHT, J. F. 'The design of tunnel burners', *Trans. Inst. Gas Engrs* 1950-51 **100**, 684.

# Engineering Outline: Jet Pumps

This article, prepared by members of the staff of BHRA Fluid Engineering, was first published in the journal 'Engineering' for 3rd May 1968 as number 123 in a series of features generally entitled 'Engineering Outline'. It is reproduced here with the agreement of the publishers of the journal.

**Definition** A jet pump is a device in which a jet of fluid (the driving fluid) is used to entrain more fluid. It consists of a nozzle, a suction box, a mixing tube (sometimes called a throat) and, in the majority of cases, a diffuser on the downstream side, **1**.

The principle of operation of this device is purely fluid dynamic and, therefore, it differs in operation from other classes of pumps, ie reciprocating, centrifugal and air lift.

The value of the jet pump lies in its simplicity and absence of moving parts. On the other hand, its efficiency is very low.

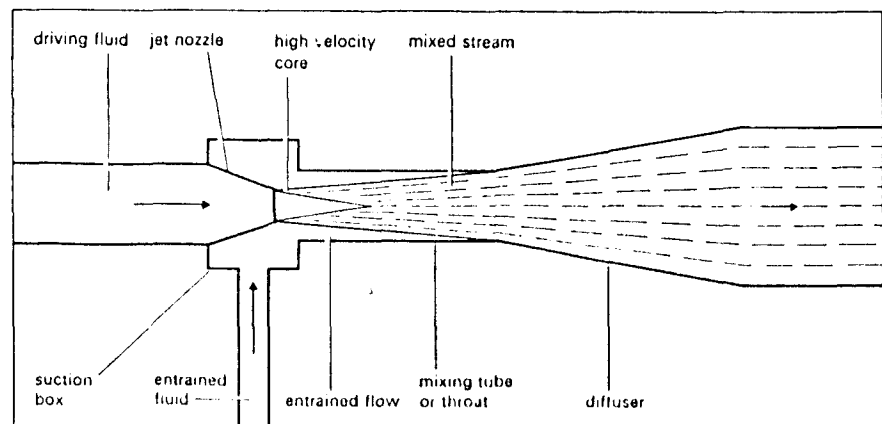
**Classification** Jet pumps are known by various names, which are usually associated with the application. Among such names are injector, ejector, eductor, and water-jet heat exchanger. The steam injector, for example, is a jet pump designed to supply feed water to a steam boiler, the driving fluid being a proportion of the steam generated by the boiler. The water-jet ejector, on the other hand, is designed to draw leakage air and other non-condensable gases from the exhaust of a steam turbine plant.

When operating as an eductor, the driving fluid, eg water, is used to entrain additional water so as to obtain a greater mass flow, but at a lower pressure than that of the driving fluid.

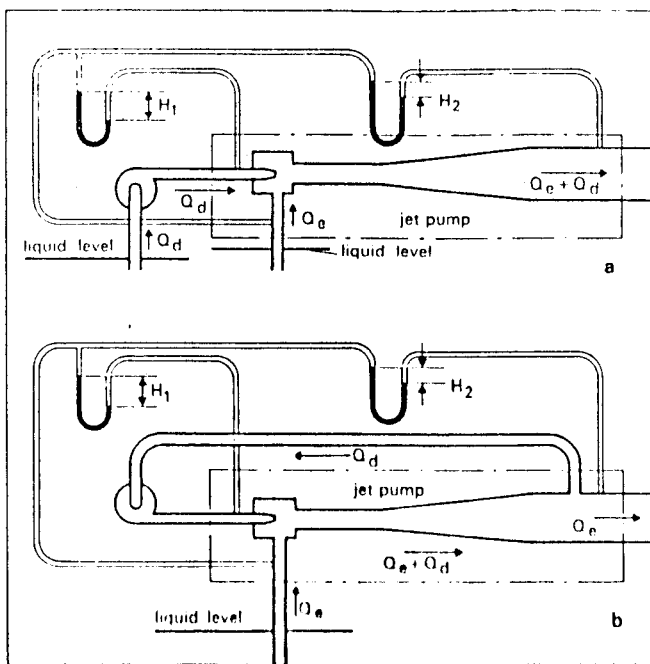
The water-jet heat exchanger is essentially the same as a steam-jet injector, the name signifying that the pump supplies heat to the feed water.

There are four basic forms of jet pump: gas-gas, liquid-liquid, gas-liquid and liquid-gas, the first mentioned fluid in each case being that used to drive the pump. Jet pumps may also be classified in accordance with the fluid components and fluid phases. For example, a steam-jet water injector is a two-phase, one-component jet pump, since steam and water are two different phases of the same fluid. A water-jet air ejector, on the other hand, is a two-component two-phase jet pump.

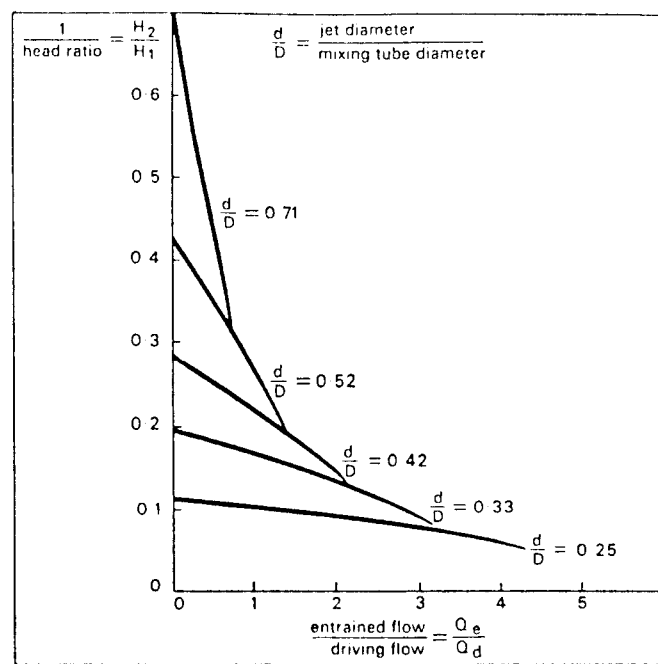
**Principle of operation** When a jet of fluid (liquid or gas) penetrates into a stagnant or slowly moving fluid, a dragging action occurs at the boundary of the two fluids, **1**. This results in mixing between the driving and entrained fluids, the momentum transfer accelerating the entrained fluid in the direction of flow of the driving fluid jet. The fluid entrainment takes place in the suction box immediately downstream of the nozzle, the acceleration of the flow



**1** Diagrammatic arrangement of jet pump, showing mixing process



2 Two methods of operating a jet pump



3 Typical head flow characteristic for a liquid-liquid jet pump

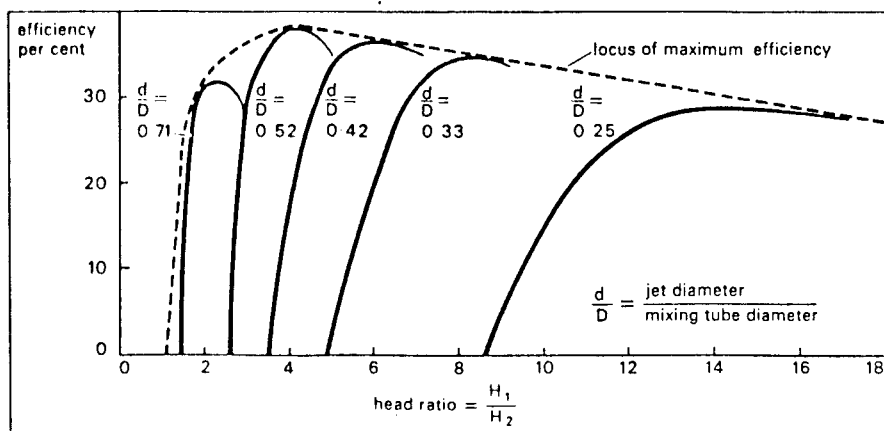
through the nozzle resulting in a high-velocity low-pressure jet. As the two fluids flow downstream, they spread into the mixing tube.

At the entrance to the mixing tube, the entrained fluid fills the annular space between the driving fluid jet and the mixing tube wall. At the mixing tube exit mixing is complete and both fluids are flowing forward at the same velocity. The diffuser serves as a head recovery device; it converts the kinetic energy to pressure energy.

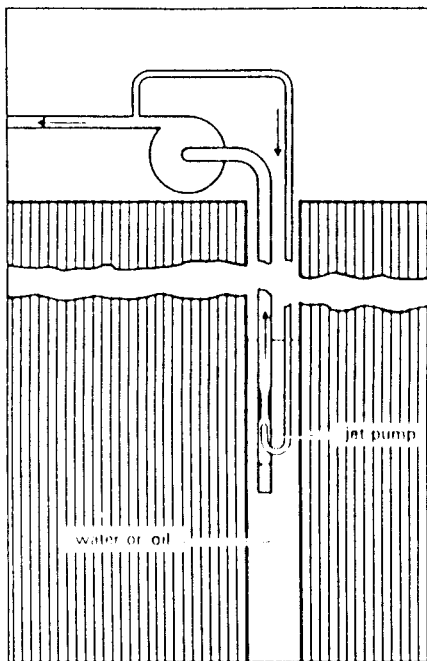
**Efficiency** To obtain the maximum benefit from a jet pump, its performance must be closely matched with the required duty. This is particularly important in view of the inherent very low efficiency of jet pumps—not exceeding some 35%. One of the factors which determines the efficiency of a jet pump is the manner in which it is used. If both the driving and entrained flows are delivered against the head at the jet pump outlet, **2a**, the overall efficiency is

$$\frac{(Q_e + Q_d)H_2}{Q_d H_1}$$

where  $Q_e$  is the entrained mass flow,  $Q_d$  is the driving mass flow,  $H_1$  is the differential head between the jet upstream and the suction inlet and  $H_2$  is the differential head between the jet pump discharge and the suction inlet. If only the entrained flow is delivered against the head, **2b**, the efficiency is reduced to  $Q_e H_2 / Q_d (H_1 - H_2)$ . This difference is due to the fact that, while in both cases the hydraulic losses within the jet pump are the same, the mass flow output is greater in the first case. Thus, in using



4 Influence on peak efficiency of the geometrical proportions of a jet pump



5 Deep-well pumping

a jet pump to pump clean water, the arrangement in **2a** would be more efficient. However, the more usual application of a jet pump would be to use clean water to pump, say, a slurry, and if the arrangement shown in **2a** were used, with clean water as the driving fluid, a substantial dilution of the slurry would result and this might prove uneconomic. In this circumstance, the second, lower-efficiency pumping method **2b** would be used.

For liquid-liquid jet pumps, correlations of pump characteristics, which closely follow experimental results, are shown in **3** and **4**. In **3** are given typical relationships between differential head ratio and flow ratio for various ratios of jet to mixing tube diameter, while **4** gives the locus of maximum efficiency for various differential head ratios and various ratios of jet to mixing tube diameter.

In accordance with practical experience, maximum efficiency is obtained when a flow ratio, in volume units, of about unity exists between the driving flow and the entrained flow for all combinations of phase and components. This is to say, when one volume of driving fluid (whether it be liquid or gas) entrains approximately one volume of the driven fluid. It is important to bear in mind that, in the case of gases, the two flows must be compared at identical conditions of pressure and temperature, ie as obtained in the suction box.

The application of momentum conservation and energy loss considerations to the mixing of two streams presents no problems when it is confined to the conditions before and after mixing is completed. The process of mixing which defines the design of, possibly, the driving nozzle and, certainly, of the mixing chamber, is far from simple. As a result of this, the theoretical design of a jet pump continues to lag behind the experimental demonstration of 'best' design. The efficiency of jet pump design would be increased if this mixing process was fully understood.

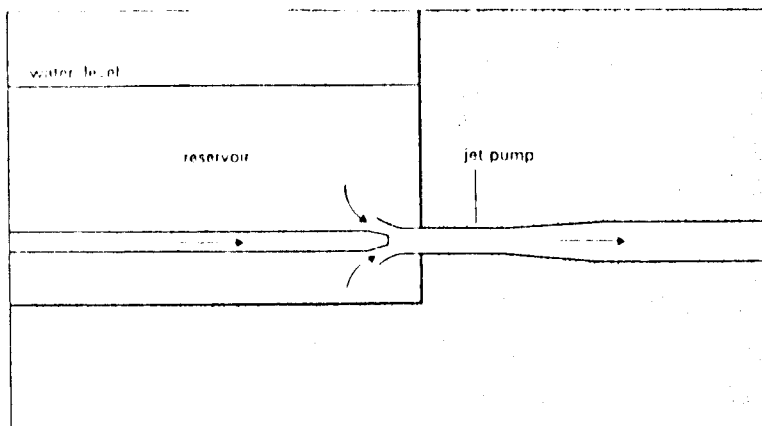
### Applications

The applications of jet pumping cover a very wide industrial field. Among the instances where jet pumping techniques may be utilized are solid materials handling, water and oil well pumping, pump priming, gas fuel installations, ventilation, distillation, generator cooling and cryogenic pumping. A few typical examples are described below.

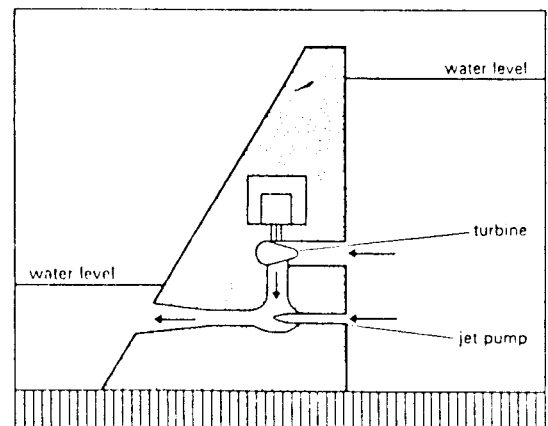
**Dredging and hydraulic transport of solids.** In the handling of solids by hydraulic means, the jet pump is of particular value. The pumps that supply the high pressure driving water to the nozzle are only required to handle a clean liquid, so that the wear and, therefore, frequent replacements normally associated with hydraulic transport are confined to the cheap and easily replaceable mixing tube assembly.

Results show that high concentrations of solids can be pumped economically with jet pump type of equipment. The jet pump is installed on the delivery side of the centrifugal pump and high pressure water is delivered from the centrifugal pump to the jet nozzle where the entrainment of solids with a relatively small amount of water takes place. On entering the mixing tube, the solids mix with the jet water and are boosted into the discharge pipe. With this arrangement, the solid material passes through pipes only and does not come into contact with any moving parts. Large particles can be transported in this manner. Recently a jet pump system for transporting molluscs from the sea bed underwent successful trials.

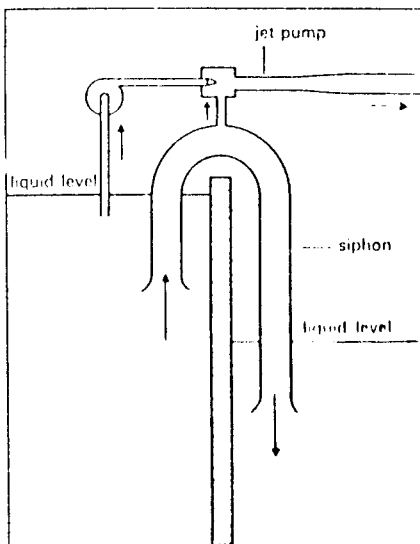
**Deep-well pumping.** When a liquid, such as water or oil, has to be



6 Booster pumping



7 Tail-water suppression



8 Priming device

raised from a deep well, 5, the suction lift may exceed the absolute vapour pressure of the liquid. In place of a submersible pumping unit, a jet pump can be used in the well in conjunction with a centrifugal pump at ground level. If the suction lift, ie jet pump delivery, is very large, a multi-stage jet pump unit can be used.

**Booster pumping.** The water jet pump can be utilized to boost the supply of water in a pipe network system. Water under pressure is supplied to a jet pump installed at the reservoir outlet, 6. The high-pressure jet entrains water from the reservoir, a flow into the system being obtained at a pressure higher than that due to the depth of water in the reservoir.

**Tail-water suppressors.** When flood-water conditions prevail in hydro-electric schemes, 7, ie when high tail-water levels exist or when relatively high water levels are required downstream for navigation or irrigation purposes, a water jet pump can be incorporated in the design to increase the effective head for power production. The system can be applied to reaction and impulse turbines as well as to tidal power units.

**Priming devices.** As a water jet pump is capable of transporting any fluid, it can be used as a general priming device; a typical case is that of a siphon, 8. There is no need to use foot valves and the accumulation of vapour bubbles at the top of the siphon is prevented by a water-air ejector maintained in operation during the siphoning process.

**Gas burner injectors.** Injectors of various types play a very important role in the utilization of gaseous fuels. In the domestic field, almost all cooker burners are designed around the atmospheric injector and many millions are in use. The atmospheric burner is also widely used in industry and its performance is often enhanced by the use of boosted gas pressure. A gas burner injector serves the dual function of mixing intimately the gas and the primary air needed for good combustion, and also of producing the mixture at a sufficient pressure to give a velocity at the burner port high enough to stabilize the flame.

**Ventilation.** Ejectors are used in ventilation work for the removal of contaminated or high temperature air. Conversely, air injectors are used as a means of diluting toxic or otherwise obnoxious fumes. A fan or, in large installations, an air compressor delivers pressurized air through a nozzle which produces a low pressure in the suction box. The toxic localities are connected to the suction box by means of pipes and the fumes are removed through the common discharge pipe on the downstream side of the diffuser.

---

**Acknowledgement** *Engineering* thanks A Linford and G Fish of the British Hydromechanics Research Association for preparing this Outline.

---

**Some centres of research or further information** British Hydromechanics Research Association, Cranfield, Bedford.  
British Pump Manufacturers' Association, London SW1.  
King's College, London University, London WC2.

---

Ejectors

Ejectors are used for many services, a rather unusual application being the use of high pressure gas to power ejectors that compress an exactly proportioned amount of air to blend with the outlet gas and provide the exact Btu content desired in the final mixture. This can be done under system control. This particular application is found in a gas distribution peak-shaving operation.

Thermal Compressors

Caption Index	Page
Introduction.....	10-1
Application.....	10-1
Characteristics.....	10-2

Introduction

An ejector is normally thought of as a compression device operating with an inlet pressure considerably below atmosphere and discharging at a level which, as a maximum, would slightly exceed atmospheric pressure. Under these conditions, while actually a compressor, an injector is classed as a vacuum producer or "pump." Its primary purpose is to pump unwanted gases and vapors out of a system into which their flow, or leakage, may be either continuous (as from a steam condenser) or practically zero (as from a very tight system being evacuated or pumped down). See Chapter 4 (pages 4-31 through 4-39) and Chapter 20. The present Chapter is concerned with the use of ejectors as *thermal compressors*, to handle gases and vapors at pressures above atmosphere.

### Application

Thermal compressors are usually allied with use or reuse of available gas or steam, or of available energy in the gas or steam, which might otherwise be wasted. Energy conserved may exist in the low-pressure induced steam or may exist in the higher-pressure motive gas.

An example involving steam is recompression and recirculation of uncondensed steam from drying drums on a Fourdrinier paper machine. The high-pressure motive steam acts as makeup for the lower-pressure steam previously condensed in the drums. A constant supply of heat from the motive steam is always available for drying.

There are many chemical processes where low pressure exhaust steam can be compressed economically by an ejector. Substantial savings are possible with a relatively small outlay.

Another application involves the use of high-pressure natural gas as motive power, the ejector acting as a reducing valve on the high-pressure line. At the same time, it compresses gas from some lower-pressure source into a mixture storage or distribution system. An adaptation is found where high-pressure gas compresses atmospheric air into a distribution line, the gas-air mixture ratio being preset and automatically controlled by the respective initial air and gas pressures.

### Characteristics

Compression ratios may be greater or less than 2 to 1, but for most applications will be less than this critical ratio. This changes the velocity pattern in the diagram of Fig. 1-N (page 1-16) in that throat velocity in area F will be below sonic. Ejector characteristics will not be the same as for an ejector with sonic diffuser throat velocity, the type discussed in Chapter 4 (page 4-31 through 4-39).

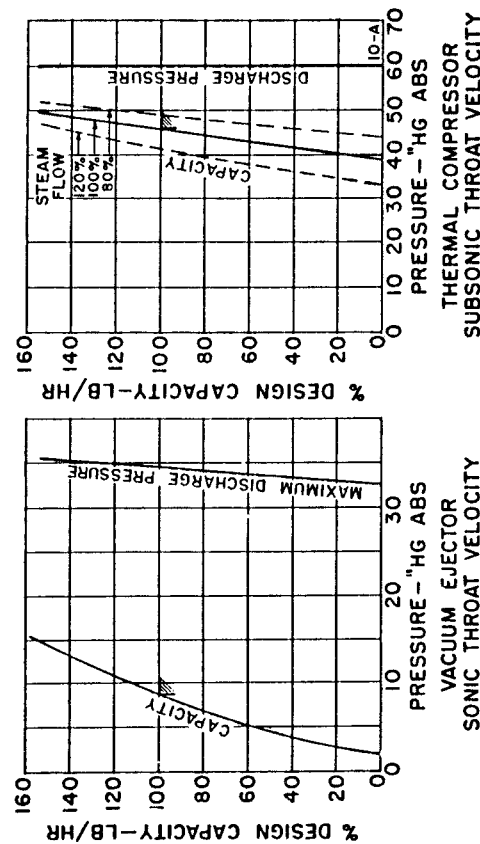


Fig. 10-A. Comparison of the operating characteristics of a vacuum ejector and a thermal compressor.

Fig. 10-A shows typical performance curves on both types of ejectors. In each, the left hand curve, or group of curves, shows variation of intake pressure with capacity. The right hand represents discharge pressure. In the vacuum ejector, it is the *maximum* discharge pressure obtainable. The *actual* discharge pressure may be lower with no change in the suction pressure-capacity curve. See page 4-36. This is not so with thermal compressors. Any change in actual discharge pressure is reflected in a similar change in suction pressure for the same capacity in lb/hr.

In each, there are four possible variables; steam weight flow, or steam pressure on a fixed nozzle; intake pressure; discharge pressure; and, capacity in lb/hr. The following chart is based on changing one of these at a time. Influence on the others is noted. (*Ratio* means compression ratio.)

Vacuum Ejector	Thermal Compressor
Increases <i>maximum</i> discharge pressure; practically no other change.	Increases Steam Flow Reduces intake pressure. Increased ratio. Alternately, can operate at constant ratio and increased capacity.
Reduces ratio; increases capacity.	Increases Intake Pressure Reduces ratio; increases capacity.
No change (until reaches breaking pressure).	Increases Discharge Pressure Entire family of curves moves with the discharge. Ratio remains practically constant.
Reduces ratio; increases intake pressure.	Increased Capacity Reduces ratio; increases intake pressure.

Two characteristics stand out in the functioning of a thermal compressor. One is the effect of varying steam weight flow for capacity control. The other characteristic is the way a change in discharge pressure causes the intake pressure-capacity curve to move, or *float*. This is at an almost constant compression ratio.

These characteristics are only within reasonable areas. For example, increasing steam weight flow on a thermal compressor too far could possibly increase throat velocity to the sonic range; the ejector would act like the normal vacuum ejector.



## COMPRESSED AIR AND GAS DATA

## MISCELLANEOUS THEORY

## Nozzle and Orifice Formulas

These data are intended to assist in the application of the jet action of nozzles and orifices as widely used in industry. (See Chapter 28 for metering and measurement of gas quantities).

The formulas presented are strictly theoretical, and are often subject to empirical modification to suit the applications, and, as usually applied, must have suitable safety factors added. They will not give absolute answers, but do permit a logical approach to many problems of flow quantity through various types of holes, the velocity of the jet, and the energy available.

## Subcritical and Critical Flow

There are two types of gas flow through any hole, the type depending upon the ratio of downstream to upstream absolute pressure. Consider an orifice discharging gas from a large vessel held at constant pressure into another large vessel where the pressure can be maintained at any desired level. Starting with the two pressures equal (no flow), slowly decrease the downstream pressure by bleeding gas out of the vessel. The flow rate will steadily increase until the ratio mentioned above reaches a value near 0.5, when a further decrease in downstream pressure will have no influence on flow rate. It remains as it was. This ratio, and there is one for every gas, is known as the *critical ratio*. Gas flow at ratios of downstream to upstream pressure greater than the critical is known as *subcritical* and follows specific laws. Those at ratios equal to or less than the critical are known as *critical* flows and follow other laws.

The critical ratio is found to be when the speed of sound (sonic velocity) is reached in the throat — smallest section of the gas stream. The velocity will depend upon the gas and the pressure and temperature conditions at the throat.

## Types of Holes

An orifice is a round sharp-edged hole in a thin plate. A nozzle is a round hole having a rounded entrance and a short straight section at the smallest area or throat. For certain applications, a flaring section may be added to the discharge side of the nozzle to expand the gas further and obtain greater velocity. Fig. 5-C shows these three types and the flow pattern through each. In this discussion, the ratio of orifice or nozzle diameter to the upstream pipe diameter is considered to be low and the velocity of approach can be neglected.

Considering first the middle sketch, there is a smooth approach to the straight throat section and flow is streamlined with the throat full of gas. The same comment holds true of the bottom nozzle in which the gas is expanded beyond the throat with increasing velocity in a divergent (flaring) section.

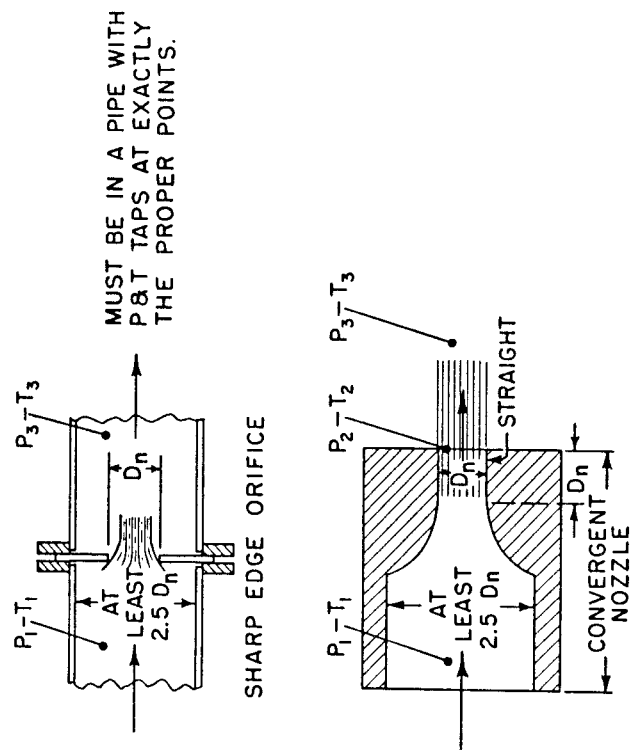


Fig. 5-C. Various Types of Orifices.

The sharp edged orifice (top) is different. The orifice does not flow full, but forms a jet of decreasing cross section known as the vena contracta. The form is similar to the jet developed with the rounded entrance nozzle, but the actual ratio of the jet area to the orifice area varies with many factors. These are allowed for in the flow coefficients applied in all flow formulas.

## Gases Covered

The formulas included are suitable for perfect gases with special adaptations for steam and air. Air is generally considered a perfect gas, although this is not strictly true. An excellent reference for properties of air and some other gases including the products of combustion is *Gas Tables* by Keenan & Kaye, published by John Wiley & Sons Inc. Where possible, suitable tables and charts should be used for steam, ammonia and other gases that deviate materially from perfect gas laws.

## The Critical Ratio

Strictly speaking, critical ratios apply accurately only to rounded entrance nozzles. Their application to sharp edge orifices is rather approximate. In practice, they are applied generally to both. The *critical ratio* can be calculated for any gas if the ratio of specific heats is known.

$$r_c = \frac{p_2}{p_1} = \left( \frac{2}{k+1} \right)^{\frac{k}{k-1}} \quad (5.13)$$

For air and steam, accepted values follow.

Gas	Condition	k	r <sub>c</sub>
Air	0° F (-17.8°C)	1.401	0.528
Air	250° F (121°C)	1.396	0.528
Air	500° F (260°C)	1.383	0.530
Steam	Saturated - 100 to 500 psiG (7 to 35 Kg/sq cm G)	1.295	0.547
Steam	Superheated - 100 to 500 psiG (7 to 35 Kg/sq cm G)	1.285	0.549

## Symbols

A	Throat or orifice area	sq in
C	Coefficient of flow	dimensionless
c <sub>p</sub>	Specific heat at constant pressure	Btu/lb/°F
D <sub>n</sub>	Throat diameter	inches
e	Mouth of a flared nozzle (exit diameter)	ft lb/sec
E <sub>k</sub>	Kinetic energy	dimensionless
F	Coefficient of conversion of adiabatic heat drop to velocity (0.85 is conservative value).	
g	Acceleration of gravity (32.2)	ft/sec. <sup>2</sup>
h <sub>1</sub>	Enthalpy at inlet conditions	Btu/lb
h <sub>2</sub>	Enthalpy at throat conditions	Btu/lb
h <sub>3</sub>	Enthalpy at exit conditions (no friction)	Btu/lb
h <sub>3F</sub>	Enthalpy at exit conditions allowing for friction	Btu/lb
k	Ratio of specific heats	dimensionless
L	Length of divergent section	inches
M	Mouth or exit area	sq in
p <sub>1</sub>	Upstream pressure	psiA
p <sub>2</sub>	Throat pressure	psiA
p <sub>3</sub>	Downstream or exit pressure	ft lb
R'	Specific gas constant	lb °F.
r <sub>c</sub>	Critical ratio	dimensionless
T <sub>1</sub>	Upstream temperature	°R
T <sub>2</sub>	Throat temperature	°R
T <sub>3</sub>	Exit temperature	°R
v <sub>1</sub>	Upstream specific volume	cu ft/lb

Throat specific volume	cu ft/lb
Exit specific volume	cu ft/lb
Throat velocity	ft/sec
Exit velocity	ft/sec
Weight flow	lb/sec

v <sub>2</sub>	
v <sub>3</sub>	
V <sub>2</sub>	
V <sub>3</sub>	
W	

## Coefficient of Flow

In metering, the coefficient of flow is highly important and has been extensively investigated. For the applications involved here, a high degree of accuracy is not so important and for a rounded entrance nozzle, a value of 0.97 may be used.

If an *orifice* is truly sharp edged, the coefficient will be close to 0.61. This only holds for a true, clean, sharp edge. A slight rounding of the corner or even a collection of dirt on the entering edge can increase the coefficient (and the flow) by 20% or more. An internal rough or burred edge on a hole in the wall of pipe can decrease the coefficient remarkably. Except under closely controlled conditions as in metering, the flow through any sharp edged orifice must be considered as an estimate.

## Flow Quantity

This is expressed as weight in lb/sec. To obtain cfm, multiply by 60 times the specific volume at the desired reference conditions.

### Subcritical Flow

p<sub>3</sub> Greater Than Critical, Equals p<sub>2</sub>

$$\text{Air Below 500°F} \quad W = \frac{2.05 P_1 AC}{\sqrt{T_1}} \sqrt{\left(\frac{P_2}{P_1}\right)^{1.43} - \left(\frac{P_2}{P_1}\right)^{1.71}} \quad (5.14)$$

$$\text{Saturated Steam Below 500 psiA} \quad W = 1.97 AC \sqrt{\frac{P_1}{v_1} \left[ \left(\frac{P_2}{P_1}\right)^{1.77} - \left(\frac{P_2}{P_1}\right)^{1.89} \right]} \quad (5.15)$$

$$\text{Superheated Steam Below 500 psiA} \quad W = 1.39 AC \sqrt{\frac{P_1}{v_1} \left[ \left(\frac{P_2}{P_1}\right)^{1.34} - \left(\frac{P_2}{P_1}\right)^{1.77} \right]} \quad (5.16)$$

### Critical Flow

p<sub>3</sub> Equal To or Less Than Critical p<sub>2</sub>

$$\text{Air} \quad W = \frac{0.53 P_1 AC}{\sqrt{T_1}} \quad (5.17)$$

$$\text{Saturated Steam Below 500 psiA} \quad W = 0.3 AC \sqrt{\frac{P_1}{v_1}} \quad (5.18)$$

$$\text{Superheated Steam Below 500 psiA} \quad W = 0.316 AC \sqrt{\frac{P_1}{v_1}} \quad (5.19)$$

### Any Perfect Gas For Either Condition

$$W = 0.668AC \sqrt{\frac{k}{k-1} \frac{P_1}{v_1} \left[ \left( \frac{P_2}{P_1} \right)^{\frac{2}{k}} - \left( \frac{P_2}{P_1} \right)^{\frac{k+1}{k}} \right]} \quad (5.20)$$

$$W = \frac{8.02P_1AC}{\sqrt{R'T_1}} \sqrt{\frac{k}{k-1} \left[ \left( \frac{P_2}{P_1} \right)^{\frac{2}{k}} - \left( \frac{P_2}{P_1} \right)^{\frac{k+1}{k}} \right]} \quad (5.21)$$

### Velocity

Nozzle and jet calculations frequently require a knowledge of velocity at the throat and/or the velocity at the mouth (for divergent nozzles).

Note that a divergent nozzle is useful only when  $p_3$  is less than the critical pressure. Its purpose is to further expand the gas to (or just above)  $p_3$ , thus increasing the velocity beyond the maximum throat value. This transforms additional heat into kinetic energy.

### Subcritical Flow

$p_3$  Greater Than Critical, Equals  $p_2$

$$V_2 = \frac{144Wv_2}{A} \quad (5.22)$$

$$V_2 = \frac{R'T_2}{144P_2} \quad (5.23)$$

$$V_2 = 223.7 \sqrt{F(h_1-h_2)} \quad (5.24)$$

### Critical Flow

$p_3$  Equal To or Less Than Critical  $p_2$

Under these conditions the flow reaches a maximum and the throat velocity reaches the velocity of sound in the fluid flowing at conditions  $p_2$  and  $T_2$ .

For Air, use Keenan & Kaye tables if available.

### Velocity of Sound (Theoretical)

#### Basic Formulas

$$V_2 = \sqrt{144gk_2v_2} = \sqrt{kgR'T_2} \quad (5.25)$$

See Fig. 6-BC, page 649, for velocity of sound in atmospheric air.

$$V_2 = \sqrt{\frac{288kg_2v_1}{k+1}} \quad (5.26)$$

### Velocity of Sound (Theoretical)

#### Specific Formula

$$\text{Air} \quad V_2 = 73.5 \sqrt{p_1v_1} \quad (5.27)$$

$$= 44.6 \sqrt{T_1} \quad (5.28)$$

$$\text{Saturated Steam} \quad V_2 = 70 \sqrt{p_1v_1} \quad (5.29)$$

$$\text{Superheated Steam} \quad V_2 = 72 \sqrt{p_1v_1} \quad (5.30)$$

### Divergent Nozzle Sections Air and Perfect Gases

$$\text{Isentropic Heat Drop-Btu/lb} = h_1-h_3 \quad (\text{frictionless}) \quad (5.31)$$

$$h_1-h_3 \text{ (frictionless)} = c_p T_1 \left[ 1 - \left( \frac{p_3}{p_1} \right)^{\frac{k-1}{k}} \right] \quad (5.32)$$

$$\text{Actual Total Heat at Exit-Btu/lb} \quad h_{3F} = c_p T_1 - F(h_1-h_3) \quad (\text{with friction}) \quad (5.33)$$

$$\text{Actual Temperature at Exit} \quad T_3 = \frac{h_{3F}}{c_p} \quad (5.34)$$

$$\text{Exit Velocity} \quad V_3 = 223.7 \sqrt{F(h_1-h_3)} \quad (5.35)$$

$$V_3 = \frac{144 W v_3}{M} \quad (5.36)$$

$$V_3 = 96.26 \sqrt{\frac{k}{k-1} p_1 v_1 \left[ 1 - \left( \frac{p_3}{p_1} \right)^{\frac{k-1}{k}} \right]} \quad (5.37)$$

$$\text{Specific Volume at Exit} \quad v_3 = \frac{R'T_3}{144p_3} \quad (5.38)$$

$$\text{Exit Area} \quad M = \frac{144Wv_3}{V_3C} \quad (5.39)$$

$$\text{Length beyond Throat} \quad L = \frac{e-Dn}{0.175} \quad (\text{basis } 10^\circ \text{ Flare}) \quad (5.40)$$

In the design of divergent nozzle sections, it is generally best to *under* expand rather than to *over* expand. Losses are much less with design  $p_3$  slightly *above* actual exhaust pressure. Also, if initial pressure  $p_1$  or downstream pressure  $p_3$  varies, allowance should be made for such variation throughout the entire nozzle design.

### Throat Temperature

#### For Air Or Any Perfect Gas

$$\text{(Frictionless)} \quad T_2 = \frac{T_1}{\left(\frac{P_1}{P_2}\right)^{\frac{k-1}{k}}} \quad (5.41)$$

With friction the temperature will be higher dependent upon coefficient F. Use a chart for steam.

### Kinetic Energy of Jet

$$\text{(General)} \quad E_k = \frac{WV^2}{64.4} \quad (5.42)$$

$$\text{(Convergent nozzle)} \quad E_k \text{ (1000 lb/hr)} = \frac{V_2^2}{232} \quad (5.43)$$

$$\text{(Divergent nozzles)} \quad E_k \text{ (1000 lb/hr)} = \frac{V_2^2}{232} \quad (5.44)$$

### Applications of Orifices and Jets

Applications of the jet action obtained by nozzle flow with compressed air abound in industry. Typical are:

1. Ejection of parts from dies of stamping, punch, and forming presses in metal and plastics manufacture;
2. Blowing chips and cleaning machinery in all types of industry;
3. Blast cleaning of metal and other materials;
4. Atomization of liquids for spray painting, lubrication, etc.; and
5. Certain types of pulverizing machinery.

Typical uses of orifices drilled in the walls of pipe or in thin plates include:

1. Agitation of acids, milk, cement slurry, asphalt, and other liquids to either mix, prevent settlement of solids, or accelerate oxidation or fermentation;
2. Limitation of flow in a line to a certain maximum quantity; and,
3. Some types of transfer machinery for pulverized materials such as cement.

The above are typical only and in most cases the equipment has already been designed by an experienced supplier. Practical comments for those making their own applications follow.

1. The air consumption of an intermittently operating jet, frequent in automatic machinery, is practically impossible to calculate. The time during which the control valve is open is usually

measured in seconds or less, the actual average pressure at the jet entrance is unknown and it is desirable that this type of application be designed by trial to do the desired work. Then consumption, if important, can be determined by test.

2. The same comment applies to the small open end tube, used sometimes to form a jet. The flow and exit velocity cannot be satisfactorily calculated.
3. There are many applications involving orifices made by drilling holes in pipe walls. These pipes may be mounted in front of a furnace opening, the jets to provide an air curtain to protect the operator, or the pipes may be laid on the bottom of a tank or vat, the air flow being used to cause agitation and mixing of the liquid. These applications can be reasonably estimated as to flow quantities or orifice size for given conditions using the formulas above. For further information about agitation, see page 32-6.
4. An orifice placed in a line to limit the maximum flow is usually (although not always) operating at the critical condition. In either case its size can be calculated by the formulas given.

### COMPRESSED AIR AND GAS DATA

#### AN INTRODUCTION TO COMPRESSORS

### The Ejector

An ejector consists of a relatively high-pressure motive steam or gas nozzle discharging a high-velocity jet across a suction chamber into a venturi shaped diffuser. The gas, whose pressure is to be increased, is entrained by the jet in the suction chamber. The mixture at this point has high velocity and is at the pressure of the induced gas. Compression takes place as velocity energy is transformed into pressure inside the diffuser.

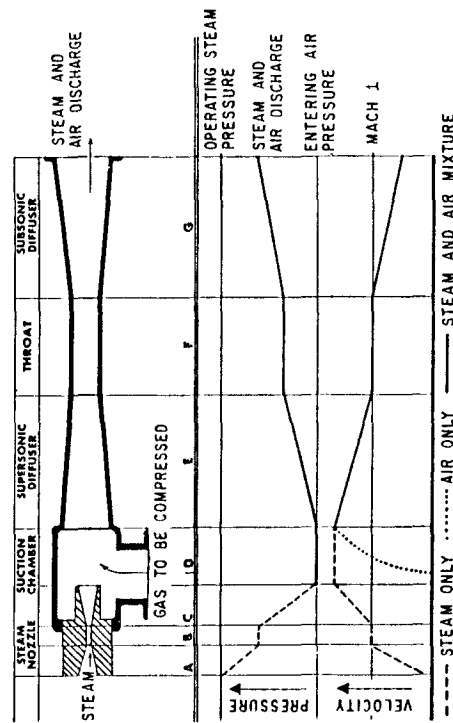


Fig. 1-N. A diagram of the pressure and velocity variations within a steam jet ejector handling air.

Ejectors may be arranged in either parallel or series. When two or more steam ejectors are placed in series to form a multistage arrangement, it is usual, if water temperature is sufficiently low, to interpose a condenser between successive elements to condense the steam used by the prior jet plus any condensable vapor in the gas being compressed. This materially reduces the steam required for the next stage since the weight of mixture remaining to be handled is much less. Fig. 1-0 shows typical arrangements. Both barometric and surface intercondensers may be used. Ejectors have no moving parts. They can handle liquid carryover without physical damage although they should not be exposed to a steady flow of liquid.

Ejectors have no moving parts. They can handle liquid carryover without physical damage although they should not be exposed to a steady flow of liquid.

## COMPRESSED AIR AND GAS DATA

### APPLICATION OF THEORY

#### The Jet Ejector

Experience has shown that the ability of jet action to induce, entrain, and compress a gas does not necessarily follow theoretically predictable lines. Ejector design is largely empirically based, backed by extensive tests. This discussion includes only the application of theory as it is involved in the properties of the gas handled. For the most part the discussion is restricted to the compression of air-water vapor mixtures, the most prevalent use of ejectors. Steam, being the most widely used power medium is the only one considered here although other gases, particularly air, may be used in special cases. Discussion is limited to vacuum applications. See Chapter 10 for thermal compressors.

#### Ejector Ratings

Ejectors are rated on the weight flow of gas compressed, rather than on volume flow as is usual with other compressor types. Ratings are expressed in lb/hr of the gas or gas mixture handled. Steam (or other motive medium) is also stated in lb/hr.

Normally, manufacturers' basic ratings are on the weight rate of "equivalent air," which is air at 14.696 psia and 70°F and containing normal atmospheric moisture. The user must specify the desired capacity in such terms that equivalent air can be calculated and the best ejector can be selected.

Capacities desired are preferably specified in one of three ways:

1. Lb/hr of a saturated air-water vapor mixture (AVM);
2. Lb/hr of a superheated air-water vapor mixture; and,
3. Lb/hr of a mixture of gases either including or excluding water vapor.

The proportion of air to vapor in (1) is known and no further information is needed for conversion to equivalent air.

In (2), it is mandatory that the relative weights of air and vapor be specified, otherwise it is impossible to determine the MW and equivalent air.

Ejectors are principally used to compress from pressures below atmosphere (vacuum) to a discharge close to atmospheric. They may, however, involve compression from a near atmospheric intake to some higher level in which case they are known as *thermal compressors*. See Chapter 10. Although the operating principles are identical for both types, the velocities reached and characteristics developed may be quite different.

A *vacuum* ejector, using steam as motive fluid and inducing air, is used in Fig. 1-N to show operating principles. Pressure and velocity changes are indicated for various sections of the device. Temperature changes follow the pressure curve closely. Mach 1, where referred to in the notes, is the velocity of sound in the flowing medium. For this particular example it approximates 1000 ft/sec. The following notes refer to Fig. 1-N.

- A. Subsonic steam velocity generated to Mach 1 in a converging nozzle as steam pressure drops.
- B. Stabilization with pressure constant, velocity constant at Mach 1.
- C. Supersonic steam velocity raised in diverging nozzle as pressure drops.
- D. Since suction chamber is at the lowest pressure in the system the air flows into the chamber and is entrained in the steam jet.
- E. Supersonic mixture pressure is increased in converging diffuser until velocity drops to Mach 1.
- F. Stabilization with pressure constant, velocity constant at Mach 1.
- G. Subsonic mixture pressure is increased in diverging diffuser as velocity drops.

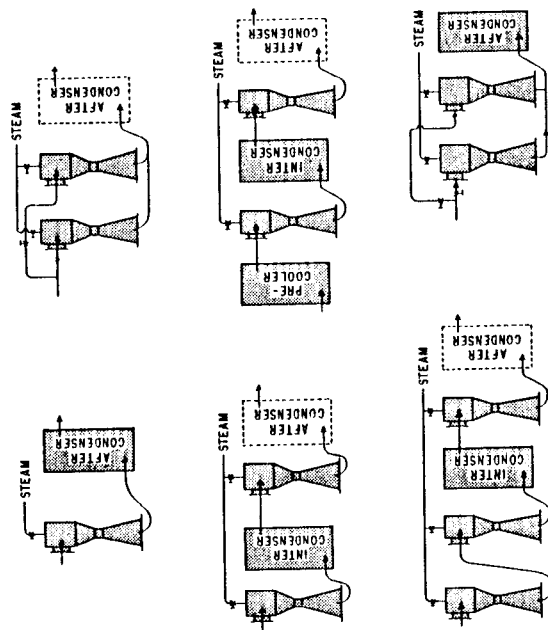


Fig. 1-0. Typical arrangements of ejectors with their coolers and condensers.

Method (3) requires that a complete analysis of the gas be given or that the user specify the average molecular weight. The analysis may be on a volumetric (molar) or a weight ratio basis.

One of the major problems in ejector selection is that information given is often insufficient to permit accurate evaluation of *MW*.

Transfer from specified lb/hr to equivalent air is based on two conversion curves involving *entrainment ratios*. These curves (Fig. 4-X and 4-Y) were established by tests run under the auspices of the Heat Exchange Institute and are accepted and used by all ejector manufacturers. Two conversion steps are involved; the first being based on molecular weight and the second on gas inlet temperature. These apply to each individual ejector as a single-stage basic element.

Molecular weight entrainment ratio is the ratio of the total weight of inlet gas that can be handled to the total weight of equivalent 70°F air that would be handled under the same conditions.

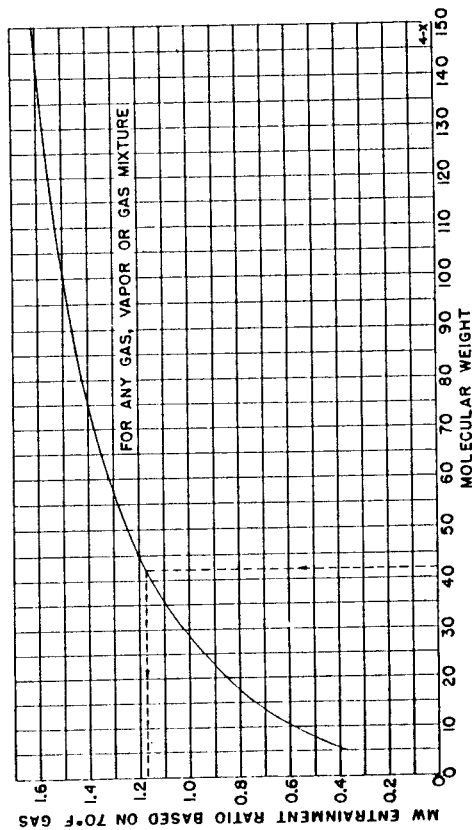


Fig. 4-X. Molecular weight entrainment ratio for steam jet ejectors handling any gas.

Temperature entrainment ratio is the ratio of the total equivalent weight of air (or water vapor) at actual temperature that can be handled to the weight of equivalent air or water vapor at 70°F that would be handled. Dry gas and steam (water vapor) must be separately converted for temperature and totaled.

Entrainment ratios are divisors to obtain lb/hr equivalent air when lb/hr of the gas handled (and its vapor component) are known.

#### To Obtain Equivalent Air

The formula for obtaining equivalent air for any gas or gas mixture whether containing water vapor or dry is given below.

$$\text{Equivalent air} = \frac{\text{lb/hr Dry Gas}}{\text{MW} \times \text{TER}_g} + \frac{\text{lb/hr Water Vapor}}{0.81 \times \text{TER}_v} \quad (4.24)$$

*MW* is molecular weight entrainment ratio (4-X).

*TER<sub>g</sub>* is temperature entrainment ratio for dry gas (4-Y).

0.81 is molecular weight entrainment ratio for water vapor (*MW* = 18).

*TER<sub>v</sub>* is temperature entrainment ratio for water vapor (4-Y).

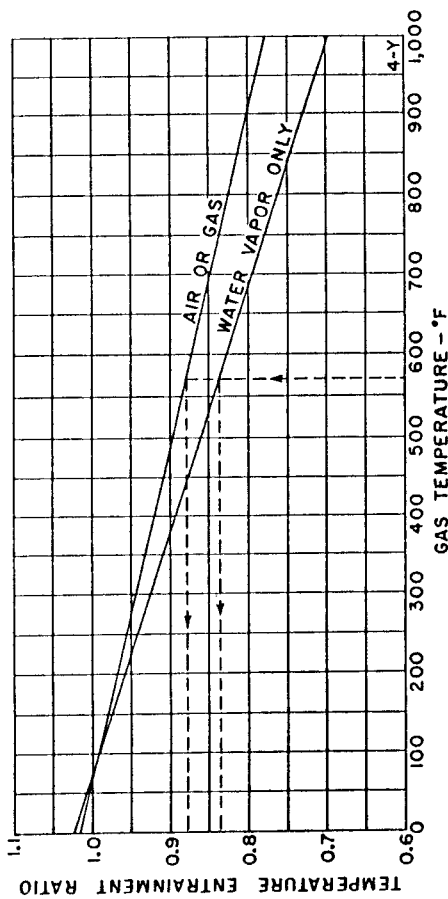


Fig. 4-Y. Temperature entrainment ratio for steam jet ejectors handling any gas.

Note:—Fig. 4-X, Y, and Z drafted from data in *STANDARDS FOR STEAM JET EJECTORS*, Third Edition, Copyright 1956 by the Heat Exchange Institute, 122 East 48 Street, New York, N. Y. 10017.

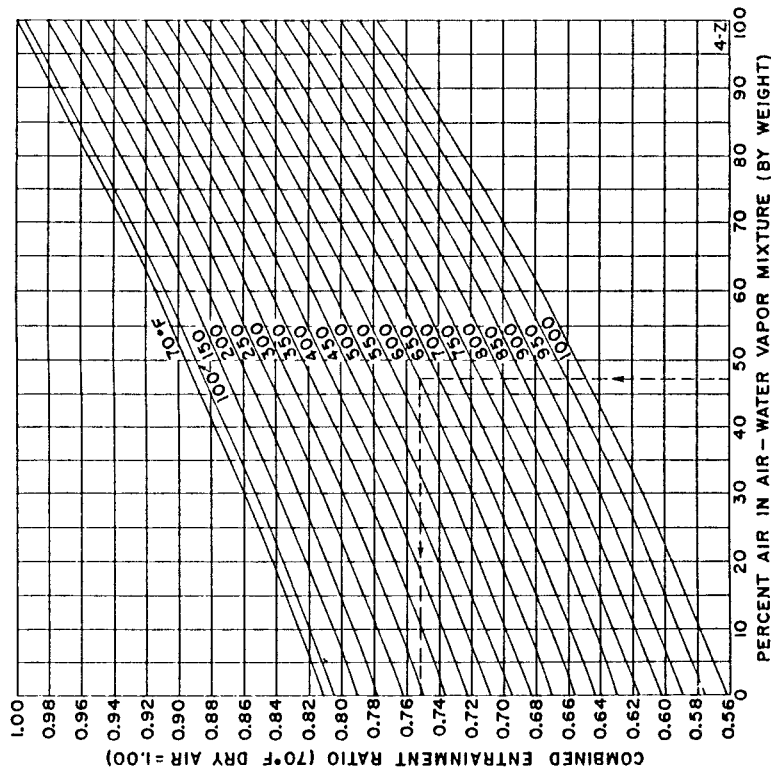


Fig. 4-Z. Combined molecular weight and temperature entrainment ratios for air-water vapor mixtures only.

is held constant. Referring first to the equivalent air (MW 29) curve in the left hand group, it can be seen that for every ejector there is a definite relation between absolute suction pressure and capacity. The right hand curve shows the maximum stable operating discharge pressure obtainable with this particular ejector with a specified steam pressure and varying capacities.

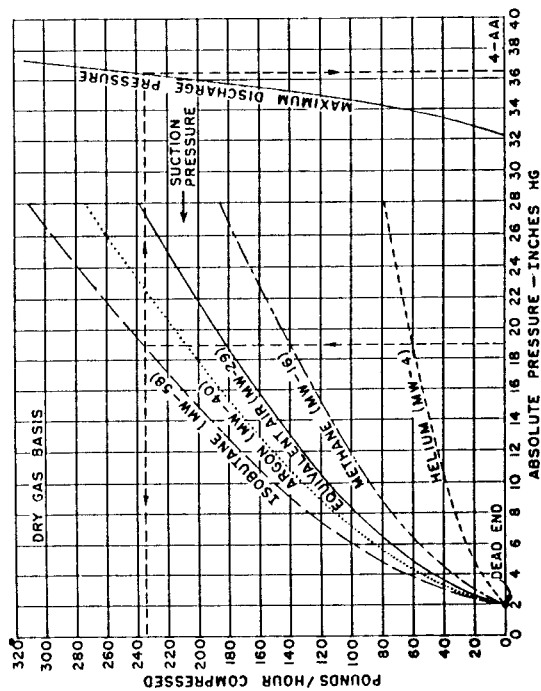


Fig. 4-AA. Typical ejector performance curve also showing the effect of changes in molecular weight (dry gas basis only).

Fig. 4-AA also shows the effect on the capacity (lb/hr) of changes in MW of the gas handled. It will be noted that the higher the MW the greater the total weight this ejector will handle. There will be no appreciable change in the maximum discharge pressure, however, when the gas composition varies.

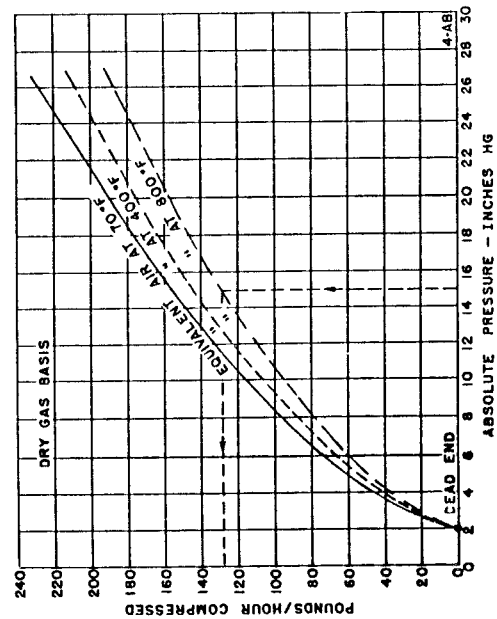


Fig. 4-AB. Typical ejector performance curve showing the effect of changes in inlet gas temperature (dry gas basis only).

In the case of a dry gas, only the left hand part of the equation applies. For an air-water vapor mixture use page 34-114 to obtain percent air in the mixture and obtain the overall entrainment ratio from Fig. 4-Z. This can be applied as a divisor directly to the total lb/hr of mixture to obtain the total equivalent air.

If an air water vapor mixture is given on a volume basis (as cfm), determine specific volume using page 34-115, convert total volume to weight (lb/hr) and then proceed as above.

In all cases, except air-water vapor mixture, the molecular weight must be known or calculated, the water vapor (steam) being separately calculated.

A dry gas analysis on a molar basis is the same as that on a volume basis. Proceed as on page 3-11 to find average MW.

If the dry gas analysis is on a weight basis, use the following method to obtain average MW.

Gas	Lb/hr	MW	Dividing gives Mole/hr
CO <sub>2</sub>	6	44	0.136
N <sub>2</sub>	24	28	0.857
Ar	62	40	1.550
He	108	4	27.000
	200		29.543

$$\text{Average MW} = \frac{200}{29.543} = 6.77 \quad (4.25)$$

If the example also contained 20 lb/hr of steam and the mixture temperature were 500°F, the following would be the step by step conversion to equivalent air.

Portion Involved	Dry Gas	Steam
a. lb/hr	200	20
b. MW	6.77	18
c. MW entrainment ratio	0.45	0.81
d. Temperature entrainment ratio (a)	0.897	0.859
Equivalent Air (lb/hr) = (c) × (d)	495	29
e. Equivalent air (Total) lb/hr	524	524

Although the user has little need to utilize the equivalent air rating, it has been presented to assist in picturing the effects of gas composition, average molecular weight, and gas temperature on the capacity of a given ejector and to call attention to information the manufacturer must have to make a satisfactory selection.

#### Effect of MW and Temperature

Fig. 4-AA is a typical performance curve of a single stage ejector showing what happens to ejector performance with changes in the characteristics of the gas being handled. In this example, motive steam flow

Fig. 4-AB shows similarly the effect of suction gas temperatures above the 70°F reference value.

Fig. 4-AA and 4-AB are on a dry-gas basis. Inclusion of water vapor with the gas would lower the two top curves on Fig. 4-AA and raise the two bottom curves because of its effect on average *MW*. It would also lower the 400 and 800°F curves of Fig. 4-AB because of the reduced entrainment ratio for the steam component.

Conversely, what these curves indicate is that for a given total lb/hr of gas, (1) the lower the molecular weight, the greater the lb/hr of steam required and the larger the ejector; and, (2) the higher the gas temperature, the greater the steam quantity required and the larger the ejector.

### Discharge Pressure

Any single stage ejector will operate stably at a given motive steam pressure and capacity against an increasing discharge pressure up to the *breaking pressure*. At this point the gas flow will stop or fluctuate. The ejector becomes unstable. If the discharge pressure is reduced slowly, the ejector will resume stable operation at a lower back pressure level. This is the *recovery pressure* and is known in the industry as *maximum discharge pressure*. The *maximum* pressure required at the ejector discharge flange must be known by the manufacturer from the specifications so that he can supply an ejector that will have a stable operating range equal to or exceeding this maximum.

### Changes in Steam Flow

Changes in an ejector's motive steam flow may be made by altering the size of the motive steam nozzle, or by changing the steam pressure.

A change by the first method alters the ejector characteristic, especially as regards compression ratio. If a simultaneous change is made in the nozzle pressure so that the steam flow (lb/hr) through the nozzle remains unchanged, there is little or no change in the ejector characteristic curve.

Changes in steam pressure (and flow) with a fixed steam nozzle do not appreciably alter the suction pressure curve, but do produce a higher or lower discharge pressure, as the motive steam pressure increases or decreases. If steam pressure is increased too far above design, the excessive steam flow will choke the ejector throat and gas capacity will be materially reduced.

With superheated steam, any increase in superheat at constant pressure will have an effect opposite to a pressure increase. That is, an increase in temperature will lower the discharge pressure due to the reduced weight of steam flow.

The reduction of discharge pressure by changes in motive steam conditions can cause the ejector to break and become unstable.

Every ejector specification must show and the ejector must be designed for the *lowest* obtainable steam pressure and the *highest* obtainable superheat at the steam nozzle. This is important if the ejector is to stay on the line at all times and have the required capacity even with the most unfavorable steam conditions.

### Minimum Pressures Obtainable

A great many ejectors are applied to remove noncondensables from a chamber of some sort. These may or may not be mixed with water vapor or the vapor of another liquid.

The ejector has a *dead-end* suction pressure obtained when the inlet is completely blanked off and the capacity is zero. This can never be attained except at shutoff. When handling a certain lb/hr of gas or mixture, there is another minimum attainable pressure that is dependent upon the properties and quantity of the gas coming to the ejector and whether moisture is contained therein. Water is the only vapor considered in the following cases. It is frequently necessary to handle other vapors; the same principles apply.

Cases 1, 2, and 3 have to do with the removal of the gaseous contents of a *closed* vessel assumed to be tight *with no inward leakage* during evacuation.

Case 1. The gas contained in the vessel is dry and no liquid is present. In this, the *pump-down* or pressure reduction proceeds along the capacity-suction pressure curve of the ejector and if operated over a sufficiently long period, the terminal pressure will reach the dead-end.

Case 2. The mixture in the vessel contains water vapor, but no water in the liquid phase. The results are as in Case 1 with capacities handled at any moment dependent on the original mixture composition, but dead-end can be obtained if operation continues long enough.

Case 3 is as Case 2, but with liquid phase water in the vessel. In this, the minimum pressure attainable is dependent upon the minimum temperature that can be reached by the vessel and contents. As the gaseous mixture is withdrawn, the pressure falls and some of the liquid evaporates, cooling both the liquid and the gas mixture. This continues until heat leakage inward is sufficient to evaporate liquid at the same rate it is being removed and equilibrium is reached. This point is close to the minimum pressure attainable (assuming the ejector has a dead-end substantially below this point) and its value will depend on the proportion of vapor in the mixture and the temperature reached.

For example, a mixture of 50% water vapor and 50% air (by weight) is contained in a vessel (with liquid water also present) and an equilibrium temperature of 40°F has been reached. The mixture has a specific humidity of 1.00 or would be said to be a 50% — 50% AVM. Reference to page 34-114 shows that a total pressure of 0.41 in Hg will have been reached.

Evacuation continues with no further reduction in temperature and will remove some of the air together with such water vapor as evaporates from the liquid. There will be a continuing decrease in the amount of air in the mixture (a lower percent noncondensables or a higher lbs of water vapor per lb of dry air) and the pressure will drop approaching, but never quite reaching the vapor pressure of water at 40°F which is 0.248 in Hg. See the table on page 34-96. If the equilibrium temperature is 32°F or lower, the liquid water will freeze.

Leakage into the vessel during evacuation in any of the above cases usually will be at a relatively constant rate and will influence results



## Precoolers

materially. *Leakage must be estimated by the user and made a part of the original specifications to permit proper ejector selection.*

It is impossible to rationalize the performance of ejectors on pump-down service sufficiently to permit the development of a reliable method for quickly estimating pump-down time under any of the above cases. The problem can best be referred to manufacturers, always advising the approximate time and minimum pressure desired. Be sure the minimum pressure specified is attainable using the applicable case above.

Cases 4, 5, and 6 involve the removal of noncondensables from a system into which there is a continuous flow, some of which usually is leakage.

Case 4, which may be somewhat hypothetical, requires the removal of a dry gas continuously and as fast as it may variably flow into the system. This is a problem of balance between inflow and removal, with the ejector holding a suction pressure depending upon the capacity which must be handled.

Case 5 involves the handling of a saturated mixture of air or gas and water vapor. An ejector serving a counter flow barometric steam condenser is typical of this application. There is a fairly constant quantity of atmospheric air leaking into the system which joins with the water vapor not liquefied by the condenser. A saturated mixture is formed at approximately 5°F above the condenser inlet water temperature. The vapor will be at the partial pressure corresponding to the mixture temperature regardless of the amount of air leakage with which it is joined. If the leakage were zero, the suction pressure of the ejector would be the saturated vapor pressure of the water at its existing temperature. The absolute minimum pressure an ejector (or any other type of evacuating machine) can maintain is therefore set by the saturated vapor pressure as determined by the mixture temperature plus the effect of noncondensables. With air in the mixture, reference to page 34-114 will show that there is an increase in total suction pressure as the air portion increases. Just follow a given temperature curve from right to left.

Case 6 in general, is the same as Case 5, but a modern surface type steam condenser is the example. Before entering the ejector, the mixture passes through a precooling coil to cool the air-vapor mixture that is saturated at the cooler outlet (ejector inlet) temperature. For a given continuous air leakage (lb/hr) inward, the minimum attainable pressure is again dependent only upon the temperature of the mixture leaving the pre-cooler. The lower the temperature, the lower the pressure. The air leakage handled influences the pressure; the higher it becomes, the higher the pressure for a given temperature. Air leakage to a surface condenser is fairly constant.

The above limiting facts are not always understood and ejectors are sometimes requested for duty at pressures below that corresponding to the saturated vapor condition. Always check this point to be sure the request can be fulfilled.

When ejectors serve condensers or other apparatus involving fluids other than water, a vapor pressure curve of the liquid involved must be made available for the manufacturer's use.

Since the suction pressure of a given ejector on a given application is determined by both the noncondensable load and the saturated vapor temperature, it is sometimes possible to precool the suction stream before compression and reduce the vapor portion of the load. A part of the vapor is condensed and removed which reduces the total weight of mixture to be handled. The saturated vapor temperature is also reduced, resulting in a smaller ejector and less steam to maintain a given pressure, or, alternately, a lower pressure with the same steam quantity.

## Multistage Ejectors

Any single stage ejector has compression ratio limitations for most efficient operation and its range may be insufficient for a given application. For compression ratios, usually exceeding 10, multiple staging is used with two to four, or even six, ejectors operating in series. The varieties of combinations are many, involving for a given primary (first-stage unit) the possible inclusion or exclusion of intercondensers between stages, various sizes of secondary ejectors, and variations in number of stages. The proper selection will depend upon the application, operating conditions, steam and water costs, load factor, etc.

Regardless of the final choice, each individual ejector is designed to and operates in accordance with the principles outlined. Each is an individual unit or element operating as part of a team and performs exactly the same function as do the stages of any other type compressor. However, the *maximum* water temperature used in intercondensers must be known and made a part of specifications. This is just as important in a multistage unit as is minimum steam pressure and maximum inlet temperature. The secondary stages must be designed to handle a certain vapor load and if designed for too low a temperature, they cannot do their job and the ejector will not function properly. See Fig. 1-0, page 1-17.

Chapter 10 discusses ejectors as thermal compressors for other than vacuum service.

## INFORMATION REQUIRED FOR BIDDING

### For Ejectors Only

#### Application

Specify the type of equipment with which the ejector will be used and any special features involved. Equipment might be a barometric condenser, surface condenser, evaporator, crystallizer, vacuum drier, still, pump primer, or impregnator.

#### Suction Conditions

Conditions must be at *ejector inlet* connection and specify clearly units of measurement involved. Piping pressure losses must be allowed for.

Gas pressure and temperature must be given. Installation altitude above sea level must be stated.

Capacity or load is preferably to be expressed in lb/hr. For dry air, molecular weight is not needed but for gas mixtures, the lb/hr and MW of each component are both necessary.

When water vapor is present, the saturated vapor temperature and the composition of the *dry* components must be specified.

When presenting gas mixtures in volume units (SCFM), include percent by volume of each component as well as molecular weight.

#### Discharge Conditions

Specify the back pressure allowing for any discharge pipe friction loss. Standard ejector design is based on 1.0 psiG maximum.

Specify *maximum* water temperature for intercondenser and after-condenser use. Specify whether barometric (direct contact) or surface condenser design is preferred or mandatory.

#### Steam Conditions

It is important that the *minimum* steam pressure and *maximum* temperature at *ejector steam* inlet be stated. Include in this determination all piping pressure losses to the jet body. Steam may be saturated but must be dry. Some superheat is desirable. Conditions must be at ejector inlet, not at the boiler.

If power medium is other than steam, specify the gas, its analysis, pressure, and temperature.

#### Additional Design Considerations

Specify whether operating cost is important. If it is, give costs of steam and condensing water for proper study of alternates. Advise whether ejector is to be in operation continuously or for shorter periods. State the hours/day.

For standby, quick pumpdown, and/or control purposes, ejectors are often installed in parallel systems, each element complete in itself. When such a setup is desired, specify the number of systems *and the capacity of each*.

## Pneumatic Handbook, 1982

### Airmovers

---

THE JETFLOW Airmover is a device which converts a small quantity of low pressure air into a large volume of fast moving air, its principal application being auxiliary ventilation of confined areas, or localized ventilation. Since the device works without power (other than a supply of low pressure air) or moving parts, it can provide safe ventilation in potentially explosive atmospheres.

The principle of operation is shown in Fig 1. A supply of primary air enters the manifold where it expands to induce a depression at the throat of the venturi section and also attaches itself to the curved aerofoil surface by Coanda effect. Secondary air from the surroundings is induced into the throat of the manifold, where it mixes with the primary air and accelerates with it through the divergent tube. The result is a high velocity mixture of primary and secondary flows emitted from the end of the tube, entraining more surrounding air.

Jetflow Airmovers can be operated singly, in series or in parallel and they perform extremely well when connected to ducting. There is, however, a limit to the resistance they will overcome but at best the Airmover will generate a static pressure (suction) of about 112 m/bar (45" W.G.). The resistance to airflow is determined by the length and diameter of the ducting and the frictional characteristic (K factor) of the duct lining.

Adequate Airmover performance depends on the correct application of these variables:-

- (a) Gap Setting.
- (b) Pressure of primary supply in manifold.
- (c) Volume of primary supply available.

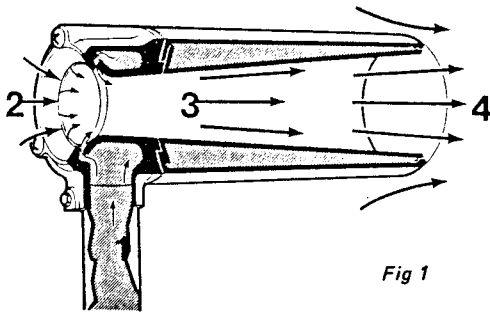
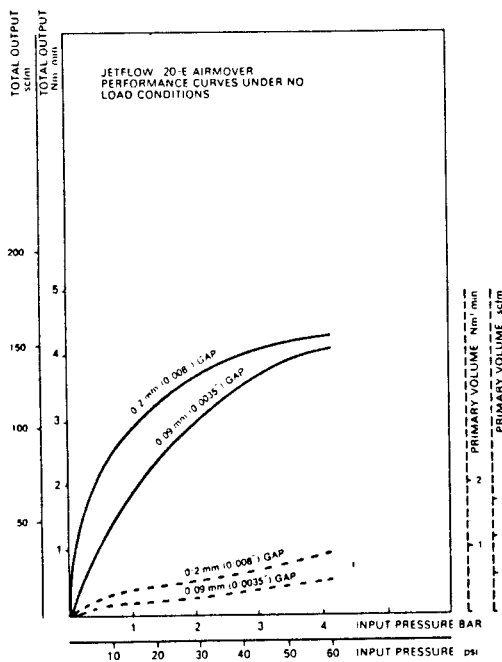
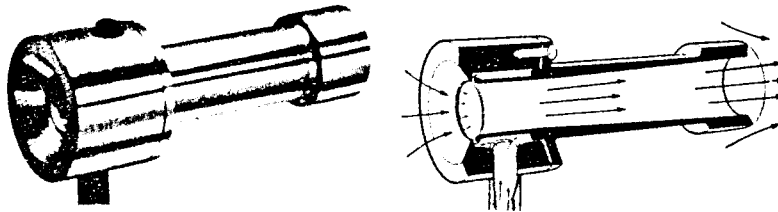


Fig 1

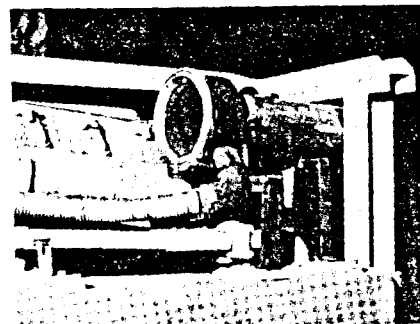
- 1 - Primary supply enters the manifold via annular gap and accelerates over the aerofoil.
- 2 - Secondary supply is induced into the throat of the manifold.
- 3 - Mixing, cooling and diluting in the divergent tube.
- 4 - Expelled at high velocity entraining surrounding air.

Olin 'Jetflow' 20 air mover.



Performance characteristics of Jetflow 20-E Airmover.

Typical installation of a 'Jetflow Air-mover' on a diesel powered mobile vehicle. Engine exhaust is connected directly to the inlet manifold providing primary supply to cool and dilute the toxic exhaust gases.



The Jetflow Airmover will operate effectively at manifold pressures varying from 0.04 bar (0.5 lb/in<sup>2</sup>) to 3.9 bar (55 lb/in<sup>2</sup>). It is recommended that the maximum manifold pressure does not exceed 4.2 bar (60 lb/in<sup>2</sup>). In many applications most efficient operation is attained within the range 0.35 bar (5 lb/in<sup>2</sup>) to 1.4 bar (20 lb/in<sup>2</sup>).

## Pneumatic Handbook

### Fluid Jet Pumps

Fluid jet pumps work on the principle of introducing a high-velocity fluid jet (liquid or vapour) into a mixing section where it meets the gas to be evacuated and entrains that gas by turbulent mixing. Some of the momentum of the jet is thus imparted to the gas which is carried down into a diffuser section and thence to a condenser if necessary, for separation. Where the operating fluid is a liquid, separation can be achieved in the diffuser, and where the operating fluid is a gas usually in a condenser, although the complete system may comprise two or more stages, with or without intercooling, depending upon the performance required. The usual types may be grouped as water jet pumps (fluid), steam ejector pumps (vapour) and vapour-booster pumps. The two former are essentially similar in principle and application whilst the vapour-booster pump comprises a two-stage system with a condenser — Fig 2.

The steam ejector pump has the most wide-spread industrial application and has, in fact, largely replaced other types of vacuum equipment in certain fields (*eg* for use with power plant condensers) because of its simplicity, reliability of operation and low maintenance costs. It can also be

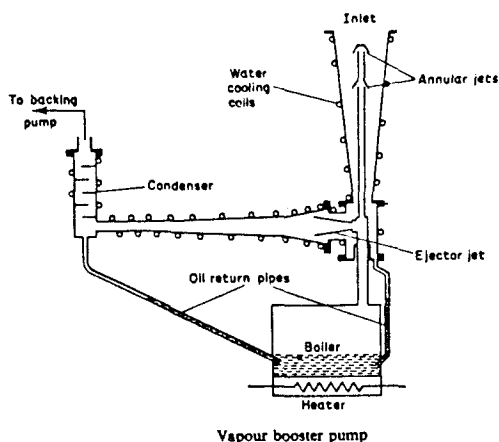
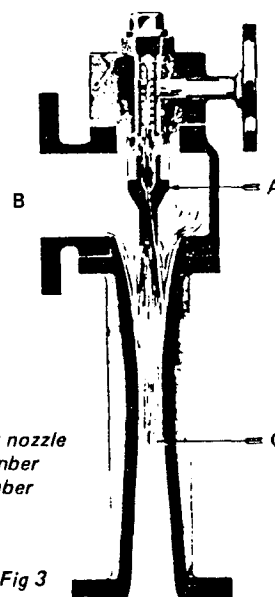


Fig 2



A — divergent jet nozzle  
B — suction chamber  
C — mixing chamber

Fig 3

used to handle corrosive or extremely hot gases, *etc*, since many materials can be adapted for its construction — *eg* the major pump elements can be made from carbon or refractory materials, glazed ceramics, *etc*, to resist corrosive attack. It may be termed variously a jet pump, ejector, augmentor (or vacuum augmentor), or thermo-compressor, depending on the duty performed. When used to produce and maintain a condition of vacuum by the removal of incondensable gases it is correctly termed an *ejector*. If used to compress vapours from a condition of high vacuum to a lower vacuum at which condensation can take place, it is correctly termed a vacuum augmentor.

The design of all steam jet pumps is essentially similar and follows the form shown in Fig 3. Steam is introduced via a divergent nozzle into a converging section of the body. The body section also incorporates a suction branch connected to the vessel or system to be evacuated and gases drawn in through this opening are entrained with the steam jet and carried down with it into the diffuser section or compression tube. During this process of entrainment the steam jet loses a proportion of its energy which is imparted to the aspired gases. In the diffuser section the kinetic energy of the mixture of steam and gases is re-converted into pressure energy. The degree of compression which can be achieved is proportional to the amount of kinetic energy each unit mass of mixture has when it enters the diffuser and thus, basically, to the quantity of steam passing through the jet nozzle. The normal range of single-stage ejectors embraces a steam consumption ranging from about 50–60 up to 8000–9000 lb per hour.

The compression ratio of the ejector is defined as the ratio of the absolute pressure of the steam-gas mixture at the discharge end to that of the absolute pressure of the aspired gas at the suction branch. Compression ratios of up to about 15:1 are practical with simple ejectors, although it is more usual to work to a lower figure in order to achieve better economy in steam consumption. Thus the single-stage ejector produces economic operation down to vacua of about 26 in. For higher vacua a two-stage or multi-stage unit is normally preferred.

When two or more stages are employed it is usual to employ a condenser between each stage so that the steam of the first stage is condensed out and withdrawn before reaching the next stage.

Thus each succeeding stage has only to deal with the incondensable vapours remaining. The usual method of cooling is to employ a cold water spray when the steam is condensed by direct contact with the cooling water, whilst at the same time the incondensable gases are cooled and reduced in volume before being drawn into the suction branch of the following stage ejector.

Three-stage ejectors are usually provided with an intermediate condenser for the first stage (although this may be omitted on smaller units) and a further condenser following the second stage. Four-stage units seldom require a condenser following the first stage since the amount of steam consumed from this stage is small and can be efficiently compressed by the following stages. Five- and six-stage units follow on the lines of a four-stage unit, with the addition of one or two non-condensing stages. The bulk of industrial applications are covered by one-, two- or three-stage injectors.

Water-operated air ejector pumps operate on a similar principle to the steam ejector except that the velocity of the water jet is due to pressure alone rather than expansion and is therefore usually much lower (steam jet velocities of over 1200 m/sec (4000 ft/sec) are commonplace in steam ejectors designed for high vacua). For a similar duty, the water ejector pump is considerably larger in order to deal with a similar volume of gas (normally air). Initially the air is in contact with the outer surface of the water jet only, until subsequently entrained in the cone.

See also chapter on *Vacuum Techniques*.

## THOMAS REGISTER 1986

### EJECTORS: AIR

#### AL: BIRMINGHAM

Rotron Industrial Division Box 43348 (Designers & Mfrs. of Regenerative Blowers) ..... NR

#### AZ: PHOENIX

Rotron Industrial Division 3009 W. Clarendon Ave. P.O. Box 27121 (Designers & Mfrs. of Regenerative Blowers) ..... NR

#### CA: BELL GARDENS

Alpa Centerless Products 7835-T Ramish Ave. .... 1/2M+

#### CA: EMERYVILLE

Western Process Design, Inc. 1525-T Powell St. (Liquid Ring Pumps) ..... 1M+

#### CA: HUNTINGTON BEACH

Rotron Industrial Division 7261 Mars Dr. (Designers & Mfrs. of Regenerative Blowers) ..... NR

#### CO: DENVER

Rotron Industrial Division 3730 Paris Unit B (Designers & Mfrs. of Regenerative Blowers) ..... NR

#### CO: LITTLETON

NORGREN, C. A. COMPANY One Norgren Plaza (ZIP 80120) (Noise Reduction; Reduces Noise Of Compressed Air/Blow Offs, Parts Ejection, Chip Removal, Etc.) (303-794-2611) ..... 1M+

#### CT: FAIRFIELD

Clarktron Products Inc. 684T State St. Ext., P.O. Box 1496 ..... 1/2M+

#### CT: MILFORD

AIR-VAC ENGINEERING CO. INC. Dept. T (ZIP 06460) (203-874-2541) ..... 1M+

#### CT: RIDGEFIELD

Rotron Industrial Division Box 66 (Designers & Mfrs. of Regenerative Blowers) ..... NR

#### CT: SIMSBURY

Rotron Industrial Division P.O. Box 905 (Designers & Mfrs. of Regenerative Blowers) ..... NR

#### FL: ORLANDO

Westinghouse Electric Corp., Turbine Generation Operations Div. The Quadrangle ..... 50M+

#### FL: SANFORD

Rotron Industrial Division 2803 Park Dr. (Designers & Mfrs. of Regenerative Blowers) ..... NR

#### FL: TAMPA

Safety Equipment Company 6509 N. Harney Rd. (Distributing Safety Products) ..... 1M+

#### GA: ATLANTA

Rotron Industrial Division 2758 Chamblee-Tucker Rd. (Designers & Mfrs. of Regenerative Blowers) ..... NR

#### IL: CHICAGO

Walsh Press & Die Co., Sub. of Katy Industries Inc. 4709 W. Kinzie St. (For Punch Presses) ..... 50M+

#### IL: ELGIN

Katy Industries, Inc. 853 Dundee Ave. (For Punch Presses) ..... 10M+

#### IL: MELROSE PARK

Darley, W. S., & Co. 2000 Anson Dr., Dept. T ..... 5M+

#### IL: PROPHETSTOWN

PENBERTHY-HOUDAILLE, INC., A SUB. OF HOUDAILLE INDUSTRIES, INC. P.O. Box 112 (ZIP 61277) (815-637-2311) ..... 50M+

#### IL: ROCKFORD

Rotron Industrial Division P.O. Box 5122 (Designers & Mfrs. of Regenerative Blowers) ..... NR

#### IN: INDIANAPOLIS

Rotron Industrial Division 6450 Around the Hills Rd. (Designers & Mfrs. of Regenerative Blowers) ..... NR

#### IA: CEDAR RAPIDS

Rotron Industrial Division 417 16th St. N.E. (Designers & Mfrs. of Regenerative Blowers) ..... NR

#### KS: MEHRRIAM

Rotron Industrial Division 6412 Carter St., P.O. Box 3114 (Designers & Mfrs. of Regenerative Blowers) ..... NR

#### KS: WICHITA

Rotron Industrial Division 1923 S. Hydraulic St. (Designers & Mfrs. of Regenerative Blowers) ..... NR

#### LA: BATON ROUGE

Rotron Industrial Division Jubon Station, P.O. Box 64985 (Designers & Mfr. of Regenerative Blowers) ..... NR

#### MA: SOUTH HADLEY FALLS

UNION ENGINEERING CORP. 3 W. Main St. (ZIP 01075) (413-533-4460) ..... 1/4M-

#### MA: WALTHAM

Jet-Vac Corp., The 69 Pond St. .... 1M+

#### MI: PORTAGE

Rotron Industrial Division P.O. Box 215 (Designers & Mfrs. of Regenerative Blowers) ..... NR

#### MN: MINNEAPOLIS

Rotron Industrial Division 4346 Xerxes Ave. S. (Designers & Mfrs. of Regenerative Blowers) ..... NR

#### MO: CHESTERFIELD

Rotron Industrial Division 300 Chesterfield Center, Suite 280 (Designers & Mfrs. of Regenerative Blowers) ..... NR

#### MO: KANSAS CITY

Labconco Corp. 8811 Prospect ..... 10M+

#### NE: OMAHA

Rotron Industrial Division 1227 S. 22nd St., P.O. Box 3588 (Designers & Mfrs. of Regenerative Blowers) ..... NR

#### NJ: EAST HANOVER

FOX VALVE DEVELOPMENT CORP. 2-T Great Meadow Lane (ZIP 07938) (Standard, Custom Designs; Stainless, Exotic Materials) (201-887-7474) .... 1M+

#### NJ: WESTFIELD

Croll-Reynolds Co., Inc. P.O. Box 868 ..... NR

#### NY: BATAVIA

Graham Manufacturing Co., Inc. 20-T Florence Ave. .... 25M+

#### NY: BUFFALO

Nortel Machinery, Inc. 1051-T Clinton St. (Pneumatic Air Movers & Air Flow Amplifiers) ..... NR

Rotron Industrial Division P.O. Box 1129 (Designers & Mfrs. of Regenerative Blowers) ..... NR

#### NY: ELMSFORD

Fire-End & Croker Corp. 7 Westchester Plaza, Dept. T-86 (Domestic & Export, Hose Stations, Nozzles, Monitors, Valves, Extinguisher & Hose Cabinets, Complete Exterior & Interior Fire Fighting Equipment For Industrial, Construction & Municipal Markets) ..... 5M+

#### NY: HAUPPAUGE

Festo Corp. 395-T Moreland Rd. .... 50M+

#### NY: NEW YORK

Vita Motivator Co., Inc. 200-T W. 20th St. .... 1/4M+

#### NY: ROCHESTER

Rotron Industrial Division 300 White Spruce Blvd. (Designers & Mfrs. of Regenerative Blowers) ..... NR

#### NY: SAUGERTIES

Rotron Industrial Division North St. (Designers & Mfrs. of Regenerative Blowers) ..... 50M+

#### NY: SCHENECTADY

Rotron Industrial Division 30 Jay St. (Designers & Mfrs. of Regenerative Blowers) ..... NR

#### NC: CHARLOTTE

Fox Trim Away Corp. Dept. T, 9724 Southern Pine Blvd. .... NR

Rotron Industrial Division P.O. Box 2324 (Designers & Mfrs. Of Regenerative Blowers) ..... NR

## ASME PERFORMANCE TEST CODES

## SECTION 5, COMPUTATIONS

**5.01** A complete presentation of the performance of an ejector system shall include a statement of the following significant quantities:

- (a) Capacity — naming motive-fluid used
  - (b) Suction pressure
  - (c) Suction temperature
  - (d) Discharge pressure — specifying if the reading is the recovery pressure
  - (e) Motive-fluid pressure — specifying if the reading is the recovery pressure
  - (f) Motive-fluid temperature
  - (g) Motive-fluid flow rate — naming fluid
- If the system includes condensers, add the following:
- (h) Cooling-water flow rate to each condenser
  - (i) Temperature of cooling water entering and leaving each condenser

The limiting conditions of stable operation shall also be given in terms of motive-fluid pressure and discharge pressure.

**5.02** Before calculations are undertaken, the instrument readings, as recorded in the log, shall be scrutinized for inconsistency and fluctuation. Where the magnitude of fluctuation, or the deviation from the prescribed operating conditions is in excess of the limitations given in Table 1, the test point shall be rejected.

**5.03** The average value of the readings of each instrument shall be computed and corrected by its calibration curve. Where more than one instrument is used for the same measurement, the corrected readings must be within the limits prescribed in Table 1 or the point shall be rejected.

**5.04** The readings of pressure gages shall be corrected for the net effect of liquid head in the connecting tubing provided the tubing is full. There shall be no pockets of water in vapor tubing nor gas bubbles in liquid lines.

**5.05** The specific weight of all manometer fluids shall be computed for the prevailing room temperature, and the pressure readings expressed in standard units. Manometer readings shall be adjusted for the differential expansion of the fluid and the scale.

**5.06** Discharge coefficients to be used for the flow nozzles (including motive-fluid) shall have their source identified and agreed upon. For ASME long-radius nozzles, the values from "Fluid Meters," sixth edition, shall be used.

**5.07 Flow Formula.** The following simplified formulae shall be used for computing flow rates with

nozzle arrangements provided in Section 4. They may be used only with gases where the physical properties do not vary, and are accurately known.

For subcritical flow where  $P_2$  is more than 55 percent of  $P_1$  for air or steam

$$m = \frac{1890 F_a C d^2 Y_a'}{(1 - \beta^4)^{1/2}} [\rho_1 (P_1 - P_2)]^{1/2} \text{ lb/hr}$$

For metric units the constant 1890 becomes 3960

$$Y_a' = \left[ \left( \frac{\gamma}{\gamma - 1} \right) r^{(2/\gamma)} \left( \frac{1 - r^{(\gamma-1)/\gamma}}{1 - r} \right) \right]^{1/2} \left[ \frac{1 - \beta^4}{1 - \beta^4 r^{(2/\gamma)}} \right]^{1/2}$$

(See Table 3 for  $Y_a'$  for air and steam.)

For critical flow where  $P_2$  is less than 50 percent of  $P_1$

$$m = 1890 F_a C d^2 Z' (\rho_1 P_1)^{1/2} \text{ lb/hr}$$

For metric units the constant 1890 becomes 3960

$$Z' = \left( \frac{2}{\gamma + 1} \right)^{1/(\gamma-1)} \left( \frac{\gamma}{\gamma + 1} \right)^{1/2} \frac{1}{\left[ 1 - \left( \frac{2}{\gamma + 1} \right)^{2/(\gamma-1)} \beta^4 \right]^{1/2}}$$

(See also Fig. 10.)

A more exact formula for critical flow is that critical flow is present if

$$P_2 \leq P_{1t} \left( \frac{2}{\gamma + 1} \right)^{\gamma/(\gamma-1)}$$

Where

	English	SI
$m$ = flow rate	lb/hr	kg/hr
$C$ = discharge coefficient		
$D$ = diameter of pipe at upstream section	in.	cm
$d$ = diameter of orifice in nozzle	in.	cm
$P_1$ = upstream static pressure	psia	kg/cm <sup>2</sup>
$P_2$ = downstream static pressure	psia	kg/cm <sup>2</sup>
$r = P_2/P_1$		
$\gamma = C_p/C_v$ , ratio of specific heats		
$\beta$ = ratio of nozzle orifice diameter to the pipe inside diameter, $d/D$		
$\rho$ = density	lb/cu ft	gm/cc

For air  $\rho_1 = 2.699 P_1/T_1$  in English units or  $\rho_1 = 0.3413 P_1/T_1$  in Metric units where  $T_1$  is the upstream temperature in absolute units. For steam, consult the 1967 ASME Steam Tables.

$Y'_a$  = expansion factor at subcritical-flow conditions, a ratio

$Z'$  = expansion factor at critical-flow conditions, a ratio

$F_a$  = area multiplier for thermal expansion of nozzle

Note: Constants 1890 and 3960 are based on gravity constant,  $g = 32.17 \text{ ft/sec}^2$

**5.08** Total pressure  $P_{1t}$  used in determining whether flow is critical or subcritical may be found directly with an impact tube or calculated as follows:

$$P_{1t} = \frac{P_1}{\left[ 1 - \beta^4 \frac{\gamma}{2} \left( \frac{2}{\gamma+1} \right)^{(\gamma+1)/(\gamma-1)} \right]}$$

**5.09** For tests using atmospheric air, the effect of humidity may be considered negligible for temperatures up to 100°F.

**5.10** For air, the value of  $\gamma$  shall be taken as 1.4 under all flow conditions. For steam,  $\gamma$  may be taken as 1.3 for all steam conditions up to 200 psia and 600°F. Other values may be obtained from the steam tables for pressure and temperature conditions upstream of the nozzle.

**5.11** Figure 7 may be used for the flow nozzle discharge coefficient obtained from

$$C = 0.9975 - 0.00653 (10^6/Re)^{1/2}$$

Where  $Re$  is the Reynolds number expressed as

$$Re = \frac{m}{235.6 \mu d} \text{ English} \quad \text{or} \quad Re = \frac{35.3 m}{\mu d} \text{ SI}$$

$\mu$  = absolute viscosity in  $\text{lb}_m/\text{ft sec}$  in English units or centipoise for SI units

See Figs. 8 and 9 for viscosity of air and steam.

**5.12** It is recommended that the value of  $\beta$  not exceed 0.25 for any flow measurements with sonic flow through metering nozzles.

**5.13** The capacity of the ejector is sensitive to the suction temperature. Where the fluid being pumped is air or steam, capacity correction values to be used are shown in Fig. 11. In using this factor, note that an ejector will handle more lb/hr of a cool gas than a hot one.

Temperature correction factors are not available for suction fluids other than air or steam or for motive fluids other than steam.

**5.14** If a mixture of air and steam is used as a suction fluid, the suction temperature,  $t_s$ , shall be computed as follows:

$$t_s = \frac{(m C_p t)_{\text{air}} + (m C_p t)_{\text{steam}}}{(m C_p)_{\text{air}} + (m C_p)_{\text{steam}}}$$

where

$m$  = fluid rate in lb per hr (kg/hr)

$C_p$  = heat capacity in Btu/lb °F (cal/gm °C)

$t_A$  = air temperature upstream of flow nozzle in °F (°C)

$t_{STM}$  = temperature calculated for steam pressure and temperature upstream of flow nozzle and expansion at constant enthalpy, °F (°C)

Note: Other than the motive-fluid nozzle, no flow nozzle shall have a diverging exit section.

**5.15** For suction fluids of various molecular weights, the capacity shall be corrected, as shown in Fig. 12. The correction factor is well established for suction pressures above 10 mm Hg absolute. Use at lower pressures must be agreed to by the parties to the test. This curve is applicable for suction temperatures between 50 and 100°F. In its use, note that an ejector will handle more pounds per hour of a higher molecular weight fluid than of a lower one.

**5.16** The capacity and stability at a single point shall be determined from a graphical plot, as illustrated by Fig. 6. Corrected capacity points are plotted and a curve drawn. The same applies to stability data. The respective scales on the curve shall be readable within  $\pm 1.0$  percent.

**5.17 Measurement of Motive-Fluid Flow Rate.** This is normally done by measuring the pressure and temperature upstream of the motive-fluid nozzle and using one of the formulae given under Section 5.07. The orifice diameter shall be measured by plug gages or other suitable means. The discharge coefficient for sonic flow is usually taken to be 0.97 for nozzles with well-rounded inlets; alternatively, Fig. 7 may be used. If the weighed condensate method is used, the suction-fluid rate shall be zero. An adequate surface condenser must be available. The minimum period of measurement shall be one-half hour, with not less than four consecutive readings made at uniform intervals. The data shall show that the motive pressure and temperature were held within 2.0 percent of the mean value.

**5.18** Cooling-water rate shall be measured only by methods given in "Fluid Meters." Allowable variations are given in Table 1.

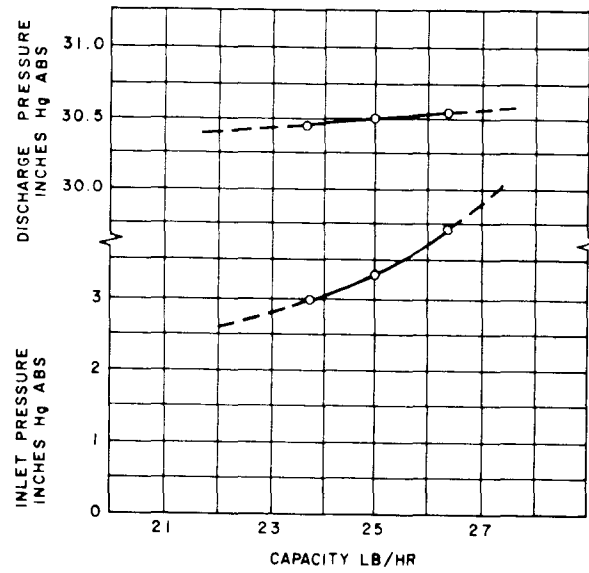


FIG. 6 CHARACTERISTIC CURVES FOR EJECTOR PERFORMANCE

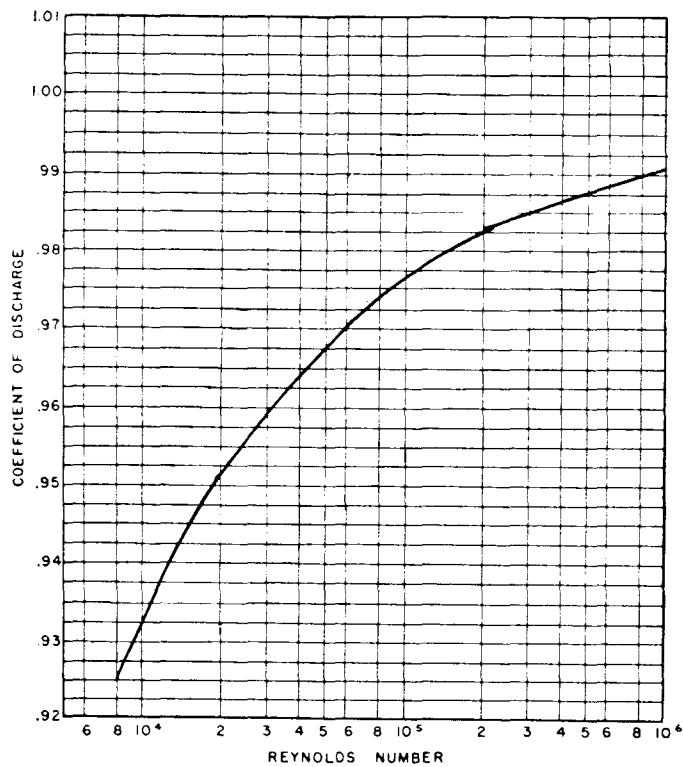


FIG. 7 NOZZLE DISCHARGE COEFFICIENT

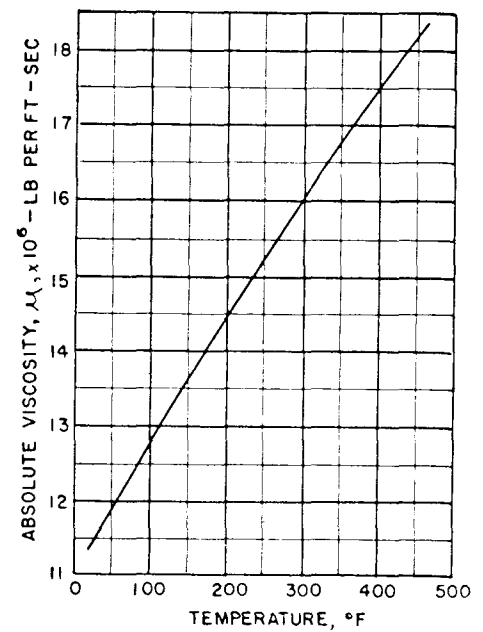


FIG. 8 ABSOLUTE VISCOSITY OF AIR



## EJECTORS

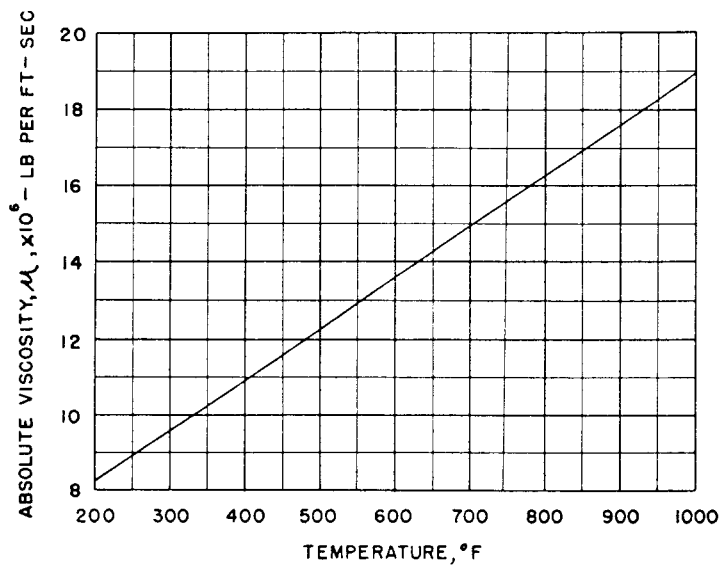
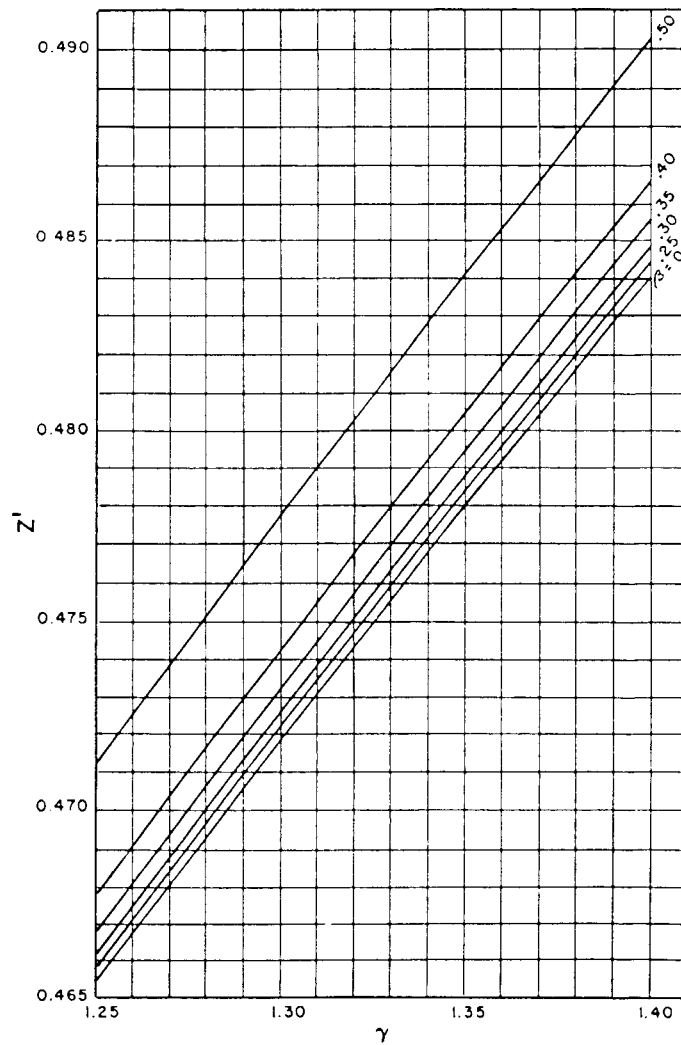


FIG. 9 ABSOLUTE VISCOSITY OF STEAM

FIG. 10 FLOW FACTOR  $Z'$  FOR CRITICAL FLOW

## ASME PERFORMANCE TEST CODES

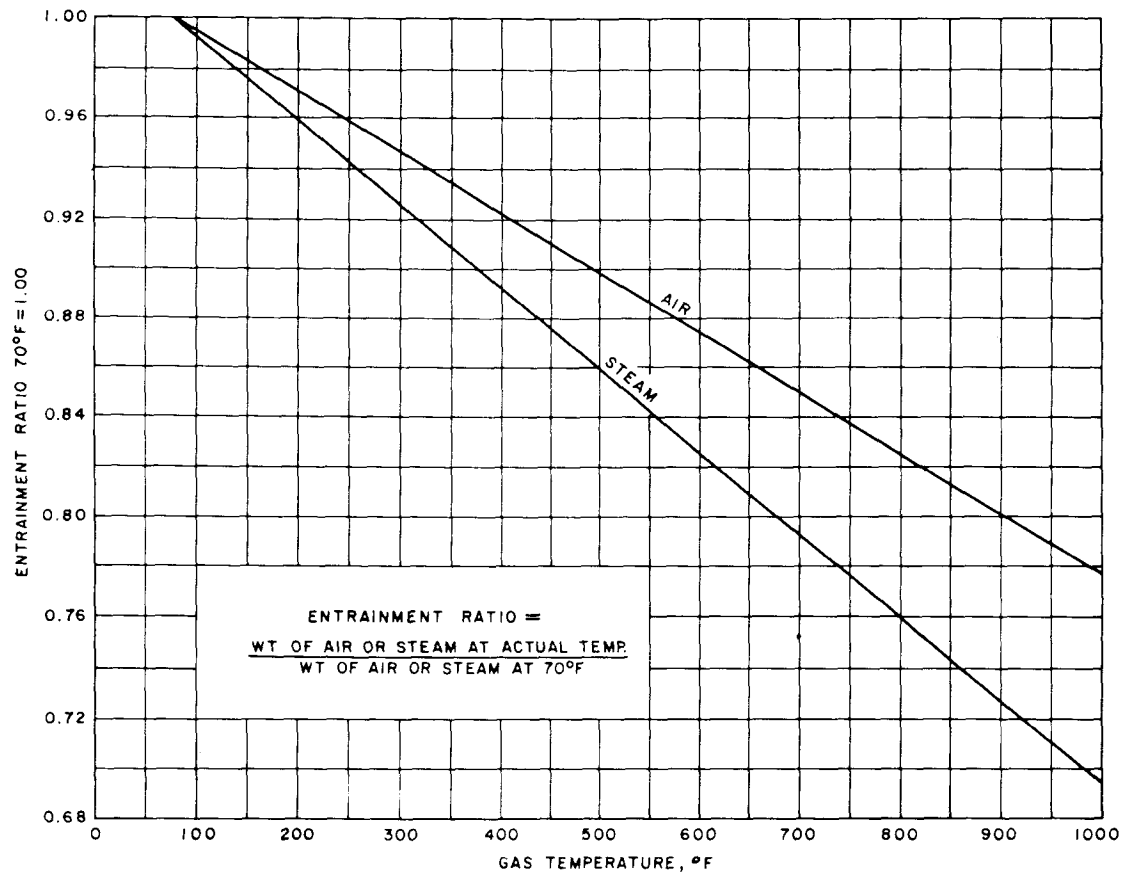


FIG. 11 TEMPERATURE ENTRAINMENT RATIO CURVE

## EJECTORS

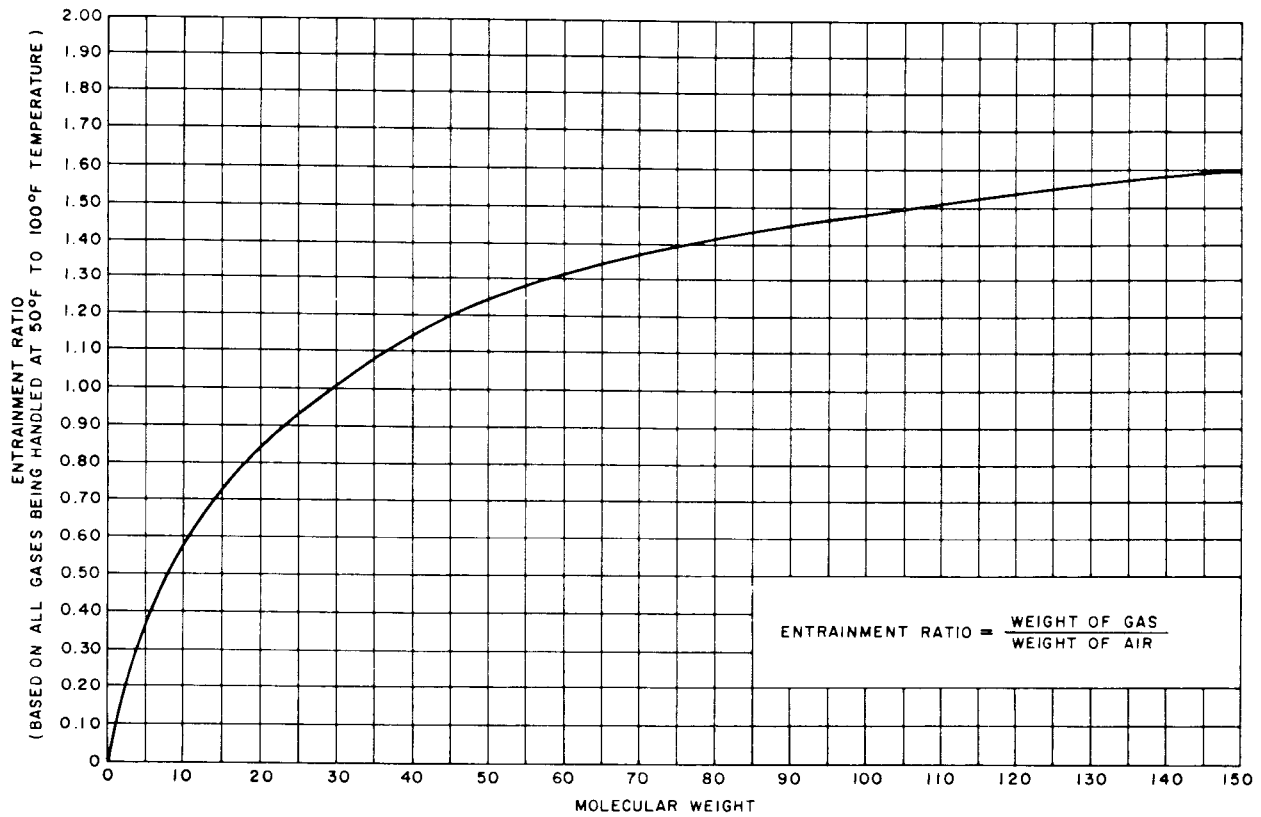


FIG. 12 MOLECULAR WEIGHT ENTRAINMENT RATIO CURVE

# ASME PERFORMANCE TEST CODES

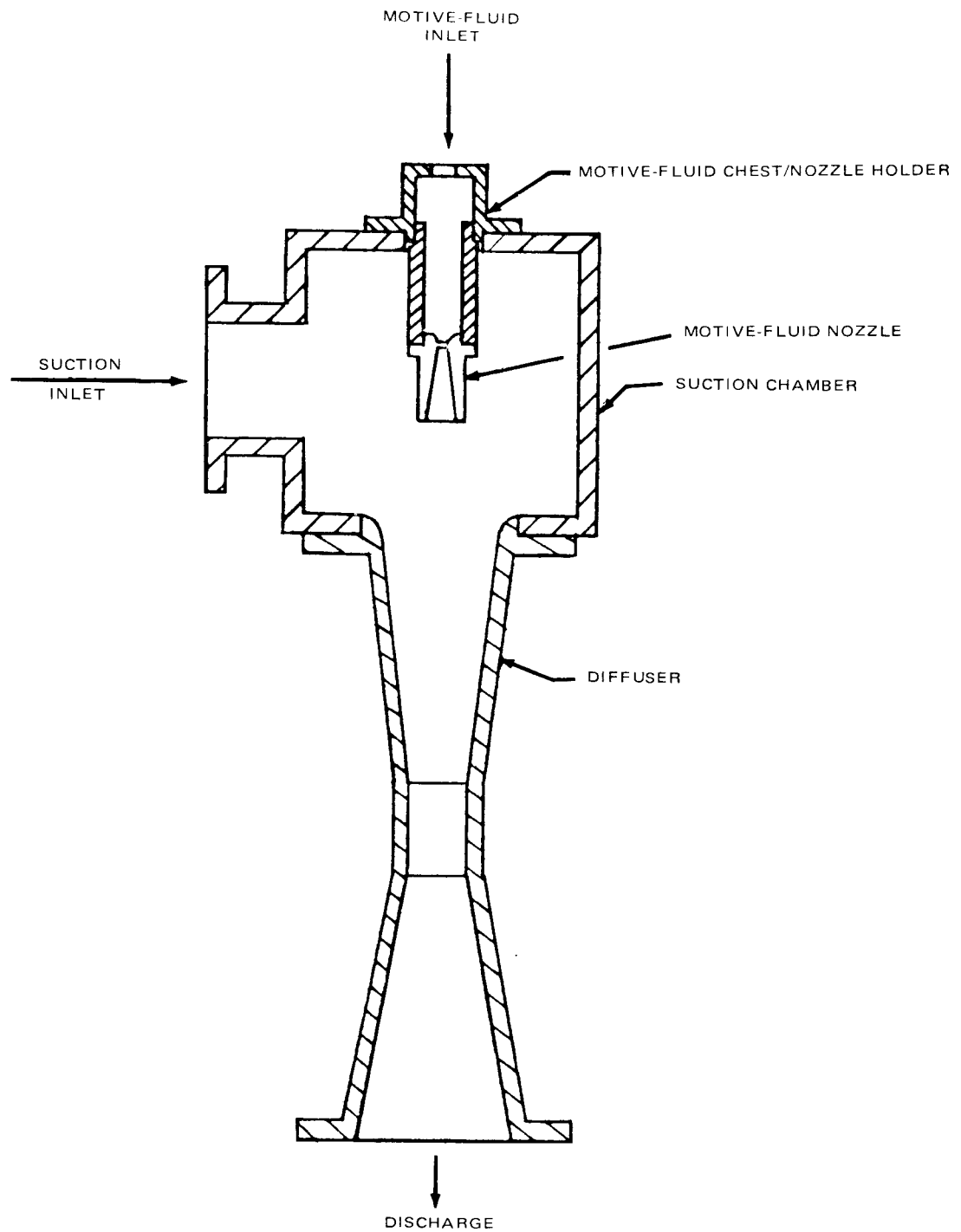


FIG. 13 TYPICAL EJECTOR

TABLE 3  
EXPANSION FACTORS FOR FLOW NOZZLES

$$Y_a = \left( r^{2/\gamma} \frac{\gamma}{\gamma-1} \frac{1-r^{(\gamma-1)/\gamma}}{1-r} \frac{1-\beta^4}{1-\beta^4 r^{2/\gamma}} \right)^{1/2}$$

$\gamma = 1.4$  for Air

$\beta$	$\beta^4$	0.95	0.90	0.85	0.80	$\frac{r}{\gamma}$	0.75	0.70	0.65	0.60	0.55
.2	0.0016	0.9728	0.9448	0.9160	0.8863	0.8556	0.8238	0.7908	0.7565	0.7207	
.3	.0081	.9726	.9444	.9154	.8855	.8546	.8227	.7896	.7552	.7193	
.4	.0256	.9719	.9432	.9137	.8833	.8520	.8198	.7864	.7517	.7156	
.50	.0625	.9706	.9405	.9099	.8785	.8464	.8133	.7793	.7441	.7076	
.55	.0915	.9694	.9383	.9067	.8745	.8416	.8080	.7734	.7378	.7010	
.60	.1296	.9678	.9352	.9023	.8690	.8351	.8006	.7653	.7292	.6920	
.65	.1785	.9655	.9309	.8962	.8613	.8261	.7905	.7543	.7175	.6798	
.70	.2401	.9622	.9247	.8876	.8506	.8136	.7765	.7392	.7016	.6633	
.725	.2763	.9600	.9207	.8819	.8436	.8056	.7676	.7297	.6915	.6530	
.75	.3164	.9573	.9158	.8751	.8353	.7960	.7571	.7184	.6797	.6409	
.775	.3608	.9540	.9097	.8669	.8252	.7845	.7445	.7050	.6657	.6266	
.80	.4096	.9498	.9022	.8566	.8128	.7705	.7292	.6889	.6491	.6097	
.82	.4521	.9457	.8947	.8466	.8009	.7570	.7147	.6736	.6334	.5939	
.84	.4979	.9405	.8856	.8344	.7864	.7409	.6975	.6557	.6152	.5755	
.86	.5470	.9338	.8740	.8194	.7688	.7215	.6769	.6344	.5936	.5541	

$\gamma = 1.3$  for Steam

$\beta$	$\beta^4$	.095	0.90	0.85	0.80	$\frac{r}{\gamma}$	0.75	0.70	0.65	0.60	0.55
.2	0.0016	0.9707	0.9407	0.9099	0.8781	0.8454	0.8117	0.7768	0.7406	0.7030	
.3	.0081	.9705	.9402	.9092	.8773	.8445	.8106	.7756	.7393	.7016	
.4	.0256	.9698	.9390	.9074	.8750	.8417	.8075	.7722	.7357	.6978	
.50	.0625	.9683	.9362	.9034	.8700	.8358	.8008	.7648	.7278	.6896	
.55	.0915	.9671	.9338	.9001	.8658	.8309	.7952	.7588	.7214	.6829	
.60	.1296	.9654	.9305	.8954	.8599	.8240	.7876	.7505	.7126	.6738	
.65	.1785	.9629	.9259	.8889	.8519	.8146	.7771	.7392	.7007	.6614	
.70	.2401	.9594	.9193	.8798	.8406	.8016	.7627	.7237	.6844	.6447	
.725	.2763	.9570	.9150	.8739	.8333	.7933	.7535	.7139	.6742	.6343	
.75	.3164	.9542	.9098	.8667	.8246	.7833	.7426	.7023	.6622	.6221	
.775	.3608	.9507	.9034	.8580	.8141	.7714	.7297	.6886	.6481	.6077	
.80	.4096	.9462	.8955	.8473	.8013	.7570	.7141	.6723	.6313	.5908	
.82	.4521	.9418	.8876	.8368	.7888	.7431	.6992	.6568	.6155	.5750	
.84	.4979	.9362	.8779	.8241	.7739	.7266	.6817	.6387	.5971	.5567	
.86	.5470	.9292	.8658	.8084	.7557	.7067	.6608	.6172	.5756	.5353	

**E-10. Condensing and Noncondensing Types**

Condensing multi-stage ejectors have intercondensers between some or all of the various stages (Figs. 5, 6, 7, 8 and 9) for the purpose of condensing as much as possible of the vapor discharged from the preceding stage or stages. In this manner, the weight of gas to be compressed by the next succeeding stage or stages is decreased. Noncondensing multi-stage ejectors have no intercondensers between stages.

**E-11. Intercondensers**

Intercondensers can be surface (Fig. 6) or direct contact (usually barometric) (Figs. 5, 7, 8 and 9) type. With three or more ejector stages, the intercondenser operating at the lowest absolute pressure is the first intercondenser and that following the next stage, the second intercondenser, etc.

**E-12. Aftercondensers**

Condensers arranged to condense the vapors discharged from one or more single stage ejectors, or from the final stage or stages of a combination of ejectors, at approximately atmospheric pressure, are termed aftercondensers. These may be of the surface or direct contact type.

**E-13. Surface Intercondensers and Aftercondensers**

Surface intercondensers and aftercondensers can be arranged in separate shells or can be combined in a common shell suitably subdivided.

## DESIGN SPECIFICATIONS

**E-14. Capacity**

The following capacity requirements shall be specified:

- (a) the absolute pressure to be maintained
- (b) the total weight in pounds per hour of the gas to be entrained
- (c) the temperature of the gas to be entrained
- (d) composition of the gas to be entrained. The weight of each constituent shall be specified in pounds per hour.
- (e) if the gas is other than air or water vapor, its physical and chemical properties shall be fully specified.

**E-15. Steam Conditions**

The following characteristics of the operating steam shall be specified:

- (a) maximum steam *line* pressure and temperature
- (b) maximum steam pressure and temperature at the ejector steam inlet
- (c) minimum steam pressure at the ejector steam inlet
- (d) design steam pressure and temperature
- (e) quality of the steam, if it is not superheated, at the ejector steam inlet.

To prevent the nozzle throat areas of the ejector from becoming too small to be practical, the ejector manufacturer may elect to use a design steam pressure lower than the available steam pressure at the ejector steam inlet.

It is recommended that the design steam pressure never be higher than 90 per cent of the minimum steam pressure at the ejector steam inlet.

**E-16. Cooling Water**

The following characteristics of the cooling water shall be specified:

- (a) maximum and minimum pressure at the ejector water inlet
- (b) maximum temperature
- (c) maximum and minimum quantity available
- (d) source and quality of water
- (e) any limitations on the cooling water for the specified capacity.

**E-17. Discharge Pressure**

The pressure against which a single stage or the last stage of a multi-stage ejector must discharge shall be specified in pounds per square inch absolute or inches of mercury absolute pressure. The normal barometric pressure in inches of mercury shall be specified.

**STANDARDS FOR STEAM JET EJECTORS**

**PART TWO**

**STANDARDS OF CONSTRUCTION**

**Table of Contents**

	PAGE NUMBER
Accessories . . . . .	7
Materials and Details of Construction . . . . .	7
Protection of Atmospheric and Subatmospheric Spaces . . . . .	9
Hydrostatic Test Pressures . . . . .	9

## STANDARDS FOR STEAM JET EJECTORS

## ACCESSORIES

## E-18. Accessories

Industrial ejectors may include a steam strainer if the steam nozzle has a throat diameter of  $\frac{3}{8}$

inches or less and may include a steam separator if required because of wet steam.

Power plant ejectors may include steam piping; steam strainer; throttle and steam stop valves.

## MATERIALS AND DETAILS OF CONSTRUCTION

## E-19. Materials and Details of Construction

Any of the following grades of materials are the minimum requirements for the parts listed below. Specifications are ASTM latest edition, unless otherwise noted.

## (a) Ejector Parts Under Steam Pressure

Max. Design Steam Temp F	Steam Pipe and Fittings	Steam Chest Nozzle Plate	Steam Nozzles
400	In accordance with USAS Pressure Piping Code B-31.1	Bronze B 62; Carbon Steel, cast A 216-WCA, forged A 181 Grade 1, bar A 107	Stainless Steel, bar A 276-303, 304, or 416
650	In accordance with USAS Pressure Piping Code B-31.1	Carbon Steel, cast A 216-WCA, forged A 181 Grade 1, bar A 107	Stainless Steel, bar A 276-303, 304, or 416
850	In accordance with USAS Pressure Piping Code B-31.1	Carbon Steel, cast A 216-WCB, forged A 105 Grade 1	Stainless Steel, bar A 276-303, 304, or 416
1000	In accordance with USAS Pressure Piping Code B-31.1	Chrome Molybdenum Steel, cast A 217-WC-6, forged A 182-F-11	Stainless Steel, bar A 276-304
1050	In accordance with USAS Pressure Piping Code B-31.1	Chrome Molybdenum Steel, cast A 217-WC-9, forged A 182-F-22	Stainless Steel, bar A 276-304
1125	In accordance with USAS Pressure Piping Code B-31.1	Stainless Steel, cast A 296-CF-8M or CF-8C, forged A 182-F-316, F-347 or F-321	Stainless Steel, bar A 276-316, 347, or 321

## (b) Ejector Parts Under Vacuum (see Note 1)

## Diffusers

Bronze B 62 or 144-3D  
Cast Iron A 48 class 30  
Steel, plate A 285 grade C flange quality  
Steel, bar A 107

## Suction Chamber

Cast Iron A 48 class 30  
Steel, plate A 285 grade C flange quality

## Interstage Valves

Cast Iron

## (c) Condensers (see Note 1)

## (1) Direct Contact Type

## Shells

Cast Iron A 48 class 30  
Steel, plate A 285 grade C flange quality

## Internal Water

## Distributing Baffles

Cast Iron A 48 class 30  
Steel, plate A 285 grade C flange quality or A 7

## Tailpipes

Cast Iron A 126 grade A  
Steel, A 120

## Water Removal Pump:

casing  
impeller(s)

Cast Iron  
Bronze



## HEAT EXCHANGE INSTITUTE

wearing rings  
shaft

Bronze  
Steel, covered with bronze sleeves

## (2) Surface Type

Water Boxes and Water  
Box Covers

Cast Iron A 48 class 30  
Steel, plate A 285 grade C flange quality

Shells

Cast Iron A 48 class 30  
Steel, plate A 285 grade C flange quality  
Steel Pipe A 53

Tube Sheets

Rolled Muntz Metal B 171  
Carbon Steel up to 2 inches thick — A 285 grade C  
flange quality  
Carbon Steel over 2 inches thick — A 201 grade A or  
B flange quality  
Stainless Steel A 240 Type 304

Tube Support Plates  
and Baffles

Steel, plate A 285 grade C flange quality or  
"Free Machining" steel plate

Tubes

Admiralty Type A, B 111  
Carbon Steel A 214  
Stainless Steel A 249 Type 304

Note 1: All flanged connections under vacuum shall be flat faced.

## (d) Standard Flanges for Vacuum Service

Material: Carbon Steel Plate—A 285 grade C flange 55000 psi tensile Bar — A 107 grade 1020 65000 psi tensile					Following notes apply to Table below: A. Dimensions W and T above 24 inches are rectangular bar sizes. B. Use medium carbon steel heat treated bolting, A 325 (SAE grade 5) over 24 inch size. Bolts are $\frac{1}{8}$ inch smaller than hole size. C. $\frac{1}{8}$ inch thick compressed asbestos gaskets to be used.		
Size Inches	O.D.	I.D.	W (A)	T (A)	Drilling (B) No. & Size Holes		Gasket (C) Size
4	USA STANDARD 125 LB DIMENSIONS			$\frac{5}{8}$	USA STANDARD 125 LB WITH CARBON STEEL BOLTS		9 x 6
5				$\frac{5}{8}$			10 x 7
6				$\frac{5}{8}$			11 x 8
8				$\frac{5}{8}$			13 $\frac{1}{2}$ x 10
10				$\frac{5}{8}$			16 x 12 $\frac{1}{2}$
12				$\frac{5}{8}$			19 x 15
14				$\frac{3}{4}$			21 x 16 $\frac{1}{2}$
16				$\frac{3}{4}$			23 $\frac{1}{2}$ x 19
18				$\frac{3}{4}$			25 x 20 $\frac{1}{2}$
20				$\frac{3}{4}$			27 $\frac{1}{2}$ x 22 $\frac{1}{2}$
24				$\frac{3}{4}$			32 x 27
30	36 $\frac{1}{4}$	30 $\frac{1}{4}$	3	1	28 - $\frac{3}{4}$	34 $\frac{3}{8}$	36 $\frac{1}{4}$ x 32 $\frac{1}{2}$
36	42 $\frac{1}{4}$	36 $\frac{1}{4}$	3	1	32 - $\frac{3}{4}$	40 $\frac{3}{8}$	42 $\frac{1}{4}$ x 38 $\frac{1}{2}$
42	48 $\frac{1}{4}$	42 $\frac{1}{4}$	3	1 $\frac{1}{4}$	40 - $\frac{3}{4}$	46 $\frac{1}{4}$	48 $\frac{1}{4}$ x 44 $\frac{1}{4}$
48	54 $\frac{1}{4}$	48 $\frac{1}{4}$	3	1 $\frac{1}{4}$	44 - $\frac{3}{4}$	52 $\frac{1}{4}$	54 $\frac{1}{4}$ x 50 $\frac{1}{4}$
54	60 $\frac{1}{4}$	54 $\frac{1}{4}$	3	1 $\frac{1}{2}$	44 - $\frac{7}{8}$	58 $\frac{1}{4}$	60 $\frac{1}{4}$ x 56 $\frac{1}{4}$
60	66 $\frac{1}{4}$	60 $\frac{1}{4}$	3	1 $\frac{1}{2}$	52 - $\frac{7}{8}$	64	66 $\frac{1}{4}$ x 61 $\frac{3}{4}$
72	78 $\frac{1}{4}$	72 $\frac{1}{4}$	3	1 $\frac{3}{4}$	60 - $\frac{7}{8}$	76	78 $\frac{1}{4}$ x 73 $\frac{3}{4}$
84	90 $\frac{1}{4}$	84 $\frac{1}{4}$	3	2	64 - 1	87 $\frac{3}{4}$	90 $\frac{1}{4}$ x 85 $\frac{1}{4}$
96	102 $\frac{1}{4}$	96 $\frac{1}{4}$	3	2 $\frac{1}{4}$	68 - 1	99 $\frac{3}{4}$	102 $\frac{1}{4}$ x 97 $\frac{1}{4}$

## STANDARDS FOR STEAM JET EJECTORS

---

### E-19.1 Protection of Atmospheric and Subatmospheric Spaces

Ejectors operating under conditions requiring a reduction from main line steam pressure to ejector design pressure, shall be protected against excessive pressure in the normally atmospheric or subatmospheric spaces.

- (a) *Ejector units without interstage isolating valves.* These unit types, either single element or twin element with separate intercondensers and separate or common aftercondenser, are to be provided with relief devices (set to relieve at 15 psi) on intercondensers if internal pressure can exceed 15 psi under any service condition. To provide for venting of uncondensed steam from aftercondenser, a vent of adequate size must be provided at the air outlet connection. When an air meter is used, an adequate relief must be provided.
- (b) *Ejector units with interstage isolating valves.* These unit types with isolating valves at discharge of both primary and secondary elements are to be provided with relief devices

on all elements set to relieve at 15 psi and sized for maximum steam flow under following abnormal conditions:

- (1) Operating motive steam pressure at ejector nozzles 25% above design.
- (2) Steam nozzle throat area 10% in excess of design.

Unit types which do not include isolating valves at discharge of secondary stages, are to be provided with relief devices on primary elements only and a vent of adequate size must be provided at the air outlet connection similar to that described in Paragraph (a). For all ejector units with interstage isolating valves, it is necessary that a relief device be installed between pressure reducing station and ejector inlet header selected to relieve at 25% above ejector design steam pressure and sized for maximum steam flow through pressure reducing station. To permit reasonable sizing of relief device, full size by-pass lines are not to be used with the pressure reducing station.

## HYDROSTATIC TEST PRESSURES

### E-20. Hydrostatic Test Pressures

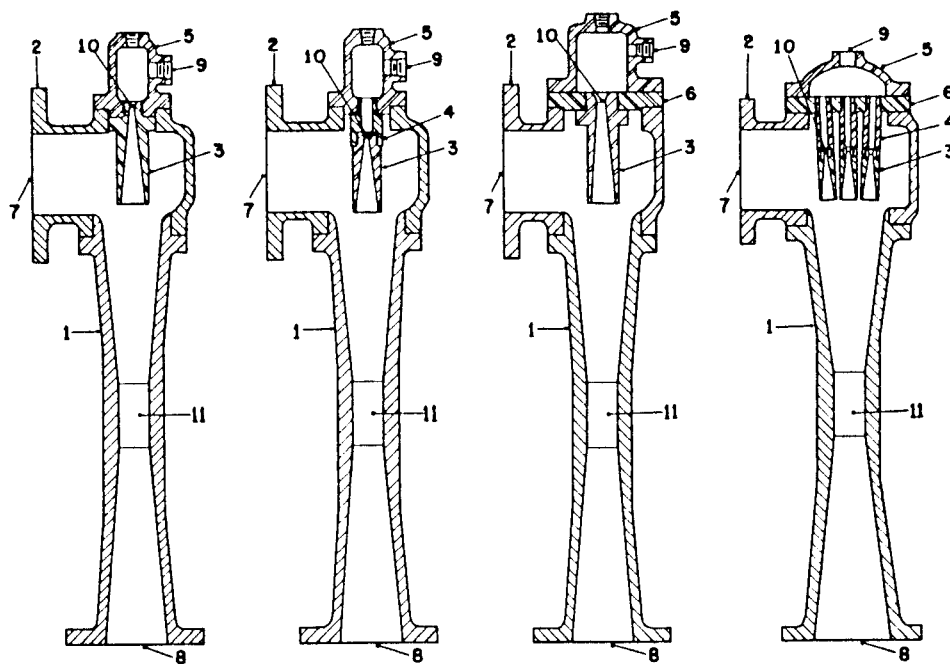
Steam piping shall be hydrostatically tested in accordance with USAS Pressure Piping Code B-31.1, latest edition. Subatmospheric spaces of the equip-

ment shall be hydrostatically tested with an internal pressure of 20 psig. Water chambers shall be hydrostatically tested at an internal pressure  $1\frac{1}{2}$  times design pressure but not less than 25 psig.

**STANDARDS FOR STEAM JET EJECTORS**  
**HEAT EXCHANGE INSTITUTE**  
 3rd Ed. c 1962  
 p. 1-3

### NOMENCLATURE

**E-1.** With the view of establishing standard terminology, the following four sketches, Fig. 1, are shown of a basic steam jet ejector stage assembly. It should be noted, however, that these sketches are merely illustrative for the purpose of indicating names of parts.



1. Diffuser
2. Suction Chamber
3. Steam Nozzle
4. Nozzle Extensions (if used)
5. Steam Chest
6. Nozzle Plate (if used)

7. Suction
8. Discharge
9. Steam Inlet
10. Nozzle Throat
11. Diffuser Throat

TYPICAL STEAM JET EJECTOR STAGE ASSEMBLIES

**Fig. 1**

## OPERATING PRINCIPLES

**E-2.** The operating principle of a steam jet ejector stage is that the pressure energy in the motive steam is converted into velocity energy in the nozzle, and, this high velocity jet of steam entrains the vapor or gas being pumped. The resulting mixture, at the resulting velocity, enters the diffuser where this velocity energy is converted to pressure energy so that the pressure of the mixture at the ejector discharge is substantially higher than the pressure in the suction chamber.

**E-3.** An ejector stage has operating limitations on the compression attainable and will operate efficiently only up to a definite maximum ratio of compression. The ratio of compression is the absolute discharge pressure divided by the absolute suction pressure.

For greater ratios of compression than can be attained in a single ejector stage, two or more stages can be arranged to operate in series. This assembly constitutes a multi-stage ejector.

**E-4.** An ejector stage is inherently a constant capacity device. The capacity is a function of the physical proportions of the diffuser.

To obtain variation in capacity, two or more ejectors, either single or multi-stage, can be arranged to operate in parallel, each series constituting an element of a multiple element ejector. This arrangement permits the operation of the number of elements needed for the required capacity, as each element is capable of completely compressing a portion of the total capacity.

## DESCRIPTION OF TYPES

**E-5.** Some of the various types of ejector units commonly used are illustrated in Figs. 2 to 9 inclusive.

### **E-6. Single Stage, Single Element Ejectors**

These consist of one basic assembly (Fig. 2) which is designed to operate at a suction pressure below atmospheric pressure and to discharge at atmospheric pressure or higher.

### **E-7. Single Stage, Multiple Element Ejectors**

These consist of two or more basic assemblies, each designed to operate at a suction pressure below atmospheric pressure and to discharge at atmospheric pressure or higher. In these combinations, each basic assembly is termed an element. The complete unit is termed a single stage, twin element ejector, (Fig. 3); single stage, triple element ejector; etc., depending on the number of elements provided.

### **E-8. Multi-Stage, Single Element Ejectors**

These consist of two or more basic assemblies arranged in series, (Figs. 4, 5, 7, 8 and 9). The first and any intermediate assembly of the series is designed to operate at suction and discharge pressures substantially below atmospheric pressure. The final assembly of the series is designed to discharge at atmospheric pressure or higher.

(a) The discharge pressure of the first stage, and the suction and discharge pressures of the intermediate stages, follow no fixed rule, but are selected to best subdivide the total compression among the several stages, according to the particular operating conditions.

(b) The first stage of a multi-stage ejector is the stage into which the vapor or gas being compressed first enters, the second stage that which it enters second, the third stage that which it enters third, etc.

(c) A complete series of stages composed of but one basic assembly per stage is termed a two stage, single element ejector; three stage, single element ejector; etc., depending upon the number of basic assemblies arranged in series.

### **E-9. Multi-Stage, Multiple Element Ejectors**

These consist of two or more multi-stage, single element ejectors, assembled in parallel as in Fig. 6, and arranged to permit the operation of any multi-stage element independently or in combination with others. These ejectors are unified by the use of common condensers with isolating interstage valves or by the use of subdivided surface condensers.



Fig. 2

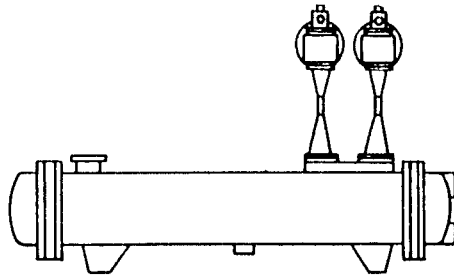


Fig. 3

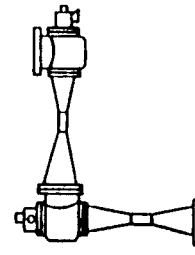


Fig. 4

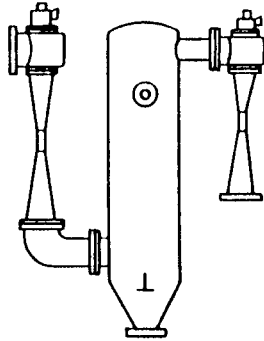


Fig. 5

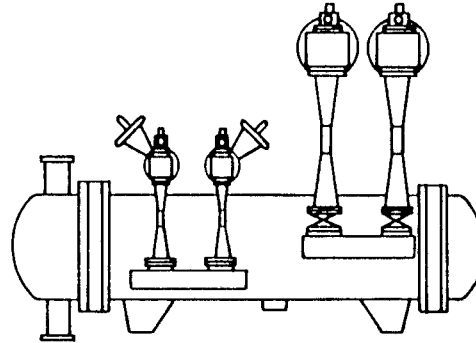


Fig. 6

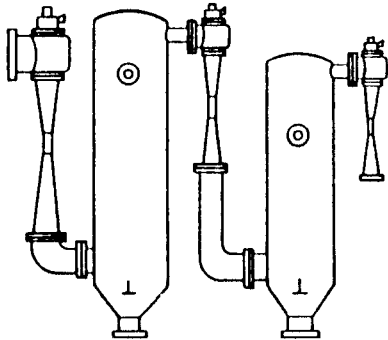


Fig. 7

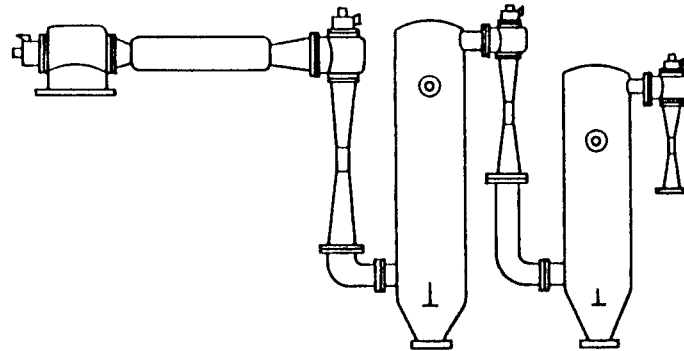


Fig. 8

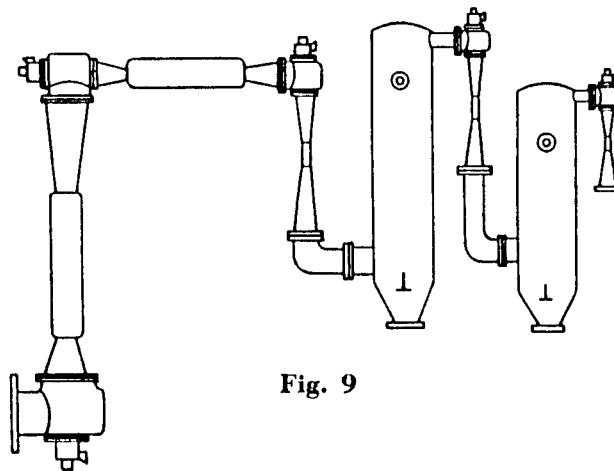


Fig. 9

COMMON TYPES OF EJECTOR UNITS

## 5. MISCELLANEOUS DESIGNS

### 5.1. Reciprocating and pulse jet pumps.

For the purposes of this review the reciprocating jet pump described in Walkden (196), (203), (272) is combined with the pulse-jet approach, for example, Johnson (235). This combination is logical to the extent that it allows the effects of frequency to be compared, although the mechanisms and intentions are considerably different.

The reciprocating pump developed by Walkden operates on the principle of alternately injecting and withdrawing fluid axially from a tube, using an orifice, the practical benefit of this being that the 'pump' to do this can be entirely sealed from the driving mechanism, for example by using a diaphragm or pneumatic drive. Its use is therefore attractive for difficult fluids.

Although the volume of fluid injected and withdrawn is the same in each stroke, a nett head is generated in the mixing tube as a result of the differing flow patterns for an orifice acting as a source and a sink. In reference (196) Walkden develops the general theory and outlines some possible practical designs (Fig. 9 shows one such arrangement) and in (272) he presents experimental results. A reasonable agreement between theory and experiment is shown to be possible if account is taken of boundary-layer effects in the driving jet. In addition to the usual operating variables the injection frequency is shown to have a considerable influence on efficiency and pump characteristics; Fig. 10 shows a simplified plot from (272) in which it is seen that the optimum pump stagnation head will occur at a frequency around 2.4 Hz, but that optimum efficiency requires a lower frequency of about 1 Hz. In other respects the pump is similar to the other momentum devices in having a straight-line relationship between head and induced flow.

This type of pump is shown to have a maximum possible efficiency of about 32% compared with 38% for a commercial jet pump, but this is offset to some extent by the potential to use a greater area ratio without such an abrupt loss of efficiency. Two stages are shown to give rather more than twice the stagnation head of one stage. Paper (337) discusses some of the practical considerations of control of the pneumatic system and describes successful tests on a model pump handling molten  $K_2SO_4$  at 1500°C.

The pulse jet pump employs a conventional jet by which a short pulse is injected into the mixing chamber producing a compression wave which travels to the mixing-tube exit and is reflected as an expansion wave. The wave action results in a nett entrainment of fluid, and entrainment ratios of 20 are quoted as possible in Johnson (235). Flow visualisation has shown the pulse to act essentially as a piston with little axial mixing and an analysis on this basis is derived. An advantage of this type of action is that very little axial length of mixing tube is necessary to reach optimum performance. Pulse frequencies in the range 60 to 100 Hz appear to be typical and there is advantage in the pulse cycle occupying something less than one third of the total cycle. Reference (235) does not discuss efficiency as such, and the emphasis is on thrust augmentation rather than generation of a pumping head.

Nagao (257) also shows the benefit of pulsating drive in the use of diesel exhaust gases to drive ejectors. Rao in (270) reports delivery ratio under pulsating conditions to be up to 4 times

those for steady flow and in (359) extends his investigation to include changes in ejector geometry and pulsation frequency.

### 5.2. Annular and Coanda effect pumps for tunnel ventilation.

While most ventilation applications employ conventionally designed ejectors Kempf (165) and Mishimua (166) should be mentioned for their exploitation of the 'Coanda' wall effect as a means of inducing flow in road tunnels where normal means of applying a driving jet would interfere with traffic requirements. The Coanda effect itself is merely the ability to turn a jet through an angle by virtue of its characteristics of adhering to a wall. In the present context the interest lies in the attempts to predict the effect of a high velocity driving stream at the wall, which is a feature of all annular jet pumps. However, the theories advanced in these papers underestimate the performance, in contrast to the overestimation resulting from the usual assumption of uniform velocity.

### 5.3. Magnetohydrodynamic pump.

This is clearly outside the context of the usual ejectors, but it is interesting to record a case in which external influences control mixing (169). In this case the applied transverse magnetic field serves to retard the primary and accelerate the secondary flows, and supercedes the usual actions of turbulence and viscosity.

## 6. MISCELLANEOUS APPLICATIONS

In the main these can be summarised as those in which the usual pumping requirement of a reasonable pressure ratio and flow ratio does not apply and thrust augmentation or mixing characteristics become more important.

### 6.1. Thrust augmentation:

#### Marine

For thrust augmentation extreme choices are a conventional screw-driven thruster and a radial-pumpdriven system with a convergent nozzle, but the latter is inefficient owing to the high efflux velocity. Witte shows in reference (256) that combining the low specific speed cargo pumps with a jet pump to produce a high mass flow can result in much more favourable thrust-to-horsepower ratios. As with all jet pump designs, optimum performance is achieved only over a limited range and this paper discusses optimum design presenting the results in dimensionless form. The thrust augments operates, of course, with a zero nett head and experiments reported in this paper give data specifically under this condition; it is significant that thrust augmentation is 10 to 15 per cent higher when the mixing tube is 3.7 diameters long, than for a length of 9 diameters, but the reasons for this are not discussed.

The degree of thrust augmentation reaches about 2.5. Reference (338) describes the theory of and experiments on propulsion devices powered by an annular jet of air.

#### Aircraft

For comprehensive treatment of the thrust-augmentation application the paper by Huang (209) is to be recommended (an extensive bibliography is included). The benefits of using

supersonic primary nozzle have been demonstrated by Deleo et al (132).

Hickman (298) deals with the very high entrainment ratios, 10 to 40, involved in aircraft applications and shows the same order of divergence between theory and experiment as found in other papers on compressible flow ejectors. The longest mixing tube employed in these tests was some 4.5 diameters but this may have been offset by the use of multiple nozzles; the tests do not cover a range sufficiently wide to enable a comparison to be made with the above recommendations (Witte (256)) of a relatively short mixing tube, but it is interesting to note that Drummond (130) shows maximum thrust to occur at a length/width ratio of 6 for a rectangular channel.

Faucher (273) achieved thrust augmentation ratios of 1.8 with a ratio of channel length to minimum width of 5.1 and ascribed this favourable result to improvements in primary flow injection techniques. Jones (376) reinforces this conclusion in a theoretical analysis which shows the important effect of inlet flow distribution. Reference (394) reports that an increase of thrust augmentation of about 20 per cent was produced by pulsating the primary jet and the authors ascribe this increase to a faster mixing. It should be noted that the mixing duct length was only about one duct width.

2nd Symposium on

PAPER A4

# JET PUMPS & EJECTORS and GAS LIFT TECHNIQUES

March 24th-26th, 1975

Held at Churchill College, Cambridge, England.  
Published by BHRA Fluid Engineering,  
Cranfield, Bedford, England.

A4-35

## DIVERSITY OF JET PUMPS AND EJECTOR TECHNIQUES

H. Schmitt,

Bertin & Cie., France

### Summary

The author first reviews the various ejection and compression methods used for extraction, compression and mixing of fluids, propulsion or lifting and so forth. This is followed by a brief discussion of a general method used in designing induction units and the appearance of operating curves, the compression ratio as a function of the ratio of the flows and variations in efficiency. The total efficiency and transfer efficiency characterizing the energy value of the system are defined.

The different techniques used in the design of jet pumps and their performances are listed: standard jet pumps using a single axial nozzle of maximum size; multitube jet pumps; annular and parietal jet pumps; cylindrical or bidimensional units; pulse jet pumps.

Efficiency, dimensions, operating noise and manufacturing cost vary so widely that the choice of a solution depends on technical and economic requirements or requirements specific to each project.



Parameters

$Q'$  ,  $Q''$  ,  $Q$  : driving, induced and total mass flow

$P'$  ,  $P''$  ,  $P$  : absolute head pressure of driving, induced and mixed flows

$p'$  ,  $p''$  ,  $p$  : absolute static pressure of the different flows

$T'$  ,  $T''$  ,  $T$  : total absolute temperature of driving, induced and mixed flows

$t$  : imaginary static temperature

$x$  : mixing ratio =  $-\frac{Q}{Q'}$

$\sigma_C$  : mixing section area ratio =  $-\frac{S_B}{S'}$

$\sigma_D$  : diffuser area ratio =  $-\frac{S_C}{S_B}$

$V'$  ,  $V''$  ,  $V$  : local average velocity of the different flows

$M$  : local Mach number

$C_p$  : constant pressure specific heat

$\gamma$  : constant pressure to constant volume specific heat ratio =  $-\frac{C_p}{C_v}$

$H$  : enthalpy of flow considered =  $C_p T$

$\eta$  : efficiency

$\phi$  : thrust ratio

$R'$  ,  $R''$  : constants of driving and induced flow

1. INTRODUCTION

Jet pumps, in use for many years for a wide variety of tasks, convert fluid energy between two flows. In general, a high-pressure fluid transfers part of its energy to a low-pressure fluid, and the resulting mixture is discharged at a pressure between the driving pressure and induction pressure. This approach is universal and does not depend on the planned application, be it fluid extraction or compression. It works with all fluids, be they gases, liquids, two-phase fluids or fluids carrying matter in suspension.

1.1. Applications

Following is a list of the principal applications.

- 1) Extraction by suction of the induced fluid.
- 2) Compression by compression of the induced fluid discharged at the expansion pressure of the driving fluid.
- 3) Ventilation and air conditioning by extraction and discharge of a mass of gas with small differences in pressure around the atmospheric pressure.
- 4) Propulsion or lifting by intermediate compression of the fluid discharged at a certain adaptation velocity.
- 5) Uniform mixing of two flows to obtain a uniform concentration or temperature or a chemical reaction
- 6) Pneumatic or hydraulic conveyance of products in powder form or fractions.

Various design methods have been developed to calculate the dimensions and performance of a jet pump. In general, all require the use of coefficients of friction and losses arrived at experimentally. Here, we will discuss a parametric design method. It uses a coefficient of total efficiency representative of the losses at the intake, in the mixer and in the diffuser, as a function of jet pump design. It is adapted to gases.

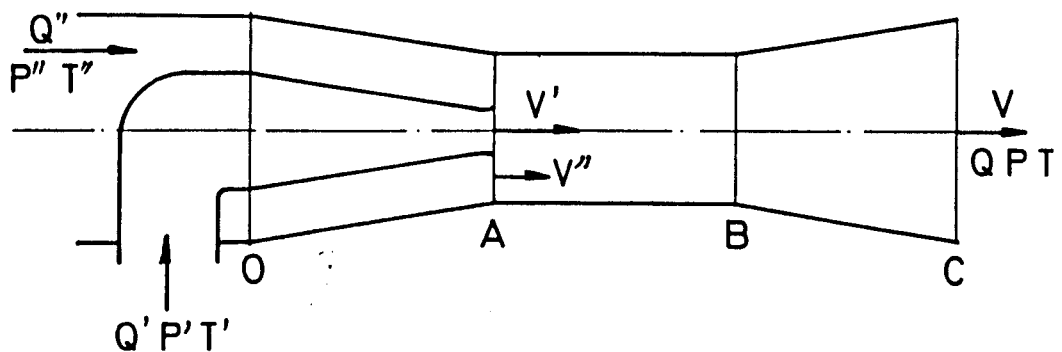
### 2.1. Design

The unit comprises :

- 1) A driving nozzle through which induction flow  $Q'$  travels at total pressure  $P'$  and total temperature  $T'$ .
- 2) A convergent suction duct OA for induced flow  $Q''$  at total pressure  $P''$  and total temperature  $T''$ .
- 3) A mixing section AB, whose section may or may not be constant, where the energy exchange takes place between the two flows.
- 4) Diffuser BC, where the kinetic energy resulting from the mixture is converted into total pressure  $P$ , the mixed flow being at average temperature  $T$ . The mixing ratio is, by definition :

$$x = \frac{Q'' + Q'}{Q'} = \frac{Q}{Q'}$$

Below appears the design of a jet pump.



### 2.2. Operation

The jet pump acts as a sort of venturi tube, in whose narrow section the velocity of the induced flow can be increased to a value close to that of the driving flow. This is favorable for high exchange efficiency between the two flows. The energy in the mixer can exceed the kinetic energy of the driving flow which would expand freely to the total pressure of the induced flow, in such a way that the losses considerably influence the energy efficiency of the unit. It is thus important to minimize losses by friction in the mixing section and conversion losses in the diffuser, both of which are proportional to the square of the velocity.

The change in pressure through the unit generally appears as shown in Figure 1. The pressures do not change across the mixer when mixing is complete, and there is a discontinuity at the inlet of the diffuser.

### 2.3. General calculation of performance

In accordance with the diagram shown above, for the analysis, the functions encountered successively in the unit can be separated into : acceleration of the two flows , their mixing and the decrease in velocity in the diffuser.

The calculation can then be made using the following assumptions :

- 1) The acceleration of the driving flow and induced flow is assumed to occur with no losses or, what amounts to the same thing for the design of the jet pump, the values of the total or generating pressures  $P'$  and  $P''$  are considered in plane A at the outlet of the driving nozzle and inlet of the mixer where the static pressure is assumed to be uniform.
- 2) The mixer is cylindrical and sufficiently long for the exchange of energy to take place in accordance with the theorem of the conservation of momentum which can be applied although the actual change in pressure along the walls of the mixer is unknown. A uniform mixture is assumed to exist at the end of the mixer.
- 3) Since the dimensions of the mixer do not enter into the calculation, friction losses in the mixer cannot be determined. An equivalent diffuser efficiency is used, including the losses undergone by the flow in these two successive elements. This is justified by the fact these losses are of the same shape and basically proportional to the square of the velocity, diffuser losses generally far exceeding mixer losses.

#### 2.3.1. Equations

The following equations are considered between planes A and B :

- Conservation of flow :

$$Q = Q' + Q''$$

- Conservation of momentum :

$$(p'S' + Q'V')_A + (p''S'' + Q''S'')_A = (pS + QV)_B +$$

$$\left[ \int_A^B p dS + \text{friction along mixer} \right]$$

(the two last terms are eliminated on the basis of assumptions 2 and 3)

- Equilibrium of static pressures at A :

$$p'_A = p''_A$$

- Conservation of energy (no exchange of work or heat with the outside) :

$$QC_p T' + Q''C_p T'' = QC_p T$$

- Relationship between the thermal capacities (permitting calculation of the final temperature of the mixture) :

$$C_p' Q' + C_p'' Q'' = C_p Q$$

- Equation of states :  $p = \rho R t$

The different operating parameters,  $P'$  and  $P''$ ,  $T'$  and  $T''$ ,  $M'$  (Mach number of induced flow), can be set, leading to  $p_A$ ,  $V'$  and  $V''$ ,  $Q'$  and  $Q''$  for a unit value  $S'$  of the driving section and a specific ratio

$$\frac{S''}{S'} = \sigma_C$$

Resolution of the system of equations permits calculation of the total pressure and velocity at B at the outlet of the mixer. The discharge pressure is then calculated for different efficiency figures of diffuser BC.

As was said earlier, the efficiency of the equivalent diffuser includes the losses in the mixer and diffuser, which depend on the profile of the velocities at inlet B, the aperture and the ratio of the sections

$$\sigma_D = \frac{S_C}{S_B}$$

Thus, varying jet pump geometries will give results which vary widely as a function of this efficiency whose influence is preponderant, especially in the case of jet pumps with short mixers.

### 2.3.3. Operating characteristics

#### 2.3.3.1. Efficiency

The efficiency of a jet pump can be expressed by the total efficiency  $\eta_G$  defined as follows :

$$\eta_G = \frac{\text{Mechanical energy available from total flow}}{\text{Mechanical energy available from driving flow}}$$

This efficiency permits easily comparing the various jet pump designs.

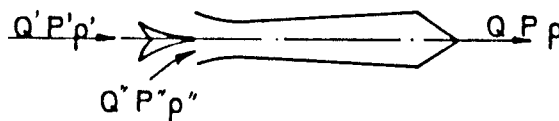
The transfer efficiency is defined in a comparable manner as the ratio  $\eta_T$  such that :

$$\eta_T = \frac{\text{Mechanical energy available from induced flow}}{\text{Mechanical energy available from driving flow}}$$

The energy terms are equal to the power of a turbine with an efficiency of 1 through which travels the flow considered between the extreme pressures.

These two expressions for efficiency are interrelated and can be written as follows :

#### 1) Incompressible flow (gases or liquids)



$$\eta_G = \frac{Q}{Q'} \frac{\rho'}{\rho} \frac{(P - P'')}{(P' - P'')} = x \frac{\rho'}{\rho} \frac{(P - P'')}{(P' - P'')}$$

$$\eta_T = \frac{Q''}{Q'} \frac{\rho'}{\rho''} \frac{(P - P'')}{(P' - P)} = (x - 1) \frac{\rho'}{\rho''} \frac{P - P''}{P' - P}$$

2) Compressible flow (gases and steam)

In this case a comparison is made of the energies equal to the drop in usable enthalpy between the pressures to be considered. Let  $H$  be the enthalpy and  $\Delta H$  its variation between two levels of pressure ; we then have :

$$\eta_G = \frac{Q \Delta H' \frac{P}{P'}}{Q' \Delta H' \frac{P}{P'}} = x \frac{\Delta H'_G}{\Delta H'_T}$$

and

$$\eta_T = \frac{Q' \Delta H' \frac{P}{P'}}{Q' \Delta H' \frac{P}{P}} = (x - 1) \frac{\Delta H'_G}{\Delta H'_T}$$

Figure 2 shows the variations in these two efficiencies for the same type of jet pump. These are envelopes for units adapted for each mixing ratio, and a particular jet pump will have an efficiency curve as shown by the dotted line.

Figure 3 shows the variations in efficiency as a function of the mixing ratio and for different ratios of generating pressures  $\eta' = \frac{P}{P'}$ . When diffuser efficiency  $\eta_D$  is high, there is a significant decrease in total efficiency when the ratio of pressures increases. However, in actual jet pumps where the efficiency of the equivalent diffuser varies between 0.3 or 0.4 and 0.7 in the best of cases, the envelope for the total efficiency of a given jet pump design is only slightly influenced by the ratio of pressure '. This greatly facilitates comparisons between various techniques.

2.3.3.2. Thrust ratio

In the design of propulsion and lifting jet pumps, the maximum ratio is sought between the momentum  $QV$  of the mixed flow and the momentum of the driving flow  $Q'V'_{th}$  which expands freely in the atmosphere.

If  $\phi$  is the thrust ratio, we have :

$$\phi = \frac{QV}{Q'V'_{th}}$$

$$\text{and } \phi^2 = \frac{Q^2 V^2}{Q'^2 V'^2_{th}} \quad \text{with } \frac{Q}{Q'} = x \quad \text{and} \quad \frac{QV^2}{Q'V'^2_{th}} = \eta_G$$

we thus have :

$$\phi^2 = \eta_G x, \quad \eta_G = \frac{\phi^2}{x} \quad \text{and} \quad \phi = \sqrt{\eta_G x}$$

These are the basic equations demonstrated by Jean BERTIN in 1955.

They show that the thrust ratio of a jet pump is in no way limited to unity and that it depends greatly on the internal efficiency of the unit. Figure 4 shows the appearance of the variations.

The pressure characteristics of a jet pump can be shown as a function of the flow using reduced coordinates. The flow is shown by the mixing ratio

$$x = 1 + \frac{Q'}{Q''} \sqrt{\frac{T''}{T'}} \sqrt{\frac{R''}{R'} \frac{Y'}{Y''}} \quad \text{expressing the influence}$$

of gases of different types on the two flows.

The effective compression  $P - P''$  is referred to overpressure  $P' - P''$  or  $P' - P$  respectively for compression and extraction units.

Figure 5 shows the characteristic curves of jet pumps used, for example, in exhausting fumes under incompressible flow conditions. The dotted line represents the case of a particular jet pump with its point of adaptation at A.

### 3. JET PUMP TECHNIQUES

The standard jet pump uses an axial nozzle, a generally cylindrical mixer and a divergent diffuser with a small angle (7 to 8 degrees). This is the simplest design, but one having the largest dimensions and poorest performance.

Thus, different techniques should be examined to improve the efficiency and compactness. Following are the major techniques listed in order of increasing performance (see figure 6).

#### 3.1. Standard jet pumps already mentioned.

#### 3.2. Jet pumps with parietal injection of the driving fluid by an annular slot at the inlet of the mixer are well suited to the pneumatic conveyance of products or the extraction and cooling of hot gases.

#### 3.3. Multitube and bidimensional jet pumps

Multitube cylindrical jet pumps can comprise three, seven, nine, 19, 37 and so forth driving nozzles. The nozzles are generally placed at the corners of a grid of equilateral triangles. Performance increases with the number of injectors. However, there are often practical limits to the increase in the number of injectors. These jet pumps are used for numerous applications, from the extraction of fumes to the filling of flexible envelopes and compression and mixing in crackers.

Bidimensional jet pumps comprise slots or injector lines. Their performance can be of the order of these of cylindrical jet pumps with equivalent space distribution of the injectors in the inlet of the mixer. They are widely used for air conditioning and in aeronautical applications for lift and propulsion (thrust augmenter and augmentor wing). In the latter case, compact ejectors are used with a diffuser, and related losses, very limited.

#### 3.4. Annular jet pumps with thin divergent flow whose performance is comparable to that of jet pumps with seven or nine divergent injectors. Divergence of the driving fluid flow is used to control the distribution of the velocities at the inlet of the diffuser and sizably increase the latter's efficiency.

#### 3.5. Jet pumps with several annular flows, concentric and divergent,

whose compactness and performance with a diffuser are the best for jet pumps handling uninterrupted flows. These are used for lift applications in aeronautics and can supply thrust ratios greater than 2 for mixing ratios of the order of 10.

- 3.6. Pulse jet pumps, whose driving flow comprises successive "bursts" or "blasts" of gases sucking in waves of induced air. Efficiency can be very high (of the order of 60 to 80 % in pulse jets with no moving parts). These jet pumps were widely used in steam engines (Kythapp exhaust) where, in fact, a source of pulsed driving gas was available. Their performance is thus very interesting, but the operating noise of these jet pumps is a major handicap to their development.

Figure 6 represents the design and relative dimensions of the various jet pump techniques discussed above. We can see that jet pumps with control of the distribution of the velocities at the diffuser inlet permit higher velocities at the inlet of the mixer whose diameter is smallest. In addition, jet pumps with multiple injectors will have a shorter mixing length. This permits designing more compact units. The mixing length is reduced approximately in the ratio of the square root of the equivalent number of injectors whose section is equal to that of a single driving nozzle.

Figure 7 shows the comparative change in the efficiency of the various jet pump techniques considered. We can see that the interest of sophisticated designs grows with the mixing ratio.

Standard jet pumps, having the poorest performance, cover a vast domain according to their manufacturers.

They are followed by parietal jet pumps and then multitube, bidimensional, compact and annular jet pumps with diffusers whose performance is rather similar.

Jet pumps with three annular, divergent nozzles have given the best performance up to now for high mixing ratios, from 8 to 12. Two remarkable applications use thrust augmentser jet pumps and pulse jets, units having little if any diffuser and thus not subject to the high losses associated with this element. In the case of jet engines, this high performance permits the use of noise-absorbent packing whose additional friction losses remain acceptable.

- 3.7. From these comparisons, due to its simplicity and low manufacturing cost the standard jet pump can be seen to be best suited for virtually all applications with a low induction or mixing ratio. However, its performance decreases rapidly with the mixing ratio while its size and operating noise are the greatest (single nozzle with the highest consumption).

For intermediate mixing ratios, with values of  $x$  of 3 to 6 or 8, we have multinozzle cylindrical or bidimensional and simple annular designs whose performance, compactness and operating noise are greatly improved with respect to the standard design.

Lastly, for high-power, high-flow industrial applications, despite the higher cost it is very worthwhile using jet pumps with multiple annular, divergent nozzle whose operating noise, in addition, is relatively low (lowest driving flow off all designs and minimum equivalent hydraulic diameter). For aeronautical applications and low-speed lift devices, these units can give thrust ratios exceeding 2 with mixing ratios of 10 to 12.

For very high mixing ratios, units with two or three stages

should be used. Their efficiency is superior to that of a single-stage unit. This is primarily due to the small size of the diffuser used with each stage, with a limited mixing ratio.

#### 4. CONCLUSION

We hope this brief discussion has clearly demonstrated the variety of jet pump designs available today. Lengthy experience permits rather good prediction of the performance of units with long mixers. However, the problems are more complicated for short and asymmetrical mixers and diffusers. Nonetheless, the potential performance combined with the simplicity and reliability of these units having no moving parts make them very attractive for many applications. As concerns the environment, modern sound-proofing techniques can virtually always provide a solution to individual problems. Given these conditions, it is almost always possible to solve an ejector problem knowing all its technical and economic aspects.

#### REFERENCES

- 1) MORRISON R. "Jet ejectors and augmentation". Report R 74. United Aircraft Corporation, Research Division, East Hartford, Connecticut, October 1941.
- 2) ROY M. "About rough theory of gas jet-pumps". (Sur la théorie sommaire des trompes à gaz). Bulletin du Groupement Français pour le Développement de Recherches Aéronautiques, n°2, 1946, pp 21-32 (in French).
- 3) Mc CLINTOCK, F.A. and HOOD J.H. "Aircraft Ejector Performance" Journal of the Aeronautical Sciences. Vol. 13, Nb 11, November 1946 pp 559-568.
- 4) KASTNER L.J. and SPOONER J.R. "An Investigation of the performance and design of the air-ejector employing low-pressure air as the driving fluid". Proceedings. Proc. of the Institution of mechanical Engineers, Vol.162, 1950, pp 149-166.
- 5) BERTIN J. "Pulsatory mixing on jets" (Dilution pulsatoire sur réacteur) C.R. Academy of Sciences, PARIS, 1955, p. 1859 (in French).
- 6) LE GRIVES E., FABRI J. and PAULON J. "Diagrams for supersonic ejectors computation" (Diagrammes pour le calcul des éjecteurs supersoniques) Technical Note n° 36, ONERA Paris, France, 1956 (in French).
- 7) BERTIN J. and LE NABOUR M. "Contribution to jet-pumps and ejectors development" (Contribution au développement des trompes et éjecteurs). Technique et Sciences Aéronautiques, T.3 - May-June 1959 pp 127-138 (in French).
- 8) BERTIN J. "Jet pumps applied to vertical flight, towards jet-wing" (Les trompes appliquées au vol vertical, vers l'aile trompe). Technique et Sciences Aéronautiques, T.2, 1960 (in French).
- 9) POLNIKOSKII V.J., PERELMAN R.G. and IVANOV I.A. "Compact ejector design" (Etude d'un éjecteur d'encombrement réduit). Industries et Thermique, n° 7, 1960 (in French).
- 10) SCHMITT H. "Recent developments of jet pumps applied to gas industries" (Développements récents des trompes à induction applicables aux industries gazières). Gaz d'Aujourd'hui, n° 4, April 1974. (in French).



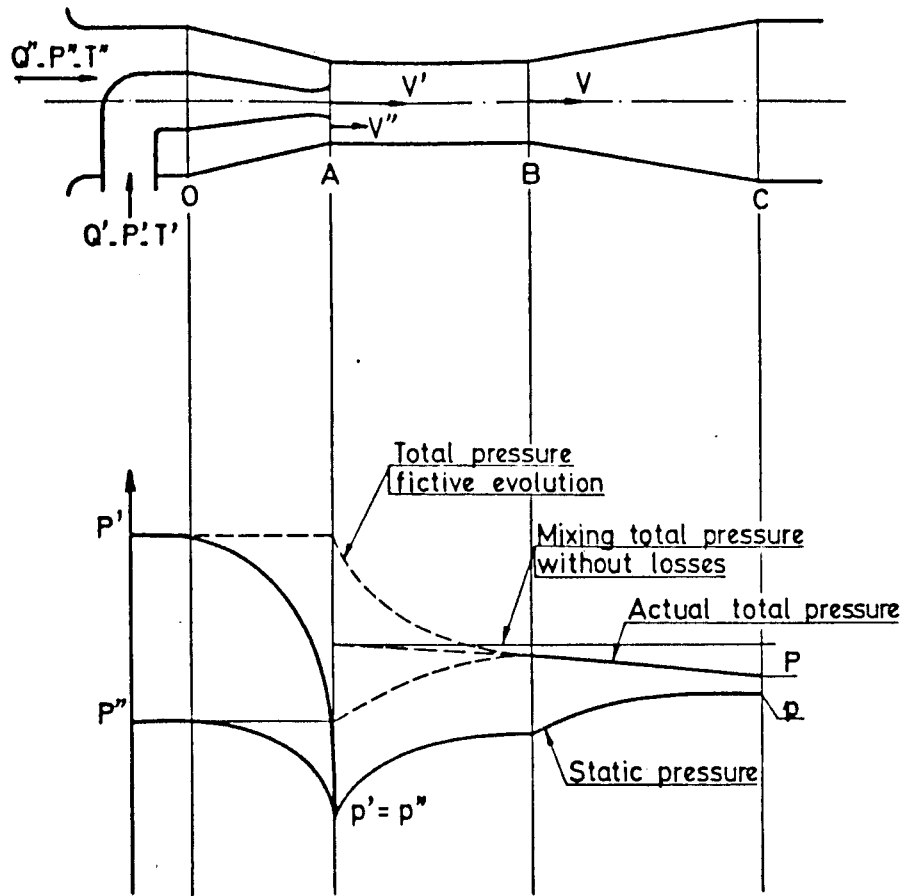


Fig.1 Pressure variations along a jet-pump

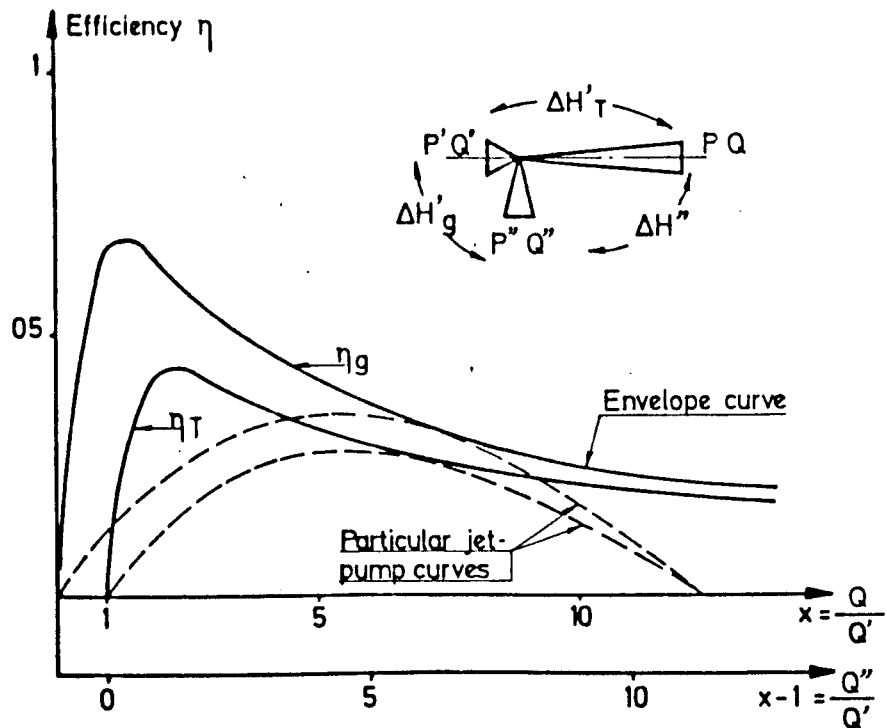


Fig.2 Efficiencies compared evolution versus mixing ratio for a given jet pump technology

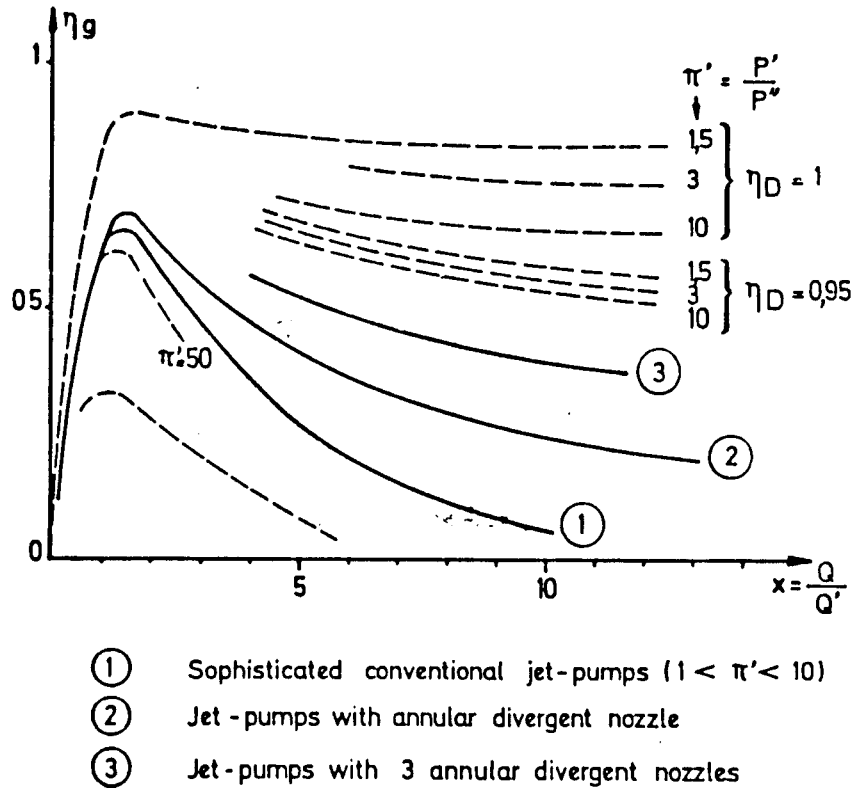


Fig.3 Compared variations of global efficiency function of driving pressure and mixing ratios

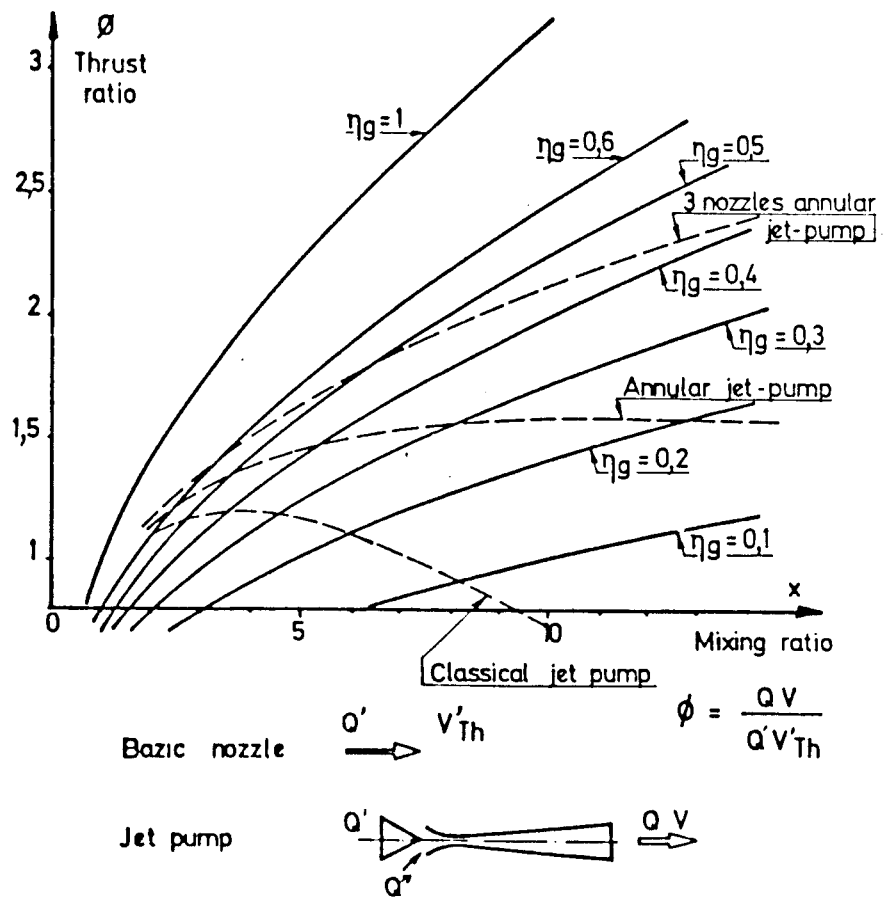


Fig.4 Thrust augmentation variations versus mixing ratio

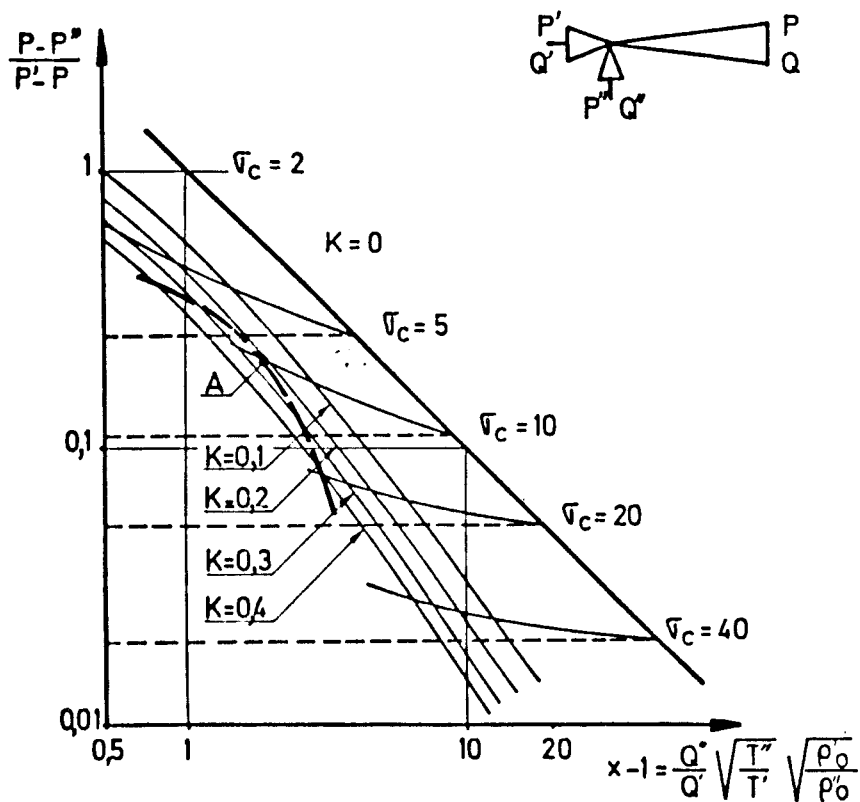


Fig.5 Characteristic pressure ratio for jet-pumps in incompressible flow

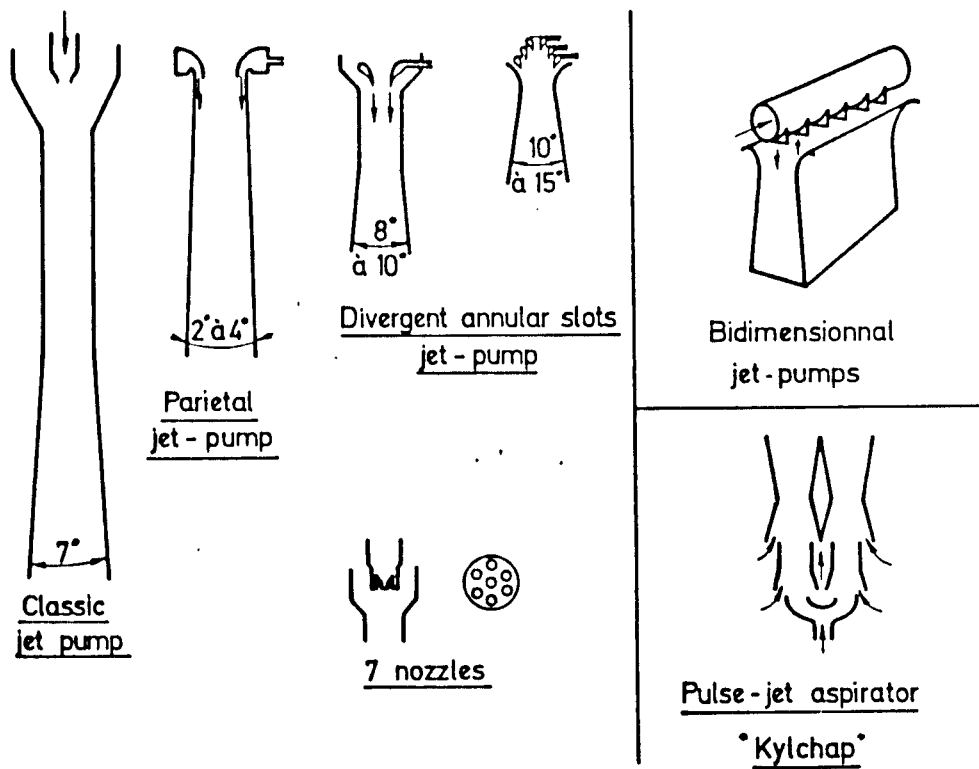


Fig.6 Various jet-pump schemes

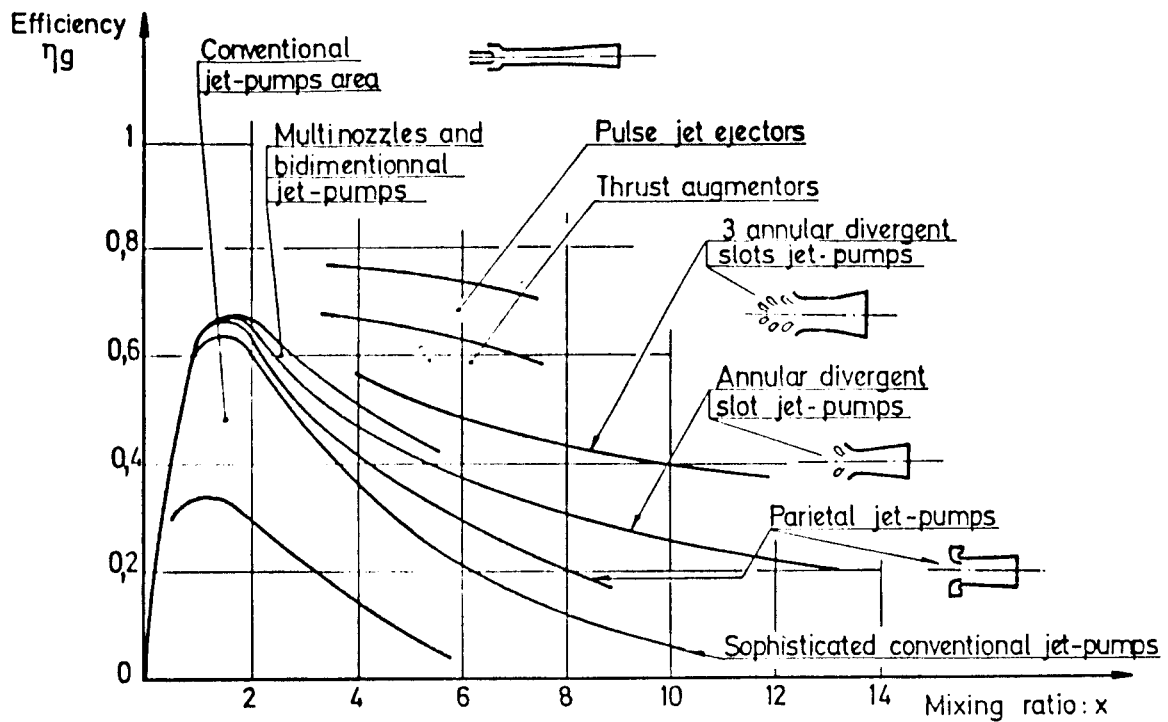
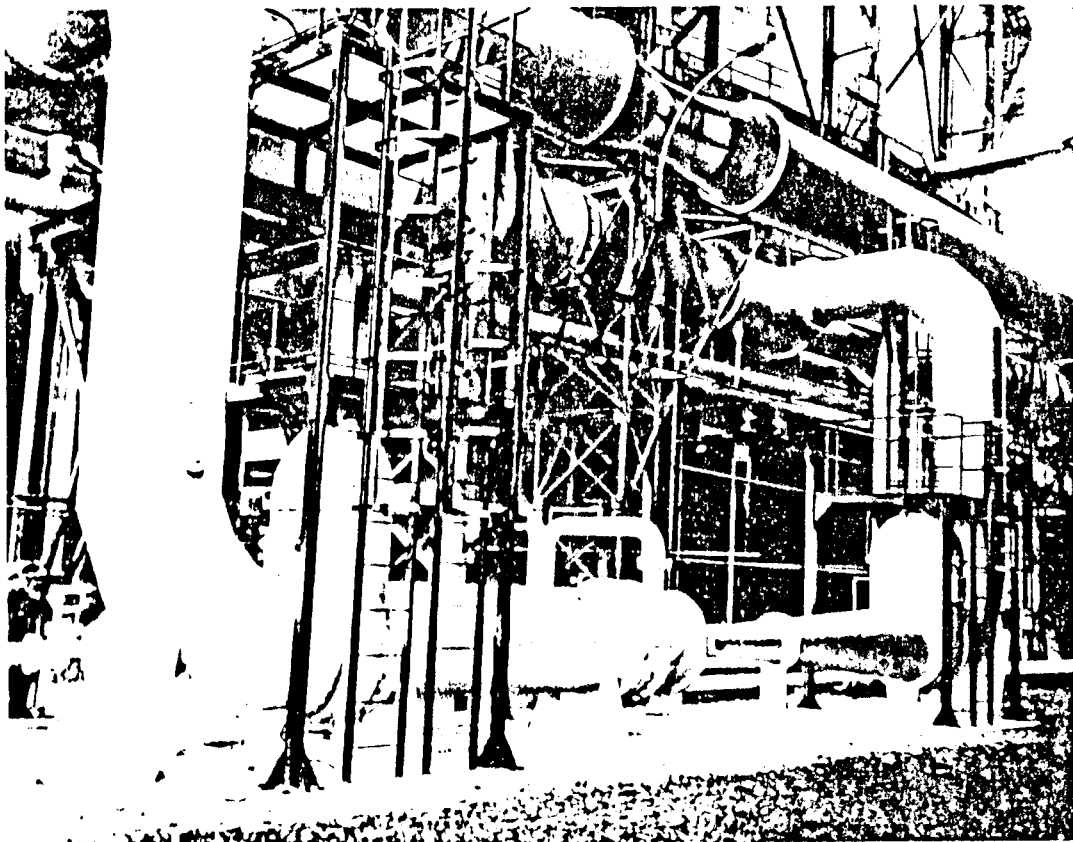
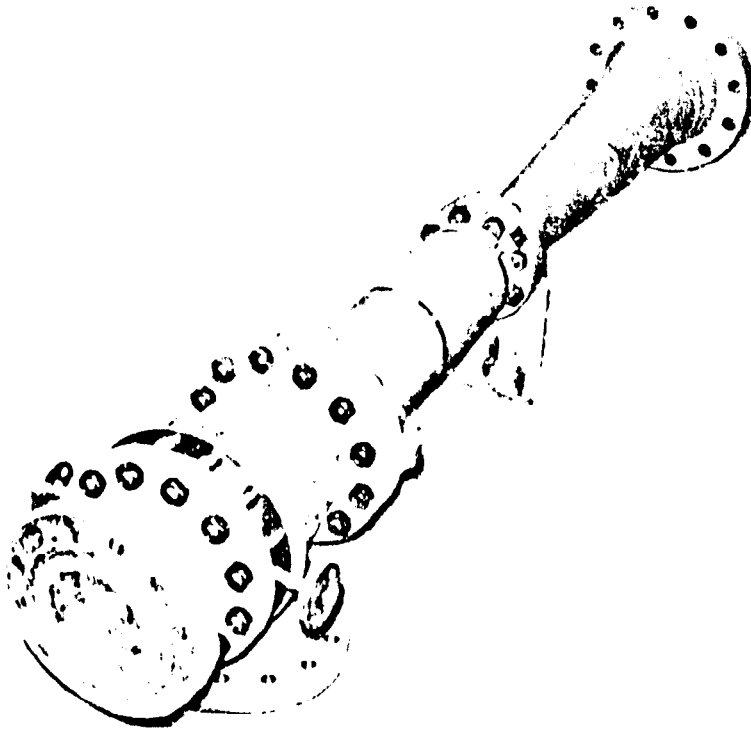


Fig.7 Global efficiency typical evolution for different jet pump designs function of mixing ratio



Three annular divergent nozzles for manufactured gas compression - 8155  
 Driving natural gas - 12 bars - 27500 St m<sup>3</sup>/h  
 Induced manufactured gas - p atm - 82500 St m<sup>3</sup>/h  
 Mixed gas - 1,29 p atm - 110000 St m<sup>3</sup>/h

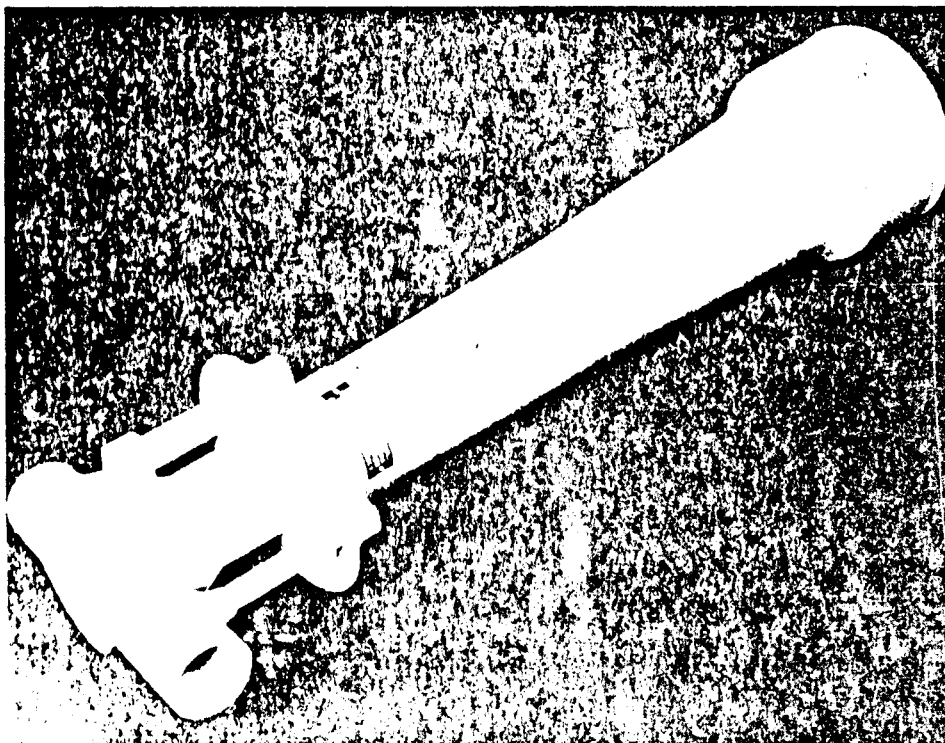


Classical jet pump for gas compression and calorific potential adjustment - 8<sup>A</sup>138

Driving natural gas - 60 bars - 90000 St m<sup>3</sup>/h

Induced manufactured gas - 15 bars - 12500 St m<sup>3</sup>/h

Mixed gas - 30 bars - 102500 St m<sup>3</sup>/h



Multinozzle (7) aspirator for rescue slides inflation - 18906

Variable mixing ratio from 12 at beginning to 3 or 4 at the end of pressurization is obtained with a variable pressure-expansion valve

Dictionaries: General Computing Medical Legal Encyclopedia

Kylchap

Word: Kylchap

Word

Look it up

Sponsored links:

**Aster Live Steam Engines**  
1:32 Scale steam locomotives  
Museum quality, limited editions.

**N Scale Community**  
Become a member of Nscale  
Community Help, Pics, Forum,  
DCC, Download

**Steam Engine**  
Yahoo! Shopping: Compare &  
Save Top brands, great stores,  
low price

**RailDriver Cyclopedias**  
RailDriver offers train cyclopedias  
with high res printable graphics

Ads by Goog

The **Kylchap** steam locomotive exhaust system was designed and patented by the famous French steam engineer André Chapelon, using a second-stage nozzle designed by the Finnish engineer Kylälä and known as the *Kylälä spreader*, thus the name KylChap for this design.

The Kylchap exhaust consists of four stacked nozzles, the first exhaust nozzle (UK: blastpipe) blowing exhaust steam only and known as the primary nozzle, this being a Chapelon design using four triangular jets. This exhausts into the second stage, the Kylälä spreader, which mixes the exhaust steam with some of the smokebox gases; this then exhausts into a third stage, designed by Chapelon, that mixes the resulting steam/smokebox gases mixture with yet more smokebox gases. The four nozzles of this then exhaust into the fourth stage, the classic *stack* (UK: chimney) bell-mouth.

It was Chapelon's theory that such a multi-stage mixing and suction arrangement would be more efficient than the single stage arrangement hitherto popular in steam locomotive draughting, where an exhaust nozzle simply is fired up the middle of the stack bell-mouth. It would also ensure a more even flow through all the firetubes, rather than concentrating the suction on one area.

The efficiency of the Kylchap system relied on careful proportioning of its components, and perfect alignment and concentricity.

Kylchap exhausts are found on many French locomotives and also on a number of British ones. Sir Nigel Gresley of the LNER was a proponent, and the Kylchap exhaust was fitted to a number of his big Pacifics, including the famous *Flying Scotsman* and the world record holding *Mallard*. Later LNER Thompson and Peppercorn designed Pacifics also had them, including preserved Peppercorn A2 Blue Peter, as will the recreated Peppercorn A1 Tornado. The last steam express passenger locomotive built in Britain, *Duke of Gloucester*, was not fitted with a Kylchap exhaust in service, but one was fitted in preservation when it was realized that poor draughting was one of the biggest reasons behind its poor performance in its service days.

Kylchap exhausts were also fitted to some British-built export locomotives, primarily Garratts for Africa, but the only other nation to take them up in quantity was *Czechoslovakia*, where they seem to have been quite common.

The Kylchap wasn't the only advanced steam locomotive exhaust: another French design, the Lemaître, had some success in France and England; noted Argentinian engineer L.D. Porta has designed several, the Kylpor, Lempor and Lemprex designs; and several US railroads including the Norfolk & Western used a concentric nozzle known as the *waffle iron exhaust*.

References

- http://www.chapelon.net/

Some articles mentioning "Kylchap":

A4 (disambiguation)	Electric locomotive	LNER A4 class 4468	Mallard (locomotive)	Steam locomotive
A4 Pacific	List of locomotives	Mallard	Mallard (train)	Steam locomotives

- Basically, it is made by stacking of four different nozzles, the first one blowing exhaust steam only and called "*primary nozzle*", a Chapelon designed item of a very particular shape generating as few as possible back pressure dividing the steam flow into four jets, followed by a Kylälä designed nozzle in which a first steam/combustion gases mix occurs, followed by another Chapelon designed nozzle where a second combustion gases suction/mix process occurs, followed by a "classical" chimney bell type of nozzle, forming the last suction and mixing point.

The image contains three technical drawings of a mechanical component, likely a turbine or pump housing, with various dimensions and labels.

- Top View (Left):** A side view of the component. It shows a central vertical axis with a horizontal base. Dimensions include a total width of 356, a base width of 380, and a height of 475. Labels A, B, C, D, and E are placed at different points on the component.
- Top View (Right):** A front view of the component. It shows a trapezoidal shape with a central vertical axis. Dimensions include a top width of 296, a base width of 390, a height of 320, and a depth of 475. Labels A, B, C, D, and E are placed at different points on the component.
- Bottom View (Left):** A perspective view of the component. It shows a cylindrical body with a flange at the bottom. Labels A, B, C, D, and E are placed at different points on the component. The text "Soudure autogène" (autogenous welding) is repeated four times, indicating the welding process used for the joints.
- Bottom View (Right):** A top view of the component. It shows a circular cross-section with a central vertical axis. Dimensions include a diameter of 130, a radius of 65, and a depth of 475. Labels A, B, C, D, and E are placed at different points on the component.

Here you may immediately perceive one of the basic ideas of Chapelon about efficient blasting systems that is the necessity of multiples suction points and/or the necessity of a progressive, multi-points mixing of fluids (have a look at a drawing of a good injector), here we have 3 different suction points conveniently well vertically spaced in front of the tubes plate. The version shown

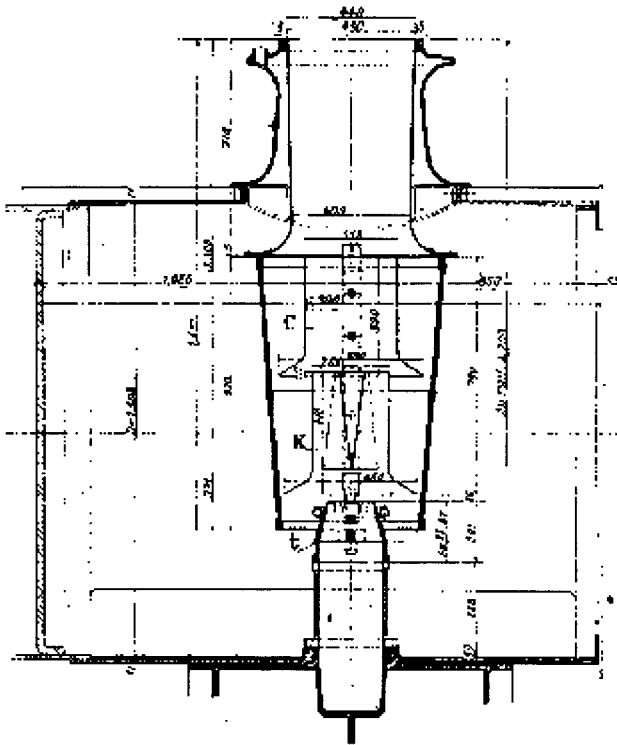


Fig. 116. — Échappement Kylehap type 1 K/1 C des locomotives 5 600 du P.-O.

here is the final one, called *1K/1C* used in single, dual (called *1K/1C-1K/1C* and not *2K/2C* as often read) or triple (*242 A 1*) paralleled configurations according to the capacity and to the quantity of steam to be produced by the boiler. Relative positions and proportions of the various nozzles, independently of general dimensions, proven to be absolutely critical parameters to obtain an efficient *KylChap*, as are their perfect concentricity and alignment (precision for "would be" *KylChap* modellers). Also note the four vital blades in the topmost *Chapelon* nozzle.

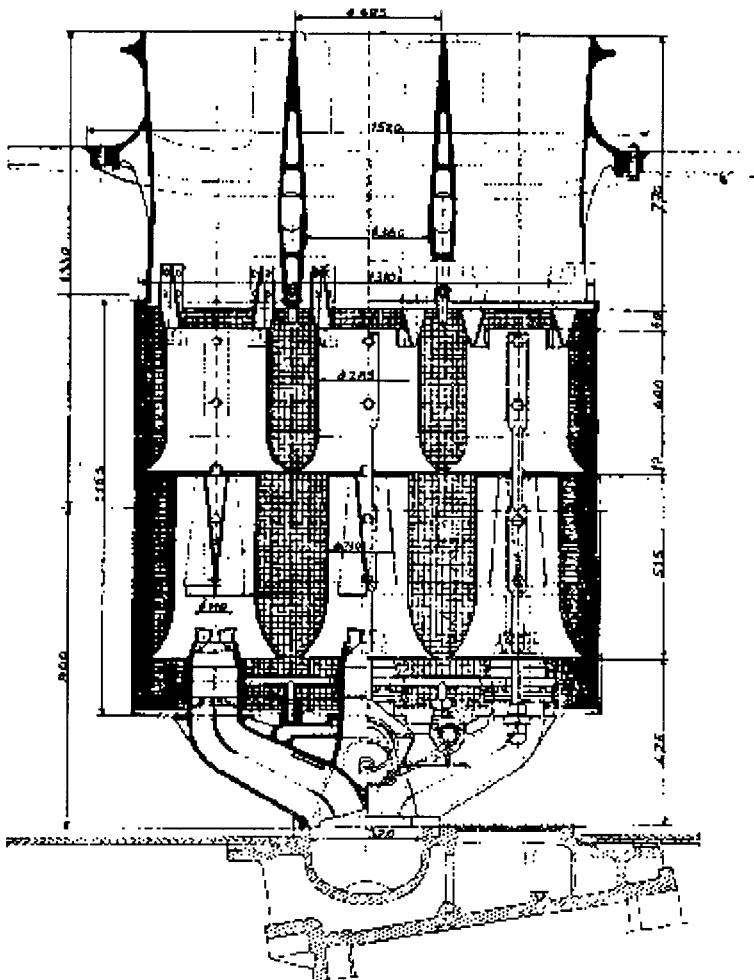
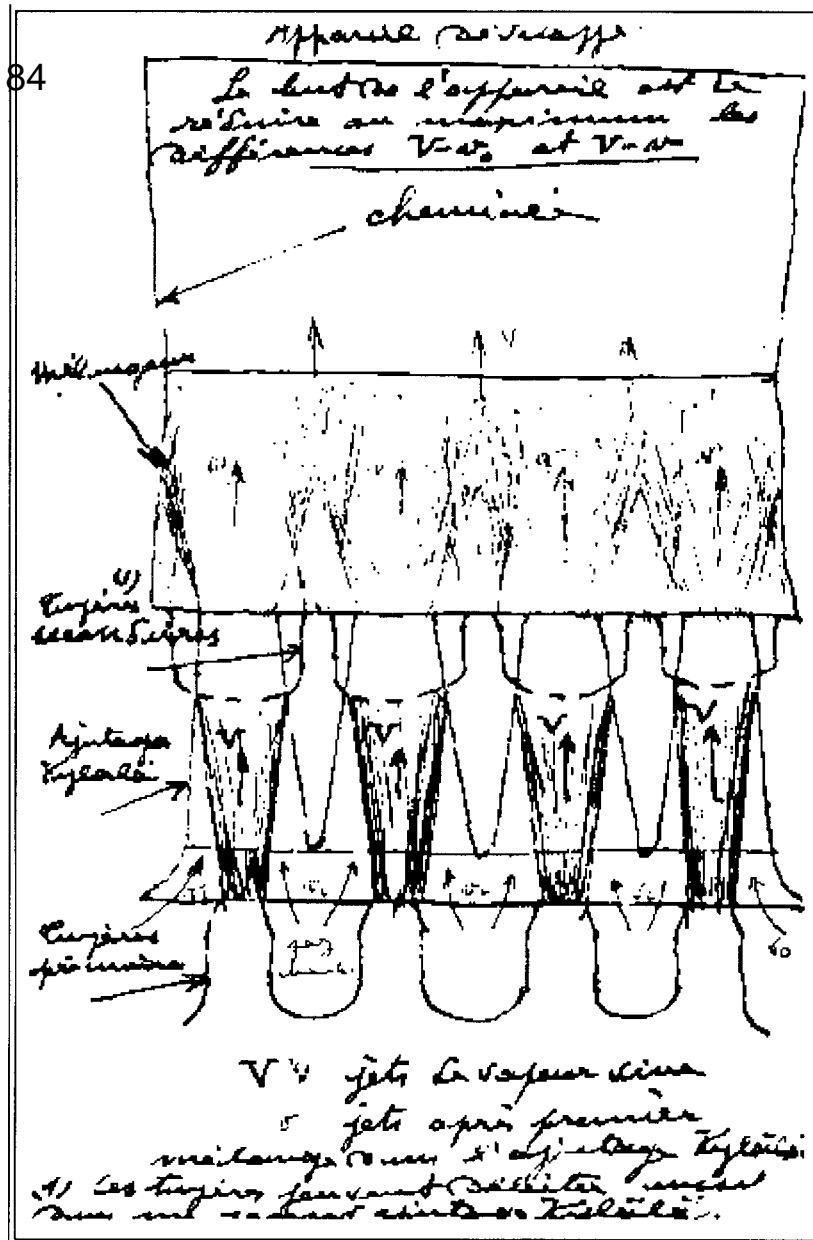


Fig. 123. — Echappement Kylechap triple de la locomotive transformée 242 A 1 de la région Ouest.

The triple KylChap of 242 A 1

The three basics paralleled KylChaps shown here being cut along three different vertical axis, most details are visible...





A very rarely shown drawing:

### The "Super KylChap"

Fully annotated sketch by the hand of the master, unique opportunity to improve your technical french! But I can also help you a bit saying that *Tuyère(s)*=*Ajutage(s)*= nozzle(s)...

*Mélange gazeux*= gases mix.

Explanation of improvements awaited by Chapelon with this design is also on hand, currently under translation. Will come.

Briefly, the major difference, not very visible on this sketch is the addition of a second Kylälä nozzle above the Chapelon tuyère resulting in a fourth suction/mixing point.

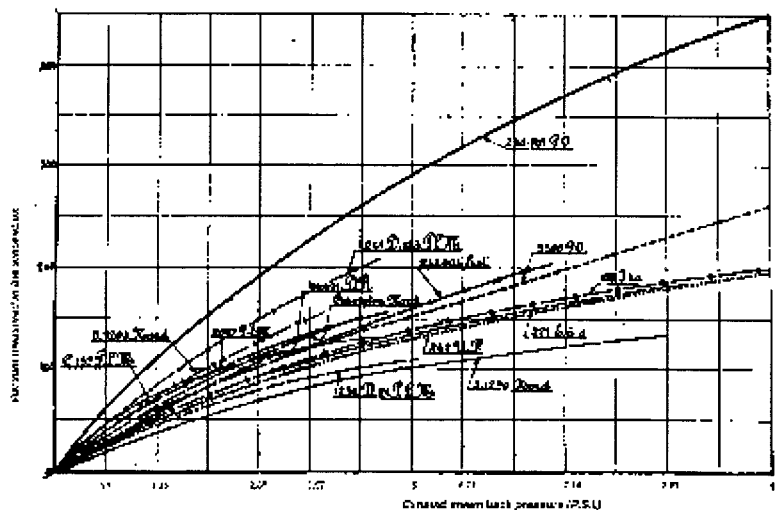
Chapelon never tried to experiment with it, saying "... Difficulties to gain agreements to give solid form to highly valuable projects are already so hard, I don't want to fight again for such a minor idea."

- Comparison of the KylChap with almost every other existing systems. You will even find graphs concerning some major foreign locomotives, U.S. and others. At least one curve concerning the LEMAITRE blasting device, used as the basis of the LEMPOR system, I'll someday add a few lines about the latest... Vacuum figures are not converted, because I really don't know what is the most used unit internationally. A brief mail about it will be welcome! A part of the text has yet to be translated. Of course, click on the sheet for a large readable version.

- 240.701 Chapelon 4 8 0, P.O. RailRoad (1932). - Dual Kylchap.
- 241 D. 133 4 8 2 P.L.M. RailRoad (1942). - Dual P.-L.-M. RailRoad's blasting system (1 nozzle containing 4 blades of rectangular section in a cross arrangement), in French "*à croisillon*".
- 241.004 Est (1937, see photo gallery). Est RailRoad's six jets (or lobes) said of clover type

(and shape) blasting.

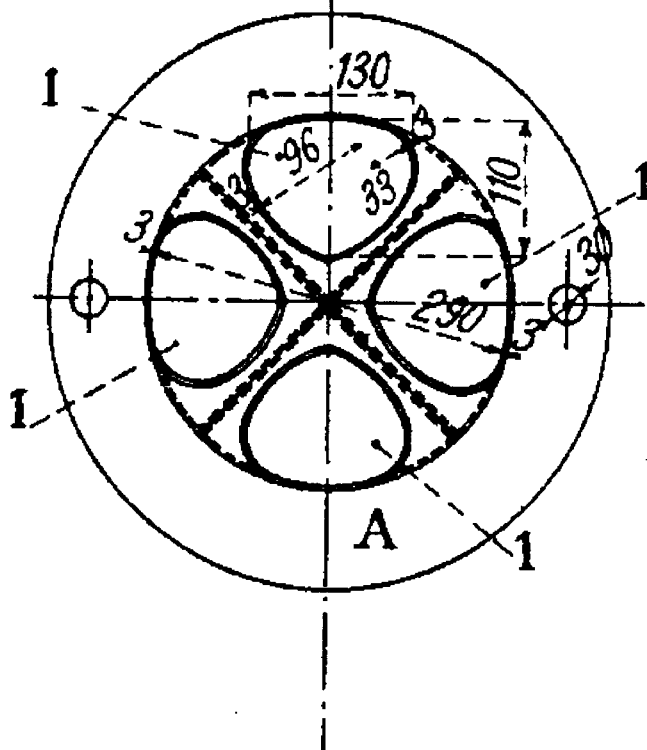
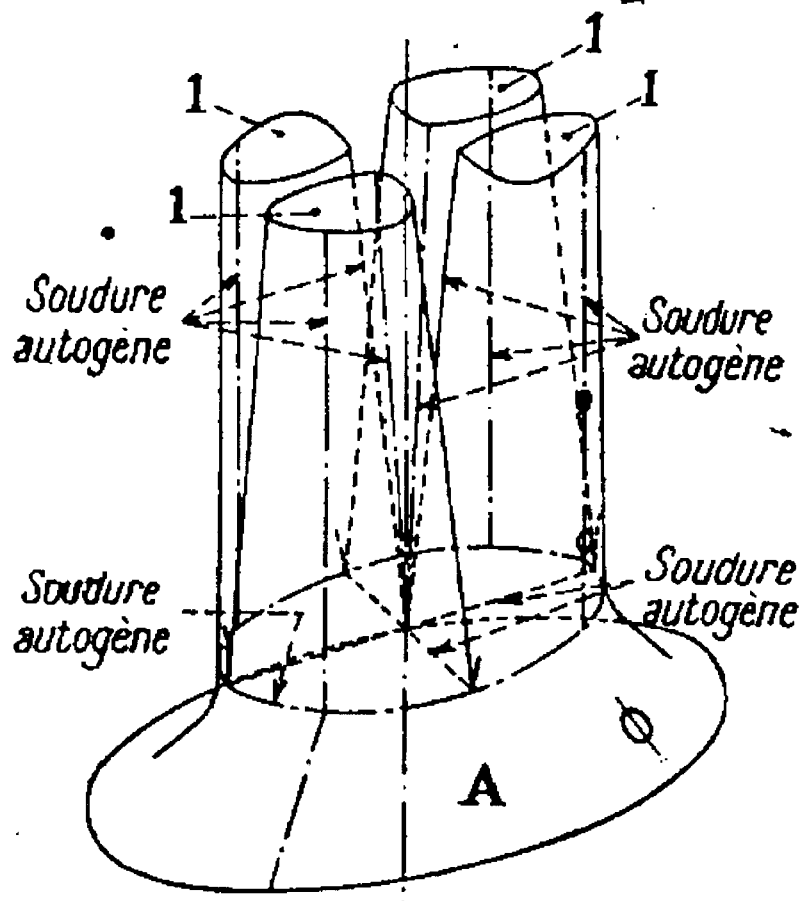
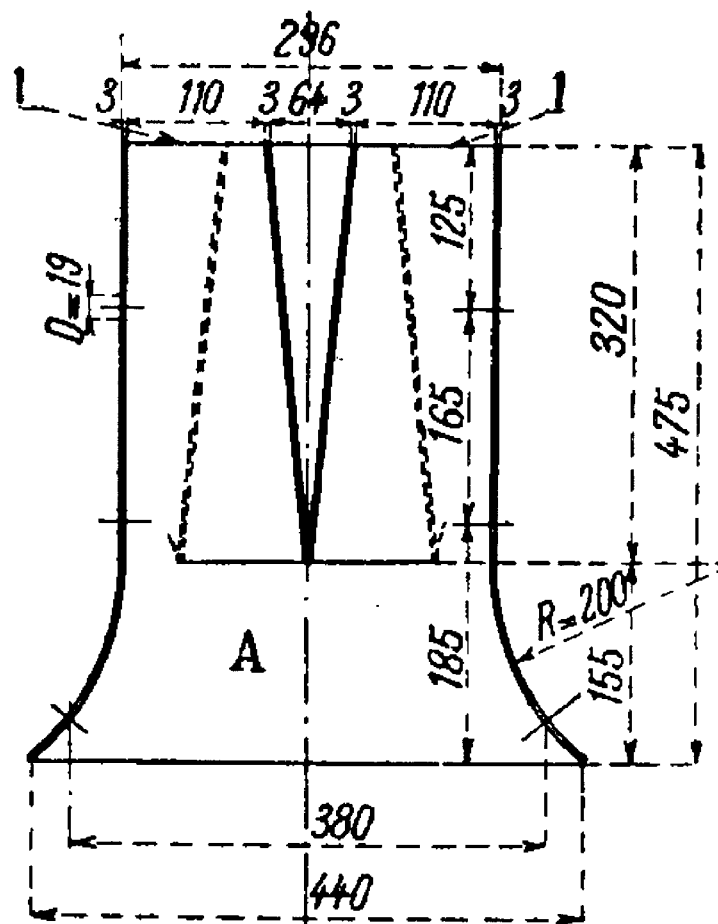
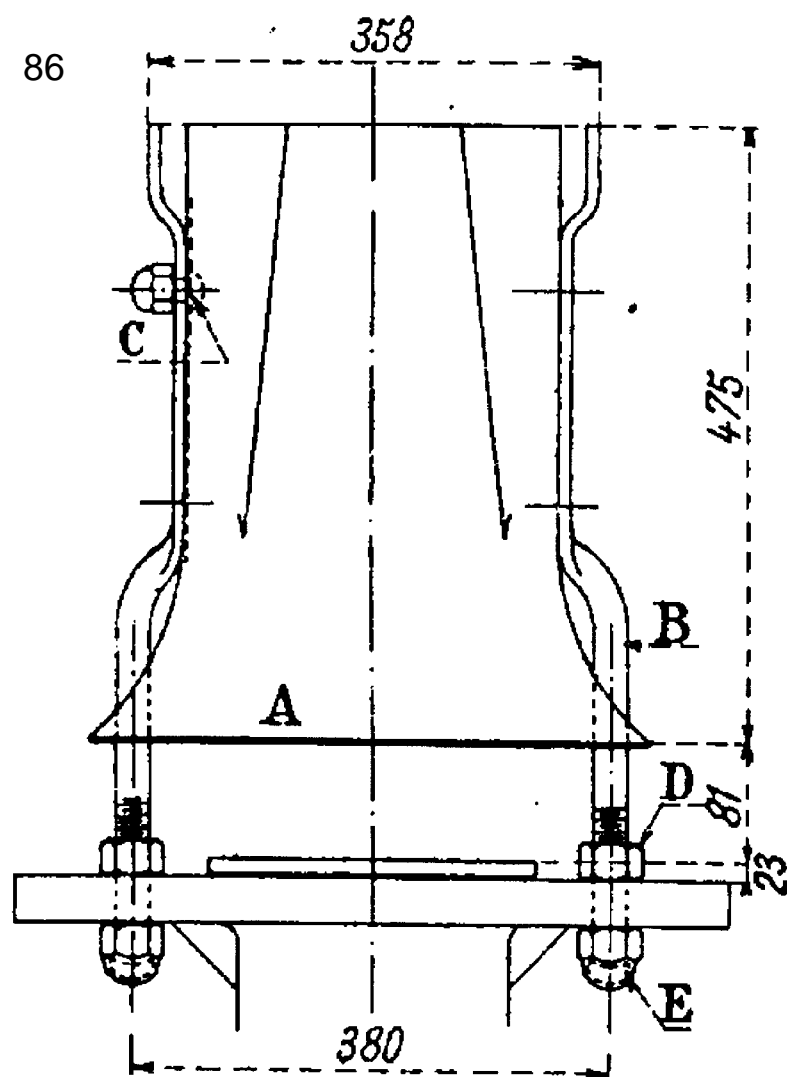
- 3.500 P.-O. RailRoad's PACIFIC (1932).  
Marcaut's clover type & shape (3 lobes) blasting.
- 5.1203, Nord RailRoad's DECAPOD (1939).  
Lemaître's blasting.
- Loc,omotive 2687 P.-L.-M. (1909). - Nord's blasting.
- Locomotive Crampton Nord (1859).- Double valve blasting.
- Locomotive C 139 P.-L.-M. (1910).  
Échappement à double valve à noyau central.
- Locomotive 01.021 de la Reichsbahn (1921). -  
Échappement circulaire fixe.
- Locomotive 150.11.s du Pennsylvania (1923). -  
Échappement fixe à amorce de barrettes.
- Locomotive 221 E. 6.8 du Pennsylvania (1912).  
-Échappement circulaire fixe.
- Locomotive 242 de l'Union Pacific (1938). -  
Échappement fixe à quatre tuyères.
- Locomotive 231. D. 21 P.-L.-M. (1922). -  
Échappement à trèfle P.-L.-M.
- Locomotive 3.1290 Nord (1931). -  
Échappement Nord.

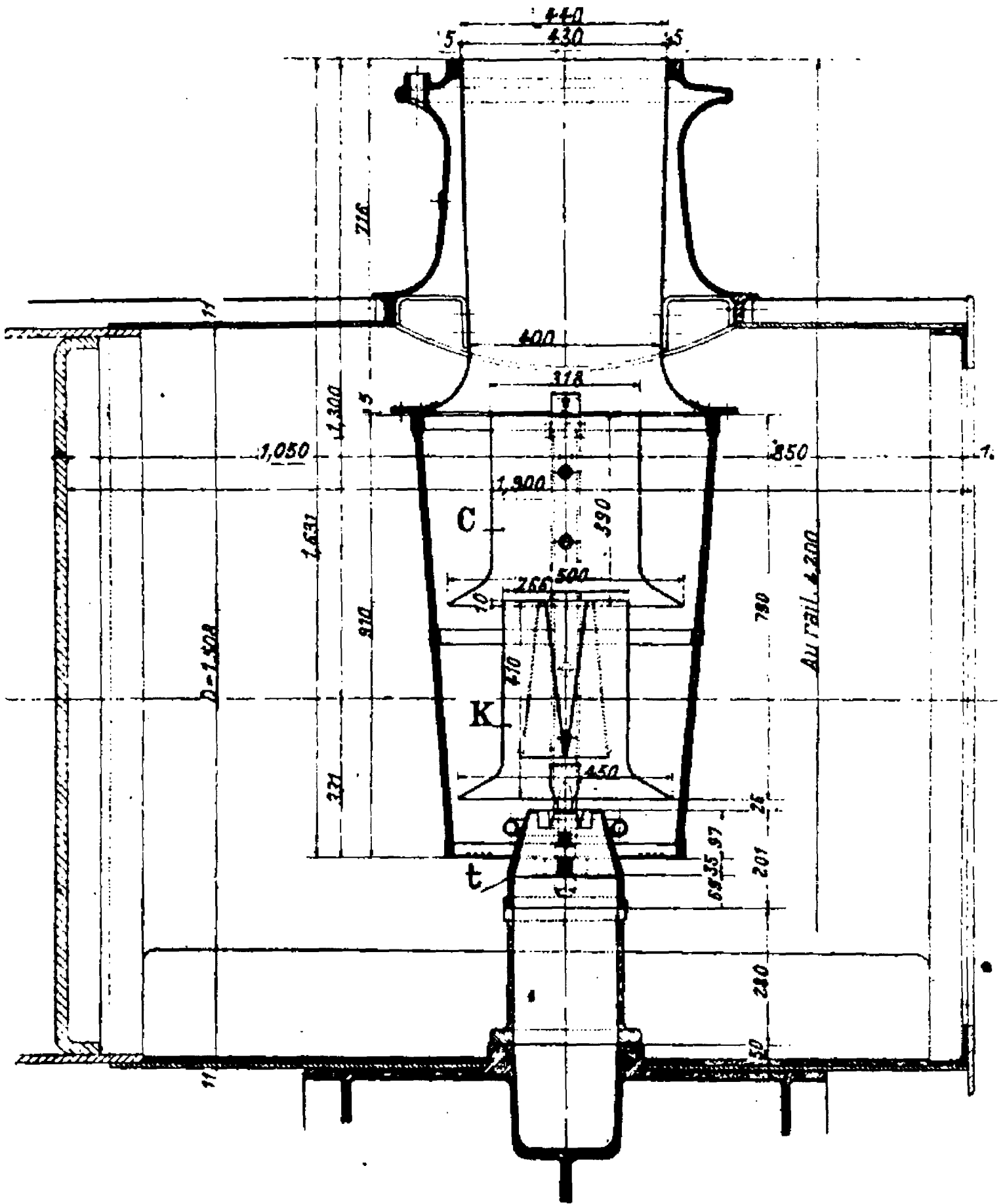


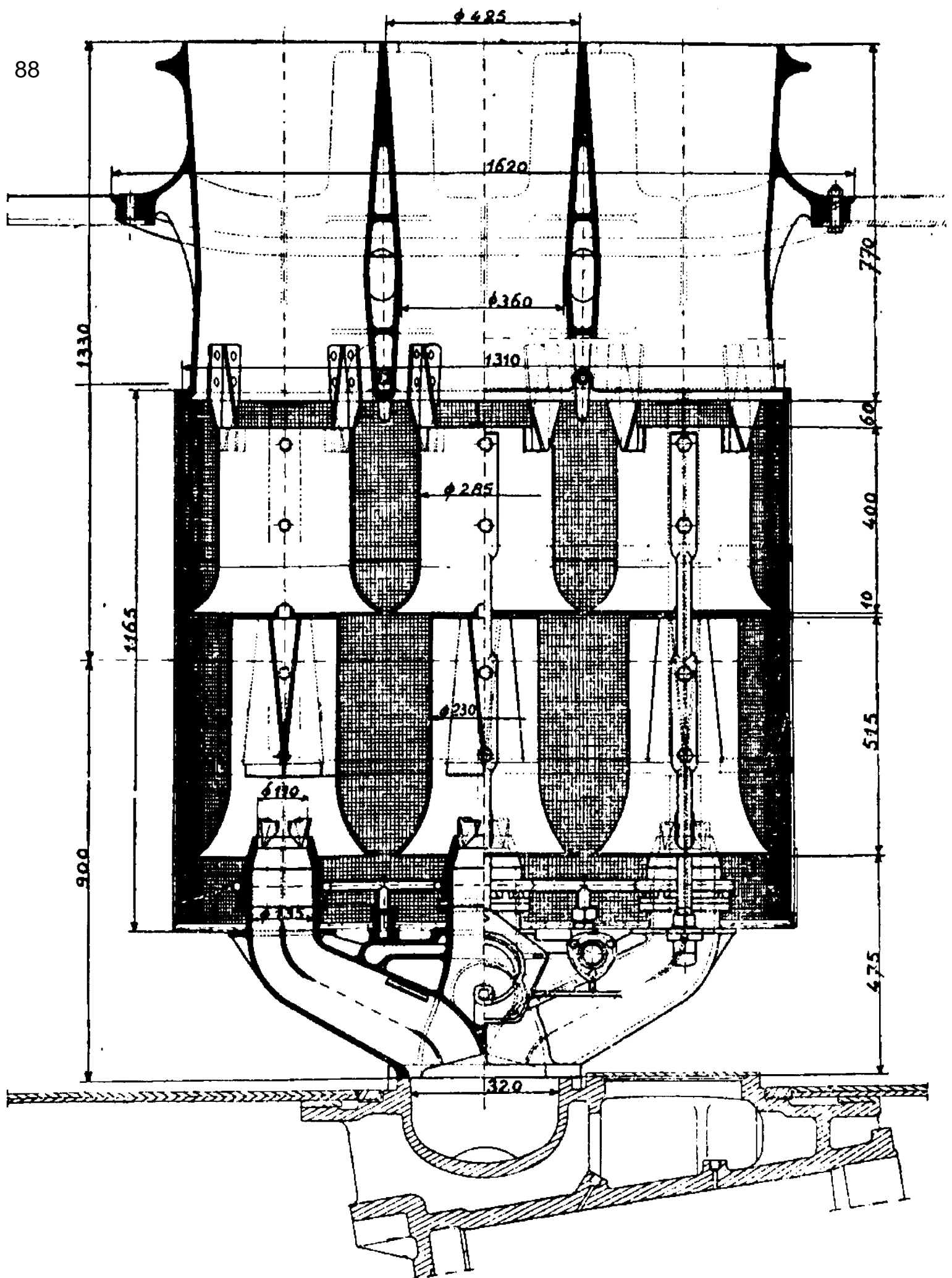
*To be continued...*

**Hit Back**  
or  
**HOME**

copyright 1997, 98, 99, 2000 by T. Stora. All rights reserved. Reproduction, translation, total or partial on any media absolutely forbidden without preliminary permission and agreement. Copyright 1997, 98, 99, 2000 by T. Stora





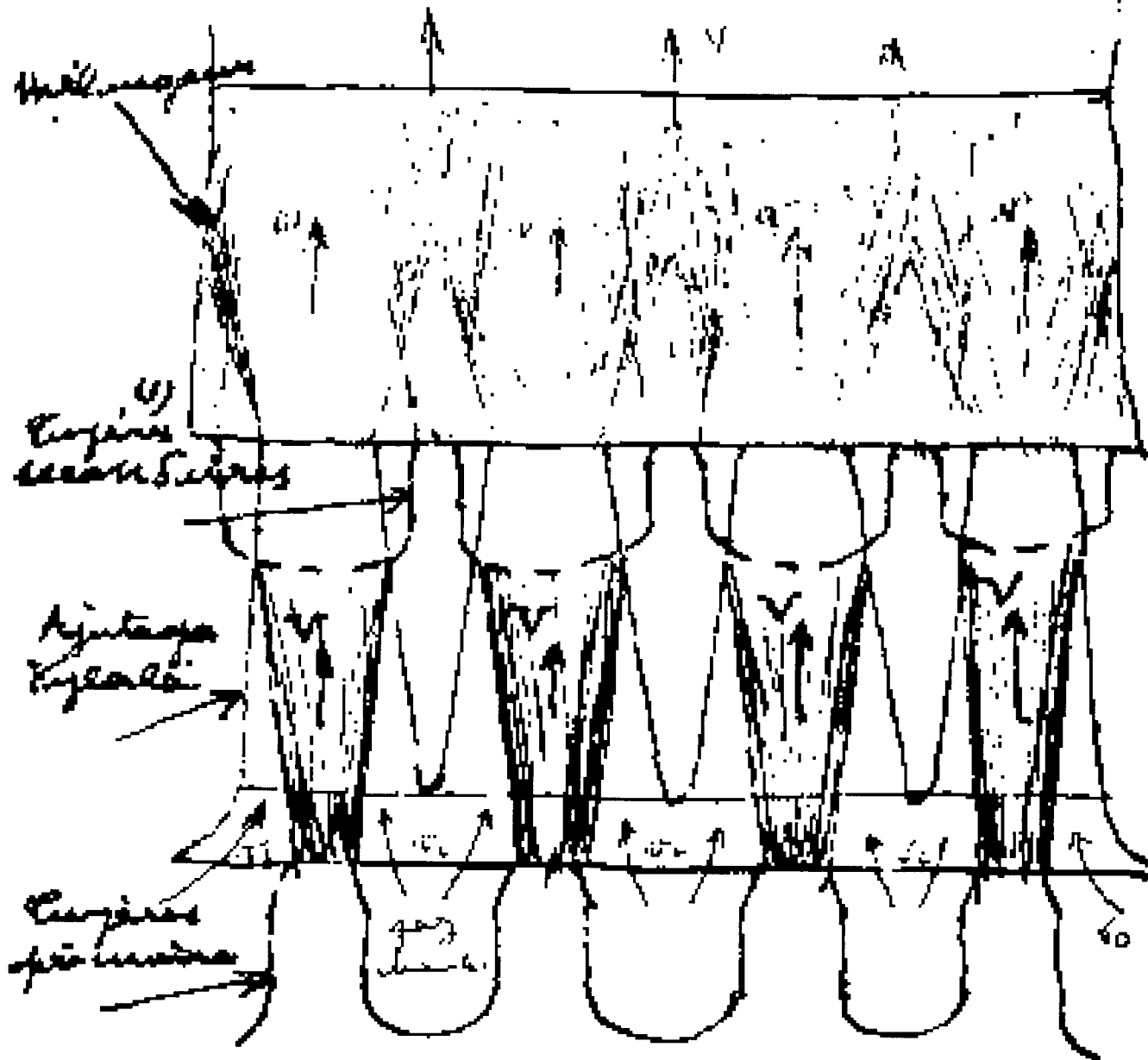


# Appareil de chauffage

89

Le but de l'appareil est de  
réduire au maximum les  
différences  $V_{1-2}$  et  $V_{2-3}$

cheminée



$V_{1-2}$  jets de vapeur d'eau

5 jets après première

mélanges avec l'ajutage Tylölä.

1) Les cupiers secondaires sont situés sous  
des jets de vapeur d'eau.



Hosted By  
**W TrainWeb**

Search

[TrainWeb.org](#) | [Member Sites](#)

## The Ultimate Steam Page

# Steam Locomotive Exhaust Drawings

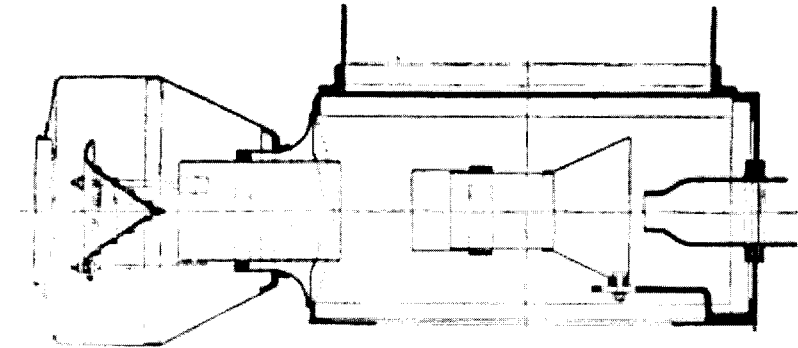
Updated February 26, 2004

One of the most important components of virtually all steam locomotives is the exhaust system. Early steam locomotive builders such as George Stephenson discovered the principal upon which virtually all steam locomotives built since have used. They found that directing the "waste" steam exhausted from the cylinders at the end of each stroke up the boiler's chimney greatly increased the air flow through the fire. This caused the fire to burn hotter and faster, allowing a locomotive boiler to generate dramatically more steam than stationary boilers of similar size.

As locomotive design progressed, builders realized that the proportions and configurations of the chimney and the exhaust pipe had a significant effect on how well the exhaust system worked. A major concern was the effect of *back-pressure* on the performance of the locomotive's cylinders. The locomotive exhaust could be built with a small exhaust nozzle, which caused the exhaust steam to jet up the stack at high velocity, which would produce excellent gas flow through the boiler (draft). However, this small nozzle would impede the flow of the exhaust steam from the cylinders, causing excessive back-pressure. This back-pressure saps power from the locomotive's cylinders, reducing the locomotive's performance. Good draft increased the locomotive's power, but high back-pressure could cancel this out.

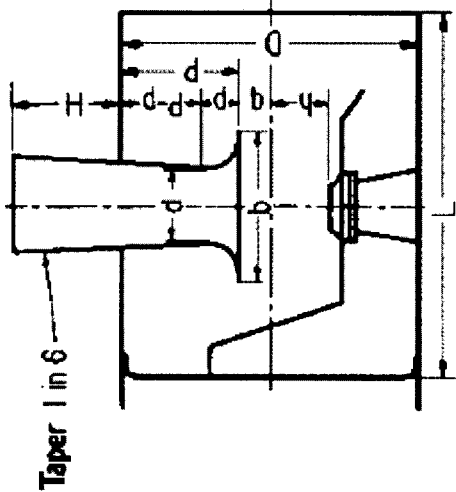
This was the chief task of locomotive exhaust designers: how to produce the maximum draft while producing the minimum back-pressure on the cylinders.

Until the 20th century, the physics of gas flow were not understood and the theories and laws which could be used to design exhaust systems did not exist. Consequently, early locomotive exhaust systems were developed through a process of trial-and-error.



This exhaust system, from a locomotive in New Zealand, is similar to that of many 19th Century locomotive exhaust systems. The steam nozzle is at the bottom, and it exhausts through a "peticoat" and finally up through the main chimney (the separate peticoat was a 20th century development). This chimney includes a spark arresting apparatus, which forces the exhaust gases through several turns in order to make sparks and cinders drop out into the bottom of the spark arrestor.

This drawing shows a typical locomotive exhaust system from a U.S. steam locomotive built in the 20th century. The drawing shows a cross-section of the smoke box at the front of a locomotive boiler (the boiler would be to the left of the view). The steam nozzle is at the bottom of the smoke box, exhausting its steam jet up the stack which is at the top. The drawing also illustrates the empirical design formulas which were used to size the components. After building hundreds of exhaust systems, designers decided that the proportions of the components listed above would

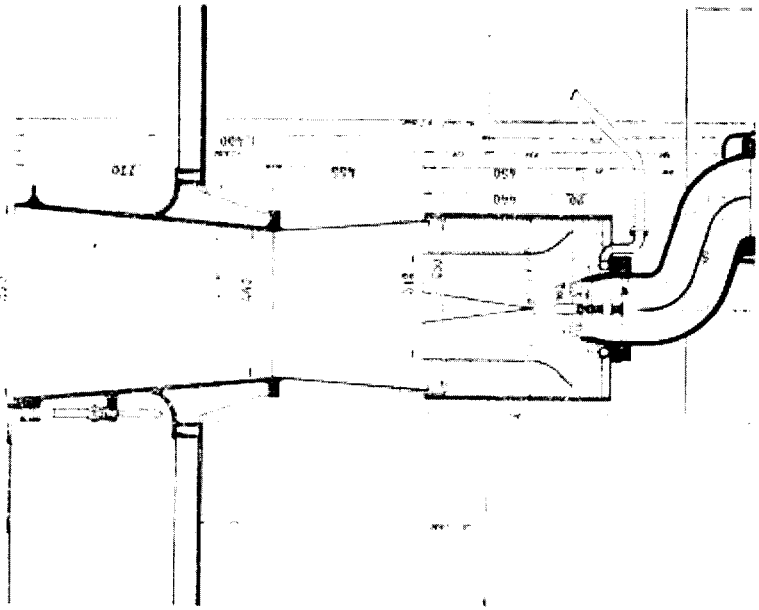


Taper 1 in 6

- 1- Make H and h as great as possible
  - 2- Make  $d = 0.21D + 0.16h$
  - 3- Make  $b = 2d$ , or  $0.5D$
  - 4- Make  $p = 0.32D$
  - 5- Make  $p = 0.22D$
- (Note from foregoing that  $q = 0.18D$ )

Fig. 8—Master Mechanics' Front End



<p>work best for most locomotives under most conditions.</p>		<p>This drawing shows an early Kylchap exhaust splitter developed by Finish engineer Kylala, which divides the exhaust stream into four parts. The Kylchap draws in gases from more than one level of the smokebox, which Chapelon believed to be an important feature in providing an even gas flow through the many tubes of the boiler. Later Kylchap exhausts used two levels of entrainment and two or even three stacks.</p>
--	---	--

The Kylala exhaust splitter was an important part of the Kylchap xhaust

system.

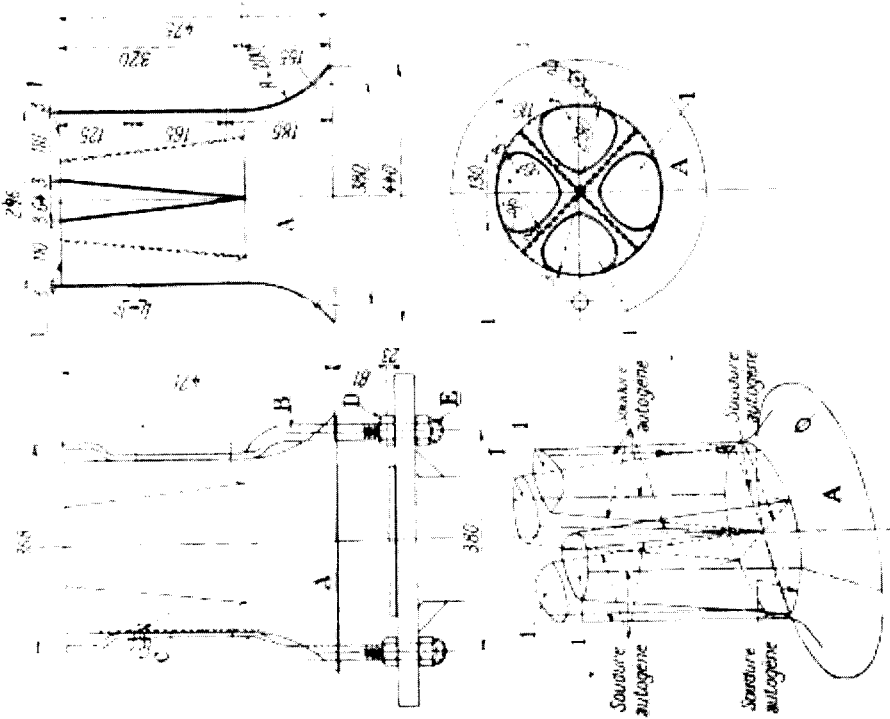
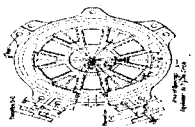


Fig. 117 - Détails de l'équipement A, B, C, D, E

In the U.S., several railways developed improved exhaust systems using annular exhaust nozzles and larger stacks.



Plan View of Annular Exhaust Nozzle  
(above)- Sectional Views of  
Smokebox (left)- Known as a "Waffle  
Iron" exhaust on the N&W

Sec. 3

BOILERS: Smokeboxes

336

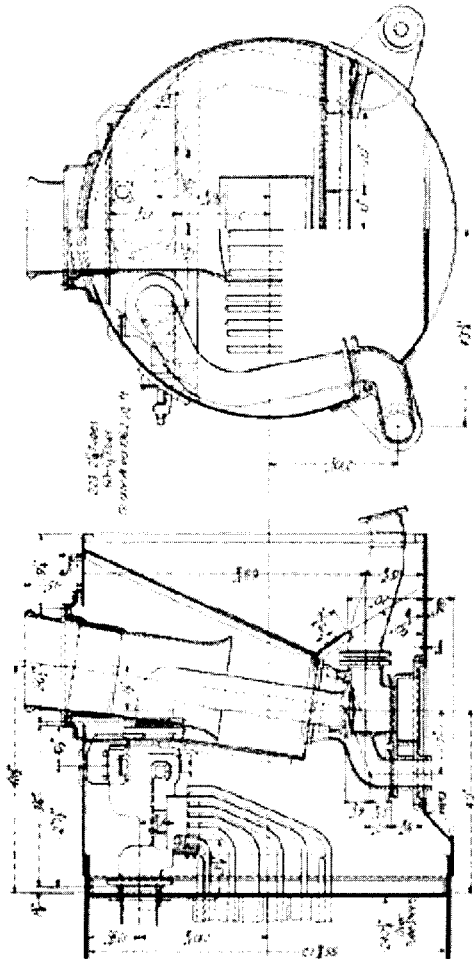
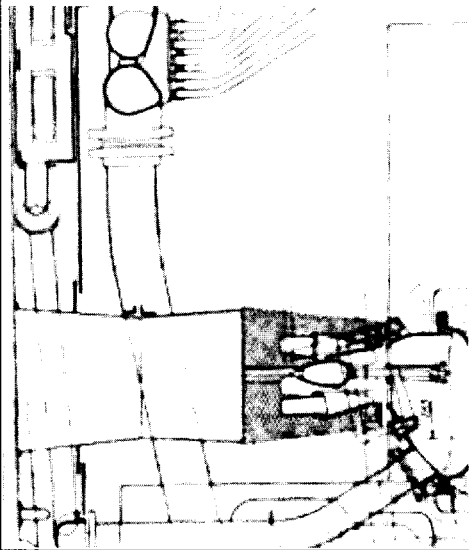
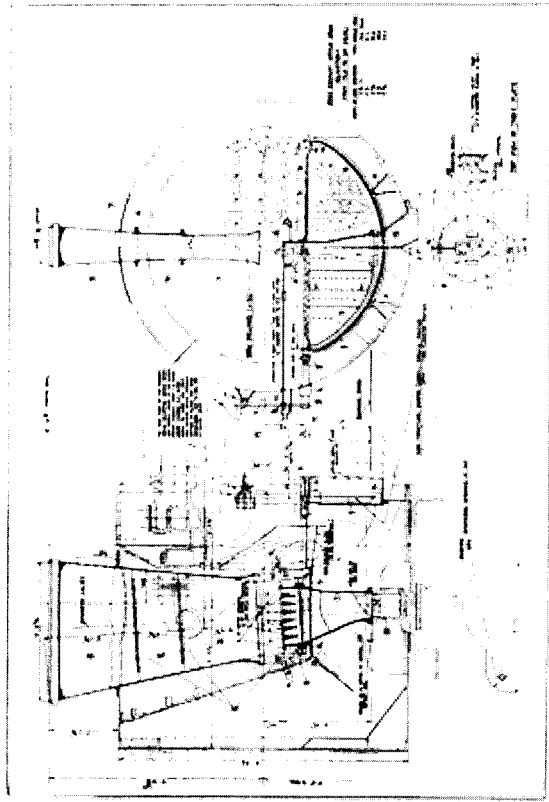


Fig. 3194 - General arrangement of Smokebox and Type A Superheater on Norfolk & Western 2-8-2 Compound Mallet Locomotive, Class V. Inclined smokestack centered above the smokebox.  
(See also Fig. 3193, Exhaust Valve)

The Lemaitre Exhaust was developed by Lemaitre, a mechanical engineer from the NORD Belge. The Lemaitre featured 5 nozzles in a circular pattern exhausting up a large diameter stack, with a variable area nozzle exhausting up the center.

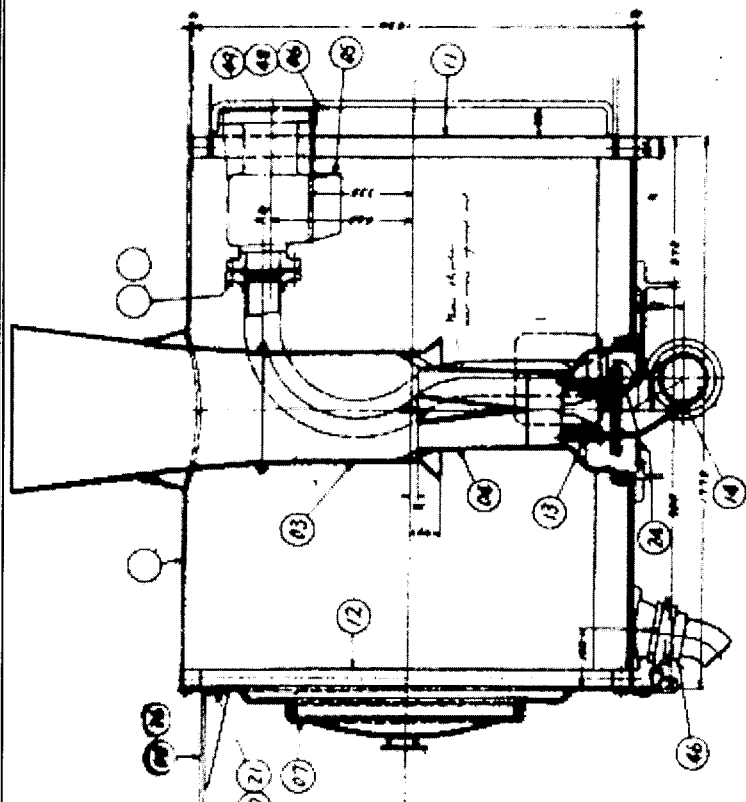


In the late 1940's, Dr. Adolph Giesl-Gieslingen developed a new exhaust design called the Giesl Ejector. He patented this device and it was applied to thousands of steam locomotives all over the world. The Giesl Ejector featured a series of small



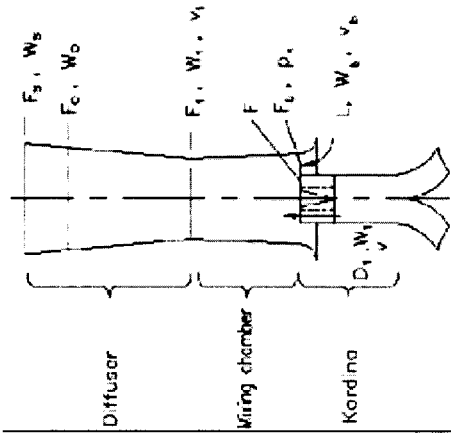
in-line nozzles exhausting up a thin, oblong chimney.

*drawing courtesy Stuart Kean*

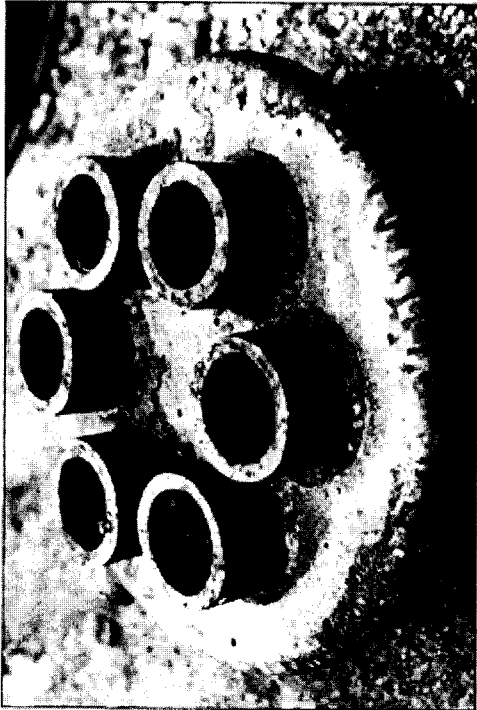


This drawing shows the Kylpor exhaust system developed by L. D. Porta from the Kylchap as applied to the 2-10-2s of the Rio Turbio Railway in Argentina.

Finally, this diagram shows the Lempor (Lemaitre-Porta) exhaust developed by Porta and applied to many locomotives. Porta also developed an extensive theory describing the performance and design of these exhaust systems.



One of the most recent new exhaust systems was developed for the Garratt locomotives of the Rhodesian Railways. These were known as "pepperpot" exhausts and were later fitted to many Garratts which were overhauled and restored to service in the early 1980's in the new country of Zimbabwe. This nozzle arrangement was used in combination with a larger chimney, and was developed as alternative to Giesl exhausts experimentally fitted to Garratts in the 1960's. The pepperpot exhaust was preferred because (1) it was locally developed (the Giesl was proprietary and royalties had to be paid for its use) and (2) the Pepperpot was less susceptible to unauthorized tampering which tended to cause problems with the Giesls in normal service.



The six jet blowdown rig as fitted to J11A, built from 1967, and much later enlarged for the 20-20A version

For the last years of his life, Porta worked on the development of a *Lemprex* exhaust system, a further advancement on the Lempor. The Lemprex incorporates features to maximize its performance within the limited height available on a steam locomotive. Basically, the taller an exhaust system can be, the better it functions. Unfortunately, the larger a steam locomotive gets, the less height is available for the exhaust system. The Lemprex exhaust may be applied to new steam locomotives planned for Cuba and Argentina.

[Back to Top](#)

[Return to the Exhaust Systems Page](#)

# THEORY OF THE LEMPOR EJECTOR AS APPLIED TO PRODUCE DRAUGHT IN STEAM LOCOMOTIVES

## Summary

This is a revision of the Porta-Taladiz theory of 1957, incorporating the effect of friction in the mixing chamber and other corrections. The theory is based on the principle of conservation of energy as applied by Strahl in 1913, with due corrections for the case under consideration. It serves for the design of an optimum ejector leaving a minimum correction of the blast pipe to be carried out in practice as usual since Stephenson's times. It serves also to predict the behavior of a given ejector.

As a matter of course, the accuracy of either the calculated or the measured performance of the boiler conditions the optimization of the ejector design. Fortunately there seems to be a reasonable latitude in the dimensions around the optimum.

The Lempor ejector resembles the Le Maître and is thermodynamically equivalent to the Kylpor, the latter resembling the Kylchap. However, its internal losses to friction in the mixing device are smaller.

Successful experiments would show 100% improvement against the best known draughting device.

L.D.Porta  
Buenos Aires  
December 1974

## Introductory Note

Note added February 1999. This theory refers to the fundamentals defining the main dimensions of the ejector. It requires the calculation (or the obtention by experimental procedures) of the boiler characteristics, a serious matter in itself. It also presupposes that a large number of details coming from a long experience are to be respected. It does not include the swirl of both of the steam jet and the gas intake. Finally, a still pending serious problem is that it assumes that the flow is steady, non-pulsating, a field open to future investigation. It is not a "kitchen recipe" guaranteeing good results without a good tuning up with measurements. However, the reader may try, provided that if success crowns his trial and error, the merit is to be credited to the theory. If not, the Author expects that the failure is not to be credited to the theory, but to the user.

### Theory of the Lempor Ejector

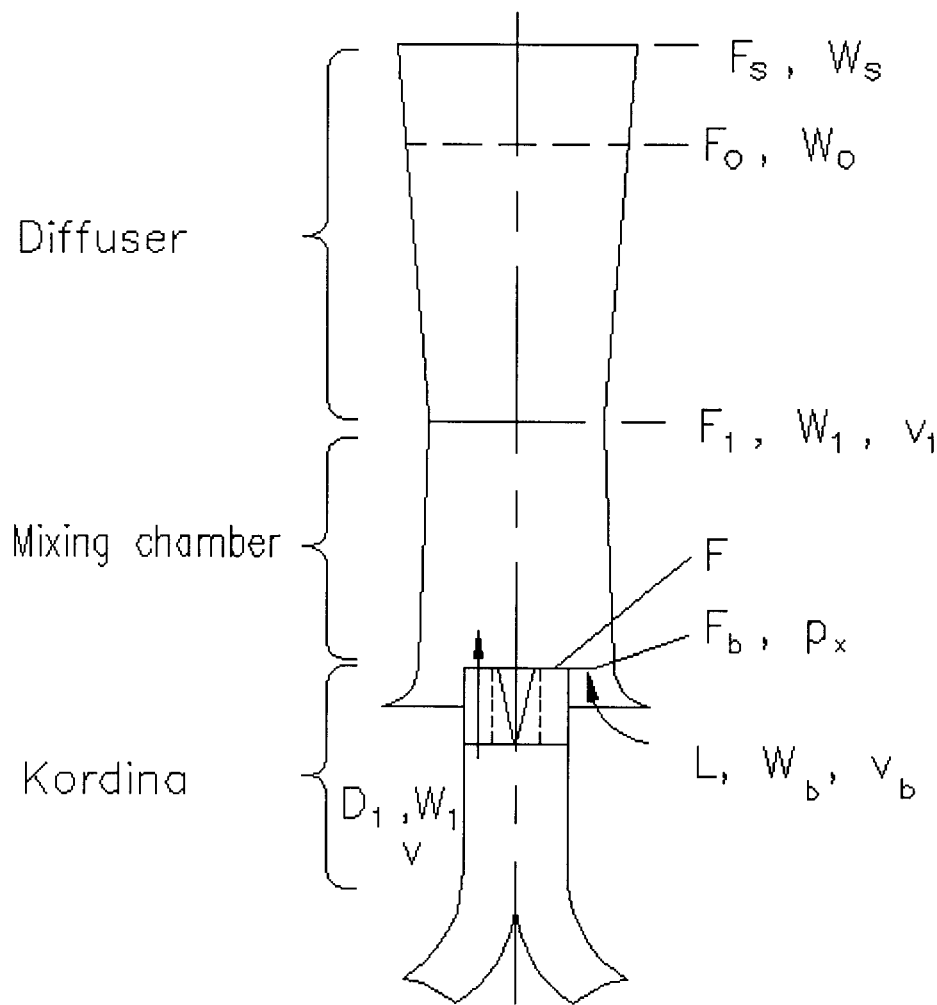


**Fig 1 The Lempor Ejector**

The principal parts of the ejector are (Fig 1)

- A. The blast pipe or tuyère made up of four nozzles with converging-diverging sections so as to account for the supersonic flow prevailing during the exhaust beats.
- B. The mixing chamber of slightly converging section whose length is a compromise between the evening-out of exit velocity and available total height.
- C. The diffuser, having the maximum possible diverging angle, yet with good diffusing efficiency.
- D. The Kordina, which is really an ejector in itself disposed so that each steam puff creates a vacuum in the other cylinder.

The interesting cross-sections are:

<u>Symbol</u>	<u>Units</u>	<u>Description</u>
$F_s$	$[m^2]$	The chimney exit area
$F_1$	$[m^2]$	Chimney throat area
$F_b$	$[m^2]$	Gas inlet area at the bottom of the mixing chamber
$F$	$[m^2]$	Steam tuyère area
$F_0$	$[m^2]$	Ideal diffuser outlet area

99

Let also be:

$L$	$[kg\ s^{-1}]$	Gas mass (rate) to be expelled
$D$	$[kg\ s^{-1}]$	Mass rate of steam flowing through the tuyère
$W_0$	$[m\ s^{-1}]$	Mixture velocity at ideal outlet
$W_1$	$[m\ s^{-1}]$	Mixture velocity at chimney throat
$W_b$	$[m\ s^{-1}]$	Gas velocity at gas inlet section of area $F_b$
$W$	$[m\ s^{-1}]$	Gas velocity at tuyère exit plane
$p_x$	$[N\ m^{-2}]$	Static pressure (absolute) at the tuyère exit plane
$p_0$	$[N\ m^{-2}]$	Atmospheric pressure
$p_c$	$[N\ m^{-2}]$	Smokebox pressure
$p_0 - p_c$	$[N\ m^{-2}]$	Draught
$p_1$	$[N\ m^{-2}]$	Pressure at chimney throat
$v_1$	$[m^3\ kg^{-1}]$	Specific volume of the steam-gas mixture
$\xi$	-	Coefficient expressing the pressure drop due to friction in the mixing chamber
$\xi_b$	-	Coefficient expressing the pressure drop at the gas entrance
$\lambda$	-	$\frac{1}{2} \left[ 1 + \left( \frac{F_1}{F_0} \right)^2 \right]$
		Ideal diffuser outlet section =
$F_0$	$[m^2]$	$\frac{1}{\sqrt{\frac{1-\eta}{F_1^2} + \frac{\eta}{F_s^2}}}$
$\eta$	-	Diffuser efficiency (e.g. 10)

Assuming a uniform velocity distribution at every cross-section, the fundamental equation of the ejector is obtained by applying the principle of the conservation of energy to the fluid streams:

**Equation**



100

$$\underbrace{(L+D)(p_0 - p_x)v_1}_{1} + \underbrace{\frac{1}{2}D(W - W_1)^2}_{2} + \underbrace{\frac{1}{2}L(W_1 - W_b)^2}_{3} + \underbrace{\frac{1}{2}(L+D)W_0^2}_{4} - \underbrace{\frac{1}{2}DW^2}_{5} - \underbrace{\frac{1}{2}LW_b^2}_{6} = 0$$

In this energy balance, there are 6 terms:

- 1- Mixture compression work which is considered to be carried out at constant specific volume  $v_1$  and from the pressure prevailing at the tuyère exit plane
- 2 & 3- Shock losses obtaining in the mixing chamber
- 4- Loss by kinetic energy of the gas having a non zero velocity at the ejector outlet. The outlet section is taken smaller than the actual one so as to account for energy losses within the diffuser.
- 5- Useful steam energy
- 6- Useful gas energy

Later a correcting term will be incorporated to account for the friction obtaining in the mixing chamber.

Expanding Equation 1, simplifying and dividing by 2 (L+D) and grouping the quadratic terms, we have:

$$(p_0 - p_x)v_1 - \frac{D}{L+D} WW_1 + \frac{W_1^2}{2} \left[ 1 + \left( \frac{W_0}{W_1} \right)^2 \right] - \frac{L}{L+D} W_b W_1 = 0 \quad \text{Equation 2}$$

The continuity equations can be written:

$$W = \frac{D}{F} v \quad W_1 = \frac{L+D}{F_1} v_1 \quad W_b = \frac{L}{F_b} v_b \quad \frac{W_0}{W_1} = \frac{F_1}{F_0}$$

Introducing these values into Equation 2, operating and setting  $\lambda$  as above,

$$p_0 - p_x = \frac{D^2 v}{FF_1} - \frac{(L+D)^2 v_1}{F_1^2} \lambda + \frac{L^2 v_b}{F_1 F_b} \quad \text{Equation 3}$$

This expression gives the vacuum at the tuyère exit plane. But it is more convenient to work with the vacuum (pressure) prevailing in the smokebox, this related to the working requirements of the boiler. It is

$$p_c - p_x = \frac{1}{2} \left( \frac{L}{F_b} \right)^2 v_b$$

Therefore it is

$$p_0 - p_x = (p_0 - p_c) + \frac{1}{2} \left( \frac{L}{F_b} \right)^2 v_b \quad \text{Equation 4} \quad 101$$

Introducing Equation 4 into Equation 3, the fundamental expression giving the smokebox draught is obtained:

$$\text{Draught} = (p_0 - p_c) = \frac{D^2 v}{F F_1} - \frac{(L + D)^2 v_1 \left( \lambda + \frac{\xi}{2} \right)}{F_1^2} + \frac{L^2 v_b}{F_1 F_b} - \frac{1}{2} \left( \frac{L}{F_b} \right)^2 v_b (1 + \xi_b) \quad \text{Equation 5}$$

At this point, the friction at the mixing chamber and gas entrance are immediately introduced.  $\xi$  is a coefficient introduced to express the pressure drop as a fraction of the velocity head at the throat  $1/2 \left( \frac{L + D}{F_1} \right)^2 v_1$  and  $\xi_b$  that corresponding to the gas entrance.

The whole of this treatment assumes that the problem is unidimensional, i.e. that the gas and steam streams are coaxial. Equation 5 can be easily solved numerically, giving arbitrary values to  $F_1$  and  $F_b$  and choosing the pair making  $F$  a maximum. While it is possible to operate mathematically the expression so as to have a formula giving  $F$  directly, the former procedure has the advantage of showing the sensitivity of the design to a change in the different variables.

It can be written:

$$F = \frac{D^2 v}{(p_0 - p_c) F_1 + \frac{(L + D)^2 v_1 \left( \lambda + \frac{\xi}{2} \right)}{F_1} - L^2 v_b \frac{1}{F_b} + \frac{F_1 L^2 v_b (1 + \xi_b)}{2 F_b^2}} \quad \text{Equation 6}$$

Equation 6 can be written

$$F = \frac{A}{B + \frac{C}{F_b} + \frac{D}{F_b^2}} \quad \text{Equation 7}$$

in which  $A = D^2 v$

102

$$B = F_1(p_0 - p_c) + \frac{(L + D)^2 v_1 \left( \lambda + \frac{\xi}{2} \right)}{F_1}$$

$$C = -L^2 v_b$$

$$D = \frac{1}{2} L^2 v_b (1 + \xi_b) F_1 = -\frac{C}{2} (1 + \xi_b) F_1 \approx -\frac{C}{2} F_1 \text{ since } \xi_b \text{ is small.}$$

The optimum  $F_b$  that makes a maximum of  $F$  is obtained by differentiating equation 7 and equating to zero.

$$\frac{dF}{dF_b} = 0 = \frac{-A \left[ -\frac{C}{F_b^2} - 2 \frac{D}{F_b^3} \right]}{\left[ B + \frac{C}{F_b} + \frac{D}{F_b^2} \right]^2}$$

It is

$$\frac{C}{F_b^2} + 2 \frac{D}{F_b^3} = 0$$

Hence

$$F_b = -2 \frac{D}{C} = \frac{-2 \left( -\frac{C}{2} F_1 \right)}{C} = F_1$$

This result shows that the optimal mixing chamber is not a constant section one. If this result is introduced into Equation 5, we get

$$\text{Draught} = (p_0 - p_c) = \frac{D^2 v}{F F_1} - \frac{(L + D)^2 v_1 \left( \lambda + \frac{\xi}{2} \right)}{F_1^2} + \left( \frac{L}{F_1} \right)^2 v_b - \frac{1}{2} \left( \frac{L}{F_1} \right)^2 v_b (1 + \xi_b)$$

$$\text{Draught} = \frac{D^2 v}{F F_1} - \left( \frac{L + D}{F_1} \right)^2 v_1 \left( \lambda + \frac{\xi}{2} \right) + \frac{1}{2} \left( \frac{L}{F_1} \right)^2 v_b (1 - \xi_b) \quad \text{Equation 8}$$

and

$$F = \frac{D^2 v}{F_1 (\text{Draught}) + \frac{(L + D)^2}{F_1} v_1 \left( \lambda + \frac{\xi}{2} \right) - \frac{1}{2} \frac{L^2}{F_1} v_b (1 - \xi_b)} \quad 1.01 \quad \text{Equation 9}$$

This equation can be solved graphically giving tentative values to  $F_1 = F_b$  so as to get the maximum for a tuyère area giving the lowest back pressure. 103

This theory is based on Strahl's theory (1) with convenient modifications. A numerical check against the application of the momentum theorem to the mixing chamber showed coincident results. Later, it was possible to demonstrate a rigorous equivalence.

The factor 1.01 accounts for a flow coefficient of 0.99 deduced experimentally from data taken at the Rugby test plant.

As a typical value for  $\xi$ , the figure of 0.10 can be taken, but a more exact estimation is possible if the theory given in (1) is accepted.  $\xi_b \approx 0.04$  can be considered a typical value for a carefully designed bell mouth.

Equation 5 allows the prediction of the performance of any ejector satisfying the assumptions stated before, while Equation 9 gives the optimum dimensions. It is clear that the design, or the prediction of performance, cannot have better accuracy than the boiler data on which are based  $L$ ,  $D$ , draught,  $v_b$ , etc. and also the steam conditions at the blast pipe tip. These can be forecasted with reasonable accuracy by means of laborious calculations, but undoubtedly actual test data are far more desirable. However, this is not enough: a locomotive ejector, the very heart of the machine, must incorporate due allowances for maintenance standards, fuel quality variations, service required from the locomotive, unavoidable steam and gas leaks, etc. Besides, it cannot be claimed that the present theory contemplates all the phenomena occurring in the ejector in full detail. Therefore it is to be used as the best available approach to an optimum, the final adjustment is to be carried out in practice by actual train running and fitting various tuyères of different area as it has been the universal practice since the days of George Stephenson. Fortunately, the main chimney dimensions are given by very flat curves and therefore it is possible to play within a fairly large latitude. To account for these phenomena, the ejector should be designed for 5% extra gas quantity and 10% more draught.

(1) 2VDI, 57 (1913), p. 1739

{Porta L.D., Heat transfer and friction in ejector mixing chambers, 1974}

The theory can take into account compressibility effects, which are actually influenced at the highest rate of working in engines operating with very high draught requirements (up to 700 mm  $H_2O$  in the SNCF 141R (see Appendix A4). Calculations should be carried out solely for the maximum rating since experience shows that the automaticity of an ejector so designed is satisfactory and not giving too large an excess of air at low working, while- and as a matter of course- no front end limit is apparent.

The calculations are to be repeated if the engine is called upon the work at very high heights above sea level, the atmospheric pressure becoming much lower (53% of sea level pressure at 4775 m above sea level on the Tocompa (?) line, Argentina). As it is well known, combustion phenomena change appreciably, yet a very limited experience seems to indicate that the same ejector behaves satisfactorily with independence of the height. But this does not prove that the optimum dimensions for sea level working remain also optimum at higher heights.

The whole design is a compromise because of the limited height available. The mixing chamber and the diffuser dispute the space on hand, and therefore the tuyère should be placed at the lowest possible position in the smokebox. So far as the written experience is concerned involving the gas producer combustion system, no fears arise of "burning too much at the front or the back" as many time has been said, but no evidence has been produced.

When carrying out the computations, due allowance should be made to account for leakage steam not passing

104. through the blast pipe, air leakage into the smokebox, stoker jets or burner steam (increasing the gas quantity to be sucked), stoker engine steam, oil heater steam, vacuum ejector steam, lighting generator steam, steam to ashpan for the gas producer combustion system, etc. which are far from being negligible.

Another point to be considered is the one concerning building up inaccuracies whose influence can in no case be favouring, and therefore the actual design should incorporate all available means to provide adequate lining up and also least perturbations in the flow.

An allowance of 1% extra section should be considered on the value of F to account for the contraction coefficient.

Finally, last but not least, nothing is known about the influence of pulsating conditions obtaining in locomotives. So far, ejectors designed on the steady flow hypothesis have behaved satisfactorily and blast pipe area so predicted required little adjustment in practice and within  $\pm 5\%$ .

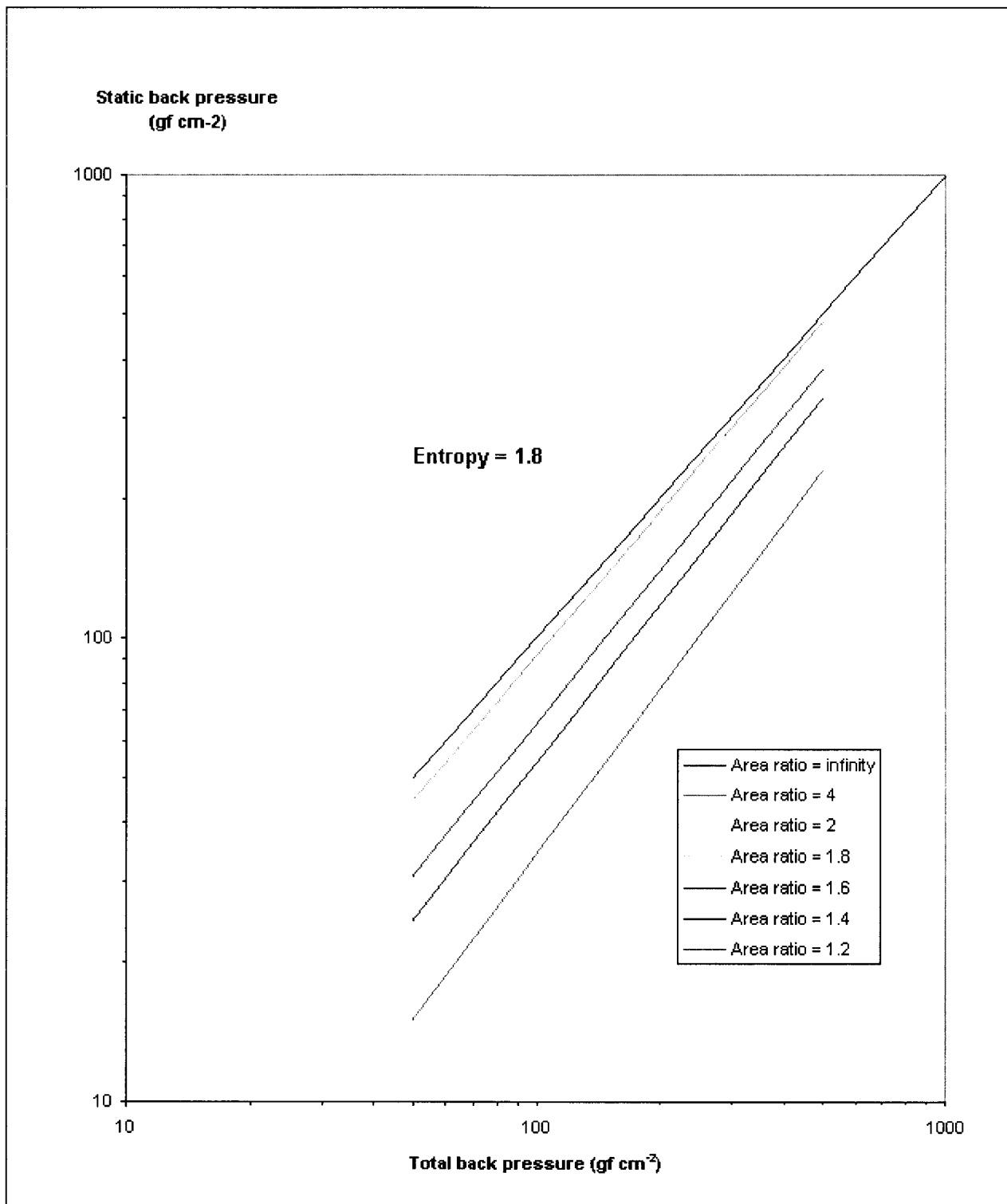


Fig 2: Relation between static and total back pressure

### Comparative measures of ejector performance

Since most locomotives operate with similar relations between gas and steam mass ( $L/D \approx 2$ ) and all of them have high superheat temperature and not too different internal cylinder efficiency, the gas and steam conditions do not differ too much. Therefore the usual back pressure - draught curve is a fair measure of ejector efficiency. The application of thermodynamic principles lead to consider the total back pressure which can either be measured with a Pitot tube in the exhaust stand (at  $\frac{3}{4}$  radius of the tube) or corrected according to the graph given in Fig 2 if the static pressure has been measured.

106

Fig 3 gives comparative curves. Those reported to be ejectors designed by the author refer to Kylpor ejectors built some 15 years ago and therefore giving a somewhat worse performance of what could be expected from a today's design. It is seen that performance is some 40% better than any other type of apparatus, possibly increasing to 50% if the present knowledge is applied.

Another comparative parameter, easier to determine, is the relation given in Table 1.

$$\left( \frac{\text{tuyere\_area}}{\text{gas\_area\_through\_the\_boiler}} \right)^2$$

The back pressure is proportional to the (tuyère area)<sup>2</sup> while the boiler draught is proportional to (gas area)<sup>-2</sup>. Due allowance should be made when comparing ejectors, to the fact that oil-burning and "gas producer" engines are so designed that part of the steam produced does not pass through the blast pipe.

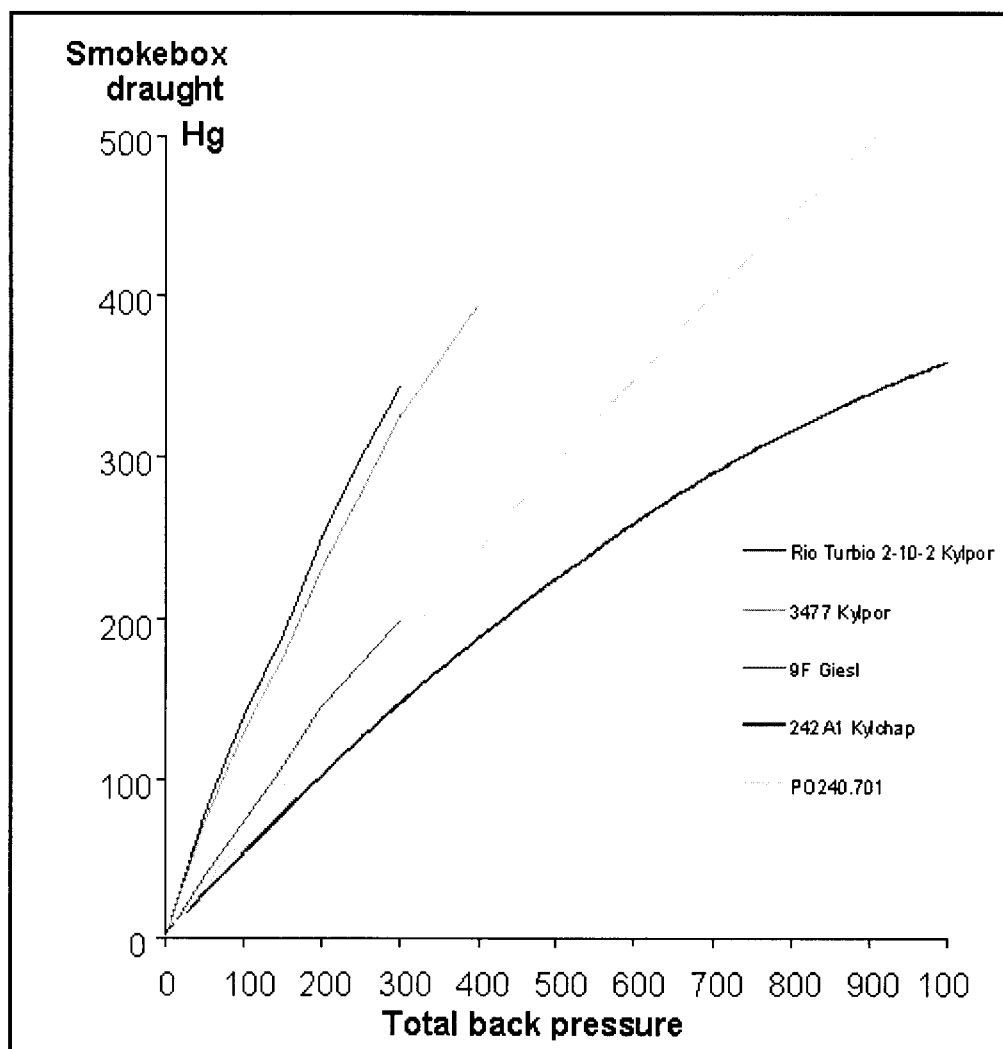


Fig 3 Comparative performance curves.

Table 1

Engine	Tuyère area F	Gas area Ω	F/Ω	(F/Ω )	Ejector	Fuel
--------	---------------	------------	-----	--------	---------	------

	cm <sup>2</sup>	cm <sup>2</sup>		<sup>2</sup> • 10 <sup>4</sup>		
PO240.701	200	4942	0.0405	16.4	Kylchap	Coal
242A1	246	5593	0.044	19.3	Kylchap	Coal
141R	179	5091	0.035	12.4	Kylchap	Fuel oil
141R	179	5910			Kylchap	
141R	229	5910	0.039	15.0	Kylchap	Coal
141R469	199	5910	0.034	11.3	American	Coal
9F	195	5091	0.035	14.7	Giesl	Good coal
1802-FC6B Argentina	216	5000	0.043	18.0	Improved existing Kylchap	Oil burning
4674FC6B Argentina	110	2078	0.054	29.0	Kylpor	Gas producer combustion system, high ash coal
4674FC6B Argentina	115	2078	0.057	32.0	Kylpor	Gas producer combustion system, high ash coal

### **The back pressure**

One of the ultimate goals of ejector design is to make a least demand to the engine in terms of back pressure or either to produce the maximum draught with a given back pressure. High draught produced economically means ample latitude to play with boiler design, gas areas, grate design, etc. essentially resulting in a smaller and lighter boiler, dispensing extra carrying wheels, good turbulence in the firebox, clean tubes, less smoke and happy crews because of an adequate steaming reserve. No effort should be spared in designing the ejector for maximum efficiency, otherwise one would fall into the trap of the "good enough engineering" which would come short of the hard competition obtaining in a near future.

The meaning of the back pressure goes further than the simple horsepower evaluation obtained after introducing its figure in the IHP formula: it is the lower boundary of the steam cycle and its importance can be clearly shown when comparing its heat drop and the engine heat drop on the Mollier and of course its value is sensible at high powers and reduced cut-off.

Back pressure is usually measured with a manometer connected to the exhaust stand, but this is thermodynamically not correct because solely the static back pressure is reported: no account is given to the energy of the steam at the measuring point which is extracted from the pistons. Figure 2 gives the proper correction factor, which is not great in usual circumstances, but not so when the area ratio of stand pipe/tuyère is near unity. This happens especially in improved engines, not to say in author's designs in which the exhaust stand area equals the tuyère area: the static pressure manometer always reads zero.

The normal design of the exhaust stand is such that each puff of one cylinder affects the piston on the other and therefore the time average back pressure, static or Pitot, is reflected in the indicator diagram. In the author's



108

designs the exhaust stand is so designed that the indicator line shows a lower back pressure than the manometer reading.

The time average back pressure can be obtained from the Mollier after an allowance for a flow coefficient of 0.99 which has been deduced from test data obtained at Rugby. This coefficient accounts for the actual reduction resulting from friction in the tuyère, the pulsating nature of the flow, the supersonic puffs, etc. One allowance should be made on the pressure around the tuyère, which is lower than the atmospheric.

### **Final comments**

The theory here presented involves an accurate mechanical realization which is somewhat difficult given the kind of apparatus working in a hostile environment and handled by usually rough boilersmiths. It is felt that there is room for improvement and development work, particularly in considering the effect of pulsations.

Since the back pressure - draught experimental curves show a definite progress which it is hoped to still improve, it is felt that this will lead to a reduction of the boiler size for a given heat duty, therefore making a contribution to the increase of the power to weight ratio.

The present paper is a draught for a book (in preparation) to be entitled "*Modern Steam Locomotive Engineering*".

Hosted By TrainWeb.com

### Appendix A1: The equivalent ideal diffuser

The conversion of kinetic energy into pressure in the diffuser is accompanied by considerable losses which must be accounted for.

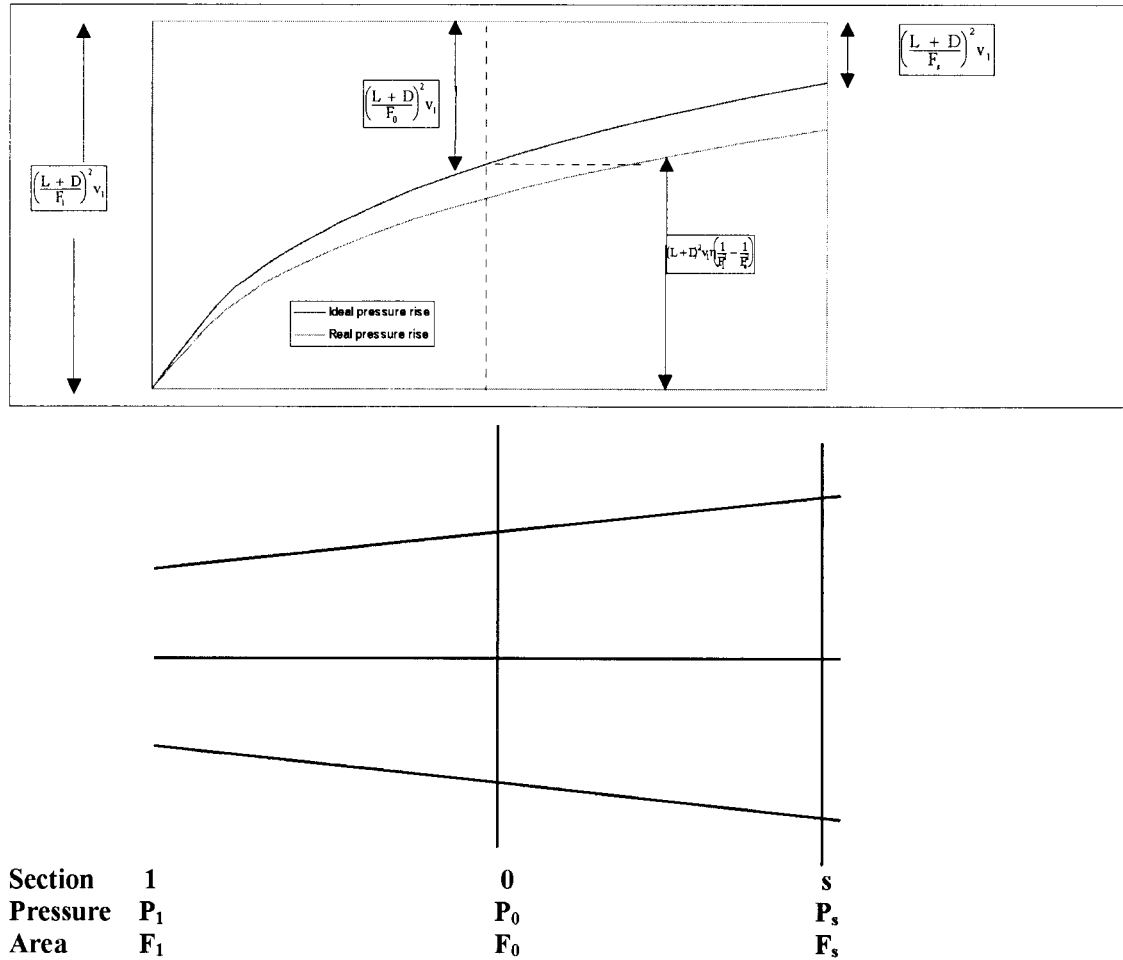


Fig 4 Equivalent ideal diffuser

The equivalent ideal diffuser is one in which the outlet section  $F_0$  is calculated so that the sum of the kinetic energy loss is equal to the kinetic energy loss at section  $F_s$  plus diffuser friction.

it is

$$p_s - p_1 = \frac{1}{2} (L + D)^2 v_1 \left( \frac{1}{F_1^2} - \frac{1}{F_s^2} \right) \quad \text{Equation 10}$$

and, in the ideal diffuser, where  $\eta=1$

$$p_s - p_1 = \frac{1}{2} (L + D)^2 v_1 \left( \frac{1}{F_1^2} - \frac{1}{F_0^2} \right)$$

Hence

$$\eta \left( \frac{1}{F_1^2} - \frac{1}{F_s^2} \right) = \left( \frac{1}{F_1^2} - \frac{1}{F_0^2} \right)$$

Therefore

$$F_0 = \frac{1}{\sqrt{\frac{1-\eta}{F_1^2} + \frac{\eta}{F_s^2}}}$$

It is most difficult with the present state of knowledge existing in this particular problem, to give definite values for the diffuser efficiency  $\eta$ , especially because it is not known what are the inlet conditions on which that efficiency depends so much. Besides the whole question of the behavior of a diffuser under pulsating conditions, the following points should be considered to favor the efficiency of kinetic into pressure energy.

- Higher Reynolds number, of the order of  $1 \cdot 10^6$
- Very high turbulence resulting from the previous mixing process.
- The application of boundary layer suction.
- Smoothness of the surfaces.

Against good efficiency, it can be set:

- The limited length available.
- The surface roughness obtaining in working conditions, especially in oil-burning engines.
- Some unavoidable inaccuracy of the whole draughting apparatus; it is a boilersmith construction operating in a hostile environment.

As a tentative figure, it is proposed to set  $\eta=0.8$  up to  $0.85$  under favourable circumstances (short smooth accurate diffusers). With an area ratio of 4, the corresponding fraction of the kinetic energy converted is  $0.80(1-1/4^2) \approx 0.75$ , which is very high.

## **Appendix A2 The Kylpor ejector**

The Kylpor differentiates from the Lempor by the fact that it makes use of the Kylala four lobe mixing device and therefore resembling the Kylchap of the type 1K/1T. Both types are thermodynamically equivalent except that the Kylpor has greater friction in the mixing chamber, this leading to the written preferences for the Lempor in recent designs. Nevertheless, the design is worthy of application in the case of a double concentric tuyère. In this design, the inner smaller tuyère is connected to the cylinder during the release phase, while both the inner and the larger- gives an extra area during the exhaust phase. This larger area determines a very low back pressure on the exhaust line and the explanation is to be sought in the fact that actually most of the work is done by the puffing steam through a very small tuyère and thereby extracting a good deal of work of the incomplete expansion toe of the indicator diagram.

It can be shown that the upper mixing chamber of the Kylpor must be cylindrical while the bottom gas section and the tuyère must be equal to that of the tip of the Kylala petticoat. This is to comply with the requirement  $F_1 = F_b$ .

Unlike former designs, there is no interest in having a uniform distribution of velocities at the Kylala exit and therefore this element should be as short as possible to reduce the unavoidable friction.

## **Appendix A3 Complementary notes**

For usual locomotive practice

$$v \approx v_b \approx v_1 \approx 1.9 \text{ m}^3 \text{ kg}^{-1}$$

$$L/D \approx 2; F_1/F \approx 7; F_b/F \approx 7; W/W_b \approx 3.5; W_1/W \approx 0.43; W/W_b \approx 1.5$$

$$(\text{Dynamic pressure at throat})/(\text{dynamic pressure at bell mouth(gas)}) \approx 2.25$$

$$(\text{Dynamic pressure at throat})/(\text{dynamic pressure at blast pipe}) \approx 0.185$$

Recovery in diffuser = 75% of dynamic pressure at throat

$$d_1/d_f \approx 2.65 \text{ (} d_f = \text{equivalent diameter of the 4 nozzles)}$$

$$d_f/d_1 \approx 0.38; (F_0 + F)/F \approx 8; d_b/d_1 \approx 1.07 \text{ (} d_b = \text{diameter of the bell mouth)}$$

$$d_f/d_b \approx 0.35; d_b/d_f \approx 2.8;$$

$$(\text{Height of mixing chamber/diameter of mixing chamber}) \approx 2.5$$

$$(\text{Chimney outlet diameter})/(\text{Throat diameter}) \approx 2; \text{Diffuser included angle} \leq 12^\circ$$

$$(\text{Draught at tuyère plane})/(\text{smokebox draught}) \approx 1.4$$

$$\text{Specific heat of steam} \approx 0.47 \text{ cal kg}^{-1} \text{ K}^{-1}; \text{Specific heat of gas} \approx 0.27 \text{ cal kg}^{-1} \text{ K}^{-1}; \text{Specific heat of steam/gas mixture} \approx 0.34 \text{ cal kg}^{-1} \text{ K}^{-1}$$

$$\text{Steam-gas mixture temperature} = 0.5(\text{steam temp.} + \text{gas temp.})$$

#### **Appendix A4 Specific volume of steam, gas and steam-gas mixture**

The steam specific volume is defined by engine performance. The latter can either be measured or, in the Mollier, the steam evolution in the cylinder represented starting from steam chest steam conditions and drawing the enthalpy drop line. Due allowance should be taken for the internal thermodynamic efficiency obtaining in the cylinder. The latter should be taken as 0.8 for modern single expansion engines and 0.88 for compounds as an average figure at high powers. Should compressibility be accounted for, the pressure at the tuyère can be obtained deducting some 1.4 smokebox draught from the atmospheric pressure. This correction may reach 10% and due account should be taken of the adiabatic temperature drop.

The gas specific volume  $v_0$  at STP (0°C, 760 mm Hg) is obtained by calculation of the performance of the boiler, better if actually measured in controlled road or plant tests. If compressibility effects are accounted for, the same corrections as for steam are applied.

The specific volume of the gas mixture  $v_1$  can be obtained by a weighted average of both the specific volume of steam  $v$  and gas  $v_b$ . An additional correction is that due to the temperature increase obtaining because of friction and shock losses in the mixing chamber. These losses are:

$$\frac{1}{2} D(W - W_1)^2 + \frac{1}{2} L(W_1 - W_b)^2 + \frac{1}{2} (D + L)W_1^2\xi \quad [\text{kg m}^2 \text{ s}^{-3}]$$

$\xi = 0.1$ ; and are to be reported to unit mass of mixture. This gives a temperature increase from which a corrected value of  $v_1$  can be obtained.

## Measurements of entrainment by axisymmetrical turbulent jets

By F. P. RICOULT AND D. B. SPALDING

Mechanical Engineering Department, Imperial College of Science and Technology, London, S.W. 7

(Received 23 November 1960)

A new technique is described for measuring the axial mass flow rate in the turbulent jet formed when a gas is injected into a reservoir of stagnant air at uniform pressure. The jet is surrounded by a porous-walled cylindrical chamber, and air is injected through the wall until the pressure in the chamber is uniform and atmospheric, a condition which is taken to signify that the 'entrainment appetite' of the jet is satisfied.

Measurements made with the apparatus have allowed the deduction of an entrainment law relating mass flow rate, jet momentum, axial distance and air density, regardless of the density of the injected gas, and including the effects of buoyancy. When the injected gas burns in the jet the entrainment rate is up to 30% lower than when it does not.

### 1. Introduction

#### *The problem*

Several accounts are available (e.g. Schlichting 1955; Pai 1954) of the turbulent jet which results from the injection of a fluid through a nozzle into a large reservoir in which a second fluid is at rest. In the present paper, attention is concentrated on one property of the jet: the mass flow rate across a section at right angles to the jet axis. This quantity will be denoted by the symbol  $m$ ; it may be related to the fluid velocity  $u$  in the axial direction, the fluid density  $\rho$ , and the radial distance  $y$  by

$$m = \int_0^\infty 2\pi \bar{\rho} u y dy, \quad (1)$$

where the over bar denotes a time-mean.

The mass flow rate  $m$  is known to increase with distance  $x$  from the nozzle. As a consequence, fluid from the surrounding reservoir is drawn radially inwards towards the jet across its conical surface; this process is known as entrainment. Entrainment is also important in many more practical situations; for example, it controls the flow patterns in combustion chambers and furnaces; it causes 'fire-storms' around large conflagrations; and many mixing devices of the chemical industry rely on entrainment for their effectiveness. If such processes are to be understood and controlled, the quantitative laws which govern the rate of entrainment, i.e. the quantity  $dm/dx$ , must be discovered.

Dimensional analysis may be employed to show that, when the fluid density is uniform, when the Reynolds number is high and when the distance  $x$  is much larger than the diameter of the orifice,  $m$  is proportional to  $x$ . More precisely, it may be demonstrated that

$$\frac{m}{x M^{\frac{1}{2}} \rho_1^{\frac{1}{2}}} = K_1, \quad (2)$$

where  $M$  stands for the excess momentum flux of the jet,  $\rho_1$  is the density of the surrounding fluid,† and  $K_1$  is a numerical constant. Consideration of Newton's Second Law of Motion shows that, since the static pressure of the flow is uniform,  $M$  must have a value which is independent of  $x$ ; it is most easily evaluated at the orifice, where the fluid has the uniform velocity  $u_0$ , from

$$M = M_0 = \frac{1}{2} \pi d_0^2 \rho_0 u_0^2. \quad (3)$$

Here  $d_0$  is the orifice diameter and  $\rho_0$  the density of the injected fluid.

The numerical magnitude of  $K_1$  can only be determined, in the present state of turbulence theory, by experimental means. Similarly, only experiment can show how equation (2) must be modified when the jet density is rendered non-uniform by a chemical reaction in the jet, or by the existence of a difference of value between  $\rho_0$  and the density of the surrounding fluid,  $\rho_1$ .

#### *Previous work*

Numerous measurements have been made of the axial-velocity profiles,  $u(y)$ , in isothermal air jets (see, for example, the bibliography compiled by Krzywoblocki 1956). These data may be inserted in equation (1), from which the mass flow rate  $m$  can then be evaluated by numerical quadrature; this has been done by Grimmer (1948), Polomik (1948) and Voorheis & Howe (1939).

Many authors have avoided the numerical quadrature by assuming that the  $u(y)$  profile has one of the forms which permit analytical integration; the velocity and radius scales appropriate to a given section are then determined from, say, the measured velocity on the axis, and the radius at which the measured velocity has half this value. The resulting values for  $m$  then depend to some extent on the profile-shape assumed.

Values for  $K_1$  obtained in this way for isothermal air jets range from about 0.22 up to 0.404, according to the investigator. The highest value, due to Schlichting (1955), is obtained by fitting to the experimental data of Reichardt (1942) a particularly full-skirted 'theoretical' curve.

The reasons for the present uncertainty about the value of  $K_1$  are of several kinds. They include the following:

(i) It is difficult to measure  $\bar{\rho}u$  at large values of  $y$  where the velocities are small and the flow may be intermittent; the presence of  $y$  as a multiplier of  $u$  in equation (1) augments the influence of inaccuracies in this region.

(ii) The above difficulty is avoided if an analytical form is chosen for the velocity profile. This choice, on the other hand, entails uncertainty as to what is the 'best' profile. Small differences in profile height at large  $y$  can greatly affect the value of  $m$  which is deduced.

(iii) Whichever of the above procedures is used, it is desirable that  $x$  should be many times greater than  $d_0$ . Since the dynamic head at a Pitot tube in the jet is proportional to  $(d_0/x)^2$ , limitations on manometer sensitivity make it difficult to work at axial distances much greater than five times the length of the potential core.

#### *Outline of the present contribution*

The above remarks show that a new method of measuring  $m$  is required, even for uniform-density flows. When jets with non-uniform density are to be studied, the case for a new method is stronger still; for a recourse to equation (1) would now necessitate measurement of a density profile as well as one of velocity, and would raise questions as to the relation of  $\bar{\rho}u$  to the measured  $\bar{p}$  and  $\bar{\rho}u^2$ .

The present paper reports a new experimental method which is not open to the objections mentioned above:  $m$  is measured more directly and simply; no integration is required. This technique is described in §2 below.

The results of the study are presented in §3 and figures 4, 5 and 7. Summarized briefly, they are: that  $K_1$  is equal to 0.282; that equation (2) holds for non-uniform density without modification provided that buoyancy effects are negligible; and that the presence of combustion reduces  $K_1$ . The role of buoyancy is not so easily summarized; it is discussed in §4.

### 2. Apparatus

#### *The principle of the method*

In the ideal free jet which is under consideration, the surrounding reservoir is large and, except in the vicinity of the jet axis, at uniform pressure; the entrained fluid flows radially inward towards the jet axis. If, however, a turbulent jet is partially enclosed by cylindrical walls, the radial inflow is impeded; the fluid entrained by the enclosed part of the jet has to flow axially in the annular space between the cylindrical wall and the conical 'boundary' of jet; the corresponding axial pressure gradients can be measured.

Now let us suppose that the cylindrical wall is made porous, and that a controlled and measured amount of fluid can be caused to flow through it in a radially inward direction. Then, if this flow is equal in quantity to that which would have passed through the area occupied by the wall if the wall had been absent, the axial pressure gradients referred to in the last paragraph will disappear.

This recognition underlies the experimental method which has been used: the flow rate through the porous wall is varied until no axial pressure gradients can be detected; this flow rate is then measured and presumed to be equal to that which would be entrained if the jet were unenclosed.

#### *Details of the apparatus*

Figure 1 shows the porous-walled chambers which were used. The axis of the jet is coincident with the axis of the cylindrical porous wall. The base of the cylinder was completely closed, apart from the orifice from which the jet originated, and the upper end of the resulting chamber was partially closed; these measures had the effect of augmenting the axial pressure gradients which prevailed when the flow through the porous wall was not 'right', while in no way interfering with the radially inward flow to the jet when it was entraining under free-jet conditions.

The porous cylinders were built up of fine-grade filter cloth on a rigid framework. A Roots-type blower was used to supply the entrainable air; this permitted the use of an appreciable pressure drop (up to 5 in. of water) across the porous cylinder and helped to ensure uniformity of inflow. Calibrated orifice plates were

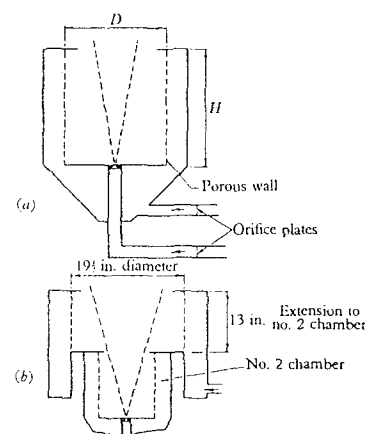


FIGURE 1. (a) Leading dimensions of three chambers. (b) Dimensions of extension to no. 2 chamber.

Entrainment chamber			
No.	1	2	3
H in.	8.7	13	3
D in.	5.8	8.9	8.9

† Now at the Laboratoire de Mécanique des Fluides, Université de Grenoble.

† The subscripts to  $\rho$  in equations (2) and (3) are not needed in the present discussion, which presumes that  $\rho$  is uniform throughout; they are nevertheless inserted for use later in the paper.

used to measure the rate of supply of this air. The orifices used were of rounded

profile, designed according to B.S.1042. Their diameters ( $d_0$ ) ranged from 0.0625 in. to 1.25 in. The corresponding range of dimensionless axial distances ( $x/d_0$ ) over which measurements could be made was from 418 to 2.4.

The axial pressure difference which was measured was that across the outlet aperture; since the pressure variations within the chamber were small, this difference can be thought of as that between the pressure in the chamber and the pressure of the atmosphere. The micromanometer used was of the direct-reading type developed by Spalding (1950).

#### Preliminary tests: the choice of aperture size

The size of the aperture in the mask at the upper end of the 'entrainment chamber' had to be chosen with care. On the one hand, it was desired that the hole should be small, since this led to an easily detected pressure difference, when the flow through the porous wall was not properly matched to the free-jet requirements; however, if the hole were made too small, the mask would interfere with the axial flow in the jet itself.

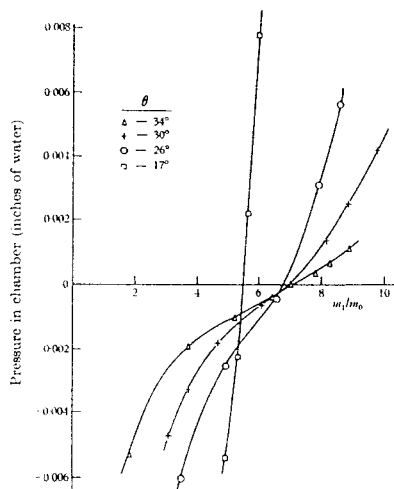


FIGURE 2. Variation of chamber pressure with flow rate through porous wall, for various apertures. Nozzle, 0.5 in. diameter;  $x/d_0 = 25.6$ ;  $u_0 = 112$  ft./sec. (No. 2 chamber.)

Figure 2 shows the results of preliminary tests leading to the choice of aperture size, the latter being expressed in terms of the angle  $\theta$  subtended by a diameter of the aperture at the centre of the base of the chamber. The ordinate is the excess pressure in the chamber; the abscissa is the ratio of the mass of air flowing through the porous wall,  $m_1$ , to the mass of gas (air) injected through the orifice,  $m_0$ ;  $m_0$ , and the orifice diameter,  $d_0$ , have the same values throughout; each curve is drawn for a different value of aperture angle  $\theta$ .

Inspection of figure 2 confirms that the smaller  $\theta$  is the more steeply the excess pressure varies with variations of  $m_1$ ; it also confirms that the aperture size influences the value of  $m_1/m_0$  which gives zero excess pressure, if  $\theta$  is too small. The latter influence is slight if  $\theta$  is  $30^\circ$  or more; thus figure 2 shows that the value of  $m_1/m_0$  corresponding to free-jet conditions for the situation in question can be taken as 7.0. These tests led to the choice of  $30^\circ$  for the aperture angle in all the tests reported below.

#### Preliminary tests: the effect of the Reynolds number

Tests were carried out, using air as the injected fluid, to establish the value of the Reynolds number above which equation (2) was valid. Some of the data are recorded in figure 3 in the form of plots of  $m_1/m_0$  versus the Reynolds number. The latter quantity is defined by

$$R \equiv \rho_0 u_0 d_0 / \mu_0. \quad (4)$$

where  $\mu_0$  is the viscosity of the injected gas. From now onwards,  $m_1$  will be used as signifying that value of the air flow rate through the porous wall which causes

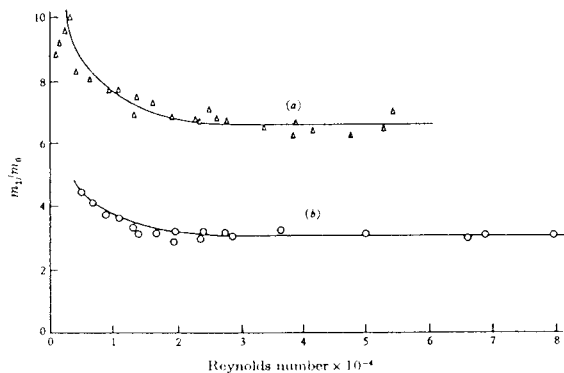


FIGURE 3. Variation of entrainment rate with the Reynolds number. (a) No. 2 chamber. Nozzle, 0.5 in. diameter;  $x/d_0 = 25.6$ . (b) No. 1 chamber. Nozzle, 0.625 in. diameter;  $x/d_0 = 13.7$ .

axial pressure gradients to disappear;  $m_1$  is therefore connected with  $m$ , the mass flow rate in a free jet of length equal to the length of the entrainment chamber, by

$$m = m_1 + m_0. \quad (5)$$

The tests of figure 3 were carried out by varying the injection flow rate, and so the Reynolds number, and then measuring the corresponding  $m_1$ . Evidently, the ratio  $m_1/m_0$  was approximately constant for Reynolds numbers in excess of  $2.5 \times 10^4$ . All test data appearing in the remainder of the paper can be taken as pertaining to Reynolds numbers greater than this value, except for those in which the injected fluid is hydrogen.

### 3. Experimental results

#### Air into air: isothermal

Experiments were made with various combinations of chamber length  $x$  and nozzle diameter  $d_0$ , when the injected gas was air at the same temperature as the air supplied through the porous wall. The results are represented by the points in figure 4 clustered near the straight line marked (a); this line may be represented by the formula

$$\frac{m}{m_0} = 0.32 \frac{x}{d_0}. \quad (6)$$

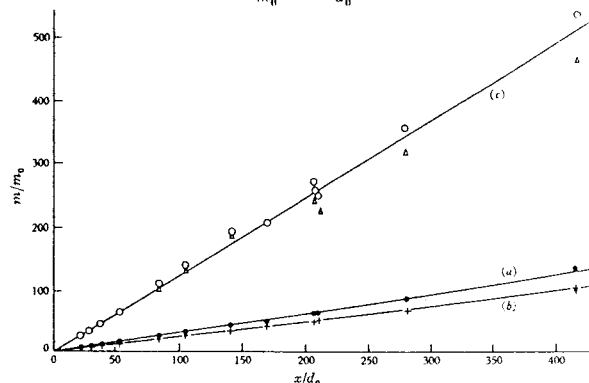


FIGURE 4. Variation of entrainment rate with axial distance for isothermal jets. Experimental results: (a) ●, air into air; (b) +, propane and carbon dioxide into air; (c) ○, hydrogen into air; (Δ), entrainment chamber inverted.

#### Heavy gas into air: isothermal

Corresponding measurements were made when the injected fluid was carbon dioxide or propane, two gases with equal densities, the temperatures being equal to that of the air supplied through the porous cylinder. The results are shown in figure 4 as a series of points clustered near the straight line marked (b); this line can be represented by the formula

$$\frac{m}{m_0} = 0.26 \frac{x}{d_0}. \quad (7)$$

Although flammable, the propane was not ignited in the experiments referred to here.

#### Light gas into air: isothermal

Figure 4 also contains results obtained by similar experiments in which hydrogen was the injected gas; the hydrogen jet was not ignited. The results are represented by the points near the straight line (c), the formula for which is

$$\frac{m}{m_0} = 1.2 \frac{x}{d_0}. \quad (8)$$

Since buoyancy was thought to affect the hydrogen jets, some experiments were carried out with the entrainment chamber inverted; it is seen that this inversion had an effect.

The high viscosity of hydrogen, and other limitations, prevented the performance of tests at Reynolds numbers in excess of 17,500.

#### Fuels into gas: combustion

Measurements were also made of the entrainment rate which prevailed when the fuel gases in the jet (propane and hydrogen) were ignited; in some cases both air and fuel were injected through the orifice simultaneously. The results of these tests, which showed a considerable effect of buoyancy, will be introduced in figure 7 below.

### 4. Discussion of results

#### Jets of uniform density

The equations (6), (7) and (8) may be cast in the form of equation (2) by introduction of equation (3) for the excess momentum flux and of a corresponding equation for the injected mass flux,  $m_0$ , namely

$$m_0 = \frac{1}{2} \pi d_0^2 \rho_0 u_0. \quad (9)$$

Equations (6), (7) and (8) then lead respectively to

$$\frac{m}{x M^{\frac{1}{2}} \rho_1^{\frac{1}{2}}} = 0.32 (1\pi)^{\frac{1}{2}} = 0.283, \quad (10)$$

$$\frac{m}{x M^{\frac{1}{2}} \rho_1^{\frac{1}{2}}} = 0.26 (\frac{1}{2}\pi)^{\frac{1}{2}} (\frac{4}{3})^{\frac{1}{2}} = 0.284, \quad (11)$$

$$\frac{m}{x M^{\frac{1}{2}} \rho_1^{\frac{1}{2}}} = 1.2 (\frac{1}{2}\pi)^{\frac{1}{2}} (\frac{2}{3})^{\frac{1}{2}} = 0.279, \quad (12)$$

wherein  $(\frac{4}{3})^{\frac{1}{2}}$  and  $(\frac{2}{3})^{\frac{1}{2}}$  represent the density ratio  $\rho_0/\rho_1$  for the respective cases of propane or carbon dioxide, and hydrogen.

Comparison of equations (10), (11) and (12) leads to the conclusion that equa-

tion (2) is valid, within the experimental error, for all the experimental results cited so far, if  $K_1$  is given the value 0.282.

The same conclusion can be expressed differently by noting that all the data can be held to obey the relation

$$\frac{m}{m_0} = 0.32 \frac{x}{d_0} \left( \frac{\rho_1}{\rho_0} \right)^{\frac{1}{2}} \quad (13)$$

This is illustrated by figure 5, which contains the data of figure 4 replotted in the manner indicated by equation (13).

#### The effect of buoyancy: theory

When the density of the fluid in the jet differs from that of the surrounding air, hydrostatic forces cause the excess momentum flux to increase with  $x$  (assuming that the jet fluid is the lighter and that the flow direction is upward). Consequently equation (2) no longer correctly expresses the variation of  $m$  with  $x$ .

Dimensional analysis indicates that, when  $x$  becomes very large,  $m$  is proportional to  $x^{\frac{1}{2}}$  (Batchelor 1954); for this to hold, however, the excess momentum flux of the jet,  $M$ , must greatly exceed the value of  $M_0$  defined by equation (3). How should  $m$  vary with  $x$  when  $M$  and  $M_0$  are of the same order?

A tentative answer to this question may be obtained by supposing that the local rate of entrainment is uniquely related to the local excess momentum flux in accordance with the differential equation

$$\frac{1}{(M\rho_1)^{\frac{1}{2}}} \frac{dm}{dx} = 0.282. \quad (14)$$

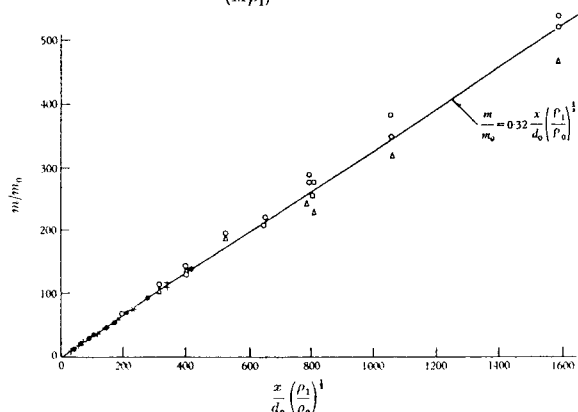


FIGURE 5. Entrainment rate for isothermal jets. Experimental results: (a) ●, air into air; (b) +, propane and carbon dioxide into air; (c), ○, hydrogen into air; (Δ), entrainment chamber inverted).

An assumption of this character has been made by Morton, Taylor & Turner (1956), and other authors, in connexion with the rise of turbulent plumes in the atmosphere.

In an unpublished study, one of the present authors has investigated the implications of equation (14), when combined with the assumptions: (i) that the velocity and temperature profiles are Gaussian, (ii) that the ratio of the widths of the temperature and velocity profiles is equal to 1.17 for all  $x$ , (iii) that chemical reaction is confined to regions of the jet which are much closer to the orifice than is the section  $x$ . The results of this study are represented by the curve of figure 6; the ordinate and abscissa quantities of this graph are self-explanatory apart from the Froude number,  $F$ , which is defined by:

in the absence of chemical reaction,

$$F \equiv \frac{c_1 T_1}{(h_0 - h_1) g d_0} \frac{u_0^2}{\rho_0} \left( \frac{\rho_1}{\rho_0} \right)^{\frac{1}{2}} \quad (15)$$

or, when chemical reaction occurs,

$$F \equiv \frac{c_1 T_1}{m_{fu} H + c_0 (T_0 - T_1) g d_0} \frac{u_0^2}{\rho_0} \left( \frac{\rho_1}{\rho_0} \right)^{\frac{1}{2}} \quad (16)$$

Here the symbols signify:

$c$	specific heat of gas at constant pressure,
$T$	absolute temperature of air,
$h$	enthalpy,
$g$	gravitational acceleration,
$m_{fu}$	mass fraction of fuel in injected gas,
$H$	heat of combustion of fuel,

and subscripts 0 and 1 refer, as before, to the injected fluid and to the surrounding air respectively.

#### The effect of buoyancy: experiment

Figure 7 presents the data of figure 4 (upward flow only) together with the results of measurements made with burning jets. Also drawn for comparison is the curve of figure 6. The following features are evident.

- The data points lie close to the curve in the forced-convection régime; this, of course, is to be expected from figure 5, for example.
- The influence of increasing buoyancy predicted by the theoretical curve, viz. an increased slope in the upper right corner, is exhibited by the experimental data. It is chiefly the hydrogen diffusion-flame data which are in question here.
- Some of the data points, particularly those for pre-mixed hydrogen-air jets, lie well below both the curve and its forced-convection asymptote.
- The scatter is considerable.

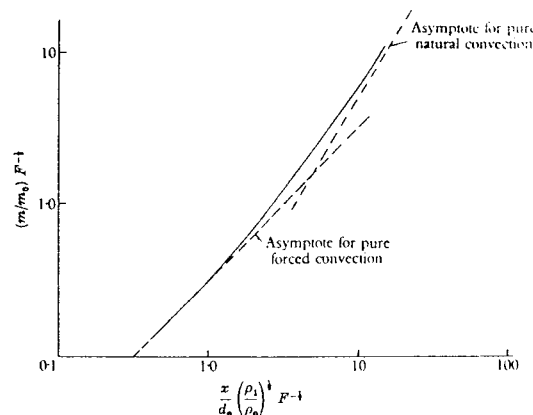


FIGURE 6. Theoretical prediction of entrainment in buoyant jets.

#### Comparison with previous work

It has already been stated that, in the absence of buoyancy,  $K_1$  has been found by previous authors to lie between 0.22 and 0.404; the value obtained from the present work, viz. 0.282, can therefore be said to lie near the middle of the range of earlier values. The ease with which the measurements were made, in the present

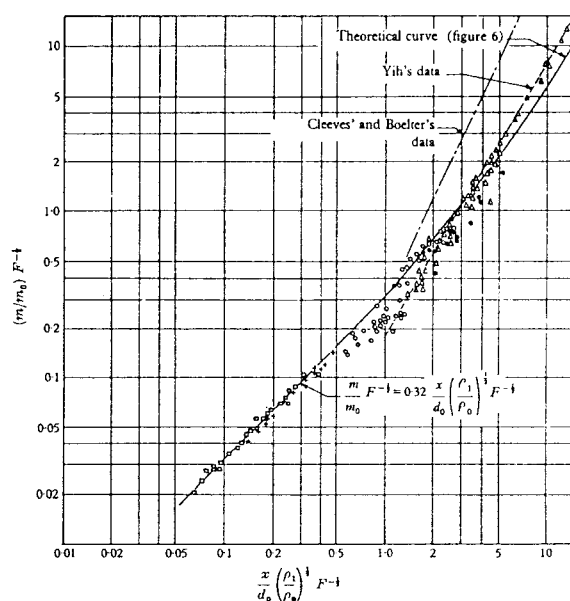


FIGURE 7. Entrainment by buoyant jets and flames. +, Unburnt propane jet; □, unburnt hydrogen jet; ○, pre-mixed air-hydrogen flame; Δ, hydrogen diffusion flame; ●, propane diffusion flame.

investigation, together with the straightforwardness of their interpretation, leads us to believe that the present value of  $K_1$  is the most reliable established so far.

The finding that equation (2) holds, in the absence of buoyancy effects, for jets of non-uniform density was expected; it accords with the surmise of Squire & Trouncer (1944), and with the suggestion of Thring & Newby (1953), that the characteristic length of a turbulent jet is not  $d_0$  but  $d_0(\rho_0/\rho_1)^{\frac{1}{2}}$ .

Other authors who have presented experimental data for the natural convection régime include Yih (1951), and Cleaves & Boelter (1947); the data of these authors are represented on figure 7 by broken straight lines which have been plotted by ignoring experimental scatter and assuming Gaussian velocity and temperature profiles.

The data of Yih agree fairly well with the present hydrogen diffusion-flame data; both sets lie appreciably above the theoretical curve, indicating that the entrainment rate is greater in a buoyant jet than a non-buoyant one of the same excess momentum. The data of Cleaves & Boelter show the same tendency to an even more marked degree; they are, however, probably the least reliable of the data on figure 7, being appreciably influenced by potential-core effects.

#### 5. Conclusions

(a) The new experimental technique for measuring the rate of entrainment by a turbulent jet was found to be easy to use, and to be applicable to jets of non-uniform density and to larger values of  $x/d_0$  than had previously been investigated.

(b) The constant  $K_1$  of equation (2) was found to have the value 0.282, irrespective of the density ratio.

(c) The curve of figure 6, based on the entrainment assumption expressed by equation (14), represents approximately the influence of buoyancy on the entrainment. However, it must be noted that: (i) there is a tendency for the curve to predict too low an entrainment rate in the natural-convection régime; (ii) the curve predicts too high an entrainment rate for some flames; (iii) the experi-



mental scatter of the results of the present and earlier work in the natural convection régime precludes the drawing of firm conclusions at present.

One of the authors (F. P. R.) acknowledges the financial support of the States of Jersey Committee of Education, and of Thomas Hedley and Company, Ltd.

This research was supported by a contract between Imperial College and the National Engineering Laboratory; the Director of the N.E.L. has given his permission for publication.

#### REFERENCES

- BATCHELOR, G. K. 1954 *Quart. J. Roy. Met. Soc.* 80, 339.  
 CLEEVES, V. & BOELTER, L. M. K. 1947 *Chem. Engng Progr.* 43, 123.  
 GRIMMETT, H. L. 1948 M.S. Thesis, University of Illinois.  
 KRZYWOBLOCKI, M. Z. 1956 *Jet Prop.* 26, 760.  
 MORTON, B. R., TAYLOR, G. J. & TURNER, J. S. 1950 *Proc. Roy. Soc. A*, 234, 1.  
 PAI, S. I. 1954 *Fluid Dynamics of Jets*. New York: Van Nostrand.  
 POLOMIK, E. E. 1948 M.S. Thesis, University of Illinois.  
 REICHARDT, H. 1942 *V.D.I.-Forschungsheft*, p. 414. (2nd ed. 1951).  
 SCHLICHTING, H. 1955 *Boundary Layer Theory*. London: Pergamon Press.  
 SPALDING, D. B. 1950 *J. Sci. Instrum.* 27, 310.  
 SQUIRE, H. B. & TROUNCER, J. 1944 Round jets in a general stream. *Aero. Res. Coun. Tech. Rep.* R. & M. no. 1974.  
 THIRING, M. W. & NEWBY, M. P. 1953 *Fourth Symposium on Combustion*, p. 789. Baltimore: Williams and Wilkins.  
 VOORHEIS, T. S. & HOWE, E. D. 1939 *Proc. Pac. Coast Gas Ass.* 30, 198.  
 YIH, C. S. 1951 *Proc. First U.S. Nat. Congr. Appl. Mech.* p. 941.

Bulletin of JSME

Vol. 12, No. 53, 1969

pp. 1153-1162

621. 694. 2: 621. 43-71

### Application of Exhaust Gas Ejector to Engine Cooling\*

By FUJIO NAGAO\*\*, YUZURU SHIMAMOTO\*\*\*, MITSUO SHIKATA†, and HIROYUKI TOYOFUKU††

Although exhaust gas ejectors have been little utilized in engines, their application is worthy of consideration because of their basic simplicity. An application for engine cooling has been investigated using a four-stroke cycle Diesel engine and an air model. Following results are obtained:

- (1) The cooling air for an engine may be supplied only from the ejector which is well designed. Fuel consumption can be decreased by using the ejector together with a fan for engine cooling.
- (2) Flow rate of air induced into the ejector becomes larger with an increase in engine load. However, flow rate per unit horse power becomes smaller.
- (3) Flow rate of secondary fluid for the ejector, whose driving fluid is intermittently supplied, is much larger than that for the ejector of steady state, because the inertia effect of fluid in the ejector is a useful factor to draw the secondary fluid.

#### 1. Introduction

As one of the methods to utilize the exhaust gas energy of internal combustion engines, it has been taken into consideration to apply an exhaust gas ejector for engine cooling and others<sup>(1)(2)</sup>. Since the necessary power for driving the fan of a small air-cooled engine is not small, the use of the ejector, in which the exhaust gas energy is employed as the activating force, instead of the fan may increase the engine output and then reduce considerably the fuel consumption. The ejector ensures reliability, because its structure is basically simple and has no moving part. Further, one of the advantages claimed for the ejector is that the flow rate of air induced into the ejector becomes larger with an increase in engine load, bringing the better cooling effect on the engine. However, the ejector has defective points in suction cooling system, and moreover there are many problems which must be solved, for instance, the exhaust noise, etc.

In this paper, fitting the exhaust pipe end of a four-stroke cycle Diesel engine with an ejector, the relation between the dimensions of ejector and the flow rate of induced air has been experimentally

investigated. Further, since it is not easy to measure accurately the rapidly changing temperature of exhaust gas, an air model has been used to compare the performance of the ejector, whose driving fluid is intermittently supplied, with that of the ejector of steady state. Through theoretical analysis and experiment, the reason why the performance of the ejector of pulsative state is different from that of steady state has been made clear.

#### 2. Experiment with an engine

##### 2-1 Test procedure

The schema of apparatus is shown in Fig. 1. The four-stroke cycle engine used is a Yanmar A2 air-cooled Diesel engine (cylinder bore × stroke = 60 mm × 66 mm, normal output 2 PS/2 600 rpm) which

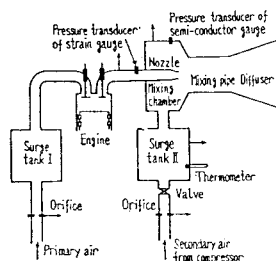


Fig. 1 Schema of experimental apparatus (engine test)

#### 68-WA/FE-33

A Mathematical Model for the Prediction of the Induced Flow in a Pulsejet Ejector With Experimental Verification, by W. S. Johnson, The University of Tennessee, Knoxville, Tenn., and T. Yang, Clemson University, Clemson, S. C., Assoc. Mem. ASME.

This paper deals with the determination of the induced flow in a pulsejet-type ejector. The momentum and continuity equations are solved by the method of characteristics and a mathematical model is set up to allow analytical predictions of performance.

Experimental results are presented and the resulting agreement between the experimental and analytical results indicate that the model is valuable in predicting the induced flow rates involved. Parametric studies indicate how the induced flow is influenced by some of the more significant variables, and show that the characteristics of the primary jet are of major significance.

is coupled with an electric dynamometer. An ejector is fitted to the end of the exhaust pipe, the inner diameter of which is 27.4 mm. The length of exhaust pipe, which is represented by the distance between the pipe end and the exhaust valve, is 150 mm. The details of ejector are shown in Fig. 2. The dimensions of ejectors have been decided on referring to the data concerning the ejectors of steady state<sup>(3)-(5)</sup>. Various area ratio of the mixing pipe to the nozzle  $m$  can be taken for the experiment by changing the combination of the nozzle and the mixing pipe shown in Table 1. The inlet diameter of mixing chamber is 40.8 mm. The exhaust gas is discharged from the ejector into the exhaust chamber of large volume through the pipe, which is 500 mm long and has the same diameter as that of the diffuser outlet.

As shown in Fig. 1, the flow rate of air induced into the engine and the secondary flow rate of ejector are measured with a sharp edge orifice respectively. Rectangular surge tanks of large volume are used to avoid the influence of pressure pulsation on the orifices. Three faces of the tanks are made of rubber membrane. The flow rate of secondary air is controlled with the valve placed between the surge tank II and the orifice.

The dynamic energy of exhaust gas as the activating force of ejector can be calculated from the gas temperature and the pressure at the nozzle inlet. However, knowing its accurate value is not easy because of the difficulty of the measurement of the changing gas temperature. In this experiment, in order to measure the dynamic energy, only the nozzle of ejector is fitted to the exhaust pipe and the exhaust gas is ejected into the cage of pendulum type<sup>(6)</sup>. Using the thrust of gas measured with the cage, the dynamic energy  $E_d$ , which is equivalent to the energy of primary flow of the ejector, is given by

Table 1 Dimensions of ejector

Nozzle diameter	mm	7, 9, 11, 13
Mixing pipe diameter	mm	12.6, 15.7, 21.3, 27.4, 35.5, 43.8, 52.8
Diffuser		
Area ratio of outlet to inlet		6
Cone angle	deg	8

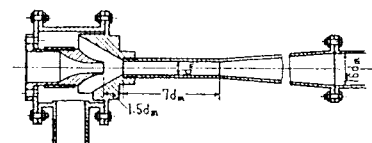


Fig. 2 Exhaust gas ejector

\* Received 21 st June, 1968.

\*\* Professor, Faculty of Engineering, Kyoto University.

\*\*\* Professor, School of Engineering, Okayama University, Okayama.

† Engineer, Yanmar Diesel Engine Co. Ltd.

†† Engineer, Kobe Manufacturing Divisions, Kawasaki Aircraft Co. Ltd.

$$E_1 = \frac{gT}{2(G_1 + B)} \quad (1)$$

where:  $B$ : fuel consumption rate

$g$ : gravitational acceleration

$G_1$ : mass flow rate of air induced into the engine

$T$ : thrust

On the other hand, the theoretical work  $E_2$  to induce the secondary air into the ejector is defined as the work to compress adiabatically the secondary air from the mean pressure  $p_{m2}$  in the mixing chamber to the atmospheric pressure  $p_0$ . By neglecting the gas velocity at the diffuser outlet, we obtain

$$E_2 = \frac{\kappa}{\kappa - 1} G_2 RT_{m2} \left[ \left( \frac{p_0}{p_{m2}} \right)^{\frac{\kappa - 1}{\kappa}} - 1 \right] \quad (2)$$

where:  $G_2$ : mass flow rate of secondary air of the ejector

$R$ : gas constant

$T_{m2}$ : mean absolute temperature in the mixing chamber

$\kappa$ : ratio of specific heats

Then, the efficiency of ejector  $\eta$  is defined as  $\eta = E_2/E_1$  (3)

## 2.2 Experimental results and considerations

Figure 3 shows the dynamic energy of exhaust gas per unit weight  $E_1/(G_1 + B)$ , and the secondary flow rate of ejector which is measured by keeping the mean pressure in the mixing chamber constant. The larger engine load gives the larger dynamic energy, causing about an increase in the mass flow rate of secondary air. However, the mass flow rate of secondary air per unit horse power decreases with an increase in the engine load, because the increase

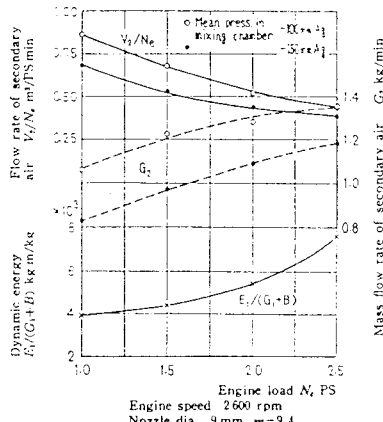


Fig. 3 Relation between engine load and ejector performance

in the dynamic energy is not proportional to that in the load. In the case of maintaining the cooling air only with an ejector instead of a fan, the secondary air of ejector is induced into the mixing chamber through the passage of constant area between the cooling fins and the cover of engine. Therefore, the mean pressure in the mixing chamber is varied with the change in the secondary flow rate. Figure 4 shows the relation between the engine load and the secondary flow rate which is obtained by keeping the pressure in the surge tank II atmospheric. Since the secondary flow rate per unit horse power increases with a decrease in the load, the ejector, which is designed so as to maintain an adequate flow rate of cooling air at the normal engine output, may supply the enough flow rate at low engine load, too.

The performance of ejector at the normal engine output of 2 PS is shown in Fig. 5. It is common to the exhaust gas ejector and the ejector of steady state that the mean pressure in the mixing chamber becomes lower with a decrease in the mass flow ratio of secondary flow to primary one  $G_2/G_1$ . As the larger dynamic energy of exhaust gas is produced by the smaller nozzle, the mass flow ratio at a constant pressure in the mixing chamber shows a tendency to be increased by the reduction of the nozzle diameter. There is an optimum mass flow ratio, at which the ejector efficiency reaches a maximum. In the case of applying the ejector for engine cooling, however, to increase the mass flow rate of secondary air is more important than to operate the ejector with high efficiency.

The area ratio of the mixing pipe to the nozzle has a remarkable influence upon the flow rate of secondary air. The results obtained by keeping the pressure in the surge tank II atmospheric are shown in Fig. 6. Both the maximum value of the flow rate of secondary air and the optimum area ratio,

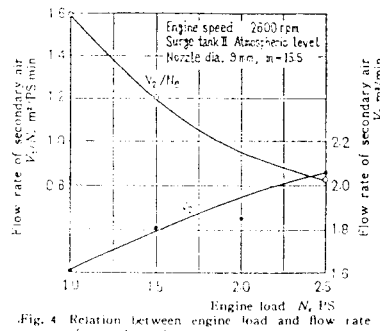


Fig. 4 Relation between engine load and flow rate of secondary air

at which the flow rate reaches a maximum, become larger with a decrease in the nozzle diameter, because of the increase in the exhaust gas energy. If the inlet of the mixing chamber is made wide enough to reduce the negative pressure in it, the secondary flow rate may become larger than that in Fig. 6. The secondary flow rate and the specific fuel consumption under the condition of the optimum area ratio have been measured for various nozzle areas. Figure 7 shows the results obtained. Specific fuel consumption has been calculated from the effective engine output, which is modified by adding the power spent to drive the fan. The dotted line in Fig. 7 represents the specific fuel consumption of the engine which is cooled only by the fan. Since the flow rate of air required to cool the engine is supposedly  $0.62 \sim 1.7 \text{ m}^3/\text{PS} \cdot \text{min}^{(7)}$ , it may be possible to maintain the necessary flow rate only using

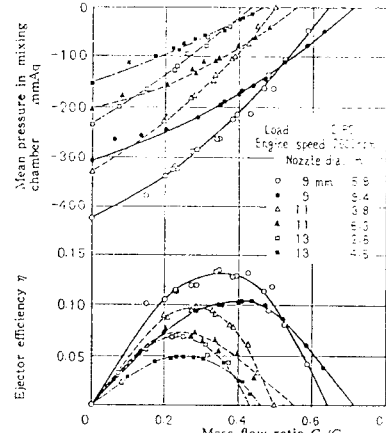


Fig. 5 Performance of ejector

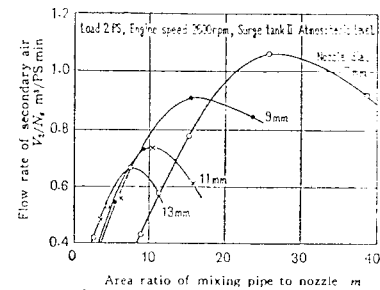


Fig. 6 Influence of area ratio of mixing pipe to nozzle

the ejector. If the ejector and the flow passage of cooling air are designed reasonably, the fuel consumption and the effective output of engine may be improved by the use of the ejector instead of the fan.

The pressure at the nozzle inlet and the pressure in the mixing chamber have been measured by pressure transducers of strain gauge type and semiconductor gauge type, respectively. Examples of recordings by a synchroscope are shown in Fig. 8. The pressure at the nozzle inlet is increased rapidly due to the blow down of exhaust gas, and after reaching a maximum, it decreases. During the discharge stroke of engine, the rise of pressure occurs again by the movement of piston. The pressure in the mixing chamber is kept positive during the early period of the blow down due to the occurrence of the reverse flow of exhaust gas, and thereafter it is lowered by the suction effect of ejector. After the exhaust valve has been closed and the pressure at

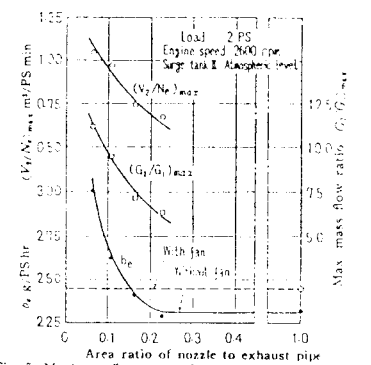


Fig. 7 Maximum flow rate of secondary air  $(V_2/N_2)_{\max}$  and specific fuel consumption  $b_1$

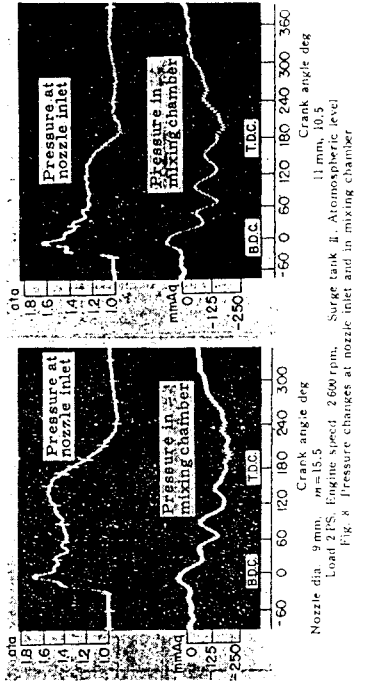


Fig. 8

the nozzle inlet has become atmospheric, the negative pressure in the mixing chamber is maintained by the inertia of gas in the ejector. The secondary air continues to flow into the ejector, while the pressure in the mixing chamber is kept negative. Therefore, it is evident that the performance of the exhaust gas ejector, whose primary flow is pulsative, is very different from that of the ejector of steady state.

## 3. Experiment with an air model

In the engine test, it is difficult to measure accurately the dynamic energy of the exhaust gas as the activating force of ejector. Therefore, an air model has been used to investigate the performance of the ejector of pulsative state in comparing it with the performance of the ejector of steady state.

### 3-1 Test procedure

The schema of apparatus is shown in Fig. 9. The piston and the connecting rod of the engine are removed, and the cylinder is replaced with a cylindrical vessel of volume of  $225 \text{ cm}^3$ . Only the exhaust and inlet valves, whose opening periods are made a little shorter by increasing the valve

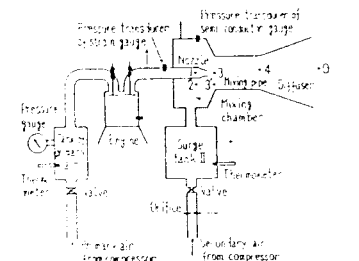


Fig. 9 Schema of experimental apparatus with air model

clearances in order to avoid the valve over-lap, are operated by an electric motor. The compressed air in the cylindrical vessel, which is supplied through the tank of primary air during the opening period of inlet valve, is discharged into the ejector through the exhaust pipe by opening the exhaust valve. Thus, the flow state similar to the blow down is produced in the ejector. The ejectors used are the same as those in the engine test. Keeping the pressure in the surge tank II atmospheric by controlling the valve, the mass flow rate of secondary air of the ejector  $G_2$  can be measured with the orifice. In order to know the flow rate of air discharged from the vessel, the pressure  $p_{e1}$  at the exhaust valve opening and the pressure  $p_{e2}$  at its closing are respectively measured with a pressure transducer of strain gauge type. The mass flow rate of primary air of the ejector  $G_1$  is given by

$$G_1 = \frac{n}{120} \frac{p_{e1} V_c}{RT_{e1}} \left\{ 1 - \left( \frac{p_{e2}}{p_{e1}} \right)^{1/\kappa} \right\} \quad (4)$$

where,  $n$ : revolving speed of model, rpm

$T_{e1}$ : absolute temperature of air in the vessel at the exhaust valve opening

$V_c$ : volume of the vessel

The mass flow rate calculated from Eq. (4) has been calibrated in comparing it with the mass flow rate measured with the orifice. The difference between two mass flow rates is within 5%.

In the case of testing the ejector of steady state, the model engine in Fig. 9 is removed and an orifice is installed between the ejector and the tank of primary air. The mass flow rate of primary air has been controlled with the valve so as to keep the Mach number at the nozzle outlet  $M_3$  constant. Mach number  $M_3$  can be calculated from the following equation.

$$M_3 = \sqrt{\frac{2}{\kappa - 1} \left( \left( \frac{p_1}{p_2} \right)^{1/\kappa} - 1 \right)} \quad (5)$$

where,  $p_1$ ,  $p_2$ : pressures at the nozzle inlet and the outlet, respectively.

### 3.2 Experimental results and considerations

The relation between the mass flow ratio of ejector and the area ratio of the mixing pipe to the nozzle has been investigated by changing the diameter of mixing pipe. The results obtained are shown in Fig. 10. There is an optimum area ratio at which the mass flow ratio becomes maximum. When a high pressure in the tank of primary air is used, the pressure at the nozzle inlet exceeds the critical value. The ejector with the divergent nozzle, which is designed with the theoretical Mach number of 1.2 at the nozzle outlet, has been investigated. Its mass flow ratios are shown with the dotted lines in Fig. 10. The deviation of mass flow ratio to the use of the divergent nozzle is scarcely seen. The pressures at the nozzle inlet and

in the mixing chamber have been measured with the same procedure as that of the engine test. An example of the changes of the pressures recorded is shown in Fig. 11. At the beginning of the blow down of primary air, the pressure in the mixing chamber increases, for a while, due to the reverse flow of primary air. Thereafter it is decreased by the ejector effect, becoming negative. After the end of the discharge of air from the vessel, the negative pressure in the mixing chamber is kept by the inertia of air in the ejector, and accordingly the secondary air continues to flow into the ejector. The above tendency of the pressure change in the mixing chamber is similar to that of the pressure change in Fig. 8. The dynamic energy of primary air per unit weight becomes smaller with a decrease in the tank pressure of primary air, that is, the pressure at the nozzle inlet. However, the mass flow ratio of secondary air to primary air increases as clearly

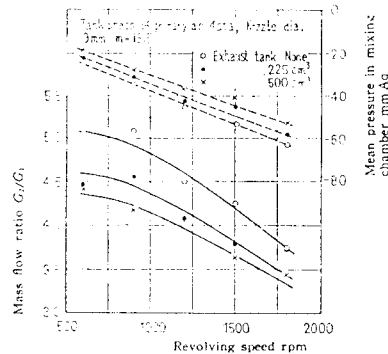


Fig. 12 Influence of revolving speed of air model

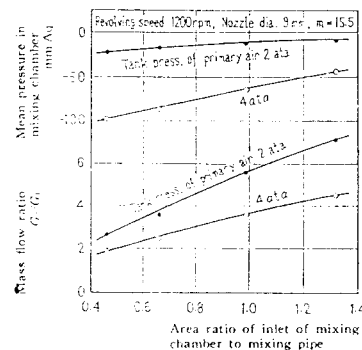


Fig. 13 Influence of inlet area of mixing chamber (air model test)

known from Fig. 10. Figure 12 is the mass flow ratio which has been obtained by changing the revolving speed of model engine under the condition of a constant tank pressure of primary air. The mass flow ratio increases with a decrease in the revolving speed. If the tank pressure or the revolving speed is made lower, both the mass flow rate of primary air and the dynamic energy per unit weight are decreased. In order to reduce the dynamic energy under the condition of a constant mass flow rate of primary air, the volume of exhaust tank is made large by subjoining an exhaust tank. In this case, the mass flow ratio becomes smaller with an increase in the volume of exhaust pipe as shown in Fig. 12.

The narrower inlet of mixing chamber brings about both the larger negative pressure in the mix-

ing chamber and the smaller flow rate of secondary air. Therefore, it is advisable to make the inlet of mixing chamber wide in order to increase the flow rate. In Fig. 13 the mass flow ratio and the mean pressure in the mixing chamber are shown by

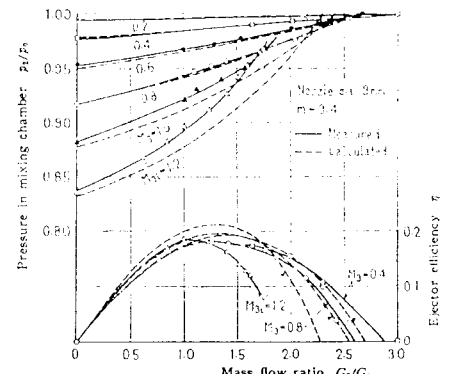


Fig. 14 Performance of ejector at state of steady flow

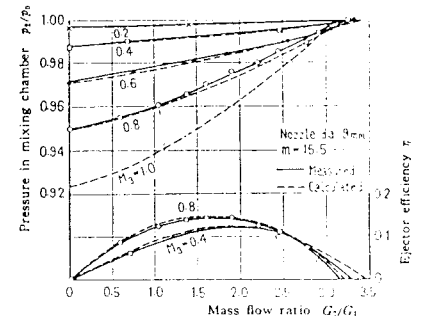


Fig. 15 Performance of ejector at state of steady flow

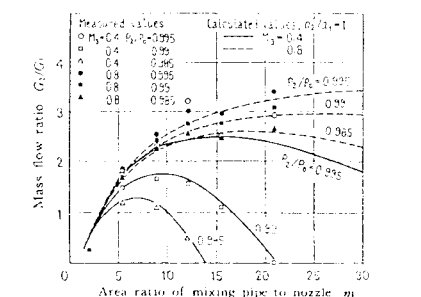


Fig. 16 Influence of area ratio of mixing pipe to nozzle in case of ejector of steady state

changing the inlet area.

The performance of the ejector of steady state is shown in Figs. 14 and 15. The pressure in the mixing chamber is represented as the ratio  $p_2/p_1$  of the pressure in the mixing chamber  $p_2$  to the atmospheric pressure  $p_1$ . The mass flow ratio for each Mach number  $M_3$  becomes maximum at  $p_2/p_1 = 1$ . These maximum values are below the mass flow ratios which are obtained in Fig. 10 for the same area ratio of the mixing chamber to the nozzle as that in Figs. 14 and 15. Therefore it is clearly known that the mass flow ratio produced in the ejector of pulsative state is much larger than that in the ejector of steady state. Figure 16 shows the influence of the area ratio. The optimum area ratio, which produces a maximum mass flow ratio, becomes larger with an increase in the pressure in the mixing chamber or with an increase in the air velocity at the nozzle outlet.

### 4. Theoretical analysis of ejector performance

Hitherto, many analytical studies on the ejector of steady state have been published<sup>(10)(11)(12)</sup> and the performance of ejector calculated theoretically has well agreed with the measured performance. In this paper, the theoretical equations, with which the operational characteristics of the ejector of steady state can be estimated, has been worked out by taking the losses in the mixing pipe and the diffuser into consideration, and thereafter the reason why the ejector performance of pulsative state is different from that of steady state has been investigated

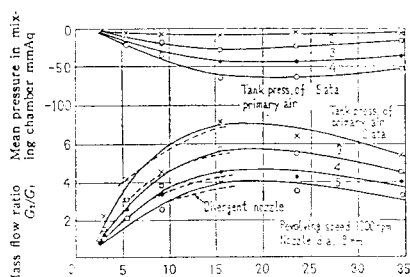


Fig. 10 Influence of area ratio of mixing pipe to nozzle (air model test)

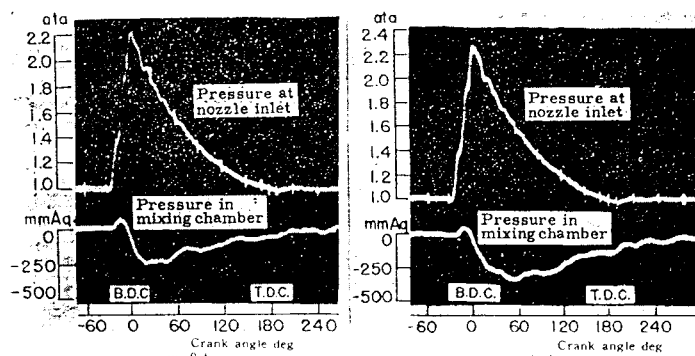


Fig. 11 Pressure changes at nozzle inlet and in mixing chamber (air model test)

## 4.1 Main notations

- $a$ : sonic velocity  
 $f_m$ : inlet area of mixing chamber  
 $f_n$ : inlet area of nozzle  
 $\bar{G}$ : momentary mass flow rate in non-dimensional form  
 $m$ : area ratio of the mixing pipe to the nozzle  
 $m_{opt}$ : optimum area ratio of the mixing pipe to the nozzle at which the mass flow ratio becomes maximum  
 $M$ : mach number  
 $p$ : pressure  
 $t$ : time  
 $T$ : absolute temperature  
 $\epsilon$ : loss coefficient of the mixing pipe  
 $\eta_d$ : diffuser efficiency  
 $\mu$ : mass flow ratio of secondary fluid to primary fluid

## Suffixes

- 0: atmospheric state  
 1: state at the nozzle inlet  
 2: state in the mixing chamber  
 3: state of primary fluid at the outlet of nozzle  
 3': state of secondary fluid at the inlet of mixing pipe  
 4: state at the diffuser outlet

## 4.2 Theoretical equations

It may be assumed in Fig. 9 that the primary and secondary fluids entering the mixing pipe are mixed completely and, after being transformed into a flow with a uniform velocity distribution, they go into the diffuser. Neglecting the heat exchange between the fluids and the wall of ejector, the equations of continuity, momentum, and energy in the mixing pipe are given respectively by

$$p_3 \frac{M_3}{a_3} + (m-1)p_2 \frac{M_2}{a_2} = m p_4 \frac{M_4}{a_4} \quad (6)$$

$$p_3(1 + \kappa M_3^2) + (m-1)p_2(1 + \kappa M_2^2) = m p_4(1 + \kappa M_4^2) \quad (7)$$

$$\left(1 + \frac{\kappa-1}{2} M_3^2\right) a_3^2 + \mu \left(1 + \frac{\kappa-1}{2} M_2^2\right) a_2^2 = (1 + \mu) \left(1 + \frac{\kappa-1}{2} M_4^2\right) a_4^2 \quad (8)$$

Mass flow ratio  $\mu$  can be written as follows:

$$\mu = (m-1) \frac{p_2}{p_3} \frac{M_2}{M_3} \frac{a_2}{a_3} \quad (9)$$

Eliminating  $a_4$ ,  $M_4$ , and  $M_2$  from Eqs. (6) ~ (9) and considering that the pressure ratio  $p_2/p_1$  is positive, we obtain

$$\frac{p_2}{p_1} = \frac{\epsilon \sqrt{\kappa^2 B^2 - (\kappa-1)((2\epsilon-1)\kappa+1)A - ((\epsilon-1)\kappa+1)B}}{\kappa(\kappa-1)(B^2 - \epsilon^2 A)} \quad (10)$$

$$\text{where, } A = \frac{2}{\kappa-1} \frac{1+\mu}{m^2} M_3^2 \left[1 + \frac{\kappa-1}{2} M_3^2 + \mu \left(1 + \frac{\kappa-1}{2} \left(\frac{\mu}{m-1} \frac{p_2}{p_1} \frac{a_2}{a_3}\right)^2\right) M_3^2 \left(\frac{a_2}{a_3}\right)^2\right] \quad (11)$$

$$B = \frac{1}{\kappa m} \left[1 + \kappa M_3^2 + (m-1) \frac{p_2}{p_3}\right] \times \left[1 + \kappa \left(\frac{\mu}{m-1} \frac{p_2}{p_1} \frac{a_2}{a_3}\right)^2 M_3^2\right] \quad (12)$$

In the case of the inlet pressure of nozzle below the critical value, the outlet pressure of nozzle  $p_3$  is equal to the inlet pressure of mixing pipe  $p_2$ . Then,

$$\frac{p_2}{p_3} = 1 \quad (13)$$

When the inlet pressure of nozzle is over the critical value, the outlet pressure of nozzle  $p_3$  is higher than the inlet pressure of mixing pipe  $p_2$ . Using the imaginary Mach number  $M_{31}$ , which is obtained by expanding adiabatically the primary fluid from  $p_3$  to  $p_2$ , the pressure ratio  $p_2/p_3$  is given as follows:

$$\frac{p_2}{p_3} = \left\{ \frac{2}{\kappa+1} \left(1 + \frac{\kappa-1}{2} M_{31}^2\right) \right\}^{1/(\kappa-1)} \quad (14)$$

If the diffuser efficiency  $\eta_d$  is given, the ratio of the pressure at the diffuser inlet to that at the outlet  $p_4/p_3$  can be calculated by the following equation<sup>(10)</sup>:

$$\left(\frac{p_4}{p_3}\right)^{(\kappa-1)/\epsilon} = 1 + \frac{\kappa-1}{2} \eta_d M_4^2$$

Eliminating  $a_4$ ,  $M_4$ , and  $M_2$  from the above equation and Eqs. (6) ~ (8), we obtain

$$\frac{p_2}{p_3} = \left\{1 + \frac{\kappa-1}{2} \frac{\eta_d}{\epsilon} \left(\frac{p_2}{p_1} \frac{B}{\kappa}\right)^{1/(\kappa-1)}\right\}^{1/(\kappa-1)} \quad (15)$$

Under the assumption that the change of state is adiabatic and the fluid velocity in the mixing chamber is negligible, the relation between the pressure in the mixing chamber  $p_2$  and the inlet pressure of mixing pipe  $p_1$  is given by

$$\frac{p_2}{p_1} = \left\{1 + \frac{\kappa-1}{2} \left(\frac{\mu}{m-1} \frac{p_2}{p_1} \frac{a_2}{a_3}\right)^2 M_3^2\right\}^{1/(\kappa-1)} \quad (16)$$

The following equation concerning the inlet pressure of nozzle  $p_1$  is given under the assumption of the adiabatic change of state.

$$\frac{p_1}{p_0} = \left\{1 + \frac{\kappa-1}{2} M_1^2\right\}^{1/(\kappa-1)} \frac{p_2}{p_1} \frac{a_2}{a_0} \quad (17)$$

In this analysis, the losses in the nozzle and in the mixing chamber are included in the loss coefficient of mixing pipe  $\epsilon$ .

Assuming  $a_2 \approx a_1$ , the sonic velocity ratio of secondary fluid to primary one  $a_2/a_1$  at the inlet of mixing pipe is given by

$$\frac{a_2}{a_1} = \sqrt{1 + \frac{\kappa-1}{2} M_2^2} \frac{a_2}{a_1} \quad (18)$$

Solving simultaneously Eqs. (10) ~ (18) with the given values of  $m$ ,  $\epsilon$ ,  $\eta_d$ ,  $a_2/a_1$ , and  $p_1/p_0$ , the relation between the pressure in the mixing chamber  $p_2/p_0$  and the mass flow ratio  $\mu$  is obtained. Instead of  $p_1/p_0$ ,  $M_1$  can be used as one of the parameters; the values of which must be given for solving the equations.  $p_2/p_0$  may be transformed as follows:

$$\frac{p_2}{p_0} = \frac{p_2}{p_1} \frac{p_1}{p_0} \frac{p_1}{p_1} \frac{p_1}{p_0} \quad (19)$$

The efficiency of ejector  $\eta$  is given by

$$\eta = \mu \left(\frac{a_2}{a_1}\right)^2 \frac{1 - (p_2/p_0)^{(\kappa-1)/\epsilon}}{(p_1/p_0)^{(\kappa-1)/\epsilon} - 1} \quad (20)$$

The measured diffuser efficiency  $\eta_d = 0.7$  is used for the calculations. The following experimental formula on the loss coefficient  $\epsilon$  has been adopted in order to make the calculated results agree with the experimental ones which are obtained in the ejector of steady state.

$$\epsilon = 1.026 + 0.0251m \quad (21)$$

$\epsilon = 1$  corresponds with the state in which no loss is produced in the mixing pipe.

## 4.3 Results calculated on the ejector of steady state

Taking  $\kappa = 1.4$  and  $a_2/a_1 = 1$ , the ejector performances for  $m = 9.4$  and  $15.5$  have been calculated with the digital electronic computer KDC-1 of Kyoto University. Dotted lines in Figs. 14 and 15 are the results obtained. Although the results calculated for the values of the Mach number  $M_3$  over 0.8 are apart from those measured, it may be possible to

On the other hand, since the mass flow rate of secondary fluid is equal to the mass flow rate at the inlet of mixing chamber, we obtain

$$\bar{G}_2 = \frac{f_m}{f_n} \frac{p_2}{p_0} \sqrt{\frac{2}{\kappa-1} \left\{ \left(\frac{p_2}{p_1}\right)^{(\kappa-1)/\epsilon} - 1 \right\}} \frac{a_1}{a_1} \quad (24)$$

Solving simultaneously Eqs. (10) ~ (19), (22) and (23), the relation between the pressure in the mixing chamber  $p_2/p_0$  and the momentary mass flow rate of secondary fluid  $\bar{G}_2$  is obtained for the given values of  $m$ ,  $\eta_d$ ,  $\epsilon$ ,  $a_2/a_1$ , and  $p_1/p_0$ . Therefore, the state in the ejector at the inlet pressure of nozzle  $p_1/p_0$  is decided by finding out the combination of  $p_2/p_0$  and  $\bar{G}_2$  which satisfies Eq. (24).

Table 2 Comparison of mass flow ratios

		Air model test		Engine test	
Area ratio of mixing pipe to nozzle	$m$	9.4	15.5	10.5	15.5
Mass flow ratio	Measured $\bar{G}_2/\bar{G}_1$	3.45	4.55	7.00	9.08
	Calculated $(\bar{G}_2/\bar{G}_1)_a$	2.34	2.69	3.23	3.95
ratio	Calculated $(\bar{G}_2/\bar{G}_1)_a$	3.45	4.61	6.46	8.41

Air model test: Tank pressure of primary air 4 ata. Revolving speed 1200 rpm. Nozzle dia. 9 mm.  
 Engine test: Load 2 PS. Engine speed 2600 rpm. Nozzle dia. 11 mm ( $m = 10.5$ ), 9 mm ( $m = 15.5$ )

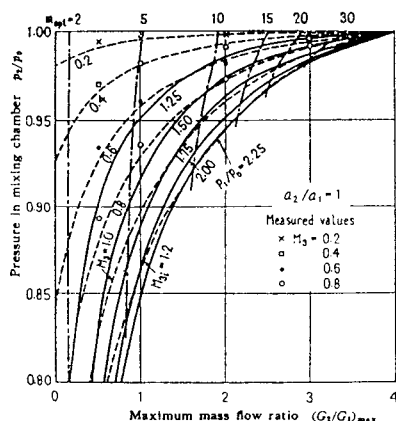


Fig. 17 Optimum area ratio of mixing pipe to nozzle for ejector of steady state (calculation)

Integrating the momentary mass flow rate of primary fluid and that of secondary fluid during one cycle of the state change, respectively, the mass flow ratio of ejector  $(\bar{G}_2/\bar{G}_1)_{el}$  is given as follows:

$$\left(\frac{\bar{G}_2}{\bar{G}_1}\right)_{el} = \frac{\int \mu \bar{G}_1 dt}{\int \bar{G}_1 dt} \quad (25)$$

Using the pressure change at the nozzle inlet shown in Figs. 11 and 8, the mass flow ratio  $(\bar{G}_2/\bar{G}_1)_{el}$  in Table 2 and the change of the pressure in the mixing chamber  $p_2/p_0$  in Figs. 18 and 19 are obtained, respectively. In the air model test,  $a_2/a_1 = 1$  is assumed and in the engine test,  $a_2/a_1$  is calculated with both the air temperature in the surge tank II and the mean gas temperature at the nozzle inlet, which has been measured with a thermocouple. On the other hand, the mean mass flow rates of primary and secondary fluids can be calculated with the change of the inlet pressure of nozzle  $p_1/p_0$  under the assumption of  $p_1/p_0 = 1$  and from Eq. (24) with the change of the pressure in the mixing chamber  $p_2/p_0$ , respectively. The mass flow ratio  $(\bar{G}_2/\bar{G}_1)_{el}$  in Table 2 is represented by the ratio of the mean mass flow rates calculated with this procedure.

In Figs. 18 and 19, the calculated pressure in the mixing chamber  $p_2/p_0$  is kept below 1, during the time that the primary fluid is flowing in the

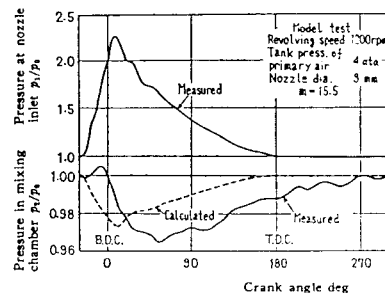


Fig. 18 Pressure change in mixing chamber

estimate the ejector performance through this analytical treatment.

The relationships of the mass flow ratio to the area ratio of the mixing pipe to the nozzle  $m$  under the condition of a constant pressure in the mixing chamber are plotted in Fig. 16. The optimum area ratio, at which the mass flow ratio becomes maximum, increases with an increase in the Mach number  $M_3$  at the nozzle outlet, that is, the inlet pressure of nozzle  $p_1/p_0$ , or with an increase in the pressure in the mixing chamber  $p_2/p_0$ . Both the optimum area ratio  $m_{opt}$  and the maximum mass flow ratio  $(\bar{G}_2/\bar{G}_1)_{max}$  given at this optimum area ratio have been calculated for various values of  $p_1/p_0$  and  $p_2/p_0$  as shown in Fig. 17. Although the optimum area ratio for the steady state is not related closely with that for the pulsative state, Fig. 17 may be utilized for the optimum design of the ejector of pulsative state.

## 4.4 Consideration on the ejector of pulsative state

About the ejector of pulsative state, both the pressure in the mixing chamber  $p_2$  and the momentary mass flow rates of primary and secondary fluids at the moment of the inlet pressure of nozzle  $p_1$  can be calculated under the assumption that the relations of steady flow are approximately applicable to the momentary state in the ejector. The momentary mass flow rate of primary fluid at the inlet pressure of nozzle  $p_1$  is non-dimensionally represented by

$$\bar{G}_1 = \frac{a_1}{\kappa g f_n p_0} \left[ \frac{\kappa g f_m p_1}{a_1} \sqrt{\frac{2}{\kappa-1} \left\{ \left(\frac{p_1}{p_2}\right)^{(\kappa-1)/\epsilon} - 1 \right\}} \right] \\ = \frac{p_1}{p_0} \sqrt{\frac{2}{\kappa-1} \left\{ \left(\frac{p_1}{p_0} \frac{p_1}{p_2} \frac{p_1}{p_0}\right)^{(\kappa-1)/\epsilon} - 1 \right\}} \frac{a_1}{a_1} \frac{a_2}{a_1} \quad (22)$$

The momentary mass flow rate of secondary fluid in the non-dimensional form is

$$\bar{G}_2 = \mu \bar{G}_1 \quad (23)$$

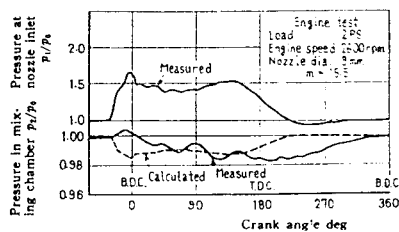


Fig. 19 Pressure change in mixing chamber

ejector and the state of  $p_1/p_0 > 1$  continues. It shows no rise at the early stage of the ejection of primary fluid. The higher pressure at the nozzle inlet produces the lower pressure in the mixing chamber due to the increase in the momentary mass flow rate of secondary fluid. The measured pressure in the mixing chamber  $p_2/p_0$  increases during the early stage of the ejection period of primary fluid due to the occurrence of reverse flow, and thereafter it is lowered below 1. After the end of ejection, the state of  $p_2/p_0 < 1$  is maintained by the inertia effect of fluid in the ejector. Therefore, the difference between the measured and calculated pressures in the mixing chamber seems to be closely related with the reason why the ejector performance of pulsative state differs from that of steady state. Comparing  $(G_2/G_1)_{st}$  in Table 2 with  $(G_2/G_1)_{st}$ , it is understood that, owing to the inertia effect, the mass flow ratio produced in the ejector of pulsative state becomes much larger than that in the steady state. The inertia effect of ejector is seriously influenced by the length and diameter of mixing pipe, the area ratio of the mixing pipe to the nozzle, etc. If the mixing pipe and the diffuser are designed so as to be suitable to the pulsative flow, it may be possible to produce the mass flow ratio larger than that obtained in this experiment.

### 5. Conclusions

For the purpose of applying the exhaust gas ejector for engine cooling, the ejector performance has been investigated with the uses of a four-stroke cycle engine and an air model. The results obtained are summarized as follows:

(1) Cooling air for an engine may be supplied only from the exhaust gas ejector, if the ejector and the flow passage of cooling system are well designed. By using the ejector together with a fan for engine cooling, it is possible to improve the specific fuel consumption and to increase the effective engine output. In these cases, however, since the negative pressure of secondary flow produced by the exhaust gas ejector is small, it is important to reduce the flow resistance of the silencer, which is

connected to the ejector.

(2) The flow rate of air induced into the ejector becomes larger with an increase in the engine load. However, the flow rate per unit horse power becomes smaller.

(3) The optimum area ratio of the mixing pipe to the nozzle and the maximum flow rate of induced air, given at this optimum area ratio, increase with a decrease in the nozzle diameter of ejector. Therefore, it is advisable to reduce the nozzle area in so far as the specific fuel consumption is not increased.

(4) Through the air model test, it is understood that the mass flow ratio of exhaust gas ejector becomes smaller with increases in both the cylinder pressure at the beginning of blow down and the revolving speed of model, but larger with a decrease in the volume of exhaust pipe.

(5) The mass flow ratio of the ejector, whose primary fluid is intermittently supplied, is much larger than that of the steady state, because the inertia of fluid in the ejector acts as an effective factor to draw the secondary fluid.

In closing, the authors wish to thank Messrs. K. Wada, T. Ishihashi, and S. Matsushima for their cooperations in the experiment.

### References

- (1) A. G. Filimonov: *Autom. Engr.*, Vol. 48, No. 7 (1958), p. 31.
- (2) A. W. Jlowich: *Autom. Trakt. Promys. (SSSR)*, No. 9 (1964).
- (3) L. J. Kastner and J. R. Spooner: *Proc. Inst. Mech. Engrs.*, Vol. 162 (1950), p. 149.
- (4) J. Keenan et al.: *Jour. Appl. Mech.*, Vol. 17, No. 3 (1950), p. 299.
- (5) I. Watanabe et al.: *Trans. Japan Soc. Mech. Engrs.*, Vol. 21, No. 104 (1955), p. 304; Vol. 22, No. 120 (1956), p. 590, p. 596.
- (6) F. Nagao and Y. Shimamoto: *Bulletin of JSME*, Vol. 2, No. 5 (1959), p. 170.
- (7) T. Yoshida: *Air-Cooled Diesel Engine*, (1961), p. 154, Sankaido Press.
- (8) M. O. Engel: *Proc. Inst. Mech. Engrs.*, Vol. 177, No. 13 (1963), p. 347.
- (9) A. W. Hussmann: *Penn. State Univ., Department of Engineering Research, Tech. Bulletin*, No. 64 (1955).
- (10) A. H. Shapiro: *The Dynamics and Thermodynamics of Compressible Fluid Flow*, Vol. 1 (1953), p. 151, Ronald Press.

# EXPERIMENTAL STUDIES ON A LOW PRESSURE EJECTOR WITH A PULSATING FLUID SUPPLY

S. PURUSHOTHAMA RAO\* AND DR C. P. GUPTA\*\*

## Abstract

Experiments were conducted on an ejector assembly having a pulsating primary fluid supply. A four stroke, twin cylinder, air cooled diesel engine was employed to supply the primary fluid to the ejector. A draft tube type ejector formed by a convergent nozzle and a straight length of maximum tube diameter was studied, over a range of engine operating conditions. The results indicate that the pulsating flow type ejector gives a superior performance. Also the draft tube ejector gives a better performance compared to a venturi type ejector. It is felt that the pulsation frequency has an effect on the overall performance of the ejector.

## Introduction

An ejector is a simple device, in which the kinetic energy of one fluid is made use of to entrain and eject a second fluid from a region of low pressure to one of higher pressure. The first fluid possessing the kinetic energy is called 'forcing fluid', and the entrained fluid is called 'secondary fluid'. The forcing fluid is admitted to the ejector through a passage known as forcing nozzle. Next to the forcing nozzle is situated the diffuser in which the forcing fluid entrains and mixes with the secondary fluid and ejects it out to a region of high pressure. The location of the forcing nozzle, in relation to the diffuser, determines the type to which the ejector belongs. There are two main types of ejectors, namely, annular type and central type.

In the annular type of ejector shown in Fig 1a, the forcing nozzle exists in the form of an annular passage surrounding the entry of the secondary fluid into the diffuser. The diffuser itself may or may not be in the form of a venturi. The forcing fluid as it issues from the forcing nozzle into the diffuser acquires a high velocity, and this enables to entrain the secondary fluid and eject it out of the diffuser against the desired pressure differential.

In the central type, the forcing nozzle is placed at the entrance to the diffuser, coaxial with it, as shown in Figs 1b and 1c. As before,

the forcing fluid, as it issues from the forcing nozzle into the diffuser, acquires a high velocity and enables to entrain the secondary fluid and eject it out against the desired pressure differential. In the central type of ejectors, there are again two varieties namely, draft tube type and venturi type as shown in Figs 1b and 1c. The draft tube type of ejector is used for low and medium pressure ratios and the venturi type for medium and high pressure ratios.

## Literature survey

Studies on ejection can be divided into two classes, namely, (i) studies on the performance of the ejector as a whole<sup>1-9</sup>, and (ii) studies on process of diffusion of free jets and mixing of one gaseous stream with the other. The flow ratio obtainable by an ejector has been computed by using the equations of continuity, momentum and kinetic energy. It is assumed that no external heat transfer occurs and that this section is so large that the pressure loss and the momentum of the secondary fluid are negligible. It is further assumed that the character of the secondary

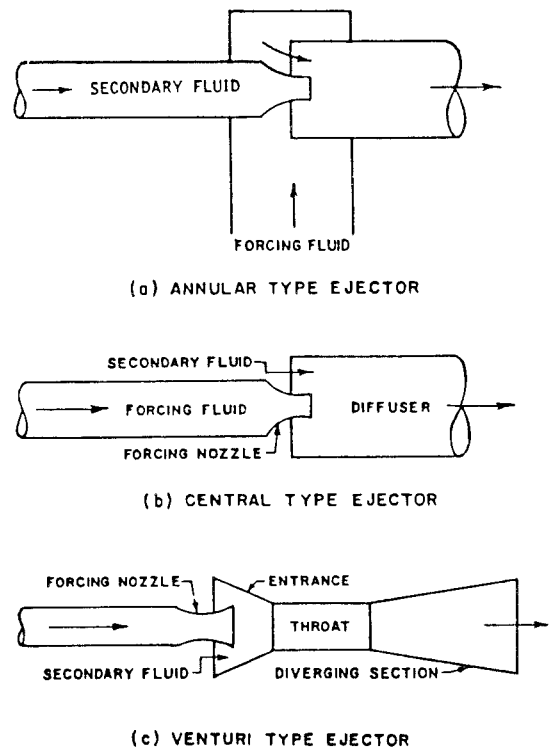


Fig 1  
Annular, central and venturi type ejectors

\*Central Mechanical Engineering Research Institute, Durgapur 9.

\*\*Mechanical Engineering Department, University of Roorkee, Roorkee.

fluid is uniform throughout the section and the exit velocity is negligible.

The mixing of the two fluids is supposed to involve the following processes.

(i) Acceleration of the particles of the secondary fluid by impact of the particles of the forcing fluid.

(ii) Entrainment of the secondary fluid by viscous friction at the periphery of the forcing jet.

(iii) Over expansion of the forcing fluid to a pressure below that of secondary fluid at entrance to the diffuser with consequent flow of the latter towards the axis of the jet.

(iv) Change of state of the forcing fluid.

However, for simplicity of analysis, it has been assumed that the mixing of the two fluids at the entrance section of the diffuser occurs either in constant area or at constant pressure<sup>1</sup>.

In the theoretical analysis based on constant area mixing, the tip of the forcing nozzle is assumed to be at the commencement of the diffuser throat and the mixing of the forcing and the secondary fluid is assumed to take place within the throat, which has a constant cross-sectional area. The throat should be sufficiently long to ensure complete mixing of the two fluids. The analysis based on this assumption is valid for ejectors having large throat proportions and hence low pressure ratios.

In the theoretical approach based on constant pressure mixing, it is assumed that the tip of the forcing nozzle is located at some distance upstream of the diffuser throat as shown in Fig 1, and the mixing of the two fluids takes place in the entrance section of the diffuser. The shape of the entrance section is assumed to be such that a constant pressure is maintained within the region between the forcing nozzle tip and the commencement of the diffuser throat. The mixing is assumed to be completed before the two fluids enter the diverging section. The distance of the forcing nozzle tip from the commencement of the diffuser throat is, therefore, one of the factors influencing the ejector performance. The venturi type of ejector, operating at higher pressure ratios is assumed to operate on this process.

Kastner and Spooner<sup>2,4</sup> have investigated the performance of large area ratio ejectors from which the following conclusions can be drawn.

(1) The single stage ejector in which the suction and the forcing fluid is air, can be designed to achieve a compression ratio of 1 to 3, if the forcing pressure is 20 psi. Under these circumstances the ratio of suction mass flow to the forcing mass flow will vary between 0 and 20, the higher mass flows are for a lower pressure

ratio.

(2) Over the range of area ratios from 2.2 to 700 it seems doubtful if area ratios above 70 for a forcing pressure of 20 psi ensure any appreciable gain in terms of mass ratio.

The optimum projection ratio, defined as the distance from the end of the forcing nozzle to the commencement of the parallel mixing tube divided by the mixing tube diameter, should be 1.5 for ejectors of small area ratio and for large area ratio ejectors the optimum projection ratio falls between 0 and 1. The values refer to cases where the maximum suction air flow is derived at a given degree of compression. The length to diameter ratio for a parallel mixing tube should be between 7 and 10. If the ratio is small some compensations can be obtained by increasing the projection ratio. The diffuser angle is important in small area ratio range and should be less than 25 degrees. No diffuser is necessary for large area ratio ejectors.

Sreenivasa Murthy and Thipperudriah<sup>8</sup> have investigated the performance of pulsating type ejectors. The primary fluid supply was obtained from a single cylinder, 4 stroke INDEC air cooled diesel engine, whose specifications are

TABLE I  
Specifications of INDEC single cylinder engine

Bore	87.3 mm
Stroke	110 mm
Power developed	6.25 hp at 1500 rpm
Compression ratio	16.5 : 1

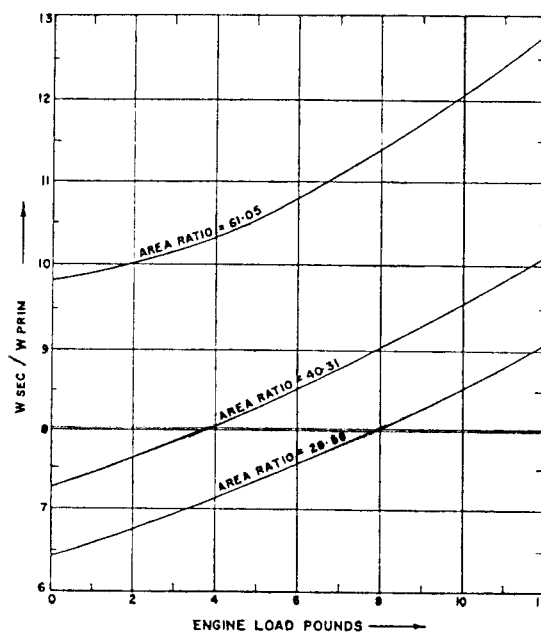


Fig 2  
INDEC single cylinder engine  
(1500 rpm)

given in Table I. Fig 2 gives a plot of the mass flow ratio vs the engine load obtained by Murthy and Thipperudriah<sup>8</sup>. Their results indicate that the mass flow ratio increases with the

increase in engine load. Nagao, Shimamoto and Shikata<sup>9</sup> have investigated the performance of small area ratio ejectors with both steady and pulsating primary fluid supply. They obtained the primary fluid supply from the exhaust of a YANMAR A-2 air cooled diesel engine whose specifications are given in Table II. From their investigations the following conclusions could be drawn:

- (1) The mass flow ratio increases with engine load.
- (2) The mass flow ratio increases with decrease in forcing nozzle diameter for a constant diameter mixing pipe.
- (3) The performance of the ejector with pulsating primary fluid supply is better than that with a steady fluid supply.

**TABLE II**

Specifications of YANMAR diesel engine

Type	A-2
Bore	66 mm
Power developed	2 PS at 2600 rpm

### Scope of work

The foregoing review indicates that very little data exists on the performance of a pulsating type ejector, with a high temperature and low pressure primary fluid supply. This type of ejector opens up a new field of research for application of exhaust gas energy of IC engines to cool the cylinders. No data, either experimental or theoretical, is available for the selection of an ejector for given engine dimensions and operating conditions. With this in view, a series of experiments were conducted to determine the influence of some of the variables on the performance of the ejector.

### Experimental

The authors were confronted with the vast number of physical variables which could affect the performance of the ejector. Some of these variables are:

- (1) Pressure and temperature of the forcing fluid
- (2) Pressure and temperature of the secondary fluid
- (3) Exit diameter of the forcing nozzle
- (4) Type of forcing nozzle—convergent or convergent-divergent
- (5) Geometry of the mixing chamber
- (6) Length of mixing pipe
- (7) Area ratio of nozzle to exhaust pipe
- (8) Area ratio of nozzle to mixing pipe
- (9) Frequency of pulsations of the primary fluid, and
- (10) Mixing length.

For the present investigation it was decided to fix the dimensions of the ejector on the basis of standard ejector practice with a continuous primary fluid supply. Hence the performance of a draft tube type of ejector formed by a simple convergent nozzle and a straight length of maximum tube diameter was studied. The convergent nozzles had throat diameter 15 mm, 20 mm, 25 mm, 30 mm, and were machined out of MS bar stock. The passage to the nozzles is through a  $1\frac{1}{4}$  inch GI pipe from the exhaust duct of the engine cylinder block. The mixing tube was of  $3\frac{3}{8}$  inch inside diameter and its length was equal to 7 times the diameter.

A two cylinder, 4 stroke, INDEC air cooled diesel engine was used to supply the forcing fluid to the ejector. The specifications of the engine are given in Table III. The engine was mounted on a suitable concrete foundation and a hydraulic dynamometer was used to load the engine. The governor was adjusted so as to obtain a constant speed of 1500 rpm. The

**TABLE III**

Specifications of the INDEC twin cylinder engine

Bore	87.3 mm
Stroke	110 mm
Power developed	12.5 hp at 1500 rpm
Compression ratio	16.5 : 1

primary and secondary air flows were measured by D-D/2 orifice plates fabricated to British standard flow code BS 1042: 1943. The pressure and temperature of the forcing fluid were recorded by a mercury manometer and a Chromel Alumel thermocouple respectively. During all the test runs the projection ratio was kept constant at 1.50.

### Results and discussion

Figures 3 and 4 show the variation of temperature of the forcing fluid vs the load on the engine, and pressure of the forcing fluid vs the area ratio of the ejector. For a given ejector area ratio, the forcing pressure was constant but the temperature varied according to the engine load conditions, as shown in Fig 3. Fig 5 shows the variation of the mass flow ratio vs the engine load, for different area ratio ejectors. The mass flow ratio increases as the area ratio of mixing pipe nozzle increases from 9.4 to 37.6. It is also seen that the mass flow ratio increases with the engine load for a given ejector, the maximum value occurring when the engine is operating at full load. Fig 6 shows the variation of mass flow ratio vs area ratio of the forcing nozzle to exhaust pipe at different engine operating conditions. It also compares the results of the present investigation with the others. Curves A, C and E compares the maximum mass flow ratios obtained. As stated earlier the maximum



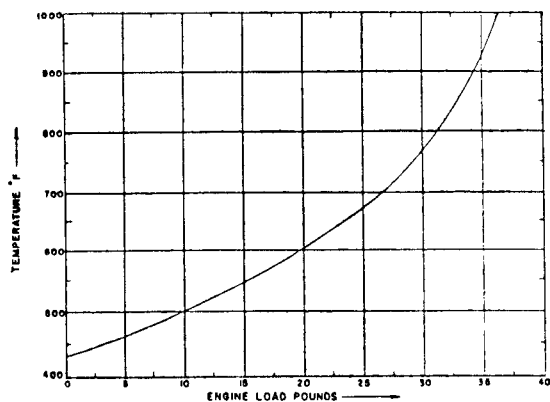


Fig 3  
INDEC twin cylinder engine  
(1500 rpm)

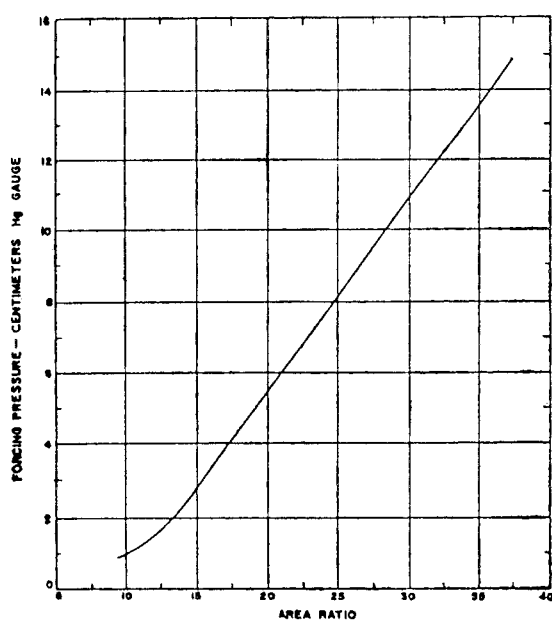


Fig 4  
INDEC twin cylinder engine  
(1500 rpm, 12.5 hp load)

secondary flow occurs when the engine is operating near full load conditions. This may be due to the fact that the enthalpy of the primary fluid is the highest when the engine is operating at full load.

The results indicate that the venturi type ejector, as used by Nagao *et al*, does not offer any advantage over the simple draft tube type ejectors. Moreover the maximum mass flow ratio obtained with the venturi type ejector is always less than the draft tube type as shown by Fig 6. Even with the draft tube type of ejector, the mass flow ratio is always higher in the case of the single cylinder engine<sup>8</sup> as compared to the twin cylinder engine, for the same

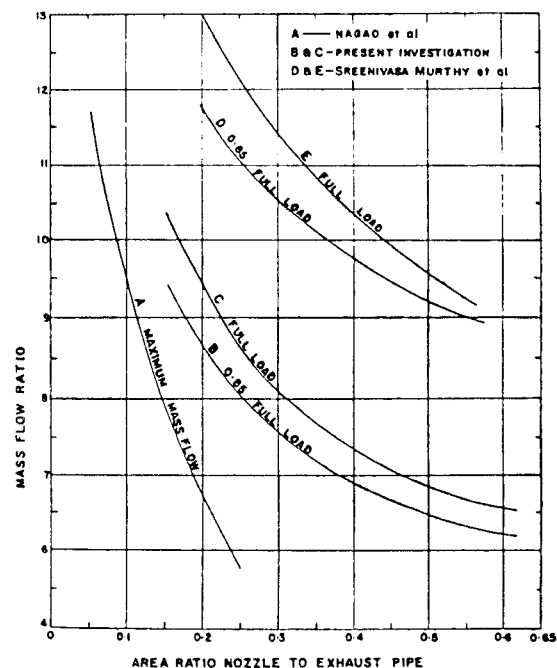


Fig 5  
INDEC twin cylinder engine  
(1500 rpm)

area ratio of the forcing nozzle to the exhaust pipe. This may be attributed to the facts, namely,

(i) The projection ratio in the present investigation was kept constant at 1.5 whereas it has not been specified by Sreenivasa Murthy<sup>8</sup>. It has been reported that the projection ratio plays a dominant part in the performance of the continuous flow type ejectors<sup>4</sup>. This fact may also be true in the case of pulsating type ejectors.

(ii) The number of pulsations in the case of a single cylinder engine is 750 whereas in the

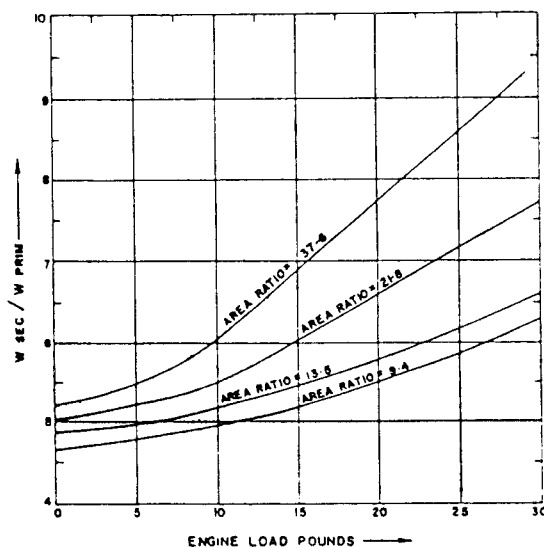


Fig 6  
Variation of mass flow with nozzle area

twin cylinder engine it is 1500. This doubling of the pulsation frequency may be acting in such a way as to bring down the performance of the ejector nearly to the steady flow conditions. However the performance of pulsating type ejector is always superior whatever may be the pulsation frequency<sup>6</sup>.

In the present investigation it was not possible to use exhaust nozzles which gave area ratios with exhaust pipe less than 0.15, as this would increase the back pressure on the engine enormously. However, Nagao *et al*<sup>9</sup> have reported data even for area ratios near 0.05. It is felt that for area ratios near 0.05, the engine would be operating with a very high back pressure with the resultant of poor combustion in the cylinder leading to loss of power and stalling of the engine.

### Conclusions

From the above, it can be concluded that—

1. Performance of ejectors with pulsating primary fluid supply is far superior compared to ejectors with steady flow.
2. The secondary flow and the mass flow ratio increases with engine load
3. The exhaust back pressure limits the throat area of the forcing nozzle and thus limits the maximum mass flow ratio obtainable at a particular load on the engine and for a given area ratio of the mixing pipe.
4. The performance of the draft tube type ejector is much better in comparison with the venturi type of ejector. Thus, it seems, it is not necessary to use a venturi type ejector when the forcing fluid is supplied at a low pressure as

previously. Kastner *et al* came to a similar conclusion while experimenting with low pressure continuous flow ejector.

5. The pulsation frequency of the primary fluid has a noticeable effect on the performance of the ejector.

6. It is possible to obtain the entire cooling air flow for an air cooled engine solely by the use of exhaust gas operated ejectors. This would eliminate the power consumed by the engine driven blower and thus help to improve the specific fuel consumption.

### References

- <sup>1</sup> Keenan and Newman, 'The complete air ejector', *Jour App Mech ASME Trans*, **9** (2), A75 to A81 (1942).
- <sup>2</sup> Kastner and Spooner, 'The low pressure air ejector', *Proc Inst Mech Engrs*, Vol 147 (1944).
- <sup>3</sup> S. A. Wood and A. Bailey, 'The horizontal carriage of granular material by injector driven air stream', *Proc Inst Mech Engrs*, Vol 142 (1939).
- <sup>4</sup> L. J. Kastner and J. R. Spooner, 'An investigation of the performance and design of the air ejector employing low pressure air as the driving fluid', *Proc Inst Mech Engrs*, Vol 162, pp 149-159 (1959).
- <sup>5</sup> L. J. Kastner and J. R. Spooner, *Ibid*, Discussion pp 160-166.
- <sup>6</sup> Schroeder, 'Self aspirating high pressure ratio ejector with high delivery ratio', *Summary in Engineering Index* 1967, p 46.
- <sup>7</sup> R. W. Upfold, 'Reducing back pressure', *Automobile Engr*, pp 184-188, May 1963.
- <sup>8</sup> N. Sreenivasa Murthy and Lt. A. Thipperudriah, 'Ejector Cooling of air cooled diesel engines', *Jour Inst Mech Engrs (India)*, **49**, (7 Part ME 4), 191-200 (1969).
- <sup>9</sup> Fujio Nagao, Yuzuru Shimamoto and Mitsuo Shikata, 'Application of exhaust gas ejector to engine cooling', *Bull Jap Soc Mech Engrs*, **12** (53), 1153-1162 (1959).
- <sup>10</sup> S. Purushothama Rao, 'Low pressure air ejector', Paper presented at the 2nd Fluid Mechanics and Fluid Power Conference, Indian Institute of Technology, Powai, Bombay, July 2-4, 1970.

(Manuscript received 7 December 1973)

P. J. Vermeulen

Associate Professor.

V. Ramesh

Research Associate.

Wai Keung Yu

Graduate Student.

Department of Mechanical Engineering,  
The University of Calgary,  
Calgary, Alberta, Canada

# Measurements of Entrainment by Acoustically Pulsed Axisymmetric Air Jets

*Direct measurements of entrainment by acoustically pulsed axisymmetric air jets flowing into surrounding air have been made for a range of orifice sizes, Strouhal numbers, and excitation powers. The entrainment was considerably increased, by up to 5.8 times at distances greater than 15 diameters axially downstream of the orifice exit plane. The entrainment of the excited jet varied linearly with downstream distance. The jet response varied nonlinearly with excitation strength, indicating that there may be a practical upper limit to the acoustic augmentation of entrainment. The response depends on Strouhal number and appears to be optimum at about 0.25.*

## Introduction

Ricou and Spalding [1] made the first direct measurements of the entrainment by steady fully developed turbulent axisymmetric free gaseous jets. Hill [2], later on, extended this work by the "measurement of local entrainment rate in the initial region of axisymmetric turbulent air jets." Indirect evidence from acoustic control of dilution-air mixing in a gas turbine combustor [3] also suggested that the jet entrainment rate was increased by acoustic modulation. Furthermore, Crow and Champagne [4], by integrating velocity profiles, showed that the entrained volume flow was increased 32 percent for a low level of periodic excitation of the jet. Also by indirect means, and using external excitation, Binder and Favre-Marinet [5] established that the entrainment rate was increased by 90 percent for stronger pulsation than in [4]. Self-excited jet flows have been studied by Anderson [6] and more recently by Hill and Greene [7] who by integration of velocity profiles showed that the entrainment rate was increased. Vermeulen and Yu [8] carried out "an experimental study of the mixing by an acoustically pulsed axisymmetrical air-jet" for external excitation strengths much greater than those used by previous workers, and showed indirectly for an excitation strength half of the maximum used that the entrainment mass flow rate was approximately doubled. This study also summarizes relevant work on excited jet flows. Thus it appears that direct measurements of the entrainment rate of pulsating jets have not been made before, and despite the evidence from indirect measurements, that the entrainment rate is significantly increased, the potential for improvement in entrainment rate by pulsing jet flows has not been thoroughly explored.

Jet entrainment is responsible for the mixing produced by a jet; acoustic control over jet flow mixing may therefore pro-

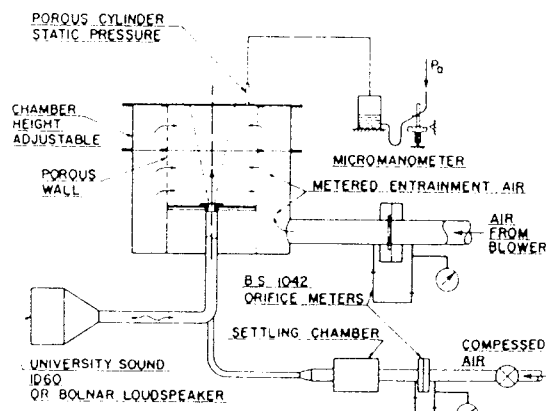


Fig. 1 Cross section through entrainment chamber

mote closer achievement of the design objectives in processes dependent on jet mixing, such as those associated with a gas turbine combustor. It is therefore of important technical interest to make direct measurements of the entrainment rate of pulsating jets and to determine the significant control variables.

## Experimental

**Entrainment Measurement Apparatus.** The apparatus used follows that developed by Ricou and Spalding [1], and consists of a porous walled chamber surrounding a 19.1-mm-dia bore tube, terminated by a smooth profile nozzle, mounted in the base plate of the porous cylinder (Fig. 1). The base of the cylinder is completely closed except for the nozzle orifice. The nozzle can be exchanged with others of different-sized bore for a range of sizes of 6.35, 9.53, 12.70, and 15.88 mm diameter. The porous wall of 300 mm diameter forms an annulus with the 550-mm-dia outer wall of the chamber. Air from the nozzle creates a jet on the chamber axis entraining air which was supplied through the porous wall from air metered to the annulus by a 76-mm-dia bore pipe. A centrifugal blower

Contributed by the Gas Turbine Division of THE AMERICAN SOCIETY OF MECHANICAL ENGINEERS and presented at the 31st International Gas Turbine Conference and Exhibit, Düsseldorf, Federal Republic of Germany, June 8-12, 1986. Manuscript received at ASME Headquarters January 17, 1986. Paper No. 86-GT-86.

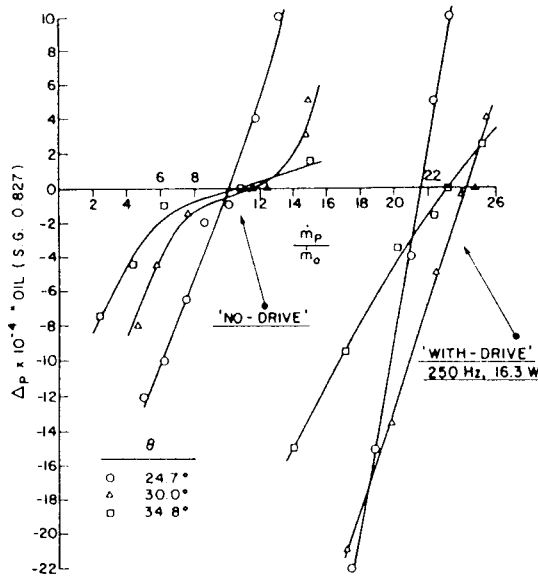


Fig. 2 Variation of pressure drop across aperture plate with mass flow rate through porous wall for various aperture included angles  $\theta$ ; orifice 9.53 mm diameter,  $x/d_o = 38.8$

delivers the entrainment air metered by a standard sharp-edged orifice meter. Compressed air was admitted to the nozzle tube via a needle valve, a standard sharp-edged orifice meter, and a settling chamber positioned to protect the flow meter from acoustic pulsations in the flow. The temperature and pressure upstream of the needle valve were kept constant, with the upstream pressure sufficiently large to ensure choked flow at the valve, ensuring constant mass flow rate. The nozzle tube bends at right angles, at the junction with the air supply tube, to couple to the acoustic excitation source of about 60 W rating.

The porous-walled annulus consists of several bolted sections, so that the chamber height is adjustable, thereby allowing the entrainment flow rate to be found for a range of jet flow lengths. The range of dimensionless axial distances ( $x/d_o$ ) over which measurements could be made was from 7.0 to 68.5. The top of the chamber was partially closed by a series of aperture plates, with carefully chosen aperture diameters that would not interfere with the jet flow. A pressure tap in the aperture plates allowed the porous cylinder static pressure to be measured with the aid of an oil-filled micromanometer gauge.

A rigid framework of 3.18-mm-dia aluminum rods and flanges supported the porous wall of three layers of fine-weave cotton cloth. Three layers of cloth were necessary in order to provide sufficient pressure drop to ensure a uniform, radially inward flow of air, passed through the porous wall. This was checked by traversing a smoke source closely all over the inside porous surface.

For safe operation of the acoustic source, power to the loudspeaker was measured by an a-c voltmeter and ammeter, a small correction for power factor having been established by calibration against an audio frequency wattmeter. The response of the system can be divided into that of the mechanical system of tube plus loudspeaker and that of the jet flow. The mechanical system response determines the frequencies at which the strongest excitation of the jet takes place. A previous investigation [8], of essentially the same mechanical system, established these frequencies to be about 250 Hz using the Bolnar loudspeaker, and about 410 Hz with the University Sound ID60 driver. The jet flow response depends on the Strouhal number, and [8] showed this to be optimum at about 0.25 for a free jet.

Upon acoustic excitation the jet velocity at the nozzle orifice pulses, which in turn excites the jet flow into wave motion growing into a train of toroidal vortices [8]. The amplitude, on the center line at the orifice exit plane, of this pulsation velocity (pulsation strength) was measured by a hot-film anemometer in a manner similar to that described in the previous work [8].

The main variables affecting the entrainment rate, and to be investigated, are the nozzle or orifice diameter  $d_o$ , the jet axial length  $x$  measured from the orifice exit plane, the average steady (unexcited) jet velocity in the nozzle exit plane  $U_o$ , the pulsation strength  $U_e$ , the driving frequency  $f$ , and the associated dimensionless parameters, Reynolds number  $Re$  and Strouhal number  $St$ .

**Measurement Method.** When the jet is flowing "free," that is when the surrounding reservoir (room) is large, it is essentially at uniform pressure (atmospheric), and the entrained air flows radially inward toward the jet axis. Now consider the jet to be partially surrounded, as in the apparatus described above, then with no air from the blower, entrainment by the jet reduces the porous cylinder pressure below atmospheric. If air from the blower is now adjusted such that the pressure in the porous cylinder is atmospheric, and the flow through the porous wall is radially inward, then free-jet flow conditions are re-established and the air mass flow rate delivered by the blower becomes equal to the entrainment mass flow rate of the jet. The method of measurement for a particular jet flow

## Nomenclature

$d_o$ = jet orifice diameter	through the porous wall	ity excitation pulsation amplitude, or pulsation strength, at the orifice exit plane (unsteady flow)
$f$ = frequency		
$F, F_1, F_2, F_3$ = functions	$\dot{m}_T$ = jet total mass flow rate crossing a plane normal to jet axis	$U_o$ = average steady (unexcited) jet velocity at orifice exit plane
$K, K_1$ = constants	$\dot{m}_{TN}$ = jet total mass flow rate for "no-drive" conditions	$\dot{W}$ = power at acoustic driver
$\dot{m}_e$ = entrained mass flow rate	$\dot{m}_{TW}$ = jet total mass flow rate for "with-drive" conditions	$x$ = jet axial length from orifice exit plane
$\dot{m}_{eN}$ = entrained mass flow rate for "no-drive" conditions	$Re$ = orifice Reynolds number = $\rho_o d_o U_o / \mu_o$	$\mu_o$ = jet viscosity at the orifice
$\dot{m}_{eW}$ = entrained mass flow rate for "with-drive" conditions	$St$ = orifice Strouhal number = $f d_o / U_o$	$\rho_o$ = jet density at the orifice
$\dot{m}_o$ = constant average mass flow rate through the jet orifice	$U_e$ = center-line jet velocity	$\rho_s$ = density of the fluid surrounding the jet
$\dot{m}_p$ = mass flow rate		

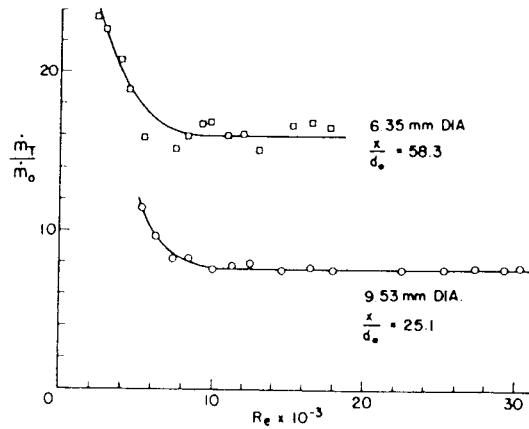


Fig. 3 Variation of total mass flow rate ratio with Reynolds number for "no-drive" conditions

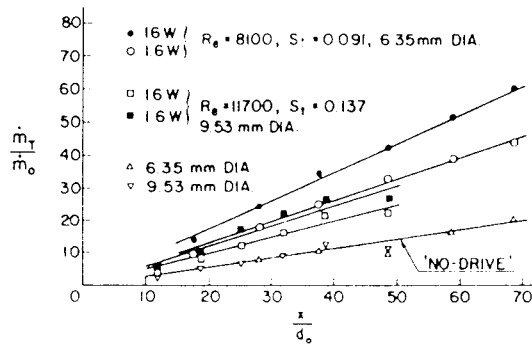


Fig. 4 Variation of entrainment rate with axial distance for isothermal conditions, temperature 26°C, atmospheric pressure 88.8 kPa,  $U_o = 17.4$  m/s, 250 Hz

length, for conditions with or without acoustic drive, is therefore simply to adjust the air flow rate through the porous wall until the micromanometer can detect no pressure difference between the porous cylinder static pressure and the atmosphere. For truly radially inward entrainment flow for this condition there must be no axial pressure gradient in the porous cylinder; measurement at two static pressure taps in the base plate of the porous cylinder confirmed that this was true.

The aperture diameter influences the pressure drop measured across the aperture plate; a minimum-sized hole was desirable in order to produce a pressure drop sensitive to changes in the flow rate through the porous wall, particularly as free-jet conditions were being approached. If the hole was too small the plate interfered with the jet axial flow, producing a reduced value for the measured entrainment flow rate. Thus if the pressure drop is plotted against the ratio of the porous wall mass flow rate  $\dot{m}_p$  to  $\dot{m}_o$ , the constant mass flow rate through the jet orifice of fixed diameter  $d_o$ , as in Fig. 2, then as the aperture size varies so does the curve crossing point for zero pressure drop. As can be seen a hole size can be chosen such that the crossing point value is little affected, and the curve slope is steep enough that an accurate value can be obtained, which is taken to be the required ratio of  $\dot{m}_e$ , the entrained mass flow rate to the mass flow rate through the jet orifice  $\dot{m}_o$  ( $\dot{m}_e/\dot{m}_o$ ), corresponding to free-jet conditions. Furthermore, for acoustic drive conditions, the aperture size which subtends an included angle of 30 deg at the orifice gives the maximum value for the measured entrainment flow rate, which is assumed to be the free-jet value. It is possible that a slightly different aperture size would give an improved value; however, the change is likely to be small, and a 30 deg aperture angle is also the best size for "no-drive" conditions (in agreement with [1]), a great convenience. An aperture angle of 30 deg was therefore chosen for all entrainment measurements.

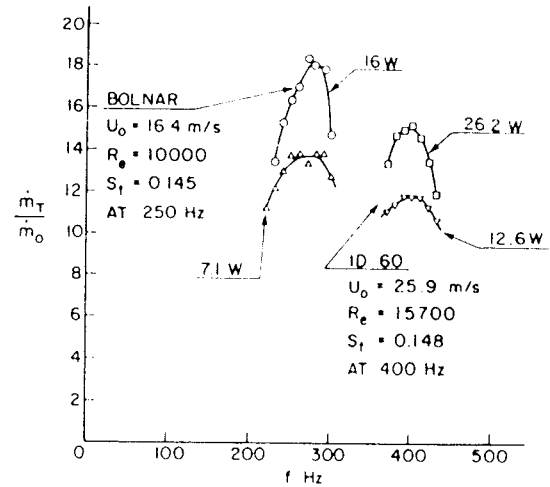


Fig. 5 Total mass flow rate ratio versus frequency for the system with either the Bolnar driver or ID60 driver; orifice diameter 9.53 mm,  $x/d_o = 25.1$

**Initial Tests to Establish the Experimental Method.** Before embarking on the main measurements it was possible to check the soundness of design of the apparatus, and to develop a good experimental technique, by duplicating some of the experimental results of Ricou and Spalding. The influence of Reynolds number, for no acoustic drive, was therefore investigated by varying the nozzle flow rate, since density and viscosity were essentially constant. Figure 3 presents data for the 6.35-mm and 9.53-mm-dia nozzles, in terms of the ratio of the total mass flow rate  $\dot{m}_T$  of the jet crossing a plane distance  $x$  from the orifice to the orifice mass flow rate  $\dot{m}_o$  ( $\dot{m}_T/\dot{m}_o$ ) versus the Reynolds number at the orifice. The distance  $x$  is identical to the entrainment chamber length, and  $\dot{m}_T$  is for free-jet conditions and related to  $\dot{m}_e$  by

$$\dot{m}_T = \dot{m}_e + \dot{m}_o \quad (1)$$

or

$$\frac{\dot{m}_T}{\dot{m}_o} = \frac{\dot{m}_e}{\dot{m}_o} + 1 \quad (2)$$

As can be seen  $\dot{m}_T/\dot{m}_o$  is constant for Reynolds numbers exceeding about 10,000. Ricou and Spalding established a critical Reynolds number of about 25,000; it is presumed that the difference is caused by higher turbulence levels in the nozzle flows of the apparatus for this investigation.

The next aspect which could be checked was the dependency of entrainment rate on jet length  $x$  for "no-drive" conditions; however, since varying the chamber height was a tedious operation it was also convenient to make simultaneous measurements for "with-drive" conditions at each value of  $x$  investigated. Thus Fig. 4 shows data for the "no-drive" condition at two orifice sizes, with an initial jet velocity of 17.4 m/s, chosen because of good driving possibilities and for possible comparison with other data [8]. A linear relationship is indicated, represented by

$$\frac{\dot{m}_T}{\dot{m}_o} = 0.29 \frac{x}{d_o} \quad (3)$$

The slope of this line is somewhat lower than the 0.32 obtained by Ricou and Spalding, which was later confirmed by Hill [2]. The degree of agreement, however, was considered to be sufficiently close to assume that the apparatus and technique were giving results as reliable as possible with the instrumentation available.

The frequencies for best mechanical system response were then verified by measuring  $\dot{m}_T/\dot{m}_o$  versus frequency, for the two acoustic drivers, at orifice jet velocities giving approximately the same orifice Strouhal number. Evidently as shown

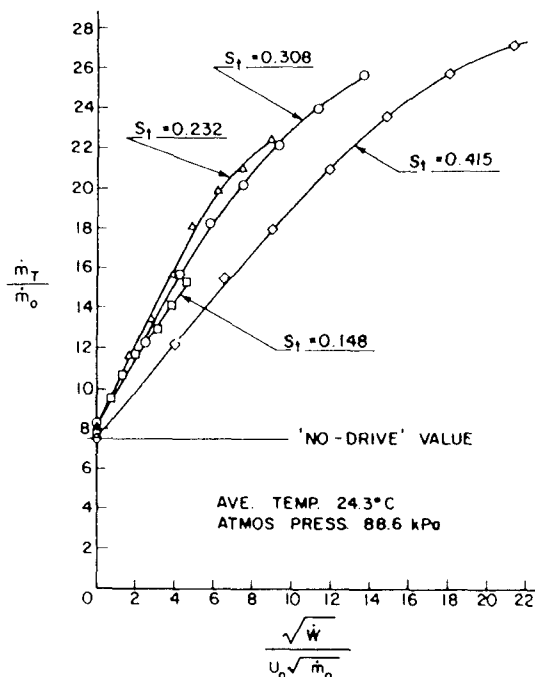


Fig. 6 Variation of entrainment rate with pulsation strength parameter for 9.53-mm-dia orifice,  $x/d_o = 25.1$ , 400 Hz, data corrected for Re effects

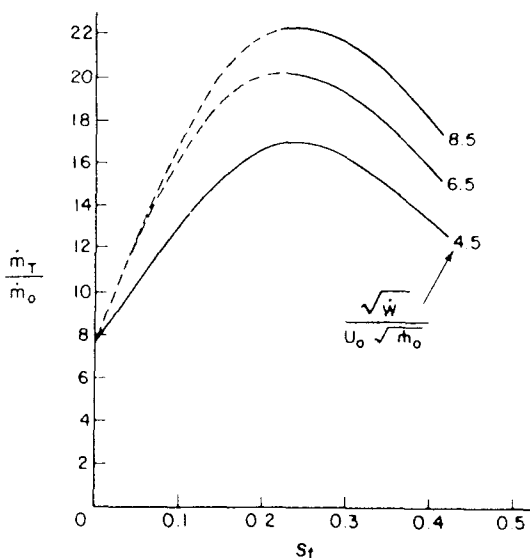


Fig. 7 Variation of entrainment rate with Strouhal number for various values of pulsation strength parameter; 9.53-mm-dia orifice,  $x/d_o = 25.1$ , 400 Hz, data corrected for Re effects

by Fig. 5 good response was obtained at frequencies of 250 Hz and 400 Hz. A frequency of 250 Hz is not quite optimum, but since a considerable number of data at this frequency for other measurements had been obtained [8] it was selected to facilitate possible comparisons.

**Experimental Results With Acoustic Drive.** The test results for  $U_o = 17.4$  m/s, shown in Fig. 4, indicate the typical effects of acoustic drive, and in general the entrainment mass flow rate was increased, relative to the no-drive condition, as shown by the increase in  $\dot{m}_T/\dot{m}_o$  for a particular value of  $x/d_o$ . It is noteworthy that over the power (or  $U_e/U_o$ ) range tested a linear relationship still exists between  $\dot{m}_T/\dot{m}_o$  and  $x/d_o$ . Because of the several orifice sizes tested the data have been obtained over a Reynolds number range of 8100 to 11,700, and a Strouhal number range of 0.091 to 0.137. The Reynolds numbers are high enough to obviate the need for

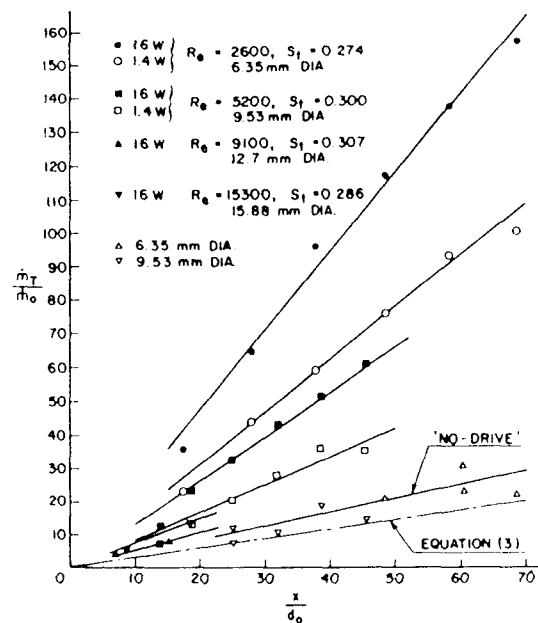


Fig. 8 Variation of entrainment rate with axial distance for isothermal conditions, temperature 26°C, atmospheric pressure 88.8 kPa, 250 Hz

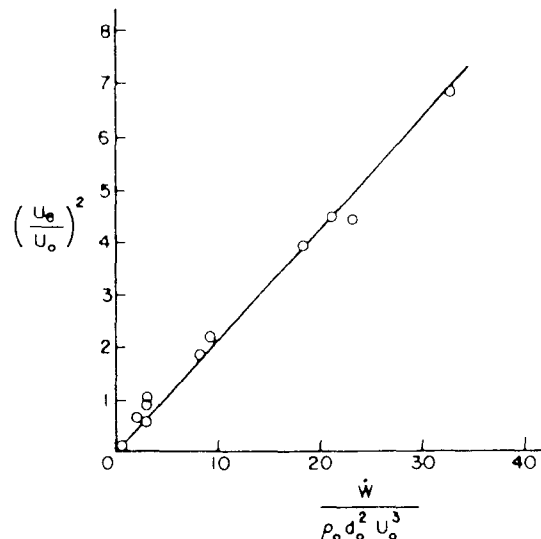


Fig. 9 Correlation between pulsation strength and dimensionless power, 9.53-mm-dia orifice, 250 Hz

corrections, but the effect of Strouhal number may be significant and was investigated further. It is apparent that the effect of power, or pulsation strength  $U_e/U_o$ , causes a nonlinear response in  $\dot{m}_T/\dot{m}_o$ , which was therefore studied in more detail.

The effect of Strouhal number, and nonlinear response with pulsation strength, were further investigated using the University Sound driver in order to examine as wide a Strouhal number range as possible. The Strouhal number was varied by changing the jet velocity, which resulted in a Reynolds number range of 5600 to 15,700. This necessitated that corrections be made to the data for Reynolds numbers less than 12,000, based on the results from Fig. 3, by assuming that the "with-drive" results are affected by viscosity in a similar manner to the "no-drive" results. It was not possible to operate at higher Reynolds numbers, thereby avoiding corrections, because of frequency limitation by the mechanical system response (Fig. 5), and because a larger diameter orifice could not be driven strongly enough by the driver power available. It will be shown later that

$$\frac{U_e}{U_o} = \frac{K_1 \sqrt{\dot{W}}}{U_o \sqrt{\dot{m}_o}} \quad (7)$$

at a particular frequency, where  $\dot{W}$  is the driver power, and  $K_1$  is a constant; hence the corrected experimental results for the 9.53-mm-dia orifice, at  $x/d_o = 25.1$ , for a range of driver powers, have been presented in Fig. 6 in terms of the parameter  $\sqrt{\dot{W}}/U_o \sqrt{\dot{m}_o}$ . The nonlinear response of  $\dot{m}_T/\dot{m}_o$  with pulsation strength is immediately apparent indicating that there may be a practical upper limit to the acoustic augmentation of entrainment mass flow rate. It will also be observed that the data for the lower Strouhal numbers have been curtailed because of the restriction on driver power ( $< 30$  W) to avoid destruction of the "voice coil." By cross-plotting the data at  $\sqrt{\dot{W}}/U_o \sqrt{\dot{m}_o} = 4.5$  ( $U_e/U_o$  constant) the response with Strouhal number can be shown, as in Fig. 7, and is seen to peak at a Strouhal number of approximately 0.25.

The variation of  $\dot{m}_T/\dot{m}_o$  with  $x/d_o$ , near optimum Strouhal number conditions, is given in Fig. 8 for several orifice sizes. Equation (3) has also been shown for comparative purposes, which immediately indicates that the experimental points for "no-drive" conditions have been affected by viscosity; presumably the "with-drive" data are similarly affected. This is the result of having to obtain a Strouhal number of 0.3 by lowering the jet velocity, resulting in low Reynolds numbers. The "no-drive" data also unfortunately suffer from undue experimental scatter caused by the difficulty in the measurement of  $\dot{m}_o$  at such low jet velocities; the lower limit of the instrumentation available was being reached. Despite this criticism the data clearly show the increased entrainment produced by acoustic drive, and that a linear relationship exists between  $\dot{m}_T/\dot{m}_o$  and  $x/d_o$  for the power (or  $U_e/U_o$ ) range used. Clearly the data are similar to those of Fig. 4 for lower Strouhal numbers.

## Discussion

**Dimensional Analysis.** The discussion is facilitated by considering the dimensional analysis of the problem, which may be conveniently divided into two parts: (a) examination of the relationship between pulsation strength and power, and (b) the relationship between pulsation strength and jet mass flow rate.

(a) Consider the nozzle flow to be incompressible and that geometric similarity applies, then since pulsation strength has been shown to depend on the power, jet velocity, and orifice diameter [8], it may be assumed that

$$U_e = F(\dot{W}, \rho_o, d_o, U_o, \mu_o) \quad (4)$$

where  $\rho_o$  is the density and  $\mu_o$  is the viscosity. Then by selecting  $\rho_o$ ,  $d_o$ , and  $U_o$  as common factors it follows that

$$\frac{U_e}{U_o} = F_1 \left( \frac{\dot{W}}{\rho_o d_o^2 U_o^3}, \frac{\rho_o d_o U_o}{\mu_o} \right) \quad (5)$$

where  $\rho_o d_o U_o / \mu_o$  is the orifice Reynolds number. By plotting  $U_e/U_o$  versus  $\dot{W}/\rho_o d_o^2 U_o^3$  it quickly becomes apparent that

$$\left( \frac{U_e}{U_o} \right)^2 = \frac{K \dot{W}}{\rho_o d_o^2 U_o^3} \quad (6)$$

(where  $K$  is a constant), as shown in Fig. 9 for data obtained at 250 Hz, for the 9.53-mm-dia orifice. Hence

$$\frac{U_e}{U_o} = \frac{K_1 \sqrt{\dot{W}}}{U_o \sqrt{\dot{m}_o}} \quad (7)$$

These data were obtained for a Strouhal number ( $f d_o / U_o$ ) range of 0.033 to 0.131. There was no discernable dependence on the Strouhal number, which justifies the omission of the frequency  $f$  as an independent parameter in equation (4). Furthermore, the Reynolds number range of the data was from 6000 to 38,000 with no noticeable effect, implying that viscous effects may be neglected. Thus equation (7) is the performance

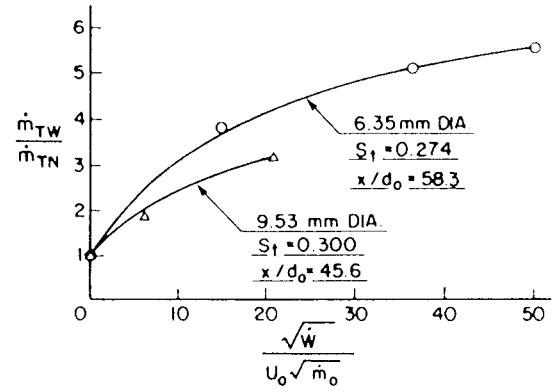


Fig. 10 Variation of mass flow rate ratio with pulsation strength parameter, frequency 250 Hz

law at 250 Hz. At other frequencies the constant  $K_1$  is expected to change because of mechanical system response, and changing the orifice size may introduce a geometry parameter since geometric similarity will not be preserved.

(b) Consider the air jet flow to be incompressible, to have the same density as the entrained air, and conditions are geometrically similar. Then since the experimental results show that the total mass flow rate through a given plane depends on the distance from the orifice, the jet velocity, the orifice diameter, the pulsation strength, the Reynolds number, and Strouhal number, a functional relationship may be assumed as follows

$$\dot{m}_T = F_2(U_e, \rho_o, d_o, U_o, \mu_o, f, x) \quad (8)$$

Again, selecting  $\rho_o$ ,  $d_o$ , and  $U_o$  as common factors it may be shown that

$$\frac{\dot{m}_T}{\dot{m}_o} = F_3 \left( \frac{U_e}{U_o}, \frac{\rho_o d_o U_o}{\mu_o}, \frac{f d_o}{U_o}, \frac{x}{d_o} \right) \quad (9)$$

In principle it would be possible to establish the effect of Reynolds number on  $\dot{m}_T/\dot{m}_o$  at a particular drive condition. However, this would involve keeping  $U_e/U_o$ ,  $S_t$ , and  $x/d_o$  constant while the Reynolds number was varied, a very difficult experimental task, which has so far not been attempted. The assumption has therefore been made that Reynolds number effects at "with-drive" conditions are similar to those at the "no-drive" conditions.

When the Reynolds number is high viscous effects can be neglected, and for fully developed flow, that is when  $x > 15 d_o$  [2],  $\dot{m}_T$  is a linear function of  $x$  for "no-drive" conditions [1]. Thus the Reynolds number can be dropped from equation (9) and there may be a simple dependence on  $x/d_o$  for "with-drive" conditions.

Furthermore, when the density of the injected fluid  $\rho_o$  is different from that of the surroundings  $\rho_s$ , being entrained, Ricou and Spalding [1], from their data, showed that the data could be normalized to those for no density difference by multiplying the mass flow rate ratio by  $\sqrt{\rho_o/\rho_s}$ , i.e.,

$$\frac{\dot{m}_T}{\dot{m}_o} \sqrt{\frac{\rho_o}{\rho_s}}$$

All the data presented here have been corrected in this manner, even though small, because of small differences in temperature of the jet flow air and the entrained air (299 K and 306 K typically).

**Entrainment Results.** Figures 4 and 8 present the entrainment mass flow rate results without corrections for Reynolds number effects. This is not important since it is the ratio of  $\dot{m}_T/\dot{m}_o$  "with-drive" to  $\dot{m}_T/\dot{m}_o$  "no-drive" which is of interest. Thus any Reynolds number factors cancel, provided viscous effects are similar. Also since  $\dot{m}_o$  was kept constant,

during a particular test, the above ratio reduces to  $\dot{m}_{TW}$  "with-drive" divided by  $\dot{m}_{TN}$  "no drive." Clearly the "with-drive" behavior is linear with  $x/d_o$  over a wide range of pulsation strength and Strouhal number, and the ratio  $\dot{m}_{TW}/\dot{m}_{TN}$  increases substantially with the driving power. Thus the entrained mass flow rate has been considerably increased by pulsating the jet flow. Some data are shown for 12.70-mm and 15.88-mm-dia orifices, but because of driver power limitations entrainment changes are small.

The variation of  $\dot{m}_T/\dot{m}_o$  with pulsation strength is clearly shown in Fig. 6, for 400 Hz, and a maximum value of 3.6 for  $\dot{m}_{TW}/\dot{m}_{TN}$  was measured. All curves in Fig. 6 should pass through  $\dot{m}_T/\dot{m}_o = 7.56$ ; the small discrepancies shown are the result of experimental error. A wider range of data variation was covered by the results of Fig. 8, which have been replotted in Fig. 10 (together with an extra experimental point) as  $\dot{m}_{TW}/\dot{m}_{TN}$  versus  $\sqrt{\dot{W}}/U_o\sqrt{\dot{m}_o}$ . Data from Fig. 6 have not been included because their abscissa scale is different, i.e., the constant  $K_1$  is known only for the 9.53-mm-dia orifice at 250 Hz driving frequency. This is because measuring the pulsation strength  $U_e$  is difficult with the instrumentation available, and would be more so in engineering situations. The measurement of driving power  $\dot{W}$  is more convenient and gives a better idea of the power requirements required to increase the entrainment rate. A maximum value of  $\dot{m}_{TW}/\dot{m}_{TN}$  of 5.59 (corresponding to  $\dot{m}_{eW}/\dot{m}_{eN} = 5.82$ ) at  $St = 0.274$  (250 Hz), was recorded for a driver power of 16 W. This is considerably greater than a ratio of 2, the maximum previously reported [8]. The pronounced separation of the curves at  $St$  values of 0.274 and 0.300 seems rather large in light of Fig. 7 and may be the result of geometric similarity not being preserved.

The driving power required for, e.g., doubling  $\dot{m}_{TW}/\dot{m}_{TN}$  may be compared with the jet power,  $\dot{m}_o U_o^2/2$ , using the data from Fig. 10. Thus for the 6.35-mm-dia orifice the power required is 32 times the jet power, and for the 9.53-mm-dia orifice it is 72 times the jet power. This is indeed large, and considered in isolation of the process being affected by acoustic control it may be misleading. For instance Vermeulen et al. [9] showed that the power required to acoustically control the dilution-air mixing of a combustor, under scaled "full-load" operating conditions, was less than 1/2 percent of the combustor energy conversion rate. Hence the power required to produce a pulsating flow may still be small when compared with the overall power of the process.

In constructing the "best-fit" lines to the data of Fig. 8 the lines have been drawn through the origin of axes, as was done by Ricou and Spalding [1]. But,  $\dot{m}_T/\dot{m}_o$  may have the value unity at  $x/d_o = 0$ , and certainly has for no-drive conditions. However, the accuracy of the data does not warrant this discrimination, and it has been ignored. For the unexcited jet Hill [2], for the initial region  $x/d_o < 15$ , showed that the slope of the entrainment law decreased from 0.32 to 0.12 at one nozzle diameter from the orifice. The present experiments were incapable of obtaining similar data for the excited jet, and measurements in the initial zone were not made. However, Vermeulen and Yu [8], by means of velocity and temperature profile measurements, showed, for the modulated jet, that increased entrainment took place over the first five diameters downstream of the jet orifice where the toroidal vortices are formed and are strongest. Hence, it is expected that future measurements in the initial zone will show that the local entrainment rate is substantially increased by acoustically exciting the jet.

Figures 6 and 10 indicate that the increase in entrainment mass flow rate begins to saturate with pulsation strength at the higher driver powers. This is in agreement with the findings of [8], and may be due to the excitation of the toroidal vibration mode of the toroidal vortices. The data are of the form  $y = ax^b + 1$  for a particular Strouhal number. This allows an

overall performance law to be found for say optimum Strouhal number conditions. The following equation was obtained for the data of Fig. 10 at  $St = 0.274$  (6.35-mm-dia orifice, 250 Hz)

$$\frac{\dot{m}_{TW}}{\dot{m}_o} = 0.13 \frac{x}{d_o} \left( \frac{\sqrt{\dot{W}}}{U_o \sqrt{\dot{m}_o}} \right)^{0.62} + 0.29 \frac{x}{d_o} \quad (10)$$

This equation is valid for  $x/d_o > 15$ , for the given system, and reduces to equation (3) for zero driving power.

An optimum Strouhal number of 0.25 was established by the results of Fig. 7. This is in agreement with the findings of [8] from velocity measurements, and is consistent with the findings of Crow and Champagne [4] who found that the turbulence intensity was optimal for  $St \approx 0.3$ . Both findings were for conditions essentially independent of Reynolds number effects. The incomplete curves in Fig. 7 suggest that the optimum value may depend on the pulsation strength  $U_e/U_o$ , but more data at lower Strouhal numbers are required before a definite conclusion can be drawn.

## Conclusions

The experimental results show that jet entrainment was considerably increased by pulsing the jet flow. Specifically for  $x/d_o > 15$  the jet total mass flow rate was increased by up to a factor of 5.6 (corresponding mass flow rate entrained by up to a factor of 5.8) for a Strouhal number of 0.274 and a driver power of 16 W. The entrainment of the excited jet varies linearly with distance downstream from the jet orifice, as for the unexcited jet.

The jet response varies nonlinearly with the excitation pulsation strength, indicating that there may be a practical upper limit to the acoustic augmentation of entrainment mass flow rate. The response depends on Strouhal number and appears to be optimum at about 0.25.

## Acknowledgments

The authors are indebted to Mr. W. A. Anson, Chief Technical Supervisor; Mr. R. Bechtold, Machine Shop Supervisor; and Mr. P. Halkett, Technician, for their careful work in the building of the test rig. The work was supported financially by the Natural Sciences and Engineering Research Council of Canada, under Grant No. A7801.

## References

- 1 Ricou, F. P., and Spalding, D. B., "Measurements of Entrainment by Axisymmetrical Turbulent Jets," *Journal of Fluid Mechanics*, Vol. 11, 1961, pp. 21-32.
- 2 Hill, B. J., "Measurement of Local Entrainment Rate in the Initial Region of Axisymmetric Turbulent Air Jets," *Journal of Fluid Mechanics*, Vol. 15, Part 4, 1972, pp. 773-779.
- 3 Vermeulen, P. J., Odgers, J., and Ramesh, V., "Acoustic Control of Dilution-Air Mixing in a Gas Turbine Combustor," *ASME JOURNAL OF ENGINEERING FOR POWER*, Vol. 104, Oct. 1982, pp. 844-852.
- 4 Crow, S. C., and Champagne, F. H., "Ordered Structure in Jet Turbulence," *Journal of Fluid Mechanics*, Vol. 48, Aug. 1971, pp. 547-591.
- 5 Binder, G., and Favre-Marinet, M., "Mixing Improvement in Pulsating Turbulent Jets," *ASME Symposium on Fluid Mechanics of Mixing*, Georgia Institute of Technology, Atlanta, GA, June, 20-22, 1973, pp. 167-172.
- 6 Anderson, A. B. C., "Structure and Velocity of the Periodic Vortex-Ring Flow Pattern of a Primary Pfeiferton (Pipe Tone) Jet," *The Journal of the Acoustical Society of America*, Vol. 27, No. 6, Nov. 1955, pp. 1048-1053.
- 7 Hill, W. G., and Greene, P. R., "Increased Turbulent Jet Mixing Rates Obtained by Self-Excited Acoustic Oscillations," *ASME JOURNAL OF FLUIDS ENGINEERING*, Vol. 99, No. 3, Sept. 1977, pp. 520-525.
- 8 Vermeulen, P. J., and Yu, Wai Keung, "An Experimental Study of the Mixing by an Acoustically Pulsed Axisymmetrical Air-Jet," *30th ASME International Gas Turbine Conference*, Houston, TX, Mar. 18-21, 1985, Paper No. 85-GT-49, pp. 1-10.
- 9 Vermeulen, P. J., Odgers, J., and Ramesh, V., "Full Load Operation of a Gas Turbine Combustor With Acoustically Controlled Dilution-Air Mixing," *29th ASME International Gas Turbine Conference*, Amsterdam, The Netherlands, June 3-7, 1984, Paper No. 84-GT-106, pp. 1-8.



## A NEW HYDRAULIC PRESSURE INTENSIFIER USING OIL HAMMER

K. Suzuki, Associate Professor  
Musashi Institute of Technology  
Tamazutsumi Setagayaku  
Tokyo, Japan

## ABSTRACT

An oil hammer generates a greater pressure than that supplied to a pipeline, and this is important in terms of the safety of oil hydraulic equipment. The author intends to actively utilize this pressure rise phenomenon to oil hydraulics and has invented an intensifier which is based on a new principle and converts oil pressure into a value more than six times higher, by means of an oil hammer. The intensifier has advantages in simple structure and in easy control since it is controllable by switching only one solenoid operated valve. In this paper, a new design for a pressure intensifier is proposed and a theoretical analysis describing the performance and operation of this design is developed. Results of experimental work on this design are then compared with theoretical results.

## NOMENCLATURE

$A_c$  = line cross-sectional area  
 $A_v$  = total open area of solenoid operated valve  
 $c$  = sonic velocity in fluid,  $\sqrt{K/\rho}$   
 $c_0$  = discharge coefficient  
 $D$  = inner diameter of line  
 $D_v = 4\nu / D^2$   
 $e_c$  = electric output signal of computer  
 $e_s$  = solenoid voltage  
 $i$  = solenoid current  
 $K$  = bulk modulus of fluid  
 $L$  = length of line  
 $N$  = number of nodes along line  
 $P_o$  = output pressure  
 $P_m$  = maximum output pressure  
 $P_s$  = supply pressure  
 $p$  = pressure  
 $q$  = volumetric fluid flow rate  
 $q_v$  = volumetric fluid flow rate through valve  
 $T_1 = 2L / c$   
 $t$  = time

$t_w$  = pulse width

$V_1$  = input volume through point 1 per cycle

$V_o$  = output volume through point 3 per cycle

$v$  = average fluid velocity at line section

$w$  = ratio of current open area of solenoid valve to its total open area

$y$  = valve (spool) displacement

$\eta$  = efficiency

$\nu$  = kinematic viscosity of fluid

$\rho$  = fluid density

subscripts

1,2,3,4,5,6: flow positions (Fig. 1)

## 1. INTRODUCTION

As an oil ( water ) hammer generates a pressure greater than that supplied to the pipeline, and sometimes causes equipment breakdown, there have been many attempts to predict such pressures and develop methods to reduce it. In the present work, however, the author proposes to actively utilize this pressure rise. A new design for a new type of hydraulic pressure intensifier is proposed, which operates on the principle that an oil hammer is generated continuously in the pipeline and only the high pressure oil is discharged through a check valve. The intensifier can convert oil pressure of several MPa produced by a low pressure pump, into a pressure which is more than six times higher.

In the case of water, a hydraulic ram utilizing this idea by means of water hammer has been invented two hundred years ago, and is used to deliver water to higher elevations. Recent investigations show that the discharge pressure in hydraulic rams are of the order of several hundred kPa [1]. In the case of oil hydraulics however, discharge pressure levels required are about 10-30 times greater than those encountered by water hydraulic devices. Consequently, a different structure is required in the case of oil hydraulic equipment. The new intensifier has the following advantages over the usual intensifier:

(a) Very simple structure: As the new intensifier consists only of a pipe line, a check valve, a solenoid operated valve and the current switching device, the structure is simple and economical.

(b) Switching of only one solenoid operated valve makes it possible to start and stop the intensifier easily and to control the discharge at the output. This control is achieved by repeated switching of the solenoid valve. Since the intensifier is controll-

able by on-off switching of only one solenoid operated valve, it is suitable for micro computer control.

In this paper the new intensifier construction is explained and its fundamental characteristics are clarified by experimental and theoretical results.

## 2. NEW INTENSIFIER CONSTRUCTION

The construction of the new intensifier which has been developed in this research is shown in Fig.1. Oil with constant pressure is supplied to the upstream side of the pipeline (position 1 ). The switching of a solenoid operated valve located at the downstream end of the pipeline (position 2 ) generates an oil hammer in the pipeline.

When current is supplied to the solenoid valve, it is in the open state, the fluid path is free and the fluid flows at high speed through the pipeline and the solenoid valve to the tank. Immediately after the valve is closed rapidly, by cutting off the solenoid current, an oil hammer is generated in the line. As long as the pressure at point 2 is higher than that at point 3 , the check valve is open and high pressure fluid is discharged through the check valve. Soon the pressure at point 2 becomes lower than that at point 3 , and the check valve is closed preventing a reverse flow. The accumulator (II) prevents sudden and local pressure rises resulting in an increased output flow.

If high pressure flow is needed, it can be loaded through point 4 , but in this research this path is closed. Although the relief valve (II) is attached in order to keep the point 3 pressure constant for slow flow change, all the high pressure fluid which is designed to be sent to a load, flows away through it because point 4 is closed.

In order that the solenoid operated valve may be operated automatically according to various patterns, the signal for switching is generated by a micro computer. An LSI ( CTC = Counter Timer Circuit ) which can read a system clock is inserted into the computer, and it is set up to detect time at intervals of 1.25 ms in order to operate the solenoid operated valve at desired time intervals. The micro computer output signal is sent to the solid state relay ( SSR ) through an interface. This signal controls the OPEN | CLOSED status of the solenoid operated valve. The OPEN-CLOSED intervals and the total number of OPEN | CLOSED operations are entered interactively by the user at the keyboard.

One of the applications of this intensifier is an application to an oil hydraulic cylinder as shown in

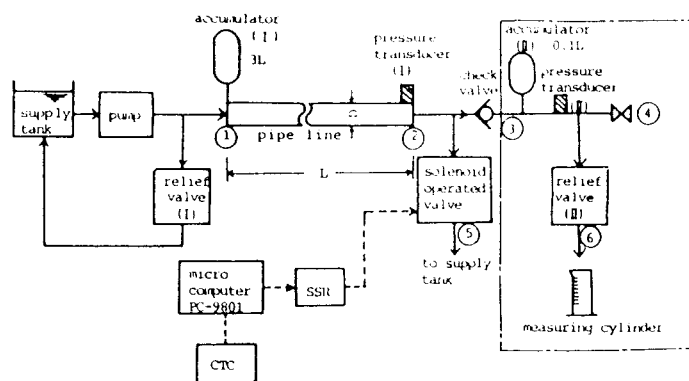


Fig.1 Schematic diagram of the test rig

Fig.2. The part enclosed by a line in Fig.1 is replaced by a hydraulic cylinder and a manually operated valve. When the solenoid operated valve is kept closed , the pressure at the pump is supplied directly to the hydraulic cylinder and it is operated by the pump pressure. If an oil hammer is generated by the operation of the solenoid operated valve, the chamber of the cylinder is compressed by the discharged fluid. The pressure in the chamber can be raised gradually for every on-off of the solenoid operated valve. The detailed performance of this application will be clarified in a future publication.

## 3. NUMERICAL CALCULATION

The method combining characteristics and finite difference has been developed to predict the dynamic response of a pipeline by Zielke [2], which considers frequency dependent laminar friction in the pipeline. This method is applied to predict the dynamic response of the pipeline when oil hammer occurs, and the performance of the system is obtained by numerical calculation.

The following conditions are assumed for numerical calculation to predict the dynamic characteristics during a cycle. At the beginning, the solenoid operated valve is in the closed position, the fluid in the line is at rest and the line pressure is equal to the supply pres-

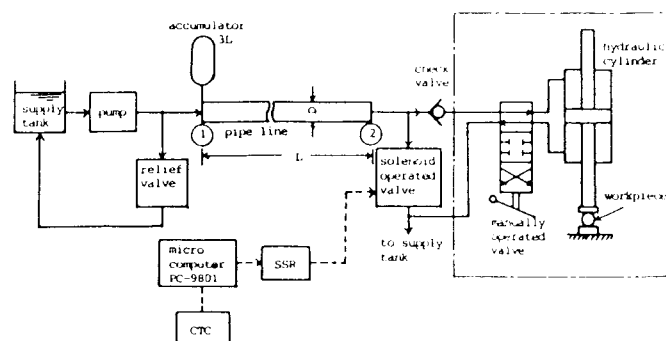


Fig.2 Example of application

sure of the pump. The valve is then opened and closed according to the pulse output of the micro computer.  $w$  in the equation (4) is the ratio of the current open area of the solenoid valve to its total open area and lies between zero and one. It is assumed that the flow through the check valve is discharged without any pressure drop when the pressure at point 2 is higher than that at point 3 due to an oil hammer.

Considering the initial and the boundary conditions, the following equations are used for the calculations together with the equations developed by Zielke. The initial conditions are

$$v = 0 \quad (1)$$

$$p = P_s \quad (2)$$

where  $v$  and  $p$  are the average fluid velocity at the line section and pressure respectively at all points along the line.

The boundary condition are at the upstream:

$$p_1 = P_s \quad (3)$$

at the downstream:

$$q_v = c_0 A_v w \sqrt{2p_2/\rho} \quad (4)$$

$$A_c v_2 = q_3 + q_v \quad (5)$$

$$p_3 = P_o \quad (6)$$

due to the action of the check valve:

$$p_2 = P_o \quad (q_3 > 0) \quad (7)$$

$$q_3 = 0 \quad (p_2 < P_o) \quad (8)$$

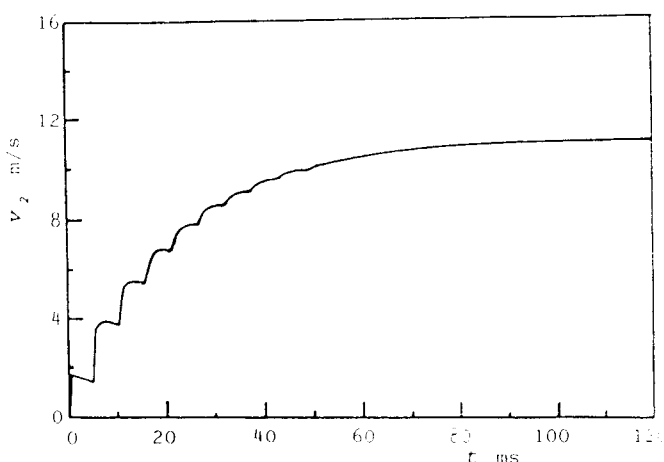


Fig.3  $v_2$  after opening the valve

#### 4. EXPERIMENTAL RESULTS and CALCULATED RESULTS

The differential transformer was connected to the spool of the solenoid operated valve to measure the valve (spool) displacement. The pressures  $p_2$  and  $p_3$  were measured by semiconductor pressure transducers (I) and (II). These signals and micro computer out-

put  $e_c$ , solenoid voltage  $e_s$  and the signal of the current  $i$  were memorized rapidly by a digital memory device. Later these were recorded slowly by X-Y recorder.

Fig.3 shows the calculated result of the fluid velocity  $v_2$  after the solenoid operated valve starts to open. The velocity increases rapidly from zero and reaches almost steady state in about 100 ms. Therefore, referring to this velocity response, the solenoid operated valve was operated with suitable time intervals.

#### 4.1 Dynamic Characteristics

First, the solenoid operated valve was operated continuously with pulse width of 125 ms and frequency of 4 Hz. The valve was intended to be closed after the flow velocity reached sufficiently steady state. Fig.4(a) shows the micro computer signal and the response at each point for one cycle, illustrated with a common time axis. The solenoid operated valve begins to open 22.1 ms after turning on the computer signal. The pressure  $p_2$  at the downstream becomes almost zero and the fluid in the line is accelerated.

By the closure of the solenoid operated valve, the pressure  $p_2$  increases suddenly and reaches a value  $P_o (= p_3)$ , which is kept constant at point 3. Because the check valve opens at this moment and the fluid is discharged through it, the pressure  $p_2$  is maintained at this value for a short time and undergoes a damped oscillatory behavior which eventually converges to the value of the supply pressure  $P_s$ . When  $p_2$  becomes lower than  $P_o$ , the check valve closes. The displacement of the poppet in the check valve was a few tenths of a mm. The fluctuation of the supply pressure  $P_s$  at the point 1 during the oil hammer was within 4 % of the steady state pressure because of the relief valve (I) and the accumulator (I).

For the numerical calculation, the observed form of the valve displacement was approximated by a trapezoidal wave. When  $y$  is greater than zero, the solenoid operated valve is open. In the figure, the solid lines show the experimental results.

Fig.5 shows the pressure responses with the different output conditions. If point 3 is shut, very high pressure is generated and after that it decreases into the value lower than atmosphere. Therefore cavities seem to appear in the fluid.

The cycle period of the vibration in the experimental result is longer than the numerically calculated result for  $P_o = 3.9 \text{ MPa}$ . When point 3 is shut, the maximum pressure of the experimental result is lower than the calculated one. These are attributed to the

Parameter	Value
$A_v$	$7.76 \times 10^{-5} \text{ m}^2$
$c_0$	0.6
$D$	5 mm except Fig. 7 & 8
$K$	$0.136 \text{ GN/m}^2$
$L$	4.15 m except Fig. 6
$N$	20
$P_s$	1.96 MPa except Fig. 8
$\nu$	$0.383 \times 10^{-4} \text{ m}^2/\text{s}$
$\rho$	$853 \text{ kg/m}^3$

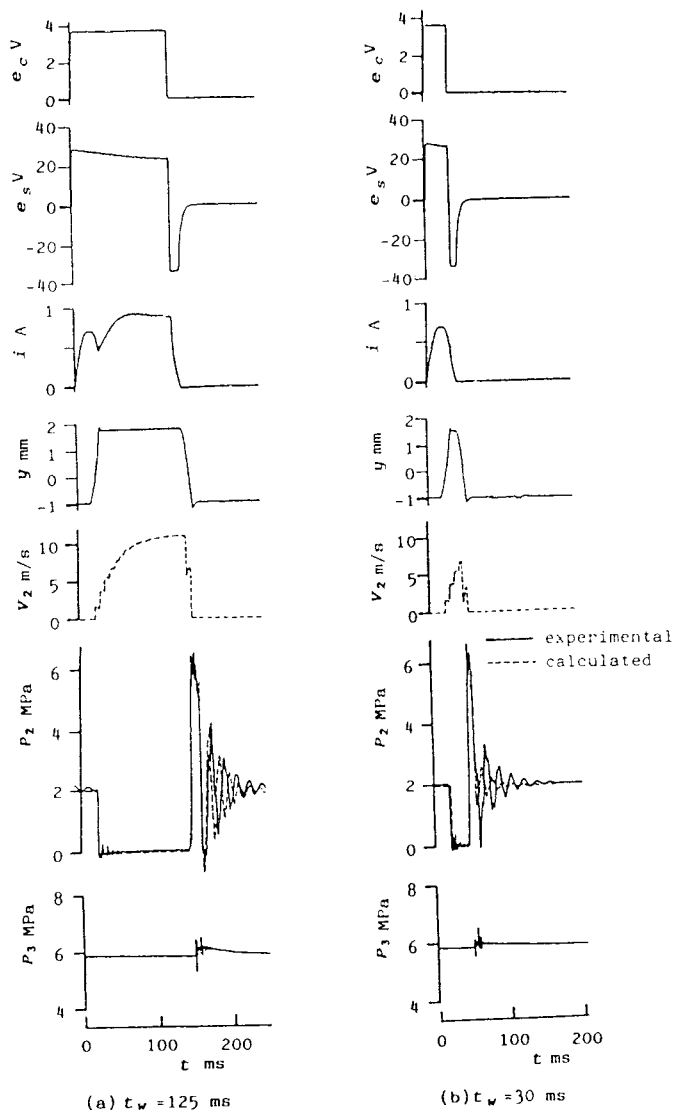


Fig. 4 Responses of the system to pulse input with different width

unavoidable volume at the connection parts in the experimental equipment. Around point 2 the distances between the downstream point of the pipeline and the solenoid and the check valve and the distance between the check valve and the accumulator (II) were made as small as possible. However, there were still some

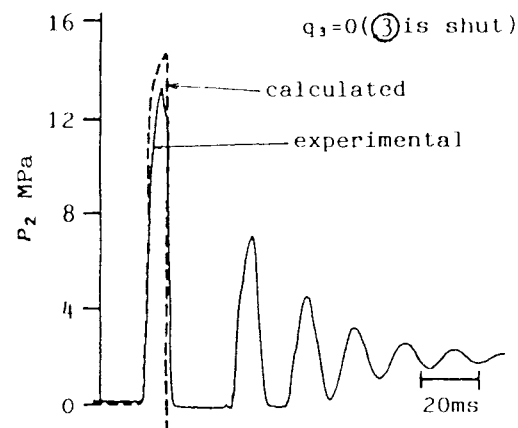
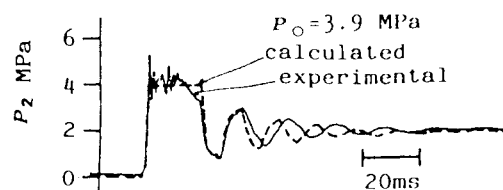


Fig. 5 Wave forms of pressure  $p_2$  for various output conditions

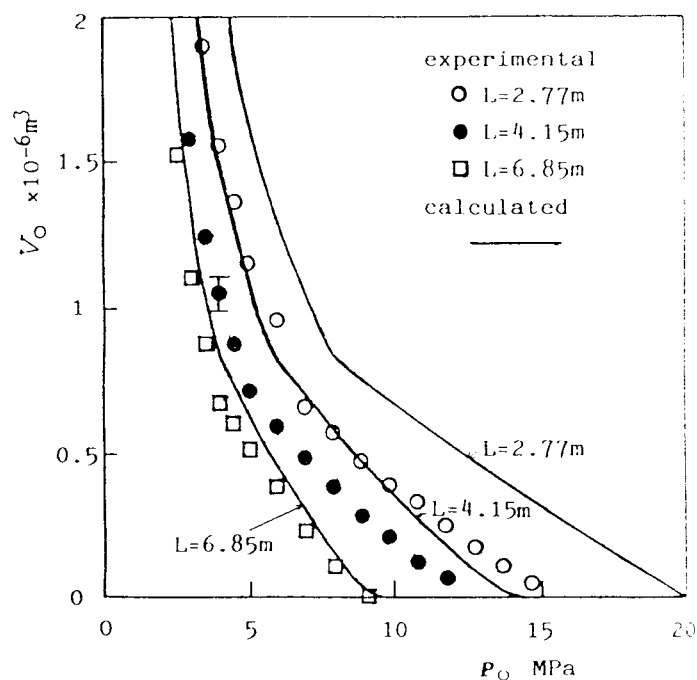


Fig. 6 Output volume  $V_0$  versus output pressure  $p_0$  for various line length  $L$

amount of unavoidable piping length between these points. The compressibility of the volume of fluid in these regions softens the abrupt change of the flow velocity and consequently weakens the oil hammer and makes the cycle period of the vibration longer. The extra piping length also produces time lags which reduce the output volume mentioned in next section.

#### 4.2 Output Volume

Fig.6 and Fig.7 show both the experimental and the calculated results of the output volume  $V_o$  per cycle for a steady output pressure  $P_o (= p_3)$ . The value of the output pressure  $P_o$  can be varied by the adjustment of the relief valve (II) to obtain experimental data. The output volume was measured at point 6. Fig.6 shows the effect of the line length. Fig.7 shows the effect of the line diameter  $D$ . Error bands in  $V_o$  for  $P_o = 3.9 \text{ MPa}$  are shown at 20:1 odds on Fig.6 and Fig.7. The same value of odds is used for error bands in the following figures.

On the whole, the output volume obtained by the experiment shows relatively lower value than that obtained by calculation. This may be attributed to the many kinds of small difference in the experimental conditions from the idealized conditions for the calculation. For example, the unavoidable small distance between each parts at the downstream 2 reduces the output volume. Dynamics of the poppet in the check valve seem complicated and need to be clarified precisely in the future, but they are idealized in the calculation because the purpose of the paper is to clarify the fundamental principles of the new intensifier. The time delay of the check valve causes the output flow reduction when it begins to open and the time delay also causes reverse flow when the check valve begins to close. Therefore, the output volume with the real check valve is less than that with the idealized check valve.

If the line length is reduced or the line diameter is increased, the output volume increases and maximum output pressure rises. However in either case, the necessary supply flow increases because the input volume to the line during the valve open increases. Moreover if the line length is reduced further, the experimental results do not increase as much as expected from the calculation. This may be attributed strongly to the unavoidable distance and volume between the components at the downstream and the dynamics of the poppet because the cycle period of the oil hammer is reduced with the line length reduced and the effect increases for a rapid change.

Another cause of the performance drop is that laminar flow is assumed in the calculation. The maximum Reynold's number is expected to be 2160 with  $L = 2.77 \text{ m}$ ,  $D = 5 \text{ mm}$  and 2390 with  $L = 4.15 \text{ m}$ ,  $D = 6 \text{ mm}$ . Around these Reynold's numbers the flow is expected to become turbulent, which results in the increase of resistance to the flow. Therefore the flow velocity does not become as high as expected by calculation.

#### 4.3 Maximum Output Pressure

As the output pressure is increased, the output volume decreases and finally becomes zero. At this state, the pressure  $P_o$  is the maximum output pressure  $P_m$  which can be generated by this system. Fig.8 shows the effect of the supply pressure  $P_s$  and line diameter  $D$  on the maximum output pressure  $P_m$ .  $P_m$  is almost proportional to  $P_s$ . The experimental results show that  $P_m$  is about 4.2 times as high as  $P_s$  with  $D = 4 \text{ mm}$ , about 6.1 times with  $D = 5 \text{ mm}$ , and about 7.4 times with  $D = 6 \text{ mm}$ . The experimental result is lower than calculated one because of the same reason as Fig.5 for  $q_3 = 0$ .

If the pressure drop through the solenoid operated valve is ignored and the valve is assumed to be closed instantaneously after the steady flow velocity is obtained, and the output flow is zero, the maximum output pressure  $P_m$  is indicated by the equation (9) because it is the typical in the oil hammer [3]:

$$P_m = \frac{cD^2P_s}{32\nu L} \left( 1 + 2 \sqrt{\frac{D_v T_1}{\pi}} + D_v T_1 \right) \quad (9)$$

The value indicated by equation (9) is a few percent higher than the results obtained by the similar numerical calculation as in section 3.

The assumption of instantaneous valve closure is reasonable in this case. Although the actual valve closure takes similar time as acoustic cycle ( $2L/c$ ) after it starts to move, the pressure drop across the valve ( $p_2$ ) is very small during almost all the process of the valve closure because the area of the valve  $A_v w$  is still big enough during it. In very short period before the valve is closed completely, the pressure drop becomes significant across the valve and stops the flow completely at last. Therefore, when the calculated result of  $p_2$  with the assumption of instantaneous valve closure is compared with the result calculated using the observed valve displacement, only a slight difference is found at the beginning portion of the pressure rise.

#### 4.4 Effect of Pulse Width

So far the pulse width was kept 125 ms. The following will be expected from Fig.3, if the open duration of the solenoid operated valve is varied by the pulse width. The maximum fluid velocity is increased and the oil hammer becomes stronger and results in the output volume increase as the duration increases. But the effect decreases when the duration is increased beyond about 100 ms. Besides the input volume to the line increases monotonically with the duration and flows away wastefully into a tank.

Now the input volume, the output volume and the efficiency are investigated when the pulse width of the micro computer output is varied. Fig.4 (a) and (b)

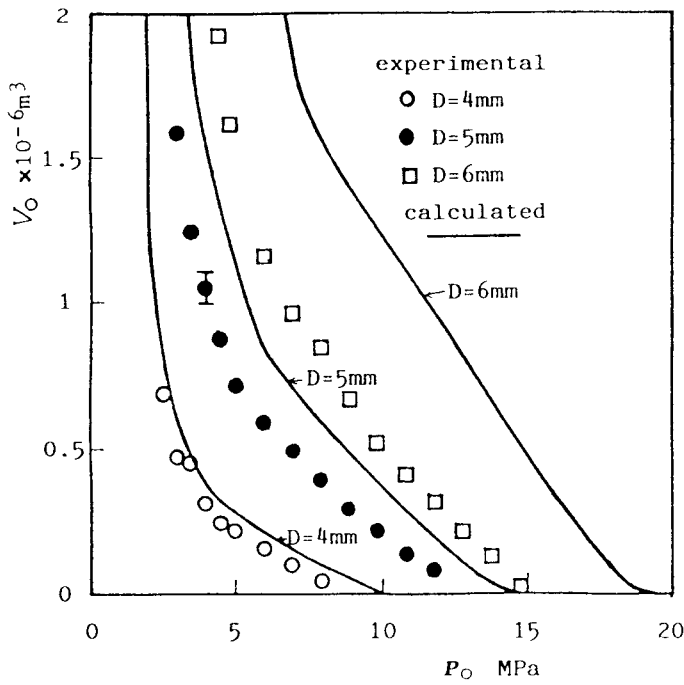


Fig.7 Output volume  $V_o$  versus output pressure  $P_o$  for different inner diameter  $D$

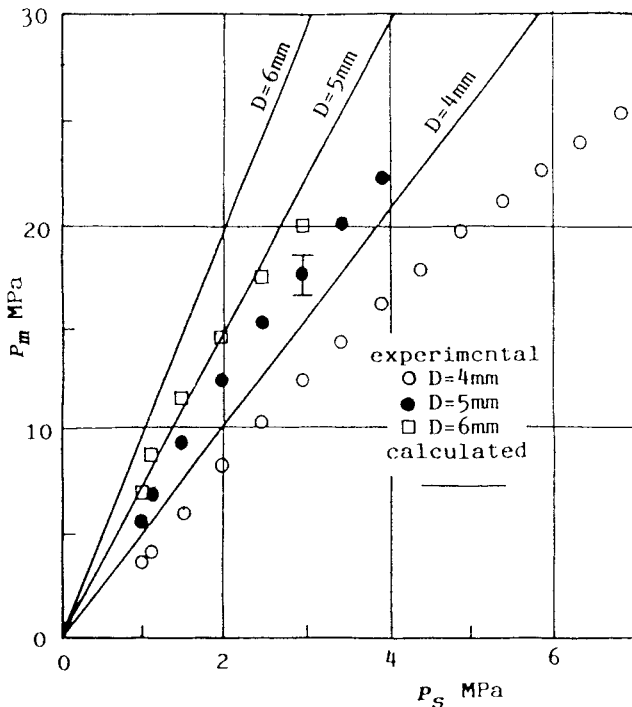


Fig.8 Maximum output pressure  $P_m$  versus supply pressure  $P_s$

show the relations between the computer output and the response at each point when the pulse width is 125 ms or 30 ms. For the short pulse width, the difference of the forms between the computer output and the valve displacement is large. If the pulse width is within 16 ms, the solenoid operated valve does not open at all because the valve displacement cannot exceed the overlap region. If the pulse width exceeds

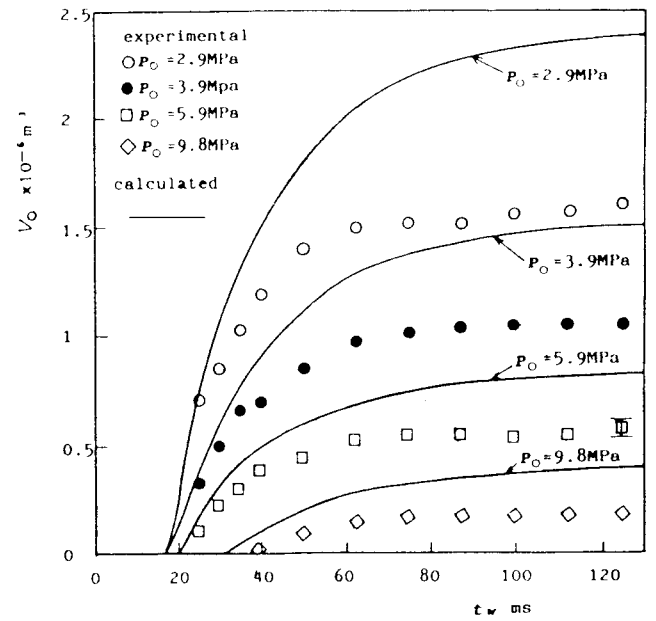


Fig.9 Output volume  $V_o$  versus pulse width  $t_w$  for various output pressure  $P_o$

about 16 ms, the open duration of the valve increases monotonically with the pulse width.

Fig.9 shows the relation between the output volume  $V_o$  and the pulse width  $t_w$ . The output volume increases as the pulse width is increased. But the output volume increases slightly as the pulse width increases beyond 100 ms. The value of the experimental results is less than the calculated results in Fig.9. This may be attributed to the similar reason mentioned in section 4.2. Fig.10 shows the relation between the input volume  $V_i$  and the pulse width  $t_w$ .  $V_i$  means the volume which flows during a cycle through the entrance of the line.  $V_i$  increases monotonically with  $t_w$ , and it is slightly more at the low output pressure than at the high output pressure.

The efficiency  $\eta$  is defined as:

$$\eta = \frac{P_o V_o}{P_s V_i} \quad (10)$$

Fig. 11 shows the relation between the efficiency and the pulse width. The figure shows that there exists a value of  $t_w$  at which the efficiency is a maximum.

## 5. CONCLUSION

A new type of intensifier has been invented and tested, which has the principle that an oil hammer is generated continuously in a pipeline and only the high pressure fluid is discharged through a check valve. As

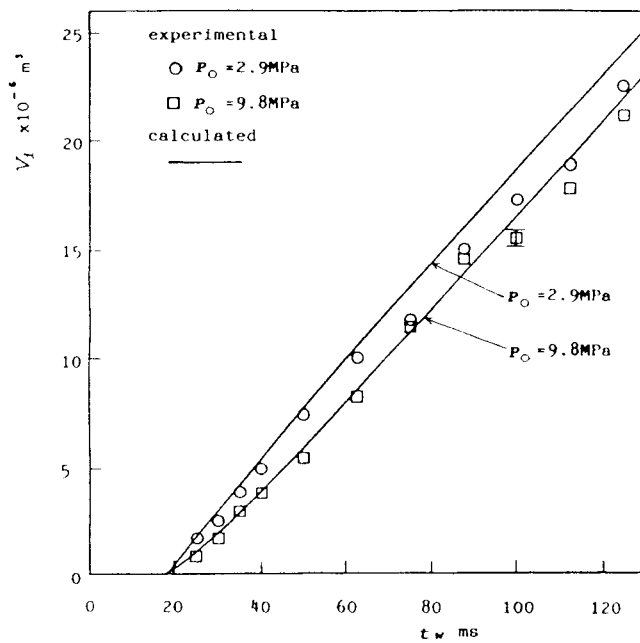


Fig. 10 Input volume  $V_i$  versus pulse width  $t_w$

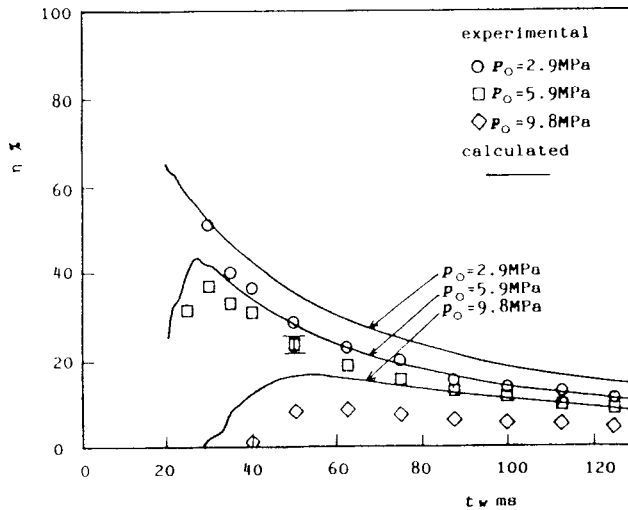


Fig. 11 Efficiency  $\eta$  versus pulse width  $t_w$  for various output pressure  $P_o$

the performance has been investigated by experiments and numerical calculations, it has been verified that the fluid pressure of several MPa supplied by a low pressure pump can be converted into pressure several times higher. Though the possible output flow is not much, application is possible where high pressure is needed by a cylinder at the final stage of pressing or during cramping in a press or a cramp equipment. As the output volume per cycle is clearly determined by the condition, the total output volume can be controlled by the number of cycles. Therefore it is favorable for computer control because the intensifier can be controlled only by switching the solenoid current on and off.

#### ACKNOWLEDGMENT

The author expresses his thanks to Prof. S. Sato and Mr. K. Kobayashi of Musashi Institute of Technology for their support in performing this research.

#### REFERENCES

- 1 Iversen, H. W. , "An Analysis of the Hydraulic Ram", ASME Journal of Fluids Engineering, Vol. 97, No. 2, 1975, PP. 191-196
- 2 Zielke, W. , "Frequency-Dependent Friction in Transient Pipe Flow", ASME Journal of Basic Engineering, Vol. 90, No. 1, 1968, PP. 109-115
- 3 Holmboe, E. L. , Rouleau, W. T. , "The Effect of Viscous Shear on Transients in Liquid Lines", ASME Journal of Basic Engineering, Vol. 89, No. 1, PP. 174-180.

# JET PUMPS & EJECTORS and GAS LIFT TECHNIQUES

March 24th-26th 1975

pp. E2-15 -  
E2-26

## IMPROVEMENT OF EJECTOR THRUST AUGMENTATION BY PULSATING OR FLAPPING JETS

G. Binder and H. Diddle

Universite Scientifique et Medicale de Grenoble, France

### Summary

The influence of pulsating or flapping motions forced on the primary jet on the performance of thrust augmenting ejectors has been investigated experimentally. The effect of the frequency and the amplitude of the forced perturbations was determined for various mixing duct lengths and diffuser geometries. The mixing duct to jet area ratios were 9 and 20 in the pulsating and flapping case respectively.

In constant area ejectors the improvement in thrust augmentation  $\phi$  over the performance obtained with a steady jet in the same geometry increases with decreasing duct length. Thus, with a total length of only ONE duct width  $\phi = 1.2$  could be obtained with unsteady jets whereas  $\phi = 1$  in the steady case.  $\phi$  was further improved by the gain in diffuser pressure recovery produced by the unsteady jets. Maximum augmentations of 1.9 and 1.65 were obtained with pulsating and flapping jets respectively as compared to 1.35 and 1.5 in the steady case.

These improvements in ejector performance are mainly due to the faster mixing produced by these jets.

### 1. INTRODUCTION

Since the beginning of aviation aeronautical engineers have sought to increase the thrust which an engine can produce. Large thrusts are especially necessary during take-off and the shorter the take-off distance the larger the thrust required is. The major problem to be solved in the design of a vertical or short take-off and landing aircraft is precisely the production of the thrust which is necessary during these stages of flight. Ejectors being simple and inexpensive thrust augmenting devices their use on such airplanes appeared early as an attractive solution to this problem.

Until recently, however, thrust augmenting ejectors have not been applied in aeronautics because their actual performance has been rather disappointing and their size excessive. Since there are no theoretical reasons setting strict limits to thrust augmentation the improvement of ejector performance has motivated a number of investigations.

### 2. INFLUENCE OF MIXING RATE ON THRUST AUGMENTATION

The thrust augmentation  $\phi$  is usually defined as the ratio of the total thrust produced together by the primary jet and the ejector divided by the thrust of the jet alone discharging into the ambient atmosphere, the head of the jet with and without ejector being kept constant. Only values  $\phi > 1$  are, of course, interesting.

For a given area ratio  $\lambda$  (see fig. 1), the thrust augmentation of a constant area ejector decreases with the non-uniformity (or skewness) of the exit velocity profile. A more uniform profile, also more complete mixing between primary and secondary streams, can be achieved by increasing the length of the duct but this conflicts with the aeronautical requirement of compactness and, in addition, beyond a certain length of about 5 Dm the gain due to better mixing is more than offset by the loss due to friction. Rapid mixing is also important for good performance.

Thrust augmentation may remarkably be improved if a diffuser is fixed behind the mixing duct. Indeed, calculations show that  $\phi$  of a constant area ejector cannot exceed two whereas with a diffuser there is no upper limit provided the diffuser effectiveness  $e$ , i.e. the ratio of actual to ideal pressure recovery is high. The beneficial effect of the diffuser on  $\phi$  falls off rapidly and becomes null as  $e$  decreases from 1 to 0.5. High diffuser effectiveness implies no separation which in turn requires uniform velocities at the entrance with thin boundary layers or velocity excess near the

### NOMENCLATURE

A	flapping angle
a	pulsation amplitude
$C_p = P_b/P_j$	blowing pressure ratio (Fig. 2)
D	diameter or width
e	diffuser effectiveness
f	frequency
L	length
P	pressure
R	radius
Re	Reynolds number
S	area
$St = \frac{Dj \cdot f}{V_j}$	Strouhal number
T	thrust
u	velocity fluctuation
v	velocity
$\alpha$	angular deflection of jet
$\phi$	thrust augmentation ratio
$\rho$	density
	Subscript
j	jet
ja	jet discharging into ambient
m	mixing duct
d	diffuser
E	ejector
t	total
l	mixing duct entrance
	Superscript
( )	space-time average

boundaries and defect in the middle of the section if the profile is non-uniform. In an ejector with a central jet rather the opposite occurs, i.e. a velocity profile with a bulge in the middle, unless thorough mixing is achieved at the diffuser entrance. But this requires a long mixing duct which, besides being cumbersome, leads to thick boundary layers and again to separation in the diffuser. High diffuser effectiveness is thus very difficult to achieve and this explains why in many experiments thrust augmentations have been deceptively low. Rapid mixing between primary and secondary streams is also a crucial factor for high ejector performance.

The recognition of this fact leads quite naturally to look for means of producing faster mixing in order to improve ejector thrust augmentation. This has effectively been tried by use of multiple jets (1), swirl (2), hypermixing nozzles (3) or a combination of these in particular multiple hypermixing nozzles (4).

The objective of the present research was to investigate the effect on thrust augmentation of unsteadiness forced on the jet such as pulsations or flapping. The investigation of free pulsating or flapping jets undertaken simultaneously in our laboratory showed that they spread faster than steady jets (5, 6). A beneficial effect of unsteadiness on ejector performance could thus be expected. Since quantitative predictions of such turbulent flows are presently beyond reach the extend of these effects could only be ascertained experimentally.

### 3. APPARATUS. FLOW CHARACTERISTICS. EXPERIMENTAL PROCEDURE.

#### 3.1 Flow Loop.

The jets were generated with the following set-up :



### 3.5 Measurements of thrust augmentation

Thrust augmentation is defined as

$$\phi = \frac{\text{total thrust}}{(\text{thrust of jet})_a} = \frac{T_t}{T_{ja}} \quad (1)$$

The index specifying that the jet exhausts into the ambient air. This may also be written :

$$\phi = \frac{(\text{thrust on ejector}) + (\text{thrust of jet})}{(\text{thrust of jet})_a} = \frac{T_F + T_j}{T_{ja}} \quad (2)$$

The generating head of the jet is kept constant. Therefore :

$$\frac{\bar{p}_j}{\rho} - \frac{\bar{V}_{ja}^2}{2} = \frac{\bar{V}_j^2}{2} - \frac{\bar{p}_j}{\rho} = \frac{\bar{V}_j^2}{2} - \frac{\bar{V}_j^2}{2} \quad (3)$$

$$\text{since } \frac{\bar{V}_j^2}{2} + \frac{\bar{p}_j}{\rho} = 0$$

the ambient pressure being chosen as reference.

$$\text{Since } T_{jo} = \rho S_j \frac{\bar{V}_j^2}{2} \quad (\text{momentum flux}) \quad (4)$$

$$T_j = S_j (\rho \bar{V}_j^2 + \bar{p}_j) \quad (5)$$

$\phi$  may be written :

$$\phi = \left( \frac{T_F}{T_j} + 1 \right) \frac{\bar{V}_j^2}{\bar{V}_{ja}^2} + \frac{\bar{p}_j}{\rho \bar{V}_{ja}^2}$$

and finally with

$$\bar{C} = T_F/T_j$$

$$b = \bar{V}_j^2 / \bar{V}_{ja}^2 = \bar{V}_j^2 / (\bar{V}_j^2 - \bar{V}_1^2)$$

$$\phi - 1 = \bar{C} + \left( \bar{C} + \frac{1}{2} \right) (b - 1) \quad (6)$$

$\bar{C}$  is the main contribution to  $\phi - 1$  while  $\left( \bar{C} + \frac{1}{2} \right) (b - 1)$  is a correction term at most equal to about  $\bar{C}/3$ . Note that  $b - 1 = \bar{V}_1^2 / \bar{V}_{ja}^2$ .

This formula shows that  $\phi$  may be entirely determined from the measurement of the thrust on the ejector, the thrust of jet discharging into the ejector (or  $\bar{V}_1^2$ ) and velocity of the entrained flow. No measurements are also needed of the jet discharging into the ambient atmosphere. This proved especially convenient with the pulsating jet because it would have been difficult to obtain the same pulsation amplitude with and without the ejector.

Equation (6) was also used to determine  $\phi$  in the pulsating case.  $T_F$  was measured directly on the thrust bench, the ejector duct being fixed to the floating beam (see below)  $\bar{V}_1^2$  and  $\bar{V}_j^2$  were measured with a hot wire anemometer. Traverses provided the data for space averaging and time averaging was performed with an integrating voltmeter. It should be emphasized that because of the large pulsation amplitudes :  $\bar{V}_j^2 = \bar{V}_j^2 + u_j^2 \neq \bar{V}_j^2$ , typically  $\bar{V}_j^2 \approx 1.3 \bar{V}_j^2$ .  $\bar{V}_j^2$  was determined by measuring  $\bar{V}_j$  and  $\bar{u}_j^2$ .

The thrust bench (Fig. 3) consists of a floating beam supported at both ends by two steel foils fixed to a rigid frame. The elastic deflection of these foils is proportional to the force applied to the beam ; it was about 0.1 mm/N and was optically amplified 4000 times to facilitate the measurements.

Independent checks made by measuring the momentum flux at the ejector exit showed that the preceding method gave values of  $\phi - 1$  about 8 to 10% too low. The results reported here are also rather underestimated values of  $\phi$ .

With the flapping jet ejector the above procedure gave poor results because of non uniformity in the spanwise direction and because of the unknown pressure distri-

- an inlet caisson with dust filters and cooling radiators designed to maintain the jet temperature equal to ambient temperature to  $\pm 0.5^\circ\text{C}$ . The purpose of these provisions was to facilitate the measurement with hot wire anemometers.

- a centrifugal blower giving  $0.5 \text{ m}^3$  discharge with a head of 80 mm of water

- control valves

- a settling caisson (cross-section  $60 \times 60 \text{ cm}$ ) with grids and a honey comb to produce uniform flow

- a terminal contraction.

### 3.2 Ejectors

The geometric characteristics of the jets and ejectors tested are summarized on Fig. 1.

### 3.3 Pulsating jet.

A pulsating jet may be defined by a velocity at the nozzle exit having a fixed direction and a modulus varying periodically in time. Such a jet was generated by a butterfly valve inserted between the caisson and the nozzle. There is a 4 : 1 contraction between the caisson and the pulsator and between the pulsator (dia. 160 mm) and the terminal nozzle (dia. 80 mm). This valve is driven by a variable speed motor which imposes the frequency.

Typical flow conditions were :

jet mean velocity :  $S \leq \bar{V}_j \leq 20 \text{ m/s}$

Reynolds number :  $Re = \frac{\bar{V}_j D}{\nu} > 3.10^4$

Jet pulsations

r.m.s. relative amplitude :  $a = \frac{\sqrt{\bar{u}_j^2}}{\bar{V}_j} \sim 60\%$

frequency :  $10 \leq f \leq 50 \text{ Hz}$

Strouhal number  $St = \frac{f D_j}{\bar{V}_j}$  :  $0 \leq St \leq 0.6$

$St = 0$  evidently corresponds to the steady jet.

### 3.4 Flapping jet

A flapping jet is characterized by an exit velocity  $\bar{V}$  having a constant modulus and a direction varying periodically about the mean flow direction Ox. If  $\alpha$  is the angle between  $\bar{V}_j$  and Ox, then for instance :  $\alpha = A \sin 2\pi ft$ . We call the amplitude A the flapping angle.

The flapping motion is produced by making use of the COANDA effect as in fluidic switching amplifiers. Essential in the design of nozzle (Fig. 2) are the two cylindrical surfaces to which the jet may attach producing thus an angular deflection. If the radius of curvature of these surfaces is approximately equal to the width of the jet it may be blown off from the surface to which it is attached by a small control jet. Since the main jet cannot stay in the middle it flips over to the other surface. The same process repeated alternatively on each cylinder produces the flapping. Alternate periodic blowing is generated with a cylindrical double valve (Fig. 2) on which one port is open while the other one is blocked. This valve is driven by a variable speed motor. The flapping angle A increases with the ratio  $C_p = p_o/p_j$ .

Typical flow conditions are :

jet mean velocity  $\bar{V}_j = 23 \text{ m/s}$

Reynolds number  $Re \approx 1.6 \cdot 10^4$

flapping motion

optimum blowing pressure  $1 \leq C_p \leq 2$

optimum frequency  $f \approx 20 \text{ Hz}$ ,  $St \approx 10^{-2}$

angle  $6^\circ \leq A \leq 8^\circ$

blowing discharge/main jet discharge  $\approx 6$  to  $8\%$

bution on the nozzle. The total thrust was then measured directly by the force exerted by the exhausting momentum flux on a perpendicular plate. The plate ( $1.80 \times 2.20 \text{ m}$ ) was fixed to the beam of the thrust bench.  $T_1$  and  $T_2$  were both measured in this way. The presence of the mixing duct did not appreciably affect the flapping so that the same conditions were easily maintained with or without ejector.

The measurement of the deflection produced by the force on the thrust bench was improved by using a capacitive displacement transducer (sensitivity better than  $1/\mu\text{m}$ ). The electrical transducer output also facilitated the time averaging of thrust which fluctuates considerably especially when the ejector has a diffuser.

#### 4. RESULTS AND DISCUSSION

##### 4.1 Pulsating jet ejectors

The best thrust augmentations from about hundred different test cases are plotted versus total length on Fig. 4.

Constant area ejectors. Comparison of the results obtained with steady or pulsating jets show that the forced pulsations:

- increase the maximum value of  $\phi$  from 1.33 to 1.46
- improve  $\phi$  for any duct length but especially in short geometries. Thus the thrust gain due to the ejector ( $\phi - 1$ ) passes from 0 to 0.16, 0.05 to 0.29, 0.17 to 0.38 for the respective lengths of 1, 2 and 3 Dm.

It may also be noted that the 2 Dm long pulsed ejector produces almost the same  $\phi$  as the 5 Dm long steady one,  $\phi = 1.29$  as compared to 1.33.

Ejectors with diffusers. Let us first mention that with the steady jet the diffusers used gave a slight improvement only with the longest mixing duct  $L_m = 9 \text{ Dm}$ :  $\phi$  moved from 1.25 to 1.35 when the diffuser  $\phi = 7^\circ$ ,  $L_D = 3 R_m$  was added. In all other cases  $\phi$  was lowered by addition of any of the six diffusers. Even the previous improvement is without practical importance since the much shorter constant area ejector  $L_m = 5 \text{ Dm}$  already produces  $\phi = 1.33$ . This was not surprising since the selected diffuser geometries were at the limit or in the region of stall on the performance chart (7).

The influence of jet pulsations on the thrust augmentation of ejectors with diffusers appears then in comparison quite remarkable as may clearly be seen on Fig. 4. In particular:

- the ejector performance was improved by the diffusers with all mixing ducts even with the shortest one which had only a length of one diameter.
- the highest thrust augmentation obtained was 1.88 whereas it was only 1.35 in the steady case. The measurement of the exit momentum flux in identical conditions gave  $\phi = 2.02$ , also a value that is even somewhat larger and a satisfactory check considering the accuracy of both types of measurements.
- values of  $\phi$  exceeding 1.7 were obtained in many cases.

The fact that diffusers worked effectively even with the one diameter long mixing duct should be underscored. Despite the faster mixing produced by the pulsations the entrance velocity profile is so skewed in this case that it would lead to immediate separation in any diffuser of a steady jet ejector. The higher turbulent intensities observed in pulsating jets (5) do certainly have a favorable influence on separation. But this may not be the whole explanation and there could be some other effect due to the flow unsteadiness.

The favorable effect of the pulsations was obtained at Strouhal numbers as low as 0.05 for  $L_m \geq 3 \text{ Dm}$ . Only in the case  $L_m = 1 \text{ Dm}$  was there a steady increase in  $\phi$  as  $St$  grew from 0 to 0.6. This is interesting because low frequency pulsations are easier to generate and minimize the noise problem.

##### 4.2 Flapping jet

The improved and simplified measurement technique developed for the flapping jet ejectors allowed the gathering of more extensive data. With the two-dimensional geometry it was on the other hand also possible to vary the diffuser angle continuously so that for every mixing duct and diffuser length the optimum angle could be determined exactly. The best thrust augmentation results are summarized on Fig. 5.

Constant area ejectors. It is seen that the maximum value of  $\phi$  is only increased from 1.45 to 1.49 by the forced flapping. But, as with the pulsating jet, the improvement due to the unsteadiness is more important in the shorter geometries. Thus,  $\phi = 1.48$  for  $L_D = 3 \text{ Dm}$  while it is only 1.36 in steady flow.

It should be noticed that the steady jet ejector performance falls off less rapidly with shorter length in this geometry than in the previous one. This may be accounted for by the difference in the  $Dm/D_j$  ratios, 20 and 3 respectively, and the lower entrainment rate in the initial region ( $x/D_j \leq 10$ ) of the jet.

Ejectors with diffusers. As in the pulsating case the performance improvement is especially significant with diffusers. The maximum thrust augmentation is, however, only 1.85 despite the larger area ratio  $\lambda$ .

Particularly interesting is the good performance obtained with short geometries. Thus for a total length of only 3 Dm  $\phi$  reached 1.56 while doubling the length only increases  $\phi$  to 1.65. Comparison with the pulsating case shows that  $\phi$  grows faster with  $L_t$  and is higher up to  $L_t = 5 \text{ Dm}$  when the jet is subjected to forced flapping but then it levels off rapidly while the performance of the former ejector increases up to  $L_t = 9 \text{ Dm}$ .

#### 5. CONCLUSION

These experiments also show that pulsating or flapping motions forced on the main jet may produce important improvements in ejector thrust augmentation. Gains with respect to steady jet performances are especially remarkable in short geometries and with diffusers. They are generally obtained at fairly low frequencies ( $St \leq 0.05$ ). Faster mixing between primary and secondary streams seems to be main mechanism responsible for these performance improvements.

The thrust augmentations considered here do not take into account losses or power requirements of the unsteady jet generation and should therefore not be confused with overall efficiency. It is not claimed so far that pulsating or flapping jet ejectors produce higher thrust for given total power but it is only shown that momentum exchange in the mixing duct and diffuser pressure recovery are more efficient.

The valve used to create the pulsating jet was especially inefficient since its working principle is a variable head loss. The evaluation of the overall efficiency is not even attempted in this case. The cost of generating the flapping is roughly the flow needed for the control blowing, also about 6% of the main jet discharge at the same generating pressure. This cost is, therefore, about 6% of the total thrust. The flapping increases  $\phi$  by about 12% in the case  $L_t = 3 \text{ Dm}$  ( $\phi$  passes from 1.38 to 1.56). The gain is also larger than the cost and the overall efficiency is better with the flapping.

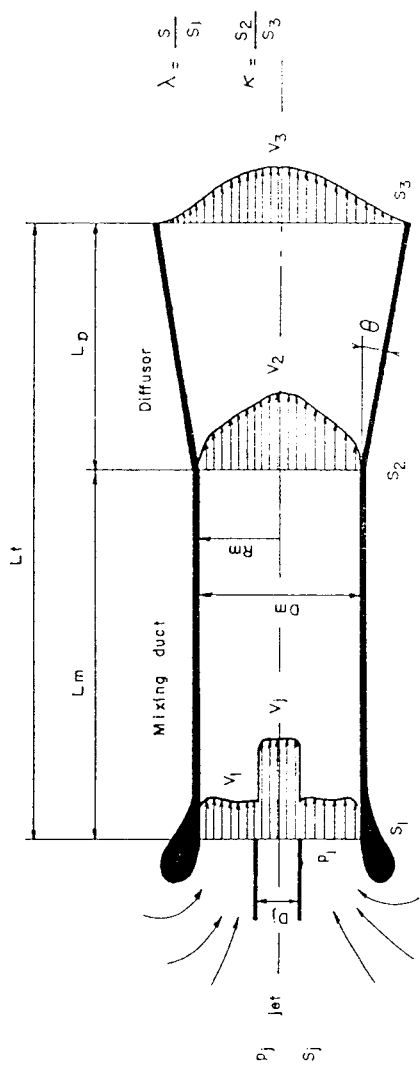
In this investigation no effort was devoted to the development of more efficient generating devices which of course does not preclude the possibility of more efficient designs based on other ideas. Resonance effects could for instance be used to produce pulsations and, on the other hand, the generation of self flapping jets by using feedback as in fluidic oscillators is a real possibility.

#### Acknowledgements

Financial support of the Direction des Recherches et Moyens d'Essais from the Ministère de la Défense is gratefully acknowledged.

#### REFERENCES

1. BERTIN J. and LE NABOUR M.: "Contribution to the development of ejectors and jet pumps" Contribution à l'étude des trompes et éjecteurs. Techniques et Sciences Aeronautiques, n° 2, pp. 127-138, (1959).
2. HOHENEMSER K.H. and PORTER J.L.: "Contribution to the theory of rotary jet flow induction". J. of Aircraft, 3, 4, pp. 339-346, (July - Aug. 1966).
3. FANCHER R.B.: "Low-area ratio thrust augmenting ejectors". J. of Aircraft, 9, 3, pp. 243-248, (March 1972).
4. QUINN B.: "Compact ejector thrust augmentation", J. of Aircraft, 10, 8, pp. 481-486, August 1973).
5. BINDER G. and FAVRE-MARINET M.: "Mixing improvement in pulsating turbulent jets", Fluid Mechanics of Mixing, pp. 167-172, (Am. Soc. of Mechanical Eng., 1973); Symp. organized by A.S.M.E., Atlanta, U.S.A., (June 20-22, 1973).
6. BINDER G. and FAVRE-MARINET M.: "Flapping jets". Flow-induced structural vibrations, pp. 57-62, (Springer Verlag, 1974). I.U.T.A.M. - I.A.H.R. Symp., Karlsruhe, (Aug. 14-16, 1972).
7. COCANOWER J.B., KLINE S.J. and JOHNSTON J.P.: "A unified method for predicting the performance of subsonic diffusers of several geometries". Thermosciences Div., Dpt Mechanical Engr., Stanford Univ., California, 94 p., (May 1965).



PULSATING JET EJECTOR		FLAPPING JET EJECTOR	
GEOMETRY	axisymmetric	two-dimensional	
JET Dj	80 mm	10 mm	height: 500 mm
MIXING DUCT Dm	242 mm	200 mm	
area ratio $\lambda$	9.15	20	
length	$1 \leq L_m/D_m \leq 9$	$0 \leq L_m/D_m \leq 9$	
DIFFUSOR $\theta$	5°	continuously variable	
length Ld	$L_d/R_m = 6, 8, 10$	$0 \leq L_m/D_m \leq 9$	
area ratio	$2.4 < 1/K < 3.6$	continuously variable	

Fig.1 Definition sketch and geometric characteristics of ejectors

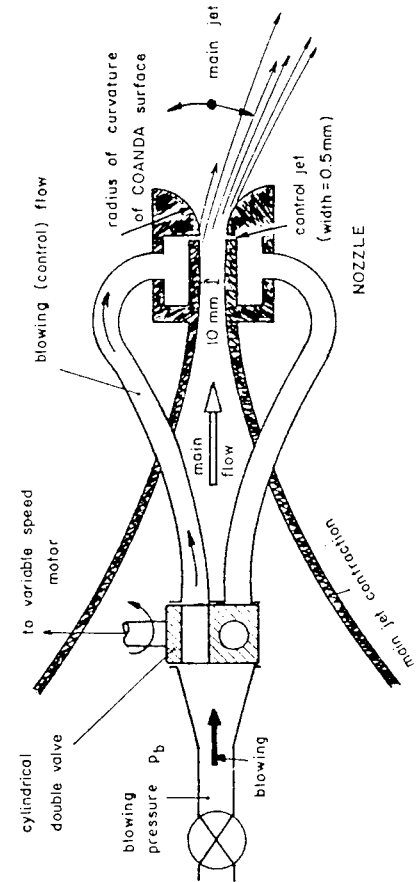


Fig.2 Flapping jet nozzle

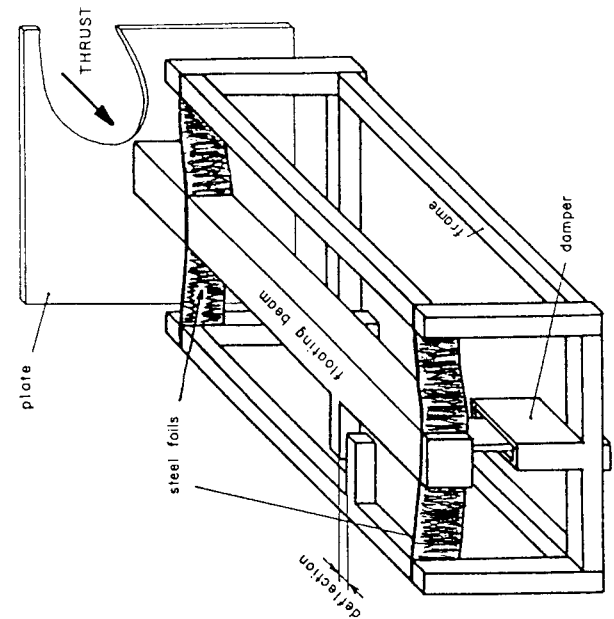


Fig.3 Thrust bench

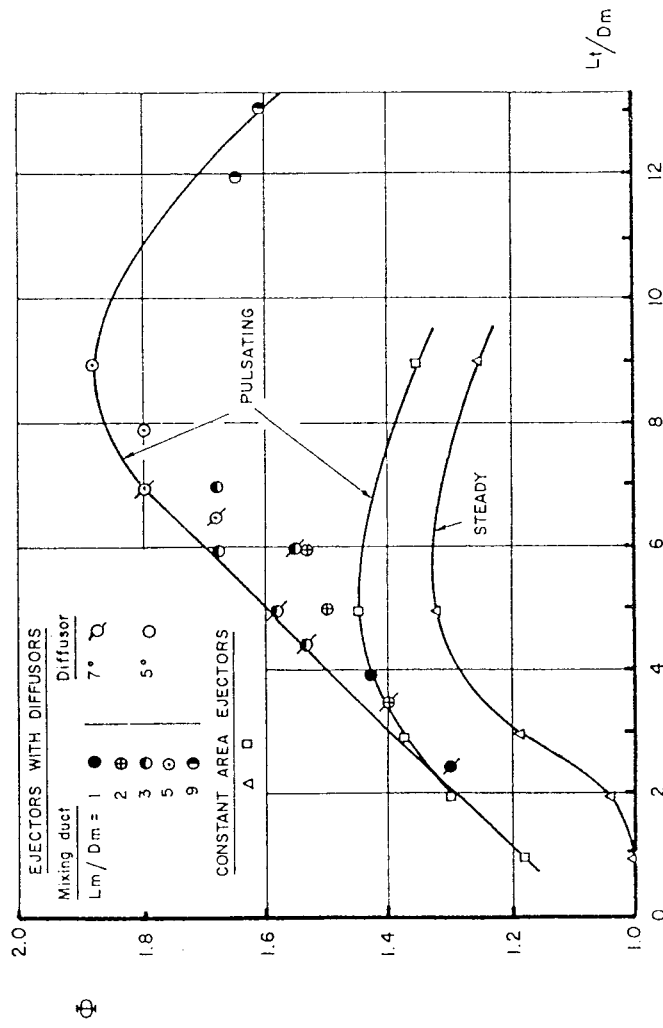


Fig. 4 Best thrust augmentations vs total length with pulsating and steady jet (Axisymmetric ejector  $\Lambda = 9.15$ )

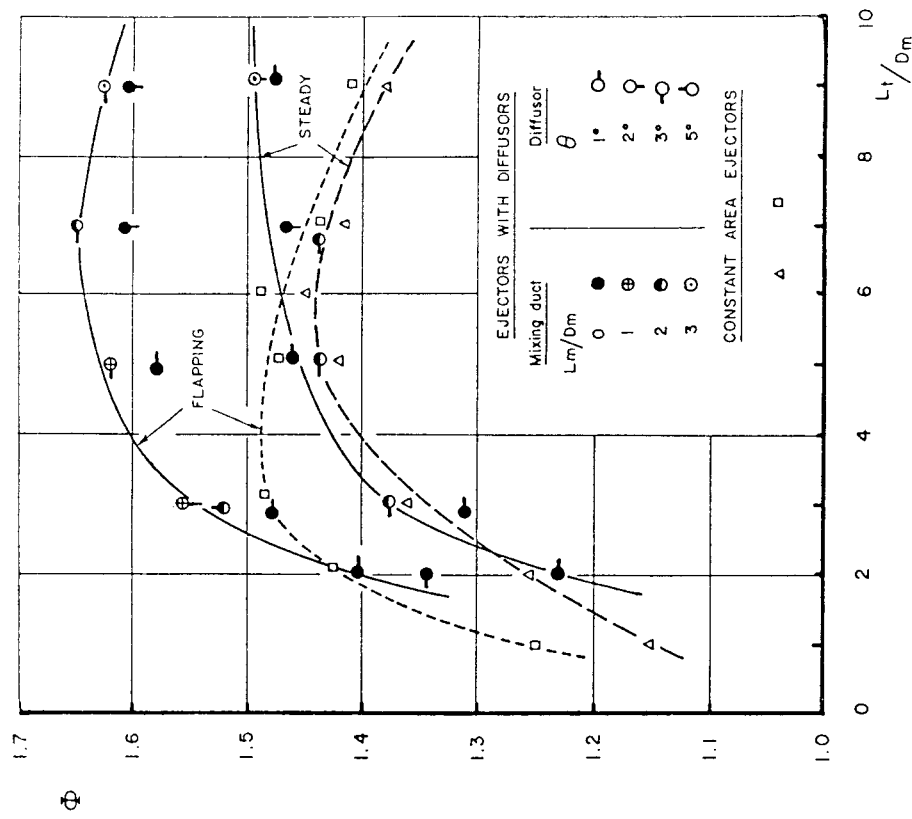


Fig. 5 Best thrust augmentations vs total length with flapping and steady jet (two-dimensional ejector  $\Lambda = 20$ )

## Some Observations on the Mechanism of Entrainment

P. M. Bevilaqua\* and P. S. Lykoudis†  
Purdue University, Lafayette, Ind.

### I. Introduction

**A**LTHOUGH entrainment of fluid from the surroundings is fundamental to the development of turbulent free shear flows, the actual mechanism of entrainment is not well understood. The fundamental process is the diffusion of turbulent vorticity; irrotational fluid that becomes rotational is said to have been entrained. Various descriptions of this process have been suggested, but these can be reduced to two basic hypotheses. Entrainment is due either to the viscous diffusion of vorticity at the smallest scales of the turbulence<sup>1-3</sup> or to the action of large-scale "mixing jets" that engulf volumes of fluid in bulk.<sup>4,5</sup> We have prepared this Note to outline our reasons for rejecting the small-scale mechanism. From considerations of similarity, we argue in the next section that a viscous diffusion mechanism is inconsistent with the observed self-preserving development of many flows. Some experimental evidence for the existence of a large-scale mechanism is described in the last section.

### II. Surface Layer Hypotheses

The existence of a well-defined boundary is characteristic of free turbulent flows. Across the greater part of the flow, the intensity of the turbulence is relatively constant. Near the boundary, however, the turbulent fluctuations diminish abruptly, resulting in a sharp interface between the regions of turbulent and nonturbulent motion. This interface is a continuous but highly convoluted surface whose irregular motion produces the intermittently turbulent signal from a fixed probe near the flow boundary.

On the basis of measurements in a plane wake, a round jet, and the boundary layer on a flat plate, Corrsin and Kistler suggested that the interface is a thin fluid layer in which the turbulence is diffused by viscosity. The characteristics of the surface layer, or superlayer, were inferred by a mixture of intuition and observation. Since, Corrsin and Kistler reasoned, the rate of vorticity production is proportional to the vorticity already present, once a fluid element has been sheared by viscous stresses at the boundary, its vorticity is rapidly increased. Thus, the interface remains sharp. Because the turbulence in the superlayer exists in a condition of equilibrium between diffusion by viscosity and amplification by turbulent straining, Corrsin and Kistler saw it as being similar to the turbulence in Kolmogorov's universal equilibrium range of the energy spectrum, which is balanced between dissipation at higher wave numbers and amplification at lower wave numbers. They concluded, by analogy, that the scale of the turbulence at the boundary and

the thickness of superlayer must therefore be small, on the order of Kolmogorov's dissipation length

$$\lambda = (\nu^3/\Phi)^{1/4} \quad (1)$$

where  $\Phi$  is the rate at which turbulent energy is dissipated in the equilibrium range and  $\nu$  is the viscosity of the fluid.

Furthermore, Corrsin and Kistler reasoned that the average rate of advance for such a diffusing surface of vorticity depends only on the fluid viscosity and the intensity of the vorticity fluctuations,  $\omega$ . The appropriate combination of these parameters, giving the speed at which the surface advances, was surmised to be

$$V_c = (\nu\omega)^{1/2} \quad (2)$$

The vorticity of turbulence in the equilibrium range must be proportional to  $(\Phi/\nu)^{1/2}$ , and so the speed of advance becomes

$$V_c = (\nu\Phi)^{1/2} \quad (3)$$

which is the Kolmogorov velocity scale.

The superlayer hypothesis has had a continuing influence on the study of the interface and the mechanism of entrainment. However, some of the underlying assumptions have been questioned. Moffatt,<sup>6</sup> for example, pointed out that the dissipation of vorticity is also proportional to the vorticity already present; on these grounds the boundary is as likely to be diffuse as sharp. Phillips<sup>3</sup> argued that the speed at which the surface advances may be more characteristic of the velocities of the energy containing eddies, although he retained the notion of a small-scale entrainment process.

The suggested equivalence between the turbulence in the superlayer and the turbulence in the equilibrium range raises a more fundamental question. Turbulence in the universal equilibrium range is, by definition, independent at conditions in the mean flow (except for the energy supplied); yet the speed at which the interface advances must adjust both to the flow geometry—wakes diffuse more rapidly than jets, for example—and to changes in the spreading rate as each flow decays. With an entrainment velocity determined by properties of the small-scale turbulence, the observed self-preserving development of many flows is not possible. This can be shown from considerations of similarity.

In the region of self-preservation, the entrainment velocity must be proportional to the scale velocity of the mean flow,  $U_c$ . According to Kolmogorov's hypothesis the dissipation is proportional to rate at which energy is supplied,  $\Phi = U_c^3/L_c$ , where  $L_c$  is the length scale of the mean flow. The requirement for self-preserving diffusion at the Kolmogorov velocity is

$$(\nu U_c^3/L_c)^{1/4} \sim U_c \quad (4)$$

In general, the self-preserving scale parameters vary as  $U_c \sim x^{-m}$  and  $L_c \sim x^n$ ; the requirement for self-preservation then becomes  $m=n$ . This is only true for the cases of the plane wake and round jet.

An assumption that the entrainment velocity is determined by simple diffusion of the energy containing eddies leads to the same result. In self-preserving flows, the vorticity of these eddies is proportional to  $U_c/L_c$ , and the requirement for spreading at the diffusion velocity is that

$$(\nu U_c/L_c)^{1/2} \sim U_c \quad (5)$$

Presented as Paper 75-115 at the AIAA 13th Aerospace Sciences Meeting, Pasadena, Calif., Jan. 20-22, 1975; received Jan. 27, 1975; revision received April 29, 1977.

Index category: Jets, Wakes, and Viscid-Inviscid Flow Interaction.

\*Presently Supervisor, Research and Engineering Department, Rockwell International, Columbus Aircraft Division. Member AIAA.

†Professor and Head, School of Nuclear Engineering, Purdue University. Associate Fellow AIAA.

The requirement again becomes  $m=n$ . Thus, except possibly in the plane wake and the round jet, another mechanism must adjust the entrainment velocity to the self-preserving rate of development.

### III. Large Eddy Hypothesis

We believe that the entrainment is determined by the large, coherent eddies whose permanence has only recently been discovered.<sup>7,8</sup> Although it was known that large-scale motions of the interface are correlated with an increase in the rate of entrainment,<sup>9</sup> it was presumed that this motion controls the entrainment indirectly, by increasing the surface area of the interface. The origin of the motion was not recognized until the coherent eddies were discovered, and various hypotheses regarding instabilities of the mean flow and the turbulence were suggested to account for the large-scale motions.

The mechanism of entrainment suggested by recent studies of the wake<sup>10</sup> and mixing layer<sup>11</sup> is illustrated in Fig. 1. The motion of the surface, which is the exposed side of a large, rotating eddy, displaces the surrounding fluid much as air is displaced by a swelling ocean wave. There is an interface for the turbulent vorticity that is kept sharp by the action of the large eddy in bringing high-intensity turbulence to the surface from the interior of the flow. At the interface, viscosity diffuses the turbulent vorticity, thus retarding the motion of the external flow relative to the surface. The decelerated fluid is then entrained into the turbulent core of the flow by the rotation of the large eddy. The newly entrained fluid is not immediately diffused by the other scales of the turbulence but continues to rotate with the large eddy.

This large eddy mechanism is consistent with earlier observations and, indeed, accounts for them. The convection of turbulent fluid to the surface and newly entrained fluid into the core would appear as a process of engulfment. In fact, Grant<sup>4</sup> reported an approximate periodicity in the occurrence of the "mixing jets" and associated a circular motion with each of them. The interface is kept sharp by this same rotation of the large eddies, rather than by the process of gradient steepening supposed by the superlayer hypothesis. Finally, the adjustment to the requirements of self-preservation is accomplished by the large eddies which are in what Townsend called a state of moving equilibrium, increasing in scale at the same rate as the mean flow diffuses.

In view of the significant role the large vortices have in the development of the mean flow, it is perhaps surprising that the permanence of these eddies was not detected sooner, especially in the wake of the cylinder, which has been so much studied. However, as seen in the photographs of Papailiou and Lykoudis,<sup>12</sup> the effect of these vortices is to cause a periodic variation in the direction of the mean velocity vector. Such variations cannot be detected by a single hot-wire sensor parallel to the cylinder axis, since the sensor responds to changes in the magnitude, but not the direction, of the velocity vector.

To substantiate the visual evidence in these experiments<sup>12</sup> the  $U$  and  $V$  components of velocity in the wake of a glass cylinder 0.635 cm in diam and 45 cm long were measured with

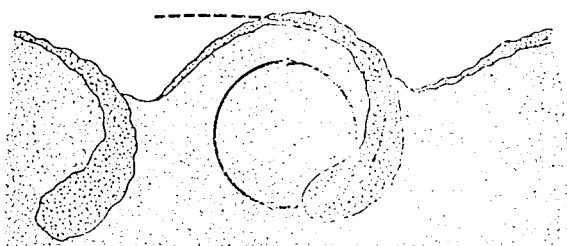


Fig. 1 Entrainment occurs by the enfolding action of the large eddies within the surface "waves".

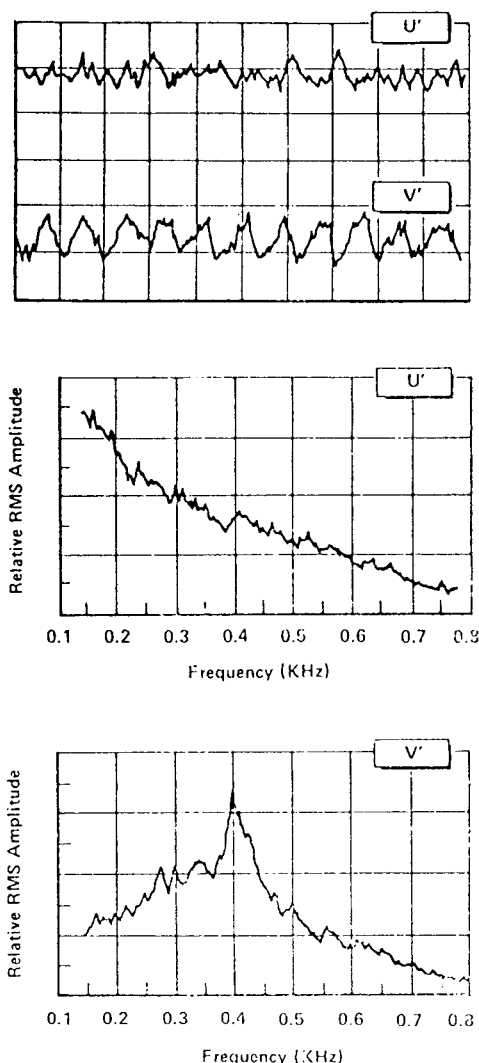


Fig. 2 Spectra of the fluctuating velocity components in the wake of a cylinder at  $Re = 10,000$  and  $x/d = 50$ .

a Thermo-Systems linearized anemometer and an  $X$  probe. The wind tunnel used was of the open return type; the test section has a circular cross section 45 cm in diam and 360 cm long. Figure 2 shows the turbulence components on the wake centerline 50 diam behind the cylinder, where the flow was generally considered to be fully turbulent. The Reynolds number is 10,000. Although the  $U$  component does appear to be completely turbulent, the  $V$  component clearly shows periodic oscillations. These oscillations correspond to the shedding frequency; that is, they occur at the first subharmonic. The anemometer signal was also analyzed with a Nelson-Ross spectrum analyzer. These spectra are also shown in the figure. The subharmonic is apparent in the spectrum of the  $V$  component, but its existence is masked in the  $U$  component. The range of this behavior was not established, due to limits on the speed of the tunnel and length of the test section, but similar oscillations were seen as far as 350 diam behind the cylinder and at Reynolds numbers up to 70,000.

### IV. Conclusions

From a critical re-examination of the assumptions and implications of the superlayer hypothesis, we have concluded that entrainment is a process that more nearly resembles a folding of the turbulent and nonturbulent fluids by the rotation of the large eddies. This mechanism is suggested by recent observations of the coherent eddies in wakes and mixing layers and provides a unified explanation of the nibbling and engulfing mechanisms that have been proposed.

- <sup>1</sup>Corrsin, S. and Kistler, A. L., "Free Stream Boundaries of Turbulent Flows," NACA Rept. 1244, 1955.
- <sup>2</sup>Townsend, A. A., "Mechanism of Entrainment in Free Turbulent Flows," *Journal of Fluid Mechanics*, Vol. 26, 1966, pp. 689-715.
- <sup>3</sup>Phillips, O. M., "The Entrainment Interface," *Journal of Fluid Mechanics*, Vol. 51, 1972, pp. 97-118.
- <sup>4</sup>Grant, H. L., "The Large Eddies of Turbulent Motion," *Journal of Fluid Mechanics*, Vol. 4, 1958, pp. 149-190.
- <sup>5</sup>Bradshaw, P., "The Understanding and Prediction of Turbulent Flow," *Aeronautical Journal*, July 1972, pp. 403-418.
- <sup>6</sup>Moffatt, H. K., "Interaction of Turbulence with Rapid Uniform Shear," SUDAER 242, also AD 626298, Stanford University.
- <sup>7</sup>*Colloquium on Coherent Structures in Turbulence*, University of Southampton, England, March 1974.
- <sup>8</sup>*Proceedings of the Project Squid Workshop on Turbulent Mixing*, Purdue University, Lafayette, Ind., May 1974.
- <sup>9</sup>Gartshore, I. S., "Experimental Examination of the Large Eddy Equilibrium Hypothesis," *Journal of Fluid Mechanics*, Vol. 24, 1965, pp. 89-98.
- <sup>10</sup>Bevilaqua, P. M. and Lykoudis, P. S., "Mechanism of Entrainment in Turbulent Wakes," *AIAA Journal*, Vol. 9, Aug. 1971, pp. 1657-1659.
- <sup>11</sup>Brown, G. L. and Roshko, A., "On Density Effects and Large Structures in Turbulent Mixing Layers," *Journal of Fluid Mechanics*, Vol. 64, 1974, pp. 775-816.
- <sup>12</sup>Papailiou, D. D. and Lykoudis, P. S., "Turbulent Vortex Streets and the Mechanism of Entrainment," *Journal of Fluid Mechanics*, Vol. 62, 1974, pp. 11-31.

Transactions of the ASME

SEPTEMBER 1977

Journal of Fluids Engineering

pp. 520-525

## Increased Turbulent Jet Mixing Rates Obtained by Self-Excited Acoustic Oscillations

W. G. HILL, Jr.

Research Department,  
Grumman Aerospace Corp.,  
Bethpage, L. I.  
Mem. ASME

P. R. GREENE

Graduate Student,  
Harvard University,  
Cambridge, Mass.

A new device, capable of greatly increasing subsonic jet mixing rates, has been discovered. This device, which we have named the "whistler nozzle," consists of a convergent nozzle section, a constant area section, and a step change to an exit section with a larger constant area. The exit section excites a standing acoustic wave in the constant area section, in a way similar to the action of an organ pipe. The result of this resonance is a loud pure tone and a greatly increased rate of jet mixing. The increased mixing rates appear related to the acoustically stimulated vortex shedding character (large scale structure or superturbulence) observed by Crow and Champagne [1] in their pioneering study of jets excited by a loudspeaker, and others utilizing upstream valves and pistons, except that the whistler nozzle is self-excited. The standing wave and the resulting increased mixing rates occur for a wide range of exit plane configurations and jet parameters.

During the course of our investigations of the factors influencing jet mixing rates, we discovered a device that we call the whistler nozzle, which greatly increases jet mixing rates. The basic whistler nozzle configuration consists of a convergent nozzle, a constant area section (this diameter is  $D_N$ ), and an abrupt backstep (Fig. 1). Most of the geometries used were axisymmetric; the proper length required to produce the resonant behavior ( $L_N$  in Fig. 1) for a given step height ( $H$ ) was determined experimentally by sliding a collar (C) over the basic nozzle cylinder. Exact geometric location is not critical (the collar can be moved several hundredths of a diameter without destroying the process). Rectangular nozzles with an aspect ratio up to about three have also been tested, but a purely planar whistler nozzle has not yet been produced.

When the proper geometry is selected, a loud pure tone is emitted and the jet mixing rate is greatly increased. Further details of our experiments are given later in this report, but qualitatively the most outstanding characteristic of the whistler nozzle is the increased mixing and turbulence level produced in the jet as it entrains the surrounding fluid.

Acoustical stimulation of a jet plume as a means of increasing entrainment is not a new idea. Crow and Champagne [1] generated discrete frequency sound waves with a loudspeaker located upstream of their plenum chamber; by taking advantage of plenum chamber resonances, they were able to produce exit plane sinusoidal fluctuations in velocity up to 5 percent of the core velocity at specific frequencies. In more recent work, Binder and Favre-Marinet, [2] and Curtet and Gerard [3] utilized a rotating butterfly valve and an oscillating piston, respectively, in the air supply to cause oscillations in the jet exit velocity that could be very large. The whistler nozzle, on the other hand, has produced

fluctuations as high as 15 percent, and more significantly, it does so without any external input. The increased mixing rate that characterizes the performance of the whistler nozzle is produced by this large self-excited velocity fluctuation and the way in which this fluctuation interacts with the exit-lip geometry. The basic oscillating behavior is a standing acoustic wave with open-open boundary conditions (organ-piping) in the straight length of nozzle. Generally the half-wave mode is excited, but occasionally the full-wave or full-wave and half-wave simultaneously are excited.

While our knowledge of the behavior of the whistler nozzle is not far enough advanced to allow optimum design or performance predictions for any given application, the ability to increase turbulent mixing rates so greatly suggests a number of applications. Several fluid dynamic problems of vertical- and short-takeoff (V/STOL) aircraft could benefit from increased turbulent mixing rates. The reduced size and weight of thrust augmenting ejectors that can be obtained by increasing the turbulent mixing rate has been demonstrated by Quinn [4]. While the benefits of decreased size and weight are obvious for aircraft application, it is also likely that a lower cost will result for commercial ground based ejectors, especially for the simple geometry of the whistler nozzle. Increased turbulent mixing rates could also contribute to improvements in the flow beneath V/STOL aircraft in ground effect, such as decreasing ground heating and erosion effects.

Another possible application is in the suppression of aircraft exhaust plume detectability. More rapid mixing of the plume with the surrounding air results in a smaller cross section of properties such as IR emission. In this application the ability to vary the plume geometry easily and apply the whistling effect only when needed, might have special importance. Jet engine combustors and chemical lasers are additional areas where the increased mixing rates hold the promise of improved performance and/or reduced size and weight. A new class of fluidic elements could be created based on the whistler nozzle. Controlled sinusoidal signals can be generated fluidically and used as a basis for AC-type or digital-type fluid systems. A movable whistler collar can be used as a mechanical-to-fluidic switch, or control jets can be used to switch the whistling behavior on and off. Many other

features of the whistler behavior may lead to other fluid concepts. The role that the acoustic output generated by the whistler nozzle will play in any of these applications is uncertain. We have not yet attempted to determine geometries that minimize noise while still increasing the mixing rates.

In the following sections we present detailed experimental results for the basic whistler nozzle geometries that we have tested. Also included are results for various perturbations of the basic geometry.

### Experimental Facility

The results presented in this report were obtained in the Grumman Research Department Jet Mixing Laboratory. The apparatus utilizes a centrifugal fan discharging through a diffuser into a two-foot (0.6 meter) square settling chamber containing a honeycomb straightener and turbulence-damping screens. A velocity of 180 feet/second (54 m/sec) was used in most of the reported results and may be assumed unless otherwise explicitly stated. The nozzle consists of a one-inch (2.54 cm) diameter ASME flow metering nozzle (elliptical contour shape) followed by constant-area sections of varying length. These constant-area sections were provided for a study of the effects of the initial boundary layer on jet mixing, but they also allow us to vary the organ-pipe frequency.

Our instrumentation consisted of a constant temperature anemometer, linearizer and hot film probes, oil-filled manometers, an x-y recorder, an oscilloscope, and a digital voltmeter. Probe traversing locations were determined from the readout of a potentiometer geared to the probe support shaft. The usual procedure was to run a continuous traverse at approximately 1/2-in. (1.22 cm) per minute and record the probe position and output signals (mean velocity or RMS level) directly on the x-y recorder. Frequencies were determined by overlaying the probe output with the output of a signal generator on the oscilloscope screen. Experimental uncertainty was estimated by measuring the variables by several methods and comparing results. Primary quantities such as pressure, length, etc., are estimated at  $\pm 1$  percent. Velocities from hot wire measurements are  $\pm 3$  percent and frequency measurements  $\pm 5$  percent. In general, the results on basic jet mixing (center-line decay and jet spreading rates) that we have obtained in this laboratory have agreed well with the summary of results collected and presented by Harsha [5].

### Experimental Results

**Basic Axisymmetric Whistler Nozzle Results.** The original whistler nozzle was an axisymmetric nozzle having a constant area section from three to twelve diameters in length, followed by a backstep-type expansion (Fig. 1). Almost all of the quantitative data obtained to date are concerned with this basic geometry. A synopsis of the experimental results is presented below. Our investigation of other geometries has been primarily qualitative. A discussion of the results of this aspect of our work is also presented. The basic oscillation is an organ piping of the constant area nozzle section, with open-open boundary conditions. The forcing, or coupling, effect of the whistler backstep section has not been studied in sufficient detail to accurately describe the process. Our feeling is that the whistler length ( $L_W$ ) is such that neither a simple free jet flow nor an annular base flow can occur. When the outer shear layer of the jet flows past, but close to the end of the whistler section, the entrained flow cannot be replaced rapidly enough and the pressure in the backstep region is lowered, turning the jet outward at its exit. When the shear layer over this backstep base region forms a reattachment point on the whistler surface, more mass is returned to the base region than the shear layer entrains and the reattachment point again moves off the end of the whistler. While even a quasistatic explanation of this sort seems to explain the effect, we also feel that the dynamics of the base flow oscillation play an important role in the coupling process.

Quantitative data on the effects of the whistler nozzle on jet

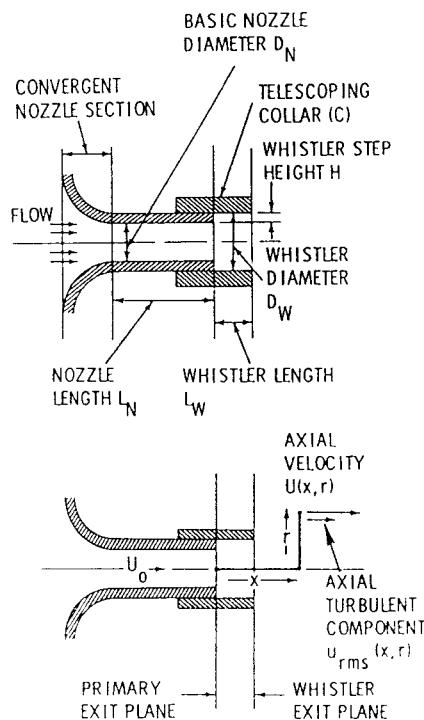


Fig. 1 Basic whistler nozzle

\*Numbers in brackets designate References at end of paper.

Contributed by the Fluids Engineering Division of THE AMERICAN SOCIETY OF MECHANICAL ENGINEERS and presented at the Joint Applied Mechanics, Fluids Engineering & Bioengineering Conference, New Haven, Conn., June 15-17, 1977. Manuscript received at ASME Headquarters March 25, 1977. Paper No. 77-FE-15.

mixing have been obtained only for one-inch (2.54 cm) diameter jets. Figs. 2 and 3 illustrate the basic effects of the whistler nozzle on jet mixing characteristics. The decay of velocity along the jet center-line for both the basic jet (backstep retracted to exit plane) and whistler nozzle is shown in Fig. 2(a). Fig. 2(b) shows the growth and decay of velocity rms levels and Fig. 2(c) shows the increase in mass flux. These results are essentially the same as the corresponding results of Crow and Champagne, except that the whistler exhibits a more pronounced decay in axial velocity than was achieved by using a loudspeaker.

The decay and spreading of the whistler forced jet are also

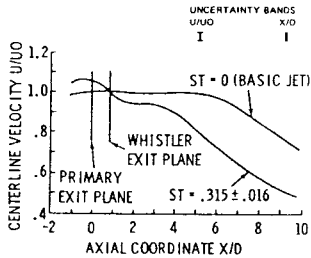


Fig. 2(a) Centerline velocity decay

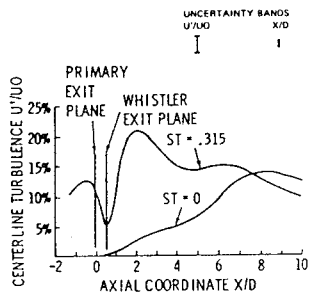


Fig. 2(b) Centerline turbulence level

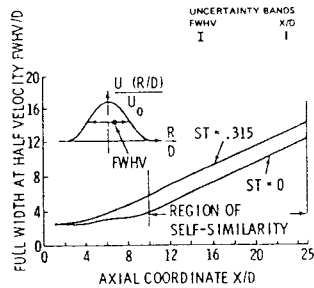


Fig. 2(c) Mass Flux

Fig. 2 Whistler nozzle effects on jet mixing

similar to the forced oscillation case of Binder and Favre-Marinet (reference [2]) but this comparison is more difficult to make since their unforced jet spreads and decays more slowly than ours.

The large RMS fluctuation levels shown in Fig. 2(b) for the whistler jet are not turbulence. The oscillations begin at the nozzle exit as pure sinusoidal oscillations, and break down gradually into turbulence as the flow moves downstream. A quantitative example of this observation is given in reference [2].

Integration of our profiles yields a variation of mass flow with axial distance (Fig. 2(c)) which is also similar to but larger than that presented by Crow and Champagne. This suggests that the primary mechanisms involved in the increased mixing rates are the same. The exit velocity fluctuations couple with the super-turbulence (orderly large scale vortex-ring-like structure, see reference [3]) and lead to rapid mixing in the initial regions of the jet. Fig. 3 illustrates the general observation that the effect of the whistler on the mean velocity profiles is a general increase in mixing rates, with no unusual profiles resulting.

Crow and Champagne's interpretation of their data indicates that the mixing characteristics of acoustically forced subsonic jets are sensitive to two frequencies: those characterized by the Strouhal numbers  $St = fD/U = 0.3$  and  $0.6$ . However, it is particularly difficult to summarize with a single parameter the mixing behavior of an entire jet plume under conditions of augmented mixing.

Crow and Champagne chose the center-line velocity at four diameters downstream as the parameter to characterize the mixing response of the jet to various excitation amplitudes and frequencies. It appears from our data that this choice is an oversimplification that leads to erroneous conclusions about the mixing response of the jet plume as a whole in the forced case. Our research with the whistler nozzle has shown that the near region of the jet ( $0 < X/D < 6$ ) is particularly sensitive to acoustic forcing, and often exhibits rather unusual behavior. Fig. 4 is a graphic illustration of how one's conclusions about the mixing of a jet are dependent upon the particular axial observation station. At four diameters downstream (Crow and Champagne's observation stations) the forcing at  $St = 0.338 \pm 0.017$  produces the greatest change in velocity; at two diameters  $St = 0.533$

$\pm 0.028$  produces the largest change of the three; at seven diameters the  $St = 0.463 \pm 0.023$  produces the largest effect. Using the virtual origin shift as a measure of enhanced mixing rate, rather than the center-line velocity at  $X/D = 4$ , we did not observe the jet to be overly sensitive at the Strouhal numbers  $St = 0.3$  and  $St = 0.6$ ; instead, the whistler seems to enhance mixing without regard to the Strouhal number over the range investigated ( $0.25 < St < 0.65$ ). This observation is also borne out by the results of reference [2] at  $St = 0.18$ . The key point is that although the local behavior (such as center-line velocity in the near field of the jet) exhibits a preferential response to forcing at certain Strouhal numbers, the gross mixing behavior is essentially independent of the Strouhal number over the interval in question. More work is required on the effects of Strouhal number and magnitude of the forcing oscillations. Crow and Champagne were restricted to resonant frequencies while they could vary magnitude (at least below 2 percent RMS) while we could vary produced almost any frequency by changing pipe length ( $L_N$ ) but had little control over the magnitude. Binder and Favre-Marinet could vary both, but report results only for  $St = 0.18$ .

**Effect of Whistler Axial Location.** The basic geometry used during most of our whistler experiments consisted of a whistler section that slid over the basic straight nozzle sections. As the whistler section was extended from the nozzle exit plane, a location was reached where a loud tone was produced and enhanced mixing behavior was observed. When the whistler section was extended further the whistling stopped. However, there were often one or two further extended stations where the whistler nozzle behavior was again encountered. We designated the first position (closest to the nozzle exit) as a "first position" whistler, and successively more distant locations as "second position," "third position," etc. All data presented in other sections of this report, unless otherwise noted, are first position whistler data. In all cases the basic oscillation was an organ piping with the frequency determined by the basic nozzle length ( $L_N$ ) and an open-open boundary condition, sometimes in a half wave mode and sometimes in a full wave mode.

Many attempts were made at correlating the location of the whistler collar, the diameter of the whistler section, the straight nozzle length, etc. No general laws of behavior were determined. The relationships between whistler position, pipe length, whistler diameter, and frequency are summarized in Tables 1 and 2. We see no obvious relation between the oscillation mode and the collar position; the phenomenon is, however, repeatable in that the nozzle always produces the same oscillation mode and frequency for a particular collar position.

Further experiments were then conducted to determine the effect of the second position whistler location on mixing rates. Fig. 5 shows comparisons of first and second position whistlers on the 8 in. (20.3 cm) and 12 in. (30.5 cm) pipes. A difference does exist in both cases, but again no general correlation behavior can be determined. The second position whistler modified the

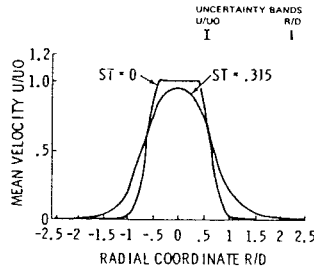


Fig. 3(a)  $X/D_N = 2$

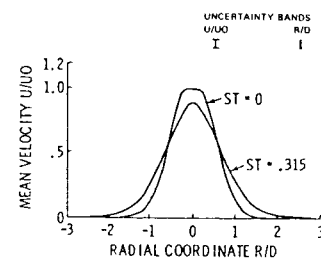


Fig. 3(b)  $X/D_N = 4$

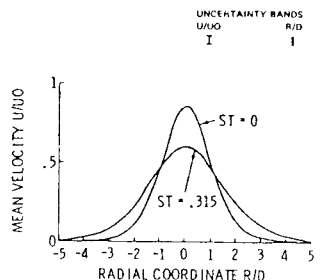


Fig. 3(c)  $X/D_N = 8$

Fig. 3 Effect of whistler nozzle on radial profiles

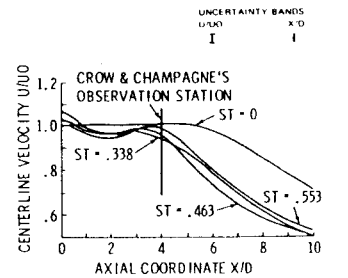


Fig. 4 Effect of Strouhal number of whistler on jet decay

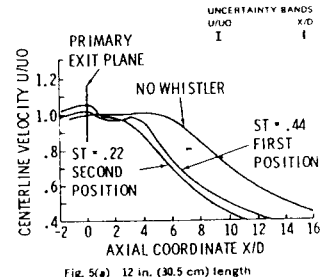


Fig. 5(a) 12 in. (30.5 cm) length

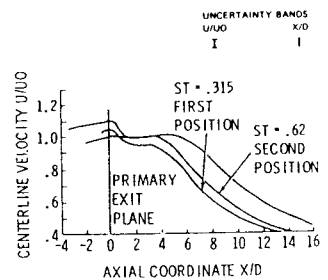


Fig. 5(b) 8 in. (20.3 cm) length

Fig. 5 Effect of whistler position on jet decay

behavior in the core region for both nozzles, and results in a faster mixing for the 12 in. (30.5 cm) nozzle and a slower mixing for the 8 in. (20.3 cm) nozzle. Note that in these tests a change from the first to second position whistler changed the frequency (and hence the Strouhal number), the RMS exit oscillation level, and the mean velocity and its gradient at the basic jet exit.

**Effect of Whistler Step Height on Mixing.** A series of experiments were performed to determine the effect of the step height (whistler diameter) on the mixing rates. Emphasis was placed on determining the size that produced a maximum increase in mixing rate. A second objective was to determine the minimum size that would still produce the whistler effect, since for many applications a small size could be beneficial. The results of these experiments are shown in Fig. 6. The maximum effect on centerline velocity decay and peak turbulence level is produced by a  $1-3/8$  to  $1-1/2 D_N$  whistler diameter. A  $1-1/8 D_N$  whistler diameter, the smallest we could conveniently construct, also produced a considerable whistler effect. Since we worked only with one-inch (2.54 cm) dia. basic nozzles we do not know if the appropriate scaling parameter is  $D_w/D_N$  or  $H$  divided by some other length parameter such as boundary layer thickness.

**Effect of Whistler on Flow Rate.** It was generally observed that the center-line velocity at the exit of the basic jet was increased by operation of the whistler, but that it dropped to approximately the original (nonwhistling) exit velocity at the exit of the whistler. This resulted in large velocity gradients in some cases. Since Crow and Champagne did not measure velocity upstream of the exit, we do not know if a similar increase in mean velocity was produced in their forcing of oscillations with a loudspeaker. Examination of their plots of velocity downstream of the exit does show a gradient of center-line velocity at the exit for the forced case. Therefore, it is possible that the same general behavior occurs for this aspect of both the speaker-forced and the whistler-induced flow fields.

#### Other Geometries.

**Ejector Whistler.** The ejector whistler (see Fig. 7) is so named because of its similarity in appearance to a conventional ejector. This configuration was not designed to function as an ejector, however, but to relieve the low pressure occurring in the backstep region of the original whistler geometry. Reduction of this low pressure could be important for propulsion applications. The ejector whistler did work, producing almost as great an increase in mixing rates as the original whistler nozzle while at the same time relieving the low base pressure. The exit velocity for the ejector whistler is well below the exit velocity for the basic whistler; this is a direct reflection of the change in exit plane pressure. Studies of the effectiveness of this arrangement as an ejector have not been conducted.

**Nonaxisymmetric Cases.** We have studied square and rectangular whistler nozzles, but a truly two dimensional whistler apparently will not function. Our first attempts at producing a



True two dimensional whistler nozzle were unsuccessful. Subsequently, we experimented to determine the degree of axial symmetry needed to produce the whistler effect. A circular plexiglass pipe was flattened, producing a "square with round corners" exit cross section. This configuration again produced the whistler behavior using a whistler section similarly constructed. A rectangular exit nozzle was then constructed with an aspect ratio of about three. This nozzle could be made to whistle when the whistler section had an outward step in all four directions. However, when the whistler section was expanded in only two opposite directions the whistling did not occur. Apparently a vortex ring effect is necessary to produce the whistler phenomenon.

### Conclusions and Recommendations

The most important feature of this investigation is the existence of the whistler nozzle phenomenon. The ability to obtain increased mixing rates without a loudspeaker or similar active input device opens many possibilities for applications to large scale engineering devices (such as aircraft exhaust plumes). A feature of the observed behavior that also contributes to possible applications is the fact that many variations of the basic geometry can be made while still producing the whistler effect. The role that the noise it generates will play in applications is not known at present.

The correlation of the observed whistler nozzle frequencies with the ideal organ pipe frequencies seems to verify the basic oscillation character. In addition, we have performed measurements of the RMS velocity levels inside the straight section of the nozzle which also support this model of the behavior.

One conclusion that arises from the organ piping aspects of the whistler nozzle is that this effect apparently cannot be produced with a sonic or supersonic nozzle exit velocity. Even though this argument is plausible, the value of applying the whistler nozzle to aircraft with sonic exit flow conditions suggests that attempts to cause a sonic jet to whistle are worthwhile. It is possible that the acoustic oscillations could be produced in a constant area subsonic passage upstream of the final sonic exit plane and still result in increased jet mixing.

Another area important for future investigation is to gain an understanding of the excitation process that occurs at the whistler lip. At present, we think that a separation reattachment cycle in the lip region couples with the organ pipe oscillation. The details and scaling laws of this behavior deserve further study. The inability to produce a two dimensional whistler nozzle is almost certainly coupled with the excitation process at the lip. This phenomenon also warrants future study.

### References

1. Crow, S. C., and Champagne, F. H., "Ordered Structure in Jet Turbulence," *Journal of Fluid Mechanics*, Vol. 48, Part 3, 1971, pp. 547-591.
2. Binder, C., and Favre-Marinet, "Mixing Improvement in Pulsating Turbulent Jets," *Proceedings of the Symposium Fluid Mechanics of Mixing*, ASME, June 1973.
3. Curtet, R. M., and Girard, J. P., "Visualization of a Pulsating Jet," *Proceedings of the Symposium Fluid Mechanics of Mixing*, ASME, June 1973.
4. Quinn, B., "Recent Developments in Large Area Ratio Thrust Augmentors," AIAA Paper No. 72, 1174, 1972.
5. Harsha, P. T., "Free Turbulent Mixing: A Critical Evaluation of Theory and Experiment," AEDC-TR-71-36, Feb. 1971.

Table 1 Details of whistler resonance conditions for whistler diameter equal to 1.25 nozzle diameter. Nozzle diameter = 1.0 in. (2.54 cm)

$L_w$ Constant area nozzle length	$L_w$ whistler length	First position		Second position	
		Exit plane RMS level	Frequency cycles/sec	Exit plane RMS level	Frequency
3 in. (7.6 cm)	0.438 in. (1.11 cm)	unknown	1100 (half wave)	0.688 in. (1.75 cm)	unknown (half wave)
8 in. (20.3 cm)	0.563 in. (1.43 cm)	13.0%	680 (half wave)	1.125 in. (3.63 cm)	3.0% 1275 (full wave)
12 in. (30.5 cm)	0.406 in. (1.03 cm)	5.83%	950 (full wave)	0.813 in. (2.06 cm)	11.3% 470 (half wave)

Table 2 Details of whistler resonance conditions for constant area nozzle length of 8.0 in. (20.3 cm). Nozzle diameter = 1.0 in. (2.54 cm)

$D_w$ Whistler diameter	$L_w$ whistler length	First position		Second position	
		Exit plane RMS level	Frequency cycles/sec	Exit plane RMS level	Frequency cycles/sec
1.25 in. (3.18 cm)	0.563 in. (1.43 cm)	13.0%	675	1.125 in. (2.858 cm)	3.0% 1300
1.50 in. (3.81 cm)	0.750 in. (1.91 cm)	10.0%	660	1.375 in. (3.493 cm)	2.2% 1350
1.75 in. (4.45 cm)	1.063 in. (2.699 cm)	3.7%	660	1.500 in. (3.810 cm)	1.7% 1300

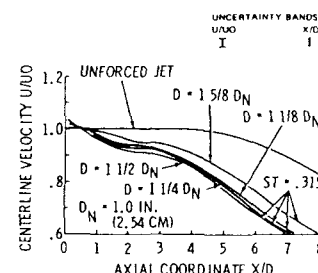


Fig. 6 Effect of whistler step size on jet decay

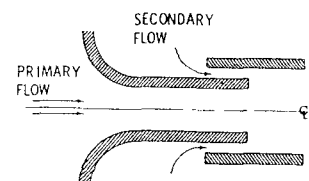


Fig. 7 Ejector whistler

AIAA JOURNAL

Pp. 1104-1106

VOL. 16, NO. 10

OCTOBER 1978

## The Mechanism of Jet Entrainment

K. Bremhorst\*

University of Queensland, Brisbane, Australia

and

W. H. Harch†

Aeronautical Research Laboratories,  
Melbourne, Australia

### I. Introduction

CONSIDERABLE research effort is being exerted to develop jet flows with higher entrainment than encountered in steady jets. Such efforts are highly empirical as the basic entrainment mechanism is not well understood. It is generally accepted that irrotational fluid which acquires vorticity is said to have been entrained. The entrainment process is, therefore, one of vorticity propagation by viscous action. Controversy exists, however, concerning the manner in which this takes place,<sup>1</sup> although the general belief is that the large structure of the turbulent/nonturbulent interface is a significant factor in the whole process.<sup>1-3</sup>

Comparison of different types of flows to permit conclusions concerning the effect of flow structure on entrainment is

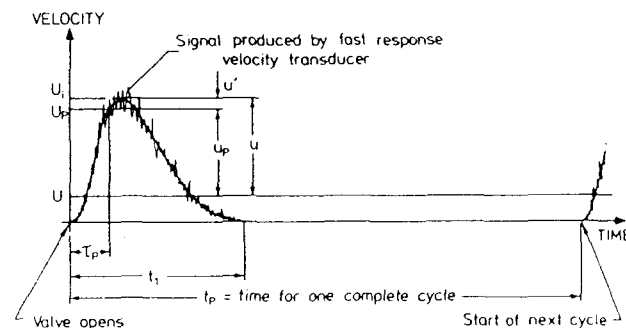


Fig. 1 Typical instantaneous velocity signal in a fully pulsed jet.

difficult, but some qualitative differences between the large interfacial structures for wakes and boundary layers to account for their different entrainment characteristics have been postulated.<sup>2</sup> Recently reported measurements<sup>4</sup> show that the entrainment and entrainment rate of a fully pulsed subsonic air jet are considerably higher than for a steady jet. The physical reasons for such an increase have not been shown so far, but are now believed to be due to a significant increase in the size of the jet structure consequent upon the pulsation.

### II. Pulsed Jet Description

The fully pulsed jet to be considered was produced by a rotating valve<sup>4</sup> which opened for one-third of each revolution © American Institute of Aeronautics and Astronautics, Inc., 1978. All rights reserved.



150 implied for the intrinsic turbulence of the pulsed jet. This component of the pulsed jet turbulence is primarily due to the action of shearing forces and could, therefore, be expected to be similar to the turbulence of steady jets. It is noteworthy that a change of scaling of the time delay to allow for the upstream shift of the effective origin has relatively little effect on the preceding conclusion; whereas the approximation introduced by use of  $R'_{II}(\tau_p, \tau)$  instead of  $R_{II}(\tau_p, \tau)$  decreases the difference between the two types of jets hence yielding a conservative result. Another possible source of variation of Fig. 2 for the pulsed-jet correlations is the use of  $U_p$  instead of the average of  $U_p$  taken over the interval  $\tau_p$  to  $\tau_p + \tau$  as is required if Taylor's hypothesis applies. However, since  $U_p(\tau_p)$  and  $U_p(\tau_p + \tau)$  differ little over the highly correlated part of the delay interval no significant error results if  $U_p(\tau_p)$  is used. Finally, if the true convection velocity is much larger than  $U_p(\tau_p)$ , better agreement between the steady jet and pulsed jet scales would be obtained, but this would be inconsistent with convection velocity measurements in steady jets for which the convection velocity is only twice the local mean velocity at the largest  $r/r_{1/2}$  reported here.<sup>6</sup> For smaller radial distances the two velocities are almost equal.

Assuming that a large streamwise length scale in the bulk of the flow also implies a large lateral spread of the surface indentations, leads to the conclusion that the mean velocity profile should have a larger tail in this region. Comparison of steady jet radial mean velocity profiles<sup>6</sup> which are well represented by

$$U/U_0 = e^{-0.693(r/r_{1/2})^2} \quad (5a)$$

with fully pulsed jet profiles<sup>4</sup> represented by

$$U/U_0 = [1 + 0.44(r/r_{1/2})^2]^{-2} \quad (5b)$$

verifies this proposition.  $r_{1/2}$  in these equations is the radial position,  $r$ , at which the mean streamwise velocity equals half the center-line value,  $U_0$ .

Unfortunately, direct comparison of the pulsed jet data is possible only with far-field steady data. However, if moving axis autocorrelations in the pulsed jet follow those in other flows,<sup>8</sup> then these will be much larger than the single-point autocorrelations of Fig. 2. It follows that such correlations would be much larger than similar ones obtained in steady mixing layers, Fig. 2, which is consistent with the preceding findings.

#### IV. Conclusion

Based on the assumption that entrainment of irrotational exterior fluid in pulsed jets is principally due to the intrinsic turbulence component, it may be concluded from autocorrelations of the intrinsic turbulence of fully pulsed jets that the size of the turbulent/nonturbulent interface indentations is significantly larger than for steady jets. In view of the generally accepted belief that the larger scale structure of this interface is related to the entrainment of irrotational exterior fluid, it is probable that the much larger entrainment of fully pulsed jets is a direct consequence of its larger entrainment interface structure.

#### Acknowledgments

The authors are grateful for support received from the Australian Research Grants Committee and to T. C. Smith for his assistance with the computations. The second author also gratefully acknowledges receipt of a Commonwealth Postgraduate Scholarship.

#### References

- <sup>1</sup>Bevilaqua, P. M. and Lykoudis, P. S., "Some Observations on the Mechanism of Entrainment," *AIAA Journal*, Vol. 15, Aug. 1977, pp. 1194-1196.
- <sup>2</sup>Townsend, A. A., "Entrainment and the Structure of Turbulent Flow," *Journal of Fluid Mechanics*, Vol. 41, 1970, pp. 13-46.
- <sup>3</sup>Kovaszny, L. S. G., Kibens, V., and Blackwelder, R. F., "Large-Scale Motion in the Intermittent Region of a Turbulent Boundary Layer," *Journal of Fluid Mechanics*, Vol. 41, 1970, pp. 283-325.
- <sup>4</sup>Bremhorst, K. and Harch, W. H., "Near Field Velocity Measurements in a Fully Pulsed Subsonic Air Jet," *Proceedings of the First Symposium on Turbulent Shear Flows*, April 1977, The Pennsylvania State University, University Park, Pa., Springer, to appear.
- <sup>5</sup>Crow, S. C. and Champagne, F. H., "Orderly Structure in Jet Turbulence," *Journal of Fluid Mechanics*, Vol. 48, 1971, pp. 547-591.
- <sup>6</sup>Wyganski, I. and Fiedler, H. E., "Some Measurements in the Self-Preserving Jet," *Journal of Fluid Mechanics*, Vol. 38, 1969, pp. 577-612.
- <sup>7</sup>Harch, W. H., "An Experimental Investigation Into the Velocity Field and Aerodynamic Noise Sources of an Unheated Fully Pulsed Air Jet," Ph.D. Thesis, University of Queensland, St. Lucia, Brisbane, Australia, 1977.
- <sup>8</sup>Wyganski, I. and Fiedler, H. W., "The Two-Dimensional Mixing Region," *Journal of Fluid Mechanics*, Vol. 41, 1970, pp. 327-361.

## Orderly structure in jet turbulence

By S. C. CROW AND F. H. CHAMPAGNE

The Boeing Company, Seattle, Washington

(Received 23 October 1970)

Past evidence suggests that a large-scale orderly pattern may exist in the noise-producing region of a jet. Using several methods to visualize the flow of round subsonic jets, we watched the evolution of orderly flow with advancing Reynolds number. As the Reynolds number increases from  $10^2$  to  $10^3$ , the instability of the jet evolves from a sinusoid to a helix, and finally to a train of axisymmetric waves. At a Reynolds number around  $10^4$ , the boundary layer of the jet is thin, and two kinds of axisymmetric structure can be discerned: surface ripples on the jet column, thoroughly studied by previous workers, and a more tenuous train of large-scale vortex puffs. The surface ripples scale on the boundary-layer thickness and shorten as the Reynolds number increases toward  $10^5$ . The structure of the puffs, by contrast, remains much the same: they form at an average Strouhal number of about 0.3 based on frequency, exit speed, and diameter.

To isolate the large-scale pattern at Reynolds numbers around  $10^5$ , we destroyed the surface ripples by tripping the boundary layer inside the nozzle. We imposed a periodic surging of controllable frequency and amplitude at the jet exit, and studied the response downstream by hot-wire anemometry and schlieren photography. The forcing generates a fundamental wave, whose phase velocity accords with the linear theory of temporally growing instabilities. The fundamental grows in amplitude downstream until non-linearity generates a harmonic. The harmonic retards the growth of the fundamental, and the two attain saturation intensities roughly independent of forcing amplitude. The saturation amplitude depends on the Strouhal number of the imposed surging and reaches a maximum at a Strouhal number of 0.30. A root-mean-square sinusoidal surging only 2% of the mean exit speed brings the preferred mode to saturation four diameters downstream from the nozzle, at which point the entrained volume flow has increased 32% over the unforced case. When forced at a Strouhal number of 0.60, the jet seems to act as a compound amplifier, forming a violent 0.30 subharmonic and suffering a large increase of spreading angle. We conclude with the conjecture that the preferred mode having a Strouhal number of 0.30 is in some sense the most dispersive wave on a jet column, the wave least capable of generating a harmonic, and therefore the wave most capable of reaching a large amplitude before saturating.

## CONTENTS

1. Introduction	
2. Flow-visualization experiments	
3. Means of forcing the jet	
4. Structure of the preferred mode	
5. Amplitude response at various Strouhal numbers	
6. Axial profiles at various Strouhal numbers	
7. Summary description of the modes	
8. Influence of forcing on entrainment and background turbulence	
9. Comparison with stability theory	
10. Concluding remarks	
REFERENCES	

## 1. Introduction

We set out to find whether jet turbulence is orderly in any sense, and whether the order can be enhanced and controlled by a slight periodic surging imposed at the jet exit. The technological motivation for the study was jet noise. To the extent that turbulent mixing can be accomplished by an orderly process, a new range of noise-suppression techniques becomes available, and the problem of predicting jet noise becomes much simpler.

How does the disorder usually attributed to turbulence originate? One approach to an answer is to consider why a vorticity-free potential flow is *not* necessarily random. An incompressible potential flow is determined at each instant by conditions on the boundary. In principle, an experimentalist could establish or annihilate any incompressible potential flow instantaneously by a suitable change in the boundary conditions. He need not reach within the boundary to control the motion. Furthermore, the potential at an interior point is a weighted average of the potential over the boundary, so a local irregularity on the boundary has only a local effect inside. From instant to instant, the gross features of the boundary conditions control the gross character of an incompressible potential flow within.

The situation changes fundamentally if vorticity sheds from the boundary into the flow, as occurs continuously from a jet orifice. The flow no longer depends strictly upon instantaneous surface conditions, and the experimentalist cannot control the rotational part of the velocity field by taking action at the boundary. *He has lost control over the flow.* The velocity at an interior point, moreover, can depend sensitively on a nearby element of vorticity and is no longer a smooth average. The flow now depends not merely on instantaneous surface conditions, but on the entire history of vortex shedding from the boundary in all detail. In order to restore control, the experimentalist must either control the three-dimensional vorticity field directly by means of body forces, or control the entire history of the boundary conditions, which is the alternative adopted in this study. Usually neither is attempted, and the flow gives way to chaos.

Despite the loss of control, the boundary conditions and mean-flow characteristics may still dispose the turbulence to acquire a somewhat orderly pattern, at least with respect to the largest scales of motion. Some classical theories of turbulent shear flow are based on that idea. Reynolds (1894) derived the original criterion for turbulence in a channel by calculating the exchange of energy between the mean flow and a train of sinusoidal eddies. Malkus (1956) based his channel-flow theory on the eigenmodes of the stability problem for the mean flow rather than an *ad hoc* sinusoidal eddy shape. The theory bearing most directly on the present work is that of Landahl (1967), who argued that the random component of boundary-layer turbulence excites relatively coherent and long-lived waves, the most lightly damped eigenmodes of the linear stability problem. The turbulence plays two roles, as a random exciter of waves, and as an ensemble of the waves themselves.

There is also a body of experimental evidence for orderly structure in turbulent flows, even at extremely large Reynolds numbers. The Karman vortex street disintegrates at Reynolds numbers above  $2 \times 10^5$  and was thought to be associated with moderate Reynolds numbers only. At a Reynolds number of  $3.5 \times 10^6$ , however, Koshko (1961) found that the vortex street behind a circular cylinder reappears with much the same structure as at moderate Reynolds numbers. In their flow-visualization experiments on turbulent boundary layers, Kline, Reynolds, Schraub & Runstadler (1967) discovered that turbulence production occurs in definite bursts near the wall. Presumably the bursts involve rapid stretching of vortex loops shed from the viscous sublayer. In any case, the bursts have a common structure and are random chiefly with respect to their origin in space and time.

The study of orderly jet fluctuations began during an evening of chamber music in the mid-nineteenth century. Among the audience was a medical doctor knowledgeable in acoustics, who noticed a gas flame dance in response to the violoncello so that '*a deaf man might have seen the harmony*' (Leconte 1858). The phenomenon attracted the attention of Tyndall (1867), who showed that ignition is not essential; any jet on the verge of becoming turbulent is sensitive to musical notes. The explanation of sensitive jets is due to Rayleigh (1896). The vortex sheet surrounding a jet column is unstable, so a sound wave passing the jet exit excites a train of interfacial waves on the column. The waves promote transition to turbulence and enhance mixing. Rayleigh could draw no certain conclusion about the precise shape of the waves, whether the column becomes sinusoidal or pulsatile, and the question has remained open since (cf. Reynolds 1962).

Questions of detail aside, it was clear by the turn of the century that sensitivity resides in an orderly oscillation of the jet column. The nineteenth-century workers dealt with Reynolds numbers around  $10^3$ , however, and it may be wondered whether any order persists at the far greater Reynolds numbers of current technological interest. A degree of order can be inferred from casual observations of turbo-jet exhausts, which often appear to disintegrate into trains of loosely packed puffs of smoke. More reliable evidence is a schlieren photograph of a turbulent jet published by Bradshaw, Ferriss & Johnson (1964)

and reproduced here with their kind permission as figure 1 (plate 1). The jet emerged with a speed of 280 ft/sec, uniform across the 2 in. diameter exit plane. The corresponding Reynolds number was about  $3 \times 10^5$  based on diameter, and the Mach number was sufficiently low that the flow can be considered incompressible. The change in refractive index was achieved by injecting Freon-12 gas into the plenum upstream of the jet. Beneath the stippled chaos of the fine mixing-layer turbulence, one can discern a train of large-scale puffs or waves.

Jet noise itself provides some evidence for natural organized structure. Mollo-Christensen (1967) observed that pressure fluctuations outside a fully turbulent jet column come in rather well-defined wave packets, as though the column were undergoing sporadic oscillations. Unlike most turbulent velocity spectra, the jet-noise spectrum has a distinct peak, at a Strouhal number of about 0.3 based on frequency, exit speed, and diameter, the exact Strouhal number depending on angle from the jet axis (Mollo-Christensen, Kolpin & Martuccelli 1964). The existence of a peak suggests that an underlying wave structure may be responsible for much of the sound.

Encouraged by the available evidence, we undertook experiments on round turbulent jets. The Mach number was always very small, not so severe a restriction, because compressibility does not alter the structure of jet turbulence until the mean flow greatly exceeds the speed of sound (Ffowes Williams 1963). We began with the flow-visualization experiments reported in §2. An orderly axisymmetric pattern was evident for Reynolds numbers between several hundred and perhaps  $7 \times 10^4$ , above which no method of visualization gave results better than those of Bradshaw *et al.* (figure 1). The next step was to modify the apparatus as described in §3 so that a sinusoidal surging could be imposed at the exit plane. We thereby assumed partial control over the history of the boundary conditions in the hope of overriding the natural tendency toward chaos at high Reynolds numbers. Even when the boundary layer at the exit was tripped and fully turbulent, axisymmetric modes of organized flow could be excited and raised to high amplitude above the random background. The mode having a Strouhal number of 0.30 could attain an especially high amplitude. The structure of that preferred mode is discussed in §4, and §§5-7 explain how a non-linear cascade establishes the Strouhal-number preference. The influence of the preferred mode on the mean field and on uncontrollable background turbulence is described in §8.

When no periodic surging is imposed, then background turbulence may trigger organized modes at random in the spirit of Landahl (1967), but the mechanism for selecting the dominant mode is different. All modes in a turbulent boundary layer are damped according to linear stability theory, so Landahl assumed that the most lightly damped mode would prevail. In the case of a round jet with a top-hat exit profile, all modes amplify, and the higher the frequency, the faster the amplification. But all modes saturate owing to a non-linear cascade, and the mode having a Strouhal number of 0.30 has the highest accessible amplitude.

The relation between the orderly structure and linear stability theory is discussed in §9, and some speculations about non-linear amplitude saturation

are offered in §10, which concludes the paper. It is worthwhile laying to rest a question here, whether the phenomenon under study consists of eddies or waves (cf. Moffatt 1969). We shall move freely between both kinds of description, sometimes calling the orderly structure a vortex train, and sometimes waves on a jet column. The two descriptions are entirely complementary as far as jet turbulence is concerned. Wave terminology conveys the fact that the periodic structure obeys the dispersion relation for linearized waves on a jet column (Batchelor & Gill 1962), whereas eddy terminology emphasizes the amplitude saturation resulting from a non-linear cascade.

## 2. Flow-visualization experiments

Viscosity influences jet turbulence primarily by affecting the boundary layer shed from the nozzle (Bradshaw 1966). The boundary layer depends on the contraction upstream of the nozzle, as well as on the Reynolds number based on exit speed and diameter. At a sufficiently low Reynolds number, however, the boundary layer of any nozzle is so thick that the exit profile resembles a Poiseuille pipe flow. We therefore began with qualitative experiments on a water jet having Poiseuille-flow exit conditions.

The jet issued from a horizontal 9 in. long glass tube submerged several inches in a large water trough. The inside diameter of the tube was 0.25 in., and the flow rates were of order 1 ft/sec. Water for the jet was drawn from a tap and sent through a fluorescein-dye injector before entering the tube, so the jet could be seen as a bright yellow column against the black bottom of the trough. To prevent the trough filling with dye under continuous operation, a cup-shaped collector was located several inches downstream from the jet and connected to a drain. Except at the lowest flow rates, the jet appeared chaotic under normal illumination, but a stroboscope revealed the underlying order for Reynolds numbers up to about  $2.5 \times 10^3$ , where the pipe flow itself became turbulent.

The first sign of instability was the sinuous, whiplash motion sketched in figure 2(a). The remaining parts of the figure show how the instability evolves with advancing Reynolds number. Flow rates were not measured accurately, and the drawings cannot be associated with specific Reynolds numbers. It is sufficient to note that the evolution from sinuous to pulsatile flow is complete at a Reynolds number of order  $10^3$ . As the Reynolds number advances toward that value, the sinuous column coils into a corkscrew shape (b), then tightens and forms bulbous lobes rather like a crankshaft (c), and finally breaks into a train of axisymmetric puffs (d). The helical types of instability could have either sense of revolution and would switch at random from one to the other when the tap was turned on and off. The evolution from a sinuous to a pulsatile instability was smooth and continuous, without the variety of motion seen by Reynolds (1962), whose vertical dye jet may have been slightly buoyant. By moving our horizontal jet up toward the surface, we could see water waves radiating outward from above the region of puff formation. The chaotic turbulence further downstream did not appear to be a strong source of waves.

Presumably because of their dispersive character, the waves were confined to narrow sectors at  $45^\circ$  to the jet axis. The dye jet and the synchronized waves on the surface above were beautiful under stroboscopic illumination and can be recommended as a lecture-room analogue of jet-noise production.

The Reynolds number of the dye jet could not be driven far above order  $10^3$  before the pipe flow itself became turbulent, so we turned to the air jet shown schematically in figure 3. Not shown are an air conditioner capable of

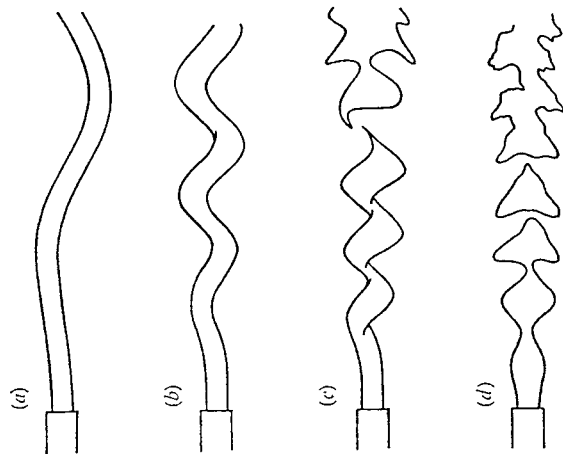


FIGURE 2. Evolution of jet instability with advancing Reynolds number. Parts (a)–(d) span the Reynolds-number interval from around  $10^2$  to  $10^3$ .

holding the jet temperature to within  $1^\circ\text{F}$  of the room temperature for hot-wire studies, a primary air filter, and a 1.5 hp centrifugal blower. Air from the blower enters a short diffuser  $S$ , is cleaned by an electrostatic precipitator  $P$ , passes through a throttle valve  $V$  and into a 46 in. long wooden box  $B$ , then passes through a 50 in. diffuser of  $6^\circ$  half-angle into a plenum chamber  $C$  36 in. long and 12 in. in diameter. The wooden box contains two plastic grids for mixing purposes, and there are two fine screens in the plenum as shown. The use of the loud-speaker  $L$  is described in §3. A nozzle  $N$  having a 12:1 diameter contraction was used for the present flow-visualization experiments, the exit diameter  $D$  of the jet being 1 in. (the schematic shows a 2 in. jet used for later hot-wire studies). A laminar boundary layer surrounds the jet column, which emerges with a top-hat velocity profile and a 0.1 % turbulence level. The jet can be driven up to a speed  $U_e$  of about 220 ft/sec.

In consideration of ambient room drafts, we decided not to run the jet below 20 ft/sec, corresponding to a Reynolds number  $Re$  of about  $10^4$ , where  $Re = U_e D / \nu$ , and  $\nu$  is the kinematic viscosity of air. We therefore could not explore the Reynolds-number range  $10^3$ – $10^4$ , but fortunately excellent photographs

have been taken in that range by Brown (1935) of a two-dimensional jet and by Becker & Massaro (1968) of the axisymmetric case. Becker & Massaro observed axisymmetric waves on the jet column for Reynolds numbers up to about  $10^4$ , beyond which the flow appeared to degenerate into chaos. Their nozzle was fed by a long pipe, however, having a diameter only 3.8 times that of the jet. It is easy to show from continuity that the Reynolds number of the pipe would have been  $10^4/3.8 = 2.6 \times 10^3$  based on mean flow speed, when the Reynolds number of the jet itself was  $10^4$ . Natural transition in a pipe occurs at a Reynolds number of about  $2.6 \times 10^3$ , so the loss of order may have been caused by transition upstream of the nozzle.

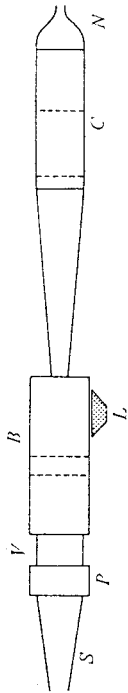


FIGURE 3. Schematic of the jet facility, which is about 16 ft long. The dotted lines represent grids or screens, and the labelled parts are described in the text.

Figure 4(a) (plate 2) is a schlieren spark photograph of our air jet under the conditions  $D = 1$  in.,  $U_e = 36$  ft/sec, and  $Re = 1.87 \times 10^4$ . The photographic technique was similar to that of Bradshaw *et al.* (figure 1, plate 1) except that the jet was seeded with  $\text{CO}_2$  rather than Freon and the knife edge was vertical instead of horizontal. The spark duration was about  $1 \mu\text{sec}$ , and high contrast Type 51 Polaroid film was used. The flow within the first four diameters of the nozzle is dominated by organized axisymmetric structure, including short interfacial waves near the nozzle, and two large-scale puffs further downstream. The puffs look rather like the underlying structure one seems to discern in figure 1. If orderly structure exists beyond the first four diameters, it is obscured by a finely textured sheath of  $\text{CO}_2$ . Figure 4(b) is a similar photograph taken under the conditions  $U_e = 102$  ft/sec and  $Re = 5.27 \times 10^4$ . The ripples on the laminar boundary layer have shortened but are still clearly visible. Any large-scale structure that may exist downstream, however, is masked by a fine-grained mixture of  $\text{CO}_2$  and air surrounding the jet. A schlieren image emphasizes fine detail, though not nearly so much as a shadowgraph. Jet-noise production, on the contrary, is heavily biased toward large-scale eddies (Effowes Williams 1963). We needed another method of visualization to search for large-scale order at higher Reynolds numbers.

After investigating several types of smoke, each of which was noxious, corrosive, or dirty, we settled upon fog as the flow-visualization medium. The fog was made by injecting steam into the airflow and passing the mixture over pans of liquid nitrogen in the box B of figure 3. By a judicious choice of the pan area and grid geometry inside the box, we could produce a light fog without freezing the plenum screens. The temperature of the fog was about  $50^\circ\text{F}$ . Air saturated at  $50^\circ\text{F}$  is 1.03 times denser than dry room air at  $70^\circ\text{F}$ , so the jet column was only about 3% denser than its surroundings. Figure 5 (plate 3) is a photograph of the facility, as outfitted for high-speed motion picture photography. The

1 ft diameter jet plenum is suspended inside a 2 ft diameter chamber containing several more pans of liquid nitrogen. They served to refrigerate the skin of the plenum, for otherwise the jet would emerge with a warm and fog-free boundary layer. Note the crossed lighting and blackened screens, necessary because fog scatters light efficiently only in directions more-or-less forward. The arrangement for stills was similar except that a single xenon flash lamp provided the illumination. The duration of the flash was measured as  $20 \mu\text{sec}$ , brief enough for an unblurred image at the highest speeds tested.

Figure 6 (plates 4-6) comprises seven photographs of the 1 in. fog jet at exit speeds ranging from 20 ft/sec to 147 ft/sec. The corresponding Reynolds numbers advance from  $1.05 \times 10^4$  to  $7.57 \times 10^4$  in roughly equal increments. Some idea of the relation between the schlieren and light-scattering methods of visualization can be gained by comparing figures 4(b) and 6(e), both of which were taken around  $Re = 5.2 \times 10^4$ . The schlieren picture 4(b) clearly shows the short waves that grow on the vortex sheet immediately downstream of the nozzle, but large-scale structure further down is left mainly to the imagination of the viewer. The fog picture 6(e) shows two dramatic large puffs 2-5 diameters downstream but cannot resolve the fine ripples near the nozzle. The large-scale puffs were photographed regularly up to the Reynolds number of  $6.52 \times 10^4$ , were infrequent at  $7.57 \times 10^4$ , and were not observed in such a striking form above that.

Using the lighting arrangement shown in figure 5, we made motion pictures of the fog jet at frame rates ranging from  $5 \times 10^3$  to  $1.1 \times 10^4$  per second. After a careful study of the motion pictures and of the fog and schlieren stills, we came to the tentative conclusion that a jet experiences two kinds of orderly process within the range of Reynolds numbers under consideration: an instability of the thin laminar boundary layer leaving the lip, and a much larger-scale process of puff formation further downstream. The instability scales on the thickness of the boundary layer, whereas puff formation involves the whole jet column and scales on its diameter.

The boundary-layer instability has been studied extensively, in particular by Sato (1960) and Browand (1966), and especially in a definitive sequence of papers put forth by Wille (1952) and his colleagues at the Deutsche Versuchsanstalt für Luft- und Raumfahrt in Berlin. Bibliographies of that work are given in a review by Michalke & Wille (1966) and in one of the later papers in the sequence by Freymuth (1966), who presents photographs obtained by a method suited especially for visualizing short waves downstream of a lip.

The work of the Berlin school concerns a free boundary layer sufficiently thin that the diameter  $D$  of the jet has no influence on the instability. In that limit the boundary layer behaves much like the two-dimensional vortex sheet of classical inviscid stability theory. The finite thickness of the boundary layer, however, distinguishes a wavelength at which the instability grows at a maximum rate. For a hyperbolic-tangent velocity profile having a thickness  $\delta$  based on maximum slope, Michalke (1964, 1965) showed theoretically that the wavelength  $\lambda$  for maximum temporal growth is  $7.07 \delta$ , and that the wavelength for maximum spatial growth is  $7.80 \delta$ . The phase velocity of the preferred temporally



growing wave is exactly one-half  $U_e$ , whereas the phase velocity in the case of spatial growth is  $0.513 U_e$ .

We made hot-wire surveys of the laminar boundary layer leaving our jet at various Reynolds numbers and found that the profile relaxes quickly into a hyperbolic-tangent form. Results for the thickness  $\delta$  based on maximum slope at a distance  $0.02$  in. downstream are presented in the table below, together with values of the wavelength  $\lambda$  measured from the photographs.

$Re \times 10^4$	$\delta/D$	$(Re)^{1/2} \delta/D$	$\lambda/D$	$\lambda/\delta$
1.05	0.041	4.16	0.44	10.9
1.95	0.031	4.34	0.24	7.7
3.09	0.025	4.36	0.19	7.6
5.14	0.020	4.47	$\sim 0.14$	$\sim 7$

TABLE 1. Boundary-layer thicknesses and instability wavelengths in dimensionless form

It is clear from the second column of the table that the boundary layer is thin compared with the diameter of the jet, so the work of the Berlin school would be expected to apply. The third column shows that  $\delta/D$  varies approximately as  $(Re)^{-1/2}$  in accord with simple viscous boundary-layer concepts. The constant of proportionality,  $\sim 4.4$ , of course, depends on the geometry of the nozzle and should decrease with decreasing contraction ratio (cf. equation (1) of Becker & Massaro 1968). The fourth column of table 1 shows that  $\lambda$  is fairly small compared with  $D$  except possibly at the lowest Reynolds number studied. Save at that Reynolds number the waves are approximately two-dimensional, and the fifth column shows that  $\lambda/\delta$  does indeed have values between 7 and 8 in accord with the stability theories of Michalke (1964, 1965). Phase velocities measured from the motion pictures were about  $0.5 U_e$  as well. These data are not nearly so accurate as those of Freymuth (1966), who used a loudspeaker to drive the instability so that phase velocities and growth rates could be measured accurately. Table 1 is intended to show that the boundary-layer instability seen in our photographs is the two-dimensional phenomenon studied by the Berlin school and that the maximally amplified mode arises without artificial excitation.

The short waves quickly steepen and combine pair-by-pair into longer waves, the subharmonics measured by Browand (1966) and Freymuth (1966). That terminates the evolution of orderly structure at a Reynolds number of  $1.05 \times 10^4$ , and the subharmonic waves propagate on downstream, gradually losing their coherence without much change in overall shape [figure 6(a)]. As the Reynolds number advances toward  $2 \times 10^4$ , a second and rather more violent combination follows the first so that four waves become packed, so to speak, into a puff. As the Reynolds number advances still higher, a cascade of pair-by-pair combinations occurs, initiated by surface waves of decreasing length, and terminated by a train of puffs as seen in figure 6. The structure of the train is relatively insensitive to Reynolds number, as though the cascade seeks a terminal state defined only by  $U_e$  and  $D$ .

The puffs are more sporadic than the initial ripples. Three or four puffs form and induct themselves downstream, an interval of confused flow ensues, several more puffs form, and so on. Formation is not periodic, but *average* frequencies  $f$  could be found simply by counting puffs during screenings of the flow-visualization motion pictures. A count depends to a certain extent on what one chooses to interpret as a 'puff', but the results have some objectivity as demonstrated by the table of timed counts below.

$Re \times 10^4$	Subject SCC	Subject SFC	$St$
1.05	50	48	0.29
1.95	55	51	0.32
3.09	60	63	0.28

TABLE 2. Average Strouhal numbers of puff formation

Subject SCC was one of us, and subject SFC was an observer without technical training, instructed briefly beforehand about the nature of a 'puff'. The agreement between the counts presented in the second and third columns is limited evidence that the puffs exist as an objective terminal state of orderly flow. Average Strouhal numbers based on the puff counts,  $St = fD/U_e$ , are shown in the fourth column and are seen to have values around  $0.3$  independent of the Reynolds number over the very limited range considered. Accurate counts at higher Reynolds numbers could not be obtained, because lighting limitations and the high frame rates required to avoid blurring ( $8 \times 10^3$  per second and above) resulted in films of poor quality, lacking some of the visual cues that facilitated the counts shown. The still pictures of figure 6 imply that structural similarity extends to Reynolds numbers much higher than  $3.09 \times 10^4$ .

In the course of watching the motion pictures, we came to understand why a conventional shadowgraph reveals no large-scale structure in jet turbulence. Some foggy air is thrown out of the jet column as each puff forms. While the puff inducts itself downstream, the ejected fog remains behind as a passive sheath around the column. Although dynamically unimportant, the sheath shows up clearly in a schlieren picture and would dominate a shadowgraph completely. A final observation from the motion pictures: for the Reynolds numbers under consideration, the conical potential core of the jet is the *interior envelope* of the waves growing on its surface.

### 3. Means of forcing the jet

The photographs led us to imagine turbulence in the transitional region of a jet as a *vortex train*, a train of loosely packed vortex rings only weakly dependent on the circumstances of their origin. The idea is attractive, because a vortex ring is a much more stable state of flow than a columnar vortex sheet. The sheet can plausibly be expected to wrap into a train of vortex rings carrying the same momentum, each ring maintaining its identity some distance downstream from its point of origin. One can easily show that a train of vortex rings would distort a fog column into spade-shaped puffs of the kind seen in figure 6.



the wake of an aircraft is known to follow a similar course (Crow 1970). An aircraft generates a pair of trailing vortices, which undergo a symmetric instability driven by their mutual induction, until they connect at points to form a ring of vortex rings oriented parallel to the ground. The rings are quasi-stable, preserving a degree of order intermediate between the original vortex pair and the chaos that finally unfolds. Because of its stability, the vortex ring may be a more universal mode of transitional flow.

The visual evidence for order in jet turbulence becomes ambiguous at a Reynolds number around  $7 \times 10^4$ , beyond which we were unable to produce a photograph better than figure 1. The vortex puffs seen in figure 6, moreover, are fed by laminar instability, and the question remains whether they would exist in the absence of a laminar boundary layer. The Strouhal number 0.3 associated with puff formation is affirmative evidence, since the peak of the jet-noise spectrum lies between 0.25 and 0.30 depending on angle from the jet axis. The evidence suggests that the vortex train is latent in jet turbulence at high Reynolds numbers and contributes to the emission of sound.

The hypothesis of latent order can be tested in at least two ways. One way would be to extract the mode of greatest likelihood from hot-wire signals, along the line advocated by Lumley (1966) and commonly used by electrical engineers, to extract signals from non-white noise. We adopted the alternative, however, of forcing the jet periodically and measuring the response. If there were no order in the unforced case, then the result of forcing would be damped as analogous to those studied by Hussain & Reynolds (1970) in turbulent channel flow. If there is a natural tendency toward order, then periodic forcing raises the latent structure above background turbulence and permit measurements without complicated signal-extraction procedures.

For the purposes of such experiments, the apparatus was modified in three aspects: the diameter of the jet was increased to 2 in., the boundary layer was tripped just upstream of the exit, and a loudspeaker was attached to the wooden box previously used for mixing fog. Doubling the exit diameter raised the operational Reynolds number of the jet to  $10^5$ , corresponding to an exit speed of about 100 ft/sec. The blower can drive the 2 in. jet up to 145 ft/sec, but the higher speed reserved for hot-wire calibration. The jet has a top-hat velocity profile and a turbulence level, higher than in the 1 in. jet, because the nozzle contraction is halved. In the absence of a trip, the boundary layer surrounding the 2 in. plenum is laminar and has a thickness  $\delta = 0.022$  in. at an exit speed  $U_e = 100$  ft/

sec. The tripped the boundary layer to achieve a measure of Reynolds-number independence and especially to destroy short interfacial waves immediately upstream of the nozzle. The trip ring fits tightly into the 2 in. nozzle about 10 in. upstream from the exit. Deep axial notches cut into the ring forestall any organized vortex shedding on its part. The ring is 0.140 in. long and 0.020 in. thick, about as thick as the laminar boundary layer just upstream of the ring at  $U_e = 100$  ft/sec. At that speed the tripped boundary layer is intensely turbulent, with a peak root-mean-square axial fluctuation of  $0.079 U_e$ . The thickness of the turbulence intensity distribution at half its peak value is 0.062 in., about

6% of the nozzle radius. The boundary layer becomes untripped at an exit speed of about 40 ft/sec, much lower than any used in the present experiments. Above 40 ft/sec, the jet is invariant to Reynolds number with respect both to mean and to root-mean-square quantities, as far as can be determined from the limited range of accessible Reynolds numbers.

Figure 7 is a plot of the mean axial speed  $U$  measured on the centreline at various positions  $x$  and at four Reynolds numbers  $Re$ . The co-ordinates represent the dimensionless quantities  $U/U_e$  and  $x/D$ . The circles are data at  $Re = 1.03 \times 10^5$ , and data at other Reynolds numbers are plotted wherever they do not overlap

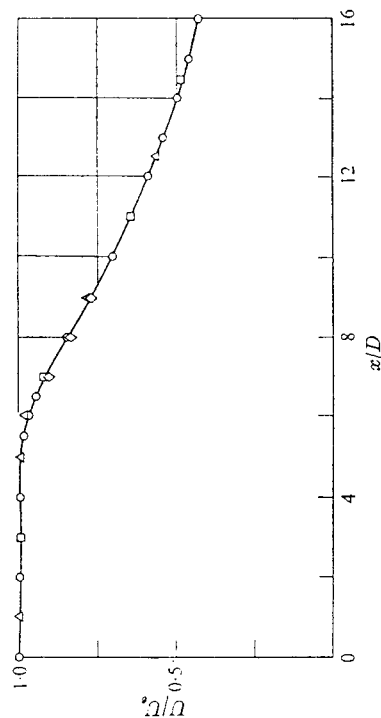


FIGURE 7. Profile of the mean axial speed on the centreline at several Reynolds numbers, as denoted by the following data symbols:  $\Delta$ ,  $6.2 \times 10^4$ ;  $\square$ ,  $8.3 \times 10^4$ ;  $\circ$ ,  $1.03 \times 10^5$ ; and  $\diamond$ ,  $1.24 \times 10^5$ .

the circles. The mean axial profiles are practically indistinguishable in the Reynolds-number interval  $6.2 \times 10^4$  to  $1.24 \times 10^5$ . Figure 8 is a similar plot of the turbulence intensity  $u$ , the root-mean-square axial component of turbulent velocity as measured on the centreline. A factor-of-two change in Reynolds number is seen to have little effect on the ratio  $u/U_e$ . The curves in figures 7 and 8 are superposed on later plots to represent the unforced state. Hopefully the tripped boundary layer resembles conditions at the exit of a turbo-jet engine, but certainly the boundary layer is fully turbulent and sustains no orderly oscillations of its own. Any large-scale structure that can be evoked has nothing to do with details of the boundary layer shed from the nozzle.

The loudspeaker  $L$  sketched in figure 3 provided the forcing. The 12 in. diameter loudspeaker was installed upstream of the plenum to keep the exit conditions clean. As a result, the transmission of energy between the loudspeaker and the exit plane is efficient only at certain discrete forcing frequencies, which are the organ-pipe resonances of the cavity. As far as internal acoustic waves are concerned, the highly contracted nozzle presents a closed face and is therefore a pressure maximum at resonance. The oscillating pressure upstream of the contraction results in an oscillating speed at the exit, since the jet must attain the constant ambient pressure downstream of the contraction. Figure 9 is a spectrum of the jet cavity, measured at an exit speed  $U_e = 60$  ft/sec, with a root-mean-square

spectrum has resonance peaks at  $f = 113$  Hz, 185 Hz, 262 Hz, and so on. The resonance frequencies are independent of  $U_e$ , but the surging amplitude  $u_e/U_e$  at a particular resonance is proportional to  $W/U_e^2$ , a result that can be deduced by assuming the fluctuating pressure upstream of the contraction to be proportional to  $W$  and applying Bernoulli's equation to the contraction process itself.

We wanted to find how the jet responds to periodic surging at Strouhal numbers ranging from 0.15 to 0.60, from half to twice the Strouhal number of 0.3 derived from puff counts. Among the quantities in the definition  $St = fD/U_e$ ,  $D$  was fixed at 2 in.,  $f$  could take on discrete values, and  $U_e$  could be varied continuously. Varying  $U_e$ , however, would result in simultaneous changes of the Reynolds number  $Re = U_e D/\nu$ . Although the boundary-layer trip makes the flow insensitive to Reynolds number, we chose to hold  $Re$  near  $10^5$  by skipping from one resonance to the next according to the following schedule:

$St$	$f$ (Hz)	$U_e$ (ft/sec)	$Re \times 10^4$
0.15	113	126	13
0.20	113	94	9.69
0.25	113	75	7.75
0.30	185	103	10.6
0.35	185	88	9.07
0.40	262	110	11.27
0.45	262	97	9.98
0.50	262	87	8.98
0.55	262	79	8.17
0.60	337	94	9.64

TABLE 3. Forcing frequencies, exit speeds, and Reynolds numbers of the hot-wire experiments

Each of the experiments described in subsequent sections was performed at the conditions specified in a row of table 3. The Reynolds-number variations are unimportant, and the periodic surging can be described in terms of a Strouhal number  $St$  and dimensionless root-mean-square amplitude  $u_e/U_e$ . Notice that the frequencies in table 3 correspond to sound waves 3–10 ft long inside the cavity. The jet turbulence outside does not interact directly with such waves and remains incompressible. The effect of the internal waves is to impose a periodic fluctuation on the strength of the vortex layer leaving the nozzle.

We measured several kinds of response downstream, each based on the axial component of velocity: the mean speed  $U$ ; the root-mean-square axial fluctuation  $u$ ; root-mean-square fluctuations  $u_{0.30}$ ,  $u_{0.50}$ , filtered around Strouhal numbers denoted by the subscripts; the spectrum  $F(f)$  of the axial fluctuation; the length  $\lambda$  and phase velocity  $c$  of organized waves. Most measurements were made on the centreline of the jet. In more general cases the cylindrical co-ordinates  $(x, r)$  of the hot wire are given,  $r = 0$  being the centreline of the jet and  $x = 0$  the exit plane.

Signals were obtained by means of a linearized, constant-temperature Disa anemometer. The mean speed  $U$  resulted from analogue integration over an interval typically 100 sec. The root-mean-square fluctuation  $u$  was measured with a Disa r.m.s. voltmeter, having a response flat to within 1% of full scale for all

potential  $W = 10.5$  V across the terminals of the loudspeaker. The abscissa is frequency  $f$ , and the ordinate is  $u_e/U_e$ , where  $u_e$  is the root-mean-square sinusoidal speed fluctuation at the jet exit, as measured by a hot-wire anemometer. The

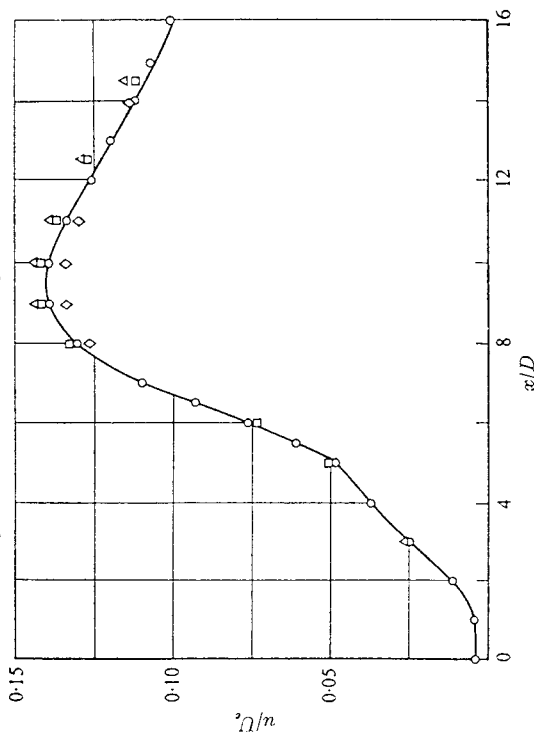


FIGURE 8. Profile of the root-mean-square axial fluctuation on the centreline. The data symbols are defined in the caption of figure 7.

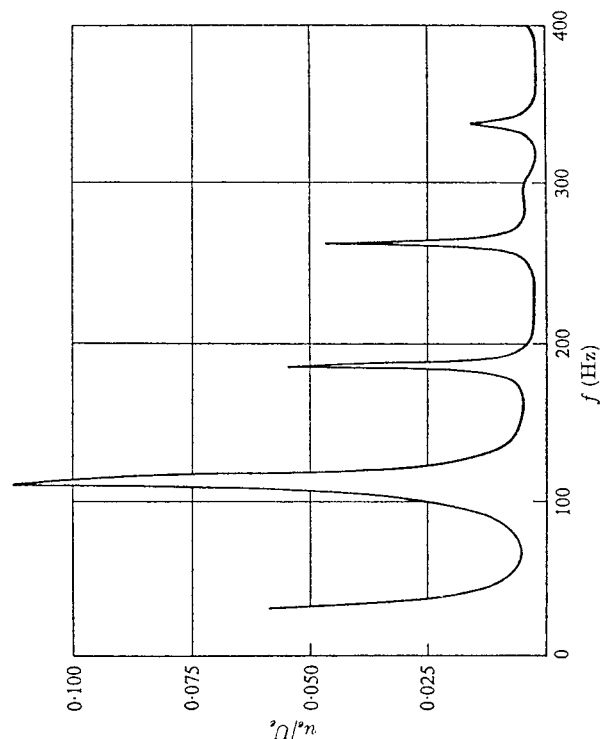


FIGURE 9. Spectrum of the jet cavity, measured in terms of the root-mean-square surging in the exit plane.

frequencies between 1 and  $10^5$  Hz. The core of the experiments is to relate the dimensionless turbulence intensity  $u/U_e$  to the axial location  $x/D$  and to the input variables  $u_e/U_e$  and  $St$ . The jet is to be regarded as a 'black box', a non-linear oscillator whose properties are to be understood in terms of the inputs  $u_e/U_e$ ,  $St$  and response  $u/U_e$ .

Now that the relevant parameters have been defined, it is worth noting exactly how this study fits with previous work involving loudspeaker excitation of jets. We deal with Reynolds numbers  $Re \approx 10^5$ , about ten times *higher* than those explored by Becker & Massaro (1968). We deal with Strouhal numbers  $St \approx 0.30$ , about ten times *lower* than those explored by Freymuth (1966), who confined his study to high-frequency waves, much shorter than the diameter  $D$  of the jet. Freymuth defined his Strouhal number in terms of boundary-layer thickness, but the lowest value of  $fD/U_e$  he reached was about  $0.9$  ( $f/U_e \approx 0.002$ , figure 16, Freymuth 1966). A fundamentally new phenomenon arises as  $St$  descends below about  $0.45$ : the forced wave becomes highly dispersive and attains an amplitude large enough to disintegrate the jet column.

#### 4. Structure of the preferred mode

We begin by explaining the consequences of forcing at  $St = 0.30$ , which table 2 suggests as the Strouhal number of natural oscillation. Except for a large accessible amplitude, the mode driven at  $St = 0.30$  is typical and serves as a useful introduction to the quantitative work.

The vortex puffs appear in the motion pictures to grow abruptly about four diameters downstream, just ahead of the tip of the potential core. On that basis, a strong response  $u/U_e$  would be expected at a point  $x/D = 4$ , under a surging imposed at  $St = 0.30$ . Figure 10 is an amplitude-response function measured under those conditions on the centreline of the jet. The abscissa is the forcing amplitude  $u_e/U_e$  measured at  $x/D = 0$  and, incidentally, found to be uniform over the exit plane. The ordinate is the response  $u/U_e$  measured by moving the hot wire back along the jet axis to  $x/D = 4$ . The value  $u/U_e = 0.038$  at  $u_e/U_e = 0$  is the natural turbulence intensity near the tip of the potential core. The amplitude response is shaped like many response functions occurring in engineering, for example, the stress-strain diagram for a ductile metal: the curve rises almost linearly with small forcing amplitudes, then yields, or saturates, under some non-linear effect (of course the figure represents time-averaged rather than instantaneous relationships). Under a forcing amplitude of 1%, that is  $u_e/U_e = 0.01$ , the response  $u/U_e$  is 13.9%, only a small part of which is aperiodic background turbulence (cf. figure 12). Under a forcing amplitude  $u_e/U_e = 2\%$ , the response  $u/U_e$  has risen to 17.2%, and it cannot be driven past 19% under any reasonable level of forcing.

One might have thought the wave-form at  $x/D = 4$  simply falls apart under forcing amplitudes above 1–2%, but quite a different process underlies saturation. Figure 11 shows four oscilloscope photographs of the wave-forms upon which figure 10 is based. The forcing amplitudes  $u_e/U_e$  are 0.005, 0.01, 0.02, and 0.04, doubling from one photograph to the next. The amplitude and time

scales are arbitrary but the same in all pictures; the axial component of velocity increases toward the vertical, and time increases from left to right. The signal at a forcing amplitude of 0.5% is a sine wave, distorted at random by ambient turbulence. As  $u_e/U_e$  advances to 1%, the signal becomes cleaner and almost

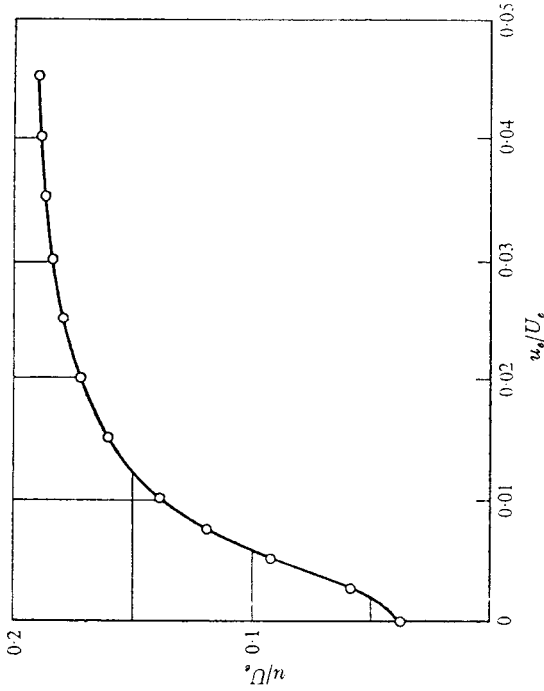


FIGURE 10. Amplitude response at the preferred Strouhal number 0.30. The response  $u/U_e$  is measured on the centreline four diameters downstream of the jet exit.

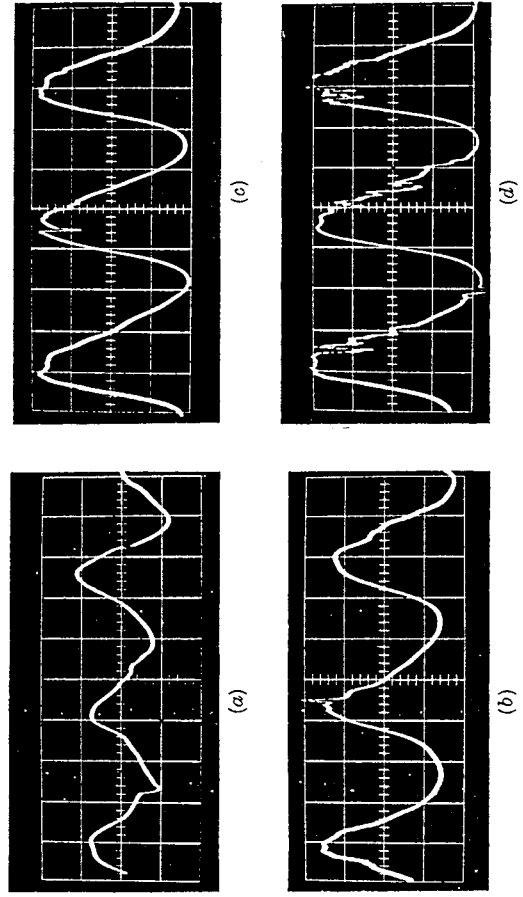


FIGURE 11. Wave-forms of the preferred mode, measured on the centreline four diameters downstream of the exit. The Strouhal number is 0.30 and the forcing amplitudes  $u_e/U_e$  are (a) 0.5%, (b) 1%, (c) 2%, and (d) 4%.

doubles in amplitude, but still resembles a sine wave. The amplitude has increased only slightly at  $u_e/U_e = 2\%$ , but now the wave-form has steepened along its rising front; a significant harmonic has arisen from the fundamental being forced. Since the Strouhal number of forcing is 0.30, the Strouhal number of the harmonic must be 0.60. Little change takes place as  $u_e/U_e$  increases from 2 to 4%, though some fine-scale turbulence begins to appear during the relaxing part of the wave cycle. The wave does not become disordered at forcing amplitudes above 1%, but instead saturates under the action of its harmonic.

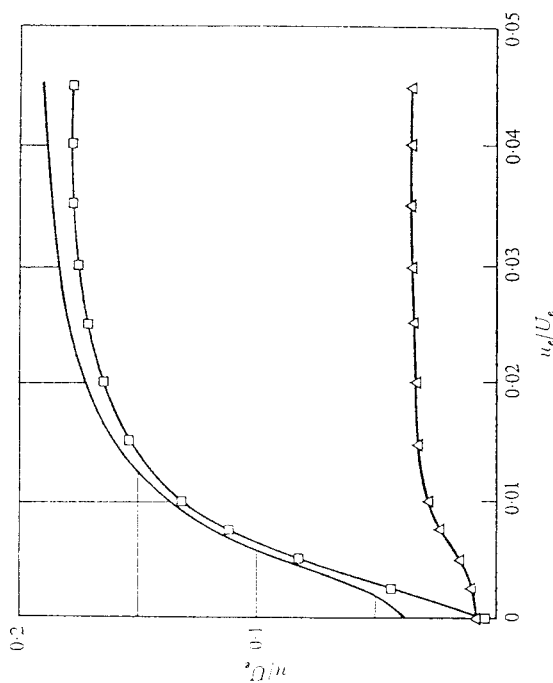


FIGURE 12. Filtered response functions of the preferred mode. The experimental conditions are the same as for figure 10, from which the curve without data points is taken, representing the total intensity  $u/U_e$ . The square data symbols denote the fundamental response  $u_{0.30}/U_e$ , and the triangular symbols denote the harmonic response  $u_{0.60}/U_e$ .

Those remarks are given quantitative form in figure 12, which is a plot of *filtered* amplitude-response data. The curve without data points is the total amplitude response  $u/U_e$  taken from figure 10, the curve defined by the square data symbols is the fundamental response  $u_{0.30}/U_e$  obtained by filtering the hot-wire output around the forcing frequency 185 Hz, and the curve with triangular symbols is the harmonic response  $u_{0.60}/U_e$  obtained by filtering around 370 Hz. The filter was a Dytronics Model 720, with a band-pass width about 7% of the centre frequency. The fundamental is accurately linear up to a forcing amplitude  $u_e/U_e = 0.5\%$ , then curves over as  $u_e/U_e$  increases from 0.5% to about 1.5%. The harmonic builds up in the same interval, and the two come into equilibrium around  $u_e/U_e = 2\%$ . The fundamental saturates at a value  $u_{0.30}/U_e = 17.9\%$ , and the harmonic at  $u_{0.60}/U_e = 3.5\%$ .

All the data presented so far were obtained on the centreline at  $x/D = 4$ , which was deemed likely to be the point of maximum response on the basis of the flow-visualization experiments. The conjecture can be verified by fixing  $u_e/U_e$  and

varying the hot-wire location  $x/D$ . Figure 13 is an axial profile of the fluctuation intensity  $u/U_e$  measured along the centreline under the forcing conditions  $u_e/U_e = 2\%$  and  $St = 0.30$ . The intensity profile for the unforced case is superimposed from figure 8 without data points. The slight but well-chosen surging at

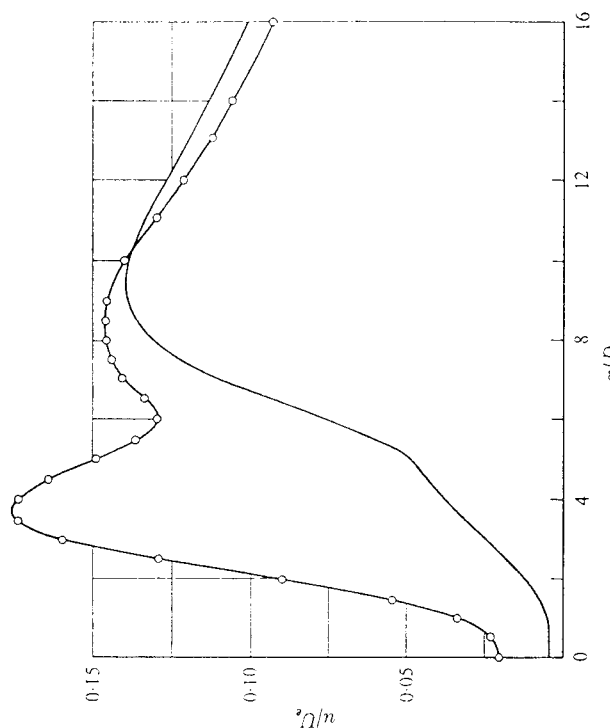


FIGURE 13. Axial profile of the turbulence intensity, measured along the centreline under 2% forcing at a Strouhal number of 0.30. The curve without data points represents the unforced case and is taken from figure 8.

the exit plane is seen to drive a powerful wave, which indeed reaches a peak amplitude near  $x/D = 4$ , more precisely, at  $x/D = 3.7$ . The intensity profile decreases from  $x/D = 4$  to 6 and there merges with the profile that exists in the absence of forcing. The natural turbulence intensity profile reaches a peak at  $x/D = 9.5$  on the centreline, and forcing under the conditions  $u_e/U_e = 2\%$ ,  $St = 0.30$  draws that peak inward to  $x/D = 8.5$ .

Axial profiles of the root-mean-square filtered fundamental  $u_{0.30}/U_e$  and harmonic  $u_{0.60}/U_e$  are presented in figure 14 for the same forcing conditions. The fundamental and harmonic rise and fall together with no apparent tendency for the spatial growth of the harmonic to lag the growth of the fundamental. Together they dominate the first six diameters of the jet and then fall toward zero. The experimental points do not quite reach zero, because the finite filter window admits some background turbulence not being driven by the periodic surging, especially in the intensely turbulent region around  $x/D = 8$ . The total intensity  $u/U_e$  is reproduced without data points in figure 14 as a solid line. The dashed line is the residual obtained by subtraction of squares:

$$\frac{u_r}{U_e} = \left\{ \left( \frac{u}{U_e} \right)^2 - \left( \frac{u_{0.30}}{U_e} \right)^2 - \left( \frac{u_{0.60}}{U_e} \right)^2 \right\}^{\frac{1}{2}}.$$

The intention was to include only the periodic parts of the filtered terms, so the fundamental and harmonic curves in figure 14 were extrapolated sensibly to zero near  $x/D = 8$  before the subtraction.

If the remaining harmonics of the forced wave are small, as seems likely, then  $u_r/U_e$  can be regarded as the intensity of background turbulence not under the control of the surging at the exit plane. The level of uncontrolled fluctuations on

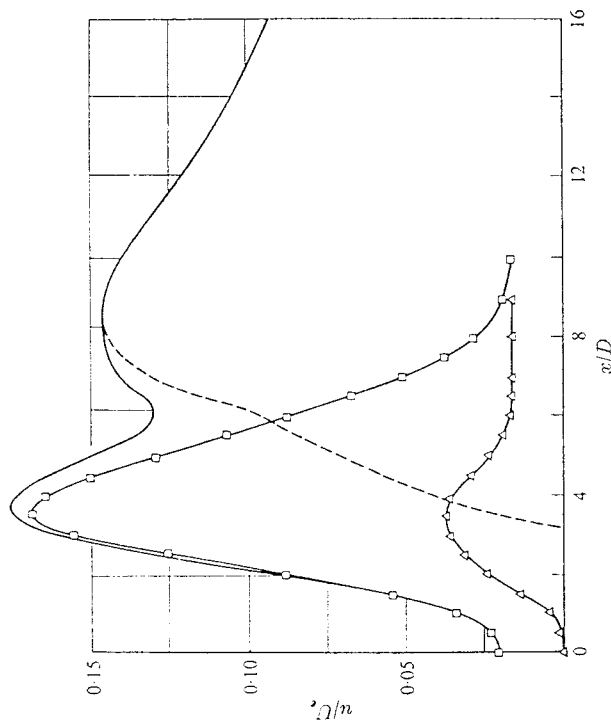


FIGURE 14. Filtered axial profiles of the preferred mode. The solid curve without data points represents the total intensity  $u_r/U_e$  and is taken from figure 13. The square data symbols denote the contribution  $v_{0.30}/U_e$  of the fundamental, and the triangular symbols denote the contribution  $v_{0.60}/U_e$  of the harmonic. The dashed curve represents the intensity of turbulence not bound in the fundamental or harmonic.

the centreline is essentially zero from  $x/D = 0$  to 3 and reaches the level of the controlled structure only at  $x/D = 6$  under the forcing conditions  $u_e/U_e = 2\%$ ,  $St = 0.30$ . The energy in the curious ramp-like portion of the natural intensity profile, seen in figure 8 between  $x/D = 0$  and 5, is bound into the strictly periodic flow. Presumably that ramp is the potential-core signature of big eddies in the mixing layer, in which case one can say that *big eddies within the first five diameters of the jet can be controlled by a slight surging applied in the exit plane at a Strouhal number of 0.30*. Moreover, *no control is possible beyond eight diameters*. By control, we mean that the surging fixes the frequency and phase of big-eddy formation.

The forced wave naturally has an effect on the mean flow. A complete discussion is deferred to §8, but an idea of the effect can be gained from figure 15, which is a profile of the dimensionless mean speed  $U/U_e$  measured on the centreline under the conditions  $u_e/U_e = 2\%$ ,  $St = 0.30$ . The line without data points

denotes the unforced case, this time taken from figure 7. Forcing draws the asymptotic decay curve beyond  $x/D = 8$  in toward the origin about two diameters. The reason for the shift in virtual origin is that forcing increases the entrainment between  $x/D = 0$  and 8, so the jet passes out of the controlled region with a volume flux appropriate to an unforced jet leaving an exit two diameters upstream from the actual exit.

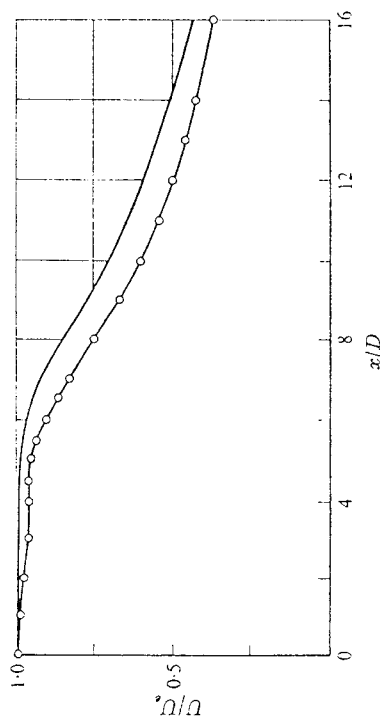


FIGURE 15. Effect of the preferred mode on the decay of mean speed along the centreline. The forcing level is 2%, and the Strouhal number is 0.30. The profile without data points represents the unforced case and is based on figure 7.

## 5. Amplitude response at various Strouhal numbers

In what sense is the mode studied in the foregoing section preferred? We first considered the question during the flow-visualization experiments, when it became apparent that puffs tend to form at an average Strouhal number of 0.3. An obvious possibility is that  $St = 0.30$  characterizes a maximally amplified mode of linear instability, but the possibility does not survive analysis. Batchelor & Gill (1962) have treated the temporal instability of doubly infinite jet columns. For a top-hat velocity profile, they found that axisymmetric waves become progressively more unstable as the Strouhal number increases. Nothing seems to distinguish the mode at  $St = 0.30$ . If the column is presumed to have a boundary layer of finite thickness, then a two-dimensional mechanism (Michalke 1964, 1965) takes over and establishes a preference as the wavelength becomes comparable to the boundary-layer thickness. The fastest growing short waves are pitched much higher than  $St = 0.30$ , however, and in any case the boundary-layer trip has eliminated them from the present experiments.

We thought about other linear mechanisms outside the theory of Batchelor & Gill. Their theory was revised for spatially growing waves, purely oscillatory in time, but the amplification rate again was found to grow monotonically with Strouhal number (cf. §9). Spatial instability of a vortex sheet leaving a semi-infinite plate was studied (Orszag & Crow 1970), in the hope that an instability downstream of a jet might interact with the nozzle to produce a large local surging when  $St = 0.30$ . The interaction between a two-dimensional vortex sheet and an

adjoining boundary was found to be disappointingly weak, however, and the interaction between a jet column and nozzle is probably even weaker. Every appeal to linear dynamics failed to establish a preference for the Strouhal number of 0.30. The reason is that non-linearity establishes the preference.

Figure 16 is a plot of amplitude-response functions measured on the centreline at  $x/D = 4$ . The total response  $u/U_e$  is plotted against the root-mean-square

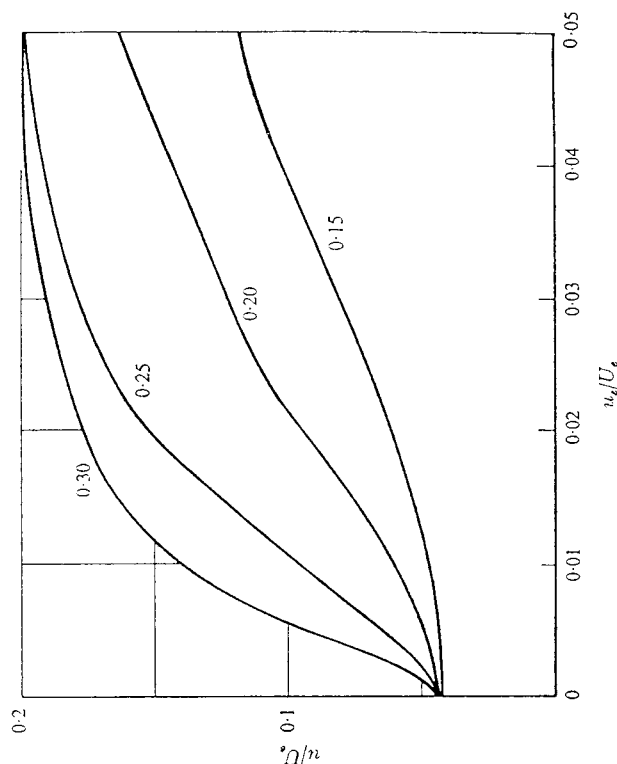


FIGURE 16. Amplitude-response functions measured on the centreline four diameters downstream of the jet exit. The response functions are labelled with Strouhal numbers, which range from 0.15 to 0.30.

surging  $u_e/U_e$  in the exit plane at four Strouhal numbers:  $St = 0.15, 0.20, 0.25$ , and  $0.30$ , the accessory experimental conditions being listed in table 3. As the Strouhal number rises from 0.15 to 0.30, the response at each level of forcing rises progressively. Within the range of small  $u_e/U_e$  where the fundamental (not shown) depends linearly on forcing, the slope  $du/du_e$  rises monotonically in accord with stability theory. The amplitude  $u/U_e$  at which non-linear saturation begins to set in rises as well.

Figure 17 illustrates the consequences of forcing at higher Strouhal numbers. The amplitude response at  $St = 0.30$  appears once again, together with response functions at  $St = 0.35, 0.40, 0.45$ , and  $0.50$ , each measured on the centreline at  $x/D = 4$ . The slope  $du/du_e$  continues to rise monotonically with Strouhal number in the linear region near  $u_e/U_e = 0$ , but non-linearity imposes an increasingly powerful restraint on the maximum attainable response. The saturation limit of  $u/U_e$  decreases continuously as the Strouhal number increases from 0.30 to 0.50. *The mode having a Strouhal number of 0.30 is preferred in the sense that it can*

attain the highest possible amplitude under the combined effects of linear amplification and non-linear saturation.

We measured response functions at  $St = 0.55$  and  $0.60$ , but they fall too near the  $St = 0.50$  curve to be plotted in figure 17. The maximum attainable response becomes very nearly constant at  $u/U_e = 10\%$  for the highest Strouhal numbers we investigated. That result accords with an observation of Freymuth (1966), that waves on a free laminar boundary layer tend to saturate at a constant amplitude at the lowest Strouhal numbers he investigated, which were mostly greater

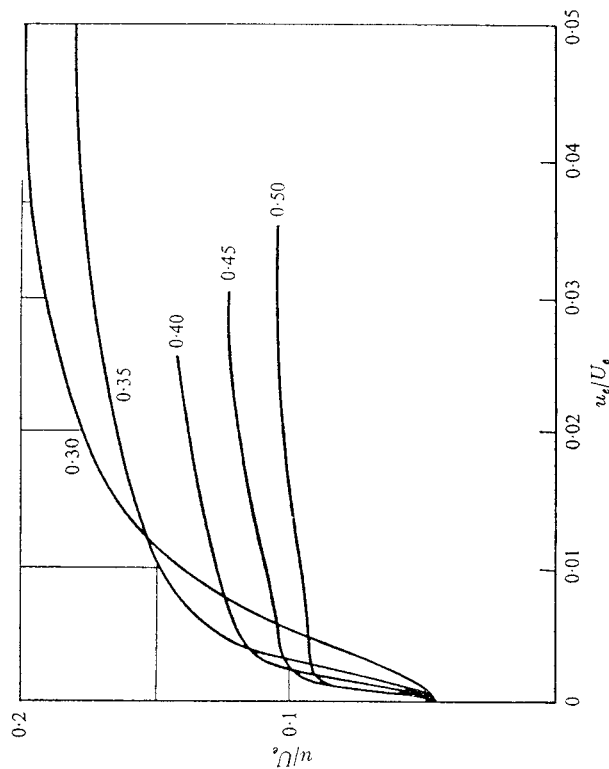


FIGURE 17. Amplitude-response functions continued through the Strouhal-number interval 0.30 to 0.50.

than 3.0 based on jet diameter, and never below 0.9. It therefore seems likely that  $u/U_e = 10\%$  persists as the upper limit of response at  $x/D = 4$  for Strouhal numbers ranging from 0.5 up to values so high that the thickness of the laminar boundary layer, if any, becomes involved.

The curves in figures 16 and 17 can be regarded as cuts through an amplitude-response surface above the plane of forcing parameters ( $St, u_e/U_e$ ). Figure 18 is a contour map of the response surface, constructed from the original response curves and their cross-plots against  $St$ . The abscissa of figure 18 is the Strouhal number  $St$ , the ordinate is the forcing amplitude  $u_e/U_e$ , and the contours are levels of constant response  $u/U_e$  measured on the centreline at  $x/D = 4$ . The higher contours point like daggers to the Strouhal number 0.30. Looking along a cut at a constant and very small  $u_e/U_e$ , one would find no Strouhal-number preference. Linear stability theory applies only along such cuts, so its failure to explain the Strouhal-number preference was inevitable. One must look along a horizontal

### 6. Axial profiles at various Strouhal numbers

We showed in the foregoing section that the Strouhal number of maximum response at  $x/D = 4$  varies somewhat with  $u_e/U_e$ , having no finite value at  $u_e/U_e = 0$  and acquiring values around 0.30 for  $u_e/U_e \geq 2\%$ . As might be expected, the preferred Strouhal number also depends to some extent on  $x/D$ . The waves all amplify with distance downstream, so a high  $x/D$  corresponds in a loose way to a high  $u_e/U_e$ . Here we examine the correspondence by presenting axial profiles of the total response  $u/U_e$  for the same Strouhal numbers as in §5, but for a forcing amplitude  $u_e/U_e$  fixed at 2%.

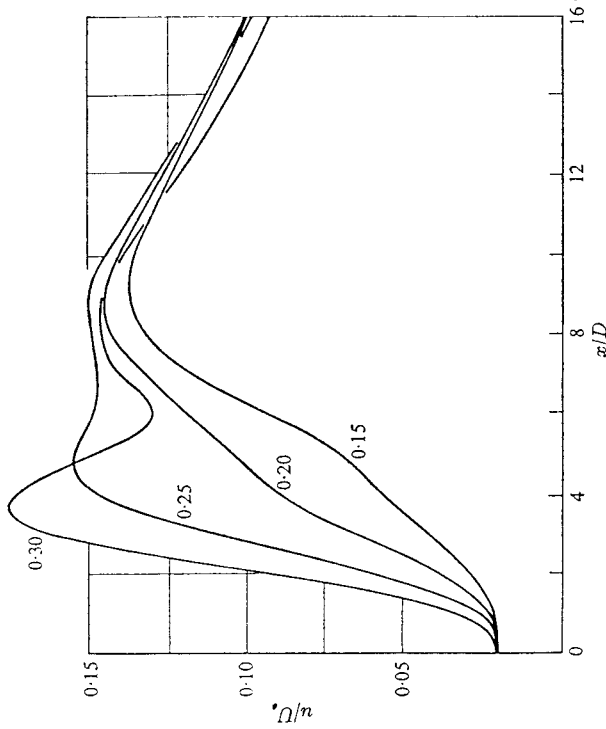


FIGURE 19. Centreline profiles of turbulence intensity, under 2% forcing in the Strouhal-number interval 0.15 to 0.30. The Strouhal numbers are given on the plot.

Figure 19 shows centreline profiles of response to 2% forcing at the Strouhal numbers 0.15, 0.20, 0.25, and 0.30 (cf. figure 16). The curve pertaining to  $St = 0.30$  has already appeared in figure 13, which shows how the data points were generally spaced. The effect of forcing at  $St = 0.15$  is very slight, and the axial intensity profile nearly coincides with the unforced case in figure 8. As  $St$  rises from 0.15 to 0.30, the ramp-like part of the intensity profile bulges upward in the interval  $x/D = 0$  to 5. When  $St = 0.30$ , the amplitude of the forced wave attains a sharp maximum around  $x/D = 4$  and then decays downstream into the secondary maximum due to natural turbulence.

Figure 20 shows the primary peak collapsing as the Strouhal number advances through the values 0.35, 0.40, 0.45, and 0.50 (cf. figure 17). At small distances  $x/D$ , the spatial growth rate  $d(u/U_e)/d(x/D)$  increases monotonically with Strou-

cut at higher  $u_e/U_e$ , say  $u_e/U_e = 1\%$ , to find a mode of maximum amplitude. Note that the Strouhal number of the mode preferred along a horizontal cut decreases somewhat with increasing  $u_e/U_e$ . At a forcing amplitude  $u_e/U_e = 0.5\%$ , the response attains a maximum at  $St = 0.37$ . When  $u_e/U_e = 1\%$ , the maximum occurs at  $St = 0.34$ , and the maximum occurs at  $St = 0.30$  exactly, when  $u_e/U_e = 2\%$ . Thereafter the variation of preferred  $St$  with increasing  $u_e/U_e$  is slow. The assertion that 0.30 is the preferred Strouhal number must be qualified slightly, because it involves the tacit assumption that the forcing amplitude  $u_e/U_e$  is 2% or more. The precise Strouhal-number preference for any given level of forcing can be deduced from figure 18.

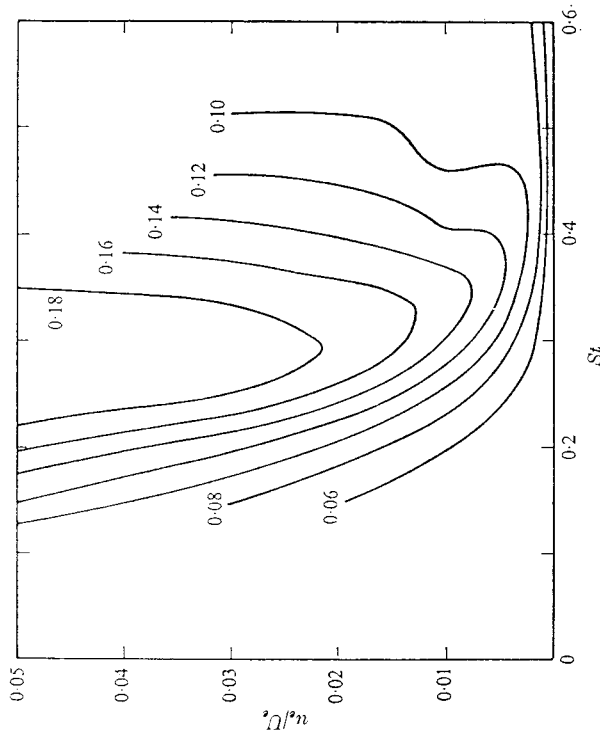


FIGURE 18. Contour map of the total response four diameters downstream on the centerline, as a function of Strouhal number and amplitude of forcing. The contours are labelled with  $u/U_e$ , which rises by 0.02 from one curve to the next. The abscissa is the contour  $u/U_e = 0.04$  approximately, the turbulence intensity in the absence of forcing.

Imagine a round jet in a turbulent state having *no* orderly structure of the kind under study. The turbulence excites waves on the jet column just as our exit-plane surging does, except that the turbulent forcing is not confined to one frequency. The turbulence hunts over the  $(St, u_e/U_e)$  plane, so to speak, triggering wave-trains at random. Those triggered at a Strouhal number of 0.30 reach an especially high amplitude, sporadically overthrowing the chaos assumed as the initial state of turbulence. The structure of big eddies can be expected to pull in around the mode at  $St = 0.30$ , which attains the highest possible amplitude under non-linear saturation.

had number throughout the range 0.15 to 0.50, as one would expect from linear stability theory. The peak response  $u/U_e$  is realized on the  $St = 0.30$  profile, near  $x/D = 4$ . The location  $x/D = 4$  was therefore the correct choice for defining the Strouhal-number preference in §5, because the mode of maximum response at  $x/D = 4$  is also the mode of maximum response over all values of the parameters  $St$  and  $x/D$ .

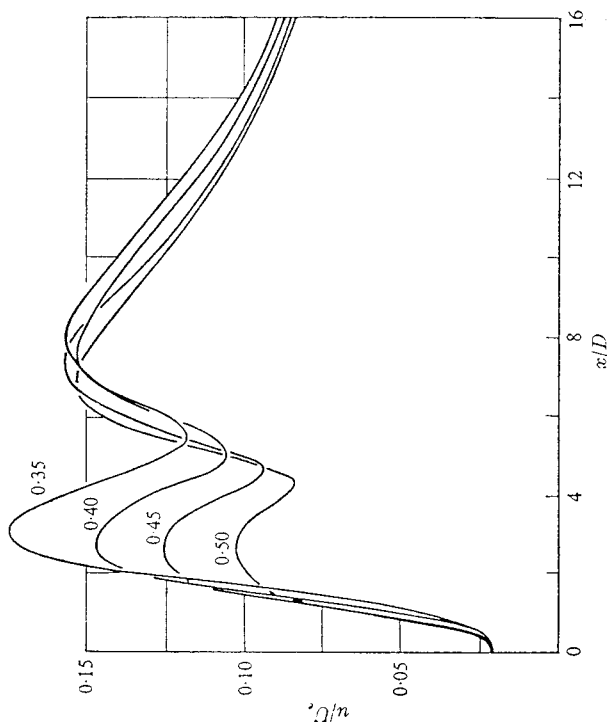


FIGURE 20. Centreline profiles continued through the Strouhal-number interval 0.35 to 0.50.

By analogy with §5, the curves in figures 19 and 20 can be regarded as cuts through a response surface above the  $(St, x/D)$  plane. A contour map of the surface is presented in figure 21, which is analogous to figure 18. The contours are again levels of constant response  $u/U_e$ , and the abscissa is still the Strouhal number  $St$ . The ordinate this time is  $x/D$ , the forcing amplitude  $u_e/U_e$  being fixed at 2%. The peak within the perimeter  $u_e/U_e = 16\%$  defines the Strouhal number of the mode preferred under 2% forcing and the location at which it attains maximum amplitude. Note that a clear Strouhal-number preference cannot be discerned by looking along a horizontal cut at small  $x/D$ . All waves are linear sufficiently close to the nozzle even when driven by a 2% surging, and the higher the Strouhal number in the linear régime, the greater the rate of spatial amplification.

Axial profiles at  $St = 0.60$  were also measured and deserve special comment. Figure 22 is a plot of the root-mean-square centreline response  $u/U_e$  measured under the conditions  $u_e/U_e = 2\%$  and  $St = 0.60$ , twice the Strouhal number of the preferred mode. The curve without data points is the intensity profile for the unforced case, taken from figure 8. The response profile at  $St = 0.60$  has two curious attributes: an abrupt change of slope at  $x/D = 4$ , and a shift of the

background-turbulence profile a full three diameters upstream toward the nozzle. The corresponding profile of mean centreline speed  $U/U_e$  is plotted in figure 23, which confirms the powerful effect of forcing at  $St = 0.60$ . The potential core has shortened by two diameters, and the asymptotic decay profile has drawn inward three diameters. The mean-speed profile may be compared with figure 15, which

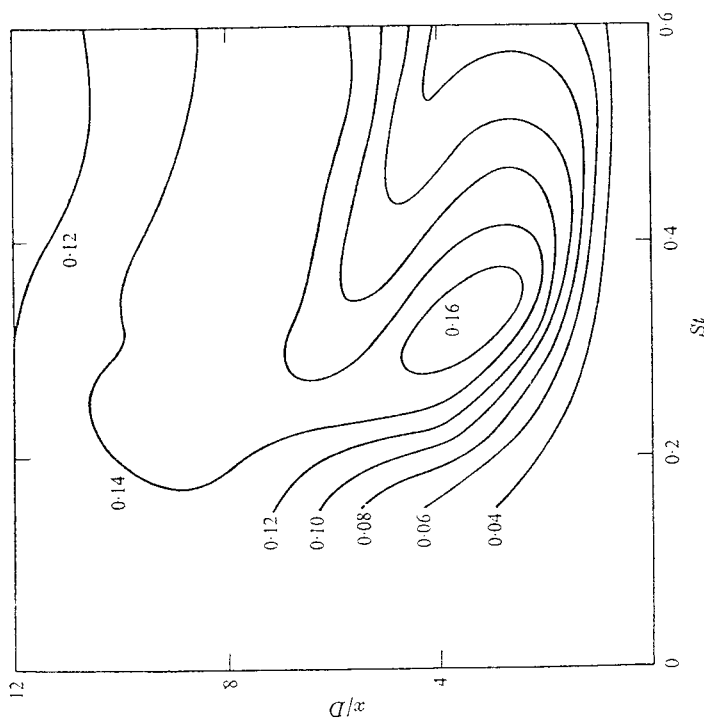


FIGURE 21. Contours of centreline turbulence intensity as a function of Strouhal number of forcing and distance downstream. The forcing amplitude is fixed at 2%. The contours are labelled with  $u/U_e$ , which changes by 0.02 from one curve to the next.

shows the more moderate changes produced by driving the preferred mode directly. The virtual origin of the decay profile shifts only two diameters upstream as explained in §4.

Judged solely on the basis of figures 22 and 23, the consequences of driving the jet at a Strouhal number of 0.60 seem paradoxical: the mode saturates at a relatively modest amplitude, say  $u/U_e = 7.5\%$ , yet deforms the jet more powerfully than the preferred mode having more than twice the saturation amplitude. The resolution of the paradox was apparent from oscilloscope traces of the hot-wire signal: the  $St = 0.60$  mode survives only up to  $x/D = 4$ , at which point a violent  $St = 0.30$  subharmonic arises, presumably by the process of engulfment seen in figure 6(a). The changes in the jet are not wrought by the  $St = 0.60$  mode directly, but instead by its subharmonic at the preferred Strouhal number



of 0.30. The  $St = 0.60$  fundamental merely serves as an amplifier between the 2% surging in the exit plane and the 7.5% surging downstream at the point of subharmonic formation.

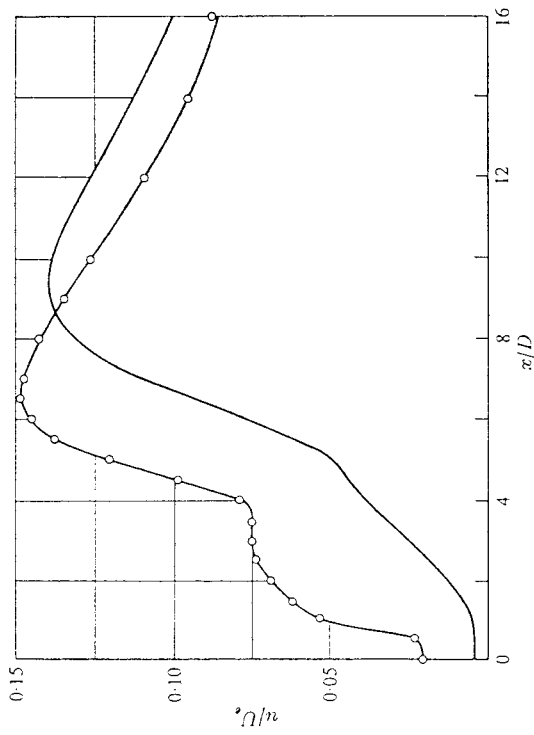


FIGURE 22. Centreline profile of turbulence intensity under 2% forcing at a Strouhal number of 0.60. The curve without data points represents the unforced case and is taken from figure 8.

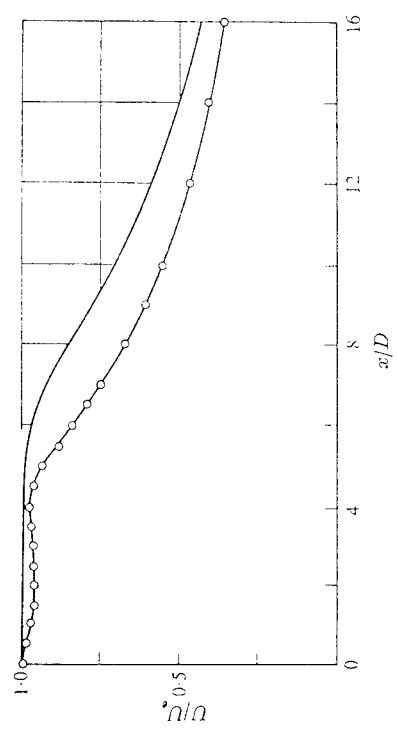


FIGURE 23. Mean-speed decay along the centreline under 2% forcing at a Strouhal number of 0.60. The curve without data points is the unforced profile taken from figure 7.

7. Summary description of the modes

In the two previous sections we studied the response  $u/U_e$ , first by setting  $x/D = 4$  and allowing  $u_e/U_e$  and  $St$  to vary, and then by setting  $u_e/U_e = 2\%$  and allowing  $x/D$  and  $St$  to vary. Here we bring the response study to its logical

completion by setting  $St = 0.30$  and varying  $u_e/U_e$  and  $x/D$ . The reason for doing so is that the other procedures have left open questions about the eventual decay of orderly structure. Why do the intensities in figures 19 and 20 decay beyond the primary peaks? What effect does the damping have on the choice of a preferred mode? The nature of the problem can best be judged from figure 14, which shows the evolution of fundamental and harmonic amplitudes under the forcing conditions  $St = 0.30$ ,  $u_e/U_e = 2\%$ . The growth of the fundamental is caused by linear instability, and the peak amplitude is determined mainly by non-linear saturation. The nature of the decay from  $x/D = 4$  to 8 remains to be studied, together with its effect on the precise location and amplitude of the peak.

Figure 14 conveys the impression that the fundamental  $u_{0.30}/U_e$  would peak at some  $x/D$  and thereafter decay, even if the mode were forced so slightly that non-linear saturation never took hold. At least two linear decay mechanisms are available. One possibility is that fine-scale background turbulence acts as an eddy viscosity and grinds the wave down. A second and less conjectural possibility is that the wave, as it propagates downstream, encounters mean velocity profiles which are progressively more stable with respect to axisymmetric disturbances. All axisymmetric modes amplify on a top-hat velocity profile, but all decay on a bell-shaped profile of the kind a turbulent jet assumes downstream of the potential core (Batchelor & Gill 1962). An axisymmetric mode could be expected to grow around the potential core, then lose its grip on the mean field in the transition region and die away. A similar mechanism terminates the growth of waves on a spreading two-dimensional laminar wake (Ko, Kubota & Lees 1970).

Figure 24 shows centreline profiles of the fundamental  $u_{0.30}/U_e$  driven at a Strouhal number of 0.30. The lowest curve represents the case  $u_e/U_e = 0$  and is included to show the root-mean-square background fluctuations admitted through the finite filter window. The remaining profiles are associated with the forcing amplitude  $u_e/U_e = 0.25\%$ ,  $0.5\%$ ,  $1\%$ ,  $2\%$ , and  $4\%$ , doubling from one value to the next. The profile for  $u_e/U_e = 2\%$  is based on the same data as figure 14. The profiles here are plotted in semi-logarithmic co-ordinates to distinguish linear and non-linear mechanisms. If the jet were a linear system, then the axial response profiles would have the same shape regardless of forcing amplitude, which would merely locate each profile along the logarithmic ordinate  $u/U_e$ . Indeed the axial intensity profiles for the two lowest forcing levels,  $u_e/U_e = 0.25\%$  and  $0.5\%$ , differ only by a constant vertical displacement out to the region  $x/D = 6$  or 7 where background turbulence takes over. Those profiles show how a forced wave behaves in the absence of non-linear saturation: the wave grows more-or-less exponentially with distance downstream, grows less rapidly near the tip of the potential core, reaches a peak proportional to forcing amplitude at  $x/D = 5.5$ , and thereafter decays under the action of a changing mean field or eddy damping. The total amplification  $u/U_e$  at  $x/D = 5.5$  is about 18.

At higher levels of forcing, the jet behaves as a linear system only within the first diameter or two of the exit. The peak of the  $u_e/U_e = 1\%$  profile is only 47% higher than the peak of the  $u_e/U_e = 0.5\%$  profile. The fractional increase of the peak intensity drops to 27% as  $u_e/U_e$  doubles from 1 to 2%, and to 14% under

the final doubling. The main effect of increasing the root-mean-square surging beyond 1% is to draw the point at which the wave saturates inward toward the nozzle. At a forcing amplitude of 0.25%, the fundamental amplitude  $u_{0.30}/U_e$  peaks at  $x/D = 5.5$ , which is therefore the point where the linear mechanisms of growth and decay just balance. At a forcing level of 1%, the peak occurs at  $x/D = 4.2$ , and it drops to  $x/D = 3.4$  when the forcing level reaches 4%. Notice how the curves associated with the two highest levels of forcing,  $u_e/U_e = 2$  and 4%, knit together into a common decay profile after saturating.

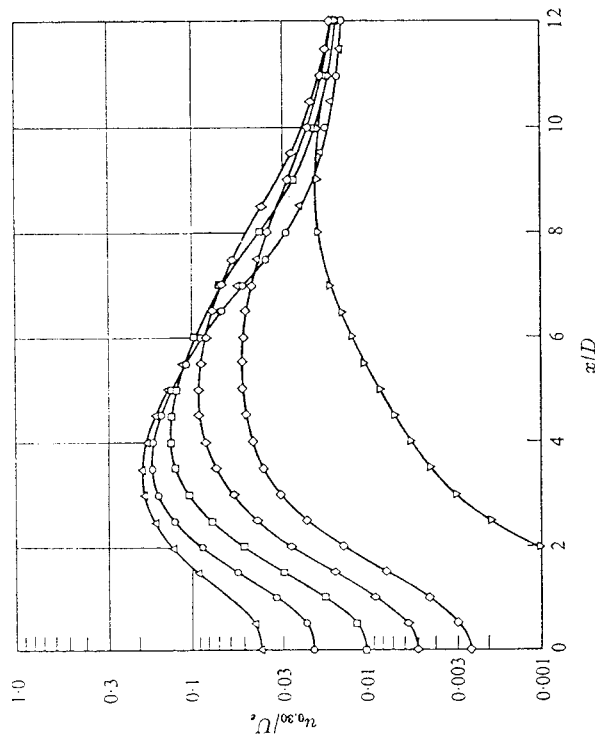


FIGURE 24. Centreline intensity profiles of the fundamental wave driven at a Strouhal number of 0.30. The data symbols denote the following forcing amplitudes  $u_e/U_e$ :  $\nabla$ , no forcing;  $\circ$ , 0.25% forcing;  $\diamond$ , 0.5% forcing;  $\square$ , 1% forcing;  $\triangle$ , 2% forcing;  $\nabla$ , 4% forcing. The ordinate  $u_{0.30}/U_e$  is logarithmic, so the forced profiles would have had the same shape had the jet been linear.

Figure 25 is a semi-logarithmic plot of the harmonic  $u_{0.60}/U_e$  under the six forcing conditions of figure 24; the lowest curve is the filter-window background, and the other five are harmonic profiles under forcing amplitudes  $u_e/U_e$  that double sequentially from 0.25 to 4%. Again the data for  $u_e/U_e = 2\%$  are taken from figure 14. The harmonic profiles have the character one would expect from the associated fundamentals. Forcing at  $u_e/U_e = 0.5\%$  or below evokes only a slight harmonic response, which is why the fundamental is free of non-linear saturation in that range. As the forcing level increases beyond 1%, a stronger and stronger harmonic arises to inhibit the growth of the fundamental. Raising the forcing amplitude from 2 to 4% brings the harmonic forth at a smaller  $x/D$  but does not greatly enhance its amplitude.

Figures 24 and 25 pertain to the  $St = 0.30$  mode, but the qualitative understanding we have drawn from them is general: a forced axisymmetric wave

amplifies owing to the linear instability of a top-hat jet column, saturates under the non-linear action of a harmonic, and finally decays owing to an essentially linear process, either mean-field changes or eddy damping.

Having reached an understanding from the hot-wire data, we returned to flow-visualization experiments for confirmation. The changes made since the photographs of §2 were taken should be recalled: figures 4 and 6 show a 1 in.

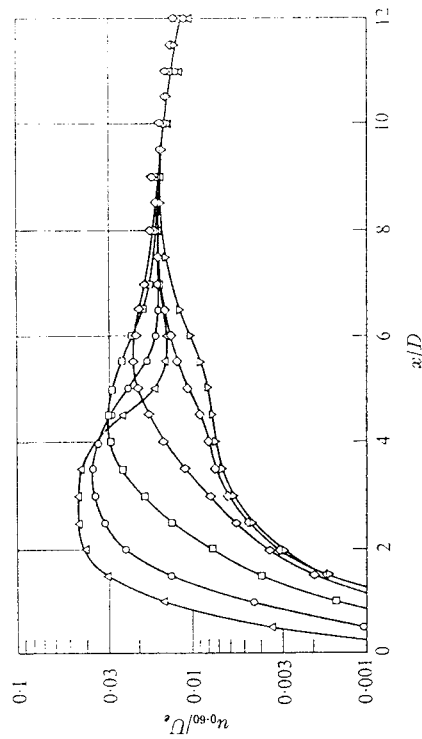


FIGURE 25. Centreline profiles of the harmonics associated with the fundamentals of figure 24. The Strouhal number of forcing is 0.60, and the data symbols denote the same forcing amplitudes as in the previous figure. The ordinate  $u_{0.60}/U_e$  is again logarithmic.

jet with a laminar boundary layer and without artificial surging, whereas the forced jet has a diameter of 2 in. and a fully turbulent boundary layer. Because the volume flow quadrupled in the transition from a 1 in. to a 2 in. jet, we could not retain fog as a means of visualization. Boundary-layer turbulence and higher Reynolds numbers put the schlieren method to even greater disadvantage than before, but schlieren photography was the only option. Happily the effects of forcing are spectacular enough to show through fine boundary-layer turbulence.

Three of the schlieren photographs are presented in figure 26 (plate 7). They were taken much the same way as those of figure 4, except that Type 52 Polaroid film of moderate contrast was used to suppress irrelevant detail. Photography under forced conditions required special care, because the introduction of  $\text{CO}_2$  causes the resonance frequencies of the plenum to shift slightly. If the loudspeaker were tuned in the absence of  $\text{CO}_2$ , then  $u_e/U_e$  would fall off the resonance peak when  $\text{CO}_2$  was introduced. The problem was easily circumvented by tuning the system while maintaining a flow of  $\text{CO}_2$  appropriate for photography. The 185 Hz resonance of table 3, for example, shifted to 181.4 Hz, which was used as the frequency for driving the  $St = 0.30$  mode. The shaft entering from the right in figures 26(b) and (c) is the hot-wire probe, located at  $x/D = 4$  and left in the flow to monitor the tuning.

Figure 26(a) shows the 2 in.  $\text{CO}_2$ -seeded jet without forcing. The usual hints of orderly structure appear, with the usual ambiguity (cf. figure 1). Figures 26(a) and (b) were taken at the same Reynolds number,  $Re = 1.06 \times 10^5$ , but the

flow seen in 26(b) was forced under the conditions  $St = 0.30$ ,  $u_e/U_e = 2\%$ . Figure 26(c) was taken under the forcing conditions  $St = 0.60$ ,  $u_e/U_e = 2\%$ . Figures 26(b) and (c) illustrate the kinematics of forced waves in a striking manner. The  $St = 0.60$  mode grows quickly near the nozzle but saturates 1–2 diameters downstream, in accord with the measured intensity profile of figure 22. A train of three saturated waves propagates toward  $x/D = 4$  and there suffers a violent transformation, leading to the enormous spreading angle evident in figure 26(c). The  $St = 0.60$  mode contorts the surface of the jet column into steep waves but cannot penetrate deep enough to disintegrate the column as a whole. The  $St = 0.30$  mode shown in figure 26(b) grows more gradually downstream of the nozzle but eventually causes contortions as steep as those of the  $St = 0.60$  mode. Because of its greater wavelength, the  $St = 0.30$  mode penetrates deep into the jet column and causes its virtual disintegration.

### 8. Influence of forcing on entrainment and background turbulence

We have concentrated so far on the structure of the forced waves themselves, and now we turn to their effect on the mean flow and on background turbulence. The work presented in this section concerns the  $St = 0.30$  mode alone. It would have been interesting to carry the study of the  $St = 0.60$  mode beyond the centreline profiles of figures 22 and 23, but time fell short.

Figures 27 and 28 display the results of radial hot-wire traverses at five stations along the jet, namely  $x/D = 0.025$ , 2, 4, 6, and 8. Part (a) of each figure shows radial profiles in the absence of forcing, and part (b) the corresponding profiles under the forcing conditions  $u_e/U_e = 2\%$ ,  $St = 0.30$ . Figure 27 shows  $U(x, r)/U_e$ , the axial component of mean velocity, and figure 28 shows  $u(x, r)/U_e$ , the root-mean-square axial component of turbulent velocity. The ordinate in each case is  $r/R$ ,  $R$  being the 1 in. radius of the jet. The profiles are staggered along the abscissas to suggest the spatial structure of the jet and global effects of forcing. Note that the axial spacing is compressed by a factor of four relative to the radial.

According to figure 27, forcing makes no dramatic change in the mean field. The mean profile spreads somewhat faster under forcing, so entrainment is enhanced, but the consequences of forcing appear much more clearly in the radial intensity profiles of figure 28. Forcing is seen to inflate the turbulence level out to  $x/D = 6$ , especially on the outskirts of the jet and inside the potential core, which can be taken as the cone generated by a straight line running from  $x/D = 0$ ,  $r/R = 1$  down to  $x/D = 6$ ,  $r/R = 0$ . The turbulence level in the mixing layer around  $r/R = 1$  is not so strongly affected.

The most interesting property of the mean flow is its volume flux, whose derivative with respect to axial location is entrainment. The volume flux  $Q(x)$  is defined by an area integral over the axial component of mean velocity:

$$Q(x) = \int_0^\infty U_i(x, r) 2\pi r dr.$$

The subscript  $i$  directs attention to the fact that volume flux makes sense only when one has in mind inner and outer solutions of a comprehensive velocity field.

The notions of volume flux and entrainment are creatures of theory, in the case of a jet, rather than experiment. In order to appreciate that important but subtle point, suppose that an expression is known for the mean axial flow  $U_i(x, r)$  within the turbulent region of a jet. Then the volume flux  $Q$  can be calculated at each station  $x$ , provided the radial integration of  $rU_i$  converges. The local entrain-

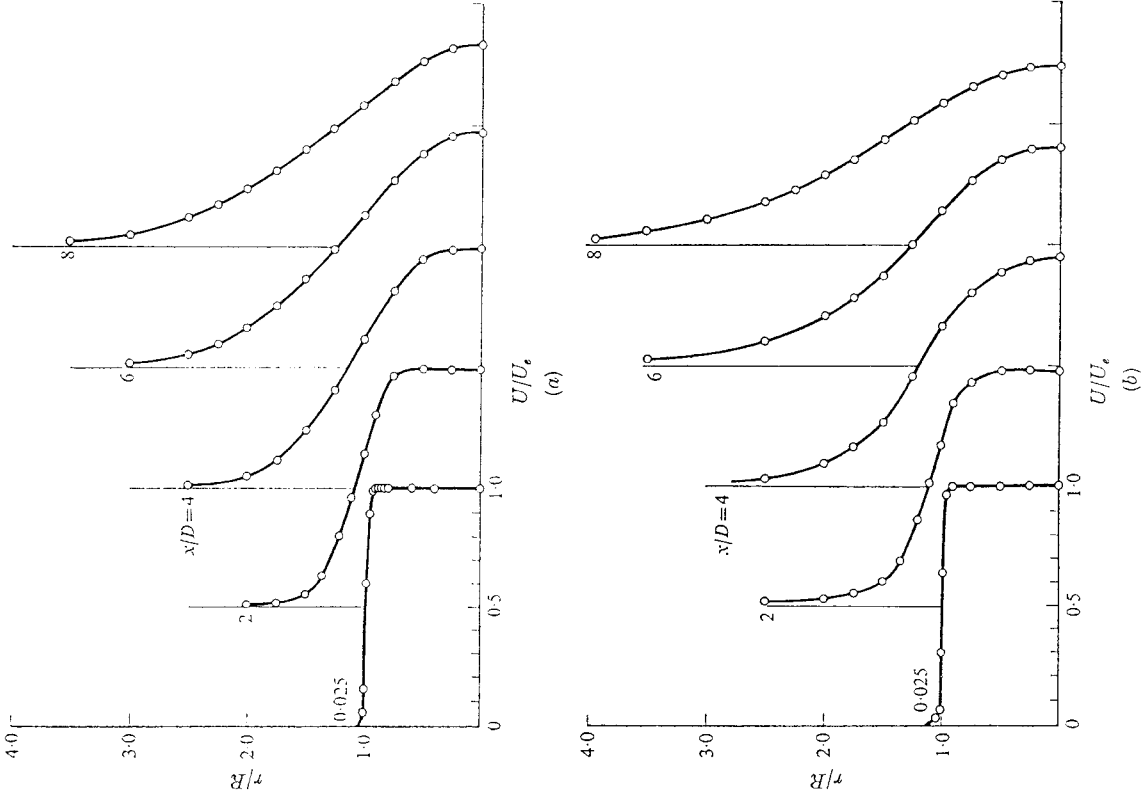


FIGURE 27. Radial mean-speed profiles at five stations along the jet axis: (a) without forcing, and (b) with 2% forcing at a Strouhal number of 0.30. The stations  $x/D$  are specified near the ordinates of the profiles, which are arranged to suggest the spatial structure of the jet.

ment is  $dQ/dx$ , which means that the jet induces an external potential flow as though it were a line sink of strength  $dQ/dx$ . One can show on the basis of similarity arguments that  $dQ/dx$  must approach a constant value  $kQ_e/D$  far downstream, where  $Q_e$  is the volume flux out the exit and  $k$  is a dimensionless constant (cf. Wygnanski 1964). As a result, the axial component of induced potential flow, say  $U_0(x, r)$ , approaches  $kQ_e/4\pi Dr$  at great distances  $r$  from the jet axis. The

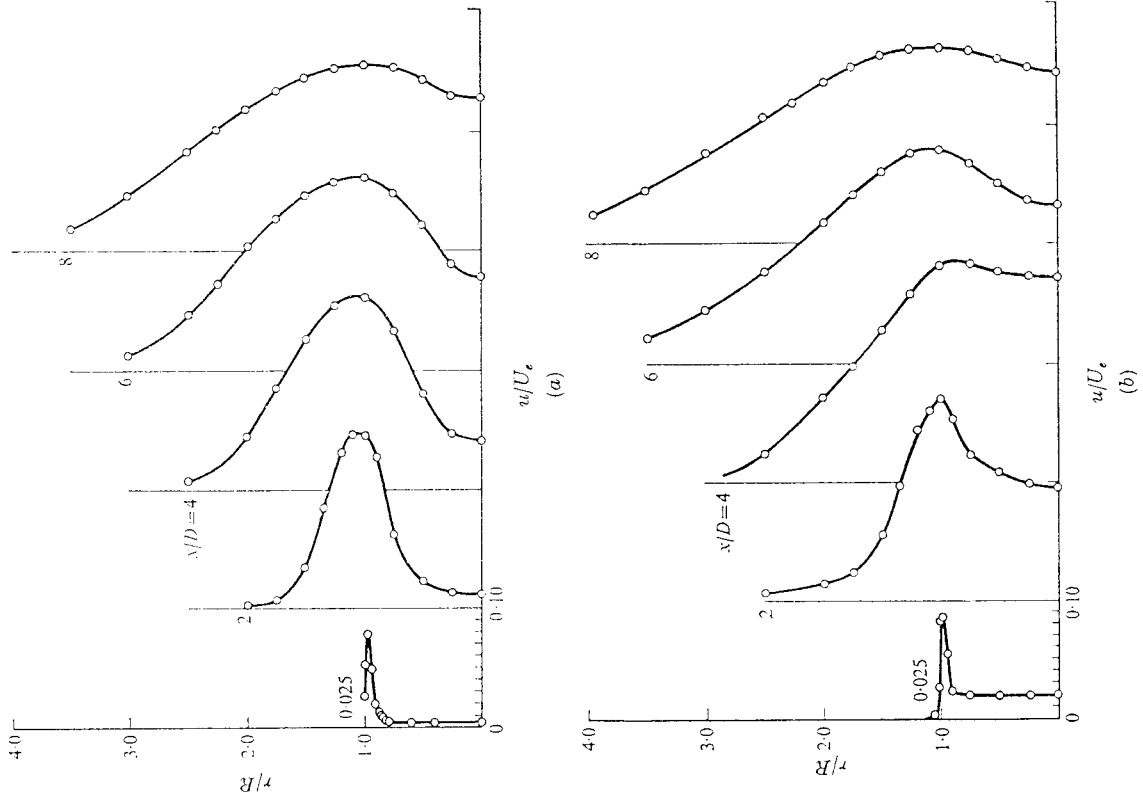


FIGURE 28. Radial intensity profiles of the axial component of turbulent velocity: (a) unforced, and (b) forced at a level of 2% and a Strouhal number of 0.30.

quantity  $rU_0$  does not fall to zero as  $r$  approaches infinity, and the *volume flux in the induced potential flow is infinite*. The flux  $Q$  therefore cannot be defined in terms of the net flow  $U = U_i + U_0$ , but only in terms of the inner rotational part  $U_i$ .

The quantity measured experimentally is  $U$ , so a somewhat arbitrary judgment must be made to isolate  $U_i$ . The judgment was not very difficult in practice. We replotted the data of figure 27 and others downstream in the form of dimensionless flux profiles  $(r/R) U(x, r)/U_e$ . The potential tails of the flux profiles were obvious, and we simply faired the curves to zero before performing

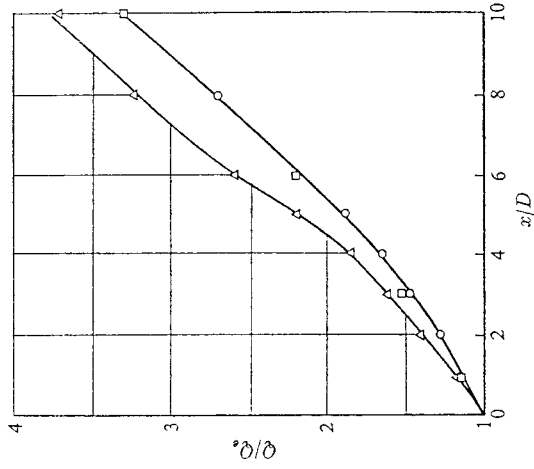


FIGURE 29. Axial profiles of volume flux, normalized on the flux out the jet exit. The round data symbols denote the unforced case, and the square symbols represent comparable data from Sami *et al.* (1967). The triangular symbols denote the case of 2% forcing at a Strouhal number of 0.30.

planimeter integrations. Hopefully the faired profiles were good representations of  $(r/R) U_i(x, r)/U_e$ , which could perhaps be measured objectively by conditioning the velocity mean on the presence of turbulence.

The resulting normalized flux profiles  $Q/Q_e$  are presented in figure 29. The circular data points represent the unforced jet, and the triangular points represent the jet under the forcing conditions  $u_e/U_e = 2\%$ ,  $St = 0.30$ . The square points were obtained by integrating the velocity profiles published by Sami, Carnody & Rouse (1967), the same standard being used for fairing the outer part of their curves as for ours. The agreement between their data and our own for the unforced jet is impressive, especially since their Reynolds number was  $2.2 \times 10^5$ .

In the absence of forcing, the volume-flux profile is seen to be linear for  $x/D$  both large and small, with slopes

$$\frac{dQ}{dx} = \begin{cases} 0.136Q_e/D & (x/D \lesssim 2), \\ 0.292Q_e/D & (x/D \gtrsim 6), \end{cases}$$

measured from figure 29. The entrainment  $dQ/dx$  is therefore constant both near

to and far from the jet exit, in accord with similarity arguments (Wyganski 1964). Wyganski cited figures implying that  $dQ/dx = 0.128 Q_e/D$  in the mixing-layer region near the jet and  $0.456 Q_e/D$  far downstream. The latter value is much higher than we measure and is found to result from an assumed functional form of  $U(x, r)$  inappropriate for calculating volume flux. To make sure of the downstream limit, we calculated the volume flux of the asymptotic jet profile measured by Wyganski & Fiedler (1969), with the result that  $dQ/dx = 0.263 Q_e/D$ . The constant is only 10% short of the value 0.292 measured from figure 29 and is probably more reliable, because Wyganski & Fiedler took pains to mitigate room drafts. The entrainment rates  $dQ/dx = 0.13 Q_e/D$  near the exit and  $0.27 Q_e/D$  far downstream should both be accurate to within  $\pm 0.01 Q_e/D$ .

Forcing under the conditions  $u_e/U_e = 2\%$ ,  $St = 0.30$  is seen from figure 29 to enhance entrainment in the interval  $x/D = 0$  to 6 and particularly in the last two diameters of that interval, beyond the point  $x/D = 4$  where the vortex puffs attain their maximum intensity. Further downstream the volume-flux profile attains the same slope as the unforced case, the virtual origin having been drawn upstream about two diameters. The shift of virtual origin has been discussed in connexion with figure 15 and can now be understood as the result of enhanced entrainment in the interval  $x/D = 4$  to 6.

We now take up the second topic of this section, the influence of forcing on background turbulence, which means any fluctuations not bound into the driven fundamental or its harmonics. Periodic forcing might reasonably be expected to suppress the larger scales of background turbulence, because big eddies would tend to become locked into the forcing frequency. The simplest statistical quantity bearing on that conjecture is  $F(f)$ , the spectrum of axial velocity fluctuations at a fixed point  $(x, r)$ . In the unlikely event that forcing bound up *all* background turbulence, then  $F(f)$  would comprise a sequence of spikes at the forcing frequency and its harmonics. If forcing had *no* effect on the background, then  $F(f)$  would consist of spikes superposed on a broad-band component identical to the spectrum that exists in the absence of forcing. The measured spectrum should lie between the extremes.

An on-line computer determined the spectra by means of fast Fourier transformation (Pao, Hansen & MacGregor 1969). The program uses the raw linearized hot-wire signal for computing the mean and a high-pass filtered version for computing fluctuation quantities; filtering trims off the direct current to improve resolution. The window of the Krohn-Hite Model 330 band-pass filter lay between 0.2 Hz and a high frequency selected to control aliasing. Both the raw and filtered signals were sent through Dynamics Model 7514 amplifiers and shielded coaxial cables to an IBM Model 1827 analogue-to-digital converter and Model 360-44 computer, the transmission system being free of distortion up to  $2 \times 10^4$  Hz. The continuous signals were converted to  $1.8 \times 10^6$  samples per second with a resolution of 14 bits plus a sign bit, and the samples were processed in lots of 8192 dictated by the computer memory capacity. Three hundred lots were typically processed to ensure convergence, which was monitored through intermediate print-outs. Since only the larger scales of turbulence were of interest, the spectra could be confined below  $9 \times 10^3$  Hz and in some cases below  $10^3$  Hz.

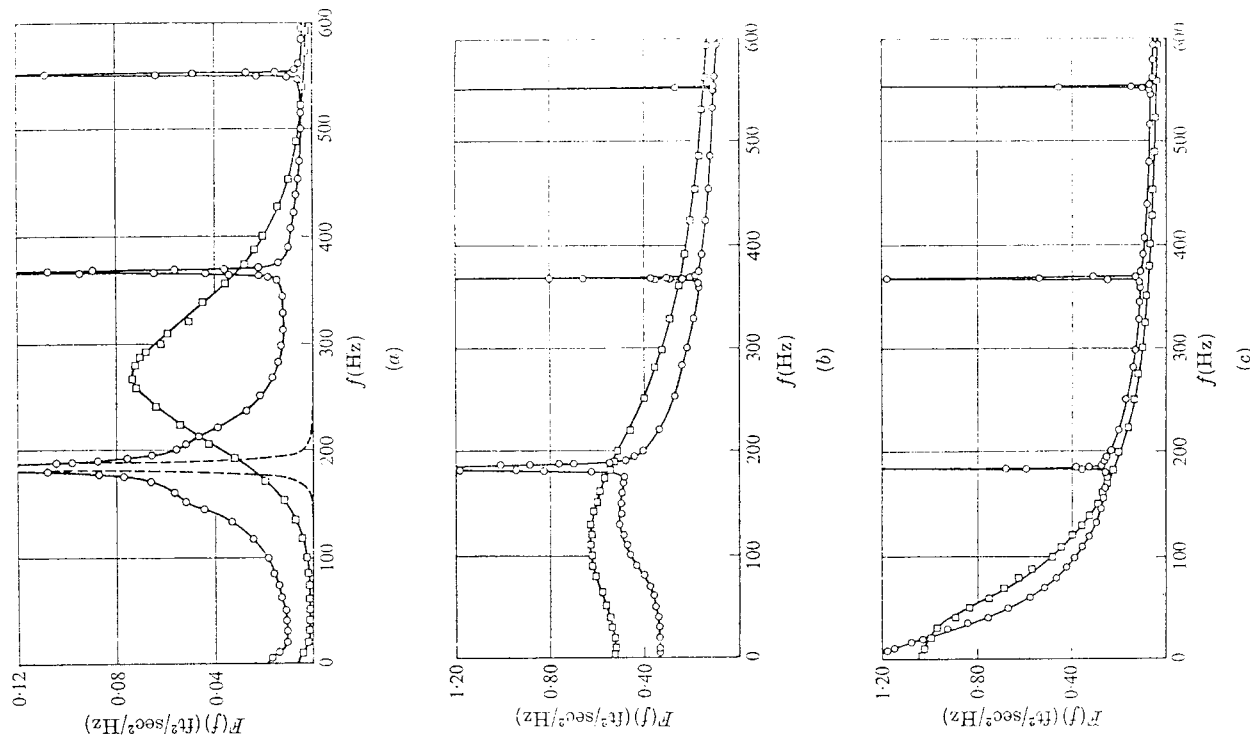


FIGURE 30. Turbulence spectra at  $x/D = 4$  and (a)  $r/R = 0$ , (b)  $r/R = 1.0$ , and (c)  $r/R = 1.5$ . The square data points denote the unforced case, and the round data points denote the case of 2% forcing at a Strouhal number of 0.30. The computer evaluated many more data than are shown. The dashed spike in part (a) represents a pure sine wave with the power of the fundamental.

In order to compare theory and experiment, we suppose that the instantaneous axial component  $u^*(x, t)$  of velocity on the centreline has the form

$$u^* = u_1^* e^{i\alpha x} \cos k(x - ct).$$

$k$  is the wave-number,  $a$  the spatial amplification rate, and  $c$  the phase velocity of the forced wave, all three parameters being real. The wavelength  $\lambda$  is defined as the distance between every other zero intercept of  $u^*$ , or as the distance between consecutive peaks. The two definitions give the same length  $\lambda$ , related to  $k$  by the formula  $k = 2\pi/\lambda$ . The phase velocity  $c$  equals  $f\lambda$ ,  $f$  being the known forcing frequency. The amplification rate  $a$  can be taken as proportional to the slope of the straight segment of a semi-logarithmic amplitude profile like those of figure 24. Admittedly the straight intervals are not extensive, and one could question whether exponential growth occurs anywhere. The profiles curve upward just downstream of the exit, probably because the uniform surging in the exit plane relaxes into the shape of a linear eigenmode. The profiles curve downward beyond  $x/D = 3$  as the jet ceases to resemble a uniform column. Within a restricted interval, however, the forced mode may behave like a linear wave on a doubly infinite jet column, and that is the issue which measurements of  $\lambda$  can clarify.

We carried out the measurements by positioning the hot wire on the centreline, noting the location of a wave peak on the screen of an oscilloscope triggered by the loudspeaker input, then translating the hot wire downstream without changing the phase of the trigger, until a new peak coincided with the location of the old. The net translation of the hot wire was the wavelength  $\lambda$ , which is tabulated below for Strouhal numbers  $St$  ranging from 0.15 to 0.80. The signal

$St$	0.15	0.20	0.25	0.30	0.35	0.40
$\lambda/D$	5.75	3.87	3.17	2.38	1.83	1.69
$St$	0.45	0.50	0.55	0.60	0.70	0.80
$\lambda/D$	1.44	1.23	1.13	1.06	0.91	0.81

TABLE 4. Wavelengths of the forced modes

displayed on the oscilloscope screen was unfiltered, since no filtering was needed for repeatable measurements. The forcing amplitude was chosen at each Strouhal number so that the wave was linear over most of the hot-wire displacement interval, which bracketed the station  $x/D = 4$  except in the cases of very long and very short waves. The measured wavelength was found to depend only weakly on the initial position of the hot wire.

The linear stability theory of waves on a uniform jet column was developed by Batchelor & Gill (1962) and extended to compressible flows by Lees & Gold (1966). For purposes of analysis, the wave is conveniently expressed in complex form,

$$u^* = u_1^* e^{i(\alpha x - \omega t)},$$

where  $\alpha$  is the complex wave-number  $\alpha_r + i\alpha_i$ , and  $\omega$  is the complex frequency  $\omega_r + i\omega_i$ . By solving for velocity potentials within and without the jet column

Spectral windows of 0.078 Hz and 0.24 Hz were used to resolve the forcing frequency and its first two harmonics, and the results were overlapped with broadband spectra obtained with a 2.18 Hz window. Each time a spectrum was measured, the root-mean-square fluctuation  $u$  was obtained both from the spectrum and by the usual analogue method. The result always agreed within  $\pm 2\%$ . Analogue checks of several spectral points fell within  $\pm 10\%$  of the digital values.

Six spectra are presented in figure 30. Each was measured at the axial station  $x/D = 4$ , and parts (a), (b), and (c) of the figure correspond to the radial locations  $r/R = 0, 1.0$ , and 1.5. The square data points represent the unforced jet, and the round data points show the spectral consequences of forcing under the conditions  $u_e/U_e = 2\%$ ,  $St = 0.30$ . The data points are spaced for visual convenience and represent only a fraction of the computer output. The dashed spike in figure 30(a) has the same power content as the turbulence fundamental but was generated by feeding a 185 Hz sine wave through the digital system. The artificial spike is included to show that the digital filter window is narrow compared with the width of the broad-band spectrum underneath.

Each forced spectrum has definite peaks at the forcing frequency 185 Hz and its first two harmonics. For the most part forcing does suppress background turbulence, the exception being at  $r/R = 1.5$  in the frequency interval 20–160 Hz, as shown in figure 30(c). Figure 30(b), obtained with the hot-wire probe at  $x/D = 4$ ,  $r/R = 1$  in the midst of the mixing layer, shows that the 185 Hz fundamental attracts both higher and lower frequency eddies, though the effect is not so pronounced as one might have wished. Suppression of the background is most evident in figure 30(a), whose ordinate is expanded by a factor of ten relative to the others. Figure 30(a) was obtained with the hot-wire probe at  $x/D = 4$ ,  $r/R = 0$ , just inside the tip of the potential core. Forcing is seen to diminish and gather up the naturally occurring bell-shaped spectrum, almost fixing the phase of the big eddies that leave their signature in the potential core.

With respect to aerodynamic sound production, the important question is whether forcing imposes order on the potential flow *outside* the mixing region, because a fluctuating exterior potential gives rise to sound. Unfortunately a hot-wire anemometer is useless outside the rotational core of the jet: the steady component of flow is too weak to sweep away the hot-wire wake, and the signal is meaningless. The appropriate measurement could be made outside a high-speed subsonic jet, where the strength of pressure fluctuations would permit the use of a microphone in the near field. We hope such an experiment will be taken up in the future.

## 9. Comparison with stability theory

The reader may have noticed the omission of one easily measured property of the forced waves, namely their lengths. Wavelength measurements have been deferred to this section so that they could be set into a theoretical framework. They have some surprising implications for the stability theory of waves on a jet column.

and matching displacements and pressures across its boundary, Batchelor & Gill derived the following eigenvalue equation for axisymmetric waves:

$$\left(\frac{U_e \alpha}{\omega} - 1\right)^2 = \frac{K_0(\alpha R) I_0(\alpha R)}{K_0'(\alpha R) I_0(\alpha R)}.$$

$U_e$  is the jet speed and  $R$  its radius, in line with the notation of this paper.  $I_0$  and  $K_0$  are modified Bessel's functions of the first and second kinds.

The real and imaginary parts of the eigenvalue equation constitute two relations among the four quantities  $\alpha_r$ ,  $\alpha_i$ ,  $\omega_r$ ,  $\omega_i$ . Before solving the eigenvalue equation, one usually assumes a restriction on the physical nature of the wave, the conventions being that it grows in time but is purely oscillatory in space,  $\alpha_i = 0$ , or that it grows in space but is purely oscillatory in time,  $\omega_i = 0$ . The first case, temporal instability, is easier to treat, because the arguments of the Bessel's functions are real and the eigenvalue equation can be solved directly for  $\omega_r(\alpha_r)$  and  $\omega_i(\alpha_r)$ . Batchelor & Gill have carried out that analysis. The second case, spatial instability, is complicated by the fact that the eigenvalue equation cannot be solved analytically for  $\omega_r(\alpha_r)$  and  $\alpha_i(\alpha_r)$ . It is necessary to solve for  $\omega$  over the complex plane  $\alpha$ , determine the locus  $\alpha_i(\alpha_r)$  along which  $\omega_i = 0$ , and finally evaluate  $\omega_r(\alpha_r)$  along that locus. We executed that program on an IBM 360-44 computer, in the belief that spatial instability would bear directly on the orderly structure of jet turbulence.

The quantities of physical interest are  $k$ ,  $c$ , and  $a$ , which have the forms

$$\left. \begin{aligned} k &= \alpha_r \\ c &= \omega_r/\alpha_r \\ a &= -\alpha_i \end{aligned} \right\} \quad (\text{spatial})$$

in the case of spatial instability. The temporal case would seem incompatible with experiment, because the hot-wire signal  $u^*(x, t)$  is indeed periodic in time but inhomogeneous in space. The definitions of  $k$  and  $c$  are the same, but the spatial growth rate  $a$  is foreign, strictly speaking, to the hypothesis of temporal instability. If temporal growth is assumed to occur locally in co-ordinates moving with the phase velocity, however, then the temporal growth rate  $\omega_i$  can be transformed into a spatial growth rate  $\omega_i/c = \alpha_r \omega_i/\omega_r$ . The result is a temporal-instability model of the forced modes, capable of being compared to experiment through the prescription

$$\left. \begin{aligned} k &= \alpha_r \\ c &= \omega_r/\alpha_r \\ a &= \alpha_r \omega_i/\omega_r \end{aligned} \right\} \quad (\text{temporal}).$$

Of course we believed that temporal instability would be irrelevant, but the belief proved wrong.

The eigenvalue equation cannot be solved in general without numerical work, but the asymptotic forms of Bessel's functions yield analytical solutions in the limits  $kR \rightarrow 0$  and  $kR \rightarrow \infty$ . The limits are worth studying, because they embody

the essential differences between spatial and temporal instability. Thus, in the limit of short waves as  $kR \rightarrow \infty$ ,

$$aR \rightarrow \begin{cases} kR - \frac{1}{2} & (\text{temporal}), \\ kR + O(kR)^{-1} & (\text{spatial}), \end{cases}$$

$$\text{and} \quad \frac{c}{U_e} \rightarrow \begin{cases} \frac{1}{2} + \frac{1}{4kR} & (\text{temporal}), \\ 1 + \frac{1}{4kR} & (\text{spatial}). \end{cases}$$

In the limit of long waves as  $kR \rightarrow 0$ ,

$$aR \rightarrow (kR)^2 \left( -\frac{1}{2} \log \frac{kR}{A} \right)^{\frac{1}{2}} \quad (\text{temporal or spatial}),$$

$$\text{and} \quad \frac{c}{U_e} \rightarrow \begin{cases} 1 + \frac{(kR)^2}{2} \log \frac{kR}{A} & (\text{temporal}), \\ 1 - \frac{(kR)^2}{4} \left( 3 \log \frac{kR}{A} + 1 \right) & (\text{spatial}), \end{cases}$$

where  $A = 1.1229$ , a constant involved in the asymptotic expansion of  $K_0$ . It is immediately apparent from the limits above that the spatial theory and its temporal analogue predict broadly similar values for the dimensionless growth rate  $aR$ , but that the dimensionless phase velocities  $c/U_e$  behave very differently. As  $kR$  increases from zero, the phase velocity  $c/U_e$  of a temporally growing instability decreases from unity and tends toward an asymptote  $c/U_e = \frac{1}{2}$ . The phase velocity of a spatially growing instability rises *above* unity and eventually settles back toward an asymptote  $c/U_e = 1$ . Short spatially growing waves propagate at the centreline speed  $U_e$ , while short temporally growing waves propagate at the average of the speeds inside and outside the jet column, which is  $\frac{1}{2} U_e$ .

The dimensionless amplification rate  $aR$  and phase velocity  $c/U_e$  are plotted against the dimensionless wave-number  $kR$  in figures 31 and 32. The solid curves are the dispersion relations for spatially growing waves. The dashed curves apply to the temporally growing analogue and are taken from the work of Batchelor & Gill (1962). The data points were obtained from table 4 through the relations  $k = 2\pi/\lambda$  and  $c = f\lambda$  explained earlier in this section.

The theoretical dispersion relations behave as anticipated from the asymptotic formulas. For both spatial and temporal instabilities, the amplification rate  $aR$  rises monotonically with wave-number  $kR$ . In accord with the discussion of §5, neither the spatial nor temporal theory singles a mode of maximum growth rate. Figure 31 shows an unexpected consequence of spatial theory, namely a band of highly unstable but very long waves ( $\lambda > 14D$ ) lying above the main sequence in the  $(kR, aR)$  diagram. Those waves correspond to a gross surging of the jet column but are probably too long to have meaning in any physical context. Figure 32 shows that the dimensionless phase velocity  $c/U_e$  of temporally growing waves decreases monotonically from 1 to  $\frac{1}{2}$  as  $kR$  increases from 0 to  $\infty$ . The phase

velocity of spatially growing waves, by contrast, always satisfies the inequality  $c/U_e \geq 1$  and reaches a maximum of 1.31 at  $kR = 1.15$ .

The surprising aspect of figures 31 and 32 is the relation of the experimental data to the theories. The black point in each figure denotes the preferred mode,  $St = 0.30$ , and is based, in the case of figure 31, upon the maximum slope of the lowest filtered profile in figure 24. No other accurate amplification rates are available. The amplification rate predicted by temporal instability theory is 47% high, and the prediction of spatial theory is much higher. Neither theory predicts the amplification rate at  $St = 0.30$  correctly, but the data plotted in figure 32 do coincide with one of the theoretical dispersion relations  $c(kR)/U_e$ , the one corresponding to temporal instability. The agreement is excellent up to  $kR = 2.5$ , beyond which the measured phase velocities lie somewhat above the theoretical. The dispersion relation  $c(kR)/U_e$  for spatially growing waves is wholly inconsistent with the data. Plausible as it seems *a priori*, an exponential spatial instability must be ruled out as the mechanism of vortex puffs.

We are faced with a curious anomaly. The temporal instability theory of Batchelor & Gill should be irrelevant to the experimental situation but appears, in an important sense, to be right. Our own spatial instability theory, tailored especially for the experiments, seems to be wrong. The issue is important, because spatial instability theory has lately come to be regarded as logically superior to temporal theory. Usually the two are compared for slowly growing waves, in which case their predictions are similar. Here the waves grow rapidly, the dispersion relations are distinct, and the data point unambiguously to the temporal instability theory.

The failure of spatial instability theory may be connected with the boundary conditions at downstream infinity. The waves are supposed to diverge exponentially to infinity, but in practice non-linearity inhibits the divergence. However small the perturbation at  $x/D = 0$ , the departure of spatial instability theory from a practical flow becomes exponentially large toward downstream infinity. The departure may induce large distortions over the whole field, *even where the original wave is weak enough to be linear*. Because the problem is elliptic, an exponential divergence downstream is inconsistent with linearity everywhere. A temporally unstable wave at least has the merit of being rigorously linear for small times. Apparently it is more advantageous to preserve reasonable boundary conditions than to simulate spatial growth by means of an exponential divergence.

## 10. Concluding remarks

An incompressible turbulent jet can sustain orderly modes of axisymmetric flow, including a preferred mode of frequency  $f = 0.30 U_e/D$ , wavelength  $\lambda = 2.38 D$ , phase velocity  $c = 0.71 U_e$ , and maximum rate of spatial amplification  $a = 0.58/R$ .

The modes obey the dispersion relation  $c(k)$  derived by Batchelor & Gill (1962), but nothing in linear stability theory seems to distinguish the mode at  $k = 1.32/R$ , which attains the highest possible amplitude under non-linear saturation. Indeed the preference is lost at sufficiently low amplitudes of forcing,

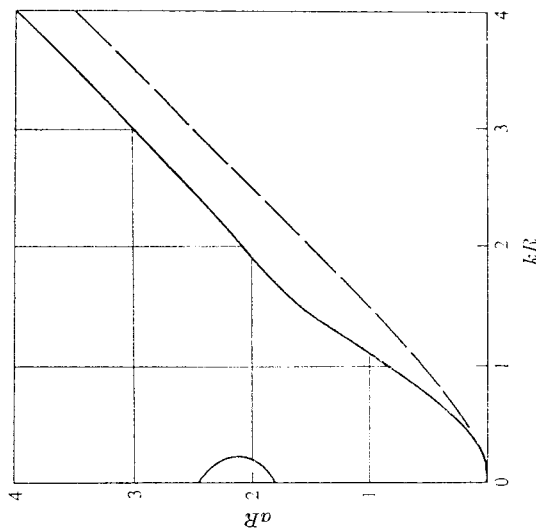


FIGURE 31. Spatial amplification rate as a function of wave-number. The solid curves result from the theory of spatially growing waves, and the dashed curve results from a transformation of temporal theory. The experimental datum is the maximum amplification rate of the preferred fundamental, as determined from figure 24.

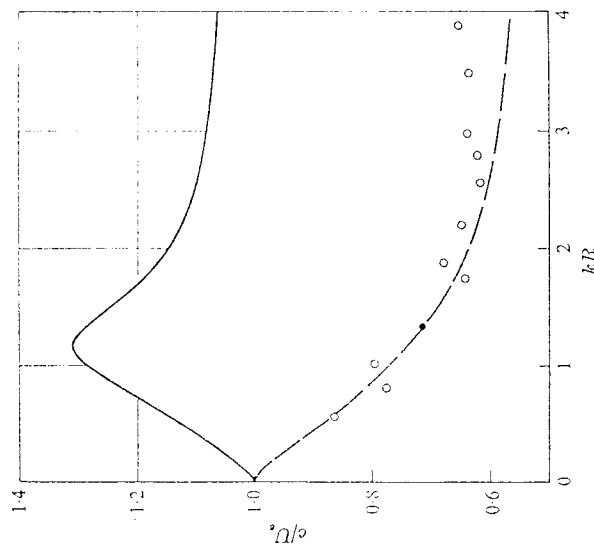


FIGURE 32. Phase velocity as a function of wave-number. The solid curve represents spatial theory and the dashed curve temporal. The data are computed from table 4.



according to the contour maps of figures 18 and 21. The preference arises outside the scope of linear theory, yet linear theory should not be irrelevant. The hot-wire signal of figure 11 is nearly sinusoidal even at the highest forcing amplitude, and the harmonic plotted in figure 12 saturates at only one-fifth the amplitude of the fundamental.

Batchelor & Gill's eigenvalue equation contains a hint of the connexion between linear stability theory and the non-linear selection mechanism. The real limits presented in §9 were taken from the following complex limits of the eigenvalue equation:

$$\left(\frac{U_c \alpha}{\omega} - 1\right)^2 \rightarrow \begin{cases} -1 + (\alpha R)^{-1} & \text{as } |\alpha R| \rightarrow \infty, \\ \frac{(\alpha R)^2}{2} \log \frac{\alpha R}{A} & \text{as } |\alpha R| \rightarrow 0. \end{cases}$$

Whatever assumption is made about spatial or temporal growth, it is clear that  $\omega/\alpha$  approaches a complex constant in either limit  $|\alpha R| \rightarrow \infty$  or  $|\alpha R| \rightarrow 0$ , which means that eigenmodes of very long or very short wavelengths tend to be non-dispersive. Modes having wavelengths comparable to the jet diameter are highly dispersive.

To appreciate the dynamical role of dispersion, consider a growing eigenmode  $u_1^* \exp i(\alpha x - \omega t)$ . The jet column is non-linear, so the fundamental eigenmode drives a first harmonic of the form  $u_2^* \exp i(2\alpha x - 2\omega t)$ . If the fundamental is highly dispersive, then the harmonic is not an eigenmode, and  $u_2^*$  is a constant and relatively small fraction of  $u_1^*$ . The ratio  $u_2^*/u_1^*$  involves a resonance denominator, however, which falls to zero when  $2\alpha$  and  $2\omega$  themselves satisfy the eigenvalue equation.  $\alpha$ ,  $\omega$  and  $2\alpha$ ,  $2\omega$  can be simultaneous solutions of the eigenvalue equation only in régimes of  $\alpha R$  where the ratio  $\omega/\alpha$  is constant, two such régimes being the limits  $|\alpha| \rightarrow \infty$  and  $|\alpha R| \rightarrow 0$ . Waves of extreme lengths are non-dispersive, resonate with their harmonics, and drive them to large amplitudes. Waves of intermediate lengths produce harmonics that are far from being eigenmodes, so the harmonics are weak.

At the next level of interaction,  $u_1^* \exp i(\alpha x - \omega t)$  and  $u_2^* \exp i(2\alpha x - 2\omega t)$  couple to drive a higher harmonic and also a wave  $u_3^* \exp i(\alpha x - \omega t)$  having the form of the fundamental. To account for non-linear selection, one need only assume that  $u_3^*$  subtracts from  $u_1^*$ , in other words, that the harmonic reacts back on the fundamental to inhibit its growth. The fundamental able to attain the largest amplitude is then the wave that generates a harmonic least effectively, the wave furthest removed from resonance with its harmonic, the most highly dispersive wave on the jet column. It cannot have an extreme length, since extremely long or short waves are almost non-dispersive. It must have an intermediate length proportional to the jet diameter, presumably the length  $\lambda = 2.38D$  of the mode preferred in the experiments.

The foregoing ideas fit the general theory of Stuart (1960) and Watson (1960) for the evolution of non-linear dispersive waves. If the assumption is retained that the jet is a uniform column surrounded by a vortex sheet, then the radial eigenfunctions are Bessel's functions, and one comes immediately to the core of Stuart and Watson's theory, the derivation of coupled, first-order ordinary

differential equations for the fundamental amplitude, the harmonic amplitude, and a property of the mean field, which in this case is the radius of the jet. Work is already under way on the temporal version of the theory, in which the eigenfunction amplitudes and mean radius depend strictly on time. The temporal theory has the advantage of a dispersion relation  $c(k)$  in accord with experiment, because the theoretical phase velocity does not vary with wave amplitude. It may be possible to account for the fact of spatial growth by means of an integral formulation (cf. Ko *et al.* 1970). In any event, we can reasonably look forward to a theoretical model of axisymmetric vortex trains, with the preferred Strouhal number of 0.30 emerging by calculation.

Our research has benefited from the encouragement and occasional active participation of Earll Murman and of Steven Orszag, during his summer visit to The Boeing Company in 1969. The course of the research was influenced by stimulating discussions with several workers in the field, notably Hans Liepmann, John Ffowcs Williams, Erik Mollo-Christensen, Peter Bradshaw, and Lester Kovasznay. We owe thanks to them and to Frederick Lange, whose technical assistance expedited every phase of the program.

This paper deals chiefly with experiments on the orderly structure of jet turbulence. A mathematical study is under way and should be presented in a second paper, to be followed in due course by a third on a technological application of the phenomenon.

#### REFERENCES

- BATCHELOR, G. K. & GILL, A. E. 1962 *J. Fluid Mech.* **14**, 529.  
 BECKER, H. A. & MASSARO, T. A. 1968 *J. Fluid Mech.* **31**, 435.  
 BRADSHAW, P. 1966 *J. Fluid Mech.* **26**, 225.  
 BRADSHAW, P., FERISS, D. H. & JOHNSON, R. F. 1964 *J. Fluid Mech.* **19**, 591.  
 BROWAND, F. K. 1966 *J. Fluid Mech.* **26**, 281.  
 BROWN, G. B. 1935 *Proc. Phys. Soc.* **47**, 703.  
 CROW, S. C. 1970 *AIAA J.* **8**, 2172.  
 FLOWCS WILLIAMS, J. E. 1963 *Phil. Trans. Roy. Soc. A* **255**, 469.  
 FREYMUTH, P. 1966 *J. Fluid Mech.* **25**, 683.  
 HUSSAIN, A. K. M. F. & REYNOLDS, W. C. 1970 *J. Fluid Mech.* **41**, 241.  
 KLINE, S. J., REYNOLDS, W. C., SCIRBAUD, F. A. & RUNSTADLER, P. W. 1967 *J. Fluid Mech.* **30**, 741.  
 KO, D. R. S., KUNOTA, T. & LEES, L. 1970 *J. Fluid Mech.* **40**, 315.  
 LANDAU, M. T. 1967 *J. Fluid Mech.* **29**, 441.  
 LECANTE, J. 1858 *Phil. Mag.* **15**, 235.  
 LEES, L. & GOLD, H. 1966 *Fundamental phenomena in hypersonic flow. Proceedings of the International Symposium Sponsored by Cornell Aeronautical Laboratory*, Buffalo, 1964. Cornell University Press.  
 LUMLEY, J. L. 1966 *Atmospheric Turbulence and ratio wave propagation. Proceedings of the International Colloquium*, Moscow, 1965.  
 MALKUS, W. 1956 *J. Fluid Mech.* **1**, 521.  
 MICHALKE, A. 1964 *J. Fluid Mech.* **19**, 543.  
 MICHALKE, A. 1965 *J. Fluid Mech.* **23**, 521.  
 MICHALKE, A. & WILLE, R. 1966 *Applied mechanics. Proceedings of the Eleventh International Congress of Applied Mechanics*, Munich, 1964. New York: Springer.

- MOFFATT, H. K. 1969 *Computation of turbulent boundary layers. Proceedings of the AFOSR-IFP-Stanford Conference*, Stanford University, 1968. Distributed by the Thermosciences Division, Department of Mechanical Engineering, Stanford University.
- MOLLO-CHRISTENSEN, E., KOLPIN, M. A. & MARTUCCELLI, J. R. 1964 *J. Fluid Mech.* **18**, 285.
- MOLLO-CHRISTENSEN, E. 1967 *J. Appl. Mech.* **89**, 1.
- ORSZAG, S. A. & CROW, S. C. 1970 *Studies in Appl. Math.* **49**, 167.
- PAO, Y.-H., HANSEN, S. D. & MACGREGOR, G. R. 1969 *Boeing Scientific Research Laboratories Document D1-82-0863*.
- RAYLEIGH, LORD 1896 *The Theory of Sound*. London: Macmillan. Reproduced by Dover Publications.
- REYNOLDS, A. J. 1962 *J. Fluid Mech.* **14**, 552.
- REYNOLDS, O. 1894 *Phil. Trans. Roy. Soc. A* **186**, 123.
- ROSHEO, A. 1961 *J. Fluid Mech.* **10**, 345.
- SAMI, S., CARMODY, T. & ROUSE, H. 1967 *J. Fluid Mech.* **27**, 231.
- SATO, H. 1960 *J. Fluid Mech.* **7**, 53.
- STUART, J. T. 1960 *J. Fluid Mech.* **9**, 353.
- TYNDALL, J. 1867 *Sound*. London: Longmans.
- WATSON, J. 1960 *J. Fluid Mech.* **9**, 371.
- WILLE, R. 1952 *Jb. Schiffbautech. Ges.* **46**, 174.
- WYGNAŃSKI, I. 1964 *Aero. Quart.* **15**, 373.
- WYGNAŃSKI, I. & FIEDLER, H. 1969 *J. Fluid Mech.* **38**, 577.

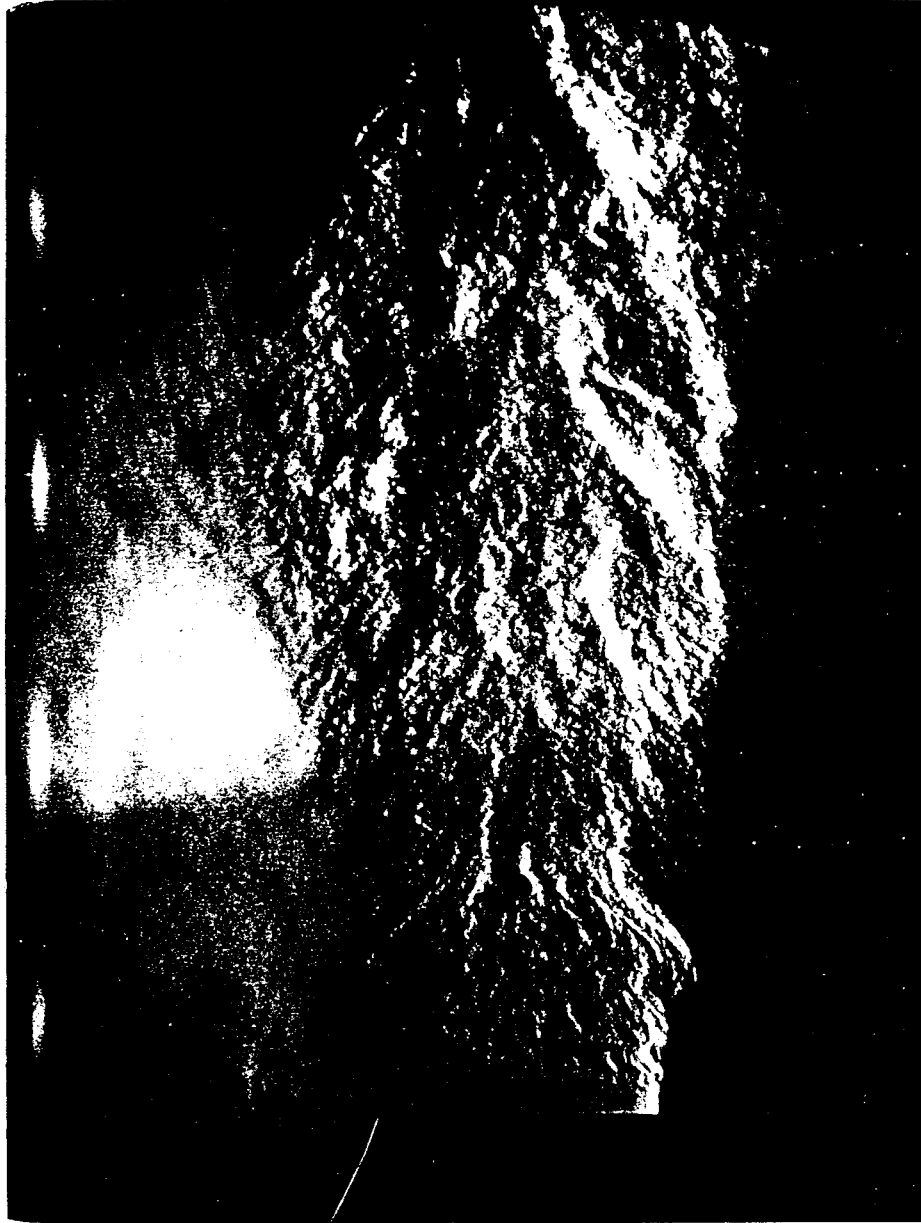


FIGURE 1. Gas-injection schlieren photograph of a 2 in. diameter air jet at a speed of 280 ft/sec (courtesy of Bradshaw *et al.* 1964). The Reynolds number is  $3 \times 10^5$ .

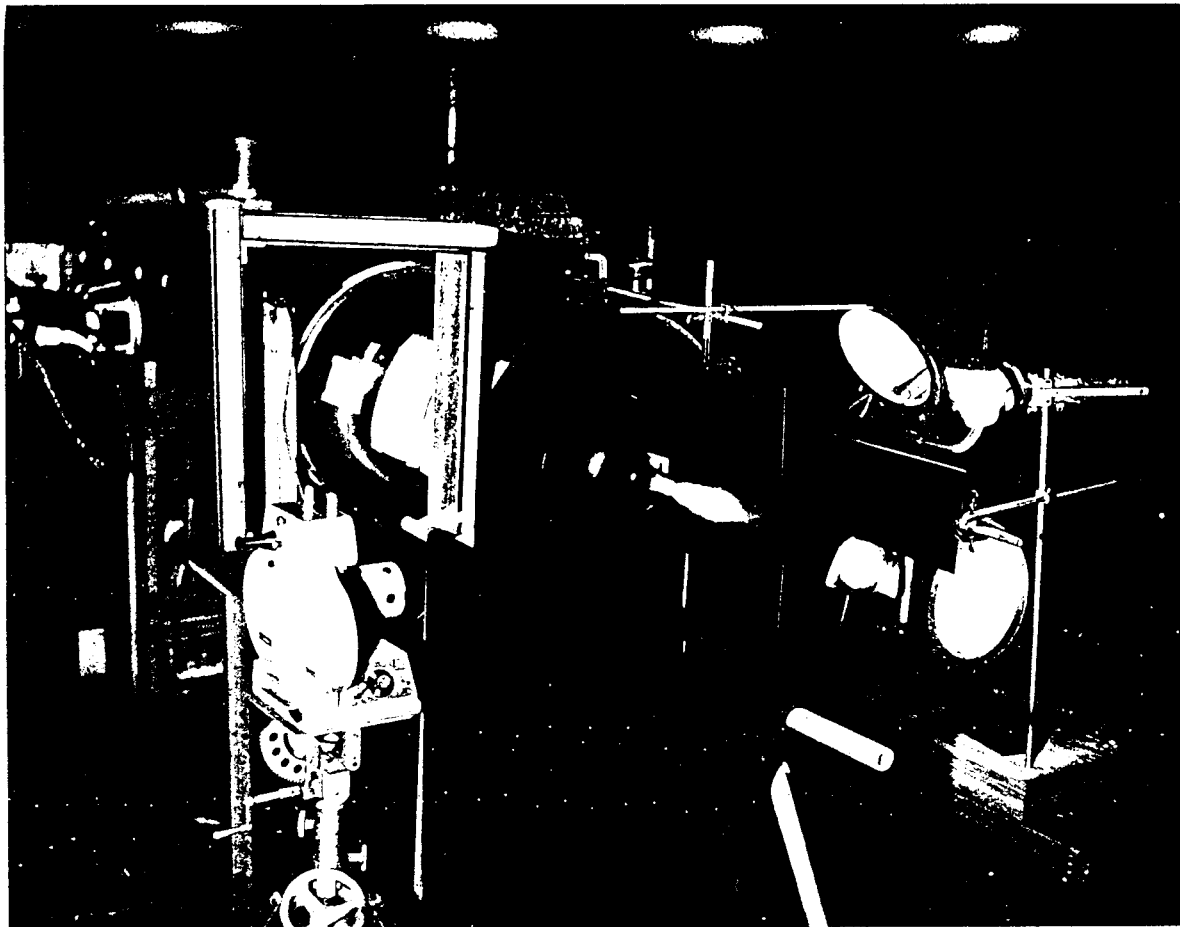
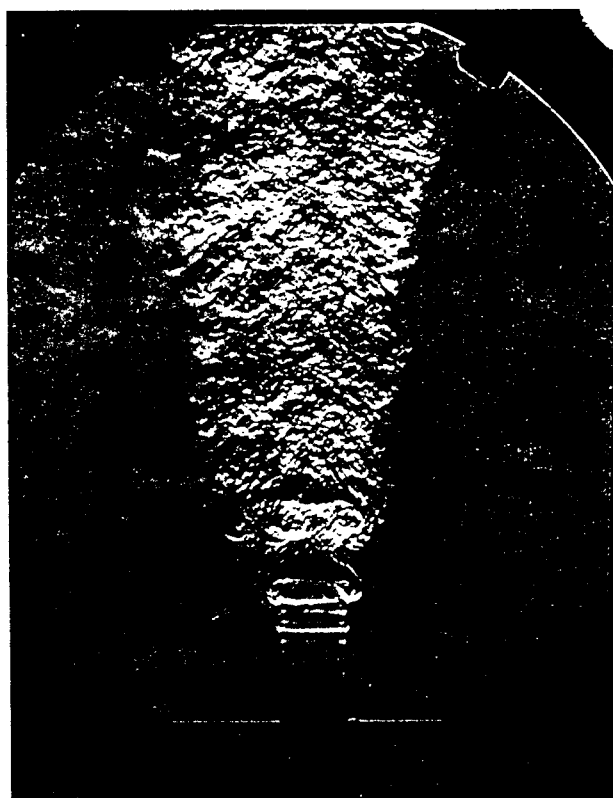


FIGURE 5. The fog-seeded jet, as outfitted for high-speed motion picture photography.

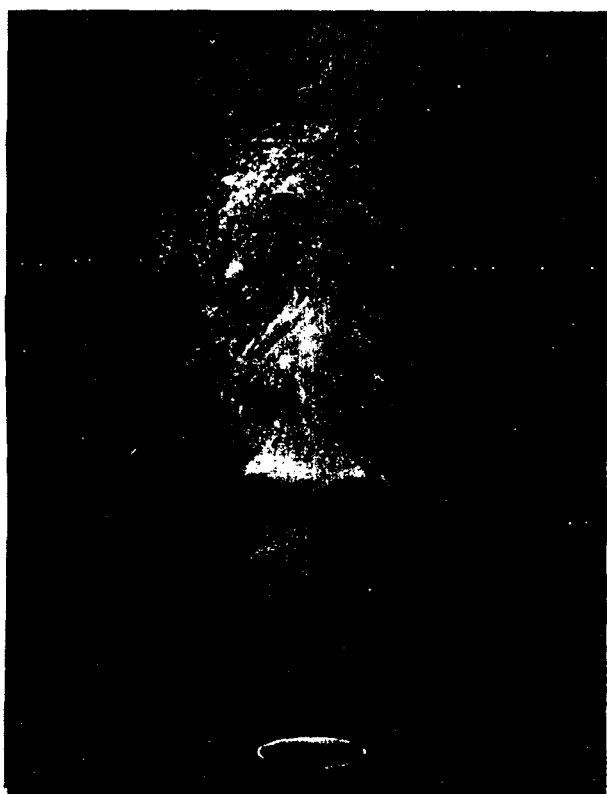


(a)



(b)

FIGURE 4. Schlieren photographs of the 1 in. air jet, made visible by CO<sub>2</sub>, at Reynolds numbers of (a)  $1.87 \times 10^4$  and (b)  $3.7 \times 10^4$ .



(a)

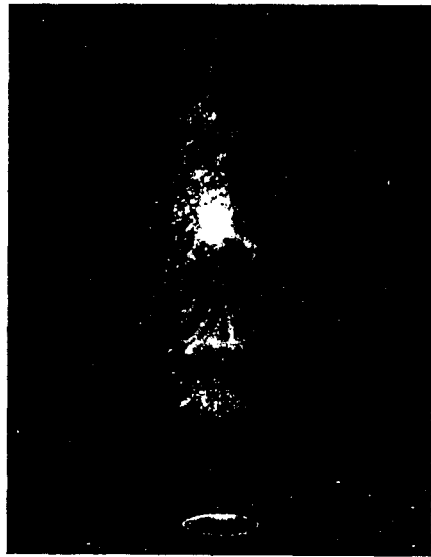


(b)

FIGURE 6. Spark photographs of the 1 in. fog jet. The Reynolds numbers range from  $1.05 \times 10^4$  to  $7.5 \times 10^4$  as follows: (a)  $1.05 \times 10^4$ ; (b)  $1.05 \times 10^4$ ; (c)  $3.00 \times 10^4$ ; (d)  $4.35 \times 10^4$ ; (e)  $5.14 \times 10^4$ ; (f)  $6.52 \times 10^4$ ; (g)  $7.5 \times 10^4$ .



(c)

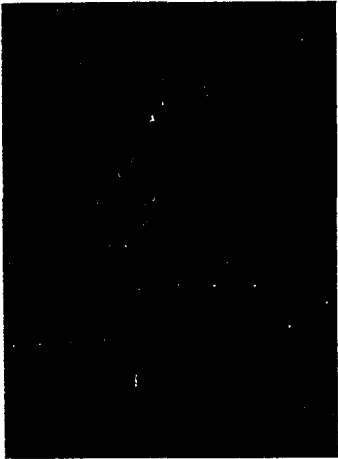


(d)

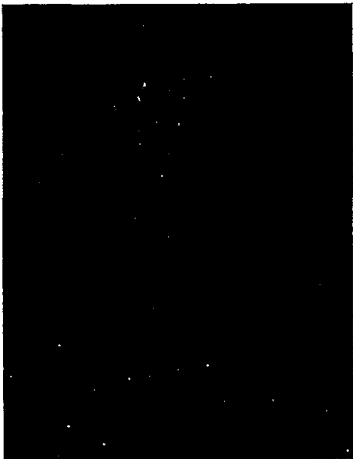


(e)

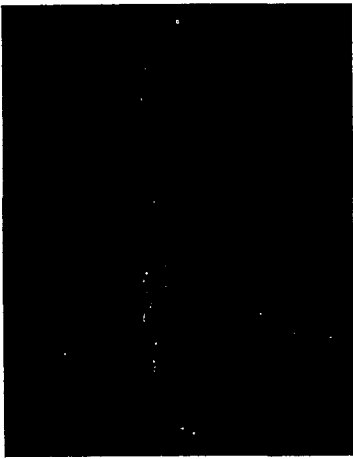
FIGURE 6(c-e). For legend see plate 4.



(a)



(b)

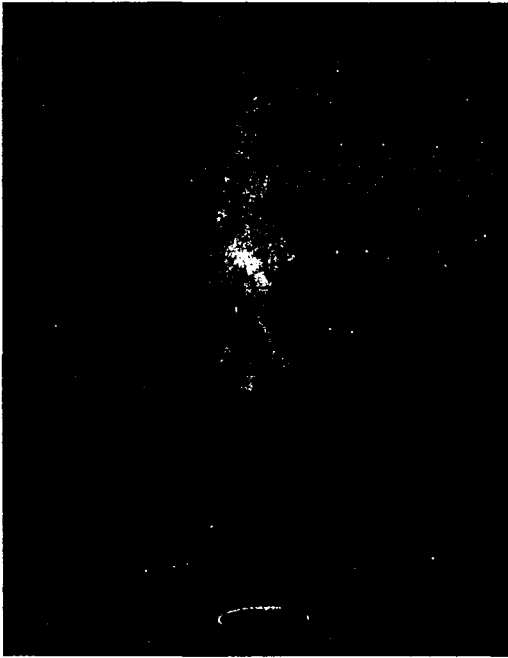


(c)

FIGURE 26. Schlieren photographs of the 2 in. jet seeded with CO<sub>2</sub>. Part (a) shows the unforced jet at an exit speed of 103 ft/sec and a Reynolds number of  $1.06 \times 10^5$ . The remaining parts show the jet under 2% forcing at Reynolds numbers of (b) 0.30 and (c) 0.60.



(g)



(h)

FIGURE 6(f, g). For legend see plate 4.

*On the Flow of Gases at High Speeds.*

By T. E. STANTON, F.R.S.

(Received March 29, 1926.)

[PLATES 6 and 7.]

In a paper on the discharge of gases under high pressures\* the late Lord Rayleigh called attention to the deficiencies in the present state of knowledge of the characteristics of the flow of a gas, from a vessel in which it is compressed, through an orifice into the atmosphere or into a receiver at a lower pressure, and suggested that further study was desirable in the direction of investigating the accuracy of the common assumptions of the adiabatic character of the flow and its dependence on the pressure in the receiver.

Assuming adiabatic flow the values of the velocity of the jet and the rate of discharge are given by the well-known relations—

$$\frac{u^2}{2} = \frac{\gamma}{\gamma - 1} \cdot p_0 \left\{ 1 - \left( \frac{p}{p_0} \right)^{\frac{\gamma-1}{\gamma}} \right\}, \quad (1)$$

$$w = g\Lambda \sqrt{\frac{2\gamma}{\gamma - 1} \cdot p_0 \rho_0 \left( \frac{p}{p_0} \right)^{\frac{\gamma}{\gamma-1}} \left\{ 1 - \left( \frac{p}{p_0} \right)^{\frac{\gamma-1}{\gamma}} \right\}}, \quad (2)$$

where  $u$  is the speed,  $p$  and  $\Lambda$  the pressure and area of the jet, and  $w$  the rate of discharge, the suffix  $0$  referring to the conditions inside the discharging vessel where  $u = 0$ .

It may be recalled that St. Venant and Wantzell† were the first to obtain the equations of discharge in the forms given in (1) and (2) and to attempt a verification of them by experiment. In discussing the value of the theoretical discharge they appear to have ignored the possibility of any variation in the area of the jet and to have confined their attention to the pressure and velocity changes in the plane of the least section of the orifice. In this section it is apparent from (2) that as the value of  $p$  diminishes,  $p_0$  remaining constant, the value of  $w$  rises to a maximum when  $p$  reaches the value  $p_0 \left( \frac{2}{\gamma+1} \right)^{\frac{\gamma}{\gamma-1}}$  and then diminishes indefinitely with further reduction of the orifice pressure, as a result of the continual reduction of the density with fall of pressure and the finite character of the velocity apparent from (1). If, therefore, the pressure in the plane of the orifice is sensibly that of the receiver, the absurd conclusion is reached that the discharge into a vacuum must be zero. Such an effect was so manifestly opposed to experience that it was decided to investigate the matter experimentally. For this purpose air at atmospheric pressure was allowed to enter a previously exhausted receiver by means of an orifice, and the rate

of discharge was determined from observations of the pressure and temperature of the air in the receiver at equal intervals of time.

The results of these experiments showed that the rate of discharge increased as the ratio of the receiver pressure (here called  $p_r$ ) to the initial pressure diminished from unity to 0·4, but that when the latter stage was reached further reduction in the receiver pressure had no effect on the rate of discharge which remained constant. They concluded, therefore, that no identity could exist between the pressure in the receiver and the pressure of the jet in the plane of the least section or throat of the orifice for values of  $p_r/p_0$  between zero and 0·4.

These observations were subsequently confirmed by R. D. Napier\* and H. Wilde,† who observed the rate of discharge to become constant at values of  $p_r/p_0$  in the neighbourhood of 0·5. No further advance, however, was made in the theory of orifice discharge until 1885, when Osborne Reynolds,‡ who apparently was not familiar with the work of St. Venant and Wantzell, obtained similar expressions to (1) and (2) for the velocity and rate of discharge in an attempt to explain the observations of Wilde, but made, in addition, two important deductions from these relations which had escaped the notice of these workers. In the first place, instead of considering a continuous fall of pressure in the throat of the orifice, Reynolds assumed a continuous fall of pressure along the axis of the jet, and treated  $\Lambda$  in equation (2) as the variable,  $w$  and  $p_0$  being constant. This at once led to the condition  $p = p_0 \left( \frac{2}{\gamma+1} \right)^{\frac{\gamma}{\gamma-1}}$  at a minimum section of the jet. Following the characteristics of the flow as the pressure in the receiver was gradually reduced from a value equal to that in the discharging vessel, it could, therefore, be regarded as made up of a series of streams in the discharging vessel converging towards the orifice and emerging into the receiver firstly in the form of a parallel jet, the pressure in which was sensibly equal to that of the receiver, and then when the pressure had attained the value  $p = p_0 \left( \frac{2}{\gamma+1} \right)^{\frac{\gamma}{\gamma-1}}$ , here called the critical pressure, developing a

minimum section and expending further down stream until its pressure had reached that of the receiver. Further from general considerations of the curvature of the streams, it appeared that the position of the minimum section would be down stream relative to the plane of the orifice.

In the second place, by remarking that the theoretical velocity of the jet at the minimum section was that of sound under the conditions existing at that section, Reynolds perceived that when this velocity was reached no further reduction of pressure in the receiver could affect the distribution of pressure and velocity on the upstream side of the minimum section, and concluded that the rate of discharge would then remain constant. The phenomenon of constant

\* 'Discharge of Fluids,' Napier.

† 'Proc. Manchester Lit. and Phil. Soc.,' 1885.

‡ 'Proc. Manchester Lit. and Phil. Soc.,' 1885; 'Phil. Mag.,' March, 1886.

\* 'Phil. Mag.,' vol. 32, p. 177 (1916).

† 'Journal de l'Ecole Polytechnique,' vol. 15, 1829.

rate of discharge observed by St. Venant and Wantzel was, therefore, explained on theoretical grounds.

It may be remarked that this argument assumes that the area of the minimum section of the jet remains entirely unaffected by the conditions of pressure in the receiver. It is, however, conceivable that, when once the velocity of sound had been attained, further reduction in the pressure of the receiver might affect the position and also the diameter of the minimum section then established. Neglecting for the present this possibility, it will be recognised that the work of Reynolds placed the theory of orifice discharge on a satisfactory basis as affording an explanation of the observed facts. An outstanding problem was the relation between the receiver pressure and that at the minimum section of the jet, and on this large amount of experimental data available might be expected to throw some light, but on examination it was found that all this work consists of measurements of the receiver pressure corresponding to the commencement of a constant rate of discharge, and no measurement of the pressure of the jet appears to have been made.

The results obtained by the early workers, St. Venant and Wantzel, Napier and Wilde, all seem to agree in indicating that a constant rate of discharge is obtained when the receiver pressure is of the order of the theoretical value for the pressure at the minimum section, i.e.,  $p_r = 0.527 p_0$ , and this would appear to confirm the view of Reynolds that prior to this stage the flow consisted of a parallel jet at a pressure equal to that of the receiver and also his tacit assumption that, when the critical pressure had been reached in the jet and the minimum section established, no further reduction in the receiver pressure would affect the area. On the other hand, some recent careful determinations by Hartshorn,\* undertaken at the suggestion of Lord Rayleigh, have exhibited a marked divergence, from the theoretical limit, of the value of the receiver pressure when the rate of discharge has become constant. Some of the results of Hartshorn's experiments are shown in fig. 1, in which the ordinate

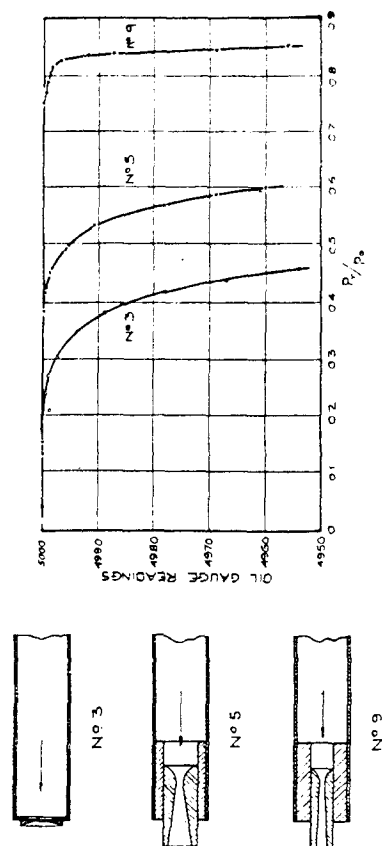


FIG. 1.

\* 'Roy. Soc. Proc., A, vol. 94 (1917).

is the pressure difference between the atmosphere and that of the reservoir supplying the nozzle, and is taken to be a measure of the rate of discharge. It will be seen that in the case of a thin-lipped orifice the rate of discharge did not become constant until the receiver pressure was reduced to one-fifth of the initial pressure. In discussing Hartshorn's results it must be borne in mind that they were essentially small scale experiments, the diameter of the throats of the orifices being of the order of 1 mm., and that their characteristics might be affected to some small extent by viscosity and heat conductivity which have been found by Buckingham and Edwards\* to have an appreciable effect on the flow through the orifices used in Bunsen's effusion method of determining the relative densities of gases. The orifices in this apparatus are, however, approximately 0.06 mm. in diameter, so that such effects might reasonably be expected to be negligibly small in the orifices used by Hartshorn. Apart from this consideration, the results of Hartshorn's experiments appear to afford evidence of an effect of the receiver pressure on the discharge which has not hitherto been suspected, and this view is strengthened from an examination of the accuracy of the method adopted by Hartshorn for detecting variations in the rate of the discharge which enabled him to detect variations of the order of 0.1 per cent. It is clear from the form of the curve (3) in fig. 1, with the very large exaggeration of the vertical scale, that observations of an accuracy of, say, 1 per cent., which may be regarded as in all probability that of the earlier measurements, would suggest a critical value of the receiver pressure in the neighbourhood of 0.5.

The results of Hartshorn's experiments with diverging nozzles of various angles of divergence are also exhibited in fig. 1, from which it will be seen that the range of constant rate of discharge extended, for small angles of divergence, from  $p_r/p_0 = 0$  to  $p_r/p_0 = 0.8$ . It is certain that when the latter stage was reached these nozzles could not have been "running full," for in that case the pressure at the outlet of the nozzle would have been considerably below the value of 0.5 instead of above it. It appears probable, therefore, that at this stage the jet in the region between the throat and the outlet of the nozzle was surrounded by a stream tending to move in the opposite direction down the gradient in pressure from the receiver to the throat. Whatever be the explanation of these results, the general impression derived from Hartshorn's experiments is that the receiver pressure is a factor affecting the rate of flow, and the desirability of further experimental work mentioned above is emphasized.

It was decided, therefore, to undertake an experimental study of the distribution of pressure and velocity in jets flowing through orifices of different forms, with special reference to the following points on which the above discussion shows that further evidence is required:—

- (1) The existence of a minimum section of the jet and its variation in position and magnitude.

\* 'Scientific Papers of Bureau of Standards,' No. 359.

- (2) The relation between the pressure in the receiver and the pressure in the jet for increasing and constant rates of discharge.
- (3) The possibility of the characteristics of high speed jets being affected by the dimensions of the orifice and the viscosity of the air.

The above investigations form Part I of the present paper.

Part II is devoted to a study, also suggested by Lord Rayleigh in the paper to which reference has been made, of the motion of jets at speeds above the velocity of sound, and the nature of the wave motion set up on their emergence into quiescent air.

## PART I.

### Section I.—The Characteristics of Jets from orifices of different form in the region of the critical pressure.

For this purpose observations were made of the pressure distribution in the jet along and at right angles to the axis and of the variation in its lateral dimensions, with distance from the plane or throat of the orifice.

For convenience of observation these experiments were made on jets discharged into the open air from a vessel of about 200 cubic feet capacity supplied with compressed air from a 50-h.p. Brotherhood Compressor. The general arrangement of the apparatus is shown in fig. 2. The air from the vessel is admitted into a cylindrical box, fitted with guide blades to damp out the eddies and irregularities of flow, so that a steady supply of air at a known pressure is delivered to the orifice which is screwed into the cover of the box. A bracket is attached to the outside of the box, and carries the pressure tube which is provided with a micrometer to enable readings to be taken along and perpendicular to the axis of the jet. Three forms of orifice were used—No. 1, a circular hole in a thin flat plate; No. 2, a plain nozzle having a faired entry and parallel outlet; and No. 3, a diverging nozzle having a faired entry and a diverging outlet consisting of a cone of total angle  $3^{\circ} 34'$ . These are shown in fig. 2. For a study of the effect of the linear dimensions of the orifice two thin-lipped orifices were used—one 0.61 cm. diam. and the other 1.22 cms. diam.

(a) *Axial Distribution of Pressure.*—The results of the observations of the pressure along the axis of the jet are given in Table I, and are shown plotted in fig. 3, in which the thin lines indicate the pressure variation at different values of the ratio of the atmospheric pressure to that of the discharging vessel, i.e.  $p_t/p_0$ , and the thick lines the position on the axis of the jet at which the theoretical critical pressure  $0.527 p_0$  was reached. It will be seen that this position depends on the shape of the orifice and within limits on the initial pressure of the jet. In the case of the diverging nozzle the position appears to coincide, within the limits of accuracy of the observations, with that of the throat of the orifice, and is approximately independent of the initial pressure of the jet within the range of observations. On the other hand, in the case of the plain nozzle and the thin-lipped orifices the position at which the critical

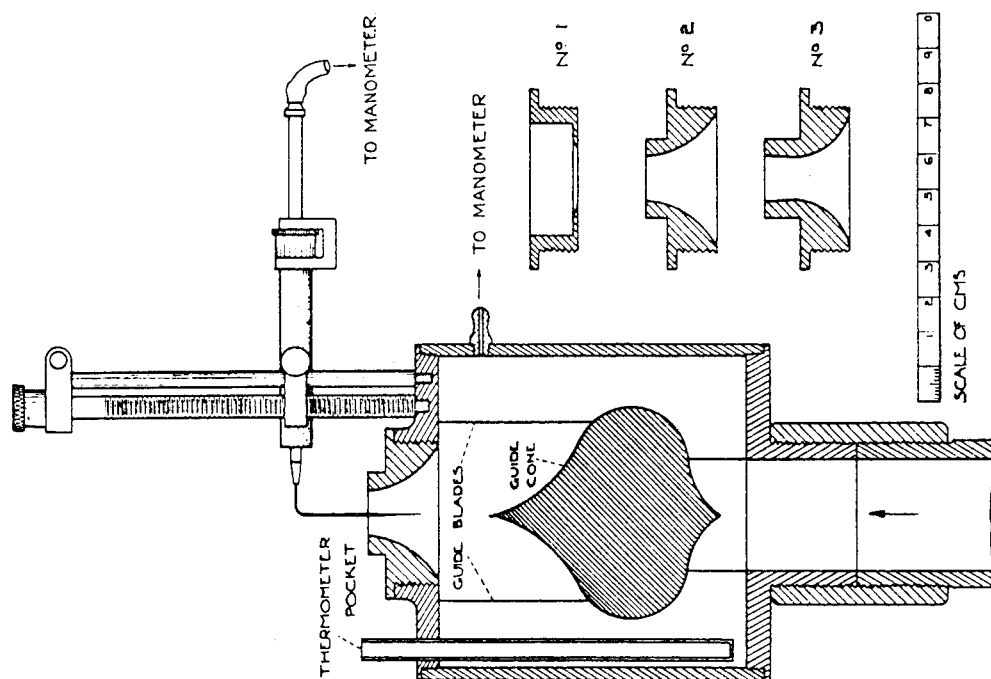


FIG. 2.

pressure is reached is in all cases appreciably down stream relative to the throats, this divergence appearing to diminish to a definite limit as the value of  $p_t/p_0$  is diminished. On referring to the curves for the thin-lipped orifices it will be seen that this limiting position is reached for a value of the ratio of the order of 0.28, which is roughly in agreement with the value of the ratio at which the limiting value of the discharge was reached in Hartshorn's experiments with an orifice of this type. It would appear, therefore, that the stage in Hartshorn's experiment on the thin-lipped orifice between values in  $p_t/p_0$  from 0.5 to 0.2, in which a small increase in the rate of discharge was noted, corresponds with a definite change in the position of the section of critical pressure.

The distance of the limiting position of the section of critical pressure from



the throat of the orifice is approximately 0.25 R for the plain nozzle and 0.4 R for the thin-lipped orifice, where R is the radius of the throat.

The comparison of the results from the geometrically similar thin-lipped orifices (fig. 3) are of interest in showing that for orifices of these dimensions and within the limits of accuracy of the observations the similarity extends also to the pressure distribution, i.e., the effect of viscosity on dynamical similarity in the motion is small.\*

\* It will be seen from Section III this similarity does not extend to the diverging nozzles.

Table I.—Pressure Distribution along axis of jet discharged into atmosphere.

Absolute Pressures in cms. of Mercury.										Description of Nozzle.
Initial.	Distance from plane of throat in cms.*									
	-0.127	-0.064	0	+0.064	+0.127	+0.190	0.254	0.317	0.380	
151.8	—	—	125.2	110.0	95.6	83.3	—	—	—	0.61 cm. thin-lipped orifice, similar to No. 1, fig. 2.
176.2	—	—	144.3	126.2	106.4	87.6	—	—	—	
201.5	—	—	163.2	141.2	116.5	92.9	—	—	—	
224.0	—	—	178.2	148.8	121.4	92.3	—	—	—	
250.5	—	—	200	170.8	138.2	106.4	—	—	—	1.22 thin-lipped orifice, No. 1, fig. 2.
150.8	—	—	—	—	—	94.0	86.4	81.3	76.2	
175.5	—	—	—	—	111.5	102.1	91.4	83.5	75.7	
200.2	—	—	—	—	—	111.2	98.0	88.1	77.9	
250.2	—	—	—	—	147.5	131.4	113.5	100.2	86.6	1.25 cm. plain converging nozzle, No. 2, fig. 2.
274.8	—	—	—	—	162.7	145.5	125.2	110.0	96.5	
149.2	—	94.2	89.8	85.0	80.5	—	—	—	—	
198.8	—	124.9	118.8	111.9	104.6	—	—	—	—	
246.0	—	154.3	146.5	137.2	120.1	—	—	—	—	1.21 cm. diverging nozzle, No. 3, fig. 2.
151.0	89.8	84.6	79.2	72.5	67.4	—	—	—	—	
175.8	104.3	97.8	91.7	83.6	77.7	—	—	—	—	
200.2	119.0	111.3	104.4	96.4	88.0	—	—	—	—	
225.6	133.7	125.0	117.2	106.5	98.4	—	—	—	—	1.25 cm. plain converging nozzle, No. 3, fig. 2.
250.2	147.8	138.0	130.0	117.6	108.8	—	—	—	—	
275.5	161.2	151.6	142.1	129.0	119.8	—	—	—	—	

\* Distances reckoned +ve down-stream.

(b) *Radial Distribution of Pressure.*—The observed distribution of static pressure across that section of the jet having the critical value of the pressure at the axis is shown, for the 1.22 cms. thin-lipped orifice and the divergent nozzle in fig. 3, from which it will be seen that the falling off in the value of the static pressure near the boundary is appreciable. It might be supposed at first sight that this was a frictional effect, but as has been pointed out by previous writers,\* the relatively large curvature of the individual streams near the boundary must involve a radial pressure gradient of the kind observed to which must correspond an upstream displacement of the throats of the elementary streams near the boundary.

\* Cotterill, 'Applied Mechanics,' p. 570.

A method of verifying this assumption which suggested itself was the measurement of the pressure in a pitot tube inserted at various points of the jet. Assuming no losses in the elementary stream in which it is placed, and provided that the velocity does not exceed that of sound, the pressure in the pitot tube

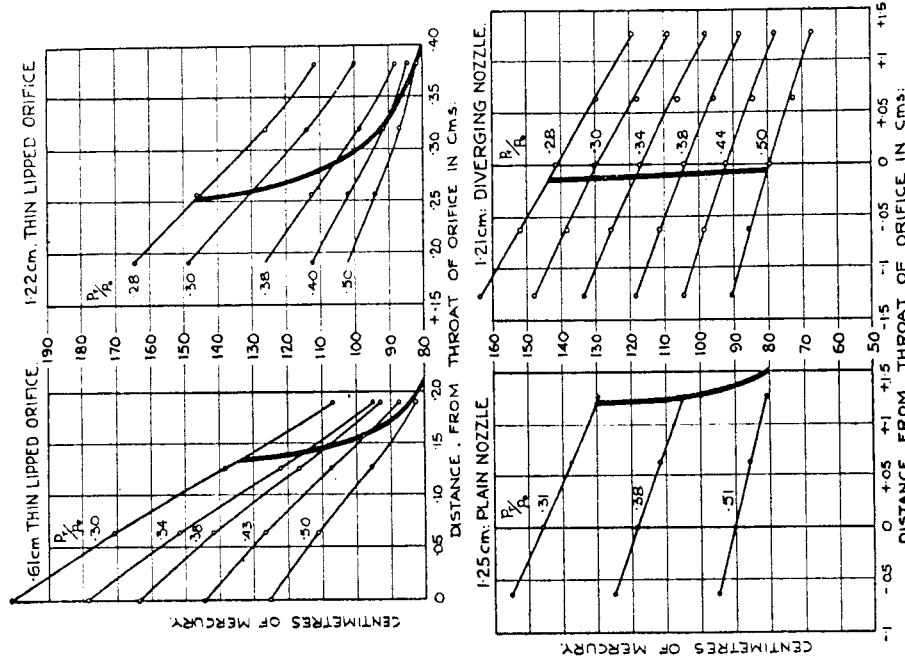


Fig. 3.—Curves of Variation of Static Pressure at Axis for Orifices of different form, discharging into atmosphere. A thick line indicates the position at which the pressure reaches the theoretical critical value.  $P_0$  = Pressure in reservoir.

Correction : the abscissal values in the upper right-hand figure should read as +.08, .13, .18, .23, .28, .33, instead of .15 ... .40.

should be equal to the pressure in the reservoir from which the stream emerges. If, therefore, the pressure in the stream near the wall is affected by friction, an appreciable difference between the pitot tube pressure and the reservoir would be observed. This method of discrimination was accordingly adopted, and the results of pitot tube observations on the two orifices considered are shown plotted in fig. 4. It was not possible to get an observation nearer to the walls than

Table II.—Measured diameter of jet from 1.22 cm. thin-lipped orifice at varying values of the initial pressure and distance from the plane of the orifice.

Distance down-stream of section from plane of orifice					Distance down-stream of minimum section from plane of orifice.					Diameter of minimum section.
0.063	0.127	0.254	0.381	0.508	0.762	1.016 cms.				
—	1.108	1.087	1.080	1.080	1.065	—	(ms.	—	Cms.	—
—	1.110	1.098	1.100	1.105	—	0.38	—	—	1.007	—
1.135	1.120	1.118	1.130	1.140	—	0.13	—	—	1.116	—
1.140	1.132	1.150	—	—	—	0.22	—	—	1.132	—

increase as the value of  $p_r/p_0$  diminishes, and this affords an explanation of the low limit of this ratio at which the discharge became constant in Hartshorn's experiments on this type of orifice (fig. 1).

On comparing the positions at which the minimum sections are located by the above method with the corresponding positions of the section at which the critical pressure exists for this nozzle, which is shown in fig. 3, it will be seen that the agreement is reasonably good. It was concluded, therefore, that the answers to the above questions were all in the affirmative.

To sum up, the conclusions derived from the experiments described in the present section are as follows :—

- (1) In each of the three characteristic types of orifice which may be used for the discharge of gases from a vessel at constant pressure into a receiver at a pressure appreciably below the critical value  $0.527 p_0$ , the section of the jet diminishes to a minimum value, at which the velocity is that of sound under the conditions existing, and then increases. This minimum section in the case of a free jet is not constant in area or position relative to the plane or throat of the orifice, but depends on the total ratio of expansion.
- (2) In a jet in which the expansion takes place within solid boundaries, i.e., a diverging nozzle, the minimum section may for all practical purposes be regarded as coincident with the throat of the nozzle for all ratios of expansion.
- (3) The flow of the fluid up to the minimum section is adiabatic in character.

#### Section II.—The Characteristics of the Rate of Discharge from Orifices of Different Forms.

The results of the experiments described above on the variation in position and magnitude of the minimum section of the jet from a thin-lipped orifice afford, as was pointed out, a partial and probably a complete explanation of the low value of the ratio  $p_r/p_0$  at which the discharge became constant for this

1.22 cm. THIN LIPPED ORIFICE. 1.21 cm. DIVERGING NOZZLE.

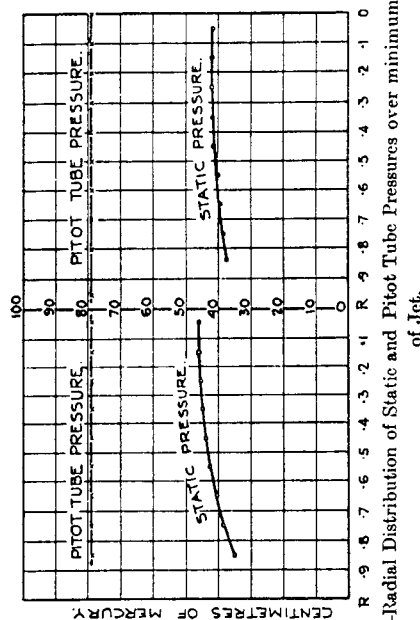


Fig. 4.—Radial Distribution of Static and Pitot Tube Pressures over minimum section of Jet.

0.025 cms., but for all radii less than this no variation of the pitot tube pressure was noted, and the observed value was within 0.5 per cent. of that of the receiver pressure. It was concluded, therefore, that the observed falling off of the static pressure near the walls was not due to friction but to the up-stream displacement of the throat of the outside streams.

(c) *The Variation in the Linear Dimensions of the Jet with Distance from the Throat of the Orifice.*—The object of these experiments was three-fold, and may perhaps best be expressed in the form of the following three questions :—

- (1) Could the existence of a minimum section of the jet be detected for values of  $p_r/p_0$  less than 0.527 ?
- (2) If so, did its position coincide with that section at which the theoretical critical pressure was observed ?
- (3) Did the area of the minimum section of the jet from a given orifice depend on the value of the ratio of the receiver pressure to the initial pressure ?

The determination of the effective boundary of the jet was obviously difficult, and after some consideration it was thought that a sufficiently accurate location of it would be the point at which the pressure in a pitot tube was a mean between that in the interior of the jet and the atmospheric pressure. The method adopted, therefore, was to move the pitot tube across a diameter of the jet by means of a micrometer and measure the distance from boundary to boundary as defined above. The measurements were all made on the 1.22 cms. diameter thin-lipped orifice, and the reduced values of the diameter of the jet at varying values of the initial pressure and of the distance from the plane of the orifice are given in Table II following.

It will be seen that there is a well-defined minimum section for all but the highest value of  $p_r/p_0$ , the value of which is so close to the critical value at which the formation of a minimum section begins that the detection of a minimum in this case could hardly be expected. Further, the areas of the minimum sections

form of orifice, in Hartshorn's experiments. On the other hand, the cause of the extremely high value of the corresponding ratio in the case of the diverging nozzles was still an obscure problem, and in attempting its solution it was thought advisable in the first instance to determine whether this characteristic applied to diverging nozzles of considerably greater dimensions than those of Hartshorn, which it will be remembered were 1 mm. diameter. In the tests previously described on the two geometrically similar thin-lipped orifices, 0.61 and 1.22 cms. diameter, no appreciable scale effect could be detected, but this might possibly be due to the absence of a solid boundary to the jet, and it was thought that for a completely enclosed jet the influence of the viscosity of the air might be much more marked. It was decided, therefore, to investigate the characteristics of the discharge from the orifices used in the present work. For this purpose the original method of St. Venant and Wantzel, in which the flow is from the atmosphere to a variable lower pressure, possesses, as pointed out by Lord Rayleigh,\* considerable advantages over that of discharging into the atmosphere from a vessel in which the pressure was varied, and it was accordingly adopted. The re-arrangement of the apparatus for the purpose was rendered comparatively easy by the device of utilising the discharging drum of the previous experiments as the receiver, by previously exhausting the latter to a low pressure and then allowing air at atmospheric pressure to pass through the nozzle into the receiver, the pressure in which would gradually rise. The arrangement of the apparatus is shown in fig. 5. The discharging nozzle is enclosed in an air-tight cylinder

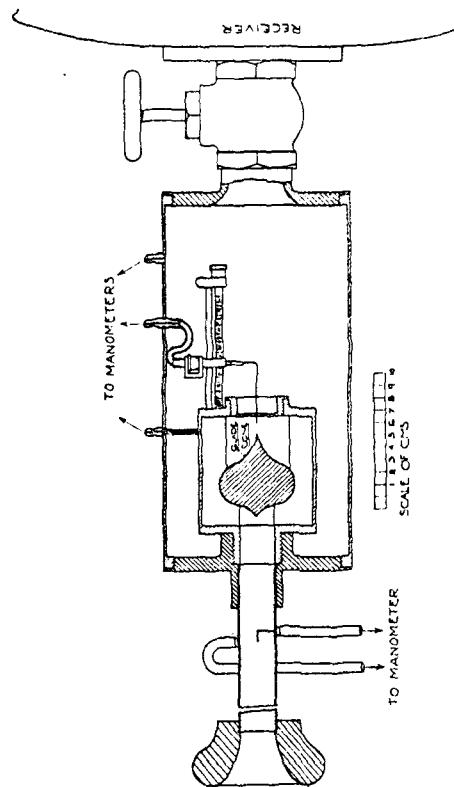


FIG. 5.

communicating with the receiver by means of a stop-valve. The orifice box is attached to the other cover of this cylinder, and is supplied from the external air by means of a brass pipe 2.85 cms. diameter and 300 cms. long provided with a bell mouthpiece at the inlet and pitot and static pressure tubes near the

delivery end, from observations on which the mass flow can be measured.

The receiver was disconnected from the air compressor and coupled to an exhausting pump so that the pressure in it could be reduced to any desired value below atmospheric pressure. A static pressure tube was inserted in the axis of the jet as shown and connected to a manometer. Provision was also made for recording the pressure in the outer cylinder, i.e., the receiver pressure, and the pressure in the orifice box, or the initial pressure, which was slightly below that of the atmosphere.

In making an experiment, the pressure on the drum having been reduced to a given value, the exhaust pump was stopped and the valve connecting the receiver to the orifice box was opened. Readings of the discharge gauge and the manometers connected to the box, receiver and static pressure tube, were then taken at equal intervals of time.

The results proved to be of considerable interest, and gave a satisfactory explanation of the peculiar behaviour of diverging nozzles which had previously been obscure.

Taking first the case of flow through a thin-lipped orifice, the results of the tests on the 0.615 cms. diameter orifice are shown in fig. 6. In this the values

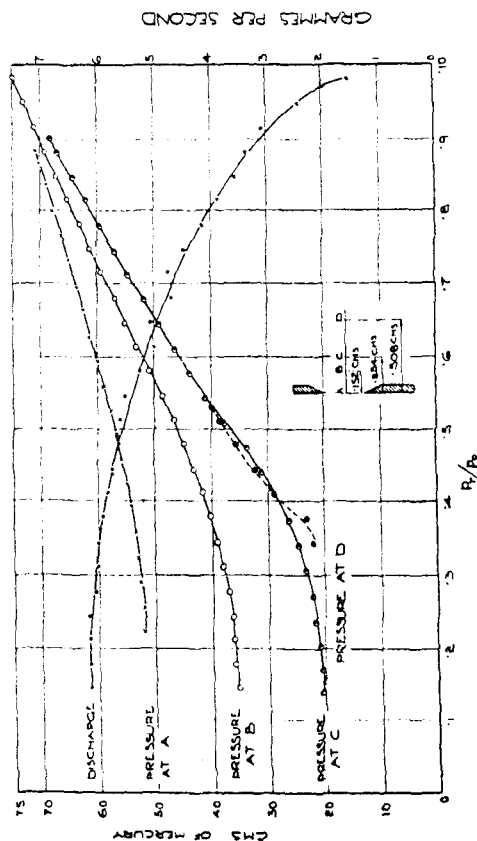


FIG. 6.

of the measured mass flow and the pressures at different positions along the axis of the jet have been plotted as ordinates on a base of values of the ratio of the receiver pressure to the initial pressure. As regards the variation of mass flow, it will be seen that the flow becomes constant at a value of  $p_1/p_0$  equal to 0.2, which, as will be seen from fig. 1, agrees closely with the value found by Hartshorn for this case.

It would appear, therefore, that, as predicted from the experiments on geometrically similar orifices described in Section I, the effect of linear dimensions on the limiting conditions of flow arc, for this type of orifice, extremely small.

The pressure curves taken at the three positions A, B, C and D, indicated in

\* 1.c. ante, p. 1.

diverging outlet throw considerable light on the action of the jet in passing through the divergence. It will be seen from the figure that the pressure at a distance of 1.27 cms. from the throat remains constant up to a value of  $p_r/p_0$  of 0.65, and then begins to rise with the receiver pressure. At 3.81 cms. from the throat there is no steady value and the pressure rises with the receiver pressure throughout the whole range. It is clear, therefore, that at no stage of the expansion does the nozzle "run full" at this distance from the orifice, and the pressure here is sensibly that of the receiver. At 1.27 cms. from the orifice the nozzle "runs full" up to a value of  $p_r/p_0 = 0.65$ , and then breaks away from the walls. As a variation on this experiment an extension piece was fitted to the end of this nozzle so that the length of the diverging cone was doubled and the observations repeated. It was found that the critical pressure at the throat was not reached until the ratio  $p_r/p_0$  had attained the value of 0.90. Further, the values of  $p_r/p_0$  at which the jet broke away from the two points to which the manometers were connected were considerably greater than those previously observed. Again, on shortening the nozzle to one quarter of its original length the critical pressure at the throat was reached for a value of  $p_r/p_0$  of 0.70. It was clear, therefore, that the critical points in the discharge and pressure curves of the nozzle were dependent upon its length. As a second variation the angle of divergence of the nozzle was increased to  $4^\circ 36'$ , and the test repeated. In this case it was found that the discharge remained constant up to a value of  $p_r/p_0$  appreciably greater than when the angle was only  $2^\circ 52'$ . On increasing the angle still more the value corresponding to the critical value of the discharge receded, showing that there was a maximum value for some definite value of the diverging angle.

It would appear, therefore, that in a diverging nozzle supplied with air at constant pressure the expansion ceases, *i.e.*, the nozzle fails to run full at some point in its length depending on the value of the receiver pressure, the angle of divergence, and the distance of the point from the end of the nozzle, and that as the receiver pressure rises the point of break away moves gradually up to the throat, and finally at a value of  $p_r/p_0$  depending on the shape and dimensions of the nozzle disturbs the pressure distribution there with consequent reduction in the flow. On the down-stream side of the point of break away the region between the walls of the nozzle and the issuing jet is therefore one of back flow towards the throat of the nozzle with a pressure gradient consisting of the difference between the receiver pressure and that of the jet at the point of break away. This action affords a satisfactory explanation of all the characteristics of diverging nozzles observed by Hartshorn.

### Section III.—The Existence of a Scale Effect in the Flow through Geometrically Similar Nozzles.

The effect of the changes in dimensions of the nozzle on the pressure and discharge characteristics described above raises the question whether the flow through nozzles at speeds above the velocity of sound may not be affected by the viscosity of the air, since this would be a necessary accompaniment of an effect due to the linear scale of the nozzle. The results of changes in dimensions

fig. 6, also afford a satisfactory check on the observations, described in Section I, of the movement, with variations of  $p_r/p_0$ , of the section at which the critical pressure exists. It will be seen that at 40 cms. of mercury, which is the critical pressure in this case, the position of the section is 0.254 cms. in front of the orifice for  $p_r/p_0 = 0.527$ , and moves to a position 0.15 cms. in front of it when the ratio has fallen to 0.38.

It may be remarked that the change in the rate of discharge between values of  $p_r/p_0$  of 0.2 and 0.537 taken from the curve of fig. 6 is of the order of 10 per cent. From Table II it will be seen that this is in close agreement with the measured changes of area of the minimum section of the jet. This is satisfactory evidence that the velocity at the minimum section of the jet remains invariable, as it should do according to the theory.

The results of a similar series of observations on a diverging nozzle of throat diameter 0.615 cms. and a diverging outlet of total angle  $2^\circ 52'$ , are shown in fig. 7, in which are plotted the values of the rate of discharge, the pressure at

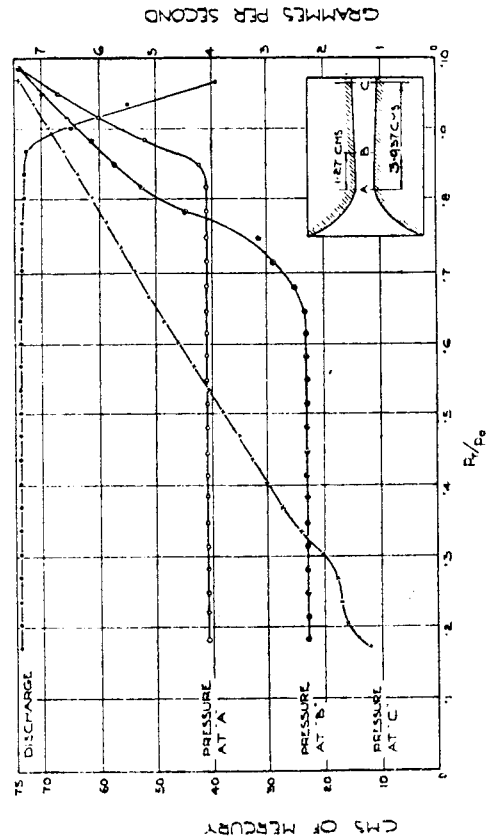


Fig. 7.

the axis of the jet at the least section of the nozzle, and the pressures at the wall of the nozzle at two points distant respectively 1.27 and 3.81 from the throat. From the curve of discharge it will be seen that this bears a close resemblance to that observed by Hartshorn for his nozzles of  $4.4^\circ$  and  $4.6^\circ$  angles of divergence in which the discharge appears to be constant up to a value of the receiver pressure equal to 80 per cent. of the initial pressure. There is, however, in the present experiments a small but perceptible fall in the discharge before this stage is reached, and corresponding with it there is also a slight increase in the throat pressure. There would appear to be some evidence, therefore, that even in such completely enclosed jets as those in diverging nozzles, there is a very slight movement of the section of critical pressure down-stream as the value of  $p_r/p_0$  increases, with a consequent perceptible decrease in the discharge. The plotted pressure variations at different distances along the

hitherto discussed, cannot, of course, be taken to prove that the conditions for dynamical similarity in the flow must include some unknown scale factor, for the reason that geometrical similarity in the various nozzles tested did not exist. In this connection it may be pointed out that the conditions for dynamical similarity of flow throughout the nozzles are:—

(1) The nozzles must be geometrically similar.

(2) At similarly situated points in the outlets (a) the product of the linear dimension and the speed divided by the kinematic viscosity, and (b) the ratio of the speed to the velocity of sound, must have identical values, i.e.:—

$$(a) \quad \frac{v_1 l_1}{\nu_1} = \frac{v_2 l_2}{\nu_2};$$

$$(b) \quad \frac{v_1}{V_1} = \frac{v_2}{V_2}.$$

It is generally assumed that when the speed is in the neighbourhood of the velocity of sound, as in the cases under consideration, the effect of the viscosity of the air is negligible, i.e., condition (a) may be ignored as an essential for similarity of flow, but as far as the writer is aware, experimental evidence bearing on this point appears to be lacking. It was decided, therefore, that as the method of observation described in the last section was exceptionally suitable for testing the above assumption, a series of tests on geometrically similar diverging nozzles should be made. In such tests it was clear that, provided the initial pressure and temperature of the air supply remained constant, the pressure distributions in such nozzles should be identical for identical values of  $p_1/p_0$ , if dynamical similarity in the flow was independent of condition (a).

Three diverging nozzles were prepared for the tests. The diameters at the throats were 0.61, 0.305 and 0.152 cm., respectively, and pressure holes were made in the walls at distances of 2.08 and 6.46 throat diameters from the throat.

The results of the tests on these nozzles are shown in fig. 8, in which for the sake of clearness only the pressure variations at the two points in the walls corresponding to the changes in the receiver pressure are plotted.

It will be seen that in the case of the pressure at the wall of the nozzle at 2.08 diameters from the throat, the steady pressures in the stage during which the nozzles are running full are different in amount, and the values of  $p_r/p_0$  at which the break away of the flow from the wall takes place are also different. The latter phenomenon is much more marked in the case of the pressures at 6.46 diameters from the throat. At this point the largest nozzle is running full up to a value of  $p_r/p_0$  of 0.45, whereas the flow has failed in the case of the smallest nozzle in the neighbourhood of  $p_r/p_0 = 0.10$ .

It is clear, therefore, that in these experiments dynamical similarity in the flow was not preserved, and the conclusion derived from the results is that condition (a) above is necessary and probably sufficient for this purpose. It

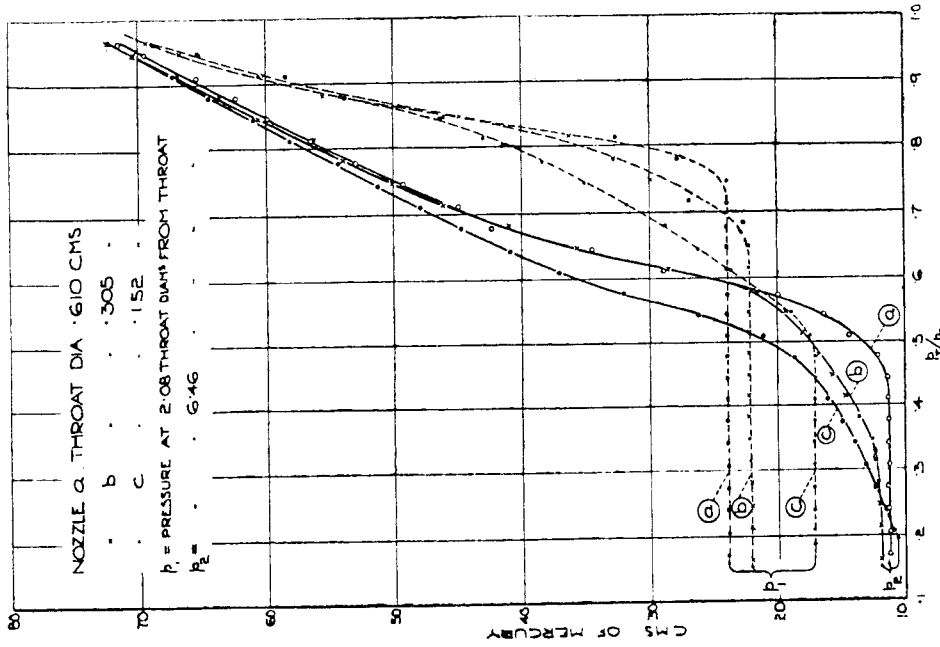


Fig. 8.—Pressures in geometrically similar diverging Nozzles.

is of interest to note that in this case instability in the flow is associated with a reduction in the value of the criterion  $v/\nu$  instead of an increase in this quantity as in the case of the breakdown of steady motion into turbulence in the case of a fluid flowing through a channel with parallel boundaries.

It follows, therefore, that, since a reduction in the value of  $v/\nu$  can equally be made by an increase in the kinematic viscosity of the fluid, a similar effect to that shown in fig. 8 for nozzles of different sizes should be obtained for a single nozzle in which the initial temperature of the air was varied.

The possibility that the effects shown in fig. 8 were due to small deviations from exact similarity in the dimensions of the nozzles was considered very remote owing to the care taken in their preparation, but it was thought that a check on the results by means of a variation of the initial temperature of the air entering one of the nozzles would be of value. Arrangements were, therefore, made for varying the initial temperature of the air by means of a coil of manganin wire through which an electric current could be circulated, wound

## PART II.—THE CHARACTERISTICS OF AIR JETS AT SPEEDS ABOVE THE VELOCITY OF SOUND.

### Section I.—The Measurement of the Speed.

In the case of gases flowing at moderate speeds, the most convenient and accurate method of measuring the velocity at a point is by means of the well-known instrument consisting of a combination of a pitot tube and static pressure tube. In the use of this instrument the changes in pressure velocity and density of the air stream are supposed to be given by equation (1), which for the present purpose may be written in the form

$$\frac{u^2}{2} - \frac{u_0^2}{2} = \frac{\gamma}{\gamma-1} \frac{p_0}{\rho_0} \left\{ 1 - \left( \frac{p}{p_0} \right)^{\frac{\gamma-1}{\gamma}} \right\}, \quad (3)$$

where the suffix  $_0$  refers to the undisturbed conditions of the air stream. Assuming that the stream is brought to rest at the mouth of the pitot tube, the pressure in the pitot tube will be given by

$$\left( \frac{p}{p_0} \right)^{\frac{\gamma-1}{\gamma}} = 1 + \frac{\gamma-1}{2} \frac{u_0^2}{a_0^2}, \quad (4)$$

where  $a_0$  is the velocity of sound under the conditions  $p_0\rho_0$ . For speeds up to 150 feet per second, where  $p - p_0$  is small, the formula reduces to

$$p - p_0 = \frac{1}{2} \rho u_0^2, \quad (5)$$

so that all that is then required for the determination of the speed is a knowledge of the density of the fluid and the pressure difference between the pitot and static pressure tubes. This relation has been found to hold a high degree of accuracy over the range to which it is applicable.

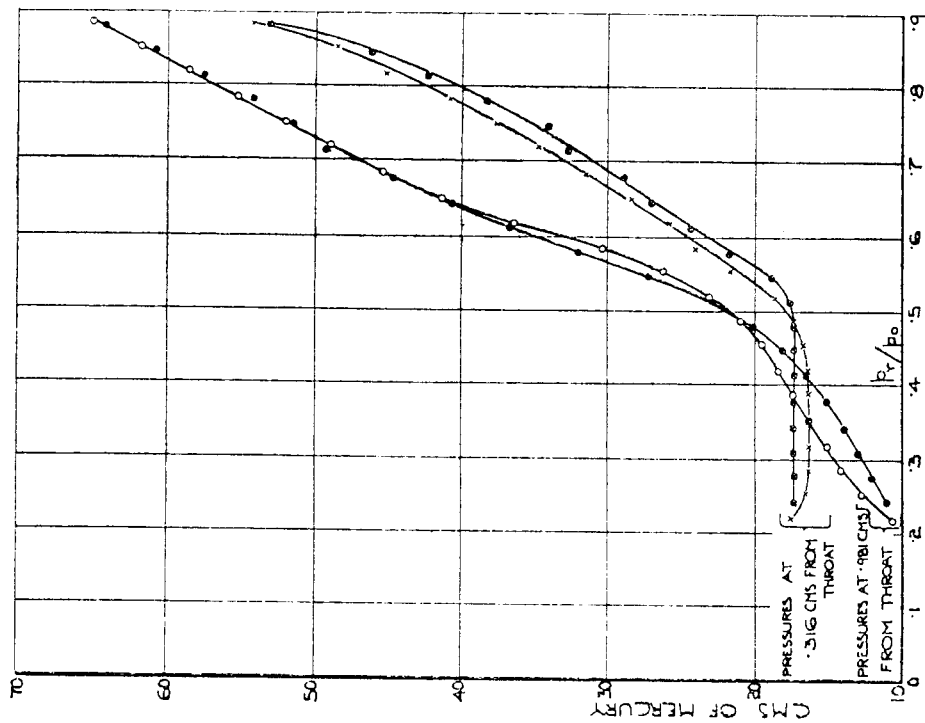
It might be assumed, therefore, that equation (4) might be applied to the determination of the velocity of jets moving at speeds exceeding the velocity of sound in a similar manner to that adopted for low velocity calculations. It is found, however, that calculations of speed so determined are not reliable in that they give values of the speed appreciably less than the real values determined by independent methods. The cause of this discrepancy was explained by the late Lord Rayleigh, who showed\* that the dynamic pressure on a small obstacle placed in a stream of air moving at those speeds will not be that due solely to the adiabatic compression of the stream impinging on it, but that this compression will be divided into two stages in one of which adiabatic conditions obtain, and in the other the conditions for a stationary wave of finite disturbance. From an application of Rankine's theory of thermodynamic waves of finite disturbance to the motion, Lord Rayleigh showed that the dynamic pressure measured at the centre of the obstacle would be related to the speed, density and static pressure of the air by the following

\* 'Roy. Soc. Proc.,' A, vol. 84 (1910).

round the inlet pipe shown in fig. 5. The temperature of the air was measured by mercury thermometers—one placed near the entrance to the nozzle and one at its outlet. The results of two tests on the 0.152 cm. diverging nozzle C—one at atmospheric temperature and the other at an initial temperature of 141° C.—are shown in fig. 9.

It will be seen that, as predicted, the effect of a rise of temperature of the air is to move the point of "break away" nearer to the throat in the same manner as a reduction in the size of the nozzle, and the results, therefore, confirm the conclusions derived from the previous tests.

It may be remarked that the dimensions of the nozzles used for these experiments are relatively small, and it is possible that in comparatively large sizes the effect of the  $vl/v$  factor may also be relatively small.



x o HOT TEST. INITIAL TEMP = 141°C — BAROMETER 76.58 CM Hg

o • COLD TEST. INITIAL TEMP = 18.3°C — BAROMETER 75.69 CM Hg

FIG. 9.—Tests on 0.152 cm. diverging Nozzle.

relation\*

$$\left(\frac{p_2}{p_0}\right)^{\frac{\gamma+1}{\gamma}} = \frac{\left(\frac{p_1}{p_0} + 1\right)^2}{4\gamma} \left\{ \frac{p_1}{p_0} \frac{\gamma-1}{\gamma} \left[ 1 + \frac{\gamma-1}{\gamma} \frac{1}{p_1} \right] \frac{p_0}{p_1} \right\} \quad (6)$$

where

$$\frac{p_2}{p_0} = \frac{2\gamma}{\gamma+1} \frac{a^2}{1+a^2} - \frac{\gamma-1}{\gamma+1} \frac{1}{a^2}$$

and  $p_2$  is the observed dynamic pressure which may be the pressure in the mouth of a pitot tube facing the stream.

The advantages of the use of a pitot tube for the measurement of the values of  $u/a$  at very high wind speeds were so obvious that it was decided to attempt to make an experimental verification of the accuracy of Lord Rayleigh's relation when used for this purpose.

To obtain a high velocity of flow a diverging nozzle 1.27 cms. diameter at the throat and having an angle of divergence of  $4^\circ 56'$  was used. At the end of the divergence the air passed into a short length of parallel channel and thence by an expanding cone into a pipe 7.6 cms. diameter in which the mass discharge could be measured. A small pitot tube was inserted at the axis near the end of the diverging cone to enable the values of  $p_2$  to be observed. This tube could be replaced by a static pressure tube for the measurement of  $p_0$ .

From the observed values of  $p_2/p_0$  and assuming a value of  $\gamma$ , the theoretical value of  $u/a$  could be calculated from equation (6) for any point in the cross section of the jet.

As no determination of the actual value of  $u/a$  at a point to the degree of accuracy required for the calculation seemed possible, it was necessary to adopt a method of mean values such as a comparison of the mean value of  $u/a$  from the pitot tube measurements with its mean value calculated from the observed mass discharge and the density, the latter quantity being estimated from the pressure and temperature of the stream. For this purpose it was essential that the nozzle should be "running full" over the experimental section, and considerable time was spent in determining a suitable angle of divergence for the nozzle and the value of the initial pressure of the air for this condition to be satisfied. Finally it was found that in a nozzle of the dimensions given above, with an initial pressure not less than 220 cms. of mercury, there was a continuous fall of pressure from the throat to the experimental section, and the pitot tube pressure over the whole section was sensibly constant except in the region close to the wall. It was considered, therefore, that the nozzle was running full and free from waves at the experimental section. An attempt was then made to measure the temperature of the flow by inserting thermojunctions in it, but any correct estimation of the true temperature was soon found to be hopeless owing to the heating up of the thermojunction by the adiabatic compression of the gas in its neighbourhood; a difficulty which was encountered in the well-known porous plug experiment of Joule and Thomson. This idea was accordingly abandoned, and consideration was given to the use of the well-known reaction method for the determination of the

momentum of the jet which, in combination with the value of the mass discharge, would give a value of the mean velocity of the jet.\* This method appeared to be more promising, and the arrangement set up for the measurement of the momentum is shown in fig. 10.

It will be seen that the nozzle is supplied with air by means of two india-rubber tubes connected to a tee-piece screwed into its inlet end, and rests on a narrow air-tight seating made at the entrance to the parallel discharge channel which is the same diameter as the outlet of the nozzle. A weigh beam is carried on knife edges attached to the bracket supporting the discharge channel, one of its arms carrying a scale pan and the other engaging with a pivot on the axis of the nozzle. By this means the vertical reaction of the jet could be measured.

In the first attempt at calibration the mean values of the speed and density were calculated from observations of the mean value of  $\rho u^2$  given by the weigh beam, the mean value of  $\rho a$  given by the discharge meter, and the known area of the channel supposed to be running full. A mean value of  $a$  was then calculated from the observed static pressure and the calculated mean density. The rate of the mean speed to the mean value of  $a$  was then compared with the mean value of  $u/a$  obtained from the pitot and static pressure measurements. This method was, of course, open to objection that the error due to the assumption that the ratio of the mean values of  $w$  and  $a$  was equal to the mean value of the ratio might not be negligible. On further consideration it was seen that this objection could be overcome by proceeding as follows:—Assume the cross section of the jet to be divided into concentric rings of width  $8r$  and the value of  $u/a$  determined for each ring from pitot and static pressure observations in each. If the momentum of the fluid passing through each of the rings is  $\delta M$  we have—

$$\Sigma \delta M = \Sigma 2\pi r \delta \rho u^2, \quad (7)$$

or  $\Sigma \frac{u^2}{r} 2\pi r \delta r = M$  the total momentum of the jet. From the observed values of  $p$  and the calculated values of  $u/a$  the summation on the left can be evaluated graphically and the extent of its agreement with the observed value of  $M$  will furnish a measure of the accuracy of the Rayleigh formula.

The observations made for the purpose of the calibration are given in Table III, in which are also given the values of the observed and calculated reactions. It will be clear that in calculating the total reaction due to the jet account must be taken of the difference of static pressure between the outside and the inside of the nozzle. The measured reaction is the difference between the vertical forces in the nozzle (1) before the jet is turned on and the external and internal air pressures are equal, and (2) after the jet is started when the external pressure will be atmospheric and the internal pressure the static pressure of the jet at the section considered. This measured reaction must, therefore, be augmented by the product of the area of the jet and the difference between the

\* 'Roy. Soc. Proc., A, vol. 84 (1910).

\* Morley, 'Proc. Inst. Mech. Engineers,' 1910.





(2) From the value of  $u/a$  given by equation VI and that of  $a$  calculated from the observed static pressure and the density calculated on the assumption of adiabatic expansion. ( $= v_2$ ).

The value of the mean speed ( $v_m$ ) over the section of the outlet was also calculated from the reaction and the mass discharge.

The observations and reductions are given in Table IV.

It will be seen that in the first two experiments the values of the calculated speeds at the axis of the nozzle are in good agreement with each other, and also the mean speed over the section is what would be expected from the comparatively slight retardation which is known to take place at the walls, i.e., the mean values are 96 and 97 per cent. of the speed at the axis. Further, the pressure at the walls is appreciably lower than the pressure at the axis, as it should be. On the other hand, in experiment (3) the pressure at the walls is considerably higher than at the axis indicating the commencement of the breakdown of the motion and the values of the calculated speeds are not in approximate agreement. It is clear, however, that the break away of the flow from the walls has not become considerable at this stage, since the mean speed is still of the same order as the calculated speeds. In the last experiment the break away is apparently complete and the disagreement between the calculated values of the speed is still more marked.

The general conclusion from these experiments is that so long as a diverging nozzle runs full the flow may be taken to be sensibly adiabatic throughout except in the immediate neighbourhood of the walls.

#### Section II.—The Pressure and Velocity Distribution in High Speed Jets emerging into Still Air.

The characteristics of air jets emerging from a circular orifice into the atmosphere have been investigated by Emden\* by means of the shadow method of Dvorak, in which a point source of light is used to throw a shadow of the jet on a screen. On examination of the features of the shadow it was found that when the speed of the jet attained a definite value a series of bright equidistant discs became visible. On increasing the air speed the distance between the discs increased and diagonal lines connecting their extremities also appeared. At still higher speeds the discs gradually broadened out into a wing-shaped formation and the diagonals became curved. These characteristics are illustrated in fig. 12, in which is shown a series of shadowgraphs of jets from nozzle No. 2, fig. 2, at increasing speeds. The discs were identified by Emden with stationary waves in the jet and their first appearance with the attainment of the velocity of sound in it, but his conclusions that this velocity cannot be exceeded and that the pressure in the emergent jet is uniform

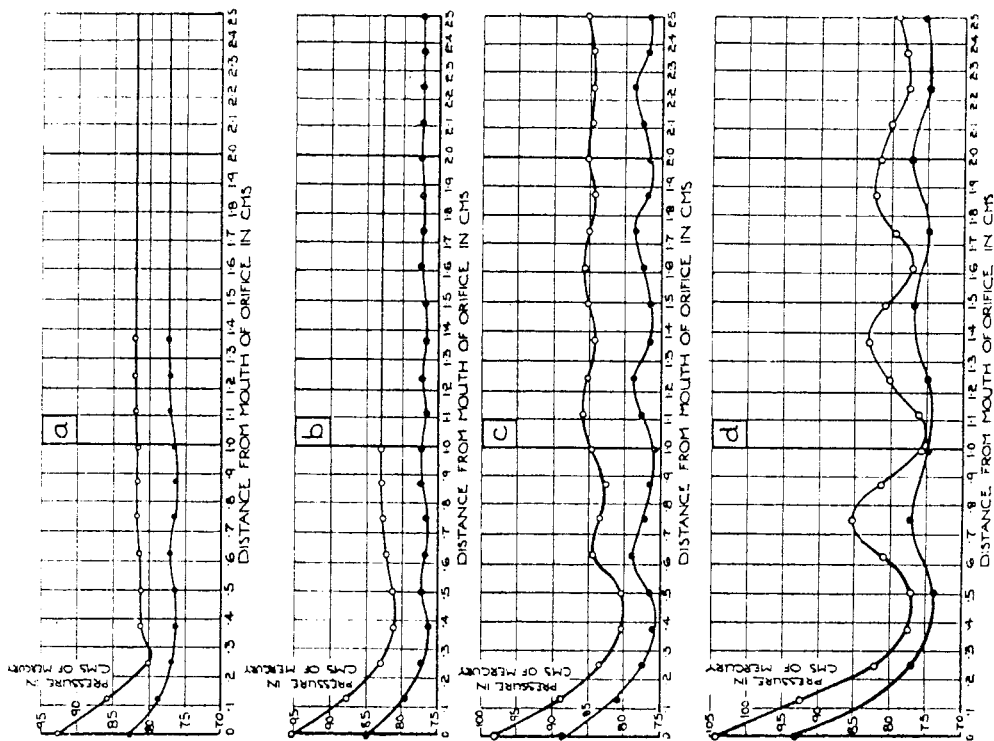


FIG. 11.—Pressure Distribution in Jets from No. 2 Orifice. Compare Plate 6, fig. 12.  
o = along axis; . = along line parallel to axis and 0.51 cm. from it.

Initial Pressures in cms. of mercury: a = 143.0; b = 147.7; c = 153.1; d = 157.8.

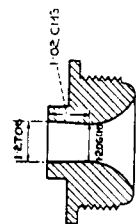
and atmospheric have been shown by Lord Rayleigh to be erroneous.\*

A theory of the formation of stationary waves in jets has been developed by Prandtl.† According to this theory the waves originate at the outer edge of the orifice and their characteristics will depend on the ratio of the pressure of the jet on emergence ( $p_1$ ) to that of the atmosphere ( $p_2$ ). If  $p_1 > p_2$  waves of rarefaction will proceed from the edge of the orifice inwards, the velocity at any point being such that its component perpendicular to the direction of uniform density is that of sound at the temperature and pressure existing there. It is also assumed that these waves of rarefaction will undergo reflection

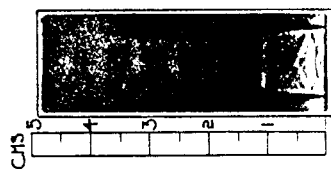
\* 'Phil. Mag.' vol. 32, pp. 177-187 (1916).

† 'Physikalische Zeitschrift,' p. 599 (1904), and p. 23 (1907).

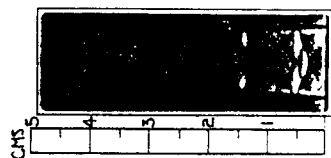
\* Wiedeman's 'Annalen,' Bd. 69, pp. 264 and 426 (1899).



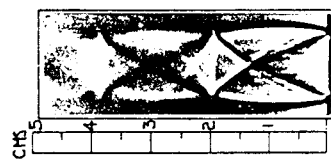
No. 1.



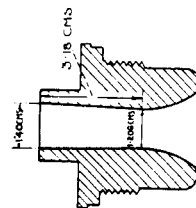
Initial Pressure: 170.7 cms.



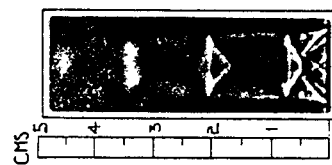
Initial Pressure: 185.4 cms.



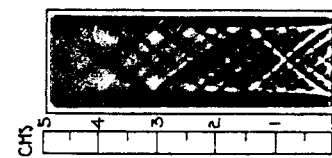
Initial Pressure: 304.8 cms.



No. 2.

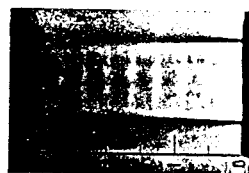


Initial Pressure: 235.7 cms.

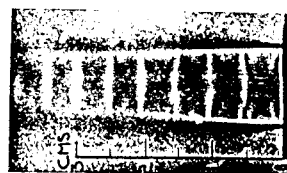


Initial Pressure: 304.8 cms.

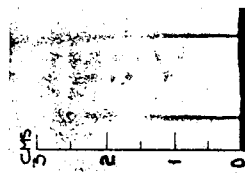
FIG. 15.—Shadowgraphs of Jets discharged into the Atmosphere from Diverging Nozzles.



(a)



(c)



(b)

(d)

FIG. 12.—Shadowgraphs of Jets from No. 2 Orifice. Compare fig. 11.  
Initial Pressures in cms. of mercury:  $a = 143.0$ ;  $b = 147.7$ ;  $c = 153.1$ ;  $d = 157.8$ .



FIG. 13.—Shadowgraph of Jet from No. 2 Orifice. Initial Pressure: 225 cms.  
Compare fig. 14.

at the boundary of the jet and become waves of condensation. On the other hand, when the pressure on emergence is less than that of the atmosphere, the initial disturbances are waves of compression which become waves of rarefaction from the boundary of the jet.

The value of the wave-length was deduced by Prandtl from the theory of the small disturbances in a cylindrical jet in which the motion is steady and under the assumptions of the existence at the boundary of atmospheric pressure and a discontinuity of velocity. Taking the axis of  $y$  as that of the jet and assuming the velocity along the axis  $V$  to be nearly constant, while  $u$  and  $w$  are small, the solution of the equations of motion gives

$$v = V + H \cos \beta y J_0 \left\{ \beta r \sqrt{\frac{V^2}{a^2} - 1} \right\}, \quad (8)$$

so that the wave length of the periodic features along the jet is given by  $\lambda = \pi/\beta$ .

At the boundary of the jet since  $p$  is constant  $v$  is constant and, therefore,

$$J_0 \left\{ \beta R \sqrt{\frac{V^2}{a^2} - 1} \right\} = 0. \quad (9)$$

The lowest root of this is 2.405, so that

$$\lambda = 2.61R \sqrt{\frac{V^2}{a^2} - 1}. \quad (10)$$

In comparing the wave-length given in this formula with the measured values obtained from photographs of the jet, which were somewhat similar to those shown in fig. 12, Prandtl assumed that the values of  $V/a$  could be estimated with sufficient accuracy from the inclination to the axis of the jet. of the characteristic lines of the photograph indicating positions of maximum or minimum condensation, and obtained what he considered to be a satisfactory check on the theory.

For the purpose of the present investigation shadowgraphs of the jets emerging into the atmosphere from nozzles of different forms and at different initial pressures were obtained by the method described above, and the interior of the jet was then explored by means of the static pressure and pitot tubes.

These observations were sufficient to determine the length and amplitude of the stationary waves and the variations in the values of  $V/a$  along and at right angles to the axis.

In the first series of tests the converging parallel nozzle No. 2, fig. 2, was used. The variation of the static pressure was measured along the axis and also along a line parallel to it in the neighbourhood of the boundary for four different values of the initial pressure, and the results are shown plotted in figs. 11 (a), (b), (c) and (d); the corresponding shadowgraphs are shown on Plate 6, fig. 12 (a), (b), (c), (d). It will be seen that the amplitude and length of the waves diminish as the initial pressure is diminished, the disturbances eventually vanishing when the pressure in the jet on emergence exceeds the critical value  $0.527 p_0$ .

The results, therefore, confirm Emden's conclusions as to the nature of the motion, but definitely disprove his prediction of a uniform pressure and, as

will be seen later, of a velocity equal to that of sound throughout the jet. There is also a marked difference between the mean pressure at the axis and that in the neighbourhood of the boundary, and this difference is still considerable even when no wave formation is apparent.

An interesting effect of this radial pressure gradient is that the velocity of sound is attained at the boundary before it is reached at the axis, and it would, therefore, be expected that the waves would first be detected at the boundary. In the case of (a), figs. 11 and 12, this is seen to be the case.

The corresponding values of  $V/a$  were calculated from the static pressure of the pitot tube pressure observations by means of the Rayleigh formula, and are shown plotted in fig. 14 for a higher value of the initial pressure.

Comparing the observed distribution of pressure with the characteristic features of the shadowgraphs, it will be seen that the position of the discs corresponds with the sections of maximum condensation, except in the case of (a), figs. 11 and 12, where the variations of pressure, although perceptible, were too small to enable the outline of the wave to be determined with precision. Further, these positions also coincide with those at which the calculated value of  $V/a$  is unity, which is a satisfactory explanation of the persistence of the "disc" effect even when the average velocity is considerably above the velocity of sound.

It will be clear that this condition prevents any precise comparison of the observed wave-length with the theoretical wave-length obtained by Prandtl's investigation, which assumes a constant value of  $V/a$  throughout the wave. It may be remarked, however, that the observed wave-length does correspond with a value of  $V/a$  intermediate between the maximum and minimum values attained. Thus in the case illustrated in figs. 13 and 14 the wave-length is 1.4 cms., so that the solution of equation (10) gives  $V/a = 1.33$ . The observed values of  $V/a$  throughout the wave ranged from 1 to 1.62.

Shadowgraphs were also taken of jets discharged from diverging nozzles, and these are illustrated in fig. 15.

In these cases it was possible by varying the initial pressure to make the emergent pressure of the jet either greater or less than atmospheric, and so to vary the position relative to the mouth of the nozzle of the section of maximum condensation, as will be seen from the shadowgraphs. It will be seen that these shadowgraphs indicate the existence of a complicated series of waves proceeding from the interior of the nozzle in addition to those formed at the outer edges. It would be anticipated from the work described in the preceding sections that the internal series of waves would disappear for a sufficiently high value of the initial pressure, and this appears to have happened in the last experiments on nozzle No. 1. In the case of No. 2 nozzle the angle of divergence was too great for a waveless jet to be formed at the maximum initial pressure available.

From the Prandtl theory of the formation of waves it might be supposed that in the case of a jet emerging into the atmosphere at a uniform pressure over its whole section equal to that of the atmosphere no waves would be

detected even when the velocity was considerably above that of sound. An attempt was made to verify this assumption by fitting a parallel portion to the end of a diverging nozzle and carefully watching the shadow of the jet on the screen, while the issuing pressure, as measured on the edge of the nozzle, was gradually raised from a value below to a value above the atmospheric pressure. This was repeated several times, but no change in the wave pattern

could be detected in changing from a condition in which the atmospheric pressure was greater than that of the jet to one in which it was less. It was concluded that the theory was inadequate to account for, at any rate, all the wave characteristics observed.

The investigation was carried out in the Engineering Department of the National Physical Laboratory, and the author desires to acknowledge the valuable assistance of Mr. R. W. Fenning in obtaining the shadowgraphs of the jets. The author's thanks are also due to Mr. A. Eaton and Mr. H. Robinson, of the mechanical staff of the Department for assistance in making the experiments.

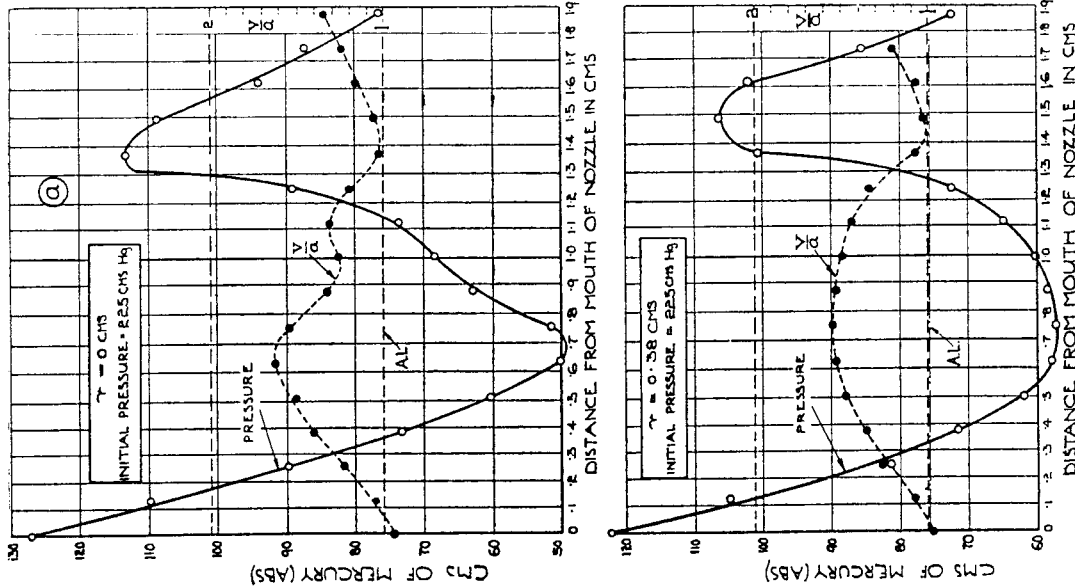


Fig. 14.—Pressure and Velocity Distribution Jet from No. 2 Orifice discharging into Atmosphere. Compare Plate 6, fig. 13.

*The Air Ejector.*

By A. D. Tutun, B.Sc., A.R.T.C.

## ABSTRACT.

This paper deals with the general characteristics of the air ejector. Except for a few published results on the performance of standard units, information on the subject is scarce, and the experimental lines followed in this investigation have been arranged to provide a systematic examination of the effect of the various dimensions on the stability and efficiency of operation.

Diffuser losses are deduced by analysis from the tests, and the main questions arising in the combination of the operating and suction fluids are discussed. Photographs of several aspects of the fluid action are shown.

*Introduction.*—The air ejector is now an indispensable adjunct to the high-efficiency steam turbine unit. With it the very high condenser vacuum necessary is made possible. It is very simple and reliable, can be placed in any convenient position, and does not require special foundations. It involves no moving machinery, requires little attention, and can be operated to its fullest capacity without stressing. According to most authorities, it also compares favourably with the reciprocating pump in the matter of steam consumption, and the only reason why it was not adopted earlier was the lack of interest in the production of a very high vacuum, the special benefits of which were not then capable of exploitation.

The ejector may be defined as a pump in which the air to be compressed is entrained by one or more jets of fluid which pass through the entrainment space at a very high velocity, the combined stream then passing into a tube called the diffuser, in which it is compressed at the expense of its kinetic energy. Steam is generally the operating fluid since it is easily available, but some manufacturers abroad claim that the water jet has its advantages.

At first, the ejector had several disadvantages. When only the single stage was employed for compression ratios above 1.8, it was found that the diffuser throat diameter required for the ejector to start was greater than that necessary for working, so that a compromise had to be made, which was not always satisfactory. Greater success was obtained with the ejector in conjunction with the ordinary reciprocating pump as a "vacuum-augmenter," patented by Parsons, but it was not until the adoption of the two-stage plant that its use became widespread. Each unit has a compression ratio under the maximum 1.8, and an intercondenser is often introduced to deal with the operating steam of the first stage.

Very little is understood about the working of the ejector, though it has been generally accepted that the suction fluid is entrained by friction. This led to the adoption of a cluster of very small bore steam nozzles in the form of a ring, in place of the single nozzle, in order to increase the surface area of the jet. Lately the advantages of this type have been questioned, and the simple friction theory has consequently

lost support. It is evident that with the theory in such an elementary state of development, the design of a plant to allow the entrainment process to be carried out in the most efficient manner is largely a matter for experiment. Naturally this has resulted in a complexity of designs. Water-cooling the throat of the diffuser is claimed to increase the efficiency and ensure stability, while the latter can also be obtained by the rather wasteful method of allowing atmospheric air to enter the diffuser at the throat and so ensure that the section is always filled.

The aim of this research has been first of all to obtain experimentally the most efficient arrangement, and by varying the leading dimensions in a series of tests to ascertain their effect on the operation of the ejector. With the dimensions which will give the best possible results for the particular conditions of working, the performances can be analysed to obtain the balance of energy, after assessing the losses which are known to exist. By this means it is hoped to reach definite conclusions in connection with the combining of the streams and their compression in the diffuser. The latter process is of particular interest, as the results of research on divergent nozzles by Professors A. L. Mellanby and W. Kerr,<sup>1</sup> and by the author,<sup>2</sup> show that the compression of a high-speed jet is accompanied by considerable losses.

*Experimental Plant.*—The air ejector generally operates on steam, which is usually available at a pressure suitable for working, but for an investigation into the fundamental principles of the ejector the use of a single fluid both for operating and for compression would appear to be the most satisfactory arrangement, with a single stage of operations. Air is supplied up to a maximum pressure of 100 lb. per sq. in. gauge in the laboratory by a two-stage compressor, which is quite suitable for the tests, and suction air can be drawn direct from the atmosphere.

Since the tests are intended to cover a wide range, more than one nozzle is required. Each nozzle is made of machined gun-metal, and is to standard so far as entry curve, throat diameter, and length are concerned. It is well known that a nozzle which over-expands, or one which under-expands considerably, loses efficiency, so that to accommodate the range in pressure ratios, the nozzles, three in number, have a different divergent taper. If, then, for each test the nearest under-expanding nozzle is chosen, the loss due to this cause will be negligible. The outlet area corresponding to a given ratio is calculated from theory, and allowance has to be made for a  $\frac{1}{8}$ -in. search tube which passes through the nozzle. Details are given in Fig. 2, where in order that the passage of the suction air may not be impeded, the nozzles are tapered down on the outside.

<sup>1</sup> This Journal, 1925.<sup>2</sup> This Journal, 1926.

The nozzles are screwed to fit a  $\frac{3}{4}$ -in. pipe about a foot in length, which is machined and ground to fit a gland in the combining chamber; a circular box flanged to receive the diffuser plate. The diffuser is screwed into this plate, and the whole can slide along the nozzle supply pipe, on which a scale of inches is marked off. The apparatus is mounted on a long horizontal arm pivoted at a swivel joint, and through this passes the air supply from the compressor receiving-tank. This enables the ejector to move freely in a vertical direction, and so the reaction

of the air leaving the diffuser can be measured on a balance, just as in the nozzle reaction tests described in the paper on nozzle compression losses previously referred to. A pressure gauge and a thermometer to determine the initial condition of the operating air are included.

Measurement of the suction air, or leakage air when referred to a condenser system, is effected by means of a series of apertures leading into the combining chamber. The arrangement of these apertures is found later to have no effect on the working of the diffuser, as demonstrated by setting them at the opposite end of the combining chamber, or by placing a baffle plate in the path of the incoming air.

Theoretically, the design of a diffuser should be followed out on the same lines as that of a nozzle, but the characteristics of a combined jet are insufficiently determinate to enable more than a rough estimate to be made. Thus, when the velocity of the combined jet is above the critical, the diffuser should be convergent at first and then divergent, for the conditions are just the reverse of those in the divergent type of nozzle; actually, this is modified in most types by a parallel or very gradually tapering extension of the throat section. The diffuser throat diameter can be only roughly approximated to by calculation, and no fixed rule can be given for the parallel length of the diffuser and its distance from the nozzle. For the particular requirements of the tests, it is, therefore, necessary to find out the "optimum" values of these dimensions for each case.

The overall length of the diffuser cannot be varied directly in a diffuser of the convergent entry and divergent outlet type, but its effect can be gauged in one of the simple parallel type by moving the nozzle along the diffuser axis. This is effected by screwing a parallel tube, 12 inches long, which can be bored out to various diameters, into the diffuser plate. Readings are taken of the chamber pressure for a range of distances of the nozzle outlet from the diffuser outlet, for various conditions of operation. The results show that unless the boundary of the jet is actually clear of the diffuser altogether the diffuser length has little influence on the working of the ejector, for in each case the chamber pressure rapidly attains a minimum steady value as the nozzle is brought further from the diffuser outlet. The point where this value is reached varies somewhat with different conditions, showing their

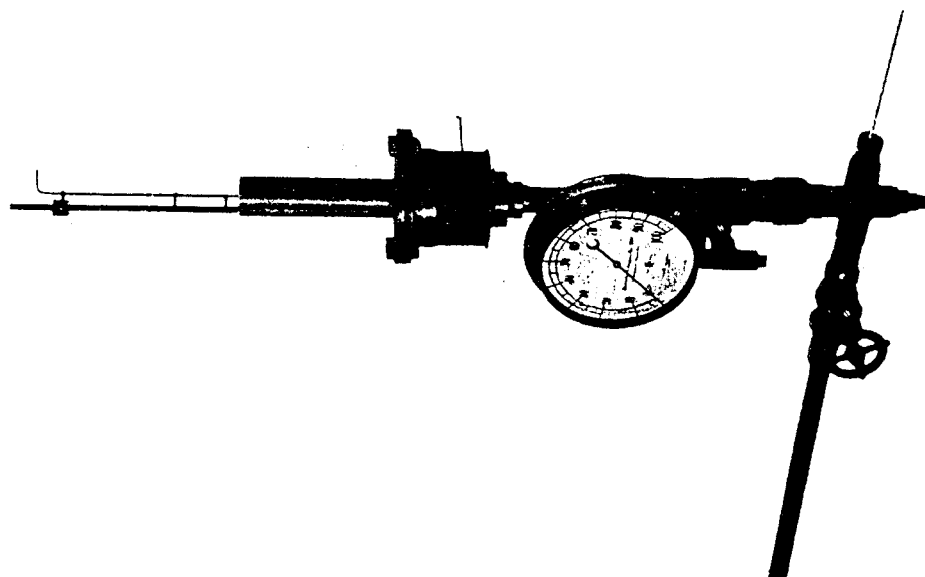


FIG. 1.—Experimental Air Ejector.

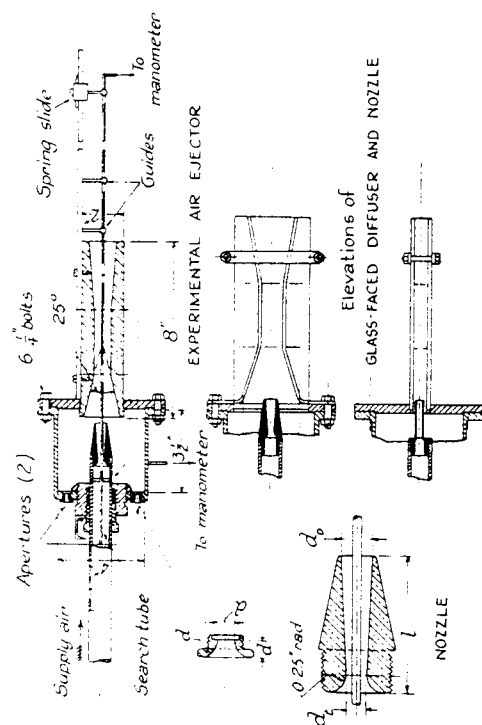


FIG. 2.

effect on the spread of the jet, but it may be assumed with safety that a parallel diffuser length of about four diffuser diameters will cover all possibilities. This feature of a steady minimum chamber pressure above a certain critical length is of much interest and importance.

From a further preliminary investigation on the subject of diffuser diameter, the critical importance of this dimension is at once apparent, and, as there is no means of making it variable, the whole series of tests to be run on the ejector will depend on the choice of a set of diffusers of suitable diameter. Later experience will show that four diffuser diameters provide sufficient optimum values for the series of tests.

There remain to be decided the convergent entrance angle and the divergence of the diffuser. A cone angle of  $25^\circ$  seems to be practically universal in the first case—a result of experience—while the latter is more influenced by the delivery conditions than by anything else, and has no direct effect on the ejector working. The diffuser is bored out of a 2-inch gun-metal cylinder to the first throat diameter, and the convergent and divergent sections turned out to leave a parallel portion four times the diameter in length, and an outlet area of, say, three times that at the throat. Successive diameters are obtained by further machining, the divergent cone being turned down in each case until the parallel length is equal to four diameters and the outlet area ratio is the same as before.

Pressures along the axis of the nozzle and diffuser are determined by means of a simple search-tube apparatus. A slide attached to the end of the tube moves up and down a graduated guide-rod, which is screwed to the side of the diffuser tube. Comparative rigidity of the tube is obtained by fixing guides in such positions as will result in no interference with the air stream. A  $\frac{1}{2}$ -in. hole is drilled in the side of the tube, and connection is made to a mercury manometer. So that the nozzle area may remain unchanged by the movement of the tube, the latter must be of exactly uniform cross-section, and it must be so long that when the hole is opposite the diffuser outlet the tube remains in the lower guide.

A table of nozzle, diffuser, and suction aperture sizes is appended.

TABLE OF DIMENSIONS (in inches).

Nozzles.			Apertures.		Diffusers.	
$d_t$	$d_n$	$l$		$d$		Throat Dia.
1	0.289	2.01	1	0.0693	A	0.629
			2	0.1245		
2	0.289	2.00	3	0.196	B	0.694
			4	0.251	C	0.750
3	0.289	1.96	5	0.299		
			6	0.352	D	0.788
Search Tube Dia.—0.135						

*Theory of the Ejector.*—In explaining the theory of the air-operated ejector, the following symbols for the properties of the air are used:—

- $P$  = absolute pressure in lb. per sq. in.  
 $V$  = volume in cubic ft. per lb.  
 $T$  = absolute temperature in  $^\circ\text{F}$ .  
 $v$  = velocity in ft. per sec.  
 $M$  = flow of operating air in lb. per sec.  
 $M'$  = flow of suction air in lb. per sec.  
 $E$  = kinetic energy per lb. operating air.  
 $p$  = pressure ratio referred to the nozzle supply pressure.  
 $r_a$  = pressure ratio referred to atmospheric pressure.

The suffix (1) denotes the nozzle supply,

(2) the nozzle jet before combining,

(3) the combined stream before compressing,

(4) the discharge stream.

If the inlet velocity to the nozzle be neglected, the kinetic energy at the outlet is given by

$$E_2 = \frac{144n}{n-1} P_1 V_1 \left\{ 1 - r^{\frac{n-1}{n}} \right\} \quad (1)$$

from standard nozzle theory, where  $n$  is the index of expansion. It has to be modified to allow for friction losses, which are represented by the term " $k_n$ ". This term is equivalent to an energy loss just as  $(1 - r^{\frac{n-1}{n}})$  is equivalent to the energy in adiabatic expansion,<sup>3</sup> so that, when  $n$  is given its value of 1.40 for air, and substitutions are made,

$$E_2 = 186 T_1 (1 - k_n - r^{\frac{n-1}{n}}) \quad (2)$$

The loss term is obtained from the dimensional equation

$$k_n = c \int_0^l \frac{p}{A} \left( 1 - k_n - r^{\frac{n-1}{n}} \right) dx \quad (3)$$

where  $\frac{p}{A}$  is the hydraulic mean depth at a point, and  $dx$  an element of length. The constant  $c$  has a value for machined nozzles of about 0.005. Values of  $k_n$ , the loss up to a point, are assumed for the moment in the integrand, and the curve of  $\frac{p}{A} \left( 1 - k_n - r^{\frac{n-1}{n}} \right)$  is integrated for the whole length of the nozzle, as the jet is in contact with the walls throughout its length. A small factor, estimated at 0.004, is added to include entrance losses. A closer approximation to  $k_n$  is obtained from this integration, so that a repetition of the process will enable the loss to be determined more accurately.

From the principle of the conservation of momentum, it is known that the sum of the momenta of the nozzle jet and the suction air is equal to the momentum of the combined stream, in any one direction. This assumes that there is no change in pressure and no losses due to combination or to reaction from the sides of the diffuser. Since the suction air quantity is small when compared with the area of entry into the diffuser, its momentum is quite negligible, so that the momentum

<sup>3</sup> McIlhenny and Kerr, "Stream Action in Simple Nozzle Forms," Brit. Assoc., Sect. G, Aug., 1920.

equation is

$$Mv_2 = (M + M')v_3 \quad (4)$$

$$\therefore v_3^2 = \left( \frac{M}{M + M'} \right)^2 v_2^2 \quad (5)$$

$$\therefore E_3 = \frac{M}{M + M'} E_2 \quad (6)$$

This is an expression for the kinetic energy of the jet which is available for compressing the combined stream.

The state of the combined stream before compression can be determined from theory, for the nozzle outlet conditions correspond to adiabatic expansion with friction reheat, and in the combining of the streams there is a further reheat equivalent to the theoretical energy loss in combining. A theoretical value for the throat area is often calculated from the velocity of the stream at this point, for

$$A_3 = 144 (M + M') V_3 / v_3, \quad (7)$$

assuming that the diffuser throat is at chamber pressure, which is seen not to be the case from pressure readings recorded later, especially when the ejector is working at high vacuum.

The kinetic energy of the combined stream absorbed by compression up to atmospheric pressure is given by the equation

$$\text{Work done per lb. combined air} = \frac{144n}{n-1} \cdot P_3 V_3 \left( \frac{1 - r_a^{n-1}}{r_a^n} \right), \quad (8)$$

$$\text{or, Work done per lb. operating air} = \frac{M + M'}{M} \cdot \frac{144n}{n-1} \cdot P_3 V_3 \left( \frac{1 - r_a^{n-1}}{r_a^n} \right) \quad (9)$$

The diffuser friction loss term  $k_a$  is calculated in the same way as that of the nozzle, by integrating the energy curve. Since the compression loss in the diffuser is unknown, it is possible only to approximate to the energy at a point, but the friction loss is a comparatively small one so that no great error arises. With the friction loss added, and substituting for  $n$ , the equation now becomes

$$\text{Work done per lb. operating air} = \frac{M + M'}{M} \cdot 186T_3 \left( 1 + k_a \frac{r_a^{0.286}}{r_a^{0.286}} \right) \quad (10)$$

The residual energy in the stream is deduced from the measured reaction of the ejector. If  $R$  is the reaction in lb., then

$$R = (M + M') v_4 / g \quad (11)$$

$$\text{i.e. } E_4 = \frac{gR^2}{2M(M + M')} \quad (12)$$

The work done in compression added to the residual energy  $E_4$  should be equal to the available energy  $E_3$  in equation (6) if there are no other losses in the operation, so that the difference will be equivalent to the losses unaccounted for.

*Method of Testing.*—Before proceeding with the tests, the temperatures for corresponding pressures at the nozzle inlet, with the compressor at normal running temperature, are plotted on a curve. The values are substituted in the flow formula  $M = 0.534 P_1 A_1 / \sqrt{T_1}$ , and

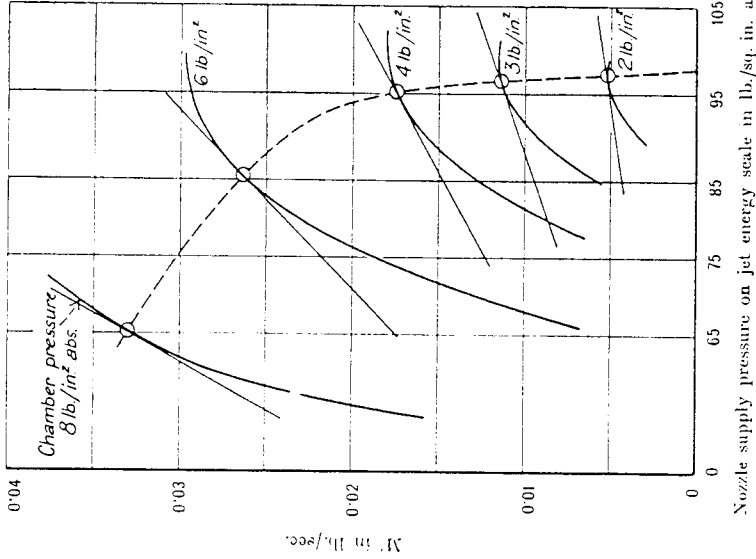


FIG. 3.—Curve of Maximum Efficiency, Diffuser "B."

with a discharge coefficient of 0.97 curves of the nozzle discharge on a pressure base are obtained.

The first object of the tests is to determine the operating conditions suitable for each diffuser diameter. With the first diffuser size, readings of the chamber pressure are taken at a diffuser distance from the nozzle which gives the best results for a range of nozzle supply pressures and suction apertures. The chamber pressures are plotted on a base of suction quantity, and curves of constant nozzle pressure are drawn through the points. From these are derived curves of suction quantity at constant chamber pressure, on a base of nozzle supply pressures scaled off in units of energy expended per lb. of operating air in expanding to atmospheric pressure. The points of contact of tangents drawn from the origin to the curves give readings of the suction quantity and nozzle pressure which represent the most efficient conditions of working for each chamber pressure, *i.e.*, the maximum ratio of work done to energy supplied. The reason for choosing the chamber pressure as constant will be evident, for the operating vacuum of a plant in practice is the first item to be fixed in specifications, the others being more or less a matter of choice. A curve drawn through the points of contact enables the



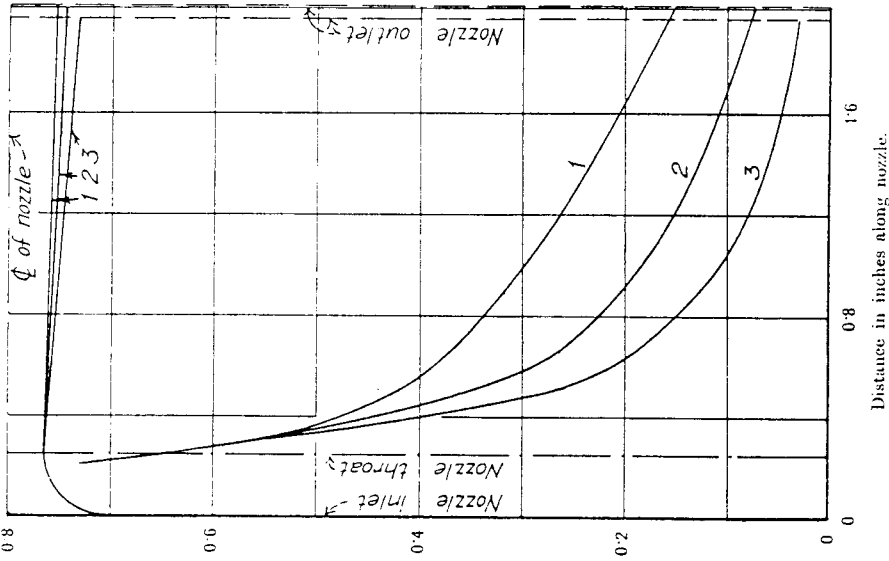


FIG. 4.—Pressure Ratio Curves, Nozzles 1, 2, and 3.

nozzle supply pressures corresponding to the suction quantities given by the various apertures to be read off, as will be observed by referring to the specimen set of curves in Fig. 3.

Under the conditions of maximum efficiency the ejector is now operated, and readings taken of the nozzle supply pressure, the chamber pressure, the atmospheric pressure, the search tube pressures at suitable intervals along the axis of nozzle and diffuser, and, in addition, the reaction of the outlet stream. The procedure is repeated for each diffuser diameter, and the results tabulated. Thereafter the calculations indicated by theory are followed out to determine the balance of energy.

Pressure ratio curves for the nozzles and one of the diffusers are given in Figs. 4 and 5.

*Effect of Dimensions.*—The effect of the length of the diffuser has been dealt with in the preliminary tests, on the simple parallel type of diffuser, and the outstanding observation made was the minimum parallel length required. This value is modified to some extent by the amount of suction air; the more air, the more indefinite seems to be

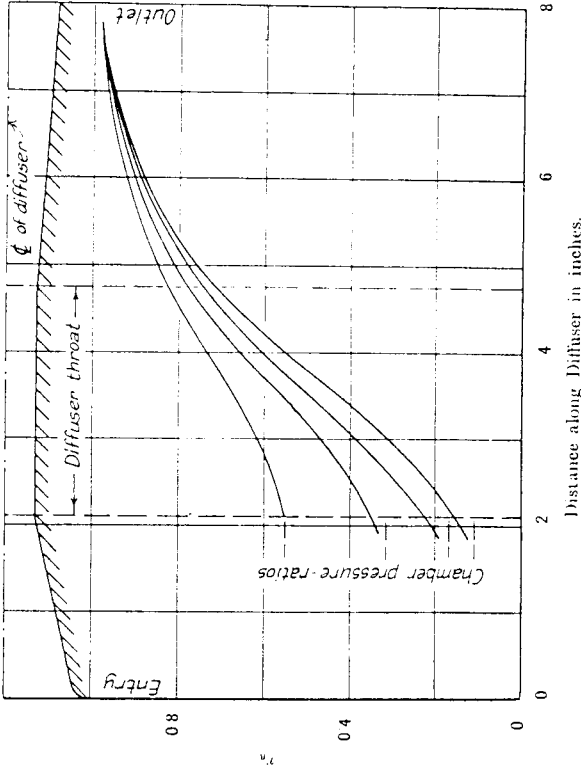


FIG. 5.—Pressure Ratio Curves, Diffuser "E."

the boundary of the jet, and hence the required diffuser length. Increased nozzle pressure requires a slightly longer diffuser, but this is partly accounted for by an increase in the cross-section of the jet, and would not be so apparent if the diffuser diameter were enlarged accordingly. In this simple type of ejector it is the diffuser section that is usually fixed, as in some forms of exhaust blower, and the jet boundary has to conform to it by the natural process of spreading out until the walls are reached. Though this type of diffuser is used only where simplicity overrules economy, its operation is seen to give some idea of the nature of the ejector action, before a study of the more efficient type of diffuser is begun.

The most noticeable fact emerging from the dimension tests is the complete dominance of the diffuser throat diameter over the working of the ejector. It is the critical and ruling dimension. This is further emphasized when it is realized that the area of the stream varies under starting and abnormal working conditions, and there is no practical means of varying the diffuser area to correspond. For this reason the ejector, in the single stage at least, cannot be termed a flexible unit. On starting, since a large volume of air at atmospheric pressure has to be dealt with, experiment has shown that a much larger area is required than for normal running.

The sectional area of the jet is influenced by various factors. Thus, the nozzle throat diameter and the inlet pressure govern the flow of jet fluid, and to this has to be added the suction air quantity. Once the flow quantity is fixed, the area of flow is governed by the relation  $V_s/r_s$ , so that at very high vacua, while  $V_s$  is increasing towards infinity and  $r_s$  slowly towards a maximum, the required area will become correspondingly large, and will vary considerably for a very small change in vacuum.

The importance of a correct diffuser area is illustrated in Fig. 3. It will be observed how rapidly the capacity of the ejector falls away when the nozzle supply pressure is reduced, at constant chamber pressure—the result of the jet area becoming too small for the particular diffuser size. Similarly, by increasing the pressure the diffuser becomes choked and functions improperly. It is obvious that the practice of making the diffuser oversize to assist in the starting of the ejector will mean a considerable sacrifice in efficiency when working under normal conditions.

The distance of the diffuser from the nozzle has not the same critical effect on the ejector operation. It is confined between two definite limits; when the diffuser is so far away that the jet has lost its definite boundary, on the one hand, and when it is so near that the jet does not strike the diffuser until it reaches the parallel portion, on the other. The curve in Fig. 6 records the chamber pressure for varying nozzle outlet position, and illustrates how comparatively steady it is over a considerable length. In general, it appears that for a constant nozzle pressure the distance is least when the ejector is working at high vacuum with little air suction, while increase of nozzle pressure, by increasing the dimensions of the jet, requires a proportionate increase in diffuser distance.

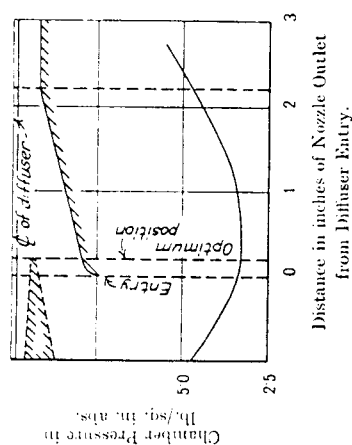


FIG. 6.—Effect of Distance between Nozzle and Diffuser.  
 $P_1 = 75$  lb. per sq. in. abs.; Suction apertures No. 2.

The convergent entry angle to the diffuser, kept constant throughout the tests at a standard angle, cannot have much effect on the entrainment action. The divergent outlet is designed to suit the discharge requirements, and any possible effect it may have on the working of the ejector could be put to test by comparing a divergent outlet diffuser with a parallel one of the same overall length. Actually, the efficiency of the ejector is found to be quite unaffected by the rate of divergence.

From the combined results of the tests an instructive chart can be evolved, as shown in Fig. 7. It is intended to show how an actual plant could be designed from specifications, *i.e.*, the nozzle throat size, the supply pressure, the amount of air to be dealt with, and the vacuum from which it has to be pumped. From the constant nozzle pressure curves of vacuum against suction quantity, the capacity of each ejector unit in the plant can be deduced, and hence the number of units required

to deal with the specified air quantity. The diffuser diameter and the throat distance from the nozzle to give the best results can then be read

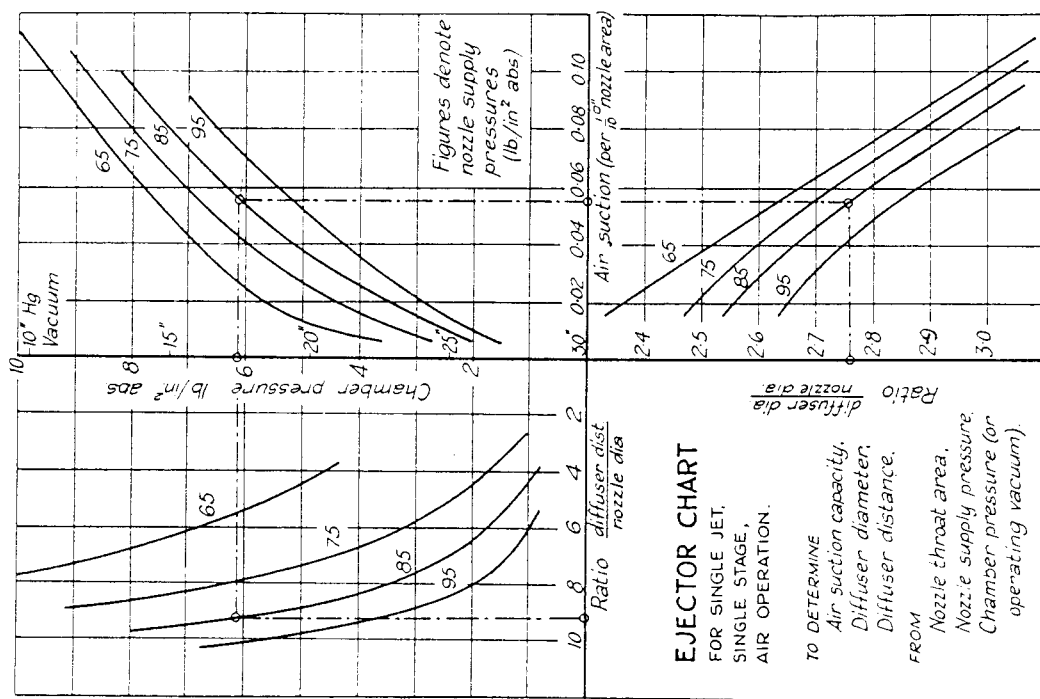


FIG. 7.

off on curves which have been derived directly from the results of the tests. For example, if the stage vacuum is to be 17.5 inches, and the nozzle supply pressure 85 lb. per sq. inch absolute, then the capacity and the dimensions for unit nozzle size are given by the dotted lines in the figure. The scope of this chart is, of course, limited by the range of the tests, and is applicable to air operation only, but there is no reason why the method could not be extended to cover practical requirements.

Further evidence of the effect of dimensions is provided by photographs of the jet, taken in the same manner as in the paper on

compression losses in nozzles referred to previously. To obtain the photographs a glass-sided diffuser is required, so that the rays of light from an arc spot-lamp are enabled to pass through the combining chamber on to a screen beyond. It would be out of the question to have the diffuser of circular section, owing to the refraction caused by the glass, but a rectangular form, both of nozzle and diffuser, is sufficient to maintain a reasonable efficiency and conform closely enough with the actual ejector form for purposes of observation. The details of the diffuser and nozzle are shown in Fig. 2, each being adapted to fit the existing apparatus. The diffuser is framed by brass strips,  $\frac{1}{2}$ -inch wide, which are secured to the combining chamber in such a way that their distance apart, and hence the diffuser throat width, is adjustable. These strips act as distance pieces for two plates of  $\frac{1}{8}$ -inch optical glass, held in position by a slot in the chamber cover plate and by a clamp. As in the main tests, several nozzles of different divergence are provided, but in each case two of the sides are parallel and  $\frac{1}{4}$ -inch apart.

With a chosen nozzle pressure and air aperture, it is necessary first of all to find the diffuser diameter and distance to give the best results, and as these dimensions are easily varied on the apparatus, they can be determined directly by trial. An ordinary camera is used to take photographs of the shadows thrown on the screen by the refraction of the light passing through the jet. During exposure, the compressor supplies air to the nozzle at steady pressure, and great care is taken to prevent the condensation of moisture on the glass sides of the diffuser.

The first exposure represents the ejector working under the best conditions, as in Fig. 8 (a); in (b) the throat area of the diffuser is reduced by bringing the sides closer together, and in (c) the distance is reduced. In all three photographs the form of the jet can be followed, more or less, by the waves formed naturally at the nozzle outlet. These compressions and rarefactions, or sound waves, as they might be termed, are always formed at the outlet of a nozzle which expands beyond the critical ratio (0.528 for air). The greater the difference between the designed nozzle ratio of expansion and the actual ratio of expansion of the air, the more pronounced do the waves become, but even when the nozzle expands perfectly, the wave formation still appears. The nozzle outlet sections in the photographs are designed to under-expand slightly, which is usually the case in practice, and the resulting waves are fairly well defined.

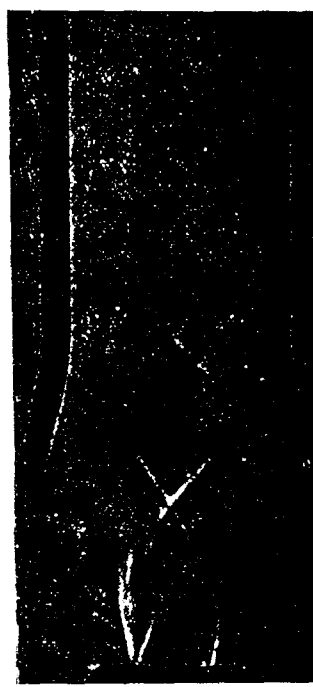
No outward effect of the entrainment of the air can be observed in the photographs; in (a) the jet is not visibly disturbed right up to the throat section. It is interesting to note also the clearance between the visible boundary of the jet—that at which the waves are reflected—and the diffuser walls. In (b) the sectional area of the diffuser is considerably reduced, and its effect of choking the ejector is plainly seen in the setting up of a boundary disturbance surrounding the stream, in front of the throat. The considerable reduction in wave length, and hence a increase in chamber pressure with less efficient working, and hence a reduction in the jet velocity and the amplitude of the waves. In (c) the effect of bringing the diffuser closer is not nearly so marked. Compression takes place sooner, of course, and the amplitude of the waves is seen to decrease rapidly as compression starts. The chamber pressure



(a) Optimum diffuser distance and throat area. Chamber press. 7.0 lb. per sq. in. abs.



(b) Diffuser throat area reduced.



(c) Diffuser distance reduced.

FIG. 8.—Shadow photographs of waves in the combining chamber of a glass-faced ejector, to show the effect of dimensions on the jet form. Nozzle press. 90 lb. per sq. in. abs.; suction 0.022 lb. per sq. in.

recorded is only slightly higher than that in (a), and this is reflected in the very similar wave form at the nozzle outlet in each case. It is significant to note that varying the diffuser distance gives a chamber pressure curve, as in Fig. 6, which shows no effect of the varying wave front at the throat section, thus proving that the waves do not influence the entrainment of air.

*Losses and Entrainment Action.*—The energy unaccounted for in the diffuser balance, which latter includes the nozzle and diffuser friction losses as well as the theoretical loss in combination, must be equivalent to some unknown loss which occurs between the nozzle outlet and the diffuser outlet. There may be some difference between the actual

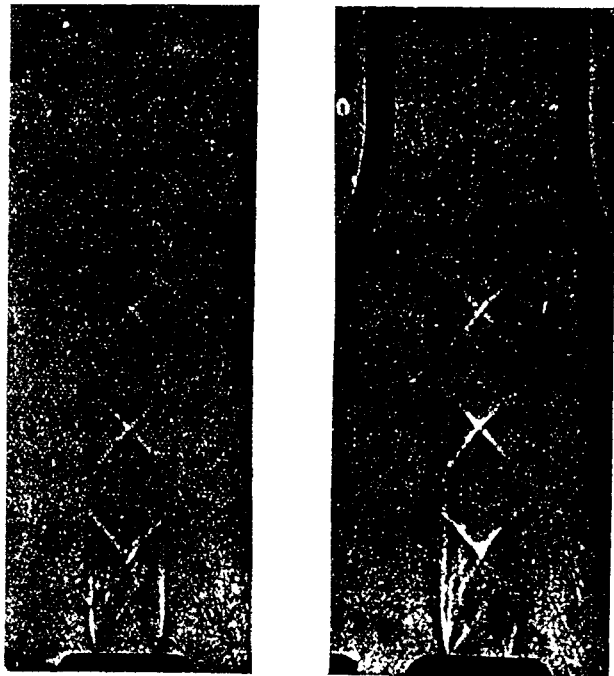


FIG. 9.—Shadow photographs of waves in the combining chamber of a glass-faced ejector, to compare the forms of free and combining jets of the same expansion ratio.

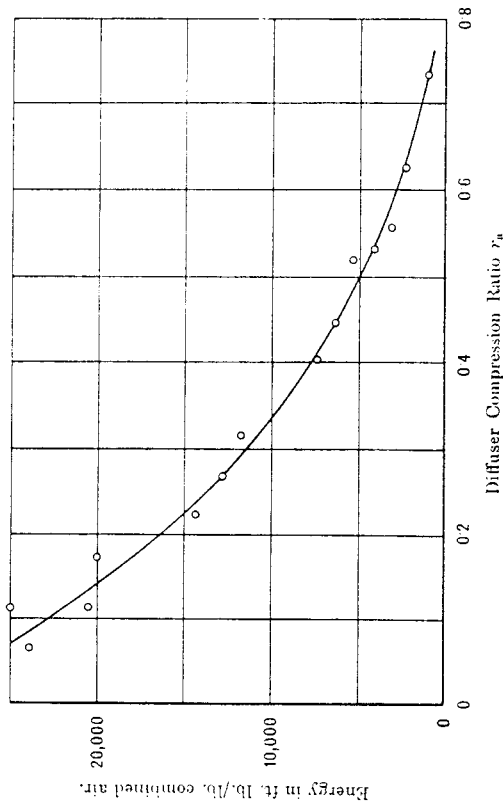


FIG. 10.—Energy unaccounted for.

combining loss and that obtained by following the law of the conservation of momentum, but it is most likely that the greatest loss occurs in the compression of the combined jet in the diffuser. It is impossible at this stage to calculate the magnitude of a compression loss, so that all that can be done is to plot the unaccounted loss on a suitable base, such as the ratio  $r_a$  of compression in the diffuser, for each test, and

note the trend of the curve. Fig. 10 shows that as the ratio decreases the loss increases, a feature which is quite compatible with a compression loss.

The efficiency of the ejector is the ratio of work done on the entrained air to the energy expended overall by the operating fluid. When steam is used as the operating fluid in a condensing plant, this does not represent the actual thermal efficiency, however, as the heat of the steam in the second stage at least is recovered in the discharge to hotwell. For a steam-operated condenser plant it is customary to assume a nozzle efficiency of 90 per cent., and a diffuser efficiency of 50—75 per cent. The latter is defined as the ratio of the work done in compressing the combined jet to the difference between the kinetic energies of the combined and discharge streams. Taking a typical example from the tests, where 29.5 lb. of suction air are dealt with per hour at 25-inch vacuum, a nozzle efficiency of 91 per cent. and a diffuser efficiency of about 60 per cent. are noted, with an ejector efficiency of 5.5 per cent. The ejector efficiency as defined above is very misleading; for useful work is done only on the entrained air, and the proportion of this varies with the chamber vacuum required, but is generally very small.

Considerable interest is attached to the problem of how the entrainment of the air surrounding the jet actually takes place. It has been stated already that the idea of friction alone being responsible for the entrainment has lost favour; it is now generally recognized that the jet of fluid leaving the nozzle expands to a pressure below that of the chamber, on the same principle as over-expansion in the divergent nozzle, and so causes an inrush of the surrounding fluid. A complete pressure traverse, in a plane containing the centre line of a jet expanding into the atmosphere, was carried out some time ago by the author, and revealed this suction effect of the jet. The over-expansion is quite distinct from the familiar nozzle outlet waves of compression and rarefaction which are observed in the photographic tests, and in the pressure curves along the centre line of the jet.

A further set of photographs, taken with the object of investigating the effect of entrainment on the visible form of the jet, is reproduced in Fig. 9. These photographs show a comparison between two jets from the same nozzle working at the same expansion ratio, one jet expanding freely to atmosphere and the other entraining air in the combining chamber. In the first case (a) the sides of the diffuser are removed, leaving the glass faces in position, and the nozzle is supplied at the highest pressure obtainable. To find the supply pressure in (b) which will give the same expansion ratio, trial tests have to be carried out first, and the diffuser finally set to the correct width.

From the results the rather unexpected conclusion is reached that the jet within the visible boundary is quite undisturbed right up to the point of disappearance of the waves—very nearly to the diffuser throat—by the entrained air. No indication is given as to the manner of entrainment of the air, but there is sufficient proof that complete intermingling of jet and entrained air does not take place, until the throat section, at least, is reached.

"Discussion on Steam-nozzles Research Fifth Report." Institution of Mechanical Engineers  
(1928 Proceedings, Part 1, Jan. 1928): 82-91.

Mr. B. HOPKINSON presented the following communication on behalf of Mr. H. L. GUY, who was unable to be present. Some time ago, tests were carried out in the experimental department of the Metropolitan-Vickers Electrical Company on some practical types of convergent-divergent nozzles, which appeared to indicate that their apparatus, which was similar to that of the Committee, could usefully be employed for testing that type of nozzle. Before an

FIG. 22.—*Standing Waves.*

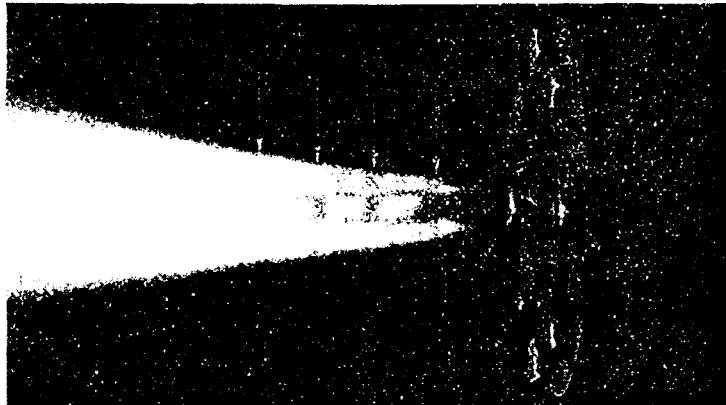
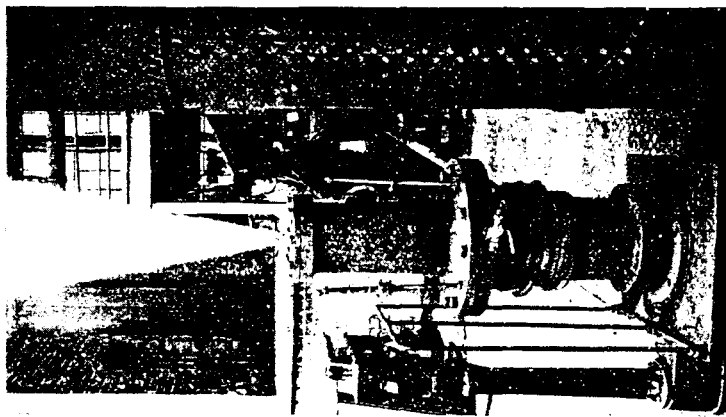


FIG. 24.—*Arrangement of Steam-Chest and Nozzle-Box in "Null" Test.*



extensive research in that field was attempted, it was considered necessary to carry out a careful investigation of the validity of the method of testing when steam velocities far exceeding that of sound were employed. From earlier discussions there appeared to be a general impression that the accuracy of such experiments would be affected by the presence of standing waves in the jet. To determine the effect of the presence of such standing waves, it was in the first

place necessary to determine their wavelength for the nozzle under examination. By allowing the nozzle to discharge into atmosphere and by gradually increasing the pressure drop across it, the standing waves became clearly visible when established, particularly when the steam was superheated at exhaust. Fig. 22 showed such a condition, the arrows indicating the successive anti-nodes. It was found that the wavelength was mainly a characteristic of the nozzle dimensions. Further, once the critical pressure-drop necessary to establish the standing waves was reached, further increase of drop within the range covered by the tests, did not sensibly affect the wavelength. For the nozzle in question, the wavelength was approximately 2 inches and was constant, though it fell off slightly on the fourth and fifth waves, where it was, of course, very difficult to measure.

In the nozzle tester installed in their experimental department, arrangements had been provided whereby the distance of the nozzle from the bottom of the cage could be readily altered, even during the progress of a test. It was therefore decided to test the nozzle at a series of distances between its exit and the top of the wire-netting pad above the impact plate, representing varying fractions and multiples of the wavelengths. In this way the impact on the plate occurred at all pertinent phase relations with the standing waves. It followed that the influence of the standing waves was measured by the difference between the successive values determined for the velocity coefficient in the different nozzle positions. Fig. 23 showed the results of several series of such tests with the nozzle distance from the netting pad varying from 7.86 inches to 0.90 inch. The tests designated by blind circles at 2.4 inches distance, and marked with a heavy figure, were made with a steam temperature 260° F. higher than those shown for 2.36 inches distance. There was, of course, a difference of superheat also because the exhaust pressure was constant. It should be added that the standardized nozzle distance was 2.5 inches, which was the same as that employed by the Committee. The tests were regarded as distinctly encouraging, and as indicating that, under such extreme conditions, the apparatus possessed the possibility of development for accurate measurements.

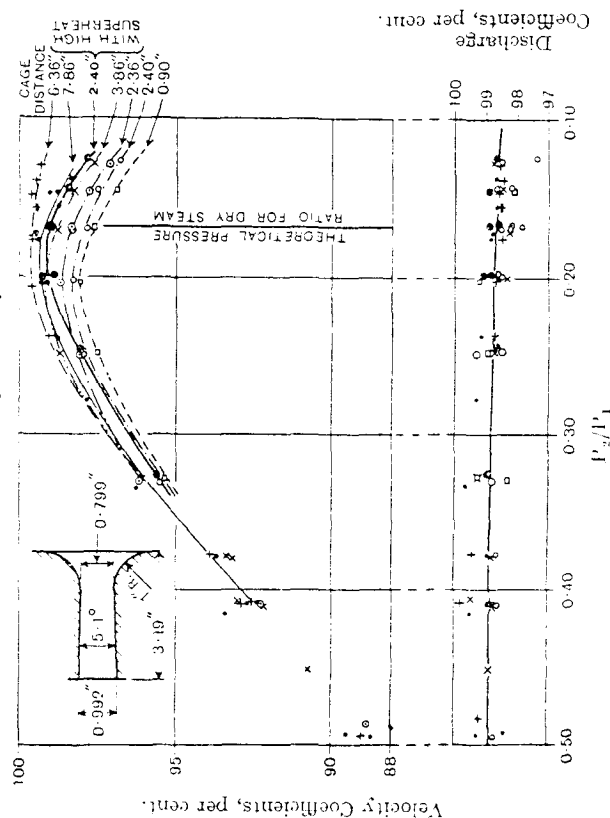
In order further to explore the matter, it was decided to carry out a "null" test on the divergent nozzle with the full steam quantity, and the apparatus used in the impulse tests. The steam-chest and nozzle-box were erected as shown in Fig 24 in the open air on a weighbridge which was sensitive to additions or subtractions of one ounce. Steam was supplied through a straight horizontal length of 18 feet of 2-inch diameter pipe which was in turn connected by

2 feet of flexible pipe to the steam-main. The flexible pipe could just be seen in the photograph at the end remote from the nozzle-tester chest. The axial thrust on the flexible pipe was restrained, and the weight of the horizontal pipe was taken up by flexible cable restraint; this, however, was a refinement as the apparatus would work without it.

The apparatus erected as shown provided a sensitive reaction tester. The reactions were measured through the same range of pressure drops as had previously been worked to in the nozzle tester.

Fig. 25 showed the reaction observations plotted as blind circles

Fig. 23.—Straight Convergent-Divergent Nozzle.

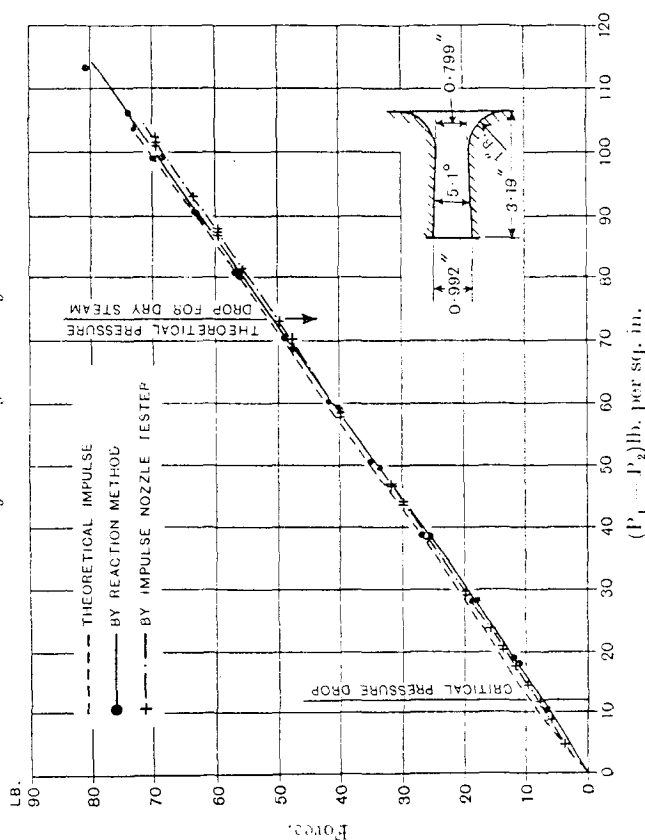


and a full-line curve. The crosses represented previous tests in the nozzle tester and were connected by the chain-dotted line. It would be noted that for the lower range of pressure ratios across the nozzle, the measured impulse was slightly greater than the reaction, whereas for the higher ratios the measured reaction was slightly greater than the impulse. For the pressure ratio corresponding to the actual "flare" of the nozzle, the measured reaction was 1.66 per cent greater than the measured impulse. In character this difference was in line with the previously stated facts that velocity coefficients measured in a reaction tester were slightly higher than those deduced from the Committee's apparatus. Here again, the correspondence between results arrived at by such widely different methods was distinctly encouraging.

The "null" test was carried out by attaching the cage in its normal position outside the nozzle-box by means of the four screws shown in Fig. 24. The cage could be carried by the four screws in

any position desired. It was found that a certain amount of condensed steam tended to hang on the slats of the cage. The method of test was therefore developed in the following way: steam

Fig. 25.—Straight Convergent-Divergent Nozzle.



was turned on the nozzle and allowed to run until steady conditions were established. The apparatus plus the steam contained in it was then accurately balanced. The steam was then shut off by a quick-closing valve, and weights were added to the pan to readjust the balance. The added weight represented the difference of the mass of the steam in the apparatus due to shutting the valve, plus the difference between the impulse and the reaction.

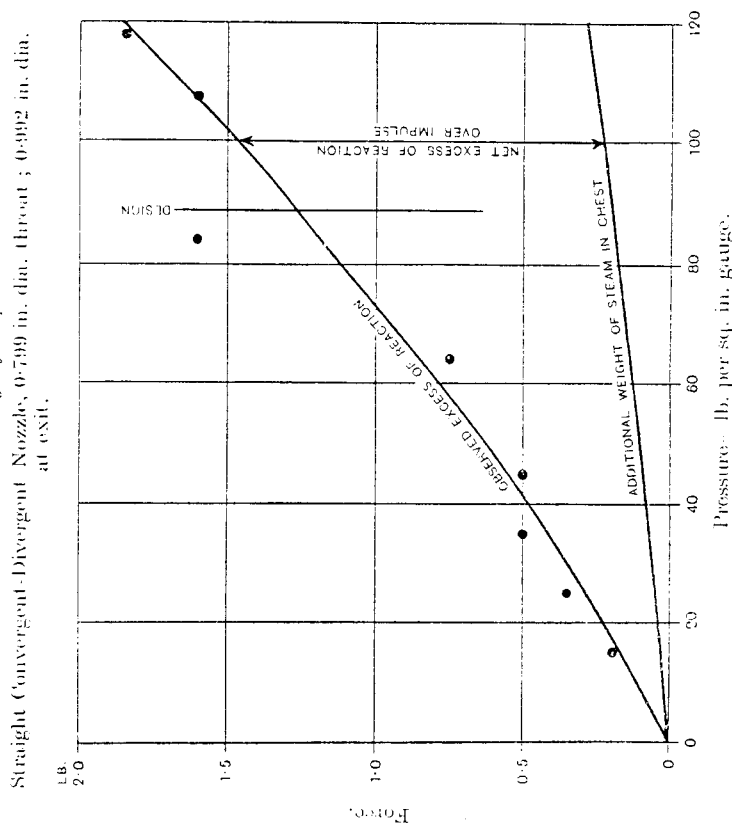
The results of an early series of such tests were plotted in Fig. 26, together with the calculated additional mass of steam in the apparatus. The allowance for this additional mass of steam was not great as the volume of the steam-chest was only 1½ cu. ft. The difference between what was observed in the tests described and the calculated figure due to the steam in the chest at a given pressure, was the "null" effect and was given by the difference between the upper and lower curves in Fig. 26. The "null" test gave, for example, the reaction at the designed pressure ratio for this nozzle as 1.66 lb. greater than the impulse, corresponding to a difference in velocity coefficient of 1.75 per cent. He had previously mentioned 1.66 per cent as having been obtained by direct measurement.

Thus, the "null" test with the cage in the open atmosphere, and the comparison between measured reaction and measured impulse

in the normal tests, gave almost exactly the same difference between reaction and impulse. Further, in both cases the difference was sensibly less than the width of the error "band" enclosing the results of the Committee's tests.

Whilst the results just given must be regarded as in the nature of an interim report of an investigation still in progress, it was felt that their character was such as to establish the flexibility of the Committee's apparatus and the general accuracy of their methods and conclusions.

FIG. 26. "Null" Test on Cage of Impulse Nozzle Tester.



of an interim report of an investigation still in progress, it was felt that their character was such as to establish the flexibility of the Committee's apparatus and the general accuracy of their methods and conclusions.

Mr. H. M. MARTIN said he had been greatly interested in what Mr. Guy had communicated and would have expected rather more difference than had in fact been found. He did not know what effect the standing waves would have, but was surprised to find it was so little. The apparatus, of course, was not designed for such conditions, and it was remarkable that it had worked so well under them. He might say that two alternative methods had been proposed for eliminating (should it be thought desirable) the correction now necessary when the pressure in the discharge box was other than atmospheric. It was a large correction in the case of small velocities; but as a matter of fact he doubted if it was necessary to make an alteration, because the efficiency seemed very little dependent on

the absolute discharge pressure.

In view, however, of certain attempts to improve on the Committee's apparatus, which seemed to have been made in ignorance of the principles governing its design, he might perhaps be permitted to give a short sketch of what those principles were. In early days, impulse testers fell into disfavour because the simple forms used by the experimenters gave anomalous results. The Rugby experiments, in which most valuable help was received from Mr. R. H. Collingham, showed that those anomalies were mainly due to eddies generated by the fluid as it escaped at high velocity over the edge of the impact plate. The eddies reduced the pressure at the back of the plate, and thus increased the apparent impulse. Accordingly the plate was covered with a porous pad which was intended to reduce the velocity of the fluid to a minimum before it reached the edge of the plate. The kinetic energy of the fluid as it left the pad would thus be too small to generate eddies of appreciable strength. In those experiments "null" results were obtained and the tests indicated that the desired end was attained. This had been confirmed by experiments made at Manchester, in which the pressure was found to be so uniform that it was deemed unnecessary to install the packings of wire-netting originally contemplated.

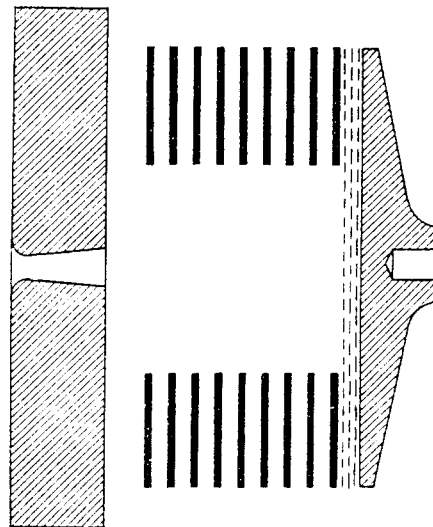
The object of the cage was to ensure that, whatever fluid might enter or leave the movable part of the apparatus, should do so solely when travelling at right-angles to the axis of the jet. Any such flow would therefore have no effect on the impulse recorded. The nozzles were buried very deeply in the cage in order to ensure that the topmost bar should be located in stagnant fluid. Were that not the case, and were there any fluid in motion in the vicinity of the bar, then, by Bernoulli's principle, there would be a corresponding reduction of pressure at the bar, and the impulse recorded would be too small, there being then a slight tendency to lift the cage.

Some special experiments, described, he thought, in the Third Report and made at the instance of Dr. Stodola, showed that there could be no appreciable motion of the fluid in the vicinity of the top of the cage. He thought there could be little doubt as to the general accuracy of the results obtained, but, as had been noted in previous Reports, there was a slight anomaly still outstanding for which it was very difficult to account. He referred to the fact that the impulse recorded was found in certain cases to vary slightly with the distance between the nozzle and the pad, which the elementary theory of the apparatus showed ought not to be the case. The amount was very small, even in the worst cases; but it was of considerable theoretical interest, and he was inclined to think some light was thrown on it by recent developments in hydrodynamic theory. He did not think it was in any way due to the residual velocity of the steam escaping from the porous pad, which answered the question Mr. Patchell had been asked abroad. He thought it was something happening inside the cage, and was inclined to

associate it with the phenomenon of "flapping." He did not mean to say that actual "flapping" occurred, but Dr. Petrie had found that, when steam flowed at a small angle past a flat surface, it was drawn in towards the surface, and that might cause "flapping." \* This occurred because under the conditions stated the pressure over the surface might be reduced far below the nominal value. The apparent angle of discharge from the nozzle might thus be subject to periodical fluctuations.

He thought modern developments of hydrodynamic theory pointed to the conclusion that a similar, but smaller, diminution of pressure might be expected even when the jet issued at right-angles to the nozzle-plate. In short, according to the modern view, a sheet of intense vorticity was developed over the surface of any jet flowing through quiescent fluid. The accompanying system of eddies would reduce the pressure over any adjacent fixed surface. The character of those eddies, or systems of eddies, would not be independent of the arrangement and dimensions of the space in which they were generated. It seemed, therefore, that every nozzle tester must be subject to a dimensional effect. In the case of a reaction tester, it would depend upon the form and arrangement of the discharge box; in the case of the apparatus used by the Committee, it would depend on the position of the nozzle inside the cage. In most cases the effect, though necessarily present, was very small and it was, of course, important to make arrangements that such should be the case. A hole in a flat plate could not therefore be considered a good form of nozzle. He was under the impression, however, that the "distance effect" had not so far been observed, save with that type of nozzle. There was a reduction of pressure over the whole of such a surface, and therefore a lift on the cage. Most of the nozzle-plates used by the Committee were not subject to that objection, because,

FIG. 27.—Showing incorrect arrangement of Nozzle and Cage.



\* Second Report, page 337.

as was well known, they were all cut away to eliminate the "flapping" effect; but he thought that the flat surface along the sides of the jet must nevertheless introduce some small dimensional effect, and that the nozzle-plate should be cut away there also. He might add that provision for this had been made in the new programme of the Committee.

He thought the detection of this dimensional effect was a striking tribute to the care and honesty of the observers, and to the sensitiveness of the apparatus employed. Further evidence in support of the conclusion in question was afforded by the fact that experiments made with a replica of that apparatus had shown that extreme care was necessary if conditions of dynamical similarity were to be secured. Not merely must the nozzles be exactly similar, but the conditions on both sides of the nozzle-plate must also be similar. It was really extraordinary what exceedingly small departures from that requirement sufficed to vitiate comparative tests and yet, when those apparently trivial corrections were made, the comparative results fell into line and became consistent.

He had already mentioned that the nozzle, in the case of the Committee's apparatus, was buried deeply in the cage. That precaution was essential, for the reasons already given. The very worst possible arrangement was that represented in Fig. 27 where, not only was the nozzle formed in a large, flat plate, but it was actually outside the cage. Moreover, the top bar of the cage was adjacent to the flat surface of the nozzle-plate. Under those conditions, the

FIG. 28.—Flow in a corrugated pipe (Yarnell, Nagler, and Wondward).



jet must induce a flow between the top of the cage and the adjacent fixed surface. A tester constructed on those lines, or anything approximating thereto, must, in his opinion, be absolutely worthless.

It was mentioned in the Report that an attempt had been made to determine the effect of roughness by grooving nozzles with threads of different pitches. He confessed he was doubtful whether that kind of roughness was really comparable to the natural roughness



occurring in commercial nozzles. In general, the friction of a pipe roughened by erosion, or other natural causes, increased approximately as the square of the velocity; but some time ago Professor Gibson made experiments on the friction of corrugated pipes, and found that in them the friction increased at a much faster rate, which appeared to indicate that the physical character of the flow in the grooved nozzles could not be the same as with a naturally roughened surface. He thought that view was supported by Fig. 28, which was reproduced from a photograph taken by Messrs. Yarnell, Nagler, and Woodward at Iowa University\* in their experiments on the discharge coefficients of corrugated pipe culverts. It would be seen that a Helmholtz-Rayleigh surface of discontinuity started from each corrugation. It was, of course, conceivable that similar discontinuities might start from each asperity of a naturally roughened surface, but the scale would be very much smaller, and, moreover, natural asperities were distributed absolutely at random, whereas corrugations had a definite pitch. In those circumstances, what it was now customary to call the "flow patterns" would not be the same, and unless the flow patterns were the same, no law of comparison existed. He did not think, therefore, that it would be possible to establish a satisfactory specification of roughness.†

\* Bulletin 1, 1926, Iowa University, "Studies in Engineering," pages 1-128.

† See also Communication by Mr. Martin, page 118.

# FLUID JETS AND THEIR PRACTICAL APPLICATIONS

By PROFESSOR A. L. MELLANBY, D.Sc., M.I.Mech.E.

Public Lecture delivered before the Institution on Friday, October 26, 1928, in the Institution of Civil Engineers, Westminster, S.W. 1, the President, Sir Alexander Gibb, G.B.E., C.B., in the chair.

The study of jet action has, of late years, assumed great importance owing to the large extent to which it is now employed in engineering processes. The primary cause of the great interest shown in this subject must be attributed to the development of the steam turbine, where the transformation of the heat of the steam into useful work is accomplished by an intermediate transformation into kinetic energy. The best way of making this change is the starting point from which originated the vast amount of research work upon steam nozzles now being carried out in this country, the Continent, and America. Apart from turbine applications, however, many other types of engineering plant depend for their efficient design upon a clear conception of jet flow. The old established steam injector used for boiler feed supply is one of the best known illustrations, while closely allied to it are the series of devices for vacuum production or for extracting and delivering at a specific pressure one fluid by the action of another fluid moving at a high velocity.

The subject of which I wish to speak this evening may be best developed by starting with a few simple illustrations of what takes place when a fluid is caused to flow from a region of high to one of low pressure through a simple orifice. Once the laws governing the pressure drop are recognised the features of the more complicated industrial applications will become much clearer.

From the experimental point of view the subject appears to have been attacked first by Napier in 1867. When passing steam at a definite pressure through an orifice into a chamber maintained at some lower pressure he found that the amount of steam passing through the orifice was a maximum when the pressure in the chamber was about half the value of the pressure at admission to the orifice. Any lowering of this back pressure produced no increase in the steam flow.

The full explanation of this experimental observation may be best forthcoming until 1886, when Osborne Reynolds showed that in a nozzle of varying section the velocity at the minimum section could not exceed the velocity of sound in the fluid. It therefore followed that, taking for example the simplest kind of orifice with rounded entry, the lowest possible pressure at the exit of the orifice itself would be equal to that at which the pressure drop would produce a gas speed equal to the velocity of sound in the gas. Any further lowering of the pressure in the chamber would have no effect upon the pressure at the orifice exit and, consequently, the amount of fluid discharged would remain unaltered. From theoretical considerations it can be shown that, for frictionless adiabatic flow, this critical pressure will be equal to about half the initial pressure, confirming therefore the original observation made by Napier.

A method of measuring the pressure drop along the axis of an orifice or nozzle was originated by Prof. Stodola of Zurich, who inserted a search tube with a very small hole in its side into a nozzle through which steam was discharging. One end of the tube was closed and the other end connected to a pressure gauge, so that by traversing the tube along the

described by a few such illustrations. The simplest case is shown in Fig. 1, where the pressure-drop curves, as determined by the search-tube method, are presented for a convergent nozzle. The ordinates indicate not actual pressures but pressure ratios, a method of plotting which possesses several advantages. Each of the two upper curves shows a gradual drop right down to the chamber pressure. When, however the chamber pressure is brought down to about 0.55 of the initial pressure, the pressure at the end of the nozzle does not fall below 0.58 of the initial pressure. Even with a still lower back pressure the nozzle pressure remains fixed, thus confirming Reynolds' statement. For superheated steam, used in this experiment, the critical pressure for frictionless adiabatic flow is 0.55  $P_1$  and it is of some interest to note that the lowest pressure to which the steam will fall before leaving the nozzle is 0.58  $P_1$ .

In Fig. 2 the curves for a convergent parallel nozzle are presented. The same general features are to be observed; with high chamber pressures the nozzle is able to expand the steam practically to the

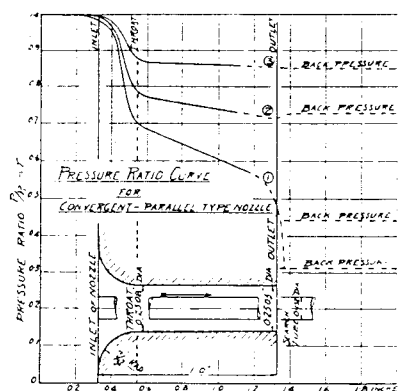


FIG. 1.

back pressure, with the chamber pressures lower than the critical the expansion limit of the nozzle is clearly shown. In this case it will be noted that the lowest pressure at the end of the nozzle is about 0.5  $P_1$ , while, as before, the critical pressure for frictionless flow is 0.55  $P_1$ . This lower pressure for the actual nozzle is, however, to be expected. The long nozzle now under consideration has a comparatively large surface and consequently offers greater frictional resistance to the steam than did nozzle No. 1. In both cases the pressure drop is that necessary to produce the velocity of sound and obviously the greater the resistance the greater the pressure drop necessary to generate the same speed.

This feature of the relationship between pressure drop and critical speed is perhaps more completely illustrated by Figs. 3 and 4. In Fig. 3 the pressure drop curves for two parallel nozzles are given. In both cases expansion was from the same initial to the same final pressure. Given frictionless flow the velocity generated in each nozzle would have been the same. Actually the velocity at the end of the longer nozzle was appreciably less than that found at the end of the short one, as shown by the full lines marked Nozzle 1 and Nozzle 2, respectively. The case where the total pressure drop is greater than the critical is shown for three nozzles in Fig. 4. In each of these three examples the nozzle is able to expand the steam to the limit fixed by the condition that the outlet velocity of the steam will be equal to the velocity of sound in the steam, here about 1740 ft. per second. The effect of the increased resistance to flow produced by nozzle length can be seen by the end pressures, which, as shown in the figure, are 0.55  $P_1$ , 0.45  $P_1$ , 0.4  $P_1$ ; again illustrating the fact that the longest nozzle requires the greatest pressure drop in order to give the steam the required speed. A further illustration of this point can be given by comparing the pressure drop curves for smooth and rough surfaced nozzles working under the same inlet and exhaust chamber conditions. The roughened nozzle will always show the lower end pressure—providing the chamber pressure is below the critical—due to the extra pressure drop required to overcome the greater frictional resistance in giving the steam the velocity of sound.

If it is required to produce a nozzle in which the steam can expand to a pressure lower than the critical it becomes necessary to add a convergent tail, so giving what is generally called a convergent-divergent nozzle. With this type of nozzle the pressure drop phenomena are very different from those previously observed, and Fig. 5 indicates some of the most interesting features. It must be recognised that such a nozzle has only one definite pressure range within which it can work efficiently. Should the pressure range be either greater or less than the correct one the nozzle will not be working at its highest efficiency.

The nozzle shown in Fig. 5 was designed to expand steam from a pressure  $P_1$  down to a terminal pressure of 0.2  $P_1$ . The lowest curve shows that, with this pressure range, the expansion curve was steady and continuous. When the back pressure was raised above the proper value curves 2 and 3 resulted. Here it will be noticed that the pressure in the nozzle does not fall gradually to the outlet value, but that it first drops much below the back pressure, and that recompression then takes place right to the end of the nozzle. Even when the back pressure is so high as 0.75  $P_1$ , there is still some over-expansion followed by recompression.

The fact that the pressure at the throat is not affected until the back pressure is raised to the relatively high value of 0.75  $P_1$  indicates that the rate of steam flow through the nozzle remains constant between this value of the back pressure and the minimum value of 0.2  $P_1$ . It must not be assumed, however, that this constant discharge indicates a constant efficiency. The extensive over-expansion and recompression entail severe losses and the curves show clearly, what has also been proved by actual turbine experience, that a nozzle of this type should not be run at a back pressure above that which allows a continuous fall of the pressure line. Practical design has been influenced by this to the extent that it is now common to make the final area of the nozzle rather less than that given by calculation in order to have under-expansion rather than possible over-expansion with recompression.

It will also be noted that the portions of the curves representing the recompression process are shown by dotted lines. This is to indicate that, during this part of the process, the pressure readings were very unsteady; the gauge pointer was in a state of continuous vibration and occasional violent movements were observed. Another point to be observed is the low value of the pressure at the nozzle throat. With the full convergence here provided there appears to be little reason why this pressure should not agree with the theoretical ratio of 0.55. So far as my own experience goes this agreement with theory never exists, although the actual throat value may vary

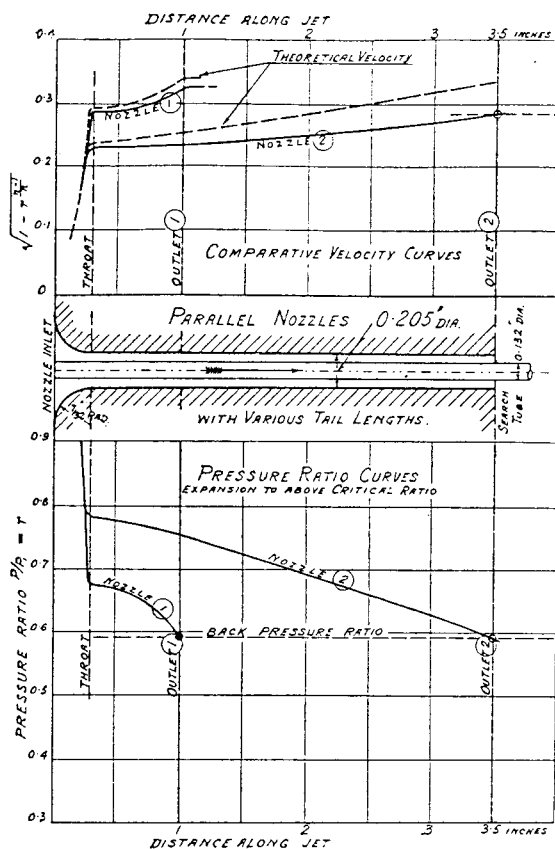


FIG. 3.

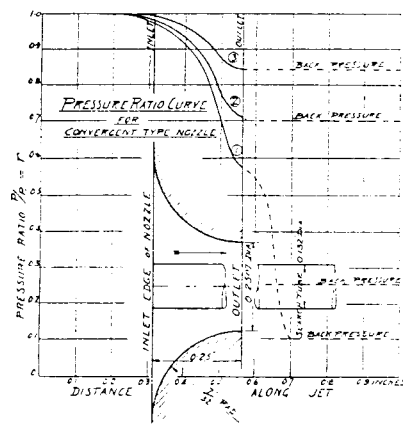


FIG. 1.

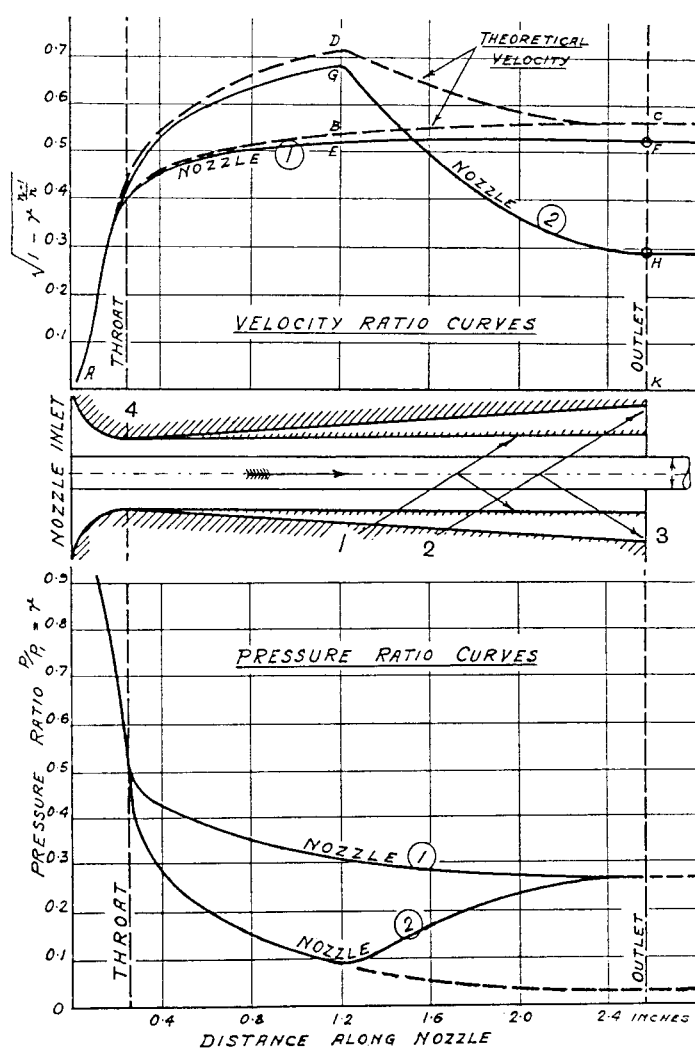
nozzle the pressures at the points occupied by the small hole could be successively observed. Given therefore this possibility of tracing the pressure drop along the axis of a nozzle, it is considered that the principal features of fluid flow can best be

between fairly wide limits for different cases. The over-expansion at the nozzle throat would indicate that during the first period of expansion the jet leaves the nozzle walls and forms its own throat at the point where the pressure ratio is 0.55. There is also practical certainty that the jet leaves the walls during the recompression period and that the space between the jet body and the nozzle surface is filled with eddies which do not contribute to the flow. Before leaving Fig. 5 attention might be called to the fact that here we have for the first time some indication of the action of the steam ejector. The low pressure portion followed by the recompression, as shown in curve 3, suggests the possibility of taking in some outside fluid at the low pressure carrying this along with the steam and ejecting it at the terminal chamber pressure.

In Fig. 6 is shown, in another fashion, the ill effects of using a divergent nozzle for incorrect pressure ratios. From the pressure ratio curves it will be observed that in Nozzle 1 the pressure drop is continuous, while for Nozzle 2 there is over-expansion followed by recompression to the common back pressure. Theoretically the exit velocities should be the same in both cases, and the dotted lines show how these velocities would increase as the steam expanded along the nozzle. The actual velocities, obtained by experiment, are shown by the full lines which illustrate how great must be the losses produced by the recompression effect.

The losses during the recompression process have been closely studied by my colleague Professor W. Kerr and myself, and a method of analysis, which we think illustrates to a large extent the nature of the problems involved, has been devised. At the previous occasion on which I gave a lecture to this Institution, the importance of what was taking place during the compression of a fluid jet was emphasised, and I promised to devote further attention to this work with the object of giving what further information I might gather to a future meeting of the Institution. In what follows I shall endeavour to show what it has been possible to do and hope to convince you that this work has thrown some light upon the action of the fluid ejector. Practically the whole of the experimental work to be described was carried out by one of my students, A. D. Third, Ph.D., as part of his research work, and credit is due to him for most of the experimental details.

One of the first investigations was upon the recompression action, and an experiment was devised with the object of finding whether the jet did leave the



1. Nozzle exit, diameter 0.302 ins.
2. Nozzle exit, diameter 0.554 ins.
3. Search tube, diameter 0.132 ins.
4. Throat, diameter 0.256 ins.

FIG. 6.  
Divergent Nozzles.

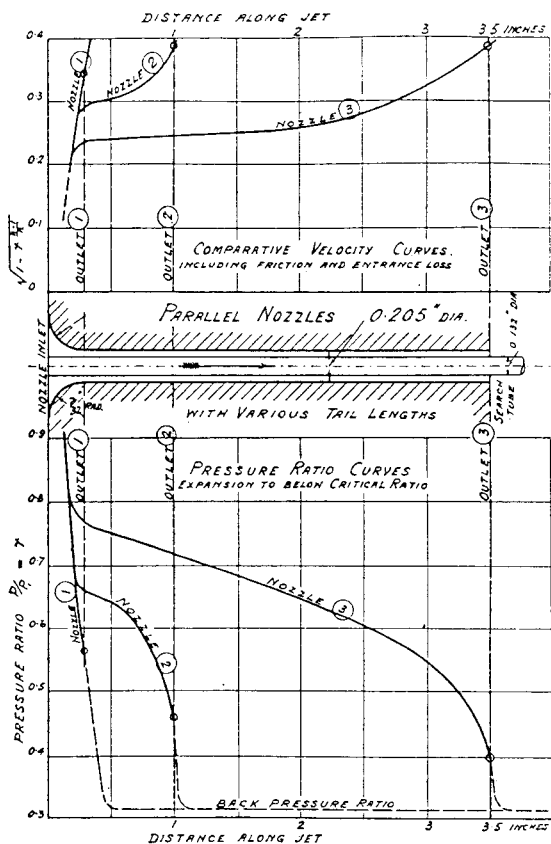


FIG. 4.

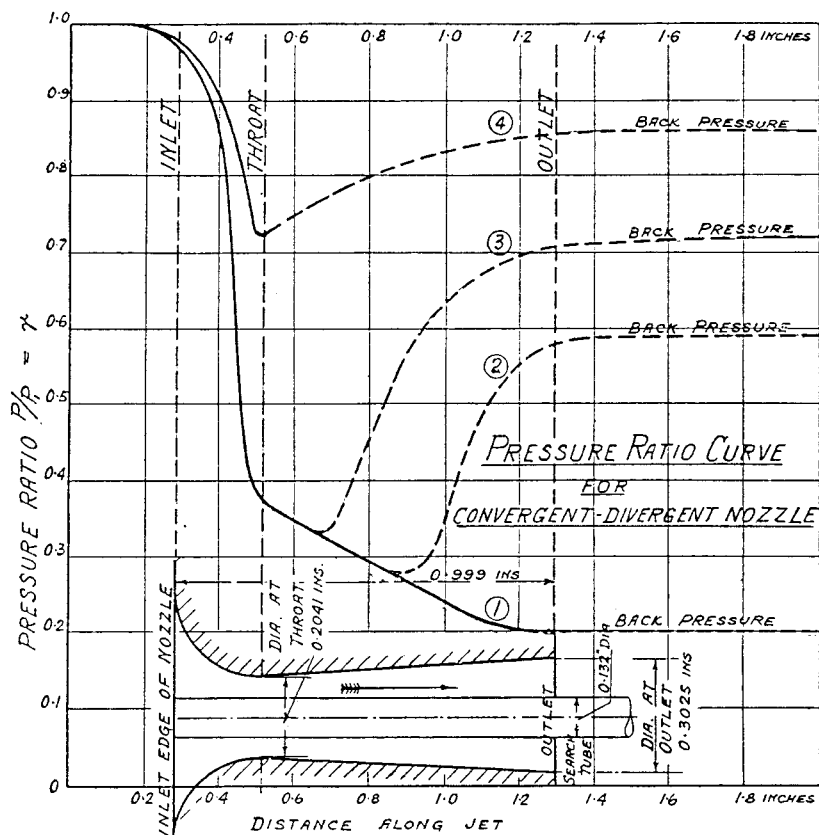


FIG. 5.

walls after the over-expansion process had been completed. For this purpose a divergent gun-metal nozzle was constructed with parallel glass faces. The internal faces of the glass were coated with a uniform film of very viscous oil and the nozzle placed between an arc lamp and an ordinary camera. A compressor and reservoir tank provided a supply of high pressure air and, by connecting it to the reservoir, air at any predetermined initial pressure could be passed through the nozzle. Exposures were made during the air flow, and the results obtained are shown in Fig. 7. The light portions in the photographs represent that part of the nozzle in which the air remained in close contact with the walls and either thinned or completely swept away the oil. The dark portions show where the jet had freed itself from the walls, leaving the oil film intact and so preventing the passage of the light. In all cases the air jet was delivered to the atmosphere, thus fixing the back pressure, and to obtain different pressure drops experiments with different admission pressures were carried out. The corresponding pressure ratio curves are shown in Fig. 8, and it is interesting to compare these with the previous figure. In the top figure where the supply pressure was 10 lb per sq. in. separation takes place well beyond the throat and at a point corresponding to that at which recompression is about to start in Fig. 8. Similar relationships will be found in the other illustrations, and especially remarkable is that shown by the bottom photograph where the nozzle is shown to be full almost to the outlet when some breakaway is evident.

Confirmation of this effect is also given by Fig. 9, where light from a point source has been passed through the jet on to a screen, so rendering the compressions and rarefactions visible. In a case like this it is necessary to introduce some sharp object to create a well-defined, sound wave and in the example shown minute knife-edged projections were placed on opposite sides of the throat section. The waves formed by the obstructions in the nozzle travel across the jet and are reflected from the other side. When, however, the jet leaves the walls of the nozzle no definite reflecting surface is available, so that at the points of recompression the waves become suddenly weaker and ultimately disappear. A comparison of Fig. 9 with Figs. 7 and 8 will show a close coincidence in the points of divergence. The photographs of Fig. 9 would appear to indicate that an enormous contraction of the jet takes place at the throat, a contraction evidently out of all proportion to the diminutive projections. Measurements of the flow quantities showed, however, that no such contraction could have taken place, and the photographic effect must therefore be attributed to the magnifying effect of the refraction of the light rays in such an area of steep density gradient. A practical inference to be drawn from these photographs is that waves must be well developed in cast or roughly finished nozzles, and that wave production and not friction alone may account for the low efficiencies of such nozzles when passing fluid at very high velocities.

#### PRACTICAL APPLICATIONS.

It is in the steam turbine that the fluid jet finds its widest practical application, and an appreciation of the expansion processes already described will make clear the main points of turbine design. Obviously the amount of pressure drop allowed in each set of nozzles will determine, to a large extent, the main features of the turbine, since this will fix the number of stages, the speed of the blading, and the overall efficiency. While it is not intended to say more than a few words upon this subject, attention might be directed towards the influence of what can be called the "quality of the jet" upon turbine performance. This is a branch of nozzle work to which little public attention seems to have been given, although its importance has been demonstrated in a paper\* presented to the Institution of Mechanical Engineers by Professor W. Kerr. It is shown by Dr. Kerr that, for turbine work, the ideal jet leaving a nozzle should be parallel in form, symmetrical in section, clearly defined and solidly directed without tendency to dispersion. The actual jet at outlet may, however, possess features quite different from those of the ideal. It may, for instance, be undergoing a compression action, or freely expanding; it may have been developed at an excessive rate of divergence, or have followed a path of extreme curvature. It should also be realised that the actual operation of a jet in turbine work is not truly represented by the action on an impact plate. The jet works throughout the length of a blade passage, and hence there is every opportunity for the development of any flaw in quality which may be inherent in the jet as supplied. The experiments of Professor Kerr show how important these features of jet quality are when applied to turbines and how the losses are diminished when the proper degree of expansion is allowed. Reference to his original paper is strongly recommended to all interested in this phase of turbine design.

#### THE EJECTOR.

It has been considered that the majority of the members of this Institution would be more interested in the application of fluid jets to the withdrawal or delivery of other fluids and solids, and consequently the remainder of this lecture will be devoted to a study of the Air Ejector.

Restricting ourselves to fluids alone, we may define the ejector as a pump in which one fluid is entrained by a jet of another fluid moving at a high velocity. The combined fluids are then compressed to the delivery pressure at the expense of the kinetic energy.

As was the case with the preceding work, it may be claimed that the recent close study of ejector performance and its consequent improvement were influenced largely by the progress in steam turbine practice. The necessity for a very high condenser vacuum directed attention to the simplest means of producing and keeping it, and in all modern stations it will be found that the ejector has proved the most suitable apparatus for such duties. In these circumstances it is employed for the withdrawal of air from the condenser, and must therefore be capable of working through a range represented by a vacuum of, say, 29 ins. of mercury and atmospheric pressure.

It was early recognised that the most serious obstacle to the development of the ejector was the design of a suitable diffuser. Experience soon showed that a single stage ejector could not be conveniently employed for compression ratios greater than 8 to 1, since the diffuser throat diameter required for starting is much greater than that necessary for continuous working under the established conditions.

How the compression ratio is influenced by the vacuum can be seen from the following figures. If a vacuum of 26 ins. has to be maintained under a barometer of 30 ins. the compression ratio will be practically  $\frac{30}{7} = 7.5$ . With a 28-in. vacuum the compression ratio rises to  $\frac{30}{2} = 15$ , and with 29-in. vacuum to 30. The great difficulty attached to the production and maintenance of so high a vacuum as 29 ins. will be readily appreciated from these figures.

The first successful application of the ejector as a vacuum producer for surface condensers was in the arrangement patented by Parsons, where the ejector worked in series with a reciprocating air pump. The ejector took care of the lowest pressure range, delivering the air to the reciprocating pump, which then compressed and discharged it to the atmosphere. This led to the development of two-stage and ultimately three-stage ejectors where each unit could work, even under highest vacuum conditions, with a compression ratio well within its range, thus insuring stability as well as efficiency.

It is remarkable that so little is understood about the working of the ejector. At one time it was generally accepted that the suction fluid was entrained by friction, and this led to the adoption of a cluster of small bore nozzles, in place of a single jet, to increase the surface area of the working fluid. Latterly the simple friction theory has fallen out of

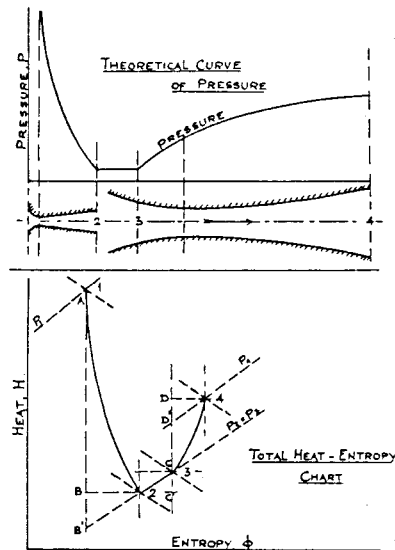


FIG. 10.

favour, and it is suggested that the entrainment of the fluid is due to a natural tendency of the jet to overexpand on issuing from the nozzle. In designing an injector advantage is taken of this property of the jet by allowing a limited quantity of the fluid to leak in at the point of lowest pressure. The ejector thus becomes similar in its action to that of a divergent nozzle working at a back pressure above that for which it was designed. A difference is to be found in the condition that provision must be made for the entrainment and compression of an additional fluid.

In the work which follows an account is given of a series of systematic observations upon the effect of the leading dimensions on the working of an air-operated ejector. From these observations attempts are made to find the most efficient arrangements for operating under given conditions. Air has been used both as the operating and the suction fluid, since this simplified not only the experimental arrangements but also the analysis of the losses that were developed during the action of the jet.

A general idea of the changes involved may be obtained from Fig. 10, the top diagram of which shows how the pressure falls and rises along the axis

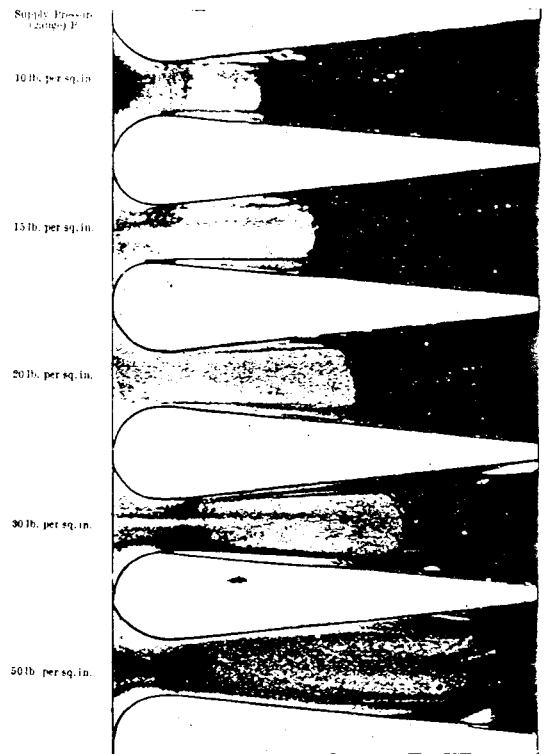


FIG. 7.

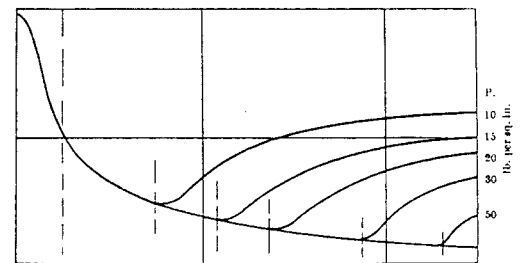


FIG. 8.  
Pressure Ratio Curves.

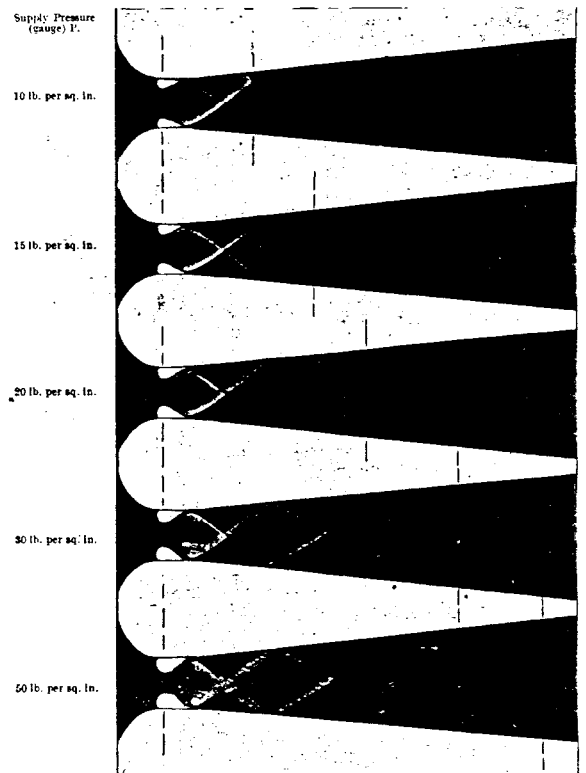


FIG. 9.

\* Jet Action in Turbine Blading. Proceedings Institution of Mechanical Engineers 1924.

of the ejector, and the lower diagram shows the corresponding changes on a heat-entropy chart. Expansion takes place between 1 and 2, and for most cases a nozzle of the convergent-divergent type is here required. With frictionless adiabatic expansion the energy liberated and converted into kinetic energy would be represented by  $AB^1$ ; but due to frictional and other losses the energy actually liberated is  $AB$ , so that the ratio  $\frac{AB}{AB^1}$  can be taken to represent the nozzle efficiency.

With the low pressure induced by this expansion the external fluid can now be drawn in and the entrainment stage is represented by 2-3. The assumption is made that there is no rise of pressure during entrainment, but there is a loss of kinetic energy during the process, and this is represented by the reheating of the combined stream shown by  $CC^1$ .

The compression stage is shown by 3-4. At the point 3 the combined stream strikes the wall of the diffuser and compression starts. The shape of the diffuser will depend upon the velocity that has been generated. Should this velocity exceed the critical a convergent channel will be required for the first part of the compression. In this convergent portion the velocity will fall to the critical and the remainder of the compression must be performed in a divergent

entry curve, throat-diameter and length were concerned. The different pressure ranges were accommodated by using three such standard nozzles with different areas of outlet. The nozzles were screwed to fit a pipe which, machined and ground, passed through a gland in the combining chamber. The latter was in the shape of a circular box, to which also the diffuser was fitted. The whole apparatus could thus slide along the nozzle supply pipe, and by mounting it to a long horizontal arm pivoted at a swivel joint it was possible to measure the reaction of the air leaving the diffuser by means of a balance.

Measurement of the air drawn in was effected by a series of standard apertures leading into the combining chamber. A preliminary investigation was made to determine if the position of three apertures had any effect upon the working of the ejector. The conditions are illustrated by Fig. 11, which also shows in diagrammatic form the nozzle and diffuser arrangement. The first arrangement is shown in (a); in (b) the positions are reversed; in (c) the air is drawn in through a single aperture which passes the same quantity as the other two combined; and in (d) the incoming air is directed against a baffle plate as shown. Although in arrangement (c) the effect of the injector was slightly impaired the general conclusion to be drawn from the tests was that the capacity of the jet for entraining the fluid is independent of the aperture conditions. This may be taken to prove that ejector action depends very little upon the design of the chamber or the position of the induction pipe.

While it is possible to estimate from theoretical considerations the correct sizes of the nozzle, the situation is different when we approach the design of the diffuser. Theory requires a convergent channel followed by a throat or minimum area section and a divergent channel. Owing to the unknown losses in the diffuser direct calculation of the correct throat area is impossible, and experiments with

diffusers of different diameters were therefore seen to be desirable. It was first necessary to decide upon the most suitable form of diffuser, that is to say upon the angle of convergence, the extension, if any, of the section of minimum area, and the angle of divergence. Previous experience has indicated that  $25^\circ$  is about the best convergence angle, and that either the throat section should be extended for a few diameters or the divergence should start very gradually.

It was at once seen that the throat area was of critical importance and, since there were no practical means of making it variable, the value of the test results depended upon the choice of a set of diffusers of suitable diameters. Preliminary trials showed that four diffuser diameters provided sufficient range for the series of tests.

The object of the first series of tests was the determination of the most suitable working conditions for each diffuser diameter. This obviously demanded a series of different pressure ranges, and for each particular case the nozzle corresponding to the selected expansion ratio was employed. The results obtained with one of the diffusers from this set of tests are shown in Fig. 12. The ordinates represent weight of air drawn in per second, and the base shows nozzle supply pressures scaled off in units of energy generated per pound of operating air in expanding to atmospheric pressure. The points of contact with the curves of constant chamber pressures of tangents drawn from the zero base reading represent the most efficient conditions of working for each of these pressures. That is to say, they show when the ratio of work done to the energy supplied is a maximum. This corresponds to what is generally required in practice, since the chamber pressure (or operating vacuum) is first specified and the best working conditions then determined. The dotted curve drawn through the points of contact with the tangents permits the nozzle supply pressures corresponding to the suction quantities given by the different apertures (in Fig. 11) to be read off. The ejector was then operated under these conditions of maximum efficiency and the data required for an analysis of its performance thus obtained. This involved records of the nozzle and apertures used, the nozzle supply pressure, chamber pressure, search tube pressures along the axis of nozzle and diffuser, and the reaction of the outlet stream. A similar programme was carried out with the other diffusers, and the calculations indicated by theory enabled the energy distribution to be determined. A typical set of pressure ratio curves showing how the pressure falls along the nozzles is given in Fig. 13, and similar curves illustrating the rise of pressure along one of the diffusers will be seen in Fig. 14.

**Effect of Dimensions.**—Some little attention might be given to the light thrown by the test results upon the effect of dimensions on the working of the ejector. The three most important variables coming under this heading are the diffuser throat diameter, the distance of the end of the nozzle from the diffuser, and the shape of the diffuser channels. So far, no accurate theoretical relationship has been found which would assign definite values to these variables and no published data have been discovered available for their estimation. The deductions from the tests appear therefore to be of some importance.

The diameter of the diffuser throat is seen at once to be the critical and ruling dimension. This is readily seen from an inspection of Fig. 13, which has been constructed from the set of curves of which Fig. 12 may be taken as an example. In Fig. 13 the

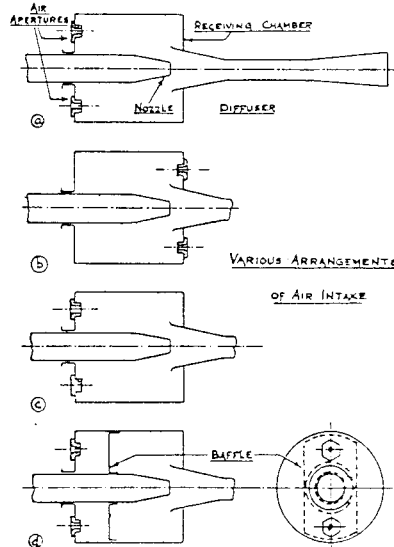


FIG. 11.

channel. A channel of the convergent-divergent type is shown in the figure. If the velocity of the stream is below the critical when compression commences the convergent part may be omitted.

The work done in compression, together with the losses during the process and the residual kinetic energy at the end of the nozzle should be equivalent to the kinetic energy at 3. On the heat-entropy chart the compression stage is represented by 3-4. The energy required for frictionless adiabatic compression is shown by  $CD^1$ , the energy actually re-

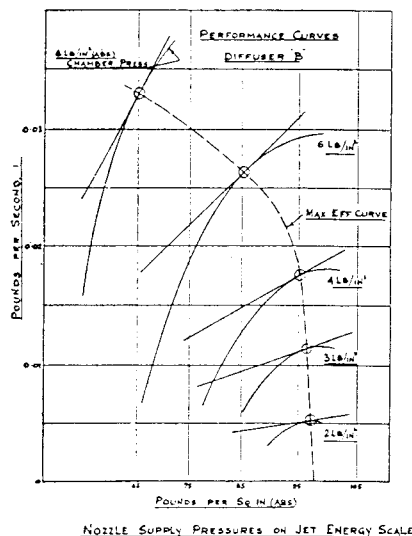


FIG. 12.

quired by  $CD$ , so that the efficiency of compression is represented by the ratio  $\frac{CD^1}{CD}$ .

#### EXPERIMENTAL APPARATUS.

The air available for the experiments was supplied to a large reservoir at a pressure of 100 lb per sq. in. Since the experiments were intended to cover a wide range of expansion, several nozzles were required, and these were made to the same standard so far as

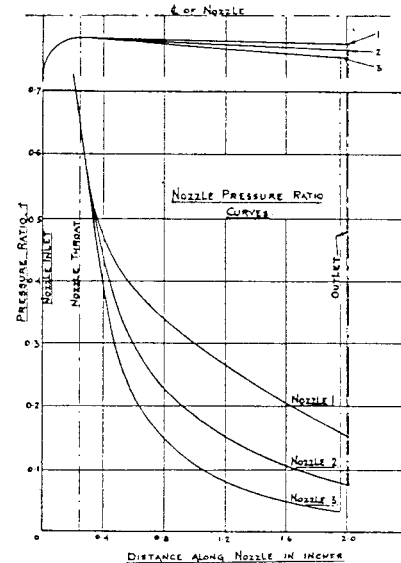


FIG. 13.

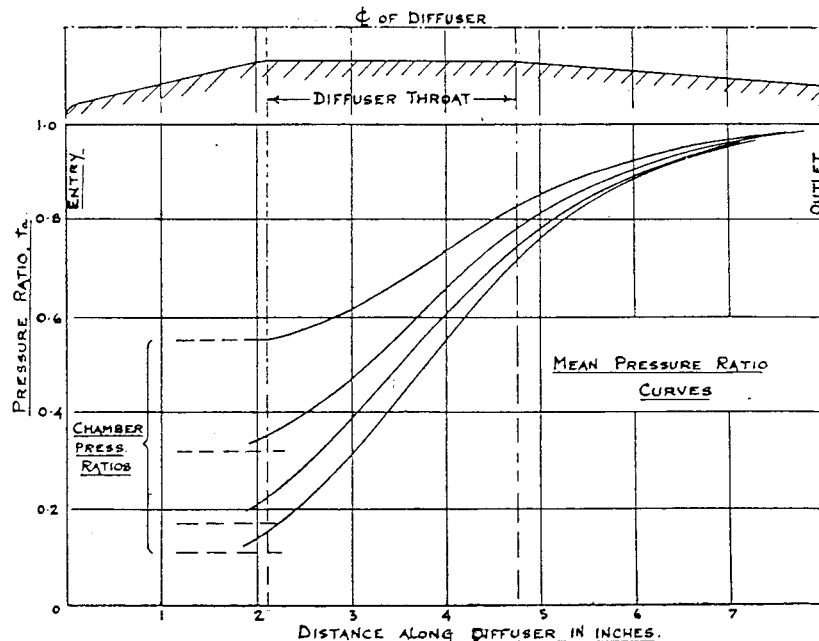


FIG. 14.

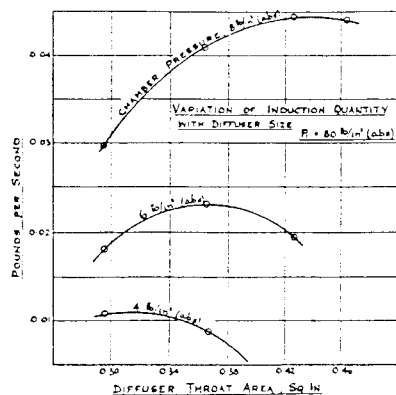


FIG. 15.

variation of air drawn in at different chamber pressure with the change in diffuser throat area is shown for a supply pressure of 80 lb. per sq. in. It will be noted that a considerable difference in the amount of air entrained results from a comparatively small change in throat area, and also that, by extending the curves the areas outside of which no air can be entrained may be estimated. This latter condition arises from the fact that the sectional area of the stream in the diffuser depends upon the quantity of induced air and the chamber pressure as well as upon the nozzle throat diameter and the supply pressure. If the diffuser is too small for the stream then choking occurs; when it is too large there is a leak back of air into the chamber.

The choking effect is illustrated by the pressure observations shown in Figs. 16 and 17. In Fig. 16 is shown the compression curve along the diffuser under normal working conditions, and the gradual damping out of the waves formed at the nozzle outlet will be observed. By increasing the supply pressure, and consequently enlarging the jet, it was possible to choke the diffuser, with the results shown in Fig. 17. Here the wave of compression in front of the diffuser throat and the increased chamber pressure due to the unfavourable conditions that have been produced are to be noted.

From a series of curves similar to those shown in Fig. 15 it is possible to obtain another set of curves illustrating what might be termed the ideal performance of the ejector. One such curve for a constant nozzle supply pressure of 80 lb. per sq. in. abs. is shown in Fig. 18, where chamber pressure is plotted to a base of induced air quantity. Each point on the curve was obtained when the injector was working with the proportions required to give the maximum efficiency. Comparison of this curve with the more usual performance curve of an injector with fixed diffuser dimensions is afforded by the dotted line in Fig. 18. This latter represents the ejector performance with a constant throat diameter under the best conditions of distance between nozzle and diffuser. The full curve shows a continuous tendency towards the origin, and the dotted one indicates a definite value of the chamber pressure at which there is no induction. Some idea is thus given of the difficulties encountered in comparing ejector performances and the relative merits of single and two-stage working. The full line shows that there is no very definite limit to the vacuum obtainable from the single stage, with dry air, and that the limiting conditions are fixed by considerations of efficiency and stability.

**Effect of Nozzle Distance.**—The effect of the distance of the nozzle from the diffuser has been studied, and in all tests quoted this distance has been adjusted to give the minimum chamber pressure. The factors upon which this nozzle distance depends are—the throat and outlet areas of the nozzle, the pressure of nozzle supply and in the chamber, and the form of the diffuser. The test results show that the distance is least when the ejector is working at a high vacuum with little air suction. An increase of nozzle supply pressure increases the dimensions of the jet, and so requires an increase of nozzle distance.

Tests illustrating the effect of nozzle distance upon chamber pressure are shown in Fig. 19. The base represents the distance of the nozzle outlet from the diffuser throat, and the variations of chamber pressure with this distance are shown by the two full curves, which represent two sets of tests. Under normal conditions no critical effects are evident, but when only a small amount of air is being induced a region of instability is produced. The upper dotted curve illustrates the action when the nozzle is drawn away from the diffuser, the lower one when it is advanced towards it.

It is probable that the explanation of this unstable region is to be found in the great change of jet size which will result from small variations in the chamber pressure at such high degrees of vacuum.

**Form of Diffuser.**—In this part of the apparatus the most important point to fix is the rate of divergent taper immediately following the throat section. The design of the experimental diffusers was based on the belief that an extension of the throat section, or a

very gradual preliminary taper, would provide the ideal form. Since the form of channel for the most efficient compression of the stream is also a question of interest this point was kept in mind when fixing the diffuser dimensions.

The outlines of the four experimental diffusers are shown at the top of Fig. 20. Diffuser D is of the type most generally used throughout the general tests; in E the parallel section is extended to the outlet; F has the same outlet area as D but a much smaller length of parallel section, while G with a similar short parallel section has a greater divergent angle. The chamber pressure readings, which are also recorded in Fig. 20, show, as might have been expected, that diffuser D is easily the best of the four types. Comparison of the compression curves for D and F shows that the defect of the latter is due to a too rapid divergence immediately after the throat section. This effect is increased in G, and the slope of

the curves for F and G, just beyond the throat, would indicate that compression in these two cases is taking place too rapidly. In diffuser E we have an illustration of the other extreme where the compression is drawn out too long. The curves for D and E might appear to be very similar, but it is the higher chamber pressure of the latter that produces a false impression of early compression. It is, however, rather surprising that diffuser E should give almost as good a performance as G. The possibility of the selected test conditions being more suitable for one diffuser than for another was not overlooked, but experiments with different supply pressures showed that the results given in Fig. 20 may be taken as representative of the performance of the various diffusers.

It seems clear from these tests that, for the ideal diffuser, divergence should not follow rapidly after convergence. This condition may be fulfilled by having a parallel extension of the throat or a very gradually increasing divergence after the throat

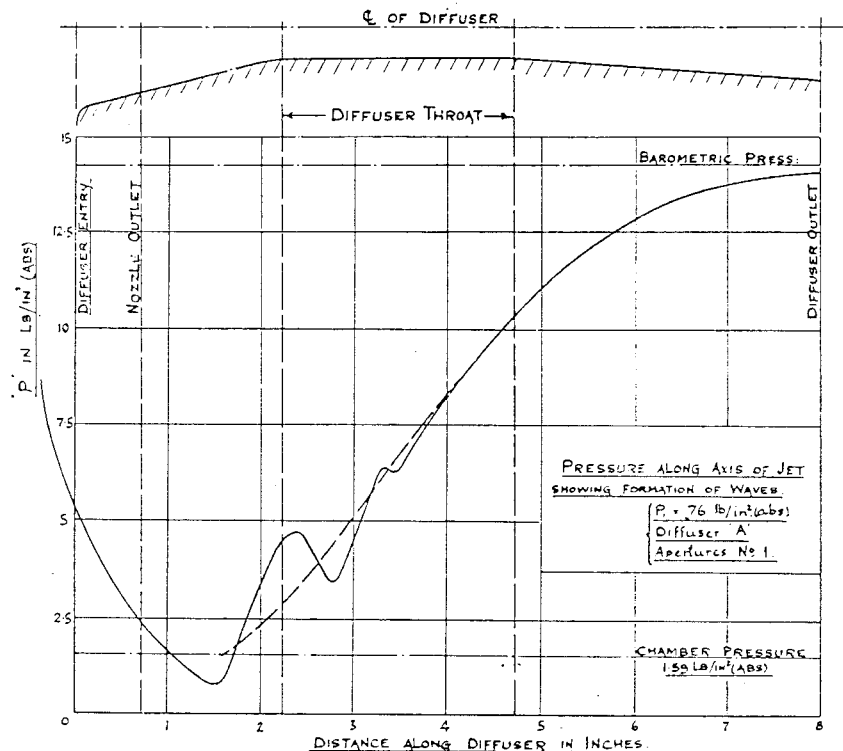


FIG. 16.

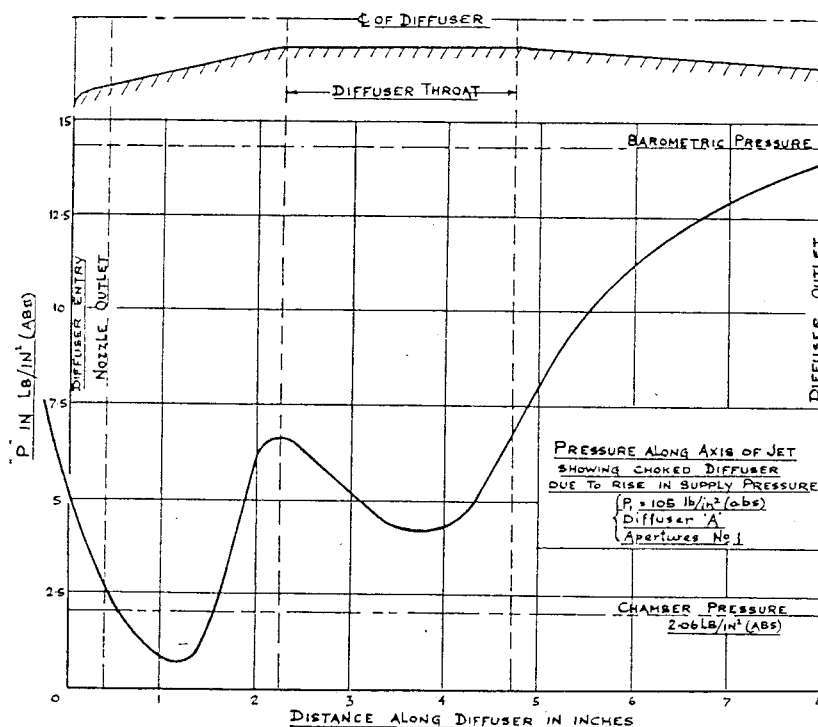


FIG. 17.

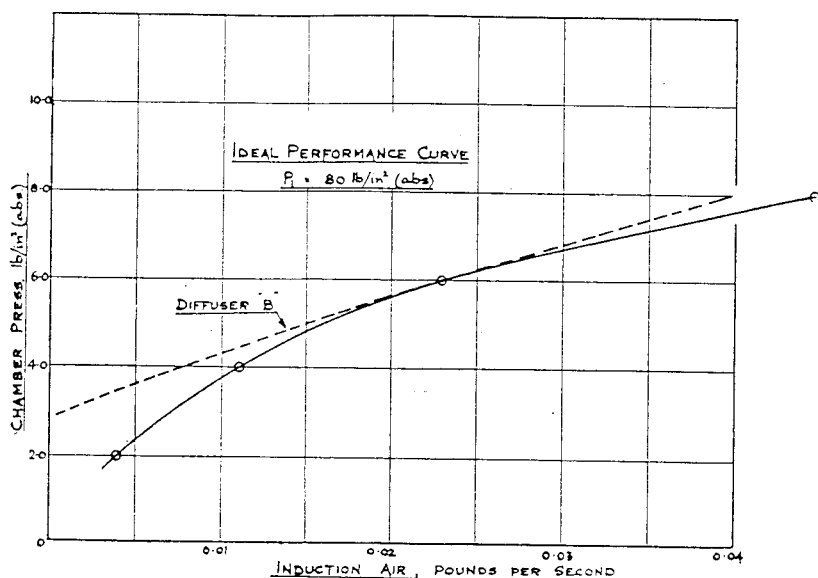


FIG. 18.

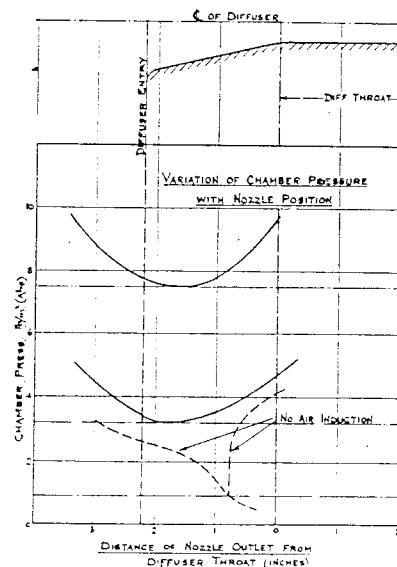


Fig. 19

section has been reached.

The results of the investigation on diffuser design have been combined in the calculation chart shown in Fig. 21. This has been drawn to show how an actual ejector plant might be designed to suit a definite specification. For actual use such a chart would require to be based on experiments made with steam as the working fluid, but it is thought that it would be better suited to design purposes than a calculation based upon theoretical principles or empirical formulae.

An ordinary specification would include the supply pressure of the working fluid, the amount of air to be handled, the vacuum from which it has to be drawn, and the throat area of each ejector unit in the plant. The chart is based upon unit nozzle throat size, which, along with the supply pressure, governs the ejector consumption.

The constant nozzle pressure curves of vacuum against induced air quantity per unit nozzle throat area have been deduced from the tests. From these the air-handling capacity of each unit in the plant can be calculated and hence the number of ejector units to deal with the specified air quantity. The diffuser throat diameter, and the distance of the nozzle outlet from the commencement of the diffuser throat section, for unit nozzle diameter, can then be found from the series of curves which also have been derived from the test results. Assuming, for example, that the stage vacuum has to be 17.5 ins. of mercury, the nozzle supply pressure 85 lb. per sq. in. abs., and throat diameter 0.25 in. Starting with the top, right-hand diagram a horizontal line is drawn to the right from the 17.5 ins. vacuum point to cut the 85 lb. sq. in. pressure line. A vertical line drawn from this point cuts the air suction base at 0.055. The area of the nozzle is 0.049 sq. in., so that the amount of air that could be drawn in would be  $0.055 \times 0.49 = 0.027$  lb. per second. Continuing the vertical line until it cuts the 85-lb. pressure line in the lower figure and drawing another horizontal line this cuts the scale of diffuser dia. at 2.77. The diameter of nozzle dia.

the diffuser throat will be, therefore,  $0.25 \times 2.77 = 0.69$  ins. Returning to the first point, and drawing a horizontal line to the left to cut the 85-lb. pressure line in the corresponding figure, the point of intersection is vertically above the figure of 9.3 on the scale representing the diffuser distance. From this nozzle dia.

it will be seen that the distance of the exit end of the nozzle from the diffuser throat should be about  $9.3 \times 0.25 = 2.3$  ins.

This completes the account I set out to give upon the influence of ejector size and proportions upon performance, and it is hoped that the results may prove of some value to those who contemplate using this system for exhausting air or other gases or for transporting fine solids.

It may be, however, of interest to examine a few further illustrations which give some idea of the actions that are taking place in a diffuser. For this purpose a glass-sided diffuser of rectangular section was prepared to work in conjunction with a nozzle of similar section. Light rays from an arc spot lamp were passed through the diffuser and an ordinary camera was used to take photographs of the shadows thrown on the screen by the refraction of the light passing through the jet. The results are shown in Fig. 22, where the top photograph shows the waves produced when the ejector was working under the best conditions for the selected nozzle pressure. In this picture it will be noted that the

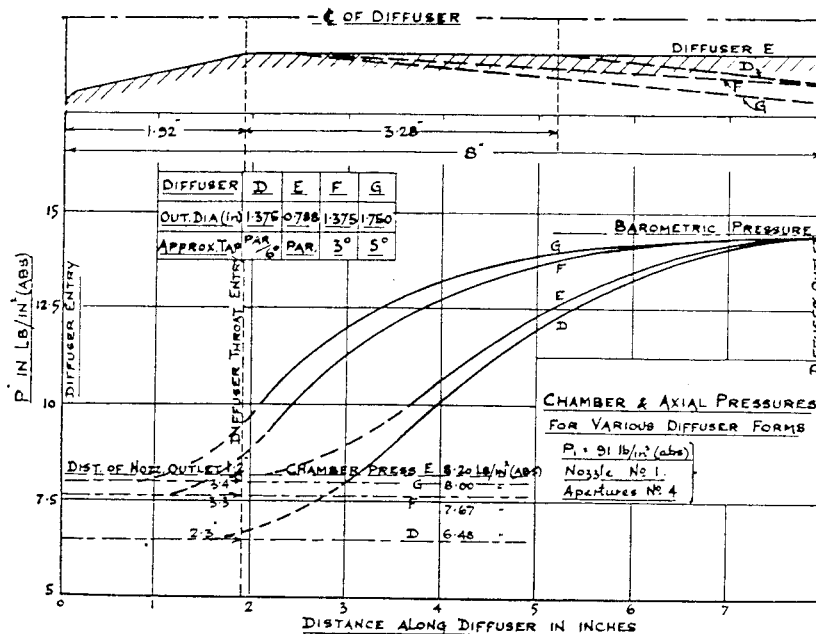


FIG. 20.

jet issuing from the nozzle is not visibly disturbed until it is close to the throat section, when entrainment takes place. The clearance between the visible boundary of the jet—where the waves are reflected—and the diffuser wall should be noted. In photograph (b) the sectional area of the diffuser has been reduced and the choking effect can be clearly seen. A disturbance has been set up around the stream in front of the throat; also the wave length has been reduced due to the increase in chamber pressure and consequent reduction of jet velocity. This figure should be compared with Fig. 17, where the pressure curves resulting from too small a diffuser are shown. In photograph (c) the nozzle has been brought closer to the diffuser, but there is no very marked difference between this and (a). Compression takes place sooner and the amplitude of the wave is seen to decrease rapidly as compression starts. The chamber pressure is only slightly higher than that with (a) and, consequently, the wave front at the nozzle outlet is very similar in each case.

Before concluding, I should again like to express my debt to Dr. Third for the greater part of the material from which this lecture has been constructed, and also to acknowledge the assistance given by my colleague, Mr. P. Caldwell, in the preparation of the diagrams by which it is illustrated.

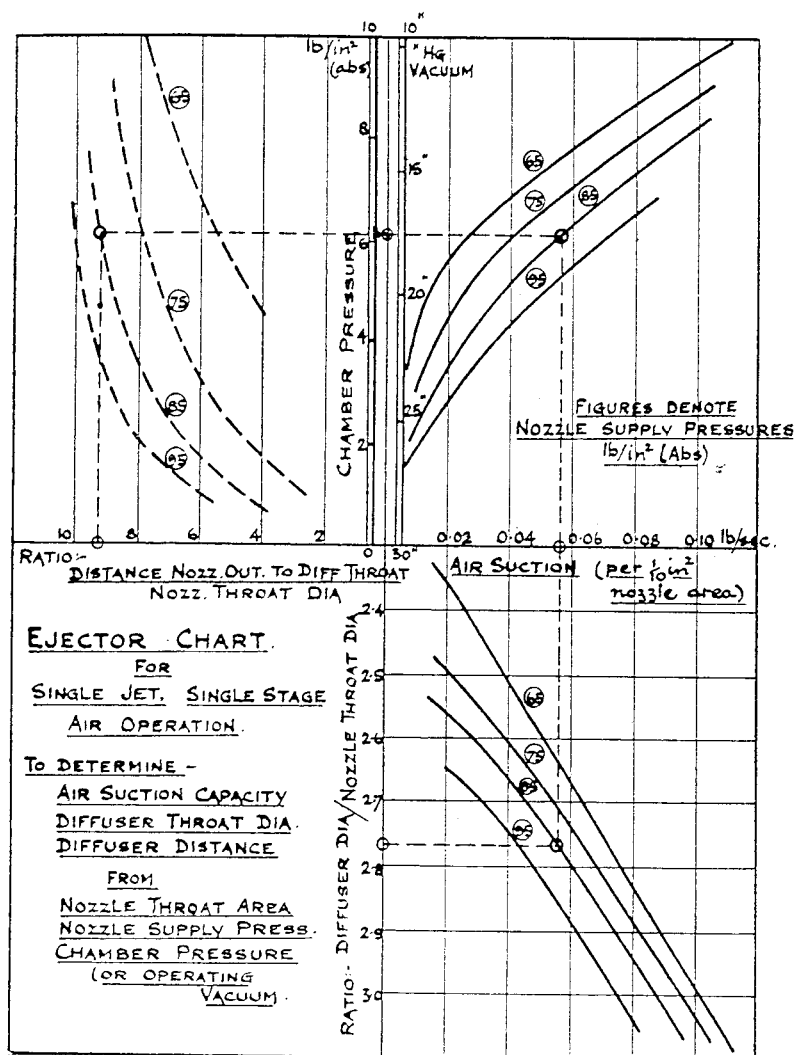
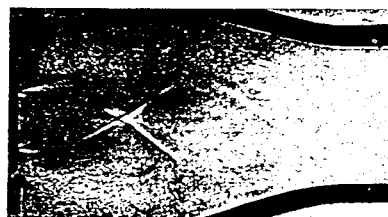


FIG. 21.

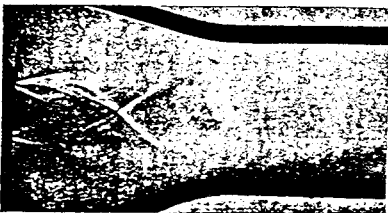
Shadow photographs of waves in the combining chamber of a glass-faced ejector, to show the effect of dimensions on the jet form. Nozzle press. 90 lb./in.<sup>2</sup> abs.; induction air 0.022 lb./sec.



(a) Optimum diffuser distance and throat area. Chamber press. 7.0 lb./in.<sup>2</sup> abs.



(b) Diffuser throat area reduced.



(c) Diffuser distance reduced.  
FIG. 22.



*Proceedings - Institution of  
Mechanical Engineers - Vol. 124  
pp. 231-300*

THE PRODUCTION OF A VACUUM IN AN AIR TANK  
BY MEANS OF A STEAM JET.

By F. R. B. WATSON, B.Sc., M.I.MECH.E.

The paper consists mainly of an account of experiments conducted by the author on a steam-jet operated air ejector with the object of investigating certain quantities which, although they affect the vacuum produced, are not included in the theory of the ejector as it exists at present. The chief of these quantities was found to be the distance from the outlet of the steam nozzle to the throat entrance of the diffuser, and in order to examine the effect of varying this length a special form of air ejector with a sliding diffuser was designed and provision was made in the design for the use of a search tube which could be passed right through the diffuser and up to the nozzle outlet. In addition to the work conducted on this apparatus the author was obliged to carry out a separate set of experiments, with the diffuser removed, and in which an air pump created the vacuum, in order to examine the change in the stationary waves in the steam jet when it was discharging at different vacua. This was done by viewing the jet through a plate-glass window fitted into a part of the ejector. Observations were made and photographic records were obtained at different outlet pressures ranging from atmospheric pressure to 27.5 inches of vacuum. These photographs are probably of interest in connexion with steam nozzles in general, as they show the form of the jet when it was over-expanded and under-expanded as well as when it expanded to the designed pressure. The ejector was also operated normally with a glass mouthpiece forming the entrance and parallel throat of the diffuser, and this arrangement was used to view the waves in the throat at the higher vacua.

Another quantity which affects the vacuum is the length of the diffuser throat and two throat lengths were used: (a)  $\frac{1}{10}$  inch, and (b) a length equal to twice the throat diameter, or  $1\frac{1}{2}$  inches. Two different forms of diffuser entrance were tried, and the vacuum and steam-air ratio at different initial steam pressures for these two different designs have been recorded in the paper.

*Introduction.*—The steam jet, as a means of creating a slight reduction of pressure in the atmosphere surrounding it and thereby inducing an air current to flow, has long been used and has many applications; but it is in its application to the production and maintenance of a high or fairly high vacuum in an adjoining chamber that it has become so important an agent for this purpose in certain

branches of motive power engineering. In its simplest form the steam-jet operated air pump, or air ejector, consists of a steam nozzle, an air chamber, and a diffusing nozzle or diffuser. The steam jet, issuing from the convergent-divergent nozzle with a high velocity, entrains the air, or mixture of air and vapour, in the air chamber and the combined stream passes into the diffuser where the kinetic energy is converted into pressure energy, with a certain amount of loss of energy, and the air, vapour, and steam are discharged at about atmospheric pressure.

Probably the two best known applications of the air ejector are its use, for more than fifty years, in producing and maintaining the partial vacuum in the cylinders and reservoirs of the vacuum brakes on railway trains, and its more recent application for the production and maintenance of the high vacua in the steam condensers of modern steam turbine installations, a duty to which it was first applied by the Hon. C. A. Parsons in 1902, when he introduced his "vacuum augments." \* For the railway brake a single-stage ejector is used, as the vacuum required rarely exceeds 25 inches of mercury, but for the modern turbine plant it is now standard practice to install a two-stage ejector, as a vacuum formed by a single stage is liable to be unstable for a lower pressure than about 26 inches of mercury on account of the liability of the stream in the diffuser to "break back." The name of Monsieur Le Blanc is well known for his valuable pioneer work on steam-jet operated ejectors, and his designs for ensuring stability at high vacua are described in many textbooks. In the two-stage ejector it is the usual practice to make the pressure ratio of compression about the same in each stage, as in the two-stage air compressor. If  $p_1$  and  $p_2$  are the absolute pressures in the condenser and of the atmosphere respectively, and  $p$  the pressure in the inter-condenser, where the steam from the first stage is condensed, then

$$\frac{p}{p_1} = \frac{p_2}{p}$$

Thus with a condenser vacuum of 29 inches (1 inch abs.) and for a barometric height of 30 inches,  $\frac{p}{1} = \frac{30}{p}$ , therefore  $p = 5.48$  or 5.5 inches abs. nearly. The compression ratio for each stage is therefore 5.5, and the inter-condenser vacuum  $30 - 5.5 = 24.5$  inches.

The theory of the steam-jet operated air ejector is not a simple one, on account of the number of variables which have to be taken into consideration, and as it exists at present it is incomplete; hence the success of the various forms of ejector in use appears to be, to a considerable extent, the outcome of prolonged experimental investigation. Unfortunately, however, very few results of such investigations are available in the technical literature connected with this subject.

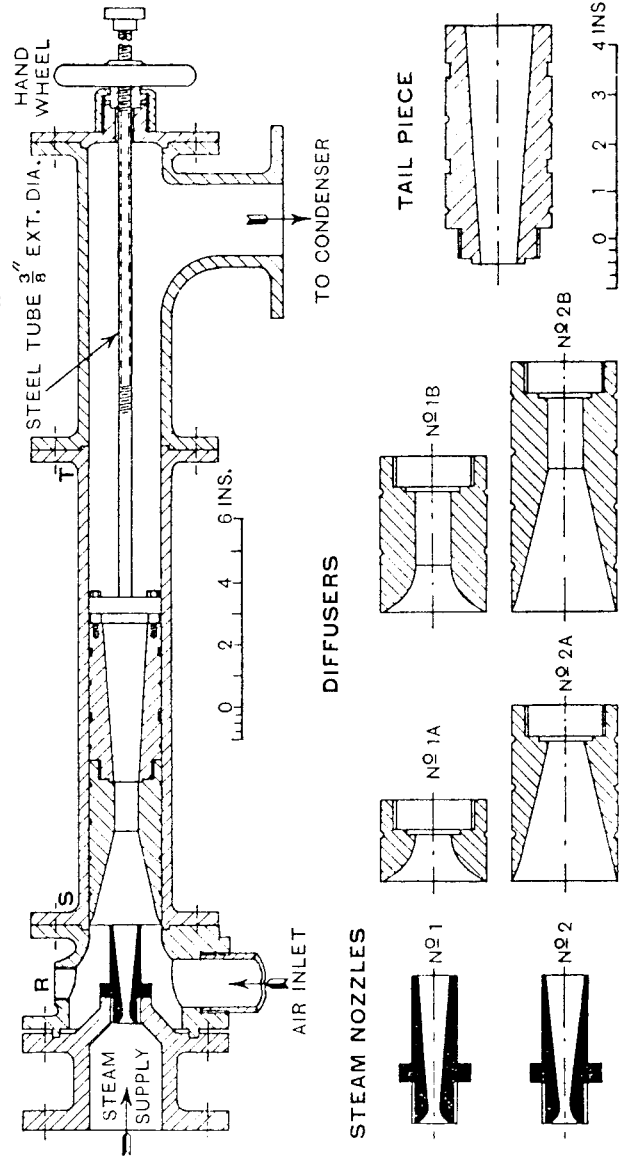
\* *Engineering*, 1904, vol. 78, p. 500.

*Objects of Experiments.*—It was therefore decided to undertake the examination of certain factors which are lacking in the theory, entirely from the physical aspect and without making any attempt at their mathematical elucidation. The chief of these factors were as follows :—

- (1) One important length, which is not included at all in the theory, and which has a very important influence on the vacuum produced, namely the distance from the steam nozzle to the diffuser.
  - (2) The reason why better results are obtained from an ejector in which the diffuser has a long parallel throat. In the theory, consideration is given only to the case of a gradual constriction tapering off to the outlet, without having any length parallel.
  - (3) How the improvement in vacuum effected by having this parallel throat can be explained physically.
- Other objects of a more practical nature were :—
- (i) The determination of the ratio of steam to air at different vacua and under different initial steam pressures.
  - (ii) Observations of the rise of pressure of the combined stream of steam and air as it passed through the diffuser.
  - (iii) Comparative results for the ejector working with a diffuser having a short rounded entrance compared with one having a tapered entrance, the latter being the more usual form in practice.

For information on sections (1), (2) and (3) it was found necessary

Fig. 1.—*Steam-Jet operated Air Ejector, with sliding diffuser.*



to carry out a careful inspection of the steam jet to observe the changes in the stationary waves in the core of the jet under different initial steam pressures and under different outlet pressure conditions. An optical method of inspection was adopted, for this caused no disturbance of the jet, and photographic records were obtained. The author considers that these photographs may be of some interest in connexion with the discharge from steam nozzles in general, as they show certain changes in the jet produced by changes of outlet pressure.

*Description of Apparatus.*—The ejector used was a single-stage one (which would, of course, correspond to a second stage unit in a two-stage ejector), and it was originally designed to extract 35 lb. of dry air per hour, the air being supposed to be saturated with water vapour at 61 deg. F., with a steam consumption of 230 lb. per hour of initially dry and saturated steam at 100 lb. per sq. in. by gauge, while maintaining a vacuum of 25.5 inches of mercury. It was afterwards realized that this project was a somewhat ambitious one. The above figures give a steam-air ratio of 6.6, and whether this performance is physically possible or not with an apparatus of this kind under the assumed conditions, the author is unable to state with certainty; but the actual performance never approached so low a figure, and the ejector had to be operated at a higher steam pressure to give the required vacuum. (This weight of air would be the allowance, by the British Electrical and Allied Manufacturers' Association rating,\* for a land surface condensing plant condensing 64,000 lb. of steam per hour.) All the experiments recorded here were carried out with atmospheric air only, and no attempt was made to use saturated air. The calculation of steam nozzle and diffuser dimensions is given in the Appendix, page 262.

In the course of these experiments two ejectors were used. The first one which was designed gave fairly good results from which much useful information was obtained. But there was a screwed connexion between the air chamber and the diffuser, and although different settings of the diffuser in relation to the steam nozzle could be made by using loose collars or distance pieces, it took too long to effect the required alterations. Hence a second ejector with a sliding diffuser, shown in section in Fig. 1, was designed by the author, in which the diffuser could be moved along horizontally while the ejector was operating, thus enabling the vacuum at any diffuser setting to be rapidly obtained.

This movement was effected by rotating the handwheel (shown in Fig. 1) which was mounted on a long brass nut at its centre. The latter engaged a screw on the outside of a thick-walled steel tube, about 1 1/4 inch internal diameter, the inner end of this tube being attached to a bridge piece fitted on the outlet end of the diffuser. A tube was used for this purpose instead of a solid rod to

\* Dry air capacity = (steam condensed per hour ÷ 2,000) lb. per hour.

TABLE 1.—Particulars of Diffusers.

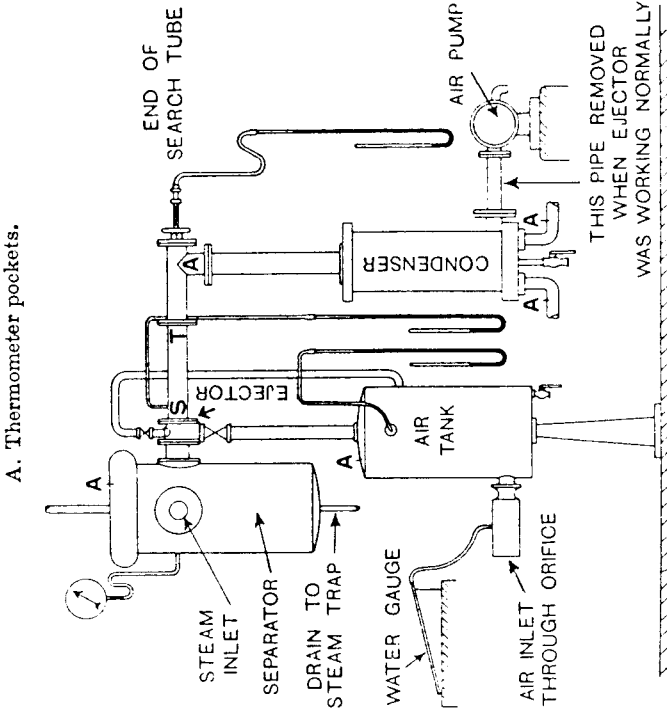
Diffuser No.	Form of Entrance.	Length of Entrance, inches.	Diameter of Throat, inches.	Length of Throat, inches.	Length of Tail Piece, inches.
1A .	Rounded	1	2	Nearly $\frac{1}{2}$	5
1B .	"	1		$1\frac{1}{4}$	
2A .	Tapered	3		Nearly $1\frac{1}{2}$	
2B .	"	3		$1\frac{1}{2}$	

TABLE 2.—Particulars of Steam Nozzles.

Nozzle No.	Diameter of Throat, inches.	Diameter of Outlet, inches.	Length from Throat to Outlet, inches.	Cone Angle, deg.	Vacuum* at Discharge, inches of mercury.
1 .	$\frac{5}{32} \pm 0.0005$	$1\frac{1}{4}$	213	9.5	25.5
2 .	$\frac{7}{32} \pm 0.008$	$\frac{7}{8}$		13.1	27.2

\* The vacua given in this Table are those for which the nozzles were designed when the admission pressure was 100 lb. per sq. in. by gauge ; when the admission pressure was 140 lb. per sq. in. by gauge the vacua for which the nozzles were suited were 24.0 and 26.25 inches respectively.

FIG. 2.—Diagram showing General Arrangement of Plant.



enable a search tube to be passed up the bore of the steel tube. The search tube itself was made of two pieces of brass tube  $\frac{3}{16}$  and  $\frac{1}{4}$  inch external diameter respectively, and was similar in form to that used by Professors Mellanby and Kerr\* for exploring a steam nozzle. The piece of larger diameter, which could just slide inside the bore of the steel tube, was jointed to the piece of smaller diameter, and the latter could be passed up through the throat of the diffuser. The exploring end of the smaller tube was formed by stopping up the bore and drilling a  $\frac{1}{32}$ -inch diameter hole diametrically at a point  $\frac{7}{16}$  inch from the end. It will be observed that any leakage which took place through the bore of the steel tube was *outwards*, as the inner end of this tube terminated in a region where the pressure was slightly above that of the atmosphere, and there was therefore no risk of any leakage through this tube affecting the vacuum. The diffuser could be moved along a considerable distance inside the 24-inch internal diameter brass cylinder, the clearance between it and the walls being from 0.003 to 0.004 inch, and the design adopted also enabled different forms and lengths of diffuser to be used which could be quickly changed. The packing in the sliding diffuser consisted of two coils of thin cotton rope wound in each of two grooves  $\frac{1}{8}$  inch deep in the tail piece, with the addition of several small grooves  $\frac{1}{16}$  inch deep turned in the surface, as shown in Fig. 1. The diffuser was made in two parts, screwed together, and they could come apart on a transverse plane passing through the outlet end of the throat. When the same diameter of throat was used, inlet ends with different throat lengths or inlet ends with different forms of entrance could be used on the same tail piece. The throat diameter of the four diffusers used in these experiments was  $\frac{3}{32}$  inch, and the two lengths of throat used were (a) nearly  $\frac{1}{16}$  inch, i.e. with practically no parallel portion in the throat, and (b)  $1\frac{1}{4}$  inches, i.e. with a length of parallel throat equal to twice its diameter. The two forms of entrance used were (i) a short rounded form having a length up to the throat (including the throat of negligible length) of 1 inch, and (ii) a straight tapered form having a length up to the throat of 3 inches. The particulars and reference numbers of the four diffusers and the two steam nozzles used are given in Tables 1 and 2.

In the experiments on both designs the ejector in use was connected to one of the openings in a steam separator about 9 inches internal diameter and 27 inches deep, and the steam pressure at the nozzle inlet was varied by throttling the steam at a stop valve on the admission pipe to the separator. The general arrangement of the testing plant is shown diagrammatically in Fig. 2. The maximum steam pressure available was 140 lb. per sq. in. by gauge, and the superheat at the separator varied from about 5 deg. F. to 20 deg. F., according to the rate of discharge by the nozzle. The separator and steam pipe were well lagged. The cylindrical air tank, of about

\* Trans. Inst. Eng. and Shipbuilders in Scotland, 1920-1. vol. 64, p. 80.

are connected respectively with two entirely different functions which the ejector has to perform, the first the admission and entrainment of the air, and the second a sealing or partial sealing of the diffuser throat (by a portion of a wave in the jet) as well as a pumping action between the regions of low and high pressure. Of course, in a particular case when once the correct value of  $D$  has been obtained, it is possible that a further slight improvement in vacuum may be effected by an adjustment of  $L$ . When using the first ejector the author carried out a separate series of experiments with a specially made diffuser having a long tapered inlet, and lengths in most cases  $\frac{1}{2}$  inch wide were machined off the inlet end and the broad collar alternately (the diffuser was screwed into the body of the air chamber). In this way the difference in vacuum in different diffuser positions within the range due to a decrement of  $D$  was compared with the change due to an equal increment of  $L$ . Over a range of movement from  $D = 5\frac{1}{16}$  inches to  $D = 3\frac{3}{16}$  inches by far the greater improvement in vacuum was due to the altered value of  $D$ , and in pursuing this somewhat drastic method of experimenting a limit was reached when no further improvement was noticed due to the reduction in the value of  $D$ . The curves obtained from the results referred to were most enlightening, and only for reasons of space are they omitted here. In the experiments recorded in this paper with the sliding diffuser,  $L$  and  $D$  were changed simultaneously, the diffuser being moved *inwards* towards the steam nozzle in all cases, and it will be observed from Figs. 3 and 4 that while  $L$  was being *decreased* the vacuum was *increased* up to a certain point, which indicated that the length  $D$  was the predominant one.

*Over-Expansion of the Steam leaving the Nozzle.*—When steam, after entering a nozzle at a certain initial pressure, expands and issues at the exit section with a pressure equal to that of the external medium, it is completely expanded. This outlet condition has been referred to in this paper as discharge at the “designed pressure,” i.e. the outlet pressure for which the nozzle was designed. When the pressure outside the exit section of the nozzle is greater than the designed pressure “over-expansion” of the steam is said to take place in the nozzle, and when it is less “under-expansion” is said to take place in the nozzle. It is sometimes stated that over-expansion is an effect which contributes to the production of a good and steady vacuum in an air ejector, and the author's experience on the whole bears this out, and also showed that the over-expanded jet was better suited to the conditions over the wide range of pressure used. Hence in all the tests recorded in the paper with air flow conditions the steam jet was in an over-expanded state, and nozzle No. 2 was used. The additional suction effect produced by over-expansion would appear to be produced by the inward pressure of the surrounding air on the steam jet (of lower pressure) and in the process the air becomes more deeply

2.5 cu. ft. capacity, into which air was allowed to leak and in which the partial vacuum was maintained, was situated vertically below the air inlet to the ejector and connected to the latter by a  $1\frac{1}{2}$ -inch diameter pipe fitted with a stop valve at its connexion to the air inlet. This valve could be closed, along with the air leak, and the tank allowed to stand for a time under partial vacuum, to test the joints on the tank for airtightness. A supplementary air inlet to the ejector (shown at R in Fig. 1) was provided, but no improvement in the vacuum was effected when this was put in communication with the air tank while the ejector was operating. The air leaking into the tank flowed through two orifices,  $9\frac{1}{2}$  inches apart, the outer one being  $\frac{3}{4}$  inch diameter and sharp-edged and the inner one  $\frac{3}{16}$  inch diameter, and they were mounted on an air box connected to the side of the tank. The pressure difference across the outer orifice was measured by means of an inclined water gauge. The steam and air on leaving the ejector passed into a small surface condenser where the steam was condensed at atmospheric pressure, and collected and weighed if necessary.

#### SURVEY OF RESULTS.

All vacua were measured by mercury columns, three of which were used, one on each of the following parts: air tank, air chamber (used during photographic work) and search tube. All vacua have been reduced to the equivalent at 30 inches barometric pressure. All steam pressures given are by gauge, unless otherwise stated.

*The Lengths L and D.*—When the diffuser of an ejector is moved relatively to the steam nozzle two quantities which affect the vacuum are altered, namely the length from the outlet end of the nozzle to the inlet of the diffuser, and the length from the outlet end of the nozzle to the entrance of the throat of the diffuser. These two lengths will be referred to as  $L$  and  $D$  respectively. In the former case the circumferential area of the jet in contact with the entering air is altered, and in the latter the setting of the diffuser throat with reference to certain wave sections in the series of stationary waves in the core of the jet. The stationary waves referred to here are caused by a sudden change of pressure. An excellent photograph of the stationary waves in a steam jet discharging into the atmosphere is included in Mr. H. L. Guy's contribution to the discussion on the Fifth Report of the Steam-Nozzles Research Committee.\* It is rather difficult to say with certainty how the air is entrained by the steam jet in an air ejector, and some writers on the subject are inclined to attach chief importance to the effect of surface friction. This varies with  $L$ , but from the results recorded here it will be seen that, with this type of ejector, the predominating quantity in producing the high vacua is apparently the value assigned to  $D$ . But it is probable that these two lengths

\* Proc. I.Mech.E., 1928, vol. i, p. 82.

embedded in the jet, and the waves, of course are more pronounced. It is important to remember that an improvement in vacuum due to any cause, such as a favourable diffuser setting, would be accompanied by a slightly increased jet velocity due to the increased heat drop, and hence the effect on the vacuum would be cumulative.

*Variation in Vacuum with D.*—In Figs. 3 and 4 are shown the variations in vacuum for different values of  $D$  for diffusers Nos. 1 and 2 with  $\frac{1}{16}$ -inch and  $1\frac{1}{2}$ -inch throat in each case, and these observations were carried out at as nearly as possible constant steam pressures of 80, 100, 120, and 140 lb. per sq. in. by throttling

the steam at admission to the separator. These curves show, in the first place, that the lower steam pressures would not produce a high vacuum when air flow took place through the tank. For the ejector to work satisfactorily the velocity of the issuing steam must be high, but with both a low vacuum and a low initial steam pressure the heat drop across the nozzle is low, and consequently the steam velocity is relatively low. The second point to be noticed in these curves is that the lower the pressure the lower is the value of  $D$  for maximum vacuum at that pressure, e.g. in Fig. 3 the point A moves towards the left as the pressure is reduced. The explanation of this result was evident from the photographic records of the jet, some of which are reproduced later in the paper, which showed clearly the shortening of the wave series in the jet with reduced pressure drop across the nozzle.

The curves in Figs. 3 and 4 afford a means of comparing the advantages or otherwise of the two different forms of entrance to the diffuser. Diffuser No. 2, with the tapered entrance, appears to be on the whole the better form, for it gave a slightly higher vacuum over a greater range, and when in use it was more stable in its action. These advantages probably account for this form of entrance being adopted by so many makers of air ejectors. A peculiarity in the behaviour of diffuser No. 1 was the sudden and rapid rise of vacuum at practically constant pressure at certain diffuser settings, when the steam pressure was slowly increased. The mercury almost rushed up the tubes of the gauges. One instance of this may be observed from a reading in the second section of Table 5, where the "vacuum in closed tank" jumped from 21.2 to 27.4 inches at a pressure of 115 lb. per sq. in. With diffuser No. 2 the mercury rose much more slowly—sometimes just moving—to above. One such instance is indicated by one reading given at 105 lb. per sq. in. in the last horizontal column in Table 5. The same tail piece was used on all the diffusers when the observations plotted in Figs. 3 and 4 were made. In Tables 3 and 4 are given the actual values of the vacuum obtained, with air flow, for various values of  $D$ .

*Effect of the Long Parallel Throat.*—It has already been stated that in most air ejectors the diffuser has a throat which is parallel for a considerable length, and the reason for this may be seen from a study of the curves in Figs. 3 and 4, in pairs at the same steam pressure, for at practically every pressure shown, with both types of diffuser, the one with the parallel throat gave the higher maximum value for the vacuum. The advantage is also clearly shown by comparing the two groups of vacuum-pressure curves, with air flow, in Fig. 5, where the full-line curves show higher vacuum than the dotted curves. It will be observed in Figs. 3 and 4 that, especially at the higher pressures of 120 and 140 lb. per sq. in., the throat tends to give a more nearly uniform vacuum over the range shown; this is due to the formation of a second "peak" on the

FIG. 3.—*Vacua at different Diffuser Settings, Diffusers Nos. 1A and 1B.*  
Constant steam pressures: 80, 100, 120, and 140 lb. per sq. in. gauge.  
Steam Nozzle No. 2.

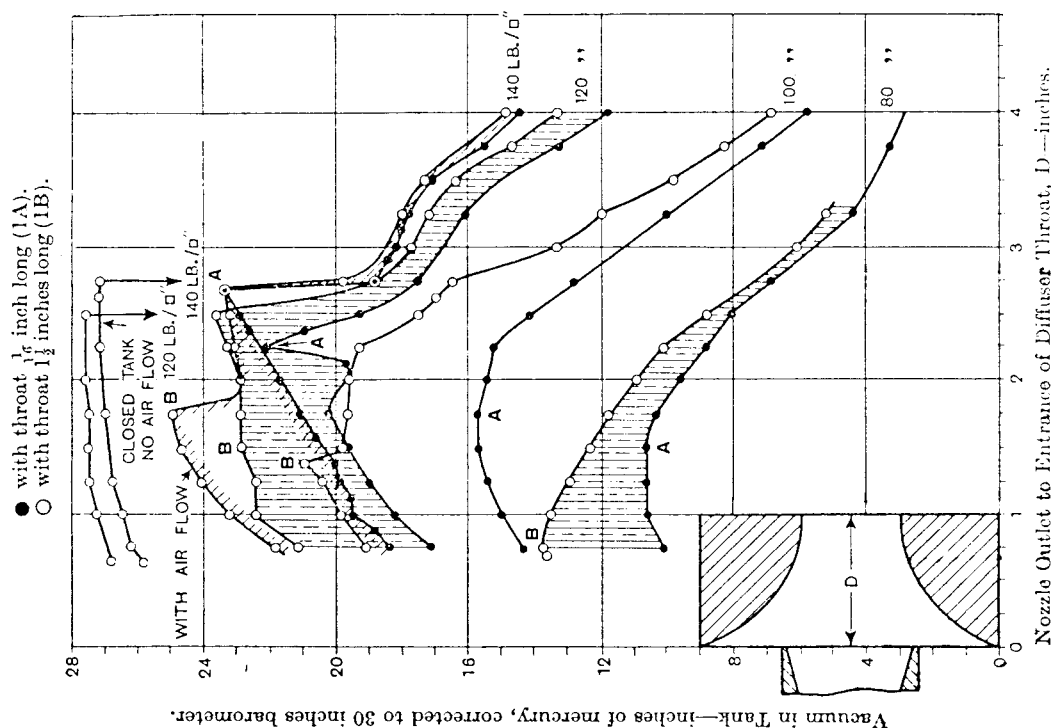
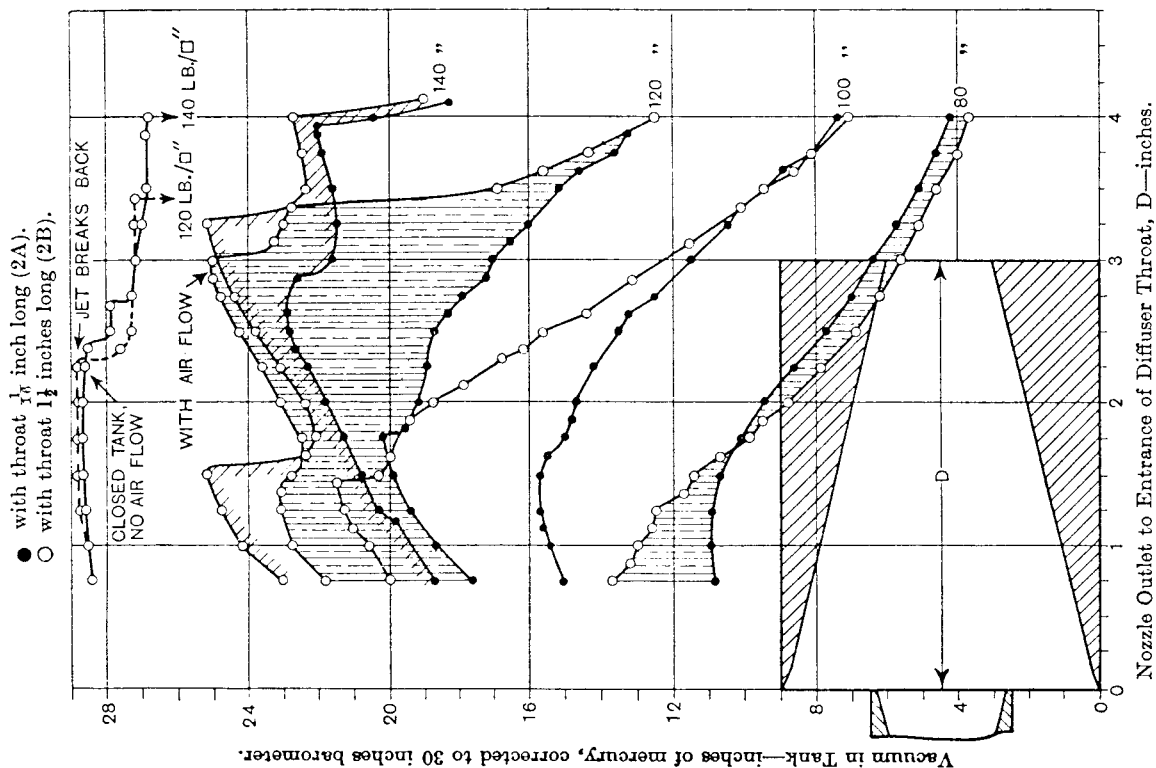


FIG. 4.—*Vacua at different Diffuser Settings, Diffusers Nos. 2A and 2B.*  
Constant steam pressures : 80, 100, 120, and 140 lb. per sq. in. gauge.  
Steam Nozzle No. 2.



curves. In Fig. 4 at a pressure of 140 lb. per sq. in. the same vacuum (25.2 inches) is reached at two positions of the diffuser, namely when  $D = 3\frac{1}{2}$  inches and when  $D = 1\frac{1}{2}$  inches, and it is interesting to note how the vacuum is produced as the pressure rises in the two cases. This is shown in Fig. 6 by the two curves marked M and N, and it is seen that the inner position ( $D = 1\frac{1}{2}$  inches) is evidently

TABLE 3.—*Diffusers 1A and 1B with Throat Lengths  $\frac{1}{16}$  inch and  $1\frac{1}{2}$  inches respectively, Steam Nozzle No. 2.*

D, inches	Vacuum in Tank, inches of mercury corrected to 30 inches barometric pressure							
	at 80 lb. per sq. in., gauge.		at 100 lb. per sq. in., gauge.		at 120 lb. per sq. in., gauge.		at 140 lb. per sq. in., gauge.	
	Diffuser 1A	Diffuser 1B	Diffuser 1A	Diffuser 1B	Diffuser 1A	Diffuser 1B	Diffuser 1A	Diffuser 1B
4	—	—	5.9	6.9	11.9	13.3	14.5	14.9
$3\frac{3}{4}$	3.3	—	7.2	8.3	13.3	14.7	15.5	—
$3\frac{1}{2}$	—	—	—	9.8	—	16.4	17.1	17.3
$3\frac{1}{4}$	4.4	5.2	10.0	12.0	16.1	17.2	17.8	18.0
3	—	6.1	—	13.3	—	17.7	18.2	—
$2\frac{3}{4}$	6.9	—	12.8	16.5	17.5	19.0	18.8	19.8
$2\frac{1}{2}$	—	—	—	—	—	—	23.3	23.4
$2\frac{1}{4}$	8.1	8.8	14.1	17.5	19.3	23.6	22.9	23.2
$2\frac{1}{8}$	—	—	—	—	21.0	—	22.6	—
$2\frac{1}{16}$	8.7	10.1	15.2	19.3	22.1	23.3	22.2	23.1
$2\frac{1}{32}$	—	—	—	—	19.6	—	—	—
2	9.6	10.9	15.4	19.6	22.9	22.9	21.7	22.9
$1\frac{3}{4}$	10.3	11.8	15.7	19.6	20.2	22.9	21.1	24.95
$1\frac{1}{2}$	10.6	12.3	15.7	19.8	19.6	22.85	—	24.7
$1\frac{1}{8}$	—	—	—	21.0	—	—	20.1	—
$1\frac{1}{16}$	10.6	12.9	15.4	20.4	19.0	22.4	19.9	24.1
$1\frac{1}{32}$	10.6	13.5	15.0	19.0	18.2	22.4	19.5	23.2
$\frac{3}{4}$	10.1	13.7	14.3	19.1	17.1	21.1	18.3	21.8

the better setting. This is rather an important result to be observed in the design of an ejector. The behaviour of the jet in passing through the long and the short throats is dealt with in the last section of the paper.

*Increase of Vacuum with Initial Steam Pressure.*—As an air ejector of this kind depends for its action on the velocity of the issuing steam, a vacuum-pressure curve should be somewhat similar in form to a velocity-pressure curve. The curves showing the growth of vacuum with the increase of steam pressure for diffusers Nos. 1 and 2 are given in Figs. 5 and 6 for about the best diffuser settings at 100, 120, and 140 lb. per sq. in., the settings used having been taken from the curves in Figs. 3 and 4. The vacua reached with closed tank and "no air flow" are also shown, and the actual observations are given in Table 5.

The curves in dotted lines in Fig. 5 are for the diffuser with practically no length of parallel throat, and it will be seen that in addition to the maximum values of the vacuum being low compared

TABLE 4.—Diffusers 2A and 2B with Throat Lengths  $\frac{1}{16}$  inch and  $1\frac{1}{2}$  inches respectively, Steam Nozzle No. 2.

D, inches	Vacuum in Tank, inches of mercury corrected to 30 inches barometric pressure							
	at 80 lb. per sq. in., gauge.		at 100 lb. per sq. in., gauge.		at 120 lb. per sq. in., gauge.		at 140 lb. per sq. in., gauge.	
	Diffuser 2A	Diffuser 2B	Diffuser 2A	Diffuser 2B	Diffuser 2A	Diffuser 2B	Diffuser 2A	Diffuser 2B
$4\frac{1}{2}$	3.9	3.5	6.7	6.4	11.0	11.0	16.5	18.4
$4\frac{1}{4}$	—	—	—	—	—	—	18.3	19.0
$4\frac{1}{8}$	4.2	3.7	7.4	7.1	12.6	12.5	20.5	22.7
$3\frac{7}{8}$	—	—	—	—	—	—	22.0	—
$3\frac{3}{4}$	4.6	4.0	8.1	8.1	13.6	14.3	21.9	22.5
$3\frac{1}{2}$	—	—	—	—	—	—	—	—
$3\frac{1}{4}$	5.1	4.6	9.5	9.4	15.1	16.9	21.6	22.4
$3\frac{1}{8}$	—	—	—	—	—	22.8	—	22.6
$3\frac{1}{16}$	5.7	5.1	10.5	10.8	16.0	23.0	21.5	25.2
$3\frac{1}{32}$	—	—	—	—	—	23.3	—	—
$3$	6.4	5.6	11.5	12.4	17.0	25.0	21.6	24.9
$2\frac{7}{8}$	—	—	12.1	—	17.2	25.0	22.6	—
$2\frac{3}{4}$	7.0	6.2	12.5	13.9	17.9	24.8	—	24.4
$2\frac{1}{2}$	—	—	13.2	14.4	—	—	22.9	—
$2\frac{1}{4}$	7.7	6.9	13.5	15.6	18.7	24.3	22.8	23.8
$2\frac{1}{8}$	8.6	7.9	14.2	17.1	18.9	23.6	22.3	23.1
$2\frac{1}{16}$	—	—	—	—	—	—	—	—
$2$	9.4	8.8	14.7	18.8	19.2	23.1	21.8	22.4
$1\frac{15}{16}$	10.1	9.9	15.0	19.8	20.2	22.5	21.3	22.1
$1\frac{13}{16}$	—	10.7	15.5	20.0	—	22.5	—	22.4
$1\frac{11}{16}$	10.7	11.4	15.7	20.3	19.9	22.8	20.8	25.2
$1\frac{9}{16}$	—	11.7	15.7	21.4	—	23.1	—	—
$1\frac{7}{16}$	—	—	—	—	—	—	—	—
$1\frac{5}{16}$	10.9	12.5	15.7	21.3	19.4	23.1	20.3	24.8
$1\frac{3}{16}$	10.9	13.0	15.4	20.6	18.7	22.8	—	24.2
$1\frac{1}{16}$	10.8	13.7	15.0	20.0	17.6	21.8	18.7	23.0

TABLE 5.—Diffusers 1B and 2B ; Steam Nozzle No. 2.

FOR ABOUT BEST DIFFUSER SETTING AT 140 LB. PER SQ. IN., GAUGE.

For 1B, D =  $1\frac{1}{2}$  inches ; for 2B, D =  $1\frac{1}{2}$  inches.

Steam Pressure, lb. per sq. in., gauge.	Maximum Steam used, lb. per hour.	Vacuum in Tank (corrected) inches mercury.		Water Gauge, inches.		Atmos. Air entering tank, lb. per hour.		Ratio max. steam atmos. air		Atmospheric Conditions.		* Vacuum in closed tank (corrected), inches mercury.	
		1B	2B	1B	2B	1B	2B	1B	2B	1B	2B	1B	2B
60	163	5.0	5.5	0.24	0.26	16.4	17.0	9.95	9.60	Dry Bulb, 64.2°F., 66.8°F. Wet Bulb, 57.6°F., 60.0°F. Rel. Humid. 67% 67% Barometer, 30.33 30.05 inches inches		6.2	5.9
70	184	7.0	7.4	—	—	—	—	—	—			8.6	8.4
80	204	11.0	11.3	0.48	0.49	23.2	23.3	8.80	8.75			12.5	12.5
90	225	15.0	16.5	—	—	—	—	—	—			18.3	17.2
100	246	19.4	19.5	0.65	0.65	27.0	26.8	9.12	9.20			23.5	23.0
110	267	22.6	22.5	0.68	0.68	27.6	27.5	9.68	9.72			25.6	25.2
115	277	22.8	22.7	—	—	—	—	—	—			—	—
120	288	22.9	23.0	0.68	0.68	27.6	27.5	10.4	10.5			27.5	28.5
130	309	23.1	25.0	0.68	0.69	27.6	27.7	11.2	11.1			27.5	28.5
135	319	25.1	25.2	—	—	—	—	—	—			27.4	—
140	330	25.1	25.2	0.69	0.69	27.8	27.7	11.9	11.9			27.3	28.5

\* In this Table, vacua in closed tank were taken with same diffuser settings as those with air flow.

TABLE 5.—continued.

FOR ABOUT BEST DIFFUSER SETTING AT 120 LB. PER SQ. IN., GAUGE.

For 1B, D =  $2\frac{1}{2}$  inches ; for 2B, D =  $2\frac{1}{2}$  inches.

		1B	2B	1B	2B	1B	2B	1B	2B	1B	2B	1B	2B
60	163	3.2	2.8	0.16	0.14	13.4	12.5	12.1	13.0	Dry Bulb, 65.3°F., 67.2°F. Wet Bulb, 57.8°F., 59.8°F. Rel. Humid. 64% 65%		4.4	2.7
70	184	5.2	4.2	—	—	—	—	—	—			6.4	—
80	204	8.1	6.0	0.38	0.29	20.6	17.9	9.91	11.4			10.4	6.1
90	225	13.1	8.3	—	—	—	—	—	—			16.3	9.0
100	246	17.3	14.0	0.62	0.56	26.4	24.9	9.34	9.88			19.2	14.0
110	267	20.1	18.2	0.66	0.64	27.2	26.6	9.82	10.0	Barometer, 30.33 30.05 inches inches		20.8	20.5
115	277	23.7	22.4	—	—	27.5	—	10.0	—			21.2 to 21.4	26.6
120	288	23.7	24.9	0.68	0.69	27.6	27.7	10.4	10.4			27.4	26.9
130	309	23.5	24.8	0.68	0.69	27.6	27.7	11.2	11.1			27.6	27.0
135	319	23.5	—	—	—	—	—	—	—			27.5	27.0
140	330	23.4	24.6	0.68	0.69	27.6	27.7	12.0	11.9			—	26.9

TABLE 5.—*concluded.*

FOR ABOUT BEST DIFFUSER SETTING AT 100 LB. PER SQ. IN., GAUGE.  
For both 1B and 2B, D =  $1\frac{1}{8}$  inches.

	1B	2B	1B	2B	1B	2B	1B	2B	1B	2B	1B	2B
60	163	6.0	5.6	0.29	0.27	18.0	17.3	9.06	9.42			
70	184	—	7.9	—	—	—	—	—	—			6.8
80	204	12.7	11.7	0.53	0.50	24.4	23.6	8.36	8.65	Dry Bulb, 65.8°F., 67.2°F.	9.9	9.1
90	225	—	16.8	—	—	—	—	—	—	Wet Bulb, 55.1°F., 69.1°F.	14.2	12.8
100	246	20.9	20.2	0.67	0.66	27.4	27.1	8.98	9.07	Rel. Humid. 55% — 62%	19.0	17.6
110	267	22.1	22.3	0.68	0.68	27.6	27.5	9.67	9.71	Barometer, 30.34 — 30.05 inches	25.8	23.0
115	277	—	22.6	—	—	—	—	—	—		27.4	24.7
120	288	22.7	22.8	0.68	0.68	27.6	27.5	10.4	10.5		—	28.3
130	309	24.0	24.2	0.68	0.69	27.6	27.7	11.2	11.1		27.4	28.3
140	330	24.5	24.9	0.69	0.69	27.8	27.7	11.9	11.9		—	28.2

\*VACUUM IN CLOSED TANK FOR ABOUT BEST DIFFUSER SETTING AT 80 LB. PER SQ. IN., GAUGE.

For 1B, D =  $\frac{3}{4}$  inch; for 2B, D =  $\frac{7}{8}$  inch.

Steam Pressure, lb. per sq. in., gauge.	60	70	80	90	100	105	110	120
Vacuum in closed tank (corrected), inches mercury.	1B 8.6	11.2	15.5	19.8	22.9	26.7	26.8	26.7
2B 7.5	10.5	14.3	19.1	28.0 (climbs slowly)	22.2	28.0	28.0	27.9

\* See footnote, p. 246.

with those for the diffuser with the  $1\frac{1}{8}$ -inch parallel throat, the slopes of the curves are less steep. One of the essentials of a good air ejector is that the vacuum-pressure curve should be steep, i.e. that the vacuum required should be reached at as low a steam pressure as possible. This is evidently the most economical result, for the higher the pressure for any given vacuum, the greater will be the weight of steam discharged from the nozzle and the higher the steam-air ratio. In Fig. 6 the two curves marked M and N are for the two diffuser settings corresponding to the two maximum values (25.2 inches) of the vacuum at the same steam pressure of 140 lb. per sq. in., and they have already been referred to.

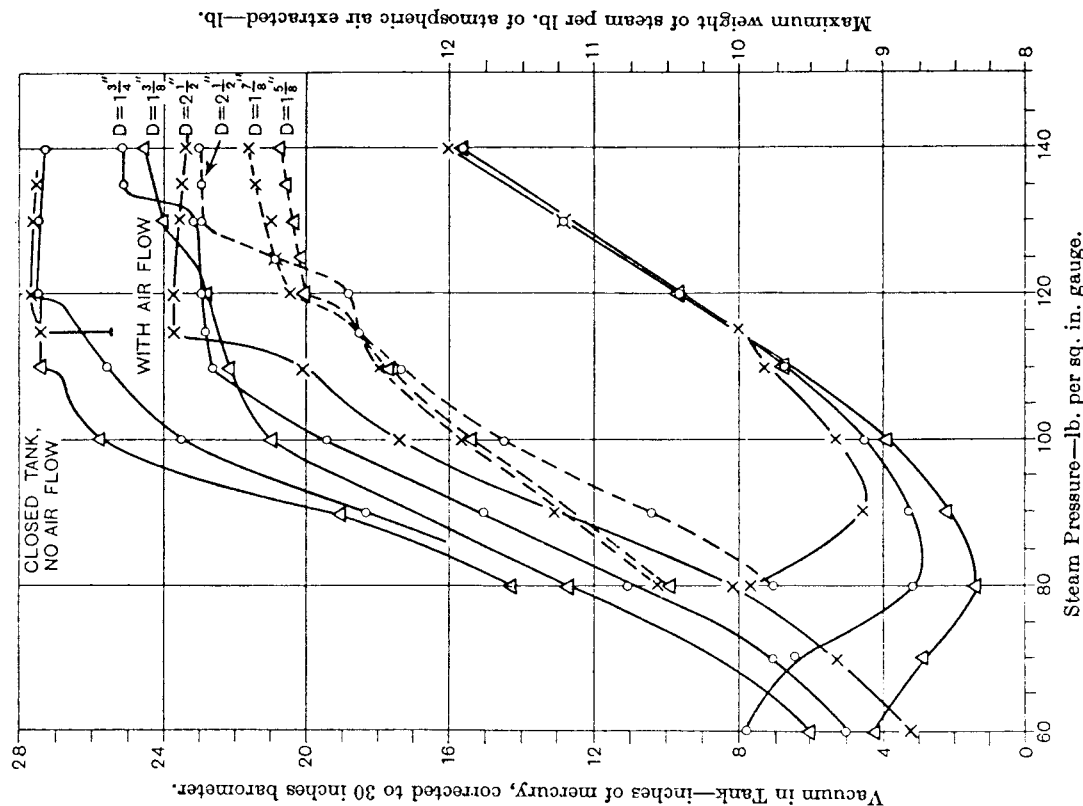
*Performance of this Ejector.*—In considering the performance of this apparatus it should be borne in mind that it was of very simple design and intended primarily for the examination of certain problems; therefore all its parts had to be readily accessible for changing quickly. Also the figures given for the steam-air ratio in Table 5 have been calculated from the maximum steam flow or theoretical discharge from the nozzle, and not from the steam collected at the condenser. The steam collected was less than the

true amount of steam used, as the steam entering the condenser was carrying over with it all the air entrained, and therefore much vapour was carried off with the air leaving the condenser. (Hence there must be a liberal allowance of cooling surface in the inter-condenser of a two-stage ejector, for the weight of steam condensed.) The percentage of missing steam at any one admission pressure appeared to vary considerably. Several measurements were made at a pressure of 120 lb. per sq. in. on different days and results giving as high a figure as 25 per cent were obtained. If the air inlet to the ejector was suddenly closed, the outlet circulating water temperature would suddenly rise by several degrees, indicating an improved heat transmission through the condenser tubes due to the exclusion of the entrained air. At a steam pressure of 120 lb. per sq. in., with inlet and outlet circulating water temperatures of 58 deg. and 102 deg. F. respectively, and when the missing steam quantity was 15 per cent of the calculated nozzle discharge, the outlet water temperature rose rapidly by 6.5 deg. F. when the air orifice was suddenly closed by placing a piece of flat rubber over it. The cooling surface in the condenser was approximately 28 sq. ft. Hence it was considered that the calculated nozzle flow was the better value to use. With



FIG. 5.—*Vacuum-Pressure Curves for about best setting of diffuser at*

100, 120, and 140 lb. per sq. in.  
 --- Diffuser 1A (throat  $\frac{1}{16}$  inch long).  
 --- Diffuser 1B (throat  $\frac{1}{8}$  inches long).  
 △ At 100 lb. per sq. in.  
 × At 120 lb. per sq. in.  
 ○ At 140 lb. per sq. in. } Steam Nozzle No. 2.



The second series of photographs was taken at the same steam pressures as the first, but the jet discharged into a partial vacuum which was produced and maintained by an air pump. With the diffuser removed it was possible to obtain a clear view of the waves for a distance of about 5 inches away from the nozzle outlet. Before this piece of work could be carried out a new  $2\frac{1}{4}$ -inch diameter

no air flow through the ejector, the measured steam was in good agreement with the calculated discharge. The superheat of the steam in the separator varied from about 5 deg. to 20 deg. F., hence an average superheat of 10 deg. F. has been assumed at all pressures in calculating the nozzle discharge. The curves of the steam-air ratio for the three higher pressures used are shown in Figs. 5 and 6, and the values are given in Table 5. The best performance, which approached most nearly the somewhat ambitious conditions assumed in the original design, was evidently with diffuser No. 1B (the second section of Table 5), when a vacuum of 23.7 inches was maintained at 115 lb. per sq. in. when exhausting 27.5 lb. per hour of atmospheric air, the steam consumption being 277 lb. per hour; these figures give a steam-air ratio of practically 10. For diffuser No. 2B at 120 lb. per sq. in. the vacuum was 24.9 inches, the steam consumption and air extracted 288 and 27.7 lb. per hour respectively, and the steam-air ratio 10.4.

#### INSPECTION OF THE STEAM JET.

*Methods Adopted.*—It appeared probable that the stationary waves in the core of the steam jet were responsible for the great changes which took place in the vacuum, and it was resolved to examine these waves and to photograph them if possible. In order to do this the principle of the "ultra" microscope was applied, i.e. rays from a source of light were allowed to pass through a narrow slit and thereby illuminate the plane section of the jet to be viewed or photographed, either operation being carried out in darkness, so that the only light rays reaching the eye or the camera lens were those from the particles on the illuminated section. This principle has been applied to a steam jet by Dr. Stodola,\* who used it to examine a jet for any evidence of supersaturation in a narrow zone close to the nozzle outlet.

The first series of photographs was taken at initial steam pressures of 80, 100, 120, and 140 lb. per sq. in. when the jet was discharging at atmospheric pressure, and Fig. 7 shows the jet from nozzle No. 2 discharging directly into the atmosphere when the light in the room was only partially excluded by dark curtains hung round the jet. What is shown is practically an outside view of the jet. For the other photographs in this series the jet was totally enclosed by means of a piece of 6-inch diameter pipe having two openings, one for the beam of light and the other for observation purposes. They were both screened, and the combined stream of steam and air passed into the condenser. The vacuum inside the screen at the highest steam pressure was equivalent to a pressure of less than  $\frac{1}{4}$  inch. The narrow beam of light for illuminating a longitudinal section of the jet was obtained in this series from an electric arc, but in the other series a filament lamp was used for convenience.

\* "Steam and Gas Turbines," Dr. A. Stodola, vol. 1, 6th ed. (Loewenstein), p. 119.

FIG. 8.—Cylinder with windows and Diffuser with glass mouthpiece.

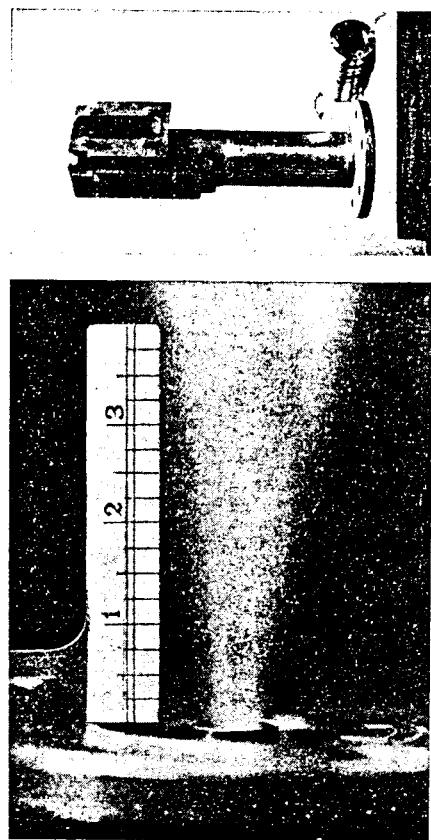
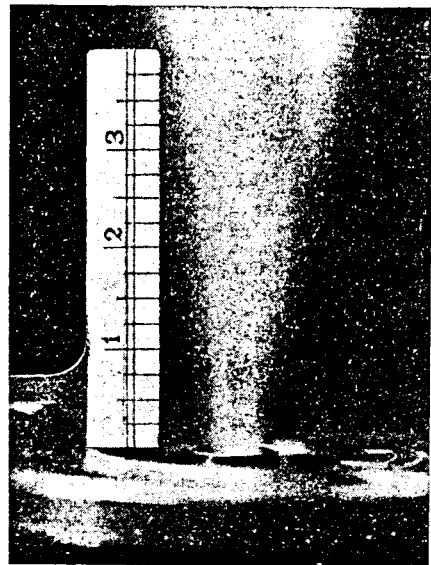


FIG. 7.—Jet from Nozzle No. 2 discharging into the atmosphere.

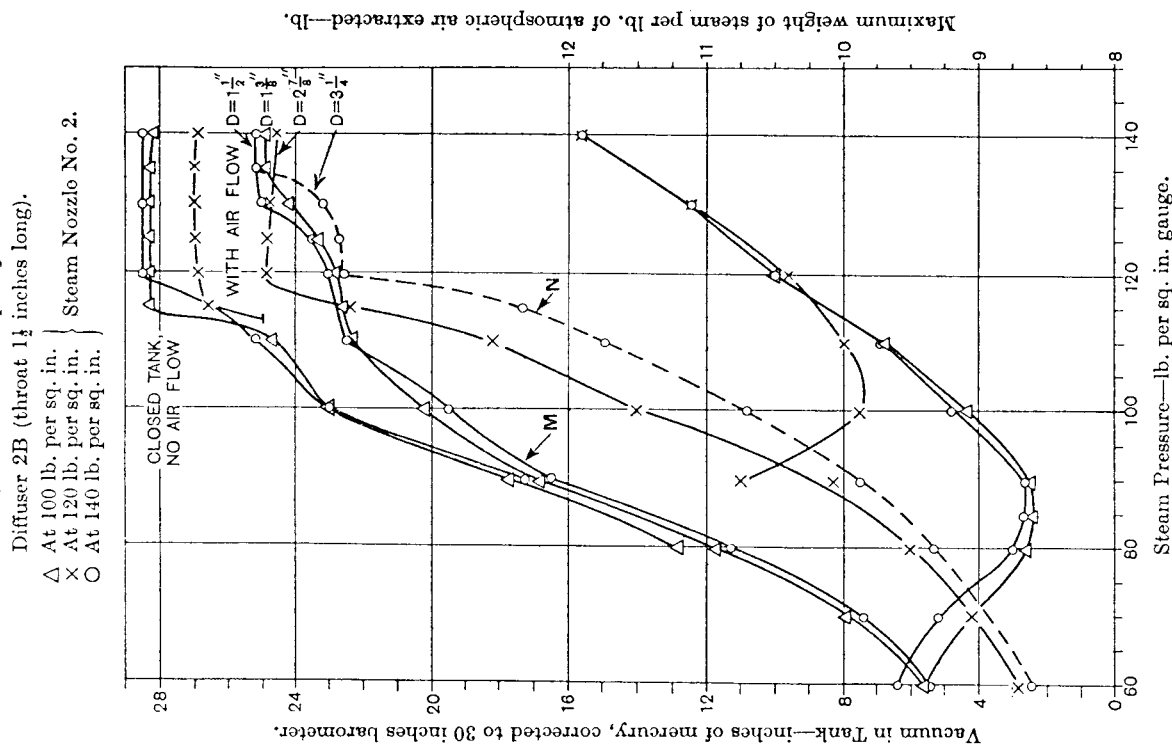


In order to render the jet visible under actual working conditions a new diffuser (also shown in Fig. 8) was made, and this was fitted with a glass mouthpiece which formed the entrance and throat of the diffuser. In form it was made as nearly as possible the same as diffuser No. 1B. When this new diffuser was used in conjunction with the new cylinder, referred to above, the jet, from the nozzle outlet to the remote end of the diffuser throat, could be seen when the ejector was working, with the air inlets full open, and performing its duty in the normal way. A third series of photographs was therefore taken, when the ejector was fitted up in this manner, at pressures of 120 and 140 lb. per sq. in. The numbers shown on the scale in most of the following photographs represent inches measured from the outlet end of the steam nozzle. The scale was fitted inside the screen immediately above the axis of the jet.

Some of the photographs here reproduced show more nearly a side elevation than a longitudinal section of the wave surface, and in obtaining these views the beam was displaced slightly from the axis of the jet in order to show the wavelength more clearly.

**Comments on Photographic Results.**—The photographs in Fig. 9 show the jet from nozzle No. 1 discharging at different vacua when the initial steam pressure was 140 lb. per sq. in. in all the four cases. In (a) the discharge pressure was practically atmospheric, and in (b), (c), and (d) the vacuum was produced and maintained by the air pump, the diffuser having been removed from the ejector. The first series of photographs (of which (a) is one taken at the highest pressure) showed that the overall length of the wave series decreased as the initial steam pressure was reduced; at 80 lb. per sq. in. only the faint tip was visible outside the nozzle. This result goes to

FIG. 6.—Vacuum-Pressure Curves for about best setting of diffuser at 100, 120, and 140 lb. per sq. in.



cylinder (shown in Fig. 8) with two plate-glass windows fitted in it to serve the same purpose as the two openings in the last screen, had to be made and fitted on the ejector in place of the cylinder marked ST on Fig. 1.

explain why the point of maximum vacuum, marked A in Fig. 3, moved towards the left as the pressure was reduced. Another result obtained by comparing (a) and (b) was that with a constant initial steam pressure the waves expanded longitudinally and transversely as the vacuum was increased or the back pressure reduced.

This was the first result sought for, in conducting the air pump experiments, and its importance in the theory of this type of air ejector cannot be too strongly emphasized.

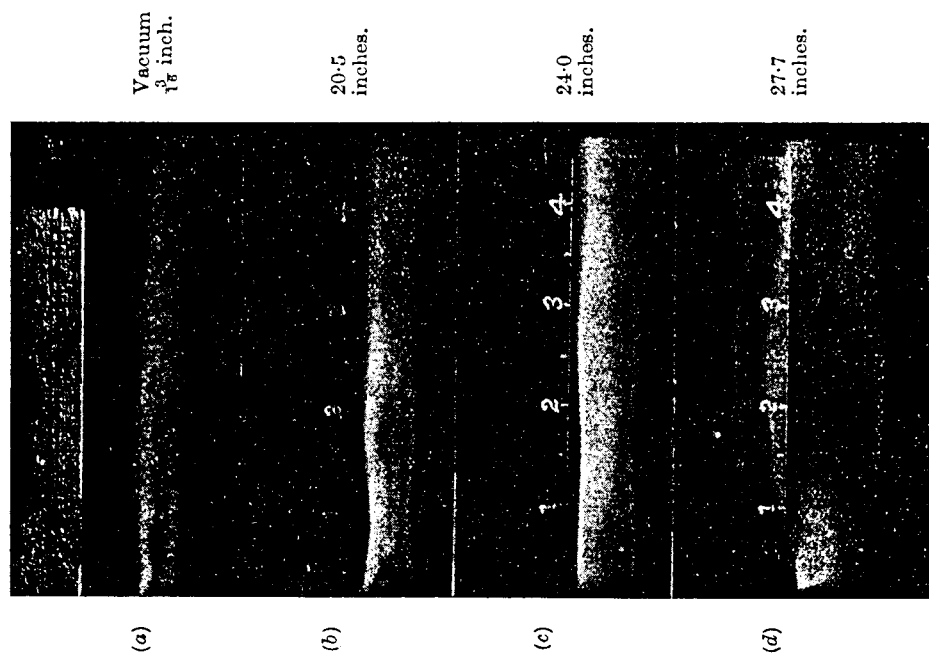
Cases (a) and (b) are instances of "over-expansion" of the jet, (c) shows discharge at the designed pressure, for the steam pressure used, and (d) shows "under-expansion" of the jet. The last three views illustrate clearly the three states of discharge that may occur in any steam jet according to the pressure conditions prevailing at the discharge end. The first state is the important one in the air ejector working under the conditions of the tests described, and is the one that prevails when the ejector is working steadily, but if violent pressure oscillations are set up in the air chamber the jet will pass from one extreme state to the other, producing a periodic pounding on the diffuser entrance during that time.

In case (b) when the search tube was set in the centre of the globular part of a wave and then moved to the neck or anti-node on either side, it was found that the pressure was low in the first position and high in the second, the difference of pressure amounting to nearly 5 inches of mercury in the wave near the nozzle, but diminishing in successive waves as the tube was moved outwards from the nozzle.

This suggested that the transverse oscillations were produced in a similar manner to those in the case of a plucked helical spring, namely an over-compression at the neck of the wave, then an outward over-expansion, then an over-compression and so on, the vibratory action gradually dying out as the tip of the wave series was reached. Hence the author's interpretation of the light and dark portions in these photographs is that a white place indicates the presence of steam (or a mixture of steam and water) and a dark one a rarefied part or an absence of steam.

In Fig. 10 are shown three photographs of the jet when nozzle No. 2 was in use, and (e) shows the magnitude of the waves at 25 inches of vacuum when the air pump was used. So far the inspection of the jet has been described when the vacuum was produced by the air pump, but it was considered unlikely that the wave formation under these conditions would be the same as when the ejector was doing its normal duty, when there would be a gradual rise of pressure along the combined stream from the nozzle outwards. Hence the views (f) and (g)—the former taken when the air pump created the vacuum and the latter when the jet created the vacuum for itself—are given to show the difference in the waves under the two different sets of conditions, for practically the same vacuum in the air chamber. It will be observed that in (g) the waves are shorter and the whole

FIG. 9.—*Jet from Nozzle No. 1 discharging at different vacua.*  
Steam pressure : 140 lb. per sq. in. gauge.  
Air pump used in (b), (c), and (d).

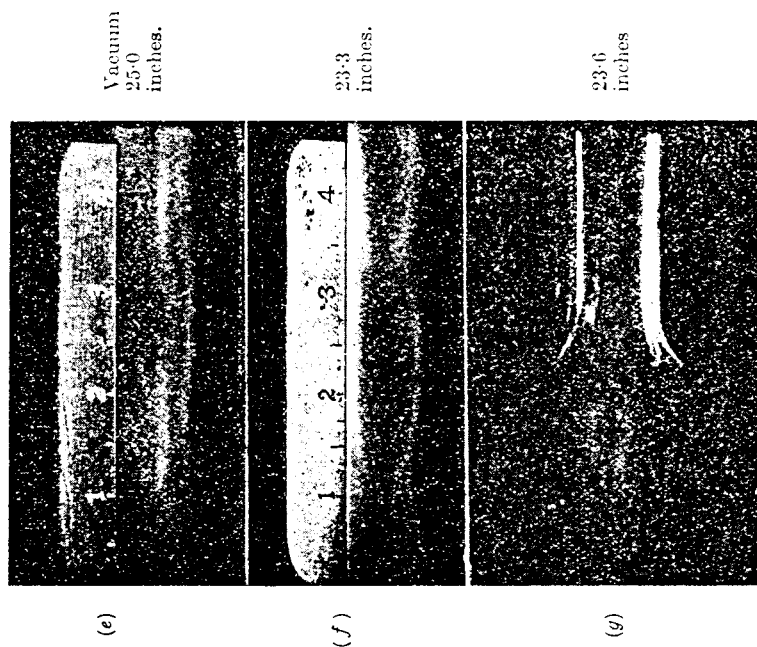


wave series appears to be thrust farther back into the mouth of the nozzle, due, most probably, to the resistance against which the jet was discharging. This particular photograph does not show the waves in the throat of the diffuser, but they were clearly visible to the eye after the sudden rise to the high vacua, though not before. In some of the photographic prints they were quite clear, but it was sometimes rather difficult to get the desired illumination in the glass throat for producing a good photograph. This view (g) is of special interest because it shows the position of the anti-node in the jet with respect to the entrance of the diffuser throat just after the sudden rise in

vacuum had taken place, as shown in Fig. 3, when D had a value of about  $2\frac{1}{2}$  inches. As the diffuser was moved forward slowly near this position it was fascinating to observe the waves lengthen slightly, swell out, and then slip into their new positions, the mercury columns immediately responding and climbing instantly from about 18.5 to 23.6 inches while the diffuser was stationary. In this manner the greatest step-up of the vacuum took place, the globular part of a wave apparently occupying a position inside the throat after the

FIG. 10.—*Jet from Nozzle No. 2 discharging at different vacua.*

Steam pressure: 140 lb. per sq. in. gauge.  
Air pump used in (e) and (f). View (g) shows the jet when the ejector was working normally.

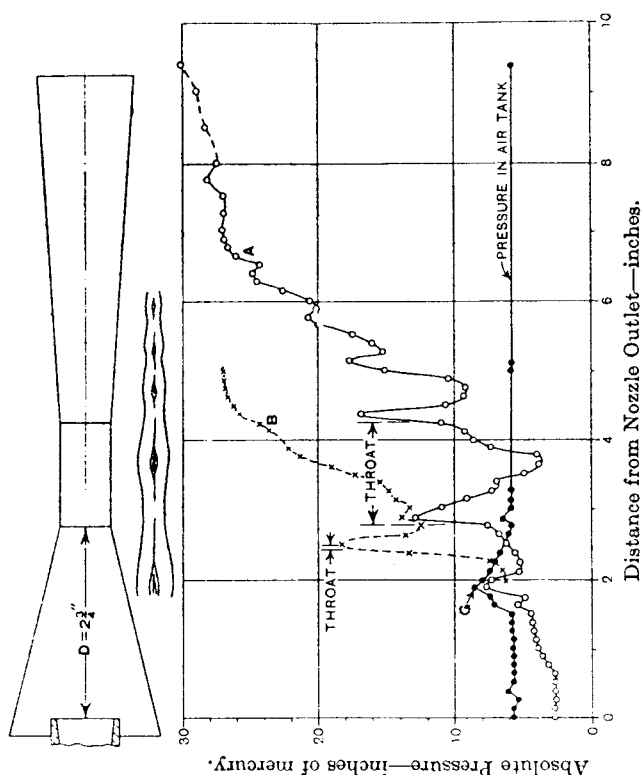


rise. The next, but smaller, rise of vacuum indicated by the peak marked B on the same curve in Fig. 3 was no doubt produced in a similar manner when the diffuser throat entrance was moved up to the corresponding position on the next wave, but it was difficult to view the jet in this case with the diffuser so close to the nozzle. The waves, under steady conditions, appeared practically stationary to the eye, and the time of exposure in taking these photographs was in most cases one minute.

*Variation of Pressure along the Diffuser by Search Tube.*—The rise of pressure along the jet from the outlet of the steam nozzle to the outlet of the diffuser is shown by the full-line curve in Fig. 11, and

FIG. 11.—*Variation of Pressure along Diffuser by search tube.*

- A. Pressure near the centre of combined stream, by search tube (Diffuser 2B).  
B. Pressure near the centre of combined stream, by search tube (Diffuser 2A).  
C. Pressure in air tank 8.2 to 8.8 inches; D,  $2\frac{1}{4}$  inches.  
With air flow; steam nozzle No. 2; steam pressure, 140 lb. per sq. in. gauge.



diffuser No. 2B was used in taking these observations. The jet with this diffuser was remarkably free from any disturbance when the  $\frac{1}{2}$ -inch search tube was passed up its centre, and confirmation of this can be seen in the tank pressure curve which is practically horizontal except for one marked disturbance in the neighbourhood of the point marked G. The pressures were measured at  $\frac{1}{2}$ -inch intervals for a distance of 7 inches from the nozzle, and at larger intervals for the remaining  $2\frac{1}{4}$  inches. They were quite steady except at a few points, where however the oscillation of the mercury column did not exceed  $\frac{1}{2}$  inch at the most. This curve shows the waves remarkably clearly, and the probable form of the jet, for 4 inches of its length, has been sketched freehand on the diagram, projections having been taken from the crests and troughs of the waves, except at the point G. It will be observed that vigorous waves penetrated the parallel throat and their wavelength was well maintained, this being quite in agreement with the photographic

results. The wavelength was rapidly reduced, indicating most probably a rapidly reduced velocity, as the jet emerged from the throat into the diverging tail piece, where the pressure rise was rapid with the rapidly diminishing kinetic energy.

The dotted curve in Fig. 11 is for the jet passing through diffuser No. 2A, with  $\frac{1}{16}$  inch length of throat, with the same steam pressure as in the last case, namely 140 lb. per sq. in., and the readings used were taken at  $\frac{1}{8}$ -inch intervals over the 3-inch range, from 2 inches to 5 inches, these distances being measured from the end of the nozzle. This jet was a weaker one than the last described, and it was more sensitive to the passage of the search tube through it. At the position in this jet corresponding to the one at G in the last it was impossible to take a reading of the mercury gauge, as the jet became unstable and violent oscillations were set up in the mercury column. While the readings used here were taken, over the range stated, the tank pressure did not vary by more than 0.6 inch of mercury. It will be observed that the jet was shorter in this case, the rapid pressure rise began much earlier, and the waves were apparently almost immediately damped out of the jet after the throat had been passed.

An important result deduced from these curves was that the pressure near the centre of the jet was high just inside the throat entrance for both diffusers, and this was in keeping with the photographic results. Hence, by both means of inspection, it appeared that when the high vacuum was being maintained the globular part of a wave was inside the throat, forming probably a sort of elastic seal with the entrained air to hold the vacuum, and a neck, or anti-node, was just inside the throat entrance.

One set of simultaneous readings of search tube pressure and pressure just inside the throat (taken through a  $\frac{1}{32}$ -inch hole in the wall of the throat) was taken at 140 lb. per sq. in. steam pressure with diffuser 2B, by traversing the diffuser and search tube together over a distance of 2 inches from  $D = 4.5$  inches to  $D = 2.5$  inches, and this range included the diffuser setting where the sudden rise of vacuum took place. The hole in the tube was kept at the same cross-section as the hole in the wall throughout this movement. For the first  $\frac{7}{8}$  inch of this distance the tube pressure was higher than the wall pressure, and for the next  $\frac{7}{8}$  inch the reverse was the case. When the sudden rise of vacuum took place the wall pressure suddenly dropped to a pressure which was nearly  $2\frac{1}{2}$  inches of mercury below the tube pressure. This indicated that the pressure round the anti-node in the throat entrance was lower than the pressure near the centre of the jet at this section.

#### SUMMARY OF RESULTS.

It appears rather remarkable that few, if any, observations have been made and recorded of the behaviour of the waves in a steam jet under different conditions of initial pressure and discharge, and if the treatment of the subject in this paper is considered deficient

in certain details, it should be stated that there were many side tracks which had to be explored and that little assistance was available from the experience of previous investigators in the field.

The main results of these experiments given with reference to continuous air flow conditions through the ejector, briefly summarized, are as follows :—

(1) Over-expansion of the steam in the nozzle took place during all the tests described, as this gave satisfactory results over a wide pressure range, but a high vacuum could also be produced by an under-expanded jet.

(2) The series of stationary waves in the steam jet, upon which the successful action of the ejector appeared very largely to depend, extended for a certain length outwards from the nozzle.

(3) With a steady admission steam pressure and over-expansion in the nozzle the photographs showed that the stationary waves varied thus: (a) wavelengths increased (and therefore the overall length of wave series) with increased vacuum; (b) waves swelled transversely with increased vacuum, and vice versa in both cases. These results were deduced from separate experiments using an air pump.

(4) A direct deduction from (3) above was that the wave series was more "tapered" in form when discharging against a gradually rising pressure along its length (working conditions in air ejector) than when the jet discharged into a region of nearly uniform pressure (air pump conditions).

(5) When a sliding diffuser was moved inwards over the jet the vacuum increased and a position was reached when the core of the jet, with its layer of entrained air, probably just filled the throat entrance. A sudden rise of about 5 inches to the higher range of vacua then took place, and the globular part of a wave was always observed to be inside the throat after this sudden rise. If the movement of the diffuser was continued, and if the diffuser had a long parallel throat, another smaller rise would take place at the next wave.

(6) It is evident from (5) that the correct setting of the throat entrance relative to the nozzle outlet is a very important length, and its determination is entirely omitted in the theory of the ejector. The maximum value of this length was found to increase with increased steam pressure, and it was evidently some function of the wavelength in the jet outside the nozzle. At a steam pressure of 140 lb. per sq. in. by gauge, for the particular nozzle used, the maximum value of this distance was practically two wavelengths.

(7) In a diffuser with a long parallel throat (a length equal to two diameters was used) at the higher vacua, vigorous waves extended right through the throat into the entrance of the tail piece. This type of diffuser admitted a longer and more powerful jet than the one with a very short throat, and it gave a higher and more nearly constant vacuum over a wider range of diffuser setting.

(8) Of the two forms of diffuser entrance used, namely (a) short

<sup>n</sup> exponent of adiabatic compression.

The suffixes *s*, *t*, and *j* refer to the steam at admission, the throat of nozzle, and the jet at exit, respectively.

*Design of Steam Nozzles.*—The steam nozzles used in steam-jet operated air ejectors are of the convergent-divergent type and are of normal design. Their theory is fully dealt with in many books on steam turbines.

$$\text{Nozzle No. 1.} \text{---Area of throat} = a_t = \frac{W_s}{0.3155} \sqrt{\frac{v_s}{p_s}}$$

$$\text{where } W_s = 230/3600 = 0.0639, p_s = 100 + 14.7 = 114.7, \\ \text{and } v_s = 3.903 \text{ (see Steam Tables).}$$

$$\text{Therefore } a_t = \frac{0.0639}{0.3155} \sqrt{3.903/114.7} = 0.03740.$$

The equivalent diameter = 0.2183 inch or  $\frac{7}{32}$  inch nearly.

Hence the diameter of throat was  $\frac{7}{32}$  inch.

The pressure corresponding to 25.5 inches vacuum = 2.20 lb. per sq. in. abs., and the frictionless adiabatic heat drop from 114.7 to 2.20 lb. per sq. in. abs. = 262 B.Th.U. per lb. (from total heat-entropy diagram). The nozzle efficiency, by H. M. Martin's formula,\* for this heat drop = 0.87. Hence the velocity of steam jet issuing from nozzle

$$= V_j = 223.8\sqrt{0.87 \times \text{heat drop}} = 223.8\sqrt{0.87 \times 262} = 3378.$$

The dryness condition (*q<sub>j</sub>*) of steam on issuing = 0.854 (from total heat-entropy diagram for a nozzle efficiency of 0.87). Hence area of outlet  $a_j = \frac{W_s \times q_j \times v_j \times 144}{V_j}$ , where  $v_j = 158.7$  (see Steam Tables).

$$\text{Therefore } a_j = \frac{0.0639 \times 0.854 \times 158.7 \times 144}{3378} = 0.3693 \text{ and}$$

equivalent diameter = 0.686 inch or  $\frac{11}{16}$  inch nearly.

Hence the diameter of outlet of nozzle was  $\frac{11}{16}$  inch.

A taper of 1 in 6, on the diameter, was chosen. This gave a length from throat to outlet of  $2\frac{13}{16}$  inches, and a cone angle of 9.5 deg. At the inlet a well-rounded entrance of about 0.27 inch radius was provided.

*Nozzle No. 2.*—This nozzle was intended to have a throat diameter equal to that of nozzle No. 1, but when finished the throat diameter was  $(\frac{7}{32} + 0.008)$  inch. The diameter of the outlet was  $\frac{3}{8}$  inch and suited for a vacuum of 27.2 inches. The length from throat to outlet was the same as in No. 1, but the cone angle was 13.1 deg.

*Design of Diffusers.*—It was assumed that :—

\* "Steam Turbines," William J. Goudie (Longmans).

rounded and (b) tapered, the latter gave, on the whole, better results than the former.

(9) The performance of a steam-operated air ejector should be based on the calculated nozzle discharge and not on the condensed steam collected. The percentage of the true steam weight carried off by the entrained air leaving the condenser varied very considerably on different days, but values as high as 25 per cent were obtained.

(10) Low steam pressures were found to be unsuitable. The lower limit in these experiments to give a high vacuum with a fairly good steam-air ratio was about 120 lb. per sq. in. by gauge. At this steam pressure the vacuum produced was nearly 25 inches and the steam-air ratio was 10.4, the steam quantity used being the calculated nozzle discharge when the initial superheat was 10 deg. F.

The author desires to express his thanks to the Governors of the Merchant Venturers' Technical College, Faculty of Engineering, University of Bristol, for the provision of the facilities required for the work described, and to Professor Andrew Robertson, D.Sc., M.I.Mech.E., Dean of the Faculty of Engineering, for his encouragement and interest. His thanks are also due to Mr. E. A. Gordon, a student at the College, for assistance in connexion with the photographic part of the work.

## APPENDIX.

### CALCULATION OF STEAM-NOZZLE AND DIFFUSER DIMENSIONS.

It was originally decided that the rating of the ejector should be approximately as follows :—

Steam consumption : 230 lb. per hour of initially dry and saturated steam at 100 lb. per sq. in. by gauge.

Air duty : 35 lb. of dry air per hour, saturated with water vapour at a temperature of 61 deg. F.

Vacuum to be maintained : 25.5 inches of mercury.

(As has already been stated the assumed steam-air ratio was too low, and the ejector had to be operated at a higher steam pressure to give the required vacuum.)

In the calculations the following symbols have been used :—

- W* weight of steam, air, or vapour flowing, pounds per second.
- p* pressure of steam, air, vapour, or mixture, pounds per square inch absolute.
- q* dryness condition of steam.
- v* specific volume of steam, air, vapour, or mixture, cubic feet per pound.
- V* velocity of flow, feet per second.
- a* area of section, square inches.

- (a) the pressure throughout the air chamber was constant up to the diffuser throat ;  
 (b) the velocity of air in the air chamber was 100 ft. per sec., and  
 (c) the velocity of the mixture of steam, air, and vapour at outlet from the diffuser was 220 ft. per sec.

(These assumptions were made after reference to Sim's "Steam Condensing Plant." †)

The additional suffixes  $a$ ,  $v$ , and  $m$  have been used in the following calculations, and have reference to the air, the vapour in the air, and the mixture of steam, air, and vapour, respectively. The numbers (2) and (3) refer to the throat and outlet end sections respectively.

From Steam Tables, the pressure of water vapour at 61 deg. F. = 0.265 lb. per sq. in. abs., and the specific volume at this pressure = 1.168 cu. ft. per lb. Hence, for the entering air, the partial air pressure ( $p_a$ ) =  $2.20 - 0.265 = 1.935$ . Also, by 144  $p_a v_a = RT$ ,  

$$v_a = \frac{53.2 \times 521}{144 \times 1.935} = 100.0.$$

$W_a = \frac{35}{3600} = 0.00973$  and weight of vapour per pound of air  
 $= \frac{100}{1168} = 0.0856$  lb.

Therefore  $W_v = 0.0856 \times 0.00973 = 0.00083$

and  $W_a + W_v = 0.01056$ .

With the assumed value of  $V_a = 100$ , the annular area required between the steam nozzle and the diffuser entrance was

$$\frac{v_a \times W_a}{V_a} = \frac{100.0 \times 0.00973 \times 144}{100} = 1.40 \text{ sq. in.}$$

Applying the principle of conservation of momentum to the collision of the steam jet and the saturated air, we have

$$W_s V_j + (W_a + W_v) V_a = (W_s + W_a + W_v) V_{m_2}$$

Therefore velocity at throat

$$V_{m_2} = \frac{(0.0639 \times 3378) + (0.01056 \times 100)}{0.07446} = 2910.$$

The volume at (2) =  $(W_s v_{s_2} + W_a v_a)$  or  $v_{m_2} (W_s + W_a + W_v)$ .

Therefore volume per pound of mixture at the throat

$$v_{m_2} = \frac{(0.0639 \times 158.7 \times 0.854) + (0.00973 \times 100)}{0.07446} = 129.3.$$

Hence area of throat

$$= a_2 = \frac{(\text{volume passing throat per second}) 144}{V_{m_2}} \\ = \frac{129.3 \times 0.07446 \times 144}{2910} = 0.4765$$

and equivalent diameter = 0.779 inch. It was decided to use, in the first instance, a throat  $\frac{3}{4}$  inch diameter. The adiabatic exponent for the mixture during compression may be obtained from the following expression

$$\frac{p_m}{n_m - 1} = \frac{p_a}{n_a - 1} + \frac{p_s}{n_s - 1}$$

where  $n_a = 1.40$  and  $n_s = 1.30$ , the usual values for air and steam respectively.

$$\text{Hence } \frac{2.20}{n_m - 1} = \frac{1.935}{0.4} + \frac{0.265}{0.3}$$

$$\therefore n_m = 1.385.$$

From  $pv^n = \text{constant}$ ,  $v_{m_2} = v_{m_1} \left( \frac{p_{m_1}}{p_{m_2}} \right)^{\frac{1}{n_m}} = 129.3 \left( \frac{2.20}{14.7} \right)^{\frac{1}{1.385}} = 32.82$ .

With the assumed value of  $V_{m_2} = 220$ , the area of outlet

$$= a_3 = \frac{v_{m_2} (W_s + W_a + W_v) \times 144}{V_{m_2}} = \frac{32.82 \times 0.07446 \times 144}{220} \\ = 1.600$$

and equivalent diameter = 1.428 inches. An outlet diameter of 1.43 inches was used.

A taper of 1 in 7.5 on the diameter was chosen, and this gave the length of tail piece as  $4\frac{1}{2}$  inches nearly. A length of 5 inches was used. The efficiency of the diffuser, calculated on the above results = 78 per cent.

Diffuser No. 1 was made with a short rounded entrance 1 inch in length. Diffuser No. 2 was made with a tapered entrance 3 inches long, the taper being about 1 in 2.2 on the diameter.

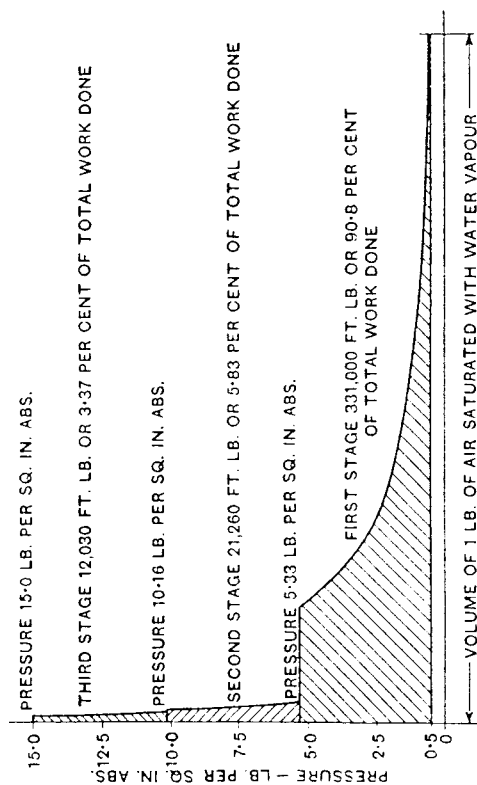
### Discussion in London.

Professor A. L. MELLANBY, D.Sc. (*Member of Council*) remarked that there were so many complicated phenomena associated with the expansion and recompression of jets that it would be no cause for surprise if every one did not share the author's opinions regarding some of the effects observed. In the early part of the paper, the author gave the proportion by which the pressure rise in a two-stage

† "Steam Condensing Plant," James Sim (Blackie).

Fig. 12.—*Work Done in Three-Stage Air Ejector, with equal pressure difference per stage.*

Initial pressure, 0.5 lb. per sq. in. abs., total; final pressure, 15.0 lb. per sq. in. abs., total; initial temperature, 70 deg. F.; total work done, 364,290 ft.-lb.



ejector should be divided as that ordinarily used for the compound air compressor. He himself did not consider this to be right for a two-stage ejector with an intercondenser (i.e. the type shown in

Fig. 13.—*Work Done in Three-Stage Air Ejector, with equal work done per stage.*

Initial pressure, 0.5 lb. per sq. in. abs., total; final pressure, 15.0 lb. per sq. in. abs., total; initial temperature, 70 deg. F.; total work done, 196,500 ft.-lb.

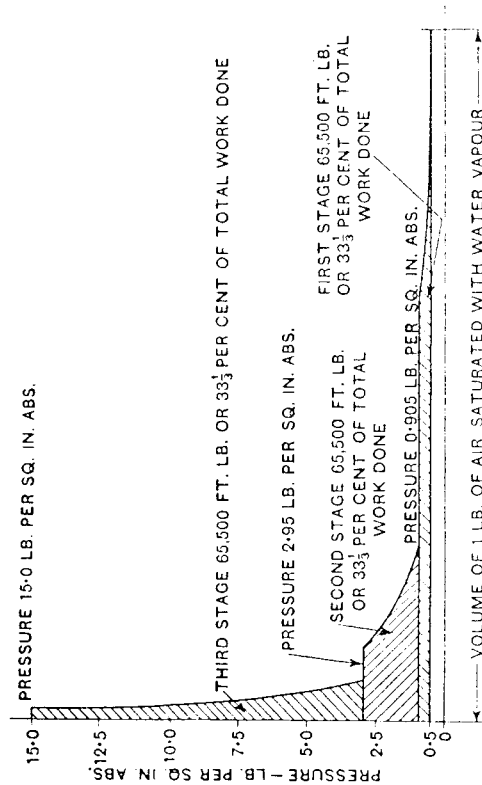


Fig. 1, p. 234), because the same fluid was not being dealt with throughout; the amount of vapour associated with the air would be quite different in the second stage from that in the first. That point had been brought to his attention some years ago when there was a dispute as to the proper proportions into which the three-stage ejectors should be divided, and he was very much surprised to find what a difference the disposition of the pressure rise in the three stages made to the work done. It would be thought, on casual consideration, that in compressing from a pressure of  $\frac{1}{4}$  lb. per sq. in. (a vacuum of 29 inches of mercury) to 15 lb. per sq. in., it would not matter very much how the pressure was divided between the three stages. Figs. 12 and 13, however, illustrated how the action depended upon the stage pressure. Here a three-stage ejector was considered in which the temperature was supposed to be reduced to 70 deg. F. after each stage. In Fig. 12 the pressure range was equally divided, and it would be noticed how very unevenly the work was divided; the low-pressure ejector had to do practically all the work. In Fig. 13 the pressures were arranged so that the compression work was equal in each stage, and it would be seen that in consequence the total work necessary to extract and compress each pound of air had been reduced from 364,290 ft.-lb. to 196,500 ft.-lb.

The author appeared to indicate that over-expansion of the steam jet was preferable, since he suggested that pressure waves in the diffuser were desirable. But it must be remembered that a diverging nozzle designed for a particular range of pressure was really suitable only for that pressure range. If the back pressure were greater than that for which it was designed, the jet would expand well below the final pressure and then recompress itself. In so doing it lost its perfection as a jet and issued into the free space in a state of partial eddying. The bad effect produced by over-expansion upon the capacity of a jet to do work in a turbine had been shown by his colleague Professor Kerr in a paper to the Institution entitled "Jet Action in Turbine Blading."\*

The manner in which the pressure fell along a divergent nozzle when it was used for pressure ranges differing from those for which it was designed was illustrated by Fig. 14. Some years ago Professor Kerr and himself when working on this problem, came to the conclusion that the jet in such circumstances left the boundary of the nozzle altogether during the period of recompression.† Two methods of demonstrating this were devised by Dr. A. D. Third, who was then working with him as a research student. Fig. 15 showed one of these methods. Air was passed through a glass-sided nozzle under the different pressure ranges shown in Fig. 14, and a method of photography employed somewhat similar to that used by the author of the paper. It would be noticed that the waves

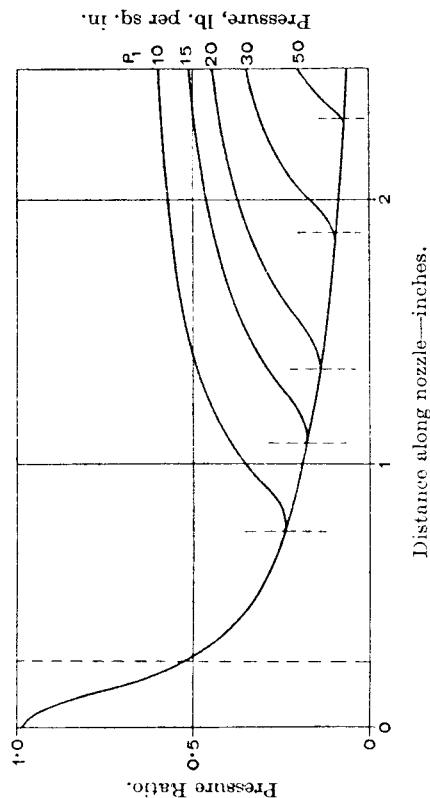
\* Proc. I.Mech.E., 1924, vol. ii, p. 673.

† JI. Roy. Technical College Glasgow, 1925, vol. 1, No. 2, p. 123.



formed could be traced up to the recompression stages, where they disappeared. These were the points at which the jet no longer filled the nozzle; thereafter it had no definite surfaces from which

FIG. 14.—Curves showing Fall of Pressure in Nozzle.



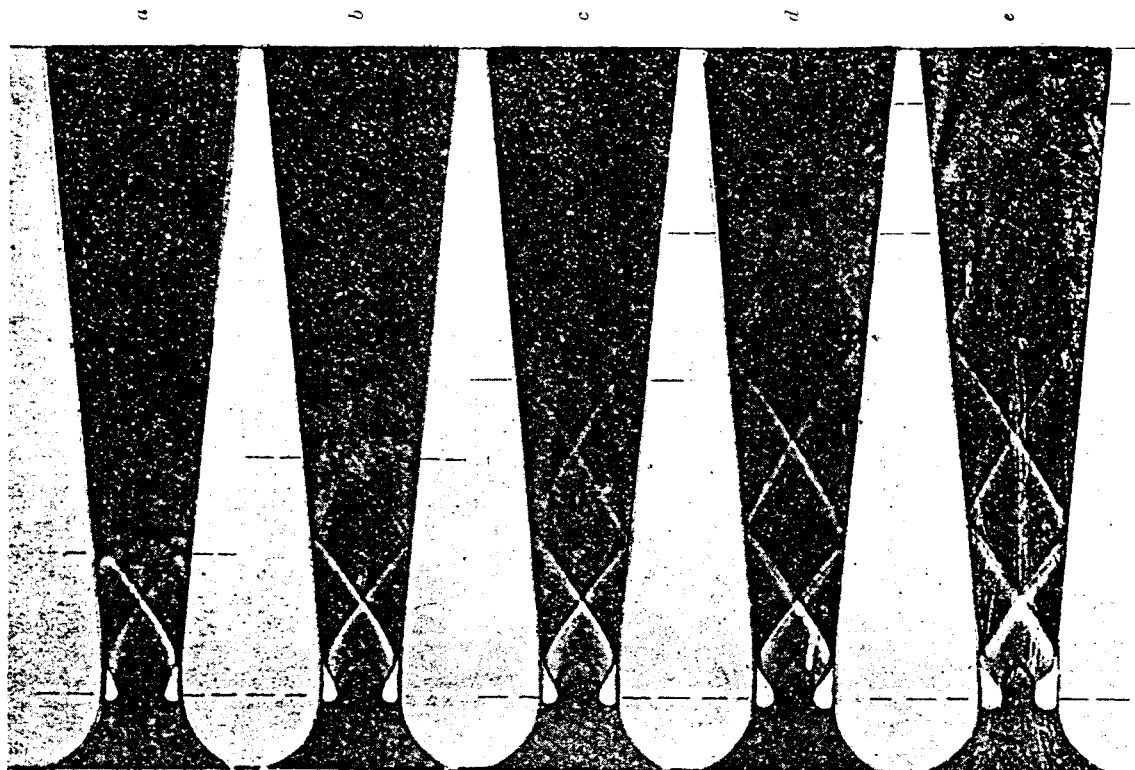
the waves could be reflected, and hence they were lost. Fig. 16 showed the same nozzle after it had been covered inside with thick oil, so as to be opaque to the light thrown against it. Here, again, it would be seen that the air jet had swept away the oil up to the points of recompression, and had then freed itself completely from the nozzle walls.

With such evidence before them, it would appear to be unlikely that a jet was in the best condition to do work in an ejector when it left the nozzle after any appreciable amount of recompression. In their own work they had found that the best results were obtained when the nozzle allowed a continuous fall of pressure throughout its length. It might, however, be noted that all jets showed a tendency to over-expand when they emerged into a free space, and it was probably this property which produced the entraining effect of the air ejector. The author had laid great stress on the distance of the end of the nozzle from the diffuser. This was certainly of some importance, but he did not think it was nearly so important as the author had imagined, provided a diffuser of a proper shape were employed. If this took the form of a short rounded nozzle at one end, then the distance mentioned might certainly make a considerable difference. The apparatus used at the Royal Technical College was shown in Fig. 17, and it would be noted that it resembled very closely that described in the paper.

The author appeared to have found that his best results were obtained when he had a series of somewhat violent waves in his diffuser. Here, again, he could not agree that such a condition

FIG. 15.—Fall of Pressure along Divergent Nozzle.

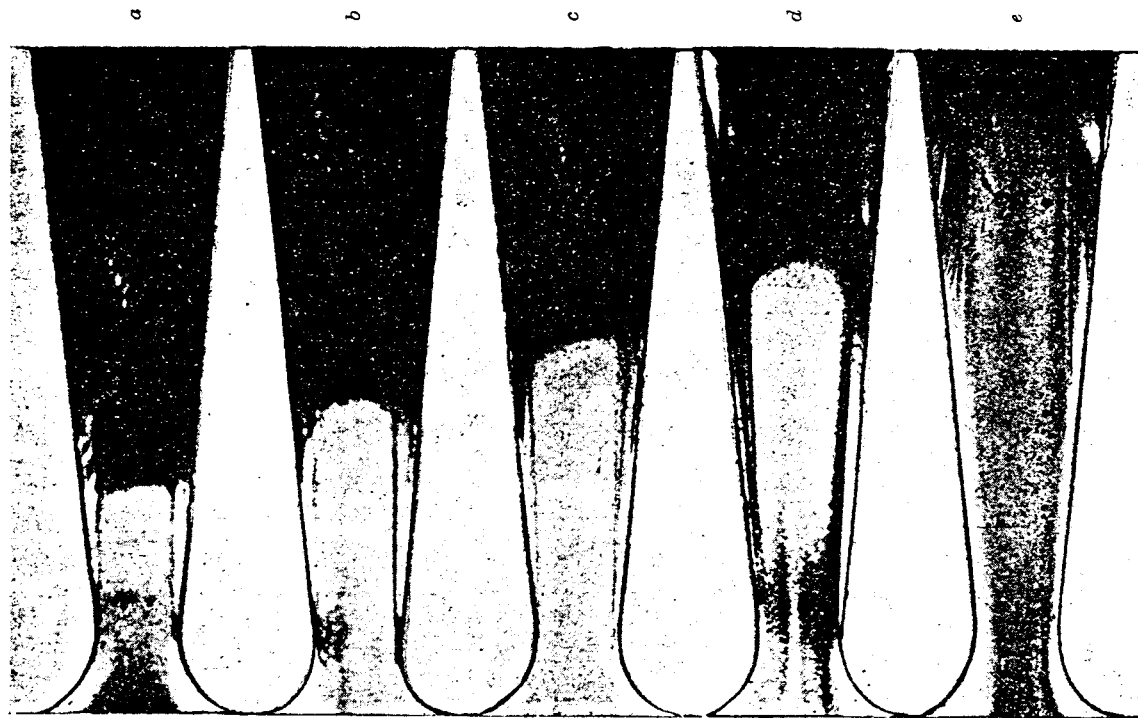
Air flowing through glass nozzle at the following supply pressures: *a*, 10 lb. per sq. in.; *b*, 15 lb. per sq. in.; *c*, 20 lb. per sq. in.; *d*, 30 lb. per sq. in.; *e*, 50 lb. per sq. in.



represented the most efficient ejector practice. Fig. 18 showed the type of expansion and compression curve which they in Glasgow had found to give the highest efficiency. It would be noticed that the waves formed after exit from the nozzle were comparatively

FIG. 16.—*Fall of Pressure along Divergent Nozzle.*

Air flowing through glass nozzle, covered inside with thick oil, at the following supply pressures: *a*, 10 lb. per sq. in.; *b*, 15 lb. per sq. in.; *c*, 20 lb. per sq. in.; *d*, 30 lb. per sq. in.; *e*, 50 lb. per sq. in.



small, and were soon damped out. With conditions producing the violent waves shown in Fig. 19, the results were not nearly so good. Some idea of what was occurring in the diffuser under good and bad conditions could be obtained from Fig. 20. To obtain this Figure, a glass-sided diffuser was employed with the method of photography previously mentioned.

FIG. 17.—*Experimental Air Ejector (Royal Technical College, Glasgow).*

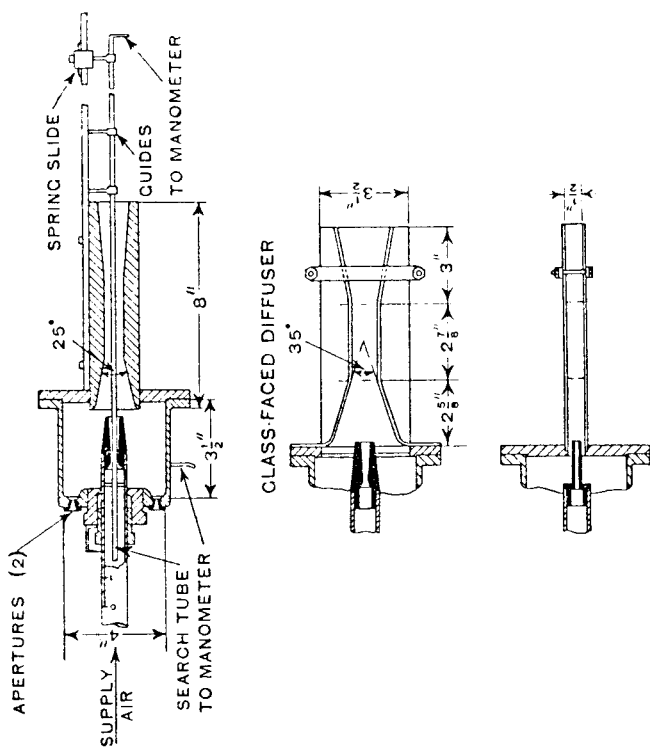


FIG. 18.—*Pressure along Axis of Jet, showing formation of waves.*  
Supply pressure,  $P_1$ , 76 lb. per sq. in. abs.

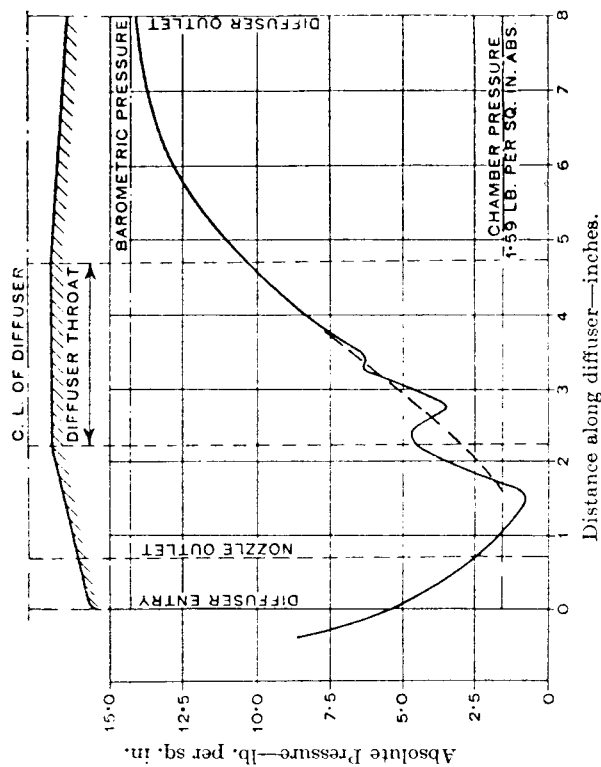
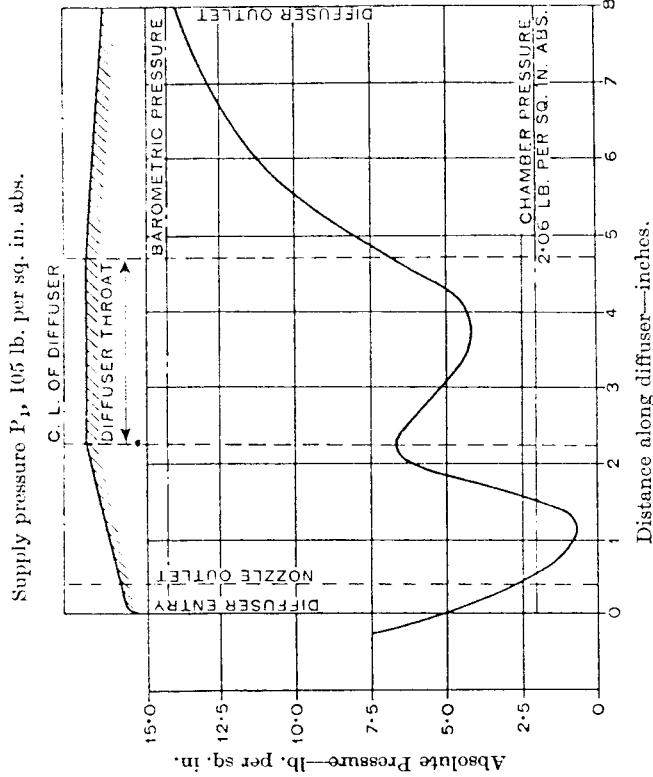


Fig. 21 gave an idea of the influence which the design of the diffuser had. Four diffusers were shown and it was evident that diffuser D was much the best, whilst E, which was parallel throughout, was the worst. It was surprising, however, that E was nearly as good as G. He thought that if the author had made the throat of his diffuser a little longer he would have obtained better results.

From Fig. 22 it would be seen how important a factor in ejector design was the diameter of the diffuser throat. A comparatively

FIG. 19.—Pressure along Axis of Jet, showing choked diffuser due to rise in supply pressure.



small change in throat area made a large difference in the amount of air entrained. If the diffuser was too small choking occurred, if it was too large there was a leakage of air back into the chamber.

A calculation chart was shown in Fig. 23 which had been drawn out to show how an actual ejector, using air as the working fluid, might be designed to suit a definite specification. Such a specification would include the supply pressure of the working fluid, the amount of air to be withdrawn, the vacuum from which it had to be drawn and the throat area of each nozzle unit in the plant. Assume, for example, that the vacuum was 17.5 inches of mercury, the nozzle supply pressure 85 lb. per sq. in. abs., and the throat diameter 0.25 inch. Starting with the top right-hand diagram, a horizontal line was drawn to the right from the 17.5 inches vacuum line to cut the 85 lb. per sq. in. pressure line. A vertical line from

FIG. 20.—Form of Jet under good and bad conditions.  
(a) Optimum diffuser distance and throat area; chamber pressure, 7.0 lb. per sq. in. abs.



(b) Diffuser throat area reduced.



(c) Diffuser distance reduced.



this point cut the air-suction base at 0.055. The area of the nozzle was 0.049 sq. in., so that the amount of air that could be entrained was 0.027 lb. per sec. Continuing the vertical line until it cut the 85 lb. per sq. in. pressure line in the lower diagram, and drawing another horizontal line, showed that the diameter of the diffuser throat would



of the air suction as shown in Fig. 24 *c*. He was sure that was wrong, because the air had not a good and uninterrupted entry into the combining tube. A smooth bore was necessary so that the mixture met with the least resistance in getting into the combining tube. The taper of the combining tube and diffuser seemed to have a very considerable influence on the result. The author commenced with a steam-air ratio of 6.6, which personally he thought was far too ambitious. He believed a ratio of 10 was more practical for a two-stage instrument.

The favourite method of scientific investigators, and probably the only convenient method of measuring pressures inside a moving fluid, was the search tube, but he always imagined that it must have some upsetting effect. When a mixture was rushing past a hole at a fairly high speed, he thought it was evident some definite phenomenon was occurring, and though the search tube might enable one to obtain a relative result, he was not sure that it was actually the result one expected.

There seemed to be two schools of thought on the subject of the over-expanded nozzle. Professor Mellanby said: "Design the nozzle correctly"; whereas the author said: "Over-expand the steam." He knew that some manufacturers who had carried out experiments said definitely that it was better to over-expand. His own theory was that if the nozzle was "gulping," as the author had shown, nodal effects with regions of lower pressure occurred, though he could not say why. He wondered if it were possible that the air collected in the positions of reduced pressure, and that the jet was split up, as it were, thus acting in some way that enabled it to collect the air better than in a nozzle of correct design. In the latter, a streamline effect occurred with a smooth flow.

Another point in connexion with the design of the combining tube emerged from experiments made by a number of manufacturers.

FIG. 24.—Good and bad Ejector Designs.

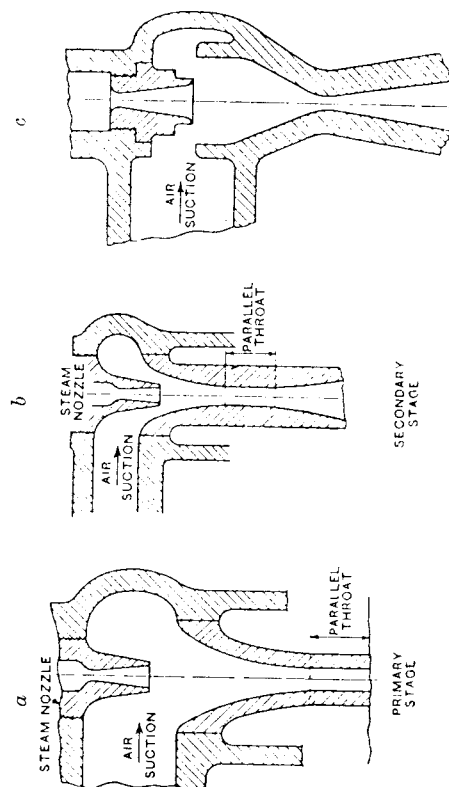
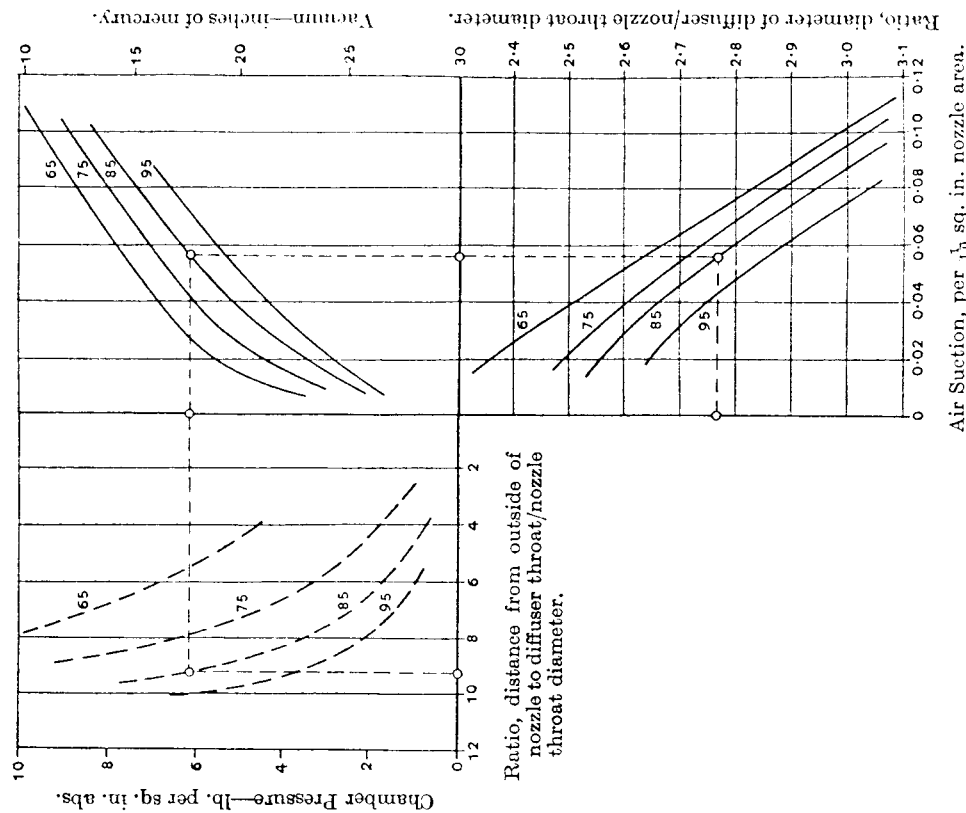


FIG. 23.—Ejector Chart for Single-Jet, Single-Stage Air Operation.

To determine air suction capacity, diffuser throat diameter, and diffuser distance, given nozzle throat diameter, nozzle supply pressure, and chamber pressure (or operating vacuum).

The figures on curves denote nozzle supply pressures in pounds per square inch absolute.



The best form was a smooth sweep with a well-rounded entry (see Fig. 24 *a* and *b*). The difficulty was that such a tube cost rather more to make than if made with a straight taper, but from experiments it seemed that the better the streamline effect the better the result. A sudden change from the taper to the parallel of the throat seemed to upset things. With regard to the tapers, while he was not sure of the limits he thought 1 in 12 to 1 in 16 for the combining tube seemed to give reasonably good results. He suggested that a

compression ratio of 5 to 6 was best where steam economy was of importance. The reason why the parallel portion improved the efficiency seemed to him to be that it gave stability to the otherwise turbulent stream and enabled it to be compressed to a higher pressure.

All those who used and operated steam ejectors knew that the bugbear was the tendency for the stability of the stream to upset suddenly. The secret of success was to keep the diffuser throat full of the mixture. It was a well-known dodge to fit an air cock to the throat and let in air, which had the effect of stabilizing the ejector again. The author said that the pressure throughout the air chamber was constant up to the diffuser throat. He himself suggested that that assumption was not altogether a reasonable one; it seemed to him the pressure must vary a good deal. Change of velocity was occurring all the time. The velocity of the air was given as 100 ft. per sec., but he would suggest it was more; while the velocity at the outlet from the diffuser was given as 220 ft. per sec., which he thought was probably too high for efficient working up to atmospheric pressure.

Mr. J. N. GRESHAM said that he and those associated with him were more particularly interested in the design of single-stage ejectors, and had been working on the theory of surface friction in connexion with the extraction of air. They had wondered what was the value of the central core of steam in producing a vacuum, and indeed, if the surface only was actually of use, whether there was any point in retaining the centre core of steam at all. At first they had inserted a plain rod in the centre of the steam jet, but found that this upset the jet completely. By shaping the rod in the form of a torpedo, however, it was possible at a critical pressure to remove the central core of the steam jet and reduce the amount of steam required to perform the work being done by the ejector. If the pressure were slightly changed, which, as the author had pointed out, would change the wavelength in the jet, a vibration like that of a tuning fork was set up and a strong hum occurred in the instrument. As a result of his investigations he was inclined to think that above moderate vacua, say 25 inches of mercury, the cone played a part which was rather in the nature of a piston action in providing the motive power necessary to drive the air through the diffuser tube. He had made at his works a diffuser having exactly the proportions given by the author and compared it with a similar ejector made some years ago in which the diffuser tube was moved by means of a rack and pinion. They had then, however, obtained some better results than were referred to in the paper, inasmuch as they got one set of nozzles to cover a higher range of vacua at given pressures. They were able, for instance, to obtain a vacuum of  $21\frac{1}{2}$  inches of mercury at 80 lb. per sq. in., 25 inches at 90 lb. per sq. in., and

28 inches at 100 lb. per sq. in. He asked the author, however, whether the figures given in the paper corresponded to the best setting of the diffuser, since in his experience the diffuser position would vary according to whether one required maximum vacuum or maximum air flow. He agreed with Professor Mellanby that the position of the diffuser was relatively unimportant, and his experiments went to show that there was no advantage in moving the diffuser between 80 and 200 lb. per sq. in. pressure whether maximum air flow or maximum vacuum was required. Where his instrument differed from that suggested by the author was chiefly in the angle of entrance to the diffuser tube, and the author seemed to use a much wider entrance than was necessary. Whether that was because he wished to be able to place his steam nozzle right in the throat for experimental purposes, he did not know, but he was sure that a much better result could be obtained with a narrower angle. There was a great deal in what Mr. Fitt had said as to the angle at which the steam was introduced to the air; the less shock imparted to the jet the better. On the question of over-expansion, he personally believed in it, but not the extent to which the author had suggested. The most important point was to keep the throat of the diffuser filled, and during certain parts of his experiments he thought the author had failed to do this. If the author was continuing his experiments, it would be of interest to ascertain the waveform imparted by the Sellers type nozzle. It was of American design and took the form of a divergent curve, and appeared to give a smoother jet than was obtained from a plain straight taper nozzle. He did not think, however, that it was of any very great practical value, since it soon wore into a perfectly conical nozzle.

Mr. I. V. ROBINSON said that from his own personal experience he could confirm the author's remarks regarding the small amount of information available as to the effect on ejectors of the distance between the nozzle and the diffuser. He spoke subject to correction by Professor Mellanby, but would call Professor Mellanby's attention to the fact that he was referring to the period prior to 1926. About that time he had been requested by a friend to help him in writing a book on condensing plant, and when he had tried to collect information regarding the variation of performance of air ejectors with variation in different features, he had naturally asked for any data connecting performance and the distance between the steam jet and the diffuser. All firms had stated that they were unable to disclose any information on this subject, as they regarded it as a matter of prime importance and did not wish their knowledge disseminated. On all other features of air ejector performance very complete information was obtainable.

The curves shown by Professor Mellanby in his contribution to the discussion showed clearly that with a certain throat area the capacity of the particular ejector to remove air became a maximum, and, in his own opinion, the reason was quite obvious. In the throat

of the ejector in operation the flowing medium consisted of a centre jet of steam at a high velocity surrounded by an annulus of air which, in his opinion, was carried through mainly by friction effects. The velocity of this air annulus was a maximum where it came in contact with the rapidly moving steam jet and a minimum at the surface of the diffuser. As in the flow of water through tubes, there would probably be a film of air in contact with the diffuser and the throat, which was stagnant. If the throat of the diffuser was so small that the steam jet occupied the whole of it, then the air could not be carried through, but would be sheared off the moving stream of steam. If, on the contrary, the throat was too large, the steam and the annulus of air would be insufficient to fill the throat, and eddies would be set up which would cause air to pass back into the convergent part of the diffuser and thus place a limit to its air-removing capacity.

As regards the effect of an appreciable length of parallel throat, there appeared to be so far no theoretical explanation, but it seemed reasonable to consider that this parallel portion enabled the flow to become more stable. The medium would be in a better condition to continue its journey through the diverging portion of the diffuser. There certainly was a very marked effect in practice. As, however, in so many other questions connected with the air ejector, the calculations became extremely involved, and as a result greater reliance was rightly placed upon practical experiments on the effect of varying different features or dimensions.

He had found the paper rather difficult to follow, and considered that it would be very difficult, if not impossible, for a designer to

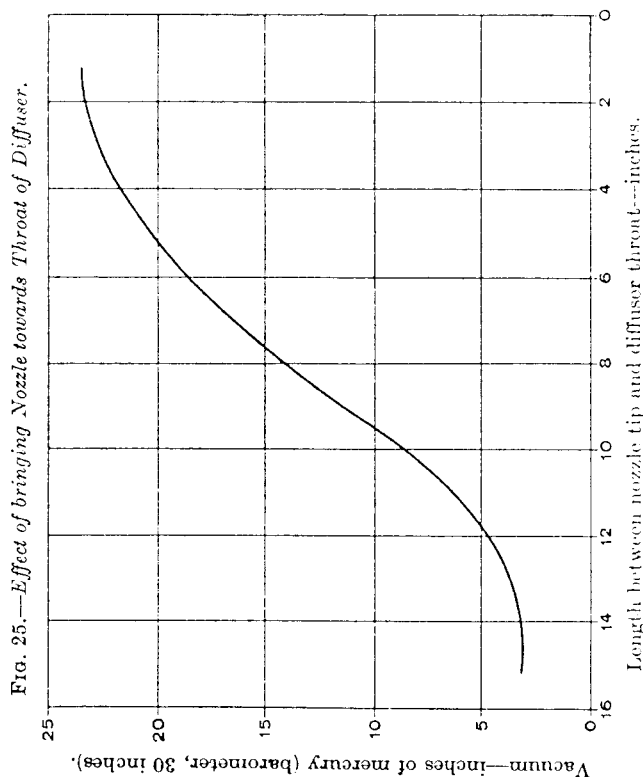


FIG. 25.—Effect of bringing Nozzle towards Throat of Diffuser.

take the paper and to apply the results to the design of an ejector to give a certain guaranteed performance. He had been intending to ask the author whether he could prepare any diagram which would be useful for this purpose, but he had been interested to see that in the earlier publications referred to by Professor Mellanby such a diagram had been published. He was looking forward to an opportunity of considering this diagram carefully when the present discussion was published.

Mr. C. E. H. VERITY stated that some years ago he had carried out a series of experiments on an apparatus generally similar to that described by the author. In his apparatus, however, it was the nozzle and not the combining tube which was moved, and the diffuser had a tapered and not a rounded inlet. It worked at a pressure of about 100 lb. per sq. in. gauge with a steam consumption of 250 to 300 lb. per hour. He had been interested to find, on looking back through his records of those experiments, that in many ways they confirmed the findings of the author.

FIG. 26.—Effect of Varying Air Leakage.

Figures on curves denote air leak in pounds per hour. Steam pressure, 100 lb. per sq. in.

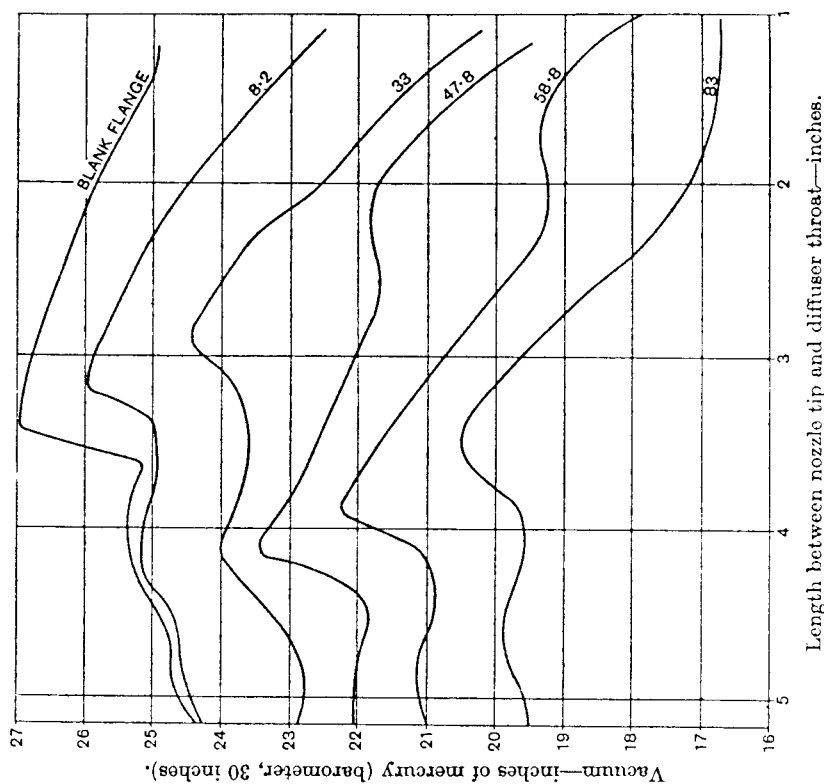
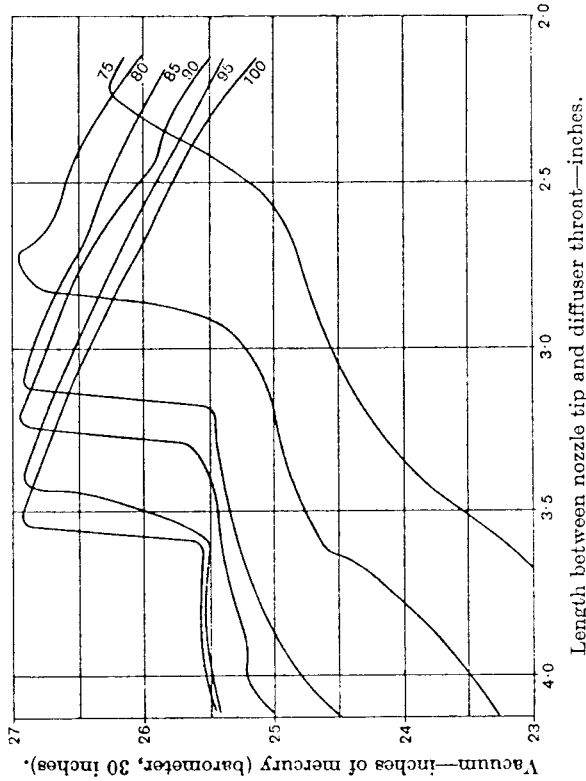


FIG. 27.—Effect of operating Steam Pressure on Correct Distance between Nozzle Tip and Diffuser Throat.

Figures on curves denote steam pressure in pounds per square inch. Air leak, 8½ lb. per hour.



of curves for varying steam pressures between 75 lb. and 100 lb. per sq. in. gauge with a constant air leakage, and it would be noticed that the point of maximum vacuum moved back, as the author had found, as the pressure was increased. Although the curves in this and the previous Figure might appear to be somewhat fantastic, they were plotted from quite stable and definite readings and they could actually be repeated again and again. He had in the course of his experiments produced hundreds of such curves.

Mr. F. R. B. Watson thanked Professor Mellanby for his criticism of the paper; most members of the Institution knew of the valuable work he had done in connexion with steam nozzles. With regard to the diagrams shown, those having reference to the pressure distribution in a three-stage ejector were interesting, but they did not have a direct bearing on the work described, as he had used only a single-stage ejector and atmospheric air (p. 235). Also those having reference to steam leaving the walls of the nozzle were important in connexion with steam turbine nozzles, but in his opinion it was rather the behaviour of the jet with its entrained air outside the nozzle that called for examination in the air ejector.

Professor Mellanby's argument with reference to recompression losses was a sound one, but when the jet was applied to an air ejector a reliable and steady vacuum, throughout a fair range of steam pressure conditions, was probably the first consideration, even if it was obtained at some sacrifice of efficiency in the jet. It was

Fig. 25 showed the general effect of gradually bringing the nozzle towards the throat of the diffuser. The horizontal scale of the curve corresponded to the author's dimension "D," i.e. it was the distance from the tip of the nozzle to the throat of the diffuser. The curve showed that the vacuum increased as this dimension was reduced.

Fig. 26 showed curves which were, he thought, interesting, since they illustrated a point which neither the author nor any other speaker had referred to, namely the effect of varying the air leakage on an ejector with a given steam consumption and operating steam pressure in addition to varying the nozzle position. As in the case of the previous curves, they showed a graph of vacuum against relative nozzle and diffuser throat positions (dimension D). The curves referred to a constant operating steam pressure of 100 lb. per sq. in. gauge, and the figures on each of the curves referred to various constant air leakages in pounds per hour.

He drew attention to the form of the curves, with particular reference to the points of maximum vacuum. Each curve appeared to have two such points and the top curve marked "Blank Flange" showed a high point at a distance D of about 3.4 inches, and a further lower point at a distance of about 4 inches. The next curve was generally similar in form, but did not show such a large difference between the maximum vacuum points. This tendency continued in the lower curves, the point of maximum vacuum gradually passing from the inner to the outer point until in the lowest curve the inner point had disappeared altogether, and a further incipient outer point was noticed to be appearing. The comparatively regular form of the curves could probably be explained by the wave theory given by the author and mentioned by Professor Mellanby, and he would be interested to have the author's comments on this point when he had had an opportunity of studying the curves.

The author and most of the speakers had spoken in terms of air ejectors designed for a certain definite steam consumption and duty, but he thought that it was well to bear in mind that the actual duty which they had to perform in service might vary considerably according to the size and condition of the plant of which they formed a part. The author had referred to the British Electrical and Allied Manufacturers' Association formula for fixing air quantities, and this formula was still being used; but even the most ardent supporter of it must agree that it was purely empirical. As the actual air leakage in service might vary so considerably from the designed figures derived from the formula, he thought that the curves in Fig. 26 were of considerable interest. With such curves it would be possible to design an ejector for a definite given set of conditions to give the maximum performance, but if the actual operating conditions varied only slightly from the specified figures the results obtained would be widely different from the estimate.

Fig. 27 confirmed very definitely the author's findings as to the effect of the operating steam pressure on the correct distance between the nozzle tip and the diffuser throat. The diagram showed a set



probably for this reason that the over-expanded jet had found favour with many ejector makers. His main objection to the under-expanded jet was its tendency to swell out, and this effect was clearly shown in Fig. 9 (*b*), (*c*) and (*d*), p. 255, where the jet with an over-expansion of 3.5 inches of mercury might be compared with an under-expanded one of 3.7 inches of mercury. He admitted that both effects were carried out rather far here, but Fig. 9 illustrated the point in question. These photographs were taken under air-pump conditions, but he had also viewed similar effects under ejector conditions when somewhat violent oscillations were set up in the air chamber. Professor Mellanby showed in Fig. 19, p. 273, unfavourable conditions which were set up by increasing the initial pressure with an under-expanded jet and this illustration indicated how rapidly conditions in the air chamber changed, probably due to the enlargement of the jet causing a partial choking of the diffuser throat. Professor Mellanby had evidently reduced the node effect in the jet to a minimum, so the length *D* would not be likely to have such a marked effect as in his own experiments. He could see no reason for modifying his statement with regard to the small amount of information available in print on work of the kind undertaken. Among other quantities investigated he had examined the possibilities of an over-expanded steam jet for producing a vacuum; compared results from two forms of diffuser entrance; determined the steam-air ratio from low vacua up to about 25 inches of mercury; examined the behaviour of an over-expanded jet, consisting mainly of steam, on its passage through two diffusers of different throat lengths, and showed photographically the three forms that might be assumed by a steam jet (outside the nozzle) according to the pressure in the region into which it was discharging. He could not see how he was to get such information from any of the results or references that Professor Mellanby had given. He had no knowledge of the paper by Professor Mellanby, or of that by Dr. Third, until a week before the meeting. He was interested in Dr. Third's photographs, shown by Professor Mellanby, of the waves in the air stream passing through a glass-sided diffuser, and he thought they were most instructive.

He had at first hoped to experiment with the two-stage ejector, but he had encountered too many problems in the single-stage to admit of this. He thanked Mr. Fitt for confirmation regarding the steam-air ratio, namely, that 10/1 was a probable value. He agreed that search tube readings had to be taken with a certain reservation, but the observations used were applied only relatively. One upsetting effect was shown at G in Fig. 11, p. 258. He was interested to hear Mr. Fitt's views on the node effect. In this connexion he considered that there was still a good deal to be learnt about the suction effect of the jet. The assumptions made in the diffuser design were no doubt open to criticism, but he would say in defence of them that the ejector suited its purpose very well and was perfectly stable under all working conditions.

He appreciated the criticism of such a well-known authority on ejectors as Mr. Gresham, and the results he gave of his investigation of the central core had a direct bearing on the work described and were of much interest. He had observed that the best positions of the diffuser for "closed tank" and "with air flow" were different and he ought perhaps to have stated in the paper that the best setting for the latter was used for *both conditions* throughout the experiments described. His only reason for this was that he had attached chief importance to air flow conditions, and he hesitated at introducing too many diffuser settings into the paper. This setting would account partly for the considerable difference between the vacua given by Mr. Gresham and those recorded in Table 5, p. 246. Also he had attempted a wide range of pressure with the same nozzle and diffuser. He had since taken some observations to find the maximum vacuum which his nozzles and diffusers would give at about 80 and 100 lb. per sq. in. when the diffuser was moved up with closed tank conditions. With nozzle No. 2 and diffuser No. 1B, he obtained 16.8 inches and 27 inches at 80 and 100 lb. per sq. in. respectively. With nozzle No. 2 and diffuser No. 2B, he got 16 inches and 27.5 inches at 80 and 102 lb. per sq. in. respectively. The vacua at the lower pressure were still considerably below Mr. Gresham's figures. The range of pressure obtained by Mr. Gresham for one diffuser setting was very good. The wide entrance-angle was used chiefly because the diffuser was worked close up to the nozzle, but he had not quite realized at this stage that the value of this angle was so important. He was also glad to have Mr. Gresham's opinion on over-expansion.

He would like to assure Mr. Robinson that he had made every effort to express the results in clear terms, and he had no doubt that on a second inspection Mr. Robinson would find them much easier to follow than he suggested.

Mr. Verity's contribution had a close connexion with the work described, and it was interesting to know that he had found certain of his results to be in very fair agreement with the author's. Mr. Verity had given consideration to the variable conditions that might arise in service, an important aspect that was probably too often neglected, and he considered the curves in Fig. 26 well worth examining. He had not tried this experiment of gradually increasing the air flow; in his own experiments he had taken only the extreme cases of no air flow and maximum air flow. His interpretation of the curves in Fig. 26 was that the wave series gradually shortened due to the gradually increased pressure in the air chamber and throat, and that the anti-node or neck in the jet, which would be formed near the peak on the right-hand of the diagram, gradually approached the nozzle tip. (Compare cases (*b*) and (*c*) in Fig. 9, p. 255). The outer point, shown on the left of the lower curves, would be the effect of the next wave in the series. The wave series would gradually withdraw itself back into the nozzle, and the outer waves would be gradually brought within the 5-inch range shown. He was not quite certain why the maximum vacuum should

He asked whether any connexion had been traced between the position of that point and the shape of the diffuser.

Mr. F. R. B. WATSON, replying to Commr. Twinberrow, said that he had had no experience of erosion in nozzles. He would recommend replacing the nozzle having a large throat by one of correct throat diameter in order to economize in steam. Probably there was, with normal steam pressure and enlarged nozzle throat, additional resistance in the diffuser throat due to the increased steam flow through it, and this resistance would cause a reduction of velocity. With increase in steam pressure the jet velocity was increased and the vacuum restored at the expense of a further increase in steam consumption. Any adjustment of D for the eroded nozzle would still mean, of course, a steam consumption above the normal.

He referred Mr. Mountney to Fig. 3, p. 241, which showed a sudden rise from 18.5 inches vacuum to about 23.5 inches vacuum at A on the 140 lb. per sq. in. steam pressure curve. This occurred when the two wavelengths were seen, immediately after the sudden rise at that point. The neck of the wave was then at the entrance of the diffuser throat, but another good setting was obtained with the second neck at the throat entrance, corresponding to the point B in Fig. 3. In fact, the closer setting generally gave the better results in both types of diffuser used.

As regards the spiral throat mentioned by Mr. Hamilton, he had never contemplated using it and had not seen any reference to anyone else having used it. He had not used ports in a diffuser, but he understood that ejectors designed on somewhat similar lines were in successful operation. The attractive feature about the ordinary form of ejector was its simplicity. With regard to the disturbance at the point G in Fig. 11, p. 238, mentioned by Mr. Worsdell, he considered that this was due to the presence of the tip of the search tube, or the small hole near the end of the tube, in a sensitive part of the jet. He did not think that the disturbance was connected with the shape of the diffuser.

#### *Communications.*

Mr. JOHN CALDWELL wrote that a considerable amount of space was devoted to the peculiarities of the action within a high-speed jet produced by a nozzle. It should be noted that this was only a repetition of work done many years ago on this subject by Prandtl and his associates in Germany, the results of which had for long been available in German textbooks and books of reference.

In the "Handbuch der Physik," \* vol. 7, there was an excellent chapter entitled "Gasdynamik" by Ackeret. This presented in a very convenient manner the knowledge accumulated on all forms

\* J. Springer, Berlin.

sometimes occur at the outer of the two points. He had noticed this in his own results, and one case was shown on the upper of the two 120 lb. per sq. in. curves in Fig. 4, p. 243. The formula given by the British Electrical and Allied Manufacturers' Association had been used only to convey to the general reader some idea of the size of the condensing plant for which such an ejector might be suited. He fully realized that the curves shown represented quite stable conditions.

#### *Discussion in Bristol on 3rd March.*

Commr. R. W. K. TWINBERROW said that he had had a certain amount of experience of steam jet operation and had found that after a few years' running an increase of steam pressure amounting to something like 5 per cent per annum was necessary to maintain the original vacuum. He assumed that this increase was necessary on account of the erosion in the nozzle. This showed that increase of the diameter of the nozzle required an increase in steam pressure, and since this in turn necessitated an increase in the dimension D, there seemed to be a relation between the diameter of the nozzle and the distance D, and hence it appeared that as wear took place in the installation, steam consumption might be economized by adjusting the nozzle rather than by adjusting the steam pressure.

Mr. C. F. MOUNTNEY asked if two complete wavelengths corresponded to the value of the dimension D, and was that the ideal number.

Mr. EDWARD HAMILTON asked the author whether he had ever contemplated making any experiments with an ejector having a spiral throat. He believed that turbulence had been largely responsible for creating the vacuum, and he therefore considered that a spiral throat might be an advantage. He would also like to know if the author had contemplated using ports in the diffuser, though the effect of the high velocities generated would probably be detrimental.

Mr. T. A. WORSDELL remarked that he had had the privilege of working for the Steam-Nozzles Research Committee in Manchester and that part of the work of the Committee had been to try to reduce to common terms the results obtained from a number of steam nozzles. In spite of the precautions taken considerable difficulty was found in discovering a satisfactory common basis. Fig. 11, p. 258, showed an interesting curve of the pressure waves along the diffuser, and there was one place where the introduction of a search tube upset the pressure in the tank and in the diffuser. It appeared as though that was the point where the greatest effect was caused by the introduction of a small foreign body, and that it was therefore an effective place from the point of view of the formation of the vacuum.

of fluid flow at high speeds, and included many excellent photographs of jets in which the wave action was shown much more clearly than in the photographs presented by Mr. Watson. In addition, jet phenomena were discussed mathematically, thereby shedding much light on the evidence presented by the photographs, the interpretation of which alone was very difficult.

Mr. R. H. B. FORSTER wrote that he had had to design injectors on several occasions to supply a large volume of air at a low pressure to low-pressure air type oil burners. This formed a highly satisfactory method where only a limited supply of high-pressure air or steam was available; but of course the power consumption was higher than if a fan were used. He presumed that in this case, i.e. when the inlet air was at atmospheric pressure, the steam should be expanded only slightly below atmospheric pressure.

As the ejector action appeared to depend on the formation of stationary waves in the steam jet, the question arose as to whether it would be possible to create or increase these by artificial means. He would like to know if the author had had an opportunity of investigating this matter. He noted that water was used in the inclined gauge for measuring the air quantities. It had been his experience that the surface tension of water introduced inaccuracies at low readings, therefore he had found kerosene more reliable.

Would not the most rational method for designing the area of the diffuser throat be to design this so that the kinetic energy of the mixture at the throat was equal to the sum of the energy to produce the vacuum required plus the losses in the diffuser?

Mr. B. HODKINSON wrote that waves appeared in the photographs whether there was over-expansion or not. In his experience it seemed only to be necessary that the stream velocity was high enough; it had to be considerably above the velocity of sound. Callendar's steam data had evidently been used. But in designing the nozzle for no over-expansion an efficiency of 0.87 had been assumed. This seemed very low, though it mattered little since over-expansion was used. It did not follow, though stated so on p. 254, that the best settings moved nearer the nozzle for lower supply pressures simply because the wave trains shrank nearer. All phenomena must extend less far outwards with feebler stream energy.

The most important deduction in the paper was perhaps that stating the relationship between the position of the entrance of the diffuser throat and the nearest wave. The best arrangement was said to be that when a globular part of a wave was inside the throat and a neck just inside (p. 259). This statement was in part repeated at the top of p. 261. It was difficult to follow. In Fig. 11, p. 258, the globular part was outside the throat and the antinode inside. Similarly in Fig. 10 (g) the globular part seemed to be just outside and the antinode just inside. Was not the conclusion rather that

the tapering part of one wave must be encircled by the throat entrance? Or was it meant that there must be a neck just inside the throat and a following globular part further inside?

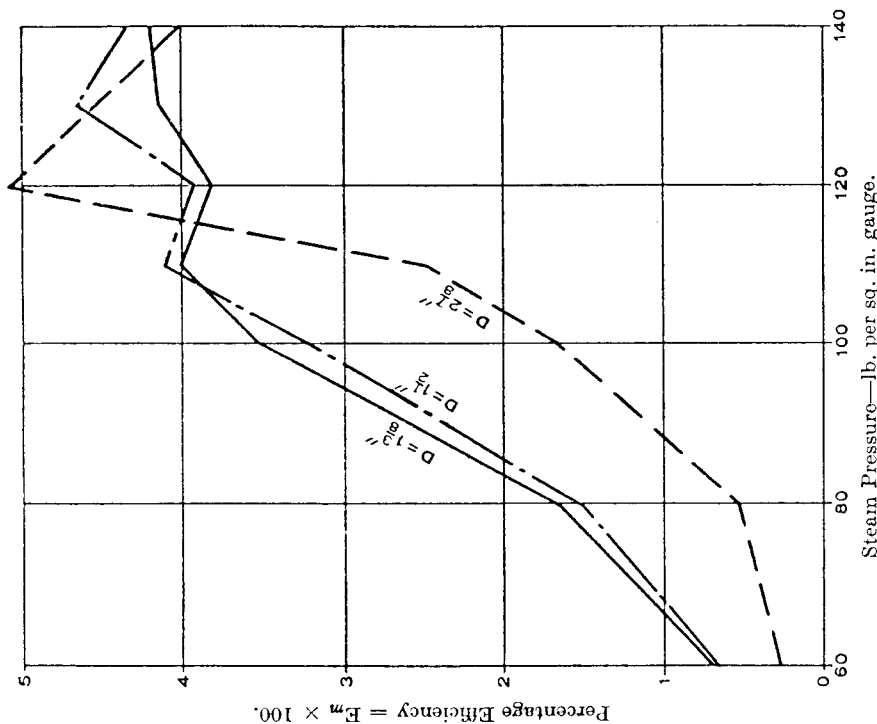
Certain details might be added in the diagrams and sub-titles to help the hurried non-specialist reader. Thus the search tube might have been sketched in somewhere, say in Fig. 11. Again, what was the air quantity in Fig. 3, p. 241? In the foot of the same Figure the drawing might be extended to show the type B (long throat) nozzle, and it might be labelled clearly as "All Type 1," i.e. rounded inlet. Similarly Fig. 4 might be labelled as "Type 2." Again, in Figs. 5 and 6, pp. 250 and 252, it seemed that the curves for maximum steam-air ratio were for the diffuser with 14 inches parallel throat. The curves should be labelled and this stated. On p. 251, line 14, the "best" performance was given as showing a steam-air ratio of 10. Yet values of 8.6 were obtained at lower pressures (about 80 lb. per sq. in.). It would have been well to state that "best" was meant from the point of view of producing the best vacuum, with a fairly normal amount of air carried.

The legends for Figs. 5 and 6 should preferably have stated that the curves were plotted from Table 5 so that the designation of the points, for example " $\Delta$  At 100 lb. per sq. in.," could be seen to mean "at the best diffuser setting for 100 lb. per sq. in." Little inset sketches of the diffuser for Figs. 5 and 6 would be helpful. The photographs in Fig. 9 might have been labelled as to expansion, with a reminder too that they were for nozzle No. 1 designed with no over-expansion at full vacuum. The same kind of remark applied to Fig. 10. In Fig. 11 curves A and B applied to diffusers 2B and 2A. Such lettering was confusing. In the same Figure the abscissa was the distance of the tapping hole in the search tube from the nozzle outlet. Then the curve of pressure in the air tank became clear.

Mr. R. LIVINGSTONE wrote that the expression "over-expansion" as applied to the steam jet might cause some confusion. It was customary to use this expression to describe the design of the nozzle, i.e. a nozzle designed for "over-expansion" was one having an outlet area greater than was required for the steam jet. If the same expression was applied to the steam jet, one was led to think of a jet which expanded more than was possible inside the nozzle instead of the reverse of this, as was intended. The term "slack nozzle" was sometimes used, and was a good description of a nozzle designed for over-expansion. Photographs of the waves in an air jet reproduced by Stodola in "Die Dampfmaschinen" were very clear in comparison with those given by the author. No doubt the author would pursue this investigation further, and it might be of benefit to establish the relation between the wavelength in air and in steam given by R. Emden as 1.35. It would also add to the value of the experiments if different weights of air were used in conjunction with the same steam jet. This could be done by using different sizes of nozzle for admitting air to the tank.

The efficiency of the ejector, although low, was nevertheless of some interest, and an examination of the shape of the efficiency curve might give a better picture of the performance than an examination of the vacuum curve alone. The efficiency could be taken as the ratio of the work done in compressing the air to the work available in the expansion of the steam. The work necessary for air compression might be taken on an isothermal basis, but it seemed preferable to take adiabatic expansion for the steam from

FIG. 28.—Efficiency Curves.  
Diffuser 2B; No. 2 steam nozzle.



the nozzle pressure to the final pressure  $P_2$ , and adiabatic compression of the air from the initial pressure  $P_1$  to the final pressure  $P_2$ .

If the air weight was taken as having a specific volume of  $\frac{202}{P_1}$  cu. ft. per lb. at the initial pressure  $P_1$ , the ratio of steam weight to air weight as  $C$ , and the adiabatic heat drop in steam from the nozzle pressure to  $P_2$  as  $dH$  B.Th.U. per lb., the overall efficiency

ratio of the ejector was

$$E_m = \frac{131 \left\{ \left( \frac{P_2}{P_1} \right)^{0.286} - 1 \right\}}{C \cdot dH} \quad (a)$$

Equation (a) had been used to plot the efficiency curves shown in Fig. 28 from the data given in Table 5, p. 246. Although the best setting for nozzle 2B at 120 lb. per sq. in. was  $D=2\frac{1}{2}$  inches, it was obvious from Fig. 28 that the rate of change in efficiency with change in pressure was too great for stable operation at this setting, and that the setting might be made the same as for 100 and 140 lb. per sq. in. without serious detriment.

In order to compare the efficiency of the test apparatus with commercial ejectors, Table 6 was given showing the results of tests on a complete line of standard ejectors made in America some years ago. The figures given without intercooler were test figures, and those with intercooler were estimated from the test data. The tests—some of which he had witnessed—were ordinary works tests,

TABLE 6.—Two-Stage Ejectors without intercooler.

Steam pressure: 120 lb. per sq. in. abs. (saturated).  
Air discharge: 31 inches mercury abs. back pressure.  
Steam heat drop  $dH$ : 152 B.Th.U. per lb.  
Average steam and air quantities } 300 to 2,700 lb. steam per hour.  
for various ejectors ranging from } 5.9 to 210 lb. air per hour.

Initial Air pressure, inches mercury abs.	1	1.5	2	2.5	3	3.5	4
Intermediate Air pressure, inches mercury abs.	5.6	6.8	7.9	8.8	9.6	10.4	11.1
Ratio, lb. steam/lb. air	51.5	31	23	18.75	16	14.25	12.9
Percentage reduction in steam consumption by intercooler	24	21	19	18	16½	15½	15
Percentage efficiency without intercooler, equation (a) $E_m \times 100$	2.80	3.85	4.20	4.85	5.15	5.25	5.35
Percentage efficiency with intercooler, equation (a) $E_m \times 100$	3.70	4.90	5.20	5.92	6.15	6.25	6.25
Compression ratio for each jet	5.6	4.6	3.9	3.5	3.2	3.0	2.8
Total compression ratio $\left( \frac{P_2}{P_1} \right)$	31	20.6	15.5	12.4	10.3	8.9	7.8

but both air and steam were measured by calibrated nozzles and the initial and intermediate air pressures by mercury gauges. The first stage of these ejectors consisted of a number of small round steam jets discharging into a common diffuser. The second-stage jet was in the form of a thin disk discharging into an annular radial diffuser. The first-stage jets could be changed in size and number to give the best value to the intermediate pressure, and the thickness of the annular second-stage jet could also be varied. In this series

of eleven ejectors, the general dimensions of the diffusers and position of the jets were fixed and only the sizes of the steam jets could be varied to suit the vacuum and weight of air. The efficiency fell with an increase in the ratio of compression, but as this was accompanied by a reduction in  $P_1$  it was difficult to say whether the change in efficiency was entirely due to change in the compression ratio. Had the author made any experiments to determine the effect of the vacuum on the steam-air ratio for constant compression ratio? This was possible by altering the pressure in the condenser to maintain a fixed ratio of  $P_2/P_1$ , and taking readings of steam and air rates for differing steam pressures.

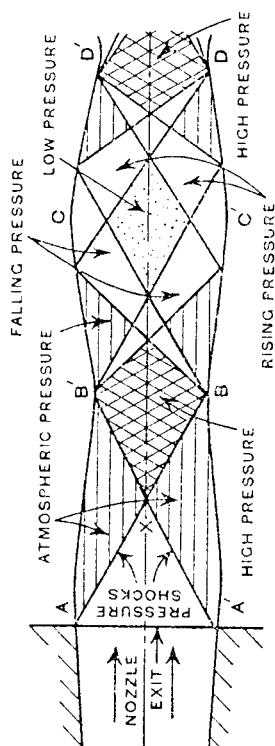
Mr. WILLIAM PEARSON (Brush Electrical Engineering Company) wrote that, as the author had employed a movable diffuser in his tests, it might be of interest to him to know that his firm carried out all their commercial tests of ejectors with movable steam nozzles, which were finally fixed in the positions which gave the best results.

Mr. S. A. WOOD (National Physical Laboratory) wrote that under the conditions of the experiments described in the paper, results indicated that the best performance was obtained by using a steam jet which had been over-expanded in the nozzle, and was therefore characterized by axially periodic variations in cross-sectional area and pressure. The conditions of pressure in a jet of this type had been studied by many, including Stodola,\* Prandtl,† Rayleigh, Stanton, and others, and their conclusions threw light on the pressure variations observed by the author. The conditions in an over-expanded jet were illustrated in Fig. 29. To enable pressure differences to be maintained stable, the velocity of the jet at efflux must be greater than that of sound; such velocities were produced by a convergent-divergent or Laval nozzle as used in the air ejector.

The steam issuing from the nozzle at AA', at below the external (or atmospheric) pressure, was subjected to a sudden "pressure shock" originating at A and A' and propagated in the directions AB and A'B', and immediately downstream of the shock waves the jet pressure was atmospheric (assuming discharge into the atmosphere). When the two shock waves concurred at X the rises due to each were superimposed, so that the pressure in the cross-hatched region between B and B' was above atmospheric.

On reaching the boundary of the jet the compression waves AB and A'B' were reflected from this, which acted as a solid boundary owing to the high speed of the jet relative to the external air. It was shown by Prandtl that the compression waves were reflected as waves of rarefaction BC and B'C', which in turn were reflected from the boundary at C and C' as waves of compression, and the whole process was repeated. The variations in diameter

FIG. 29.—Conditions in an Over-expanded Jet.



of the jet were consequences of the successive compression and rarefaction undergone by the steam. The wavelength of the periodic features of the jet was a function of the ratio of its mean velocity to that of sound, and this accounted for the shortening in wavelength as the velocity was reduced by friction and eddy losses.

An examination of Fig. 29 explained the variation in pressure recorded by the author across the diameter of the jet at an "anti-node" or neck; the pressure recorded at a hole in the wall at the beginning of the diffuser throat with the setting for maximum tank vacuum was that in the neighbourhood of B and B', which was the same as that of the surrounding air, while midway between B and B' the search tube orifice was in the shaded region of high pressure. When the author's search tube and diffuser pressure hole were moved  $\frac{3}{8}$  inch axially (approximately half a wavelength of the jet) the conditions met with were those of a section such as CC', where the higher pressure was at the circumference of the jet.

The author explained the presence of light patches in his jet photographs at the anti-nodes (regions of high pressure) by the presence of condensed particles at these positions. It would appear more feasible that this was a refraction effect due to density changes in the jet between the illuminated axial plane and the camera. Any light coloration due to the presence of condensed particles would show itself in the regions of low pressure, i.e. at the broad portions of the jet, in accordance with the law of adiabatic expansion of steam, which might be assumed to hold approximately in the first part of the jet. Similar light patches were shown in air jet photographs by Stanton.\* Photographs by Stodola referred to by the author showed dark patches at the necks of the jet.

The occurrence of optimum injector conditions when there was an anti-node of the jet at the throat entrance suggested that the diffuser throat used in the author's experiments was too small relative to the mean jet diameter; this theory was supported by the fact that the design assumed a 6.5/1 steam-air ratio, while in practice a ratio of above 10/1 was found necessary. With the throat diameter too small for the mean jet diameter, the best working would be

\* "Pumps and Gas-Turbines," 6th ed., p. 105.

† *Physikalische Zeitschrift* 1904, vol. 5, p. 599; and 1907, vol. 8, p. 23.

obtained when the local jet diameter was as small as possible at the most critical position, i.e. the throat entrance. This condition corresponded to a setting with an anti-node at the entrance. With a wider diffuser throat, the axial setting of the diffuser would not be so critical—a view which was confirmed by Dr. Third's results, referred to by Professor Mellanby at the beginning of the discussion in London.

With reference to the author's conclusion that a considerable length of parallel diffuser throat was an advantage, the results of tests carried out in collaboration with Mr. A. Bailey suggested to himself that the long throat was merely increasing the efficiency of the diffuser as a compressor, by lengthening the distance between the throat entrance and the outlet.

Mr. F. R. B. Watson wrote in reply that the work of Prandtl, which he had consulted, did not give him the information he wanted, but he hoped to examine the reference given by Mr. Caldwell. He considered the photographs in Figs. 9 and 10, pp. 255 and 257, were worth including in the paper as they showed the forms assumed by the jet from the actual nozzles used in the ejector experiments, and rendered the paper more complete, especially for readers who did not have easy access to German publications. With regard to the photographs, they were not intended to be *detail* photographs. They were taken primarily to determine wavelength and form of jet. He agreed that the mathematical investigation should proceed, if possible, hand in hand with the photographic, but in this paper he had decided to omit work of a mathematical nature.

The wave effect could be increased by allowing for a slight over-expansion of the jet, i.e. by using a nozzle having a wider outlet than that called for by the pressure conditions at discharge. With regard to the area of the diffuser throat, he was not quite clear as to the statement given by Mr. Forster. This should surely read "the kinetic energy of the mixture at the throat was equal to the work done in compressing and discharging the mixture plus the residual energy of the stream plus the losses in the diffuser." This expression was sometimes used for obtaining a value for the efficiency of the diffuser, but for obtaining a fair approximation to the throat area he would suggest the method used in the Appendix.

Mr. Hokinson had evidently made a close examination of the contents of the paper, and he appreciated the way in which he had touched on important points. In the jet shown in Fig. 9 (c), p. 255 (discharge at designed outlet pressure), there was a wave in the jet, and the pressure difference as determined by search tube between the slight anti-node shown and the nearly parallel portion on the right of it was about 0.6 inch of mercury. With regard to the anti-node near the diffuser throat entrance, this was observed when the rise to the higher vacuum took place and he considered it worth while to remark upon it. Why it should have been in that position was not easy to explain with certainty, but Mr. Wood, in his

communication, gave a probable explanation. The air quantities were not taken out when the observations in Figs. 3 and 4, pp. 241 and 243, were made. He agreed that, although curves were given, the reader's attention might have been drawn to the fact that for a vacuum of, say, 14 inches a lower steam-air ratio than 10 would suffice, as lower vacua than 25 inches were often used in industrial operations. He could not see, however, that further explanation of the results on p. 251 was necessary, for they were stated with reference to the original design conditions, given on pp. 235 and 262.

The term "over-expanded jet" was probably not a very satisfactory one, but he did not know of a better expression in common use. He had used it in the sense that the jet expanded below the final pressure (or "over-expanded") in the nozzle before recompression took place. Wave sections would show up more clearly than the outside views which he had attempted to produce. Also by grouping these photographs reproduction was made more difficult, for the same time of exposure was not suitable for all the photographs in a group. In making slides from the original photographs different times of exposure were allowed, and this was quite successful. He had other sets of orifices for the air tank, but he had not made much use of them so far. He hoped to examine later the results given by Mr. Livingstone for a two-stage ejector. He was interested in Mr. Livingstone's efficiency ratio expression and in the curves he had plotted in Fig. 28. The main point in his own mind when using the 2½-inch diffuser setting was not one of efficiency, but the lowest steam pressure that would give a vacuum of 25 inches with the air orifices used. He had been unable to get this vacuum at 100 lb. per sq. in. At 120 lb. per sq. in. and with  $D = 2\frac{1}{2}$  inches he had practically obtained that vacuum; at the closer setting he would not have obtained it. This outer setting gave high figures for steam-air ratio at lower pressures, shown clearly in Fig. 6, p. 252, and, as stated above, it was used for what appeared to be a limiting value for the steam pressure, but the ejector was quite stable in operation at this (2½ inches) diffuser setting. He had not attempted any experiments on steam-air ratio using a constant compression ratio. The object of the experiments originally was to get some information as to how the jet did its work and there had not been much time given to the consideration of efficiency.

He was pleased to know how the adjustment between nozzle and diffuser was effected in the ejectors made by Mr. Pearson's firm. He considered Mr. Wood's communication a useful contribution to the discussion, and he appreciated the criticism it contained. The statement on p. 256 might have been misleading and he did not intend it to convey the meaning that condensation was taking place in the jet at an anti-node, but that at this portion there was probably compressed steam. As stated on p. 254, many of the photographs taken were intended to be more nearly side elevations than sections of the jet, and therefore the same inter-

pretation could not be given to the colours as in Stodola's sectional photographs. The light colour showing across an anti-node in most of the views was probably a lighting effect, for one photograph taken under conditions similar to that of Fig. 9 (c), p. 255, but with an axial beam of light, showed the dark neck (with white boundary) outside the nozzle very clearly. These photographs were originally taken to show wavelength and form of jet, and not for examining the differences of density referred to in the communication.

Mr. Wood's explanation of the presence of an anti-node at the throat entrance was of considerable interest. Of course, it was also possible that the relatively low pressure region round the anti-node facilitated the passage of the air into the throat.

# STEAM-JET SYSTEM OF REFRIGERATION

40. Principle of Steam-Jet Refrigeration.—Another type of refrigeration system that is used is known as the vacuum, or steam-jet, system. Ordinary water forms the refrigerant, and the evaporation of the refrigerant is caused by lowering the pressure on it, and consequently reducing the temperature at which it will vaporize. This reduction of pressure is produced by the action of steam jets of high velocity.

A diagram of the system, showing the several parts and illustrating the method of operation, is given in Fig. 11. The water to be chilled flows into the air-tight vessel *a* through the pipe *b* and is discharged from the header *c* in a fine spray by a series of spray heads. A very high vacuum is produced in the vessel *a* by the action of a steam-jet ejector *d* that draws out the air and vapor in the vessel above the level *e* of the water. In other words, the pressure inside the vessel is reduced to only a fraction of a pound, absolute; and as this pressure is lower than that at which the water will boil, some of the water at once flashes into vapor. The heat required to cause this evaporation is

taken from the water in the vessel, and thus the temperature of that water is reduced.

41. The amount of cooling possible may be very easily shown by an example. Suppose that the water enters the vessel *a*, Fig. 11, at a temperature of 80° F., and that a pressure of .4 pound, absolute, corresponding to a vacuum of about 29 inches of mercury, is maintained in the vessel. At that pressure, water will boil at a temperature of 72.86° F., say 73° F. Consequently, when the water at 80° F. enters the vessel, about 3½ per cent. of it will flash into steam; that is, from every pound of water entering, about .035 pound is vaporized. The latent heat of vaporization of water at a pressure of .4 pound is very nearly 1,053 B. t. u. per pound, and so the vaporization of .035 pound will absorb  $.035 \times 1,051 = 36.9$  B. t. u. This 36.9 B. t. u. removed from the water reduces the temperature of each pound from 80° F., evaporates about .035 pound at 73° F., and chills the remaining .965 pound. Reduction of the temperature of 1 pound through  $80 - 73 = 7$  degrees takes 7 B. t. u., and so the amount left for chilling is  $36.9 \div 7 = 29.9$  B. t. u. Hence, the .965 pound of water remaining is lowered  $29.9 \div .965 = 31$  degrees, nearly, which means that the water in the vessel is chilled to a temperature of  $73 - 31 = 42^\circ$  F.

42. The operation of the ejector *d*, Fig. 11, known as the booster ejector, in removing air and vapor from the upper part of the vessel *a* is based on the entraining action of the jet of steam escaping at high velocity from the nozzle *f*. Steam expands while passing through the nozzle, thereby changing its pressure to velocity. The high velocity steam picks up the flashed vapor from the vessel *a* and carries it from the space *h* around the nozzle to the converging section *g* of the ejector, the mixture of air and vapor being discharged through the narrow throat *i* into the diverging pipe *j*. In so doing, the velocity of the mixture is converted into pressure. The ejector is so designed that the pressure attained in this manner is sufficiently high to enable the vapor to be condensed in the condenser *k* by the available condensing water. The vapor fills the interior of the cylindrical condenser shell, surrounding the tubes *l* through which the condensing water flows. This water enters through the pipe *m*, makes two passes through the condenser, and escapes at *n*, carrying with it the heat of the discharged steam. The steam is thus condensed, and the great decrease in volume following condensation assists in producing and maintaining the vacuum in the condenser and in the vessel *a*. The water of condensation, or condensate, is removed by the pump *o*.

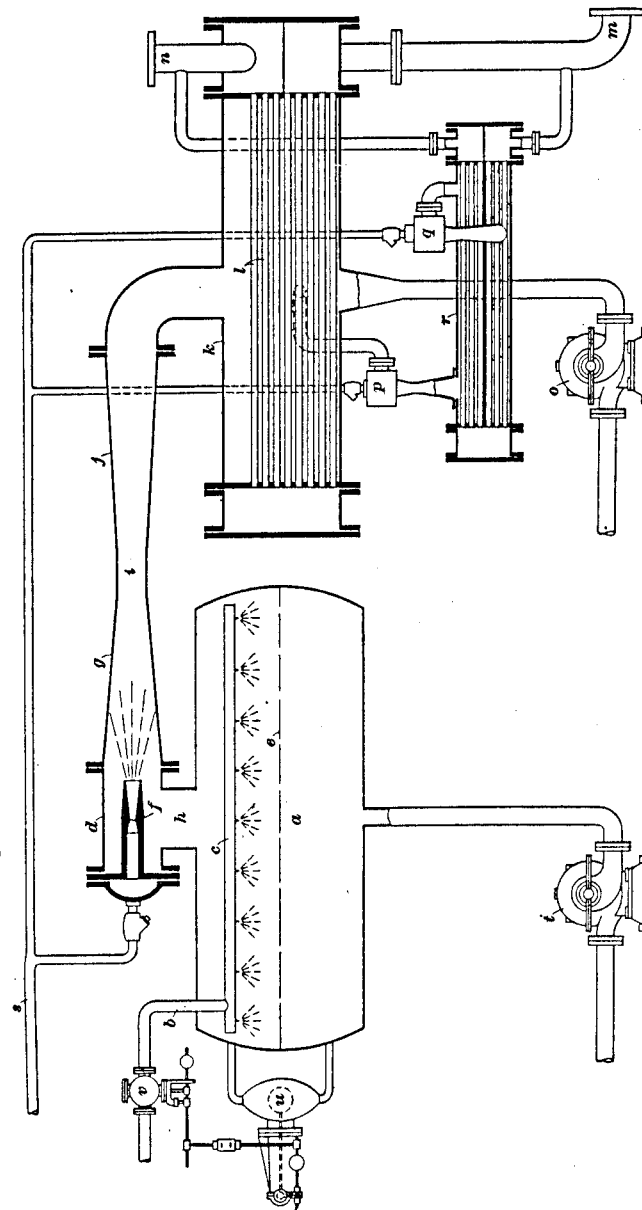


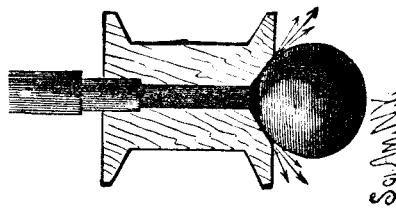
FIG. 11



may be confined in the reservoir by doubling the discharge tube or applying to it an ordinary pinch cock. A light ball of cork may be supported in the air jet while the nozzle is held in an inclined position, as shown in Fig. 99.

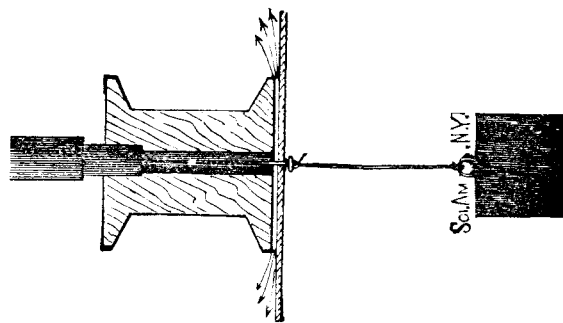
By connecting the discharge pipe of the reservoir with a spool, in the manner shown in Fig. 100, the familiar experiment of sustaining a card, together with an attached weight, by blowing down on the card may be performed.

FIG. 101.



Ball Experiment.

FIG. 100.



Card Experiment.

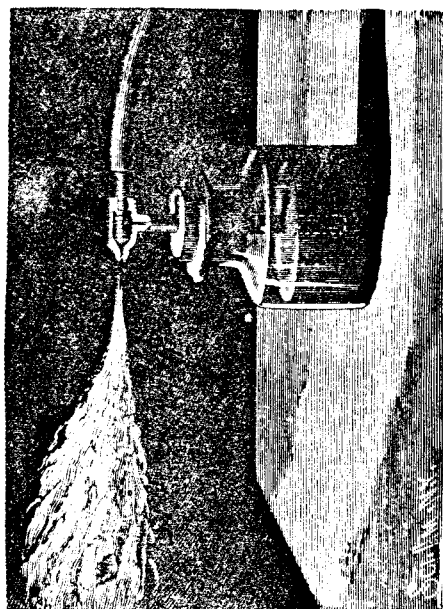
A pin passing through the card into the central aperture of the spool prevents the card from slipping.

Fig. 101 shows a simple way of exhibiting the ball experiment. The ball is held in the concavity of the spool by blowing forcibly outward against it.

In these cases the air issues in a thin sheet, which adheres to and carries away the air adjoining the upper surface of the object supported, thereby producing a partial vacuum into which the object is forced by atmospheric pressure.

In Fig. 102 is shown an atomizer which may be used in connection with the reservoir and air compressor for atomizing liquids for various purposes. In the present case it is represented as an atomizing petroleum burner. A burner of this kind yields a very intense heat, and produces a flame 2 or 3 ft. long. The oil in the vertical tube adheres to the air forced through the horizontal tube and is carried

FIG. 102.



Atomizing Petroleum Burner.

forward with the air in the form of fine spray, which readily burns as it is ejected from the nozzle. The vacuum formed in the vertical tube is supplied by oil forced up by atmospheric pressure.

#### ASPIRATORS FOR LABORATORY USE.

Wherever a head of water of ten feet or more is available, an aspirator is by far the most convenient instrument for producing a vacuum for filtration and fractional distillation. It is also adapted to a wide range of physical experiments.

Besides the advantage of convenience and compactness, the aspirator has the further advantage over piston air pumps in the matter of cost. It may be had at prices varying from \$1.50 to \$4 or \$5.

Two kinds are in general use—one of glass, known as Bunsen's filter pump, and shown in Figs. 103 and 104; the other of brass, shown in Figs. 105, 106, and 107.

The glass aspirator can be purchased of almost any dealer in druggists' sundries or chemical glassware. Any expert glass blower can make it in a short time.

This instrument consists of an elongated bulb terminating in a crooked tube at the bottom and having a tapering nozzle

FIG. 103.

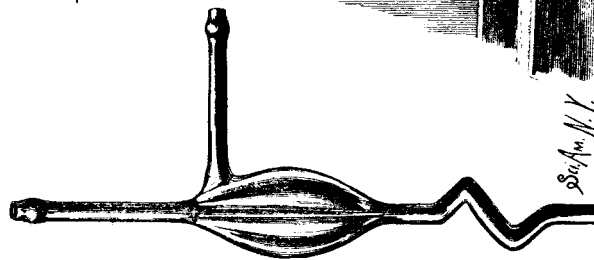
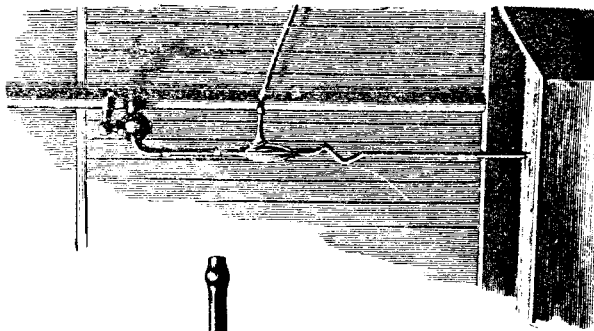


FIG. 104.



Bunsen Filter Pump.

inserted in the top and welded. The lower end of the nozzle is located directly opposite and near the crooked discharge tube. A side tube is connected with the bulb at a point near the junction of the nozzle and bulb.

This aspirator is used in the manner indicated in Fig. 104, *i. e.*, the upward extension of the nozzle is connected with a tap by a short piece of rubber tubing, and the side tube is connected by a piece of rubber tubing with the vessel to be exhausted. When the water is allowed to flow through the

aspirator, it leaps across the space between the nozzle and discharge tube and carries with it by adhesion the air from the bulb, which is continually replaced by air from the vessel being exhausted.

It is necessary to securely fasten the ends of the rubber tube connected with the tap, or the water pressure may force it off, thus causing the breaking of the instrument. To secure the best effects with this pump, it is necessary to connect a vertical tube 25 to 30 feet long with the discharge end of the pump.

The metallic aspirator shown in Figs. 105, 106, and 107 is of course free from all danger of being broken in use, and it has other qualities which render it superior to the glass instrument, one of which is a much higher efficiency, another is its ability to retain the vacuum should the flow of water be accidentally or purposely discontinued.

FIG. 105.

It can be screwed directly on the water tap, and needs no additional pipe to cause it to work up to its full capacity; and where a head of water is not available, it may be inserted in a siphon having a vertical height of ten feet or more.

This instrument is known as the

Chapman aspirator. Like all instruments of its class, it is based on the principle of the Giffard injector.

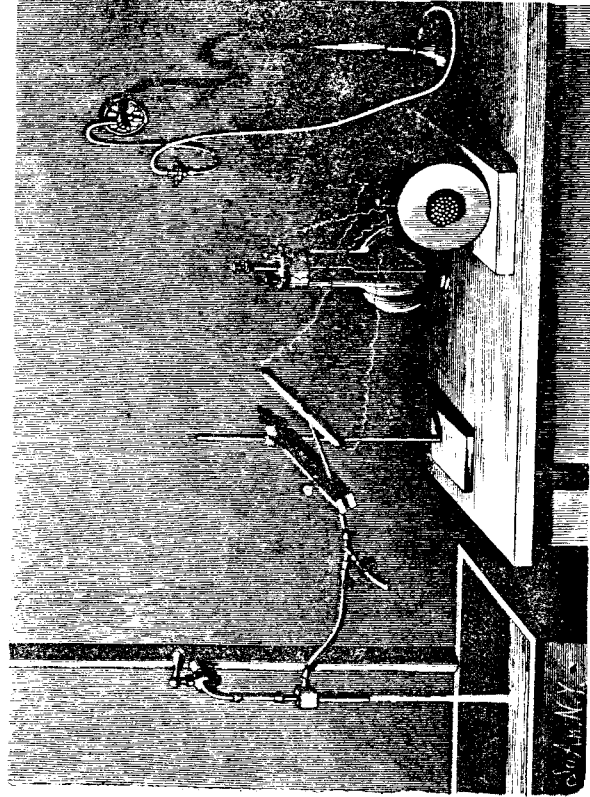
The construction of the aspirator is shown in section in Fig. 105. The water enters at A, as indicated by the arrow. The air enters at B, and both air and water are discharged at C. The water in going through the contracted passage forms a vacuum at the narrower part into which the air enters. The starting of the instrument is facilitated by a diaphragm which half closes the discharge tube. The water is prevented from entering the air pipe by a small check valve shown in the interior of the lateral tube. Much of the efficiency of this instrument is due to the accuracy with which the contracted passage is formed. A

slight change in the shape of this passage seriously affects the results.

The vacuum produced by this aspirator is equal to that of the mercurial barometer, less the tension of aqueous vapor. That is to say, when the barometer is at 30 inches, the vacuum produced by the aspirator will be about  $29\frac{1}{2}$  inches. Such a vacuum can be produced by water under a pressure of five and one-half pounds.

In Fig. 106 is shown the aspirator applied to a Geissler

FIG. 106.



Exhausting Geissler Tube.

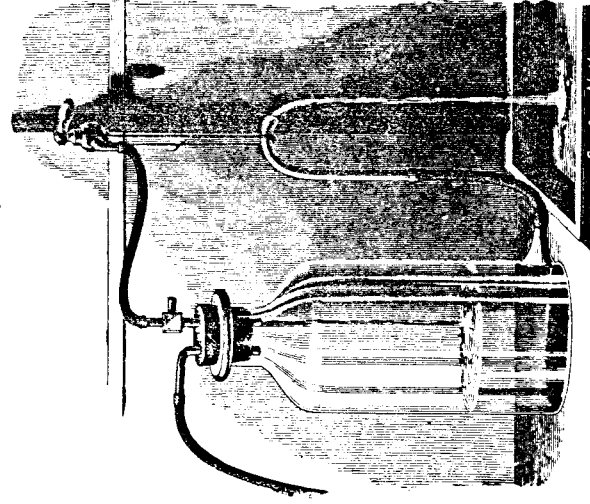
tube. It quickly exhausts an 8 inch tube, so that the discharge of an induction coil will readily pass through. By placing a tee in the connecting pipe, the Geissler tube can be filled with different gases. Each will exhibit its peculiar color as the spark passes. The vacuum is not high enough for a perfected Geissler tube, but it is sufficient for the greater part of vacuum experiments. The aspirator can be arranged to produce a continuous blast sufficient for the

operation of a blowpipe, and for other uses requiring a moderate amount of air or gas under pressure.

The method of accomplishing this is illustrated in Fig. 107. The instrument is arranged to discharge into a bottle or other vessel having an overflow, and the air for the blast is taken out through the angled tube inserted in the stopper of the bottle. The amount of air pressure is regulated by the water pressure and the height of the overflow pipe.

For many vacuum experiments a plate provided with a

FIG. 107.



Blast produced by the Aspirator.

FIG. 108.

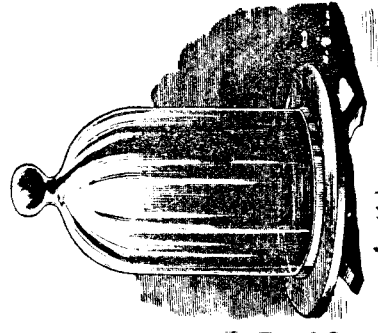


Plate and Receiver for Aspirator.

central aperture, and having a tube extending from the aperture to the edge of the plate, will be found useful. The tube is provided with a suitable valve, which closes communication with the aspirator, and which also serves to admit air, when required, to the receiver fitted to the plate. This plate and various accessories are like the plate and accessories of a piston air pump. Communication is established between the tube of the plate and the aspirator by means of a pure rubber tube, which is practically air tight.

# Exhaust Ejectors for Steam Engines

The Feasibility of Using the Kinetic Energy of the Exhaust To Create a Vacuum Is Real—Success of Experiments Indicates the Possibility of Lower Steam Consumption and Reduced First Cost

By W. TURNWALD

IT IS only recently that attempts have been made to increase the over-all efficiency of steam engines by utilizing energy which under certain conditions is contained in the steam as it is being exhausted. This energy is usually termed the loss due to incomplete

expansion, and the exhaust ejector is one of the means at disposal to convert this loss into usefulness. Comparisons between the steam engine and the two-stroke-cycle gas engine as far as application of ejector exhaust is concerned, have been made at times and in order to avoid misunderstanding it may be well to point out that the exhaust ejector is applicable primarily to multi-cylinder engines of the uniflow type.

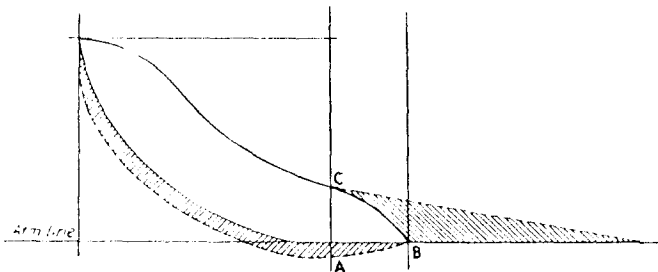


Fig. 1—Uniflow diagram showing loss due to incomplete expansion

expansion, and the exhaust ejector is one of the means at disposal to convert this loss into usefulness.

Comparisons between the steam engine and the two-stroke-cycle gas engine as far as application of ejector exhaust is concerned, have been made at times and in order to avoid misunderstanding it may be well to point out that the exhaust ejector is applicable primarily to multi-cylinder engines of the uniflow type.

## MODERNIZING AN OLD PRINCIPLE

Its principle is as old as the locomotive. Every locomotive, with its blast pipe, stack and smokebox, contains the very elements that go to make up the exhaust ejector as it is now used with multi-cylinder uniflow engines. The difference is that the ejector action with the locomotive is exerted upon the flue gases of the boiler, while with the uniflow engine it is used to evacuate a cylinder different from the one furnishing the blast.

In Fig. 1 is shown schematically an indicator diagram with the loss due to incomplete expansion and the increase in diagram area obtainable by utilizing the otherwise wasted energy contained in the steam. It will be apparent that best results will follow if it is possible to create the lowest pressure in the engine cylinder at the point where the piston closes the exhaust port,

## POSSIBILITY OF OBTAINING A VACUUM

Coming back to the locomotive, we usually find a two-cylinder engine with cranks at 90 deg., giving four exhaust puffs per revolution. Such an engine running at 200 r.p.m. will create a very even draft for the fire, because at this speed it furnishes 13 exhaust puffs per

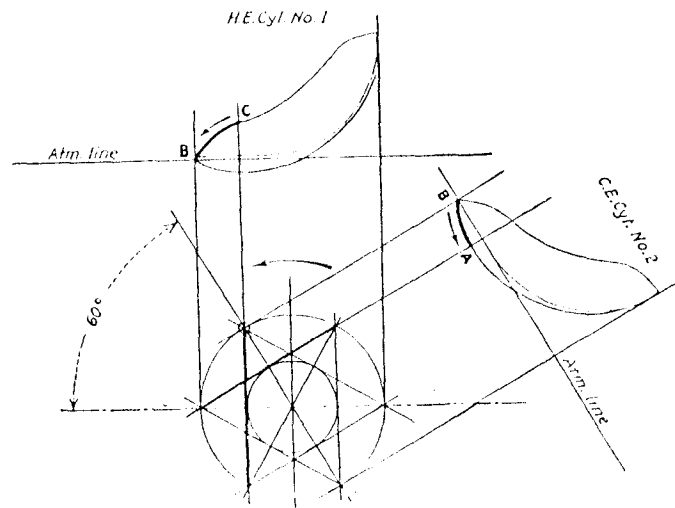


Fig. 2—Interrelation of the exhausts of two cylinders in a 6-cylinder engine

second. Similarly, with a stationary multi-cylinder uniflow engine we are able to create, at customary speeds, as much as 40 to 50 puffs per second. From this it would appear that continuity of ejector action is more than assured. In particular, for three cylinders with

cranks at 120 deg., it appears from Fig. 2 that we may count on almost continuous sequence of positive exhaust periods. The term positive exhaust period is intended to apply to the part *CB* of the diagram shown in Fig. 1. Furthermore, at any time, during which the exhaust phase *CB* takes place in one cylinder, another cylinder runs through the phase *BA*, so that we may be assured of the best possible co-ordination of exhaust ejector action. The simultaneous occurrence of the two exhaust phases is also indicated in Fig. 2.

A cross-section through a cylinder block, comprising three cylinders, equipped with exhaust ejector, is shown schematically in Fig. 3. Again, the similarity between this apparatus and the locomotive smokebox is striking. The simplest way to express the action of such an apparatus is to state that each cylinder, instead of exhausting against the static pressure in the exhaust pipe, exhausts against the dynamic pressure that is maintained in the equalizing chamber.

#### EJECTOR DECREASES STEAM CONSUMPTION

The effect of the exhaust ejector on engine performance is shown on the curve sheet, Fig. 4. The curves give the per cent water rate in pounds per i.h.p.-hour plotted against mean effective pressure. The dashed

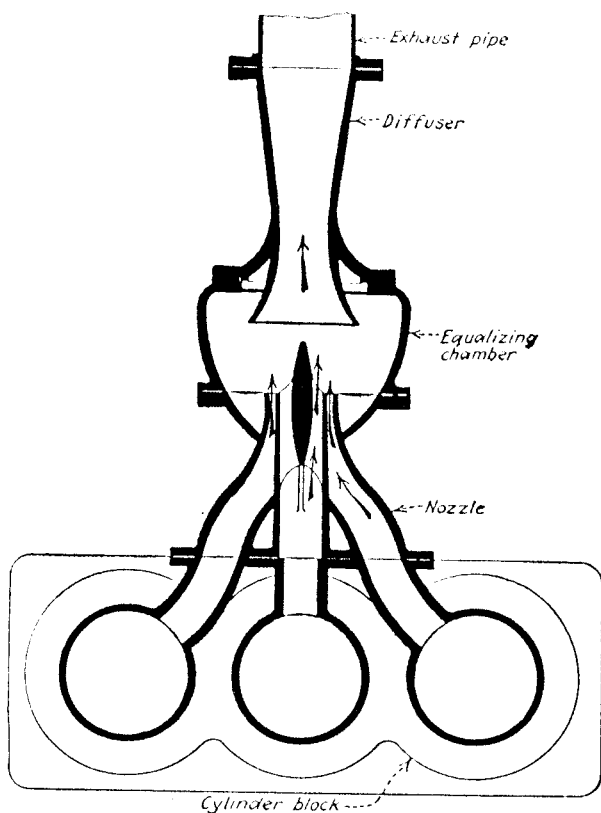


Fig. 3—Schematic layout of an exhaust ejector

curve applies to the engine without exhaust ejector, while the full line curve denotes water rates of the engine equipped with the exhaust ejector. It is apparent that the divergence between the curves increases with increasing mean effective pressure. Both curves have a common origin, the point of complete expansion, in which there is no exhaust ejector action. It may be well to state that these curves apply to the perfect engine, or the engine having clearance and compression like the real engine, but no condensation losses.

There are two ways in which the action of the exhaust

ejector may be utilized. One is to retain for a given power output the cylinder dimensions of the ordinary engine, equip it with the exhaust ejector and obtain the benefit of increased economy, as indicated for one distinct m.e.p. in Fig. 4 by a vertical line, or gain the

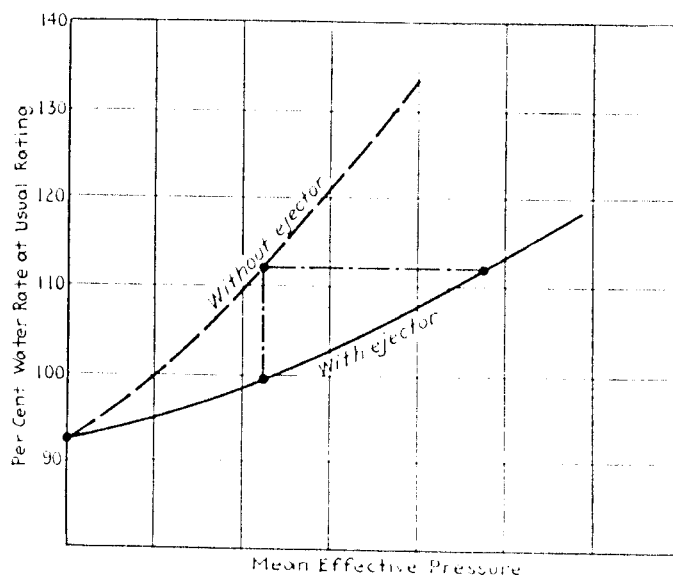


Fig. 4—Increased efficiency with ejectors

benefit of greatly reduced engine size without increase in the water rate, as indicated in Fig. 4 by a horizontal line.

From present experience it would be safe to state that for average steam conditions an increase in economy at full load of about 10 per cent will be obtainable or a reduction in cylinder size of about 40 per cent. This latter figure must not be construed to mean that it will bring about a reduction in overload capacity of the engine, because this 40 per cent increase in m.e.p. is obtained with a very slightly later cutoff. Uniflow engines of the multi-cylinder type are rated usually to develop full load with a cutoff not to exceed 15 per cent; therefore the overload capacity of the engine in all cases by far exceeds the overload capacity of the generator.

[Although the application of the ejector exhaust is still largely in the experimental stage, it would seem to have practical possibilities.—Editor.]

#### Heat Transfer in Condensers

The results of tests to determine the rate of heat transfer in condensers are usually expressed as heat transfer coefficient; that is, the rates as B.t.u. per hour per square foot of condensing surface, per deg. F. average temperature difference between the ammonia and the cooling water.

A question arises as to the proper average temperature difference to use, since the condenser is complicated in action, and may be divided into three zones, in which the ammonia is precooled, condensed and after-cooled. However, since it is probable that over 80 per cent of the surface is used in condensing the ammonia, and moreover even a larger percentage of the total heat transfer takes place in the condensing zone, according to T. K. Sherwood, it seems reasonable that no great error is made in using the logarithmic mean difference between the temperature of the condensing ammonia and of the entering and leaving cooling water.

Ca

# Design of Industrial Exhaust Systems

FOR DUST AND  
FUME REMOVAL

By John L. Alden

This book shows how to design, build or buy an Exhaust System that will remove dust, shavings, fumes, etc., so as to meet the requirements of the law or of industrial hygiene.

The descriptive matter is accompanied by 120 drawings and diagrams relating to the various details of exhaust system design. In its 252 pages of specific information the author has aimed to dispel the mystery surrounding the design of exhaust systems and cover this subject in straightforward engineering terms and tabulated designing data of practical value.

# DESIGN OF INDUSTRIAL EXHAUST SYSTEMS

How to Design, Build or Buy an Exhaust System that Will Adequately and Economically Perform the Functions Required by Law or Prescribed by Specialists in Industrial Hygiene. This Treatise Covers Exhaust Ventilation, Low-Pressure Pneumatic Conveying, the Design of Hoods, Piping and Structural Details, and the Selection of Dust Separators, Centrifugal and Axial-Flow Exhaust Fans.

By JOHN L. ALDEN

Member, American Society of Mechanical Engineers

12148  
SECOND EDITION

THE INDUSTRIAL PRESS  
148 LAFAYETTE STREET, NEW YORK 13, N. Y.  
Publishers of  
HEATING AND VENTILATING

different loads so that only one valve is open at a time. Gravity unloaders deliver intermittently. A power-driven unloader such as Fig. 89b delivers continuously and is more positive in action than the gravity valve just described. The wear is moderate if the rotational speed is not excessive. The ordinary screw conveyor, also, is a satisfactory seal if the discharge end is kept submerged in material.

Pressure systems may be fed through seals similar to Fig. 89a and b or by screw conveyor. Another type is the venturi feeder, Fig. 89c. When constructed as part of the fan discharge pipe this device reduces the static pressure at the material inlet to atmospheric or below so that no inlet seal is needed. The venturi tube may be used alone or in combination with mechanical feeders like Fig. 89b. In the latter case the power-driven feed wheel functions solely as a metering device to regulate the flow of material into the system. Since it is no longer needed as a seal, clearances may be liberal and the wear reduced correspondingly.

### Venturi Tube Theory

A simple venturi tube is shown in Fig. 90. It consists of convergent and divergent cones joined by a short parallel throat section. The pressure relationships in the various sections, for the condition of perfect pressure conversion, are shown in the illustration. These follow Bernoulli's theorem. When the static and velocity pressures at the discharge end of the unit are known and the desired static pressure in the throat has been established, the throat velocity pressure may be obtained from the expression

$$h_{v2} = h_{v1} + \frac{h_{s1} - h_{s2}}{1 - k_1}$$

where  $k_1$  is the loss factor in tapered enlargements as taken from Fig. 66. The static pressure at the inlet includes the outlet static and all intermediate conver-

sion losses. It is derived from the throat static and velocity pressures as follows:

$$h_{s1} = h_{v1} + (1 + k_2)(h_{v2} - h_{v1})$$

The constant,  $k_2$ , is the loss factor for tapered contractions and lies between 0.04 and 0.06 for included angles less than 45°.

Good proportions for venturi feeders are.

Entrance cone included angle, 20°

Discharge cone included angle, 6°

Throat length  $\frac{2}{3}$  throat diameter.

The process of computing throat diameter must start at the delivery end of the venturi since the only known factors are the discharge resistance, including collector back pressure, and the flow conditions downstream from the venturi. When the throat pressures have been established, the pressure against which the fan must work can be computed.

The venturi feeder differs from the simple venturi tube by the addition of a feeding hole in the wall of the throat. The presence of this opening introduces an additional loss because of the discontinuity of the throat surface and because of the admission of air and material at this point. For convenience, this loss may be included in the factor  $k_1$  used in the computation of the throat velocity pressure. The loss factor taken from Fig. 66 may be increased by 0.05 to 0.10. The static pressure drop from inlet to outlet of a well designed venturi feeder is usually from 15% to 20% of the static pressure at the delivery end of the tube.

### Typical All-Pressure Conveying System

There appears in Fig. 91 a typical system for conveying bulk granular material under pressure. The feeding device consists of a power wheel and venturi tube. The proportions of the latter are shown in enlarged detail in Fig. 92. The velocities in the entrance and exit cones and in the throat are shown in the lower diagram. The upper curves show the corresponding pressure changes.

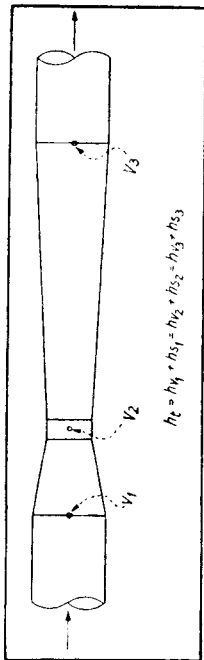


Fig. 90. Pressure relationships in simple venturi tube without losses.

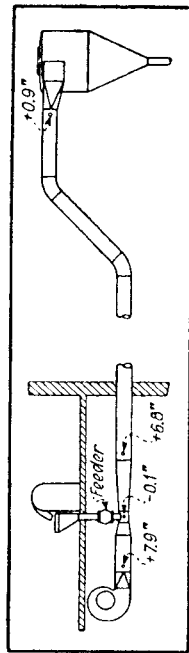


Fig. 91. Pressure conveying system.

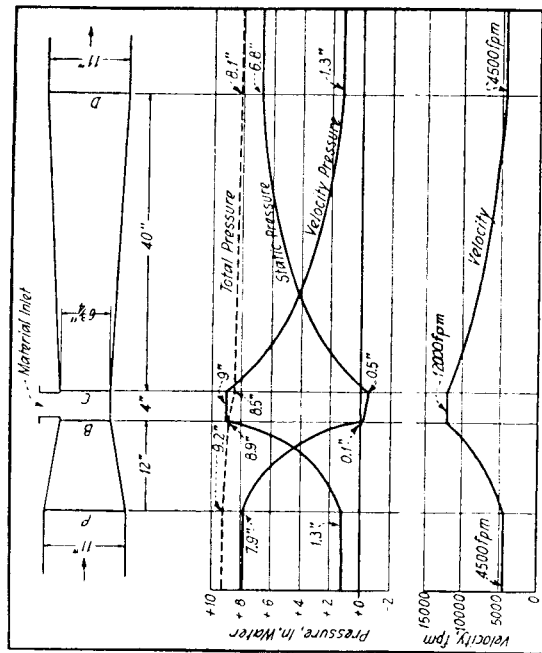


Fig. 92. Velocities and pressures in venturi charger.

### Tandem Fans

The distance through which a conveying system can operate with a single fan is limited by the maximum static pressure difference which the fan can produce. This, in turn, is limited by the safe tip speed at which the wheel can be operated. If long, stringy materials such as rags, jute or hemp fiber or long damp shavings must be passed through the fan, it is best to limit the tip speed to about 10,000 f.p.m. This speed will produce a total static pressure (sum of inlet and discharge static pressures) approaching 8 in. of water. All-suction or all-pressure systems such as Fig. 88a and b permit maximum fan speeds. Well built and well balanced wheels may be run as fast as 15,000 f.p.m., producing static pressures of from 17 to 20 in. of water depending upon the blade design. If higher pressures are needed, two or more fans may be connected in series. When so connected, the pressures are additive. Thus, if two identical fans, run at equal speeds, are connected in tandem, the pressure difference between the inlet of the first and the outlet of the second is exactly twice that produced by either fan operated alone.

The general arrangement of a long distance conveying system using tandem fans is shown in Fig. 93. The drawing also shows a diagram of the static pressures present in the different parts of the system. So far as the building arrangement will permit, the fans are spaced so as to produce the smallest departure from atmospheric pressure. The greatest compression is 10.8 in. of water or about  $2\frac{1}{2}\%$  of atmospheric. The maximum rarefaction is nearer  $1\frac{1}{2}\%$ . Had the fans been concentrated near the inlet or near the collector, the compression or rarefaction might have reached 12% or more. The corresponding change in volume would have produced a progressive increase or diminution of velocity along the system.

Inspection of the pressure diagram shows that the static pressure passes through zero between the outlet of one fan and the inlet of the next. If material is to



(Model.)

J. A. MARSH.

STEAM JET PUMP.

No. 334,597.

Patented Jan. 19, 1886.

Fig. 1.

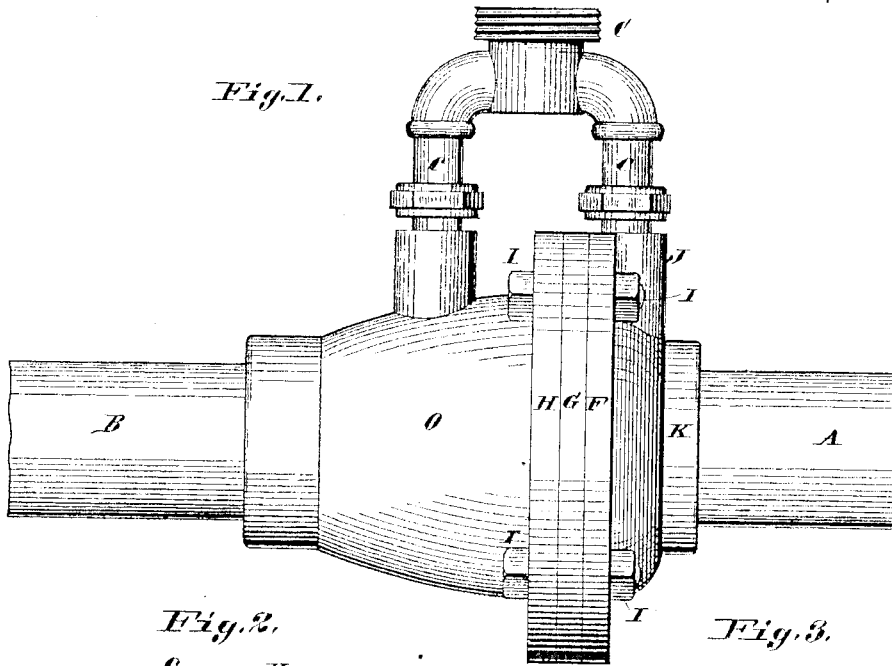


Fig. 2.

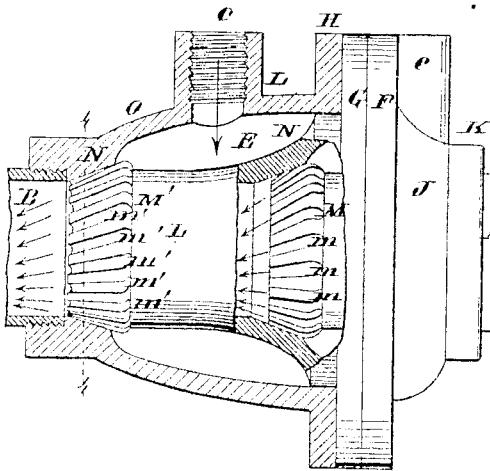


Fig. 3.

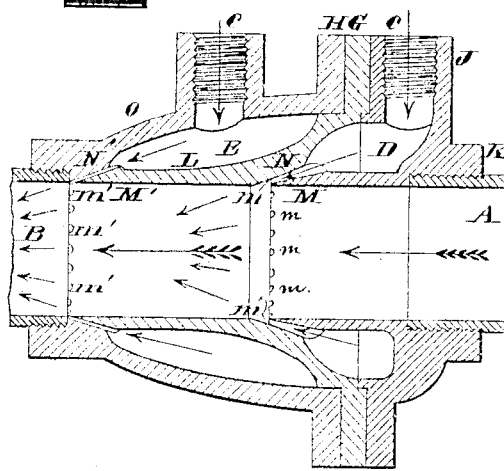
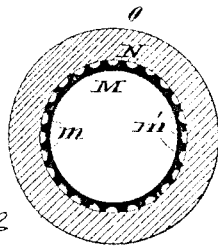


Fig. 4.



Attest;

*Geo. L. Wheelock*  
*Geo. L. Wheelock*

Inventor:

*John A. Marsh*  
*By Knight Bros*

*Atty.*

# UNITED STATES PATENT OFFICE.

JOHN A. MARSH, OF LONG LAKE, ILLINOIS.

## STEAM-JET PUMP.

SPECIFICATION forming part of Letters Patent No. 334,597, dated January 19, 1886.

Application filed March 30, 1885. Serial No. 160,621. (Model.)

*To all whom it may concern:*

Be it known that I, JOHN A. MARSH, of Long Lake, Madison county, State of Illinois, have invented a certain new and useful Improvement in Steam-Jet Pumps, of which the following is a full, clear, and exact description, reference being had to the accompanying drawings, forming part of this specification.

Figure 1 is a side view of the improvement. Fig. 2 is part in side view and part in axial section. Fig. 3 is an axial section. Fig. 4 is a transverse section at 4 4, Fig. 2.

A is the suction-pipe. B is the discharge-pipe. These may be bent or connected with other pipes or appendages in any suitable manner.

C is the steam-pipe, which is branched at c, and connects with two annular steam-chambers, D and E.

The case consists of three castings connected together by their flanges F, G, and H, secured together by bolts I. The flange-joints are made tight by rubber or other gaskets. The casting J has a screw-socket, K, into which the end of the suction-pipe A is screwed, and both it and the middle casting, L, have a bore of the same diameter as the inside of the suction and discharge pipes A and B. The casting J has a tapering jet-nozzle, M, fitting in a flaring socket, N, of the casting L. In the circumference of the nozzle M are a number of inclined grooves, m, through which the steam from the chamber D passes into the bore with a spiral movement, so that its centrifugal force will tend to make it hug the

outside of the bore and prevent in a great degree the friction of the water against the sides of the bore. These jet-passages m are shown as about semicircular in section; but I do not confine myself to this shape. I have shown the passages as varying about twenty degrees from a line parallel with the axis as to their spiral direction. It will be seen that they must also incline toward the axis of the bore, as they lead from an annular chamber surrounding the bore; but their spiral inclination is sufficient to carry the steam to the outside of the bore, (as before explained.) The nozzle or end M' of the casting L is similar to that M of casting J, and has similar grooves for the passage of steam, these grooves being marked m'. The nozzle or end M' fits in the socket N' of the casting O, into which the discharge-pipe B is screwed.

It will be seen that as the bore is of equal diameter in the supply-pipe, the pump, and the discharge-pipe, there is no possibility of the pump getting clogged, as any object entering the supply-pipe would pass through without obstruction.

I claim as my invention—

A steam-jet pump having a uniform bore throughout, surrounded by one or more annular steam-chambers, with series of jet-passages leading from said chamber or chambers to the bore.

JOHN A. MARSH.

In presence of—

BENJN. A. KNIGHT,  
GEORGE D. KNIGHT.

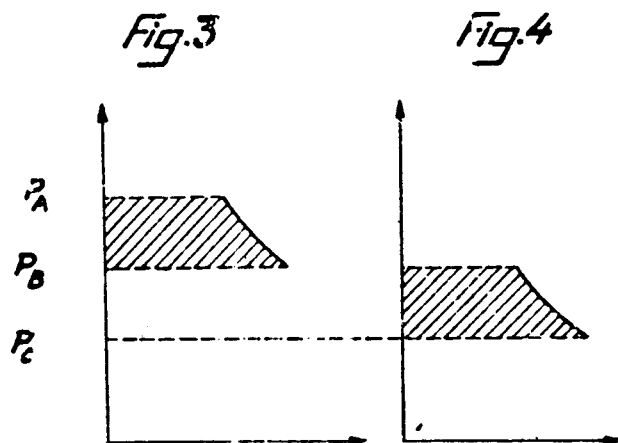
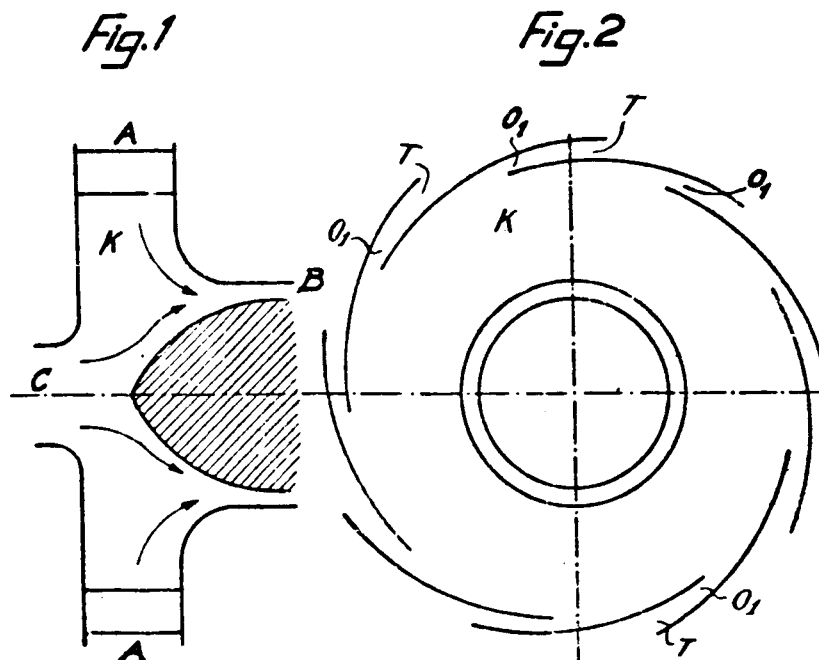
Aug. 28, 1951

J. H. BERTIN ET AL

2,565,907

APPARATUS FOR TRANSFER OF FLUIDS

Filed Feb. 16, 1948



INVENTOR

J. H. Bertin + R. H. Marchal

By Watson, Cole, Grindle + Watson

## UNITED STATES PATENT OFFICE

2,565,907

## APPARATUS FOR TRANSFER OF FLUIDS

Jean H. Bertin and Raymond H. Marchal, Paris, France, assignors to Societe Nationale d'Etude et de Construction de Moteurs d'Aviation, Paris, France, a company of France

Application February 18, 1948, Serial No. 8,627  
In France September 5, 1946

Section 1, Public Law 690, August 8, 1946  
Patent expires September 5, 1966

1 Claim. (Cl. 239—95)

1

This invention relates to an aerodynamic process for transferring fluids from a zone into another one wherein a higher pressure than in the first zone prevails.

According to this invention, for effecting such a transfer, use is made of the pressure distribution which is produced as a function of radius, by swirling axipetal flow of a primary fluid within a cylindrical chamber.

An apparatus adapted for carrying out this process may conveniently be used in any machine or plant wherein fluids are to be introduced into a chamber under a higher pressure, and it enables such an introduction to be effected without having resort to any rotary or reciprocating mechanical device.

It is possible in particular, although this example is not restrictive, to employ the process according to one invention for completing exhaust from internal combustion engine cylinders into an exhaust manifold where a pressure higher than inlet pressure prevails; which is particularly desirable where an exhaust gas turbine is provided since further expansion of gas is permissible.

Further advantages and features of our invention will become apparent from the following description thereof with reference to the appended drawing which shows diagrammatically and solely by way of example, form of construction of an aerodynamic ejector according to our invention.

Fig. 1 is a lengthwise section of said ejector.

Fig. 2 is an elevation of the revolution chamber.

Fig. 3 is a diagram illustrating how the pressure of the primary fluid employed as a prime mover for transfer varies, the specific volumes being plotted as abscissae, while pressures are plotted as ordinates.

Fig. 4 is a similar diagram showing how the pressure of the secondary fluid to be transferred varies.

Primary air is let into the periphery A of a cylindrical chamber K through apertures O preceded by tangential nozzles T which taper into said chamber, converting the pressure of primary fluid into velocity.

Such primary air is discharged through an annular passage or outlet B after it has developed a strong swirling field in chamber K. Next to

2

the axis of said chamber, a considerably lower pressure prevails than in passage B. A gas flow is thus set up from axial inlet C to annular passage B, and it proceeds as far as the pressure prevailing in the chamber (not shown) located upstream with respect to opening C and containing a fluid to be transferred to another chamber (not shown) located downstream with respect to passage B where a lighter pressure prevails, has dropped enough to assume a characteristic level which depends on the ratios between aperture radii:

$$\frac{R_A}{R_B} \text{ and } \frac{R_B}{R_C}$$

and on the rate of flow of primary air.

The pressure variation in the primary fluid flow from A to B is illustrated by the diagram of Fig. 3, while the pressure variation in the secondary or induced gas flow from C to B is shown on the diagram of Fig. 4.

We have thus actually provided a compressor borrowing energy from expansion to which primary fluid is subjected. Its efficiency is in some cases lower than that of a conventional mechanical compressor, but it meets a number of essential objects, particularly:

1. It comprises no moving mechanical member so that it is long lasting and quite simple in its construction.

2. It is very light.

3. It always operates under optimum conditions even where it is applied with flows varying at very high frequencies, having regard to the very small inertia of gas therein.

It should further be understood that our invention is not restricted to the form of construction above described, and many modifications relying on the same principle may be provided without departing from the scope of this invention.

What we claim is:

An apparatus for inducing a stream of secondary fluid by a stream of primary fluid, which comprises a hollow body containing a chamber which has approximately a shape of revolution, means providing an axial inlet for conveying axially into said chamber a stream of secondary fluid, means providing, opposite to said inlet, an annular outlet for a mixture of primary and sec-

2,565,907

3

ondary fluids, said outlet being coaxial with said inlet and having inner and outer diameters larger than that of said inlet, and a plurality of tangential inwardly convergent nozzles for directing said stream of primary fluid into said chamber, said nozzles being rigid with said body and distributed around the periphery of said chamber to define a ring coaxial with the inlet and outlet of said chamber and of larger diameter than the outer diameter of said annular outlet.

JEAN H. BERTIN.  
RAYMOND H. MARCHAL.

4

REFERENCES CITED

The following references are of record in the file of this patent:

UNITED STATES PATENTS

Number	Name	Date
334,597	Marsh	Jan. 19, 1886

FOREIGN PATENTS

Number	Country	Date
794,512	France	Feb. 19, 1936

## United States Patent

Eskeli

[15] 3,650,636

[45] Mar. 21, 1972

## [54] ROTARY GAS COMPRESSOR

[72] Inventor: Michael Eskeli, 2932 Sandage Ave., Fort Worth, Tex. 76109

[22] Filed: May 6, 1970

[21] Appl. No.: 35,112

2,007,138 7/1935 Becker.....417/78

3,001,691 9/1961 Salmon et al. ....417/78

3,081,932 3/1963 DeLancey.....417/78

Primary Examiner—C. J. Husar

Attorney—Wofford, Felsman &amp; Fails

[52] U.S. Cl. ....417/78, 415/1, 415/213

[51] Int. Cl. ....F04b 23/04

[58] Field of Search .....415/1, 72; 417/78

## [56] References Cited

## UNITED STATES PATENTS

1,009,908 11/1911 Lafore .....417/78

984,278 2/1911 Leblanc .....417/78

1,115,942 11/1914 Kieser .....417/78

1,192,855 8/1916 Buss .....417/78

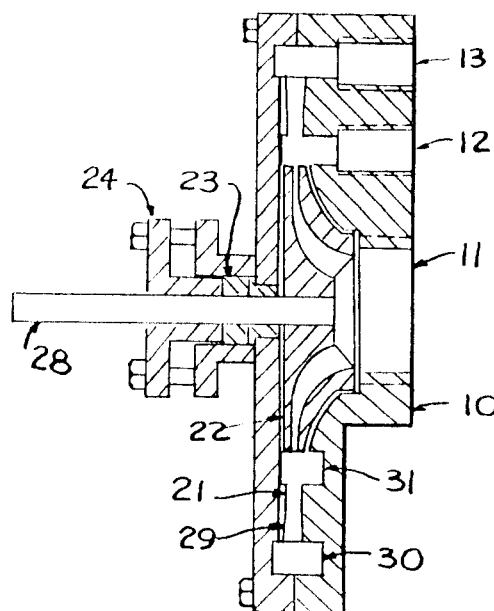
1,488,388 3/1924 Hariveau .....417/78

1,521,270 12/1924 Bogdanoff .....417/78

## [57] ABSTRACT

Method and apparatus for a compressor for compressing air, gases and vapors isothermally using a liquid stream to compress the gas; the liquid issuing from an impeller intermittently, with the gas being entrained between these liquid pulses and compressed by the liquid; the liquid having high kinetic energy when leaving the impeller and in slowing the kinetic energy is converted to pressure for both the liquid and entrained gas. Also, this compressor may be used advantageously to compress vapors, wherein the liquid is the same fluid as the gas, in which case condensation of the gas to the liquid occurs, and work of compression is reduced.

2 Claims, 4 Drawing Figures



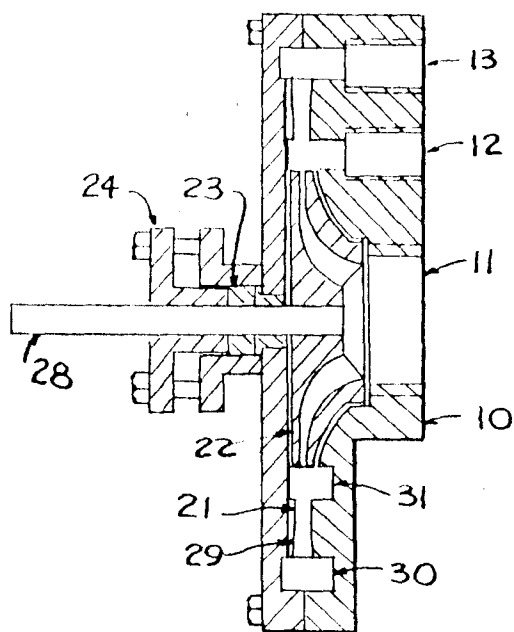
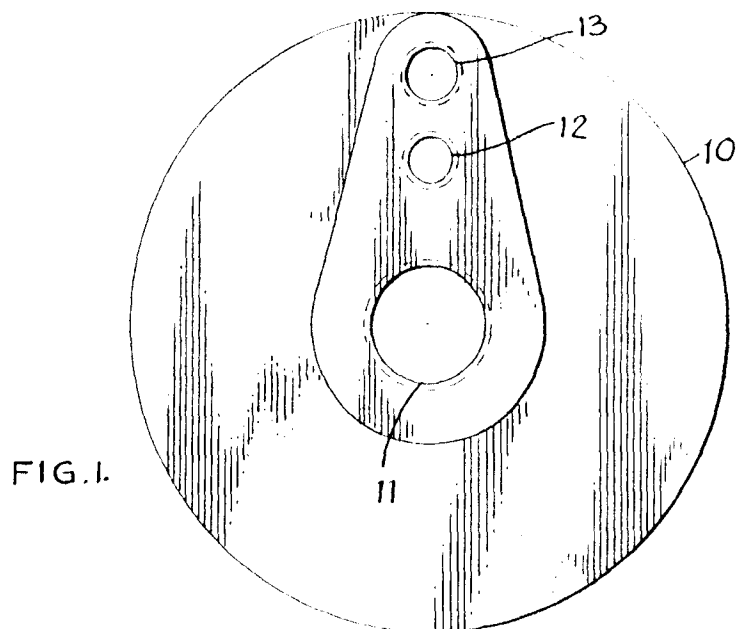
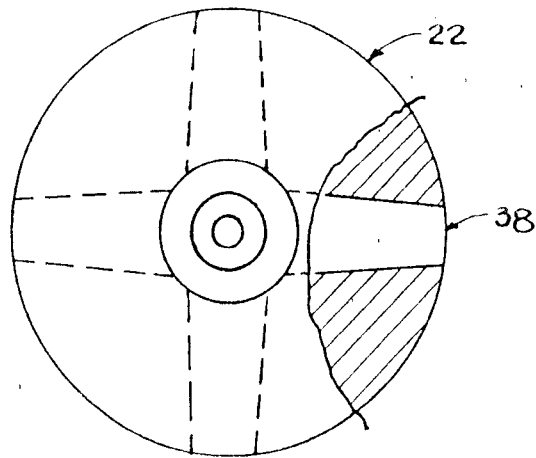
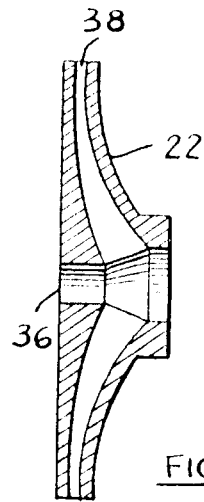


FIG. 2.

INVENTOR.

BY *Michael Eskeli*  
MICHAEL ESKELI



INVENTOR.

BY *Michael Eskeli*  
MICHAEL ESKELI



# ROTARY GAS COMPRESSOR

## BACKGROUND OF THE INVENTION

This invention relates generally to devices for compressing gases, air and vapors, in which a liquid is in intimate contact with the gas or vapor to be compressed.

### DESCRIPTION OF PRIOR ART

There are numerous devices and machines available for compressing a gas or a vapor. In some of these machines a liquid is rotated inside an eccentric casing, so that the machine rotor will cause the liquid to pulsate and the space between the rotor blades is increased or decreased, and this variation compresses the gas. These machines are called liquid piston type machines. Another device is the jet ejector compressor, where a stream of liquid or gas is used to entrain the gas or vapor to be compressed, and the kinetic energy of the stream is converted in a diverging nozzle to a pressure.

The main disadvantage of the liquid piston type machine is its poor efficiency, since the liquid is rotated in the machine and requires relatively large power input for compressing the gas. In the ejector compressor, the velocity of the liquid stream is limited and it entrains poorly of any gas; therefore the efficiency of the device is very poor. The available kinetic energy in the liquid stream is high, but due to poor entrainment of the gas by the liquid, results for the device are poor.

### BRIEF DESCRIPTION OF THE DRAWINGS

FIG. 1 is an end view of the compressor casing, showing the exterior.

FIG. 2 is a side view and a section of the casing and the impeller of the compressor.

FIG. 3 is a side view and a section of the impeller, and

FIG. 4 is an end view of the impeller, showing the fluid passages.

### DESCRIPTION OF PREFERRED EMBODIMENTS

It is an object of this invention to provide a method and a device for compressing gases or vapors essentially isothermally in which the kinetic energy contained by a liquid stream is used to compress said gas to a higher pressure where the liquid in slowing in speed will increase its pressure and increase the pressure of the gas being entrained in it. Also, it is an object of this invention to provide a method and a device in which the gas may be partially or fully be condensed in the liquid stream thereby lowering the work of compression; this occurring when the gas or vapor being compressed is the same fluid as the liquid; that is, the gas being compressed is the vapor phase of the fluid, and the liquid being used for as the motive fluid is the liquid phase of the fluid.

Referring to FIG. 1, there is shown an end view of the compressor. 10 is the compressor casing, 11 is the liquid inlet, 12 is the gas or vapor inlet, and 13 is the outlet.

In FIG. 2, a side view of the compressor is shown. The impeller 22 is rotated by shaft 28, supported by bearings and sealed by packing 23 and stuffing box 24. Alternately a mechanical seal could be used. The liquid that is used as the motive fluid enters through opening 11, passes through the impeller 22 and leaves the impeller at a high velocity and entering the throat section 21 and from there the diffuser section 29 in the casing 10. After leaving the diffuser at a higher pressure, and at a lower velocity, the gas and liquid mixture is collected in annular space 30, and from there passes out through opening 13. The liquid entrains gas from annular space 31, and the gas enters the annular space from outside through opening 12.

In FIG. 3, the impeller 22 is shown in more detail. 38 is the fluid passage, and 36 is the opening for the drive shaft.

In FIG. 4, the impeller is shown, with 22 being the impeller and 38 being the fluid passage.

In operation, the compressor functions in a manner similar to a jet ejector compressor. A motive fluid is accelerated in a passage in the impeller to a high velocity; this corresponds to the motive fluid nozzle in a jet ejector. However, the fluid stream issuing from the impeller, when it rotates, is not con-

tinuous as seen by the compressor casing, since in this particular instance, the impeller has four fluid passages, with solid material between. Therefore, the flow from impeller, as seen by the compressor casing, is pulsating, with empty spaces between the high speed liquid; these empty spaces being filled by the gas from the annular spaces, item 31, FIG. 2, and the gas being rapidly moved with the liquid to the outer annular space 30, and from there to discharge. This pulsating action improves the entrainment of the gas by the liquid, and more fully utilize the kinetic energy available in the liquid stream.

The sizing of the fluid passages and the calculations pertaining to same are fully described in thermodynamics literature for jet ejectors and for steam injectors. The space of the passage 38 in FIG. 3, would be either converging for liquids that do not vaporize when leaving the passage; or the passage could be diverging at its outlet for fluids that will vaporize either partially or fully when leaving the passage. Of the non-vaporizing liquids, water would be an example, and of the partially vaporizing types, butane would be an example, both at atmospheric temperatures, and at low pressures. As illustrated in FIGS. 2-4, passageways 38 comprise a converging section nearest the center of the impeller but are at least non-converging at the discharge section. Preferably, the at least non-converging section is a diverging section for better taking advantage of the energy available in the motive fluid to effect higher effluent velocities thereof.

The fluid passages shown in FIG. 4, item 38, can be radial as illustrated, or be forward or backward curved, depending on the fluid used or the shape of the passages. Also, the throat section 21, FIG. 2, may have vanes of proper shape to prevent circular motion of the fluid after it leaves the impeller. Vanes of this type are commonly used in turbines and pumps and are not described herein. Number of fluid passages in FIG. 4 is indicated to be four, but this number would be as required when calculations are made pertaining to the size of the passages, and the frequency of pulses of liquid required to maintain suitable pressure and volume relationships inside the compressor; also, the rotational speed of the impeller would enter into these calculations.

Normally, the amount of liquid as compared to the amount of gas or vapor, is large. Therefore, when compressing a gas, the heat of compression from the gas is transferred to the liquid, resulting in a temperature increase for the liquid, as well as the gas. This temperature increase is much less than it would be for the gas alone, resulting in nearly isothermal compression, and therefore reduced work of compression, as compared to isentropic compression that is often used in rotary compressors. Also, if a liquid that will expand in the impeller is used, with an expanding fluid passage, the temperature of the motive fluid is lowered, and the fluid velocity greatly increased, resulting in much better efficiency for the compressor; this is similar to the function of converging-diverging diverging nozzles in jet ejectors.

The operation of the compressor may be inferred from the above descriptive matter. A liquid source is connected to the impeller inlet, and a gas or vapor source is connected to the gas inlet, FIG. 1, 11 and 12, respectively. Discharge from the compressor is from 13, FIG. 1. A suitable power source, such as an electric motor, is connected to shaft 28, FIG. 2, causing the shaft to rotate. The liquid is accelerated by the action of the impeller, and as it passes through the annular space 31, FIG. 2, in pulsating flow, it entrains the gas and carries it to annular space 30, and from there to discharge.

Materials of construction for the compressor would be similar to those used to make pumps for pumping liquids. Cast iron, steel, bronze, brass, stainless steel and various plastics could be used.

What is claimed new is as follows:

1. A machine for compressing gaseous fluid and having the major components of:

a. an impeller for accelerating a motive fluid to a high velocity; said impeller having a plurality of passageways that comprise respective initially converging sections as

3

the passageways extend outwardly from the center of said impeller and at least non-converging sections exteriorly of said converging sections; said non-converging sections defining the discharge passageways of said impeller for more effective use of the available energy of said motive fluid which has been accelerated to high velocity whereby a motive fluid may be partially vaporized at the decreasing pressure due to said high velocity to attain even higher velocities for more effective entrainment of said gaseous fluid; and

b a casing for the compressor, said casing including a diffuser section for slowing the high speed mixture of fluids

4

and converting the kinetic energy of the stream to pressure, said diffuser section containing a throat section where the mixing of the motive fluid from the impeller and the vapor to be compressed occurs, and a plurality of suitable annular spaces disposed peripherally exteriorly of said impeller respectively for the entering gaseous fluid and for the mixture of motive fluid and gaseous fluid and respective apertures for the entering gaseous fluid and the effluent mixture of fluids.

2. The machine of claim 1 wherein said at least non-converging section is diverging.

\* \* \* \* \*

15

20

25

30

35

40

45

50

55

60

65

70

75

## INJECTORS

**179. An injector** (Fig. 214) is a boiler-feeding device which, by means of a jet of steam, feeds water into a boiler without the use of pumps. The steam is piped from the same boiler into which the water is to be fed. It passes into the injector, which consists essentially of a steam nozzle, a combining

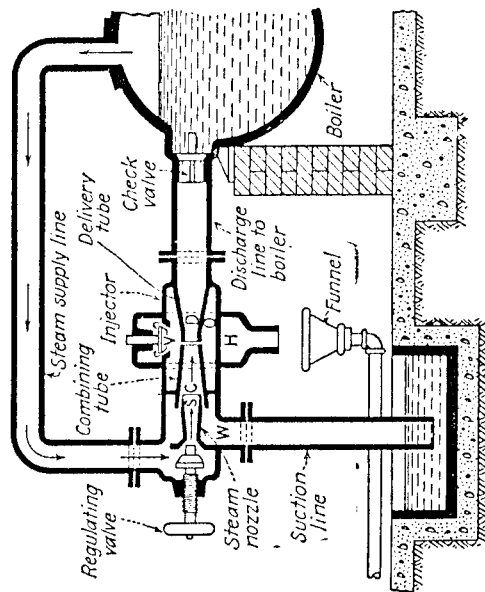


FIG. 214.—Illustrating the principle of the injector.

tube, and a delivery tube, the steam nozzle being surrounded by the incoming feed water. In condensing, the steam imparts its velocity and energy to the feed water, and forces it into the boiler against a pressure higher than that of the original jet of steam.

**NOTE.**—Ordinary injectors can discharge against a pressure greater than 130 per cent of the steam-supply pressure. Special injectors are obtainable which will utilize exhaust steam at atmospheric pressure and therewith pump water into a boiler containing steam at 150 lb. per sq. in., and with the help of a small supplementary jet of live steam will feed against a pressure of 250 lb. per sq. in.

**180. The theory of the injector** may be explained thus: A pound of steam is a reservoir of considerable energy. Expanding, in a well-designed nozzle, from 150 lb. per sq. in. (gauge) down to a 24-in. vacuum, 20 per cent or about one-fifth of its heat content is changed into mechanical energy of motion, or kinetic energy, amounting to 188,000 ft.-lb. If all this kinetic energy could be utilized, it would force 500 lb. of water back into the boiler. Over 97 per cent of it, however, is changed back again into heat when the steam jet, traveling at the rate of 40 *mi. per min.*, projects itself against the slowly moving mass of water.

Exhaust steam has no velocity under atmospheric pressure, but it acquires a high velocity when it is issued into a vacuum. Such a vacuum is produced when the steam is condensed by contact with the feed water, and the velocity thus acquired by the exhaust steam imparts sufficient force to the water to carry it into the boiler against pressure.

**NOTE.**—The impact of two bodies always results in the generation of heat at the expense of kinetic energy. Now the remaining 3 per cent of kinetic energy, after the 97 per cent has been reconverted into heat, is theoretically sufficient to force 15 lb. of water back into the boiler. But pipe friction and other losses cut this down to about 13 lb. of water pumped per pound of steam consumed at 150 lb. per sq. in. pressure. The remaining 97 per cent of the energy that was changed back into heat and the four-fifths of the original heat content of the steam are not lost, but are absorbed by the feed water and returned to the boiler.

**181. The essential parts of an injector** are shown in Figs. 214 and 215. These are purposely drawn out of proportion so that the characteristic shapes of the nozzles can be discerned more clearly.

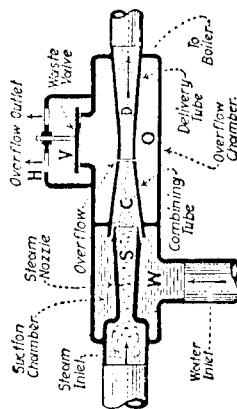


FIG. 215.—Sectional view of elementary injector.

**Explanation.**—The steam nozzle *S* (Fig. 215) at the left is so designed that the steam loses pressure and gains a tremendous velocity in passing through it. When a pound of steam expands from boiler pressure to a partial vacuum and to the corresponding lower temperature, it liberates heat that is converted into kinetic energy and thereby causes the steam to attain a very high velocity. For an explanation of the conversion of heat energy into kinetic energy by expansion through a nozzle, see the author's "Steam-turbine Principles and Practice." The combining tube *C* is a cone-shaped nozzle in which the swiftly moving steam jet strikes

But when the injector must be manually restarted before it will continue to operate, it is said to be *positive*. Automatic adjustment for variations in steam pressure or in height of lift and temperature of feed water is a feature of *self-adjusting* injectors. All double-tube injectors, and a special type of single-tube injector which has a moving combining tube, belong to this class. The Sellers self-acting injector is both self-adjusting and restarting.

**183. How an automatic injector works** is indicated by Fig. 217, which shows a section through a Penberthy automatic injector.

This is a single-tube, restarting, lifting-type injector.

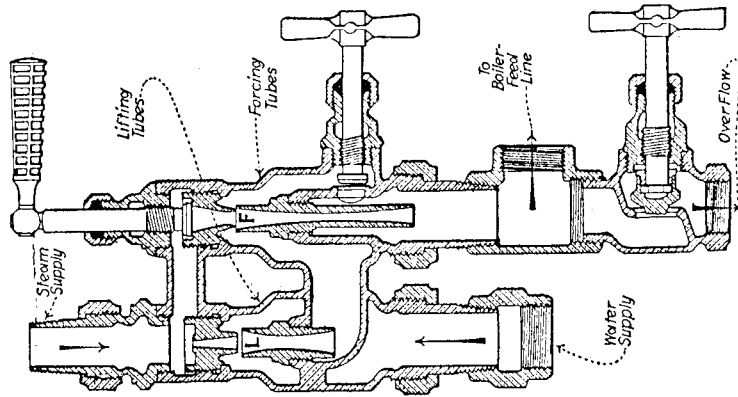
*Explanation.*—Steam enters at the top and, expanding in the steam nozzle *R*, rushes through the draft tube *S*, carrying with it enough entrained air to create a partial vacuum in suction chamber *B*. Unable to discharge against the boiler pressure, this steam escapes through the large opening above the sliding washer *T* and through the overflow opening *D*, via *P* and *O* to the atmosphere. The partial vacuum in *B* has already lifted water into it, and this water has condensed part of the steam. As more and more of the steam condenses, the jet becomes more compact and finally becomes sufficiently small to pass through the least diameter of the combining tube *C*. Thence it passes through the delivery tube *Y* and a check valve (Fig. 226) to the boiler.

The swiftly moving jet of water and condensed steam creates a partial vacuum in tube *C*. This draws the loose washer *T* up against its seat, thereby preventing any inrush of air that would scatter the jet. The closing of *T* also prevents any loss of feed water through it. If the steam or water supply becomes interrupted, the jet is destroyed and the vacuum above *T* is lost, thus allowing *T* to drop down to its original position. Hence, upon the resumption of the steam or water supply, the operation just described is repeated.

**184. How a positive injector works** is indicated in Fig. 218 which shows a section view through a Metropolitan model *O* injector. This is of the positive, double-tube lifting type and is operated entirely by one handle.

the water and is condensed. The delivery tube *D* is a diverging nozzle. It receives the combined jet of water and condensed steam and gradually converts most of the kinetic or velocity energy of the jet into static energy or pressure. This is needed to overcome the head against which the injector is discharging. Overflows *H* are slots or spill holes, usually located in the combining tube, to permit excess water or steam to escape when starting up. The waste valve *V* may be a stop valve but is usually a lift or swing check which closes automatically in case a partial vacuum is formed in the overflow chamber *O*. Thus *V* prevents the inrush of outside air that would tend to scatter the jet. The water in the suction chamber *W* is drawn into the combining tube by the partial vacuum caused by the continuous condensation of the steam therein.

FIG. 216.—Vertical double-tube injector.



**182. Injectors are classified** as (1) lifting or (2) nonlifting, depending on whether or not a partial vacuum is created in the suction pipe when starting up. A nonlifting injector must always be placed *below* its source of feed water on this account. Injectors that have one set of nozzles (*L*, Fig. 216) for lifting the water and another set *F* for forcing it into the boiler are called *double-tube* injectors. Those that accomplish the same result with only one set of nozzles (Fig. 217) are called *single-tube* injectors. If the operation of an injector automatically reestablishes itself after an interruption in steam or water supply, it is said to be *restarting*, or, more usually, *automatic*.

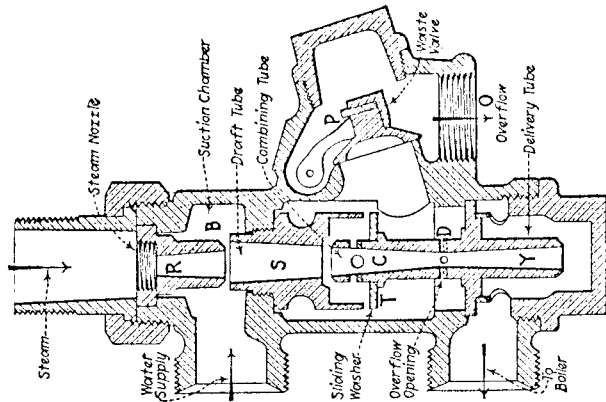


FIG. 217.—Single-tube automatic injector.

flow or waste valve *V*. As soon as water is lifted, it will reach the overflow through *C*. The operator then pulls the handle back gradually, admitting steam into the main nozzle *M* through the steam valve *V*. The action of this steam in passing through the remaining nozzles has already been explained. By the time the handle has been pulled back as far as it will go, the injector is feeding into the boiler through check valve *D*, and the link *L* has moved to the left far enough to close the waste valve *F* by means of the bell crank *B* and the stem *S*. Regulating valve *R* is used to control the supply of water to the injector.

A Garfield double-jet injector is illustrated in Fig. 219, with parts

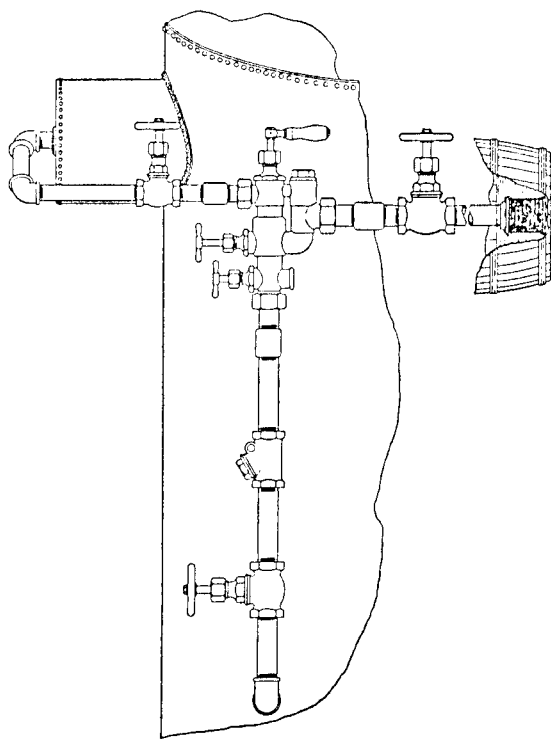


FIG. 220.—Application of Garfield double-jet injector to boiler. (The Ohio Injector Company.)

numbered and identified in the caption. This same injector is shown installed in a boiler line in Fig. 220.

**185. The advantages of an injector are** (1) simplicity, (2) compactness, (3) low first cost, (4) high temperature of feed water delivered, (5) ease of operation, (6) low cost of upkeep and repairs, and (7) high thermal efficiency, about 99 per cent of the energy put into it being utilized. The absence of any moving parts is responsible for most of these advantages. There are practically no packing glands to be renewed and no parts to be lubricated.

**NOTE.**—Cold feed water sets up strains that endanger the structural strength of a boiler. Hence an injector is of peculiar advantage on locomotives, where the lack of space and the use of the exhaust steam for stack draft prevent the installation of feed-water heaters. These same

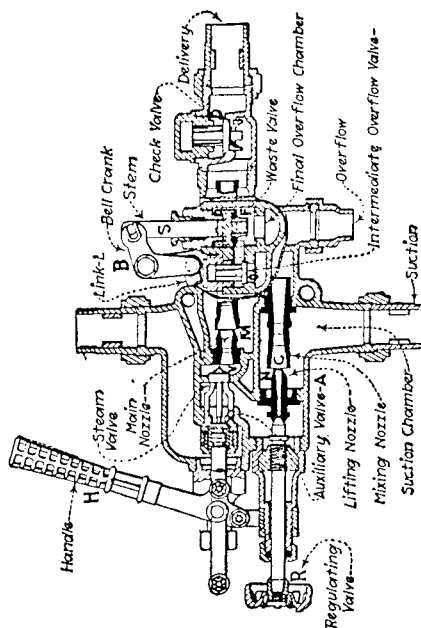


FIG. 218.—Horizontal double-tube injector.

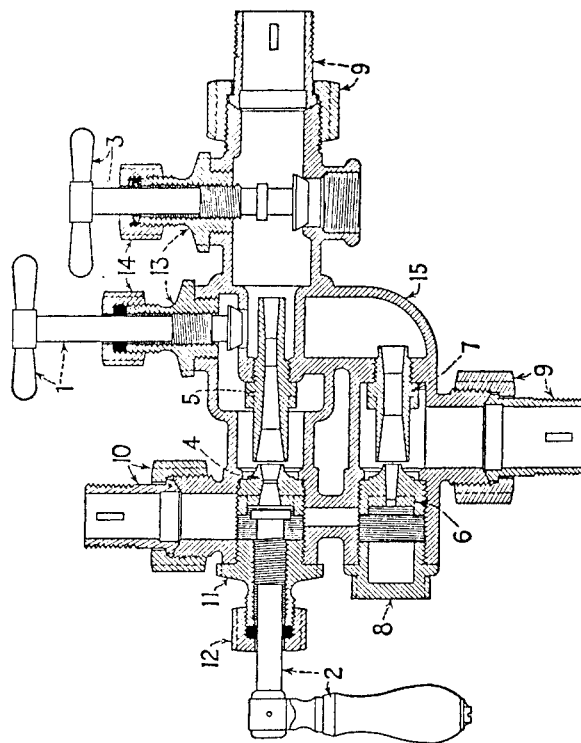


FIG. 219.—Garfield double-jet injector: (1) relief-valve stem and handle; (2) steam-valve stem and handle; (3) overflow-valve stem and handle; (4) upper steam jet; (5) forcing tube; (6) lower steam jet; (7) lifting tube; (8) cap; (9) coupling nut and nipple, suction or delivery; (10) coupling nut and nipple, steam; (11) steam hub; (12) steam-hub packing nut; (13) overflow and relief hubs; (14) overflow- and relief-hub packing nuts; (15) body. (The Ohio Injector Company.)

**Explanation.**—When handle *H* is pulled back slightly, steam is admitted to the lower lifting nozzle *N* through the opening of the auxiliary valve *A* and of the regulating valve *R*. The lifting nozzles *N* and *C* now begin to operate. The excess steam escapes through the intermediate overflow valve *O* and thence to the atmosphere through the final over-

two conditions render the injector peculiarly applicable on locomotives because of its compactness and because it is many times more economical than the feed pump if the exhaust from the latter is not used to heat the feed water. Used as an emergency feed, an injector involves a minimum of overhead expense.

**186. The disadvantages of the injector** are (1) inability to handle very hot water; (2) irregularity of operation under extreme variation in steam pressure, in temperature of inlet water, and in quantity of water handled; (3) efficiency as a pumping unit is extremely low, never over 1 or 2 per cent; that is, when used in ordinary pumping service—not for boiler feeding—an injector does not compare at all favorably with ordinary pumps in economy. Few injectors can handle water at 150°F., and most of them become inoperative at much lower inlet-water temperatures. This is the real reason why injectors are not extensively used in large power plants. Such plants always have an ample supply of exhaust steam available from the auxiliaries. If this steam is not used to heat the feed water it will be wasted.

**187. The efficiency of an injector**, considered merely as a pump, is very low, about 1 to 2 per cent; as a boiler-feed pump, where the heat of the steam is utilized in the boiler, the efficiency is nearly 100 per cent. It is commonly not the most economical means of feeding a boiler, since it can handle only cold or moderately warm water; the effect is equivalent to heating the feed water by live steam. A pump can handle water that has been heated by waste exhaust steam from the main and auxiliary engines. Steam consumption is about 400 lb. per water horsepower per hour; a small direct-acting steam pump consumes from 100 to 200 lb. (From Marks' "Mechanical Engineer's Handbook," fourth edition, 1941.)

The efficient heating of feed water by live steam makes it impossible to take full advantage of otherwise wasted exhaust steam to heat the feed water.

NOTE.—A feed-water heater placed on the suction side of an injector would make the water too hot for its successful operation. Placed on the discharge side, a feed-water heater would be inefficient because the injector would deliver water to it at such a high temperature that the heater would not abstract much additional heat from the exhaust steam. To heat feed water with live steam, when exhaust steam is available, results in poor economy. The irregularity of operation due to variations mentioned above is not a serious drawback in situations for which the injector is adapted, and necessitates only a reasonable amount of attention from the operator.

**188. The applications of injectors of the different types** will now be considered. Whenever it is necessary or desirable to locate the injector above the source of feed, the lifting type must be used. This is especially true in locomotive practice, where it is very advantageous to have the injector where the engineer can see the overflow outlet. The nonlifting type is simpler, cheaper, and of special advantage where scale-forming feed water is used, because it will not clog up readily and is very easy to clean. Double-tube injectors will handle hotter feed water through higher lifts than will those of the single-tube type. Hence they are used exclusively on locomotives as a main feeding device, and extensively on ships and in stationary power plants for emergency boiler feeding. Restarting injectors are used on small boats, traction and logging engines, and in small power plants. They are of special advantage for boats, road engines, and similar applications because the sudden interruption of water supply, due to jar or to movement of the boat, will be taken care of by the automatic feature. The self-acting injector was designed for locomotive use but is applicable where any double-tube type is necessary. Injectors are often used for testing and washing boilers, feeding compound into boiler, and similar services.

**189. A simple approximate equation of the injector**, which shows the relation between pounds of water pumped per pound of steam, the initial temperature of the steam, and the final temperature of the condensed steam, is given below. It is similar to one proposed by Julian Smallwood in his "Mechanical Laboratory Methods." In this equation radiation losses and the amount of heat which is changed into work are neglected. These two quantities amount to only 1½ per cent of the total heat energy involved. See derivation below.

$$W_{*w} = \frac{xH_v + (T_s - T_{fd})}{T_{fd} - T_i} \quad (\text{lb. water/lb. steam}) \quad (62)$$

where (see Fig. 221)  $W_{*w}$  = pounds of water pumped per pound of steam;  $x$  = quality or dryness of steam, expressed decimally; if steam contains 1 per cent of moisture, then  $x = 0.99$ ; a working average value for per cent of moisture is 2 per cent, in which case  $x = 0.98$ ;  $H_v$  = latent heat of vaporization of steam at the absolute pressure  $P_a$ , at which the injector is receiving steam, as taken from a steam table, in B.t.u.;  $T_s$  = temperature of the steam, at absolute pressure  $P_a$ , in degrees Fahrenheit;  $T_{fd}$  = final temperature of condensed

steam = temperature of feed water discharged into boiler, in degrees Fahrenheit; and  $T_i$  = temperature of intake water to injector, in degrees Fahrenheit.

NOTE.—The measure of the economy of an injector is the *weight of water pumped per pound of steam used*. This value may be determined by applying formula (62).

*Derivation.*—When 1 lb. of steam at some absolute pressure  $P_s$  lb. per sq. in. is condensed and then cooled down to a temperature of  $T_{fd}$  °F., it gives up a quantity of heat = B.t.u. =  $xH_s + (T_s - T_{fd})$ . Now each 1 lb. of water pumped into the boiler absorbs heat energy = B.t.u. =  $T_{fd} - T_i$ . Then, neglecting the radiation losses and the amount of heat changed into work (both of which amount to only 1½ per cent of the total heat energy involved), the following approximate relations exist in the injector, because the heat absorbed by the water must just equal the heat given up by the steam:

$$\text{Heat absorbed by water pumped} = \text{Heat given up by steam used} \quad (63)$$

$$\text{Heat absorbed per 1 lb. of water pumped} = T_{fd} - T_i \quad (64)$$

$$\text{Heat given up per 1 lb. of steam used} = xH_s + (T_s - T_{fd}) \quad (64A)$$

Then if  $W_w$  = weight of water pumped, in pounds, and  $W_s$  = weight of steam used, in pounds, it follows from formula (63) that

$$W_w (T_{fd} - T_i) = W_s [xH_s + (T_s - T_{fd})] \quad (65)$$

Now, transposing

$$\frac{W_w}{W_s} = \frac{xH_s + (T_s - T_{fd})}{T_{fd} - T_i} \quad (66)$$

But if  $W_w$  is taken to represent pounds of water pumped per pound of steam used, then  $W_w/W_s = W_w/W_s$ . Now substituting this  $W_w$  for its equivalent in formula (66), there results formula (62):

$$W_w = \frac{xH_s + (T_s - T_{fd})}{T_{fd} - T_i} \quad (\text{lb. water/lb. steam}) \quad (67)$$

NOTE.—To determine the value of  $W_w$  for any injector, it is (assuming that the quality of the supply steam is known, author's "Practical Heat," Div. 19) merely necessary to observe (Fig. 221) the intake- and the discharge-water temperatures at the injector, observe the steam pressure, substitute in formula (62), and solve.

*Example.*—In testing an injector (Fig. 221) the inlet-water temperature was 63°F., the discharge-water temperature was 202°F., and the steam pressure, as indicated by the gage, was 105 lb. per sq. in.

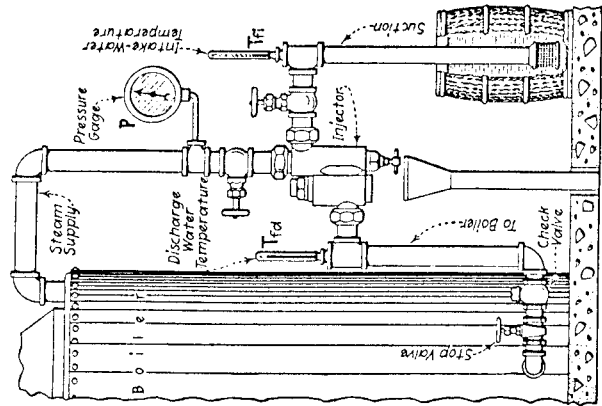


FIG. 221.—Injector arranged for testing.

The moisture content in the steam was 2 per cent. How many pounds of water was this injector pumping per pound of steam which it used?

*Solution.*—The quality of the steam =  $x = 1.00 - 0.02 = 0.98$ . The latent heat of evaporation of steam, as taken from a steam table at 105 lb. per sq. in. gage (= 105 + 14.7 = 119.7 lb. per sq. in. absolute), is 877 B.t.u. The temperature of steam at 119.7 lb. per sq. in. absolute, as taken from a steam table, is 341°F. Now substitute in formula (62):  $W_w = [xH_s + (T_s - T_{fd})]/(T_{fd} - T_i) = [0.98 \times 877 + (341 - 202)] \div (202 - 63) = [859.5 + 139] \div (139) = 998.5 \div 139 = 7.18$  lb. of water per lb. of steam.

**190. To compute the horsepower actually delivered by an injector, apply formula (24).** The amount of water that the injector is handling may be determined by weighing the water before it is pumped.

**191. The performance of an injector is influenced by the following important factors:** (1) Temperature of inlet water, (2) height of suction lift, (3) steam pressure. The action of an injector depends upon the condensation of the steam jet by the incoming water. If this water is too warm, the injector will not start. This limit is called the *overflowing temperature*. After the injector has started, it is possible to operate with an intake water of a higher temperature, up to a certain limit called the *breaking or limiting temperature*.

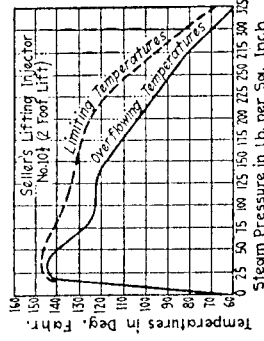


FIG. 222.—Limiting and overflowing temperatures.

NOTE.—Figure 222 shows how these two temperatures vary with the steam pressure. Figure 223 shows how variations in the feed-water tem-

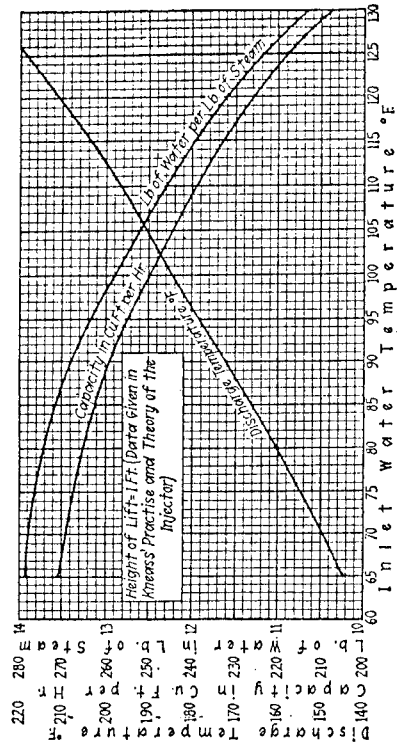


FIG. 223.—Test results of a self-adjusting injector.

peratures affect delivery temperature of feed water, capacity of injector, and pounds of water pumped per pound of steam. The height of suction lift affects the capacity of an injector, as shown in Fig. 224, taken from eight tests of a Penberthy size D automatic injector operating at 80 lb. per sq. in. steam pressure and taking feed water at 74°F. Figure 225 shows the variation in capacity of the same Penberthy injector operating under different steam pressure but with the height of lift and inlet water temperature constant at 4 ft. and 74°F., respectively.

NOTE.—The reason the water pumped per pound of steam decreases with an increase in steam pressure (Fig. 223) is that the mechanical work done by the injector, in pumping a given weight of water into the boiler, increases almost in proportion to the steam pressure, while the heat content of the steam, and therefore its ability to do work, increases but

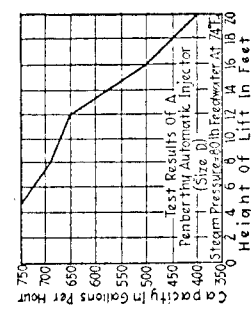


FIG. 224.—Graph of test results for an automatic injector showing relation between capacity and height of lift.

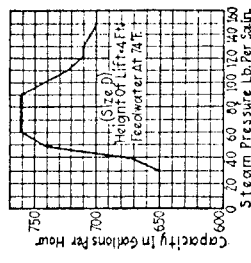


FIG. 225.—Test results of an automatic injector showing relation between steam pressure and capacity.

slightly. Between 100 to 200 lb. per sq. in. pressure, the heat content of the steam increases by less than 1 per cent.

**192. The selection of an injector** requires a careful consideration of the three factors discussed in the preceding section. Select an injector with a capacity in gallons per hour that is 30 per cent in excess of the amount of water normally used. If the amount of water evaporated per hour is not known, approximate values computed from the following equations, taken from Sellers' "Restarting Injectors," may be used. For horizontal or vertical tubular boilers:

$$\text{Gal. per hr.} = \frac{A_{bh}}{3.2} \quad (68)$$

For watertube boilers:

$$\text{Gal. per hr.} = \frac{A_{bh}}{2.42} \quad (69)$$

For flue boilers:

$$\text{Gal. per hr.} = \frac{A_{bh}}{1.17} \quad (70)$$

Where  $A_{bh}$  = area of boiler heating surface, in square feet.

**193. The question of what type of injector to use for any given service** has been previously discussed in Sec. 188. It

is always best to inform the manufacturer as to the height of lift and average temperature of feed water and the maximum, minimum, and average steam pressures, as well as the required capacity of the injector. The injector of course will not operate at more than its maximum or less than its minimum capacity. Table 194 shows data for automatic injectors of a well-known make.

**194. Capacities, pipe connections, and approximate weight of injectors.**

Manufacturer's size, designation	Pipe connection, in.	Capacity, gal. per hr., 1 to 3 ft. lift, 60 to 110 lb. per sq. in. steam pressure	
		Maximum	Minimum
O	1/4	60	35
OO	3/8	80	45
A	1/2	135	70
AA	1/2	180	100
B	3/4	260	140
BB	3/4	360	180
C	1	475	250
CC	1	600	325
D	1 1/4	800	425
DD	1 1/4	1,000	525
E	1 1/2	1,400	740
EE	1 1/2	1,900	850
F	2	2,400	1,275
FF	2	3,000	1,600
G	2 1/2	3,600	1,875
GG	2 1/2	4,200	2,150

**195. In installing injectors** the typical piping scheme shown in Fig. 226 may be followed. The size of pipe to use for injectors of one make can be found in Table 194, under Pipe Connections. The steam, suction, and discharge pipes are all of the same size except that, in the case of a suction lift exceeding 10 ft. or of a long length of suction line, a pipe one or two sizes larger should be used.

*Explanation.*—In Fig. 226, the steam line should be tapped into the highest part of the boiler and lagged all the way to the injector, if possible. C is a globe-valve. The discharge line should follow as near a straight line as possible to the boiler-feed inlet and should be securely fastened throughout its entire length. A check valve E must be installed as shown. A is a globe stop valve which can be used to cut off the boiler pressure from the check valve so that it may be opened for repair. The



metal or one of the special nonsplash types (Fig. 227).

The suction line must be absolutely airtight and as free from elbows and bends as possible. The globe angle valve *B* takes the place of one elbow. The strainer *S* should not have any opening in it as large as the steam nozzle in the injector and should have a combined opening area several times as great as the suction pipe itself. Figures 221, 228, and 229 show commercial strainers. The distance *h* should always be below 20 ft. and much less than that if possible. Injectors that will lift 25 ft. are on the market. But high lifts reduce the capacity of an injector as well as its ability to handle hot water. Further, they make starting difficult and operation impossible when there is even a small leak in the suction line.

If the injector is fed from an overhead tank (Fig. 230) or from city supply under pressure, it is advisable to insert an additional valve (*D*, Fig. 226), which can be permanently set so as to throttle the pressure down to the desired limit. Then the valve *B* is used only for opening and closing the feed line. All injectors should be braced, especially those operated by handles. After the piping is installed, it should all be blown out with steam before connecting up the injector.

**196. In operating injectors, the procedure is as follows:**  
*To start an automatic injector* be sure that valve *A* (see Fig. 226) has been left open. Open slowly steam valve *C* wide; next open suction valve *B* wide. Then throttle valve *B* down until there is no discharge from the overflow. If the suction valve is wide open and steam still escapes from the overflow, it will be necessary to throttle the steam-supply valve. If the discharge from the overflow is cool water, the suction valve must be throttled. If there are no unusual changes in conditions, the suction valve *B* can be adjusted to give proper supply and then be permitted so to remain. An injector like that shown in Fig. 218 is operated entirely by one lever, as described in Sec. 184.

**197. Injector troubles and their correction** are discussed below. The more important ones are listed. The correction of other difficulties can usually be effected through a consideration of the information given here.

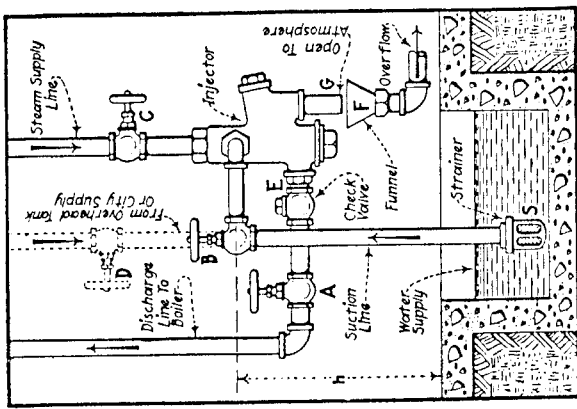


Fig. 226.—Piping of an injector.

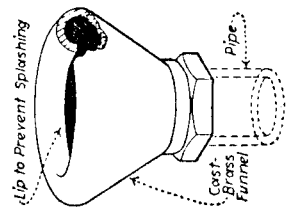


Fig. 227.—Non-splash funnel for injector overflow pipe.

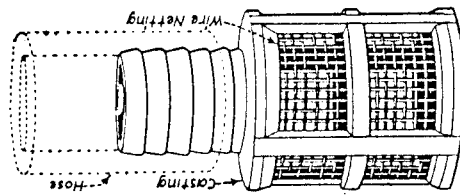


Fig. 228.—Hose-connection strainer for injector suction pipe.

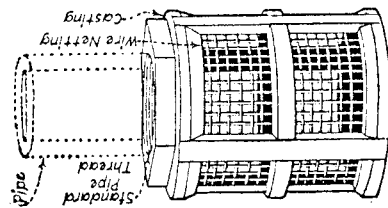


Fig. 229.—Pipe-connection strainer for injector suction pipe.

overflow is usually piped as shown. Usually it is best not to discharge the overflow into the hot well or feed supply, as the suction water may then become too hot to be lifted. The overflow line must always be open at *G* to the atmosphere. The funnel *F* may be an ordinary one of sheet

Failure of an injector to lift water may be due to the following causes: (1) Leak in suction line, (2) water too hot, (3) steam pressure too low for the lift, (4) suction strainer clogged, (5) wet steam, (6) nozzles of injector clogged up or covered with scale, (7) waste or overflow valve stuck or leaking, (8) end of suction line not below water, (9) suction hose collapsed by partial vacuum. To test for leaks in the suction line, screw a cap on the end of line in place of the strainer. Then wedge the waste valve shut with a piece of wood. When steam is turned on, the leaks will be detected easily. Steam is liable to be wet unless taken from the top of the boiler and led directly to the injector. If nozzles are clogged with scale they can be removed and cleaned. Coatings of lime can be removed by soaking the nozzle several hours in a solution of 10 parts water and one part muriatic acid.

If an injector lifts water but does not deliver to the boiler, the trouble may be due to (1), (3), (5), (6), and (7) of the above and may also be caused by (10) faulty boiler check valve or (11) obstruction somewhere in delivery pipe. In case of the last two difficulties, close valve *A* and examine the check valve. If it is lifting properly, leave the cap off and take out the disk. Then start the injector. If a full stream of water shoots out of the check valve, there is an obstruction between it and the boiler (most probably inside at the opening of the feed pipe).

If the injector starts but breaks, the trouble may be due to (1), (3), (6), (11), and also to (12), an improper adjustment of the water supply. If water at the overflow is hot, the supply is inadequate and should be increased by opening valve *B* wider. If it is cold, the supply should be throttled by means of valve *B*.

When steam appears at the overflow the fault may be (2) or (4) or (13), too high steam pressure for the lift. In this case throttle down the valve *C* until the overflow discharge ceases. Every user of injectors should preserve a set of directions for removal of injector parts and should have available spare nozzles for repairs. Directions are always furnished by the manufacturers.

**198. Ejectors.** An ejector (Fig. 231) operates on the same principle as an injector, but its construction is much simpler and it does not discharge against a very high pressure. It is therefore not suited to boiler feeding. It can, however, be used for many purposes where space is limited and only small

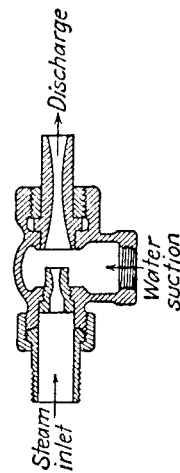


Fig. 231.—Sectional view of elementary ejector.

quantities of water have to be handled. The type shown in Figs. 231 and 232 operates on either steam or compressed air, although steam is preferable. As steam consumption is quite

high, it should be used only where it operates intermittently for short periods. (Alex Higgins, *Power*, February, 1945.)

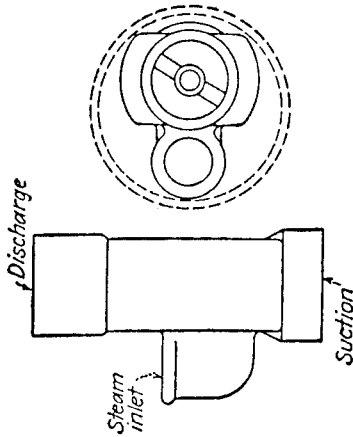


Fig. 232.—Garfield ejector, side (left) and top (right) views. (*The Ohio Injector Company*.)

Figure 233 shows the application of a Garfield ejector for raising water from a deep well by means of steam pressure from a boiler. The ejector will lift the water 15 to 20 ft., but it is usually preferable to place the ejector within 6 ft. of the water and to force the water to the required elevation. No valves are required except in the steam line itself. The ejector should always be placed in an upright position as shown, suspended by the delivery and steam pipes. The suction pipe must be tight, and if the lift is to be more than 10 ft., a larger size ejector than that ordinarily required should be used. This type of ejector is made in three classes, designated regular or stock, low-elevator, and high-elevator types. It is designed to operate at steam pressures ranging from 50 to 175 lb. per sq. in. The capacity of all ejectors is decreased when the lift or the temperature of the water is increased; and whereas an injector will force water into a boiler against its own steam pressure, an ejector will force water against only possibly one-third its operating steam pressure.

**199. Ejectors are used to convey water or liquids close to the specific gravity of water from one level to another, to fill or empty tanks, and to perform other functions of a pump where the latter might be too expensive and less efficient to use.**

**200. The steam jet air ejector is a much more complicated piece of equipment than the simple ejector discussed above, although it operates on the same general principle. Steam**

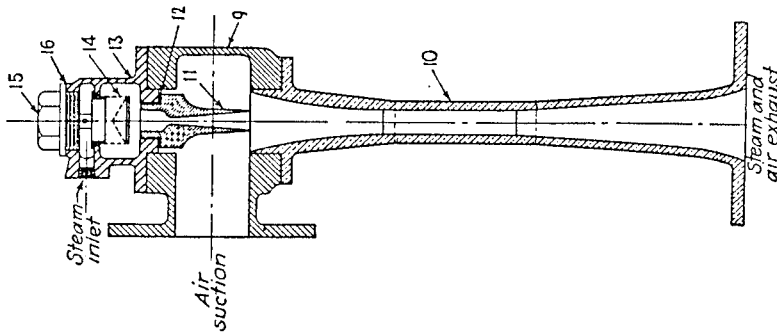


FIG. 234.—Typical single-stage steam jet ejector, with parts identified as follows: (9) suction body; (10) diffuser; (11) steam nozzle; (12) steam-nozzle washer; (13) steam chamber; (14) steam strainer; (15) steam-chamber nut; (16) steam-chamber washer. (Foster Wheeler Corporation.)

two-stage ejector, consisting of two elements similar to the one shown in Fig. 234, is used. A three-stage ejector, consisting of three elements in series, is used for vacuums from 29.3 to 29.9 in. Condensers are placed between stages in the latter design, and are known as intercondensers.

The applications of the steam jet air ejector will be discussed in greater detail in Div. 8, on Steam Condensers.

### QUESTIONS

1. Explain how it is that an exhaust steam injector can pump water into a boiler against the boiler pressure.
2. Name four important parts of an injector, giving functions of each.
3. Distinguish between an automatic and a positive injector.

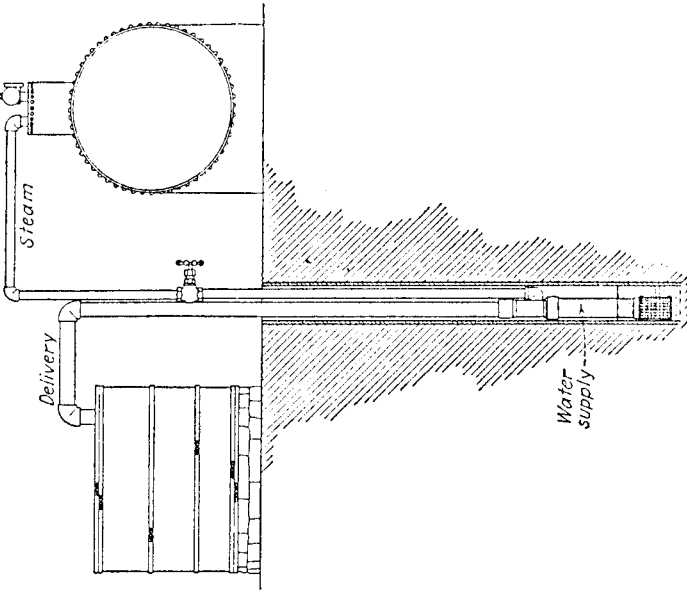


FIG. 233.—Application of Garfield ejector to deep well. (The Ohio Injector Company.)

4. What is a self-adjusting injector, and why are all double-tube injectors of this class?
5. Name and explain six advantages of injectors over feed pumps.
6. Why are injectors seldom used in large stationary plants?
7. Why are injectors always used on locomotives?
8. Explain effect upon the capacity of an injector of (1) steam pressure, (2) height of lift, and (3) temperature of inlet water.
9. Give eight general rules that should be followed in installing injector piping.
10. Give eight possible causes for an injector's inability to lift water, and state the correction for each.

### PROBLEMS

1. The following data were observed during an injector test: Temperature of inlet water, 60°F.; temperature of discharge water, 200°F.; steam pressure, 100 lb. per sq. in. gage; moisture in steam, 2½ per cent. Find value of  $W_{sw}$  or pounds of water pumped per pound of steam.
2. Assume all data in Prob. 1 except temperature of discharge water. Find what this temperature will be if  $W_{sw} = 10$ .
3. A water-tube boiler has a heating surface of 500 sq. ft. What size of injector, as given in Table 194, should be used to handle the feed water?
4. What size of steam, suction, and delivery pipes should be used in Prob. 3 if the height of lift is 8 ft.? If it is 15 ft.? If it is 20 ft.?

sources (Fig. 235) such as hot well, feed-water heater, and city water mains, so that feed water of some sort is always available during repairs or emergencies.

**210. When an injector is used only as a pump for raising and forcing water, it is very inefficient inasmuch as it requires about five times as much steam—or coal—as does an ordinary simplex or duplex steam pump to do the same work. Hence, as a device for merely handling water where boilers are not to be fed, the injector is, on an economic basis, entirely out of the question. Furthermore, the injector has a number of troubles (Sec. 197) that further limit its usefulness. The injector cannot, in practice, effectively handle water at temperatures exceeding about 100°F. This means that it cannot be used advantageously with water that has been previously heated with the feed-water heater. Hence the injector cannot be used at all with an open feed-water heater. It may be used with a closed heater installed between the injector and the boiler.**

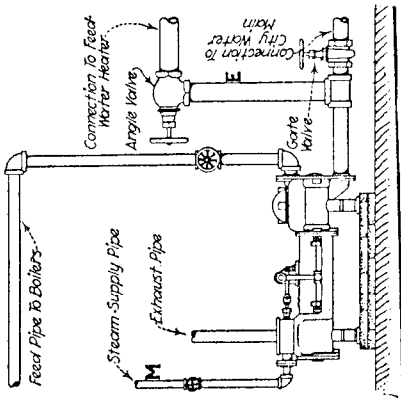


Fig. 235.—A direct-acting steam pump for boiler feeding.

**211. An injector will not start when served by a steam pressure much lower than that for which it was designed. Assuming that an injector is started on the pressure for which it was designed, then if the impressed pressure increases or decreases materially the injector will cease to work. Nor will it start again automatically upon resumption of the steam pressure at which it originally started and for which the engineer temporarily adjusted it. To make it pump water again, the engineer must perform anew the starting and adjusting process. Furthermore, any material change in the pressure of the suction water being handled by the injector will cause it to cease operation, thus necessitating a new adjustment and a new start. When an injector has been working and has become hot, and then stops or is stopped, it often cannot be restarted until it has been cooled completely by being soured with cold water. Obviously, all the above disadvantages restrict the desirable applications of the injector**

for boiler-feed service. On the other hand, the simplicity, small space occupied, absence of moving parts, and low first cost of the injector render its use desirable under certain conditions.

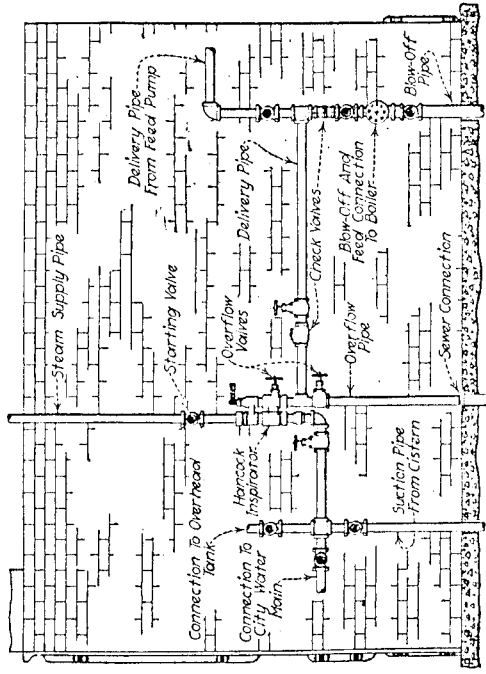


Fig. 236.—An inspirator type of injector piped for boiler feeding.

**212. The injector is economical for feeding boilers in a plant not equipped with means of feed-water heating. Under this condition the injector (Fig. 236) acts as a combined pump and preheater, and as such is almost 100 per cent efficient. The conditions favorable to injector installation often obtain in temporary or out-of-the-way plants where the equipment must be minimized, and where the saving which would occur through the installation of a feed-water heater is more than offset by its annual cost (see Sec. 269). Its feature of preheating its feed water makes the injector additionally valuable where cold water is to be fed into the boiler. By preheating, the strains that cold water would cause in the boiler are avoided. The proper combination of a pump with a feed-water heater is, however, usually more satisfactory than an injector for stationary power plants. Injectors are effectively employed on boilers for traction engines, small sawmill engines, hoisting and logging engines, and on locomotives.**

213. Relative economies of a noncondensing plant using boiler-feeding devices of different types. (See Figs. 237 to 241.) In each case the values are for the same plant delivering the same power output from its engine. The only differences between the cases are in the boiler-feeding and feed-water heating arrangements.

Equipment	Relative steam consumption from boilers	Per cent steam saving	Reference letter
Without feed-water heater			
Direct-acting steam pump receiving water at 60°F. and forcing it directly into boiler at 60°F. ....	1.000	0.0	Fig. 237 A
Injector receiving water at 60°F., heating it to 146°F., and forcing it directly into boiler at that temperature. ....	0.985	1.5	Fig. 238 B
With feed-water heater			
Injector feeding water through a heater in which it is heated from 146 to 200°F. ....	0.938	6.2	Fig. 239 C
Direct-acting steam pump feeding water through a heater in which it is heated from 60 to 200°F. ....	0.882	11.8	Fig. 240 D
Geared power pump mechanically driven by engine feeding water through a heater in which it is heated from 60 to 200°F. ....	0.868	13.2	Fig. 241 E

NOTE.—The direct-acting steam pump (first item) has a duty of 10,000,000 ft.-lb. per 100 lb. of coal when used upon a boiler with 80 lb. per sq. in. gage pressure. This corresponds to a over-all efficiency of about 1.3 per cent. Figures 237 to 241 show how a set of values such as those above may be obtained. One pound of steam delivered to the engine is taken as the unit. The heat in both feed water and steam above the feed-water temperature is considered.

214. The function of a boiler feed pump is to take the water it receives either from a deaerating or other type heater or from a surge tank or secondary pump in a closed type of

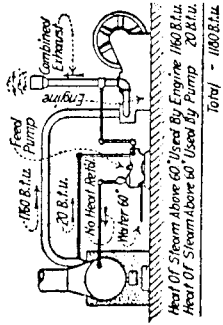


FIG. 237. Direct-acting feed pump, no heater.

(B.t.u. values in this, and the four following illustrations, are B.t.u. per pound of steam delivered to the engine.)

FIG. 238. Injector, no heater.

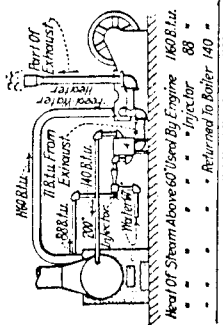


FIG. 239. Injector and exhaust heater.

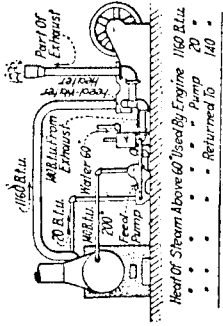


FIG. 240. Direct-acting feed pump and exhaust heater.

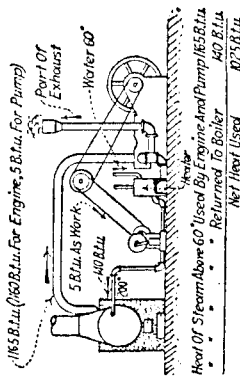


FIG. 241. Geared power pump mechanically driven by engine feeding water through a heater in which it is heated from 60 to 200°F.

FIG. 241.—Power feed pump and exhaust heater. (It is here assumed that 1,160 B.t.u. must be supplied per pound of steam required to drive the regular engine load as in the four preceding figures; but, on account of the additional engine load due to its having to drive the pump, the engine will now require more steam in the proportion of 1,165 to 1,160.)

# Traction Engine Troubles

BEING A REPRINT FROM THE  
QUESTION AND ANSWER  
DEPARTMENT OF THE  
AMERICAN THRESHERMAN  
AND PUT INTO BOOK FORM  
IN 1909



REPUBLISHED 1978 BY

THE IRON-MEN ALBUM  
MAGAZINE

Box 328  
Lancaster, Pa. 17604

## PUMPS AND INJECTORS

*Question.*—What is wrong with the injector when it blows steam through the suction hose?

*Answer.*—It is probable that the overflow check valve is stuck shut.

*Question.*—Why is the valve of a steam engine designed to give as early a cut-off and as early exhaust as possible, while the valve of a steam pump is designed to take steam and exhaust full stroke?

*Answer.*—A steam engine usually runs quite rapidly and is provided with a heavy fly wheel to carry it over center. It uses a large amount of steam and in order to be economical it cuts off the steam before the end of the stroke and thus takes advantage of the expansive property of the steam. If it took steam full stroke the steam at exhaust would contain a large amount of heat energy that would be wasted.

Steam pumps, on the other hand, run slowly, usually at a piston speed of only one hundred feet per minute. They have no fly wheel in many cases and require a steady even force to drive them to the end of the stroke. This can most easily be obtained with a square valve that admits steam full stroke. Since they are slow moving and work against the resistance of the water they do not need any cushion at the end of the stroke and so exhaust full stroke also. Since the steam consumption is usually small, comparatively, very little thought is given to steam economy.

In very large pumps used in city pumping plants, the pumps are designed to use steam expansively.

*Question.*—What is the cause or reason that an injector or pump will not put more than one and one-half gages of water into the boiler, injectors and pump and piping also being in good condition? I am unable to find out the trouble. I could always fill the boiler until last fall, and I thought it was due to the injector and pump being worn out, so I purchased new ones with no better results.

*Answer.*—This is a difficult question to answer without actually seeing the engine. We would suggest that the steam pipe which supplies the injector or pump with water either extends down into the boiler, or else the steam is taken from a point on the side of the boiler. When the water level reaches this pipe, steam is cut off and the pump or injector stops working until the water level falls.

*Question.*—Will you kindly explain why a positive injector will handle hotter water than an automatic or single tube injector? It appears to me that in the double tube injector the steam is used twice but I don't know just how and would like an explanation.

*Answer.*—The automatic injector has one set of tubes and an overflow valve that seats automatically with atmospheric pressure, that is, when a vacuum is formed inside of the injector, the pressure of the air on the outside seats the overflow valve. In the positive injector there are two sets of tubes and an overflow valve that does not seat automatically, but must be closed by hand.

In starting the positive injector the overflow valve is opened and steam blows through the second set of tubes until the air is aspirated from the suction pipe and water appears at the overflow. Then the steam is turned on to the first set of tubes and the overflow is closed. The water is now up in the injector and the steam rushing through the first set of tubes imparts its velocity to the water and at the same time is itself condensed, but even if it is not all condensed owing to the water being too hot, the mixed steam having a high velocity will have momentum enough to enter the boiler. If, however, the overflow valve were not held fast the pressure in the delivery tube might rise above atmospheric pressure and open it, causing a by-pass through which the water and vapor would pass into the air instead of continuing into the boiler.

*Question.*—I have a  $\frac{3}{4}$ -inch pipe leading from the well to the water tank, and a one-inch upright pipe to force it into the tank. If I had a two-inch pipe instead of the one-inch pipe, would it be just as easy for the wind mill to force it into the tank?

*Answer.*—Yes, the amount of resistance that the pump must overcome depends only upon the vertical head of water against which it must act, and this is not increased by the size of the delivery pipe, but by its height.

*Question.*—Can you give me the address of the company manufacturing the Clark independent pump?

*Answer.*—The Northwest Thresher Company, Stillwater, Minnesota.

*Question.*—Can you tell me how an injector works, or what makes it work and force water into the boiler?

*Answer.*—The reason for the working of the injector is that the heat energy of the steam is turned into mechanical work which is directed upon the stream of water that is being forced into the boiler. This action can best be explained by referring to the accompanying sketch, figure 14, which represents a crude form of the injector principle.

If the boiler is under pressure of 120 pounds steam pressure and the valve at A were opened the water would flow out with a velocity of about 133 feet per second. This can be easily figured out by anyone familiar with the laws of fluids. If the valve at B were opened the steam would flow out with a velocity of about 2,200 feet per second. The steam being less dense than the water will flow much faster on account of the large amount of heat which it carries. If this steam were directed back into the boiler it would not enter because it would not have sufficient momentum to overcome the resistance inside the boiler. If, however, it were first directed through a pipe C which has a place in it that is very cold and is so arranged that it can always be kept cold, the stream of

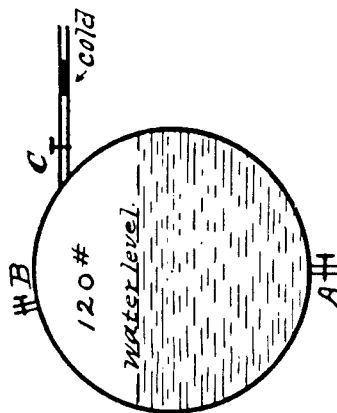


Fig. 14.

steam will be condensed and the resulting stream of water will have the same velocity as the steam out of which it was formed, namely 2,200 feet per second. A stream of water of this velocity can easily enter the boiler against boiler pressure for the reason that the water that would flow from the boiler would normally have a velocity of only 133 feet per second. It is easy to see, therefore, that the stream having the higher velocity could easily overcome the slower stream and at the same time carry a considerable load of water in the boiler, before its velocity was reduced below 133 feet. This is then the principle upon which the injector works.

The cold portion that I have mentioned is the combining chamber of the injector, which is kept at a uniformly low temperature by the incoming water. This condenses the steam and in doing so attains a velocity greater than the velocity the water would have if it were free to flow from the boiler through the valve A. If the quantity of water supplied is so great that the steam can not give it sufficient velocity it will, of course, flow from the overflow. On the other hand, if there is not enough water supplied to condense the steam the injector will fail to work on account of the fact that the stream has not sufficient weight and momentum to force its way into the boiler.

*Question.*—I have a 10-horse power engine fitted with an injector to supply the feed water to the boiler. At present the water enters the boiler in the side of the fire box. What would be the result if I ran the supply pipe along the side of the boiler, thence into the smoke box and back through the center flue, which is eight inches in diameter, and then carry the pipe back through the main flue to the smoke box, and then let the water enter the boiler near the front end?

*Answer.*—We would not advise this method of handling the feed water for the following reasons:

First. It would be hard to give the feed pipe the necessary upward pitch from where it first enters the smoke box to where it enters the boiler.

Second. This pipe being very hot would soon fill with mud and scale and burn out, probably scalding the fireman or engineer quite badly when it burst.

Third. You would obtain very little more heating surface in this way and the risk of trouble later would be too great for any possible slight advantage.

*Question.*—What is the difference between an injector and an inspirator in their construction and working parts?

*Answer.*—An injector has a single set of tubes extending from the steam end to the delivery end, while the inspirator has a double set of tubes. In the case of the former it is easy to so construct it that if it breaks suction it will take up automatically and go on working again, while with the latter, if the suction breaks, the steam must be turned off and the apparatus started again in the usual way.

*Question.*—Why are there more injectors than inspirators in use?

*Answer.*—An inspirator will handle somewhat hotter water than an injector and has a greater range. It is used largely on locomotives and in places where the suction hose is not liable to be uncovered as it is in the case of a traction engine on the road. This is the reason why traction engines are almost always equipped with injectors.

In the case of an inspirator there is one set of tubes whose office it is to bring the water to the apparatus while the other set delivers the water to the boiler. Many double tube injectors are called by that name. The Hancock double tube injector has been given the name inspirator.

*Question.*—Will you kindly explain exactly what is meant by the term atmospheric pressure?

*Answer.*—Atmospheric pressure is due to the weight of the atmosphere. The layer of air which surrounds the earth is estimated to be not less than forty miles nor more than two hundred miles in thickness. This is acted upon by gravity just the same as water or any other substance we are acquainted with and consequently has weight. If it were possible to take a column of air one inch square and as high as the air reaches and put it on one pan of a set of balances at sea level it would require 14.7 pounds in the other pan to balance the scales. A mercury barometer is simply a device for measuring the weight of the air. Gages, similar to ordinary steam gages, called vacuum gages, measure the weight of the air also. They are sometimes graduated in pounds and sometimes in inches by mercury. A column of mercury thirty inches high will just balance 14.7 pounds. Consequently thirty inches of vacuum are practically a perfect vacuum. In condensing engines, if a vacuum of twenty-six inches can be maintained, it is considered very good. This represents practically thirteen pounds.

The higher we go in the air the less air there is above and the less the pressure. If we go into a deep mine, on the contrary, the weight of the air above us increases.



# Injectors: Their Theory, Construction, and Working

W. W. F. Pullen, 1893

Reprinted 1997 by Camden Miniature Steam Services

Available from Lindsay Publications, USA

142

THE INJECTOR.

## CHAPTER XIX.

### AIR INJECTORS.

THE same reasoning may be applied to the pumping of air or other gases by the action of the steam jet.

Let  $\beta$  lb. of air be pumped by 1 lb. of steam, the velocity of the steam being  $V$ , that of the mixture being  $v$ , and that of the air as it approaches the steam jet being  $V_0$ , then we have the equation of momentum—

$$(1 \times V) + \beta V_0 = (1 + \beta) v,$$

or,

$$v = \frac{V + \beta V_0}{1 + \beta}.$$

The equivalent head of steam is  $\frac{V^2}{2g}$ , that of the delivered

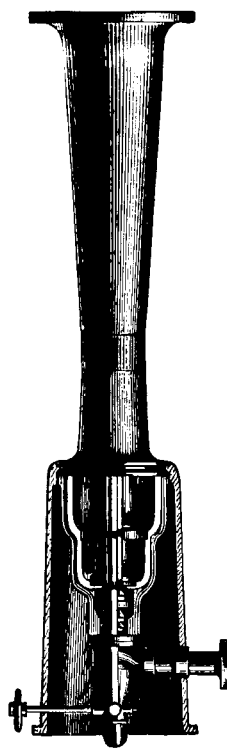


FIG. 62.

air  $\frac{v^2}{2g}$ . The efficiency of the apparatus as a pump must then be

$$\beta \frac{v^2}{2g} = \frac{\beta (1 + \frac{V_0}{V} \beta)^2}{(1 + \beta)^2} \cdot \frac{V^2}{2g} \quad \dots \dots \dots (80)$$

This shows that the efficiency increases with the velocity  $V_0$  of the incoming air. This, of course, will increase with the diminution of the pressure in front of the steam jet orifice, or, in other words, the increase of the vacuum there.

These steam-jet air pumps may be used for two distinct purposes, namely, (1) for forcing or inducing a current of air through chambers or pipes, such as for ventilating

THE INJECTOR.

143

producing a blast, or (2) they may be set to take the air out of a given vessel, and so produce a partial vacuum there. The construction of an example of one of the first of these is shown in fig. 63, the top portion being in section. The double conical trunk contains a series of cones, the first of which is supplied with steam from the small pipe on the left. The small hand wheel is merely for regulating the supply of steam. The use of a number of cones will be readily understood from what immediately follows.

With an ordinary steam-water injector the delivery jet moves down the diverging cone with considerable velocity, generally of more than 100 ft. per second. We could use this jet of water as the motive power jet of a water injector,

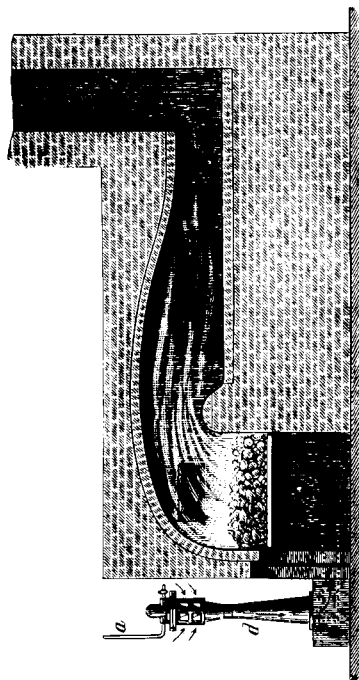


FIG. 63.

and thus pump an additional quantity of water, but, of course, against a less head than when the extra cones were not used.

The head against which air is forced in blowing a fire is at the most only a few inches of water, and sometimes only a fraction of an inch, and it is conducive to economy to force as much air as possible with the least amount of steam, and hence the use of a number of cones to augment the supply of air. The general arrangement of one of these steam-jet blowers, as applied to a heating furnace, is shown, fig. 63,  $a$  being the small steam pipe; the direction of the arrows denote the course of the air current. The illustrations have been kindly supplied by the makers, Messrs.

Korting Brothers. These blowers are used as a means of produce forced draught, and will, with a pressure of steam of 45 lb., produce a blast of about 2 in. of water. Forced draught enables more fuel to be burnt in a given time than with the ordinary draught, while by its aid the worst coal and combustible material may be used in the fire. The amount of air delivered per minute, together with the relative sizes of the apparatus, may be gathered from the subjoined Table X.

TABLE X.

Purpose of apparatus.	Air delivered per minute in cubic feet.	Diameter of steam nozzle in inches.	Minimum diameter of	
			Steam pipe in inches.	Air conduit in inches.
Undergrate blower....	130	1½	¾	
	400	¾	¾	
	550	1½	1	9
	800	¾	1¼	10
	1,200	¾	1½	12
	1,600	¾	1½	13
	2,400	¾	1½	16
	3,200	¾	1½	18
	1,000	¾	¾	14
	2,000	1½	¾	21
Ventilator.....	4,000	¾	1	30
	8,000	1½	1¼	40
	12,000	¾	1½	48
		¾	1¾	
	20,000	¾	1¾	60

CHAPTER XX.

AIR EJECTORS.

WHEN the steam jet is used for producing a partial vacuum, it is designed to remove as much air as possible out of a single vessel into which there is no leakage, rather than the carrying of a large quantity of air some distance. An example of this may be cited in the ejector used to exhaust the chambers of centrifugal pumps of air, and so charge them with water at starting. Another instance is the ejector used so universally for producing a partial vacuum in the cylinders and reservoirs of railway brakes. It is for this purpose it has received its widest application, and the brake itself would be of little use were it not for this appliance. A vertical section of the ejector used on the engines of the Great Western Railway is given (fig. 64). The main casting is fixed to the back outside firebox plate, the pipe A passing right through the boiler. Another hole, B, in the boiler plate conveys steam to the channel C, and to the back of the valve D, the latter being operated by the handle H. A port in the valve (for a certain position of the handle) directly coincides with the conical aperture E, whose axis is parallel to the axis of the pipe A. When the valve is turned into this position, steam is allowed to flow through the ejector, and thus exhaust the train pipe F and reservoirs of most of the contained air. The flap valve G prevents a return of the atmosphere into the train pipe when the steam is not passing through the ejector. The brake is applied by a movement of the handle H, whereby ports in the plate K are uncovered and a free passage is provided for the atmosphere into the chamber L, and thence, by a side port (the end of which is shown at M), into the train pipe. The vacuum brake on this railway is generally applied to the train only, the engine being fitted with a steam brake, which is applied and released by the handle (H) at the same time that the vacuum brake is undergoing the same operation. This is accomplished by casting another port, which is controlled by the valve D, which admits boiler steam to the steam brake cylinder.

Another example of an ejector for the same purpose is shown in section (fig. 65), and is made by Messrs. Gresham and Craven, for use with their vacuum automatic brake. This ejector exhausts the train pipe and brake apparatus at starting, and also maintains the vacuum during the time

146

THE INJECTOR.

the train is running by ejecting any air which may leak into the train pipe. The first of these operations is performed by admitting steam into the cavity A from which it issues

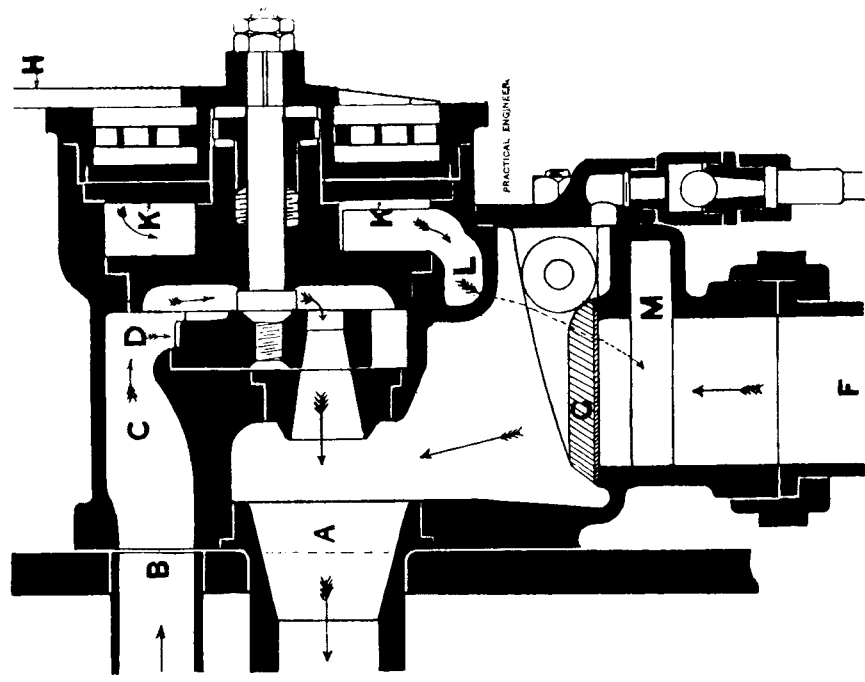


FIG. 64.

into the exhaust pipe B by the small annular orifice (C). The diminution of pressure in the exhaust pipe, just beyond

THE INJECTOR.

147

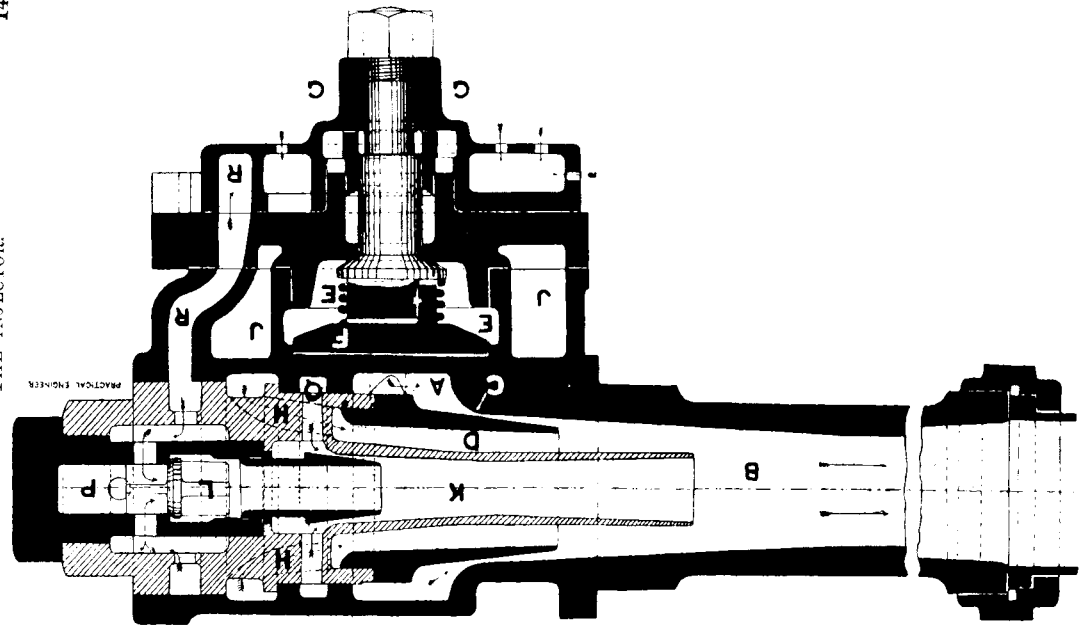


FIG. 65.

the orifice, causes a flow of air from the region of high-pressure D to the region of low-pressure B, the air being carried along with the steam into the atmosphere through the pipe B. The space D is in communication with the main train pipe, a non-return valve being interposed to prevent the return of the air when the ejector is not at work. The cavity A is in communication with the steam space E, the supply of steam being controlled by the disc valve F, which is operated by the brake handle. The space E is directly open to the boiler from which it receives its steam.

The brake is wholly manipulated by the brake handle (not shown), which forms part of the casting G, in which there are a multitude of small holes for the inlet of air when the brake is applied. There are three principal positions for the handle, namely, running position, brake on, quick release. In the second of these the handle is turned into such a position as to admit air to the main train pipe, and at the same time to shut off the supply of boiler steam to the cavity A. The third position necessitates a reversed movement of the handle, while in the first position, named above, provision has to be made for the extraction of any leakage which may take place in the apparatus. This is done by always keeping the small cavity Q in communication with the boiler, so that a jet of steam will continually flow through the annular orifice leading out of Q, and so induce the leakage to flow into the region of low-pressure at K. The valve L prevents the return of any of the exhausted air. The chamber P is in communication with the main train pipe by means of the passage R and the handle disc G.

A side elevation of this ejector is given (fig. 66), with the three positions of the handle G shown. The patches, which are cross-hatched from left to right *upwards*, show the dimensions of the ports in the seating underneath the handle disc; while the cross-hatching from left to right downwards denotes the ports in the disc itself. To the flange S is attached a small drip pipe.

Fig. 67 shows a transverse vertical section. The steam passage to the large ejector is clearly shown at E, and the channel R leads from the vacuum reservoir on the engine and tender only to the small ejector. The air passage from the disc G to the air pipe is also shown by the arrows. A vertical longitudinal section is given in fig. 68. The valve spindle N regulates the supply of steam to the small ejector.

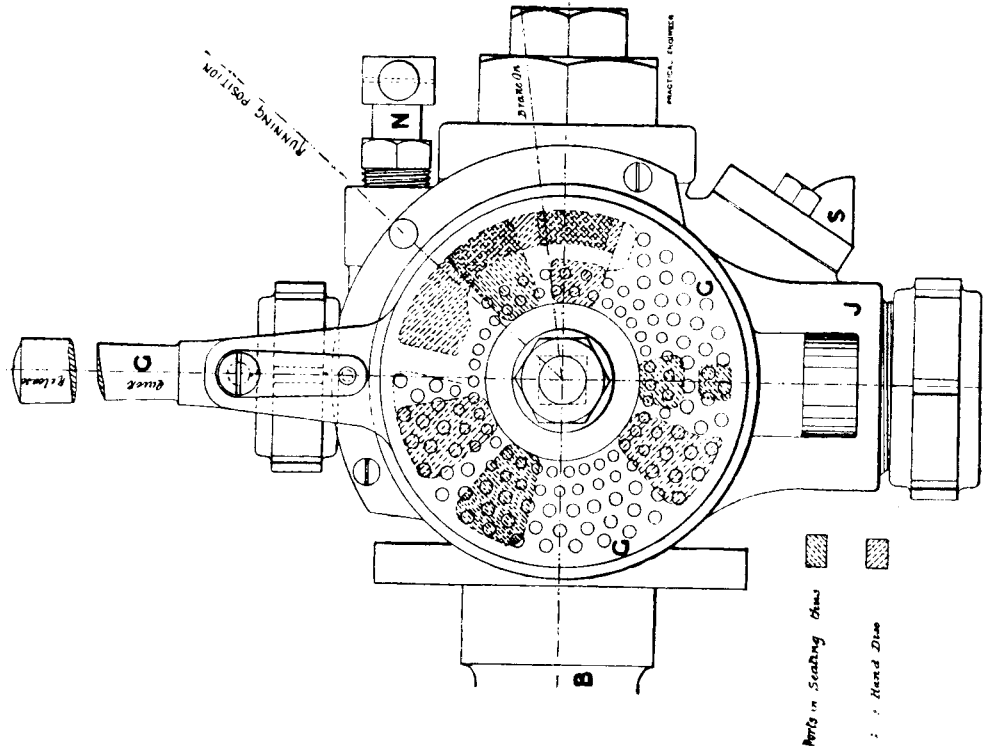


FIG. 66.

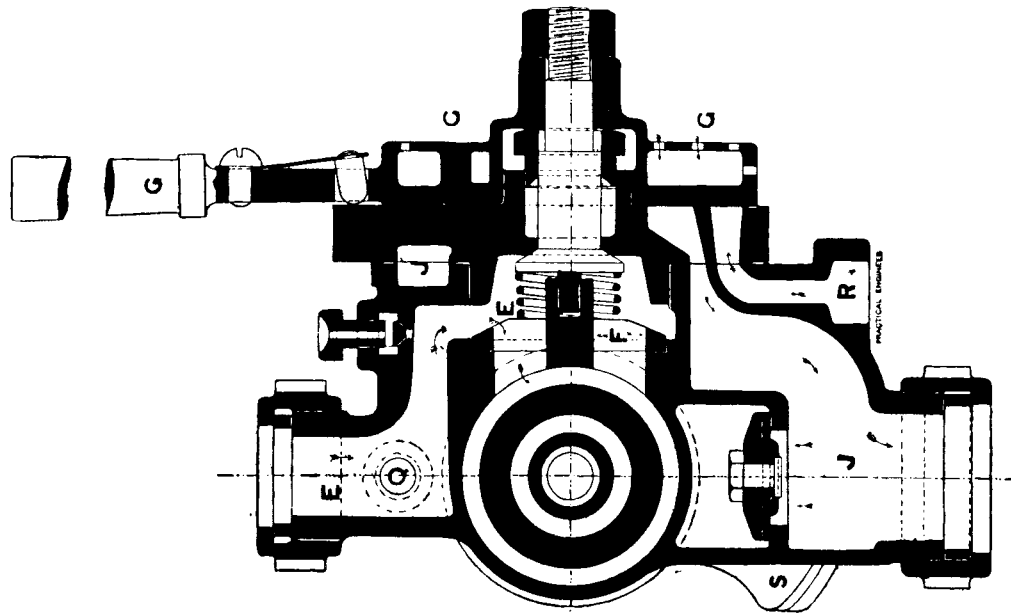


FIG. 67.

It is possible with this ejector to produce a vacuum of nearly 28 in. of mercury with a steam pressure of 140 lb. per square inch, but it rarely exceeds 25 in. under ordinary

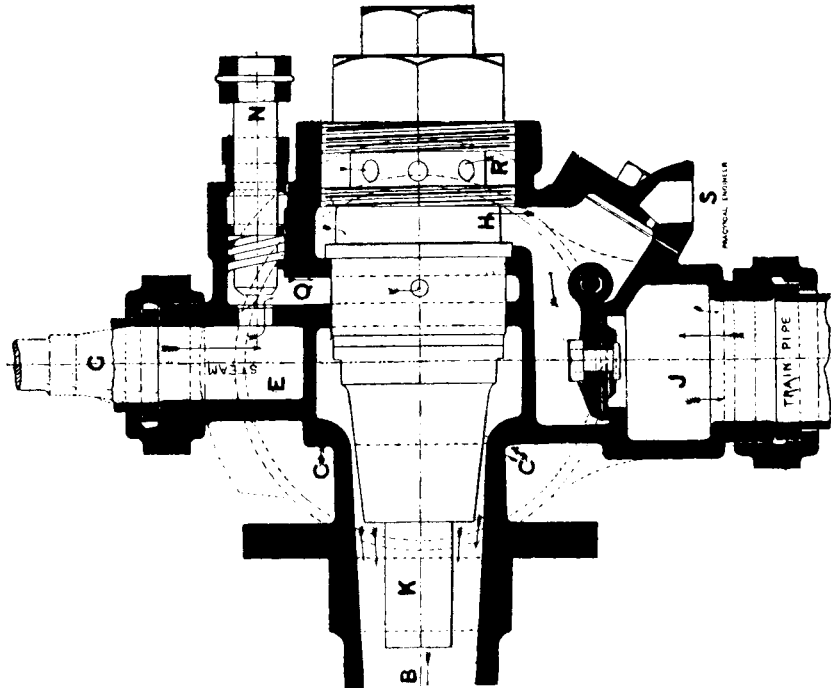


FIG. 68.

working conditions. On more than one railway a valve regulated by a spring is attached to the ejector to prevent the vacuum exceeding 20 in., this being the working pressure in general practice. The reason for this is that, should the

ejector be not able to provide so high a vacuum after a particular application that it maintained before the application, the brake blocks would be constantly pressed upon the wheels with a pressure of so many inches of mercury, and the engine would be doing useless work; besides, the longer the train, generally speaking, the more difficult it is to produce a high vacuum. With an engine and eighty-six carriages in a single train, a vacuum of 21 in. has been maintained, the boiler pressure being 140 lb., which seems to indicate that the length of train is practically unlimited as regards the capability of maintaining a working vacuum. A vacuum of 17 in. has also been maintained on a train of fourteen carriages, when the steam pressure was 70 lb., and 18 in. can be obtained on the engine alone with steam at 60 lb. All grease and deposit on the cones have to be removed periodically, and this can be done with an ordinary penknife.

## CHAPTER XXI.

### HISTORICAL SUMMARY.

(INCLUDING MISCELLANEOUS APPLICATIONS OF THE INJECTOR AND EJECTOR.)

THE preceding articles have been more especially devoted to the study of the boiler-feeding injector, and it is principally the development of this apparatus which we now propose to trace out in these few concluding paragraphs.

First made for commercial purposes in 1859 by the inventor, M. Jacques Giffard, in France, it soon found its way into this country, under the championship of Mr. John Robinson, managing director of the firm of Sharp, Stewart, and Co. This firm secured the patent rights for Great Britain, and began to manufacture the injector to patterns obtained from M. Giffard, while at the same time they set about developing new ones from experiments carried out by themselves, the results of which were placed before the Institution of Mechanical Engineers by Mr. Robinson, in January, 1860.

The novelty of the apparatus, and the then apparent mystery which seemed to surround its mode of action, account for the temerity exhibited in the discussion of the paper, in which only such veterans as Sir Frederick

Bramwell and the late Sir William Siemens took part. This may not have been altogether unexpected, if we judge from the concluding paragraph of the paper in question, which runs thus: "It has not been attempted to give any calculations of the power obtained by the injector, and, indeed, the writer has been discouraged from attempting this by the opinion expressed to him by an eminent hydraulic engineer, that the injector is a valuable application of a force which very few persons understand, and which has never been explained in books; and when it was found possible with steam of 24 lb. pressure to inject water into a boiler at 48 lb. pressure, it was felt that it would be premature to bring forward calculations based upon the result of experiments so hastily made, which require much consideration and discussion before any safe conclusions can be arrived at."

From a perusal of the above paper, and of a supplementary paper of a few months later date, we gather that

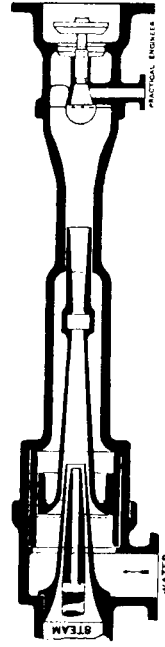


Fig. 68.

the author had not then become acquainted with the laws governing the evaporation of water or condensation of steam; for we find on page 75\* that "great surprise was evinced at the remarkable uniformity in the increase of temperature of the feed water in passing through the injector; the average rise being 75 deg., and the extent of the variation being only between 71 deg. and 86 deg., with a range of pressure from 15 lb. to 51 lb. per square inch, and a change of initial temperature of feed from 74 deg. to 110 deg."†

It was left for Sir William Siemens to point out in the discussion for the first time that the theory of the mode of action could be easily investigated by ascertaining whether the quantity of steam condensed in the jet was sufficient to

\* Minutes of Proceedings, Mechanical Engineers, 1860.

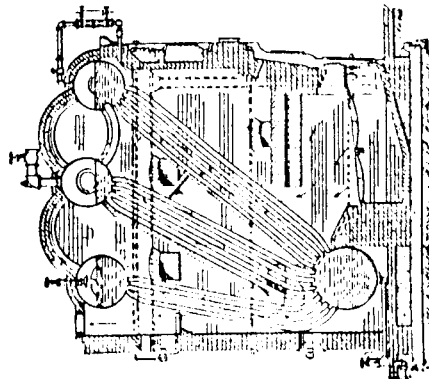
† These pressures appear to have been measured by an ordinary gauge, and are therefore above the atmosphere. — W. W. F. P.

Section V.

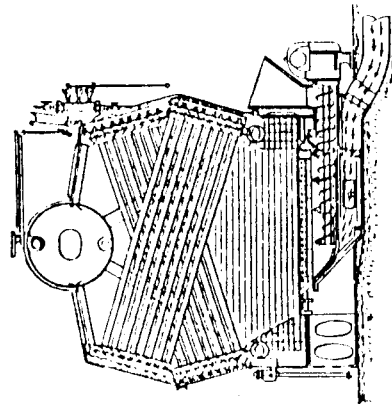
STEAM APPLIANCES.

INJECTORS, STEAM PUMPS, CONDENSERS, SEPARATORS, TRAPS, AND VALVES.

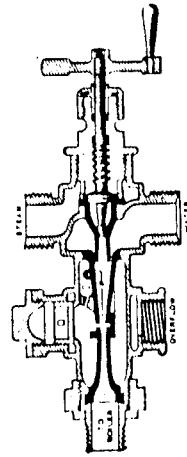
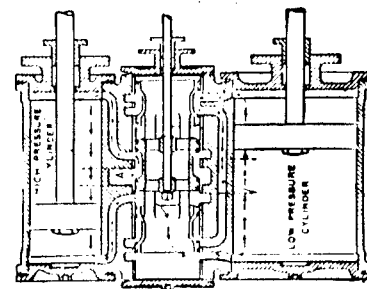
371g. THE STERLING BOILER.—The hot gases of combustion pass lengthwise through the three stacks of tubes guided by the fire brick partitions. All the fire surface divided by 12 equals the boiler horse power. Tubes are cleaned by steam blow pipes. Circulating pipes outside the setting.



371h. THE WORTHINGTON WATER TUBE BOILER.—The water tube sections are between headers and cross each other in series; the lower ends of the diagonal sections are connected with a cross pipe for circulation from the steam drum. Has the American stoker attached.

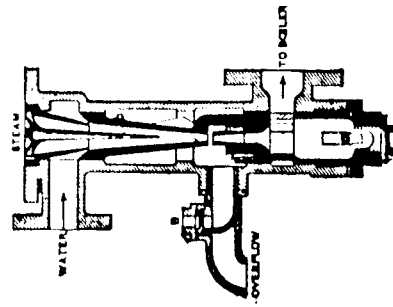


371i. VAUCLAIN'S COMPOUND LOCOMOTIVE CYLINDERS.—A single piston valve for both cylinders with direct steam passages through the valve chamber. High pressure steam enters at the central port A. Steam inlet and exhaust indicated by the arrows.

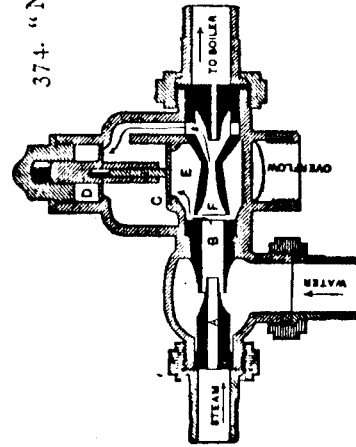


372. "PEERLESS" INJECTOR.—An exhaust steam injector. A hinged section of the combining tube allows a free flow of the exhaust until a water current is

started, when the hinge closes and the overflow valve closes, as in other injectors.

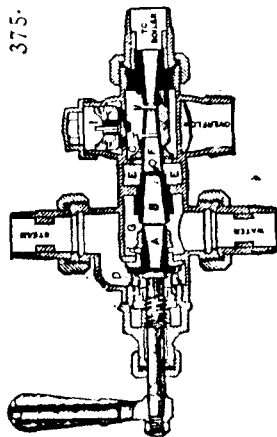


373. "SHAEFFER & BUDENBERG" INJECTOR.—An exhaust injector by which the exhaust steam establishes a feed jet to the boiler. A hinged section in the combining tube allows a free flow of steam to draw the water; the hinged section then closes and the injector operates the same as others for feeding a boiler.

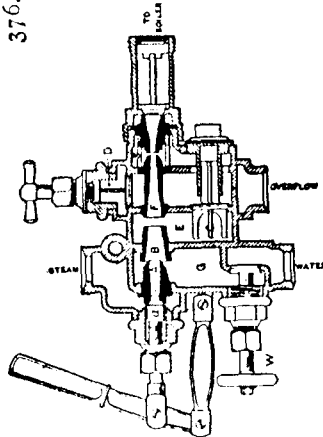


374. "NATIONAL" AUTOMATIC INJECTOR, has four fixed tubes. The two check valves, C, D, open and close successively as the lift is started and the current established.

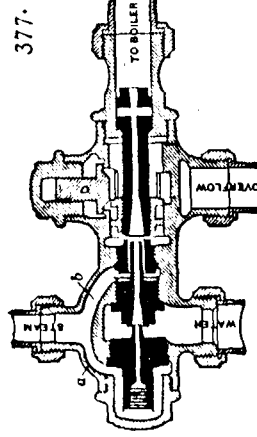
375. "METROPOLITAN" INJECTOR.—The steam is turned on by a screw spindle valve. It has three fixed nozzle tubes, A, B, F. A disc relief-check valve, C, and a wing check, I.



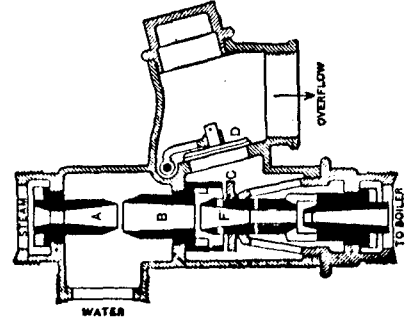
376. "LUNKENHEIMER" INJECTOR.—Four fixed nozzle tubes with a lever-moved valve, A; W, water-regulating valve; D, stop check to overflow; C, automatic check; W, water valve.



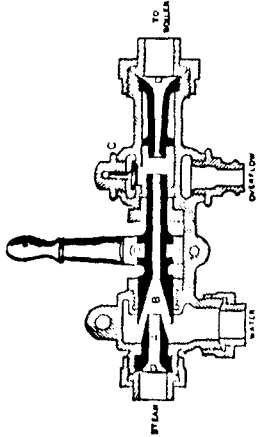
377. "EBERMAN" INJECTOR.—The combining tube slides for regulating the lift and overflow. A single gravity check valve, D, closes the overflow when the current to the boiler is established.



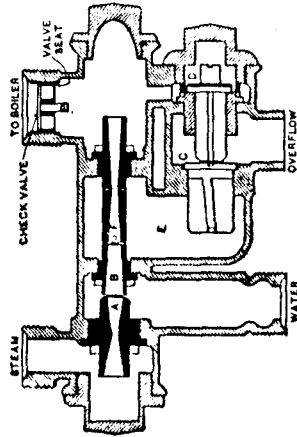
378. "NATHAN" INJECTOR.—A vertical model with four fixed nozzle tubes, tandem. A disc valve, C, closes at the moment the current is established, and the flap valve, D, makes the final closure of the overflow.



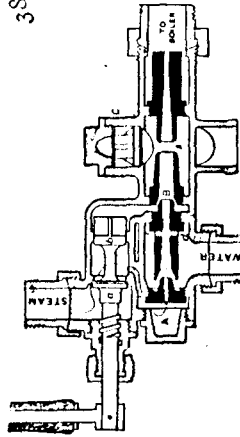
379. "LITTLE GIANT" INJECTOR.—This model has two fixed tubes. The central or combining tube is movable for adjustment. A single automatic check valve regulates the overflow.



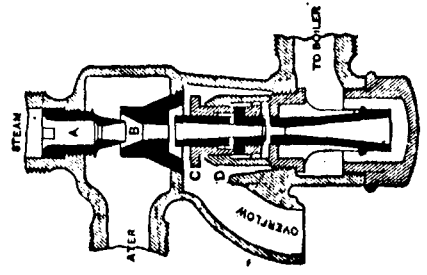
380. "PENBERTHY" SPECIAL INJECTOR.—Has three fixed nozzle tubes. The opening of a detached valve gives steam pressure in the chamber E, and opens both overflow check valves. When the current is established check valve C closes, followed by check valve D.



381. "PARK" INJECTOR.—A double tube in tandem, in which the handle has two movements to operate the lift and force nozzles. A self-lifting check valve governs the overflow.



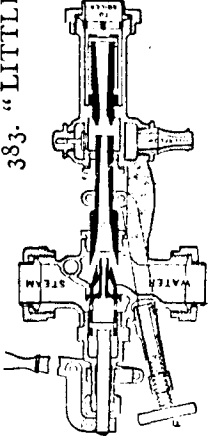
382. "SELLERS" RESTARTING INJECTOR.—In this model all the tubes are fixed. Two concentric check valves, C, D, guided by the combining tube, are operated by the pressure in the combining tube at the moment that the water reaches it, closing the overflow.





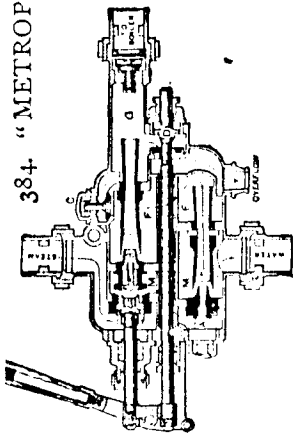
383. "LITTLE GIANT" LOCOMOTIVE INJECTOR.—In this

model the lift is started when the separate steam valve is opened. The forcing or combining tube is movable for regulation by a screw and yoke, and closes the injection nozzle, and closes the lift nozzle ports.



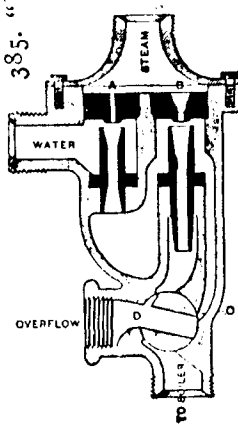
384. "METROPOLITAN" DOUBLE-TUBE INJECTOR.—The first move-

ment of the handle opens the first section of a double-beat valve at *b*, and gives steam to the lifting nozzle *A*; the overflow passing freely through the check valve *C*, and the open valve at *D*. A further movement of the handle opens the second section of the double-beat steam valve *B*, and closes the overflow valve *D*.



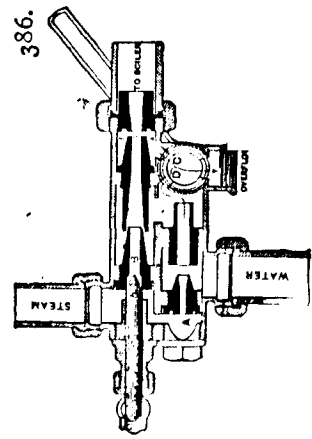
385. "BROWNLEY" INJECTOR.—

The steam flows to the double-jet nozzles without any regulating device other than the overflow cock, which by this peculiar construction relieves both lift and force tubes.



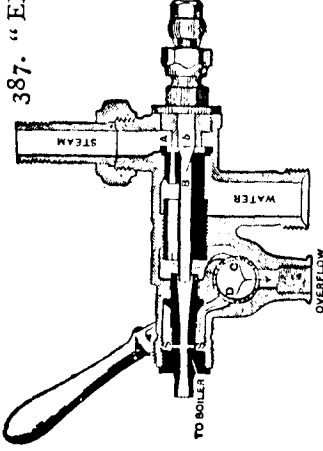
386. "LEADER" INJECTOR.—

A double-tube injector. A separate valve gives steam to the lifting nozzle *A*, with the overflow cock open. The first movement of the handle opens the force valve *b*; a further movement closes the overflow to both lift and force tubes.



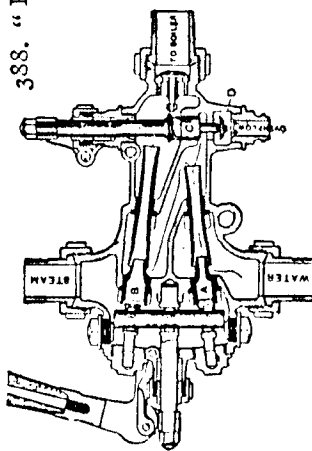
387. "EXCELSIOR" INJECTOR.—

A separate valve gives steam to the lifting nozzle *A*, the overflow cock *D C* being open. The first movement of the handle opens the conical valve *b*; a further movement closes the overflow cock *D C* to both the lifting and force overflow *S*.



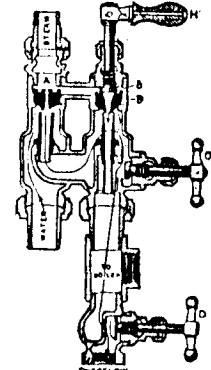
388. "KORTING" INJECTOR.—

A double-tube automatic movement by which the difference in area of the valve discs at *A* and *B* allows the balance lever to open the lifting nozzle first and, by a further movement of the handle, opens the force nozzle *B*. The overflow is self-adjusting for both nozzles.



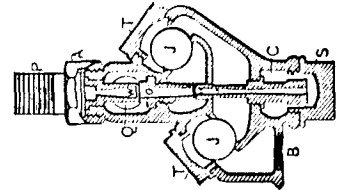
389. "HANCOCK" INSPIRATOR.—A double-tube injector.

The tube *A* lifts the water and starts the circulation through the overflow, when the steam nozzle *B* is opened and valves *C* and *D* are closed.

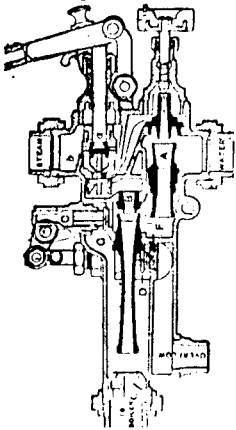


390. BALL-VALVE INJECTOR, automatic in action.

*J, J*, ball valves.  
*P*, steam inlet.  
*W*, inverted nozzle.  
*Q*, suction inlet.  
*B*, overflow.  
*C*, side outlet to boiler.  
*S*, cap.



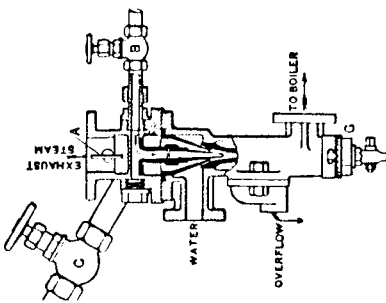
391. "HANCOCK" LOCOMOTIVE INSPIRATOR, a double-tube injector.



- A, the lifting nozzle and tube.
- B, the forcing nozzle and tube.
- C, the lift overflow.
- D, the force overflow.

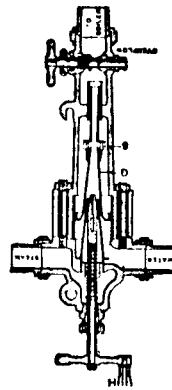
Two movements of the handle are required for starting; the first opens the starting valve *a* and overflow D, with valve H open. A further pull of the handle opens the force valve *b*, and the pressure closes the overflow valve D.

392. "STANDARD" INJECTOR.—An exhaust injector with live-steam starter and supplementary attachment for a live-steam injector.



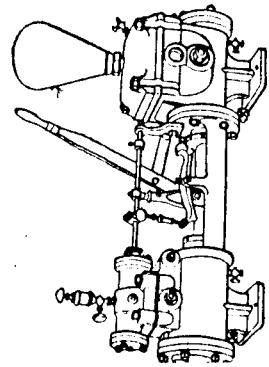
- B, live-steam starter.
- C, live steam for full work.
- A, throttle valve.
- G, regulator.

393. "SELLERS" SELF-ADJUSTING INJECTOR.—

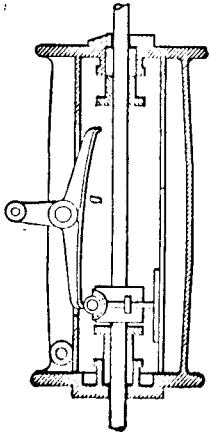


The water nozzle G has a free movement in the case and cage at S. With too much water for the steam, the nozzle is pushed back and partially closes the water area. Self-adjusting.

394. STEAM PUMP, with rotating piston valve and curved tappet. An arm on the valve stem is linked to the end of the curved tappet. The tappet is thrown by a roller clamp on the piston rod.

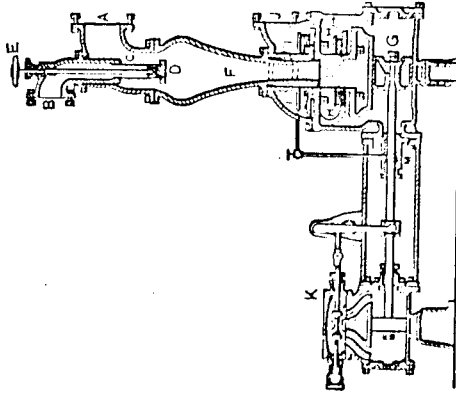


395. "MISCH'S" VALVE TAPPET, for a steam pump. A three-armed lever rocked by a roller travelling with the piston rod.

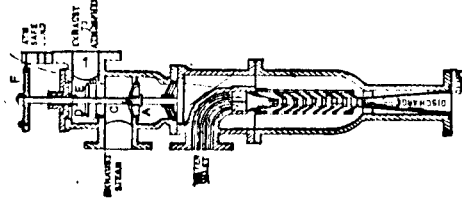


396. INDEPENDENT JET CONDENSER PUMP.

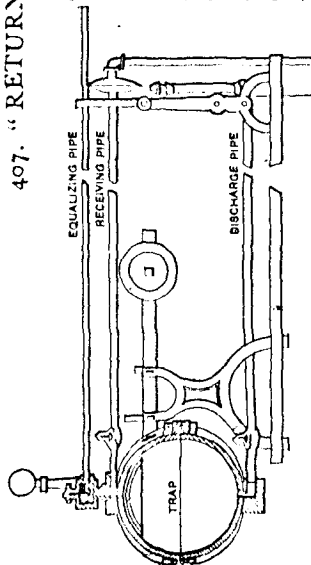
- A, exhaust inlet from engine.
- B, water inlet.
- C, water nozzle.
- D, spray valve regulated by screw spindle and wheel E.
- F, spray chamber.
- J, water discharge from pump.



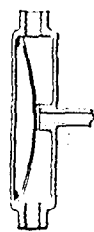
397. EJECTOR CONDENSER, with automatic three-way valve. By the operation of two valve discs on a single stem the exhaust steam is passed to the atmosphere, or is condensed by the multiple nozzle water jet. "Korting" model.



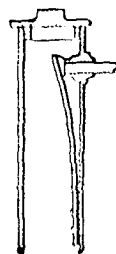
407. "RETURN STEAM TRAP,"  
"Blessing" pattern.



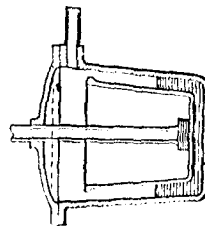
The movement of the globe up and down trips valves that alternately charge the globe with the water from a heating system and discharges it into the boiler.



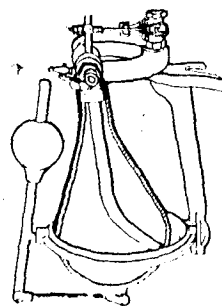
408. SPRING STEAM TRAP.—The shell of iron expands by the heat of the steam at a less rate than the brass spring valve, so that the hot steam closes it and the cooler water opens it by contraction.



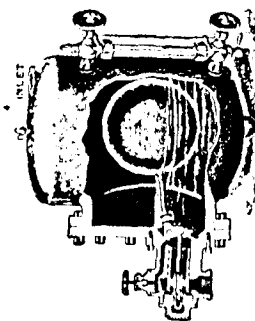
409. SPRING STEAM TRAP.—A differential expansion of the spring itself causes it to open with the water temperature and close with steam temperature. The spring is made of two strips of metal, the upper one of brass and the lower one of steel, riveted together.



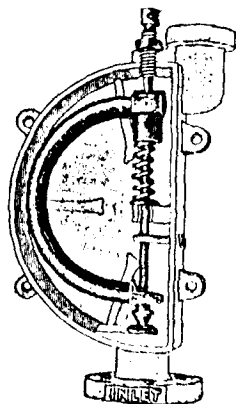
410. STEAM TRAP.—The water condensed in a heating system flows into the trap case and closes the valve by lifting the float. By the overflow into the float, it sinks, opening the valve, and the water is discharged from the float, allowing it to rise and to close the valve.



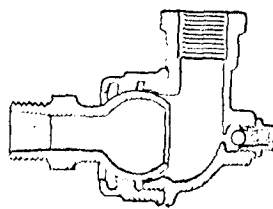
411. "BUNDY" STEAM TRAP.—The pear-shaped bowl rises when empty, and falls when full of water. It swings on trunnions carrying an arm, which operates a valve for charging and discharging the water to and from the bowl.



412. STEAM TRAP WITH VALVE,  
operated by a float. The ingress of  
water lifts the float and opens the dis-  
charge valve. "Curtis" model.



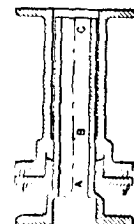
413. "HEINTZ" STEAM  
TRAP.—The differential expan-  
sion of two metals in the semi-  
circular arc opens or closes the  
inlet valve. Adjustment is made  
by the set-screw.



414. "MORAN'S" FLEXIBLE STEAM JOINT  
and automatic relief valve. A ground globular  
pipe fitting held in a spherical union joint.



415. CORRUGATED EXPANSION  
COUPLING, "Wainwright's" model. A  
hard brass tube, corrugated, gives the tube  
a longitudinal elasticity to take up the ex-  
pansion of steam pipes.



416. FLANGED EXPANSION JOINT.—  
Used in pipe lines to take up the change in  
length due to difference in temperature.

Steam Power Plant Auxiliaries and Accessories. ed. Terrell Croft, revised by D. J. Duffin. 2nd ed. p. 518-519, 532-543. (NY: McGraw, 1946).

## STEAM TRAPS

When saturated steam gives up its heat and changes back to water in any steam system, water is formed in the process of condensation. In order to obtain the maximum possible efficiency from steam-heated equipment, to reduce fuel costs, and to prevent the damage that may be caused by this condensate in the supply lines to turbines, pumps, and other steam power plant machinery, it is necessary to drain off this condensed water either continuously or at regular intervals. If the condensate and the air that is mixed with the steam are permitted to build up in steam apparatus or piping, not only are the heating efficiency reduced and fuel dollars wasted, but serious damage from water hammer, blown gaskets, or burst tubes, pipes, and jackets is likely to occur, which eventually causes costly plant shutdowns. Many methods have been employed to remove this condensate which collects at the lowest points in the system, ranging from hand-operated throttling valves to various types of automatic valves, or steam traps, which are designed to discharge condensate and air but prevent steam from passing. Traps are also used to drain water from compressed air and gas lines, and occasionally to remove water and oil or grease from separators. The traps discussed in this division are limited mainly to those used in steam systems.

**415. Steam traps** are devices for entrapping and automatically disposing of the water that results (1) from condensation and entrainment in steam piping systems; (2) from condensation in steam-heating apparatus; and from condensation in steam power apparatus.

**416. Types of steam traps.** There are two main groups of steam traps, *return traps* and *nonreturn traps*. The former are those that discharge the condensate directly into the water

spaces of steam boilers at a pressure equal to or higher than the boiler pressure. The latter group of traps separate the condensate from the steam system but discharge it into receptacles at pressures less than that of the boiler.

**417. Nonreturn traps**, which are the most widely used, are in turn classified into types according to the principle upon which they operate. These are *thermostatic traps*; *open-float* or *bucket traps*; *ball-float traps*; *inverted bucket traps*; *tilting traps*; *orifice traps*, and *impulse traps*. They will be discussed in turn.

**418. Thermostatic traps** are the most common form of steam trap in general use. They are generally constructed (Fig. 509) with an internal element in the form of a corrugated bellows of flexible metal, usually bronze, which expands or contracts with the temperature of the steam, thus opening or closing the valve of the trap and allowing air and water to pass but without allowing any steam to be lost. The flexible metal bellows *A* in Fig. 509 is partially filled with a volatile fluid and sealed tight. When the trap becomes hot, the liquid boils, creating a vapor pressure slightly higher than the steam pressure surrounding the bellows on the outside. Therefore when steam reaches the trap, the bellows *A* is expanded and the valve head *B* contacts the seat *C*, thus closing the discharge valve so that no steam can escape. When more condensate follows, its slightly lower temperature contracts the bellows *A*, thus opening wide the discharge valve. The shield *D* extending the entire length of the bellows protects it from the abrasive action of the steam. Prongs *E* formed on the lower end of

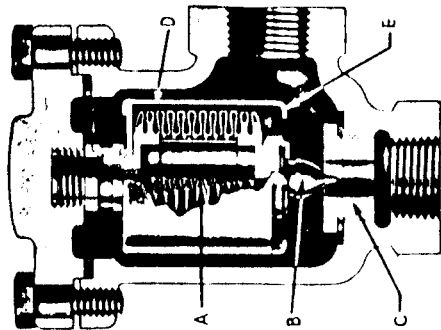


FIG. 509.—Sectional view of Sarco thermostatic steam trap for pressures up to 225 p.s.i. (Sarco Company, Inc.)

able metal bellows *A* in Fig. 509 is partially filled with a volatile fluid and sealed tight. When the trap becomes hot, the liquid boils, creating a vapor pressure slightly higher than the steam pressure surrounding the bellows on the outside. Therefore when steam reaches the trap, the bellows *A* is expanded and the valve head *B* contacts the seat *C*, thus closing the discharge valve so that no steam can escape. When more condensate follows, its slightly lower temperature contracts the bellows *A*, thus opening wide the discharge valve. The shield *D* extending the entire length of the bellows protects it from the abrasive action of the steam. Prongs *E* formed on the lower end of

what older type of installation by a different manufacturer is shown in Fig. 528.

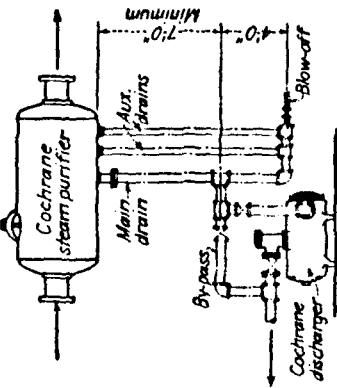


FIG. 527.—Typical drainage arrangement with Cochrane steam purifier and discharger for pressures above 200 p.s.i. (Cochrane Corporation.)

gravity or by the lift of another trap or traps. After a predetermined level has been reached, the flow of the

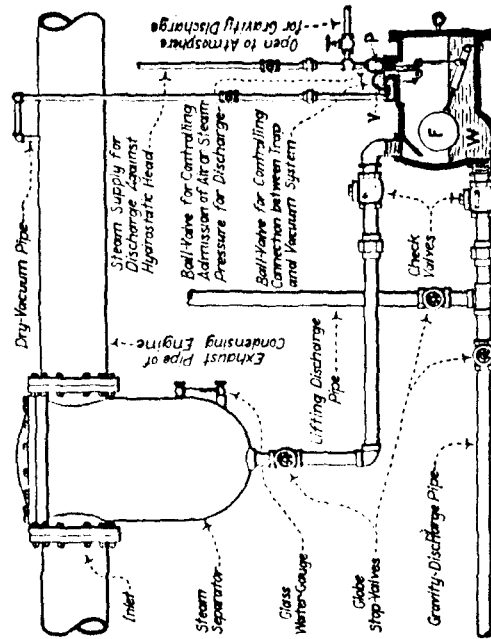


FIG. 528.—Strong vacuum trap installed for draining separator in condensing engine exhaust line. When *F* rises, *V* closes and *P* opens, permitting live steam or atmospheric air pressure to discharge accumulated water *W*.

condensate is shut off, the receiver vent is closed, and the steam at boiler pressure is admitted to the tank, forcing

the condensate out the discharge opening. As the receiver empties, the foregoing process is reversed. A check valve prevents backflow through the discharge opening, the tank vent is opened, and the condensate again flows into the receiver.

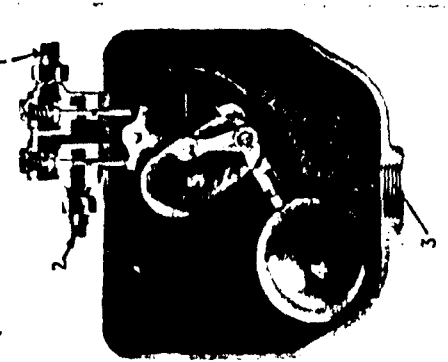


FIG. 529.—Sarcos alternating receiver or return trap for steam pressures up to 100 p.s.i. (Sarco Company, Inc.)

As condensation enters the inlet 3, it gradually raises the float 4, and when the latter reaches its maximum height, it trips the weight 5, which falls over, reversing

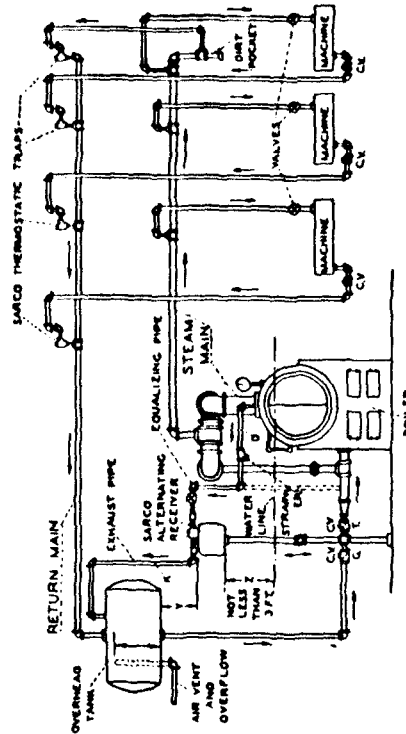


FIG. 530.—Sarcos alternating receivers or return traps returning condensate to a high-pressure boiler. (Sarco Company, Inc.)

the position of valves 1 and 2, opening 1 while simultaneously closing 2. Pressure on the water in the receiver is

thus equalized with that in the boiler, and since the receiver is always installed above the water level in the boiler, the condensation will flow through valve 3 (now the outlet) to the boiler.

In the tilting return trap (Fig. 531), the tank or receiver is pivoted on trunnions and counterbalanced by a weight on a lever. As the tank fills, its weight overcomes the balance weight and the sinking of the tank actuates the valve mechanism. Various mechanical devices and arrangements operate the valves. One type, not shown, has a pilot valve to control a steam-actuated main valve.

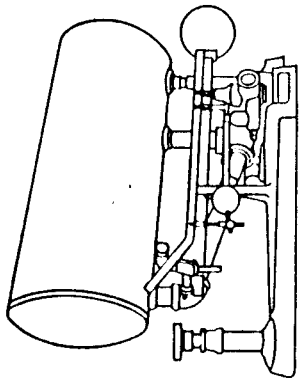


FIG. 531.—Tilting return trap.

A tilting trap in which the tank or receiver is not pivoted is shown in Fig. 532. It has a counterweighted bowl which when filled with condensate rolls in its frame and actuates the valves. Motion of the bowl in the opposite direction reverses the cycle.

An older type of installation using tilting-bucket steam traps for draining live-steam separators is shown in Fig. 533. **426. The volume, in cubic feet, of steam required for each discharge of a return trap is approximately equal to the volume, in cubic feet, of the water discharged.**

*Example.*—Assume that a return trap is discharging into a boiler under 100 lb. pressure. Then the weight of the steam that is admitted to the trap is (as taken from a steam table) about 0.25 lb. per cu. ft. The returned water of condensation weighs about 60 lb. per cu. ft. Now as stated above, 1 cu. ft. (60 lb.) of water requires 1 cu. ft. (0.25 lb.) of steam. Hence 1 lb. of water requires  $0.25 \div 60 = 0.0042$  lb. of steam.

*NOTE.*—A portion of the heat of the steam is lost by radiation from the trap. Steam may also be lost at each discharge through the vent-valve. The cumulative loss from these sources may amount to 1 per cent of the total evaporation of the boiler.

**427. The economy of return steam-trap service** consists mainly in the saving effected by returning the water of condensation from high-pressure steam apparatus directly to

the boilers, instead of returning it thereto in relays, as through a receiver or feed-water heater under atmospheric pressure.

*Explanation.*—In industrial processes that require steam for heating, drying, or boiling, the steam is frequently supplied from the boilers

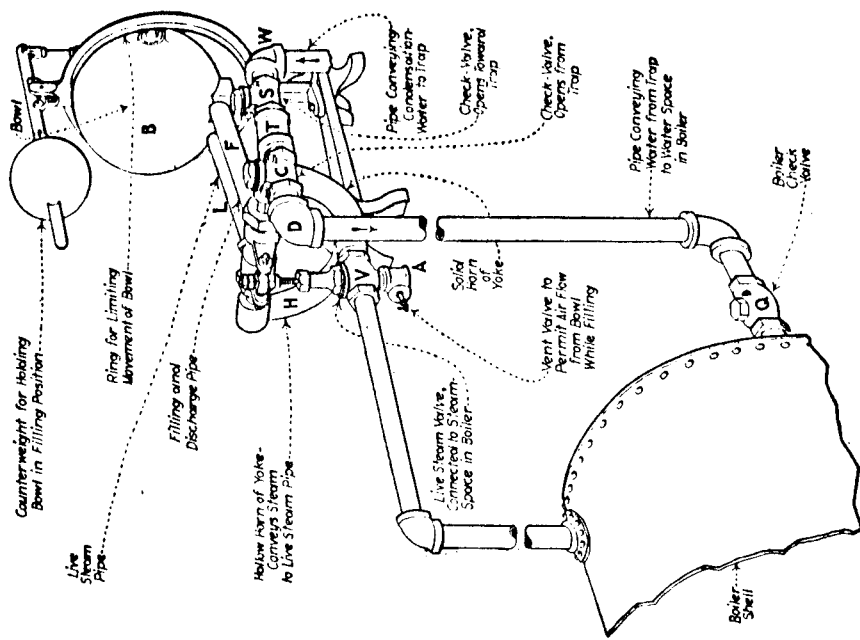


FIG. 532.—Bundy return trap. When B fills with water and falls, V opens and A closes. Steam then passes into bowl through H and L, and water is forced out through F, T, C, and D. When B empties and rises, V closes and A opens. Condensation water then passes into bowl through W, S, T, and F, and is condensed in the manufacturing apparatus under pressures ranging from a few pounds up to 100 lb. or more.

Where steam of, say, 80 lb. pressure is used in heating coils, as in a high-temperature dry-room, the water of condensation may leave the coils at a temperature of 300°F. If such water is trapped to an open

receiver or feed-water heater, it will, immediately it is discharged by the trap, expand and cool to the boiling point under atmospheric pressure. Also, its temperature must be still further reduced to about 210°F. in order that its delivery to the boilers by a feed pump may be facilitated. Thus the water will have thrown off the heat corresponding to a temperature reduction of about  $300 - 210 = 90^\circ\text{F}$ . Furthermore, it will have lost a considerable portion of its own bulk and some heat through vaporization. While most of the water thus vaporized may be recovered, some of it will be a dead loss.

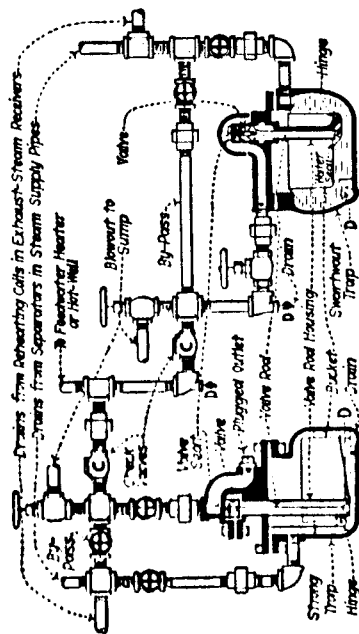


Fig. 533.—Arrangement of tilting-bucket-float intermittent-discharge high-pressure steam traps for draining live-steam separators and reheating coils of two cross-compound engines.

The saving that might be realized, in this case, by returning the water of condensation directly from the heating coils to the boilers is, therefore, represented by (1) the quantity of coal required to supply the heat corresponding to a temperature reduction of  $90^\circ\text{F}$ . plus (2) the heat lost through vaporization.

**428. A proper location for a return steam trap (Fig. 530)** is at least 3 ft. above the normal water level in the boiler to which the trap is attached. This location will ensure a positive gravitational flow of the returned water from the trap to the boiler.

**429. The economy of nonreturn steam-trap service** consists mainly in the saving effected by preventing the steam from blowing through drips and drains directly to the atmosphere. It is contingent upon two principal considerations: (1) Selection of the proper type of trap for the particular service requirements and (2) the area of the trap discharge-valve orifice and the condition of the valve.

**Example.**—Where a  $\frac{3}{4}$ -in. drain pipe from a steam piping system under, say, 165 lb. per sq. in. gage pressure is blowing directly to the atmosphere, the resulting loss of steam may amount to about 1,120 lb. per hr. This is the equivalent of approximately 35 boiler horsepower. Assuming that a boiler horsepower costs, say, \$3.25 per month, the total monthly loss from this source will amount to about  $3.25 \times 35 = \$113.75$ . With the drain pipe connected to a properly selected steam trap, the loss of steam due to condensation in the drainage connections might be reduced to about 32 lb. per hr.

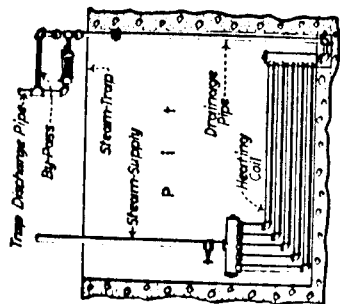


Fig. 534.—Method of trapping condensation from heating coil located on bottom of deep pit.

**NOTE.**—The area of the valve orifice of a trap for low-pressure service should equal the cross-sectional area of the size of pipe for which the outlet orifice of the trap is tapped.

The area of the valve orifice of a trap for medium or ordinary high-pressure service, as where the drainage from a live-steam separator is discharged into an open feed-water heater, may be smaller than the openings in the pipe connections. It should, however, in any case be large enough to prevent the passage from becoming clogged with particles of scale.

**430. Steam traps that are dependent upon temperature changes for their operation should not serve separators or similar apparatus, in the draining of which the trap should operate instantly after the accumulated water has attained the head at which it should discharge.**

**Explanation.**—Assume that either a float-operated trap or a tilting trap is installed for draining the steam separator in a supply line which ordinarily conveys 90-lb.-pressure steam. The trap will continue to function without intermission if the pressure rises to, say, 100 lb. or falls below 90 lb. But if an expansion trap is substituted, it must necessarily be set to open at the temperature of the condensation from the 90-lb.-pressure steam, which may be as low as  $310^\circ\text{F}$ . Consequently if

the pressure rises to 100 lb., at which the condensation may reach the trap at about 320°F., the expansion trap will remain closed until the temperature of the condensed water drops to 310°F. During the requisite time interval, however, the condensate accumulation might become dangerously excessive. On the other hand, if the pressure falls below 90 lb., condensation may reach the trap at some temperature below 310°F. Hence the expansion trap will blow steam so long as the diminished pressure continues.

**431. The proper location for an ordinary high- or low-pressure steam trap** (Figs. 528, 530, and 533) is, with reference to the location of the apparatus which the trap is intended to serve, such that the drainage water will flow to it by gravity.

**NOTE.**—If the apparatus to be drained is located at an inconveniently low elevation, as on the bottom of a narrow pit or trench, an expansion trap may be located (Fig. 534) at a higher elevation if the drainage water leaves the apparatus under sufficient pressure. There should be at least  $\frac{1}{2}$  lb. per sq. in. pressure for each foot of vertical height.

**Example.**—A steam pressure of 5 lb. per sq. in. in the heating coil (Fig. 534) will practically balance a column of water  $5 \div 0.5 = 10$  ft. high. Hence the water of condensation will be forced to the trap, if the trap inlet is located less than about 10 ft. above the drainage outlet of the coil.

**432. The location of a thermostatic trap** should be such that its operation will not be affected by excessive variations of temperature occurring in the surrounding atmosphere.

**433. The capacity of a steam trap** may be rated (Table 434) either in terms of the *quantity of water to be trapped per hour* or in terms of the *extent of radiating surface* in the apparatus from which the trap may drain water of condensation.

**NOTE.**—It is usually assumed that each square foot of direct radiating surface in a heating system will condense about 0.33 lb. of steam per hour. It is also assumed that the radiation from each lineal foot of 1-in. pipe in a heating coil will ordinarily condense about 0.19 lb. of steam per hour. Where very wet products are to be dried in a kiln or drying room, a trap for draining the heating coils should be selected on a basis of 0.56 lb. of steam condensed per hour per lineal foot of 1-in. pipe.

**434. Dimensions and capacities of various steam traps working under medium pressure** are given in the following table:

Rated capacities per hour						
Dia., in., of valve orifice	Size, in., of pipe connections	Steam pressure, in lb. per sq. in. (gauge)	Gal. of water discharged	Lb. of water discharged	Lineal feet of 1-in. pipe drained	Sq. ft. of radiating surface drained
1 1/4	1 1/4	50	375	3,114	5,538	1,846
		75	459	3,811	6,776	2,258
		100	530	4,402	7,827	2,609
		125	593	4,976	8,847	2,949
3/8	3/8	50	584	4,847	8,618	2,873
		75	715	5,936	10,554	3,518
		100	826	6,853	12,184	4,062
		125	923	7,662	13,624	4,542
1 1/2	1 1/2	50	709	5,883	10,460	3,486
		75	868	7,205	12,810	4,270
		100	1,002	8,320	14,793	4,931
		125	1,122	9,302	16,540	5,514
2 1/2	2 1/2	50	844	6,998	12,442	4,147
		75	1,034	8,379	15,754	5,085
		100	1,194	9,986	17,692	5,898
		125	1,334	11,075	19,692	6,564
7/8	1 1/4	50	1,149	9,335	16,954	5,651
		75	1,407	11,680	20,767	6,922
		100	1,625	13,486	23,978	7,993
		125	1,816	15,073	26,799	8,933
3/4	1 1/4	50	1,501	12,537	22,290	7,430
		75	1,838	15,252	27,118	9,039
		100	2,122	17,616	31,322	10,441
		125	2,363	19,694	35,017	11,672

**435. The quantity of condensation water to be trapped from a piping system** may be approximately computed by the following formula:

$$W_w = A_r K \quad (\text{lb. per hr.}) \quad (108)$$

where  $W_w$  = weight of condensation in pounds per hour;  $A_r$  = area of piping surface, in square feet; and  $K$  = condensation, in pounds per hour per square foot of pipe surface, corresponding to the observed steam pressure, as given in Table 436.



**436. Rate of condensation, in uncovered pipe lines, of steam at various pressures.** Adapted from Elliott Company's Bulletin G on Steam Traps.

Steam pressure, lb. per sq. in. (gage)...	5	10	20	30	40	50	60	80	100	125
Condensation, lb. per hr., per sq. ft. of pipe surface.....	0.7	0.8	0.9	1.0	1.1	1.2	1.3	1.6	1.7	1.9

*Example.*—It is found by computation that the high-pressure piping in a boiler and engine plant exposes 2,683 sq. ft. of radiation area. The steam pressure is 115 lb. per sq. in. gage. What size of trap, as listed in Table 434 should be used for draining the system?

*Solution.*—By Table 436, the condensation rate for steam at 100 lb. pressure = 1.7 lb. per hr. per square foot of exposed surface, and for steam at 125 lb. pressure = 1.9 lb. per hr. per square foot of exposed surface. Hence the condensation rate for steam at 115 lb. pressure =  $(1.9 - 1.7) \div (125 - 100) \times (115 - 100) + 1.7 = 1.82$  lb. per hr. per square foot of exposed surface. Applying formula (108)  $W_v = A/K = 2,683 \times 1.82 = 4,883.06$  lb. per hr. Hence by Table 434, a  $1\frac{1}{2}$ -in. trap having a  $\frac{1}{4}$ -in. valve orifice should be used.

**437. The piping of a steam trap** should be adapted to the particular service for which the trap is installed. Numerous right-angled turns and runs of excessive length in the discharge piping should be avoided. To obviate interference the discharges from low-pressure and high-pressure traps should be piped independently.

*NOTE.*—Every steam trap should have an external by-pass. Also, stop valves should be inserted between the by-pass connections and the inlet and outlet orifices of the trap.

Strainers in trap-inlet connections may be used to prevent particles of scale or other solid substances from entering the trap and fouling the valve.

Provision for draining trap-discharge pipes while the traps are inoperative should be made when the traps are exposed to freezing in cold weather.

Check valves should be inserted in the discharge pipes of steam traps where two or more high-pressure traps discharge (Fig. 533) into a common discharge line or where a return trap (Fig. 532) is used for boiler feeding.

*NOTE.*—For ordinary high-pressure service, the check valves (C, Fig. 533) in the discharge pipes of steam traps may be of standard weight and may be filled with renewable composition disks. For boiler-feed service however, the check valves (S and Q, Fig. 532) should be extra heavy and should have solid brass disks. Check valves with composition disks are ill adapted to withstand the stresses of boiler-feed service.

A vent pipe connecting a high-pressure trap with the apparatus drained is often necessary to ensure regular operation of the trap.

*Explanation.*—With a scant flow of water from the separator the upper part of the trap will contain steam of the same pressure as that in the separator. Should a slug of water enter the separator, direct communication between the steam-occupied space in the trap and the steam space in the separator will be closed in the absence of a vent pipe. The flow from the separator will therefore cease until the steam in the trap condenses. Restoration of an unimpeded flow may be further delayed by air mingled with the trapped steam.

**438. The care of steam traps** involves periodic inspections and, when necessary, repair or replacement of the valves or seats. Inspection should be made frequently because the flow of water through steam traps cuts into the valves and seats, which may then leak or blow steam. Since the traps are enclosed—as are usually also the discharge pipes—a leak would not ordinarily be noticed. But by placing the ear to a trap, the blowing can frequently be detected. A still better method for detecting the leaks consists of providing an opening in the discharge pipe, from which the leak is then visible. Since, as stated in Sec. 429, losses from leaks readily become excessive and expensive, a leaky trap should be taken from service immediately and repaired upon discovery of the leak.

**QUESTIONS**

1. What are the general uses of steam traps?
2. What is the distinction between a return trap and a nonreturn trap?
3. What types of traps operate on the principle of buoyancy?
4. Through what media is the expansion principle utilized in the operation of steam traps?
5. What is the essential operating principle of return traps?
6. What approximate volumetric ratio exists between the water discharged by a return trap and the steam required to operate the trap?



height of steam is less at higher pressures, and smaller-sized piping may be used.

Pipe supports should be designed to carry the weight of the piping *full of water*. They should be spring-mounted for heavy service in order to provide proper support during vertical motion of the pipe resulting from expansion. Langer-type supports should be adjustable by means of a turnbuckle or nut threaded to the top of the hanger rod so that compensation may be made for settling of the supporting structure.

Expansion of pipe anchored at each end may set up severe stresses. It is good practice to provide an expansion joint of the slip, bellows, or loop type for long horizontal runs of steam piping. The length of expansion is calculated

$$(t_1 - t_2) \times L \times 0.0000065 = \text{expansion, in.}$$

where

$t_1$  = steam temperature

$t_2$  = room temperature

$L$  = horizontal length of pipe section, in.

A Holly loop is a piping arrangement used to return condensate from steam-line separators to the boiler (Fig. 12-19a).

In operation, the flow of the condensate-and-steam mixture from the separator to the surge and separation tank is established by causing a slight pressure drop in the surge tank. This is accomplished by having the vent valve open slightly in a small line from the top of the surge tank to a heater hot well. The surge tank is located at an elevation sufficient to give static head pressure so that the condensate will return against boiler pressure by gravity.

Use of a Hartford loop is confined usually to heating boilers and eliminates the need of a check valve to prevent condensate returns from backing up the return line in case the steam valve is closed (Fig. 12-19b).

Package boilers or economizers may be located *outdoors* between the boiler house and stack. In freezing temperatures, the economizer or boiler should be drained when out of service. When it is in use, a bypass around the blowdown valves should be provided, and this bypass should be opened slightly to prevent freezing of the blowdown line. Also, all exposed pipes out of the main circulation system should be heavily insulated. Soot accumulations should be removed periodically, for they may impede heat transfer and draft. Large quantities of soot in the base of economizers may be washed out with a water hose.

*Safety-valve care* in the operating schedule should include frequent periodic tests of safety valves. In boilers of moderate pressure, the valve should be lifted by its lever at least once each week of operation, and the pressure should be raised to the popping point to test the safety valves at least once each year of operation. If the safety valve does not blow at its set pressure, the lever should be tried at that pressure, for the spindle may be stuck slightly

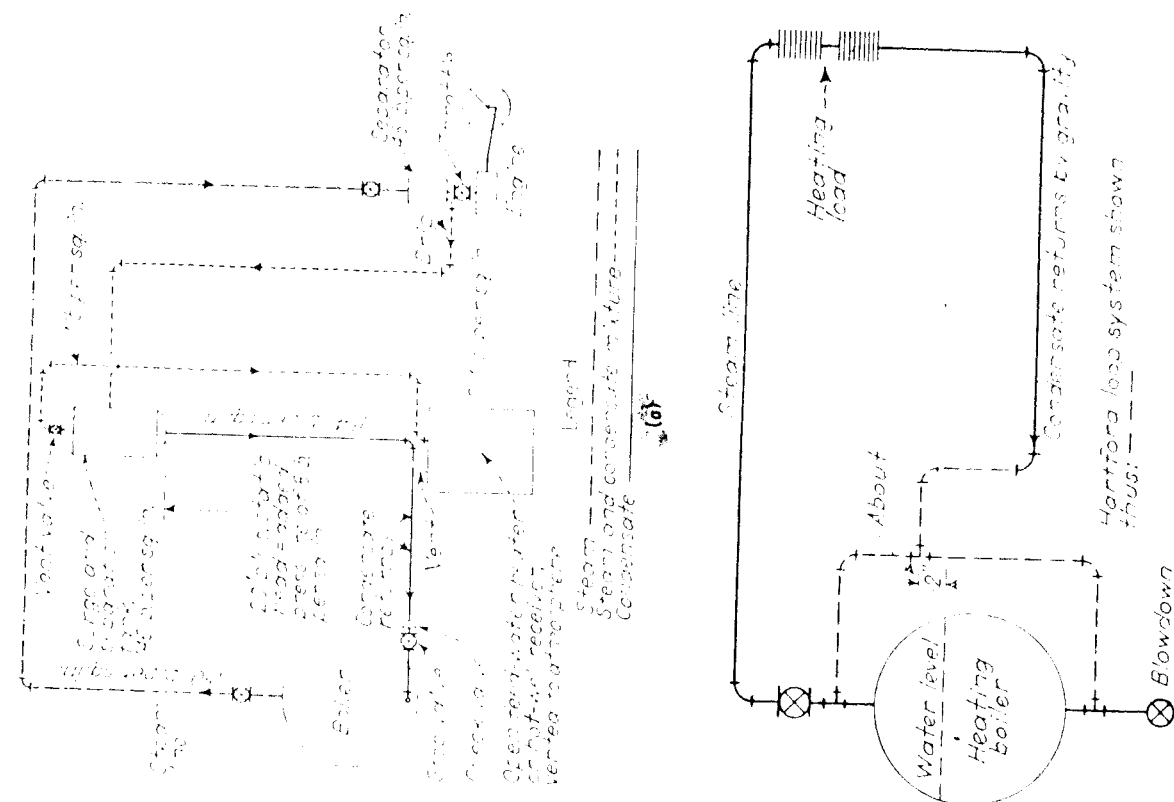


Fig. 12-19 (a) Holly loop returns condensate to the boiler from steam-line separators. (b) Hartford loop is used to return condensate in gravity return system.

## THE STEAM LOOP.

This is an attachment to a steam boiler, designed to return water of condensation. It invariably consists of three parts, viz.: the "riser," the "horizontal" and the "drop leg," and usually of pipes varying in size from three-fourths inch to two inches. Each part has its special and well-defined duties to perform, and their proportions and immediate relations decide and make up the capacity and strength of the system. It is, in fact,

nothing but a simple return pipe leading from the source of condensation to the boiler, and, beyond this mere statement, it is hardly possible to explain it; it has, like the injector and the pulsometer pump, been called a paradox.

The range of application of the steam loop practically covers every requirement for the return of water of condensation. It is much used in connection

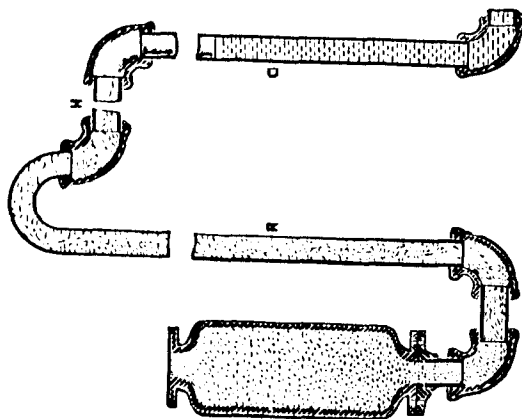


Fig. 394.

with steam-heating apparatus.

As the steam loop is merely an arrangement of piping, there are no working parts, and consequently no need of lubrication. Furthermore, there is nothing to wear and get out of order.

*NOTE.*—Difference between a cock and valve.—The cock is a valve, but a valve is not a cock; the cock is a conical plug slotted and fitted with a handle for turning the cone-shaped valve with its opening into or out of line with the opening of the pipe.

## STEAM LOOP.

The cost of returning the condensed steam to the boiler is practically nothing compared to the cost of maintenance of the pump. The illustration, Fig. 394, shows the working of the steam loop. It will be noticed that the riser R does not contain a solid body of water, but, on the contrary, a mixture

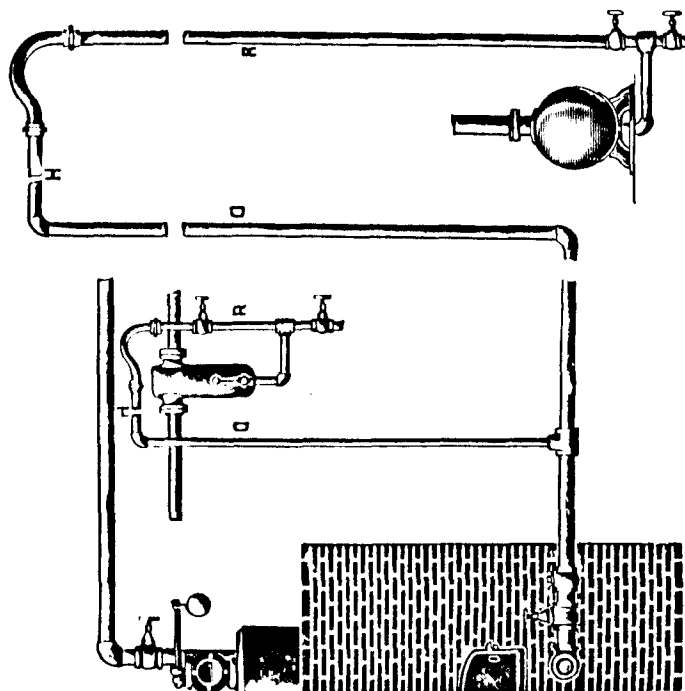


Fig. 395.

of water and steam. This mixture is readily condensed and the whole converted into water, which process is constantly going on in the horizontal pipe H. The condensation of steam at that point would soon produce a vacuum were it not for the fact that the mixture of steam and water from the riser immediately takes

### STEAM LOOP.

the place of the steam as it condenses. The riser is constantly supplying steam, conveying large quantities of water in the form of a fine spray to take the place of the steam condensed in the horizontal pipe H. As soon as the steam and spray pass the goose-neck section of the horizontal pipe, they cannot return to the riser; hence the contents of the pipes constantly work from the separator towards the boiler.

A drip should be connected with the separator so as to drain the latter and the riser when they become filled with water, as will generally be the case after steam has been shut off for some time and the main piping has become partly filled with accumulated water.

In order to proportion a steam loop properly by calculation, the specific gravity of the mixture in the riser should be ascertained, the difference of pressure between the boiler and the separator, and the pressure under which the system is to work, the latter quantity being used to determine the weight of water at the existing pressure and temperature. (See note.)

The current of steam and spray ascending the riser is due to the lower pressure in the horizontal pipe *h* caused by the condensation of steam, as previously explained. If the difference of pressure between the separator and the pipe is, say, 2 pounds, then it will sustain a column of water at a temperature of 297° F., equal to  $2.509 \times 2 = 5.018$  feet high.

**NOTE.**—The weight of a cubic foot of water at 60° Fahr. and at the pressure of the atmosphere is 62.3 lbs. Consequently a column of water one inch square and weighing one pound will measure  $144 \div 62.3$ , or 2.311 feet in height.

With steam at 50 lbs. pressure, the temperature of the water is 297°, and the weight of a cubic foot is 57.35 lbs.; the height of a column one inch square becomes  $144 \div 57.35$  lbs., or 2.509 feet for each pound weight.

### CALCULATING STEAM LOOP.

The riser, R, however, does not contain water alone, but a mixture of steam and water, the specific gravity of which varies, but may be taken as one-fourth that of water, about three-fourths of the volume being assumed to be steam. In that case the column sustained will equal  $5.018 \times 4 = 20.072$  feet. Deducting 10 per cent. for friction, the net height of the riser pipe may be 18 feet.

In the larger illustration, Fig. 395, will be seen two applications of the steam loop; one from a separator on a line of steam piping, to which the previous calculations apply; the other from a radiator which is set below the water level. It is the calculation of this latter condition which most troubles engineers. (See example given in the note.)

As shown previously, 10 per cent. should be added for friction, and it is better to allow 5 feet in any case to provide for it.

**NOTE.**—Assuming that in this case there is a difference of 5 lbs. pressure between the top and bottom of the riser pipe, and that the lower point in the return system is 12 feet below the water level in the boiler; the same pressures and temperatures as before.

If the loop is full of steam only the water will rise in the drop leg,  $D, 5 \times 2.509 = 12.545$  feet to balance the difference in pressure. Adding this height to the required lift, it will be found that the top of the water column should stand  $12.545 + 12 = 24.545$  feet above the bottom of the riser when the system is in equilibrium. Now, as the mingled water and steam in the riser pipe weighs more than the steam, the pipe must be lengthened still more; assuming the previous specific gravity of one-fourth that of water, this additional height will naturally be  $24.545 \text{ feet} \div 3$  or 8.182 feet, one-fourth of the extra height being above the present level, and three-fourths below. Adding together  $24.545$  and  $8.182$  feet, the result gives 32.727 feet for total height of riser pipe, or subtracting the 12 feet lift, gives 20.727 feet as the height of the drop leg above the water level in the boiler.

SURFACES AND CAPACITIES OF PIPES.

The size of pipes should not exceed  $1\frac{1}{4}$ " to  $1\frac{1}{2}$ ", although the horizontal H may be as large as  $2\frac{1}{2}$ ", to facilitate condensation. If the pipes are insufficient, add more pipes rather than increase the bore.

No condensation should take place in the riser pipe, and it should be carefully clothed, but the horizontal pipe needs only to be protected against freezing.

The presence of air in the loop often leads to failure, and a small cock should be placed at the highest point to expel air when starting, also to be opened at intervals, during continuous working, for a similar purpose.

SURFACES AND CAPACITIES OF PIPES.

SIZES OF PIPES.	$\frac{1}{4}$ in.	$\frac{3}{8}$ in.	1 in.	$1\frac{1}{4}$ in.	$1\frac{1}{2}$ in.	2 in.	2 $\frac{1}{2}$ in.	3 in.	3 $\frac{1}{2}$ in.	4 in.	4 $\frac{1}{2}$ in.	5 in.
1. Outside circumference of pipes in inches.	2.632	3.259	4.138	5.215	5.909	7.461	9.932	10.99	12.56	14.13	15.70	17.47
2. Length of pipe in feet to give a square foot of outside surface.....	4.52	3.63	2.90	2.30	2.01	1.61	1.32	1.09	.954	.849	.763	.686
3. Number of square feet of outside surface in ten lineal feet of pipe....	2.21	2.74	3.44	4.34	4.97	6.21	7.52	9.16	10.44	11.78	13.09	14.56
4. Cubic in. of internal capacity in ten lineal feet of pipe....	36.5	63.9	103.5	179.5	244.5	422.6	573.9	846.6	1186.4	1527.6	1912.6	2308.8
5. Weight in lbs. of water in ten lineal feet of pipe.....	1.38	2.31	3.75	6.5	8.8	14.6	20.8	32.1	43.6	55.4	69.3	86.9

Pipe manufactured from double thick iron is called X-strong pipe, and pipe made double the thickness of X-strong is known as XX-strong pipe. Both X-strong and XX-strong pipe are furnished with plain ends—no threads unless specially ordered.

PLUMBING.

*Lead working* is an ancient art, both in sheets and in pipes. The word plumbing is derived from the Latin word for lead, hence a plumber is a lead worker. Lead is one of the elementary metallic substances; it is used largely in combination with tin, copper, etc., and is the main alloy used in a measure to debase and cheapen nearly all the higher metals, even silver and gold. It is 11.4 times heavier than water, bulk for bulk; lead melts at a temperature of 617° Fahr.

The tenacity of lead is extremely low, in comparison, its tenacity is only one-twentieth that of iron; it is so soft that it may be scratched with the thumb nail. If sufficient heat is applied lead boils and evaporates; it transmits heat very slowly; of seven common metals it is the worst conductor, therefore it is good for hot water pipes. Mixed with quicksilver it remains liquid. An advantage to be found in the use of lead is its durability and comparative freedom from repairs. In London, soil and drain water pipes which have been fixed 300 to 500 years are as good now as the day they were first made.

The processes of lead working are executed by manual dexterity acquired by long practice, and to do the work properly requires special tools. Some of these are used in common with other departments of mechanics, but are none the less necessary in lead working. Among the principal tools are *saws* such as a compass saw and double-edged plumber's saw; *spirit levels*, *looking glasses* used in making underhand joints, etc.; the *plumber's torch*, used also by engineers to explore the interior of boilers and other dark places about the steam plant; *chisels*,

where  $W_c$  = weight of condensation, in pounds per hour;  
 $A_f$  = area of external surface of pipe, in square feet;  $T'_a$  =  
 steam temperature at given pressure, in degrees Fahrenheit;  
 $T''_a$  = temperature of surrounding air, in degrees Fahrenheit;  
 and  $H_c$  = latent heat of steam at given pressure, in B.t.u. per  
 pound.

*Example.*—The external-surface area of 4-in. pipe is 1.178 sq. ft. per  
 ft. of length. What will be the quantity of condensation in 40 ft. of  
 bare 4-in. pipe carrying steam at 105 lb. gage, when the surrounding air  
 temperature is 60°F?

*Solution.*—A table of the properties of saturated steam (from the  
 author's "Practical Heat") gives the temperature of steam at the given  
 pressure as 341°F., and the latent heat as 877.2 B.t.u. By formula (100),  
 $W_c = 2.74(T'_a - T''_a) \div H_c = 2.7 \times 1.178 \times 40 \times (341 - 60) \div$   
 $877.2 = 40.75$  lb. per hr.

**391. Excessive loss of heat from steam pipes may be prevented**  
 by covering the pipes with heat-insulating material. Incombustible mineral substances, such as magnesia and  
 asbestos, are commonly used for this purpose. All steam-  
 pipe coverings should be at least 1 in. thick for temperatures  
 up to 300°F.; 2 in. thick up to 500°F.; and 2 or 3 in. thick,  
 depending on whether the pipe is less or greater than 6-in.  
 diameter, for temperatures above 500°F. With a good cover-  
 ing, the heat loss may be reduced to about 15 per cent of that  
 occurring with bare pipe, or even less.

Among the newer materials for insulation of steam-pipe  
 lines developed during the past several years are the following:  
*Laminated asbestos*, made up in layers of 20 to 40 to the inch,  
 cemented together with silicate of soda, is recommended for  
 temperatures up to 500°F. *Eighty-five per cent magnesia* con-  
 sists of approximately 85 per cent by weight of carbonate  
 of magnesia and 10 to 15 per cent of asbestos fiber, and is  
 used for temperatures up to 600°F. *Corrugated asbestos* is  
 made of alternate layers of corrugated and plain asbestos.  
 paper cemented together with silicate of soda, and is limited  
 generally to temperatures of about 300°F. *Mineral wool*,  
 made by blowing steam through fused clayey limestone or  
 furnace slag to fiberize it, comes in molded blocks for pipes  
 and fittings and is recommended by the manufacturers for

service temperatures up to as high as 1600°F. *Glass wool*,  
 made by blowing steam through streams of molten glass, is  
 also made in blocks but is used only up to about 600°F.  
*Expanded mica*, *wool felt*, *hair felt*, and *cork* are used for moder-  
 ate temperatures up to about 200–250°F. *Asbestos blankets*  
 are recommended for serv-  
 ice up to 900°F., depend-  
 ing on the quality used.  
*Amosite asbestos* is a long-  
 fiber brown asbestos, used  
 for temperatures up to  
 1200°F. *Insulating ce-  
 ments* are graded as high,  
 medium, and low, and  
 consist of long- or short-  
 fiber asbestos with clay  
 binders, and in some cases  
 Portland cement.

The condensation in  
 high-pressure steam pip-  
 ing may be returned to the  
 boilers with a Holly Loop  
 (Fig. 461). The conden-  
 sation gravitates to a re-  
 ceiver *A*, where it is  
~~broken into a spray by~~  
~~passing through a perfor-~~  
~~ated plate.~~ Con-  
 nections should be made to  
 the receiver from all parts  
 of the piping system in  
 which water might be-

come pocketed. Because of the discharge of steam from the  
 discharge chamber *C* through the vent pipe *P* and the reducing  
 valve into the feed-water heater, the pressure in the discharge  
 chamber is less than that in the receiver. Hence a current of  
 water spray, mixed with steam vapor, ascends through the riser  
*R*. The steam and water separate in the discharge chamber.  
 The water gravitates to the boilers through the drop leg

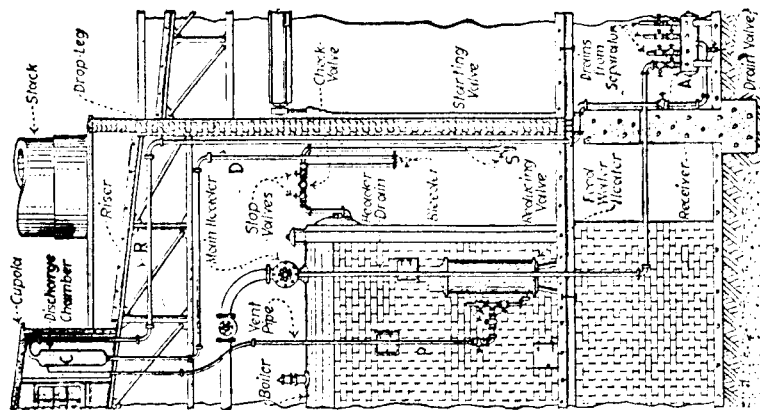


FIG. 461.—The Holly steam loop for draining high-pressure piping.

D. The discharge chamber is placed at an elevation that will ensure a sufficient hydrostatic head to overcome the excess of boiler steam pressure over the discharge-chamber steam pressure. Circulation in the loop is started by opening valve S. When steam appears, valve S is closed and the reducing valve is opened. **No pump or injector is therefore necessary.**

**392. Steam piping systems for power plants.** The connections to a boiler, as well as the piping immediately adjacent to it, are governed by the A.S.M.E. Power Boiler Code and in addition require the approval of an insurance underwriters' company. The rest of the steam piping in power plants comes under the American Standard Code for Pressure Piping, referred to previously in this division. Both Codes should be read and understood by the engineer in charge of the installation of new or additional steam power piping in any plant. These Codes set minimum safety standards for the selection and installation of suitable materials, and make reference to the standard specifications of the A.S.M.E. or A.S.T.M. by which these may be secured. They also designate the proper dimensional standards for the elements comprising the piping systems, the supports, methods of erection, and performance of operating tests. Among the provisions are the following: Valves are required to be marked by the manufacturer with reference symbols indicating the service conditions for which they are guaranteed; stop valves for services over 212°F. must have bonnets backseated to provide for repacking under pressure; escaping steam from relief or safety valves must have protection to prevent injury to men or damage to the plant; relief valves must be of adequate capacity to protect low-pressure systems if the reducing valve fails to close; a pressure gage must be installed in all cases on the low-pressure side of a reducing valve. For the latest and most complete information, the reader is referred to the latest revision of the Codes themselves.

**393. Main steam piping.** The steam piping between the boilers and the turbines constitutes the most important piping in any power plant. Several different methods are in common use for connecting boilers and turbines, the simplest of which is the type wherein one or two boilers are connected

directly to their respective turbines as indicated in Fig. 462. This is commonly known as the unit boiler-turbine system. It is considered good practice to provide a crossover, indicated by the dotted line in Fig. 462, in order to permit the operation of either turbine from the adjoining boiler or group of boilers. These crossovers may, in a plant having a number of turbines and boilers, appear to be a continuous header system, although steam is rarely carried farther than the next adjacent unit.

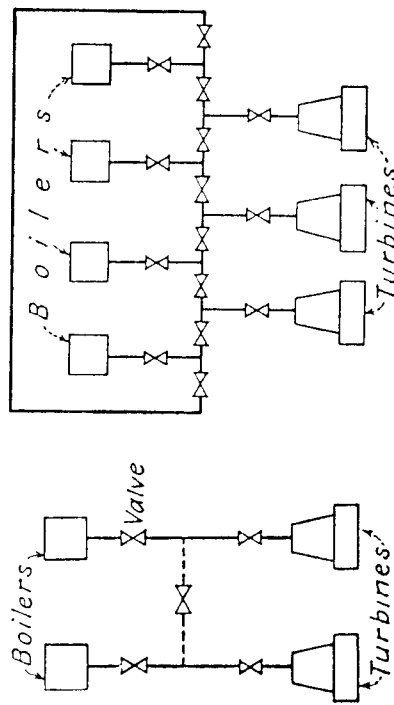


Fig. 462.—Unit boiler-turbine system.

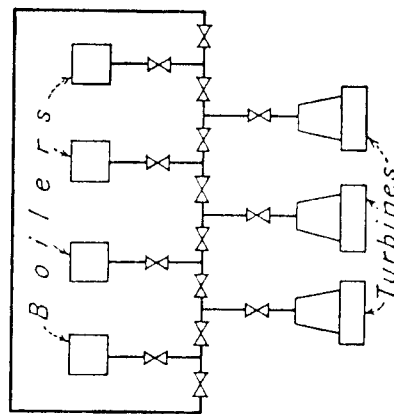


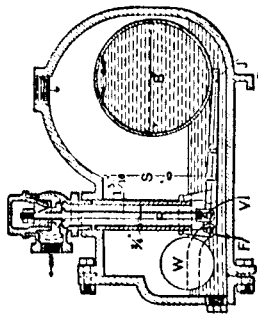
Fig. 463.—Ring-header system.

Figure 463 shows an alternate type of arrangement, known as the ring-header system, which is designed to provide great flexibility of operation between boilers and turbines. Steam may be supplied from any one of a number of boilers to any particular turbine with little appreciable pressure drop. The valves are arranged so that work can be performed on any one valve without shutting down more than one boiler or turbine. The horizontal section with eight valves seen in Fig. 463 is known as the "header." A typical steam header in an industrial plant is shown in Fig. 464. A steam header in an industrial plant is illustrated in Fig. 465.

The single-header system (Fig. 466) is still found in some older installations, and is the least expensive though hardly the most convenient arrangement, since if it were necessary to repair the section between boilers C and D, boilers A, B, and C would not be available for supplying the prime movers

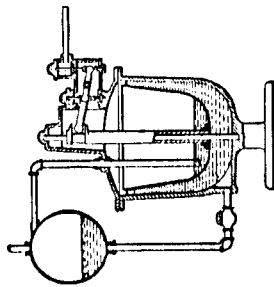


128. **BALANCED STEAM TRAP.** The float B is always full of water and not liable to collapse. It is balanced by the counterweight W, at the other end of the valve lever, so that the float B opens the valve by the differential flotation of the weight and float, when the chamber, S, fills with water.



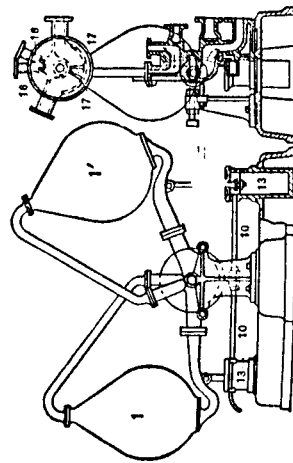
129. **RETURN TRAP.** Blessing type. For raising the water of condensation to a higher level than the water line of a boiler, to be returned to the boiler by gravity under equalized pressure.

The movable bucket operates a lever and the equalizing valves for discharging the water to a receiver by the boiler pressure and from the receiver to the boiler by gravity.



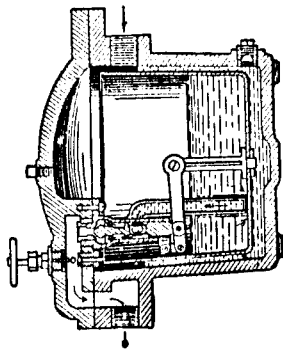
130. **AUTOMATIC BOILER FEEDER.** Feeds water to a boiler on the same principle as the pulsometer.

The feeder is placed about 4 feet above the water line of the boiler with water flowing to it by gravity or pressure. The weight of the water alternately filling the chambers, carries them down and opens a steam port in the axial valve to the boiler pressure, when the water flows into the boiler by gravity. At the same time the upper chamber is being filled by the condensation of its steam. It is made self-acting by having the steam pipe connect to the boiler at the high water gauge, at which point steam can not enter the chamber and the action repeats. The dashpots regulate the motion of the feeder.



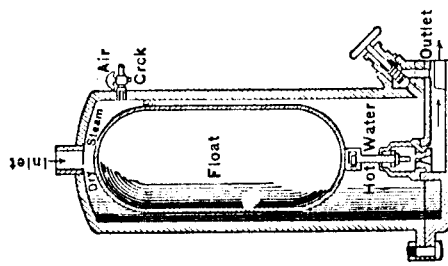
the water flows into the boiler by gravity. At the same time the upper chamber is being filled by the condensation of its steam. It is made self-acting by having the steam pipe connect to the boiler at the high water gauge, at which point steam can not enter the chamber and the action repeats. The dashpots regulate the motion of the feeder.

125. **AUTOMATIC STEAM TRAP.** Lawler type. The open float by its overflow and filling, sinks, and opens the discharge valve by its lever connection. When the float is emptied by the steam pressure, the float rises and closes the valve.

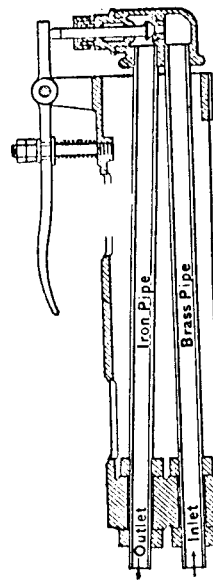


126. **FLOAT STEAM TRAP.** One of the several types of steam traps with sealed floats, this having a direct attachment of the float and valve which is designed to give a small amount of motion to the float for operating the valve.

The valve has a cage guide and its stem is loosely socketed to the float, so that any side motion of the float does not unseat the valve.



127. **DIFFERENTIAL EXPANSION STEAM TRAP.** The opening and closing of the valve for discharging the water of condensation



tion is effected by the differential expansion and contraction of the brass and iron tube, being 3 to 2. The setting of the valve is controlled by the adjusting lever, so that the water is discharged and when steam enters the brass tube it expands by the additional heat and closes the valve by lifting the seat.

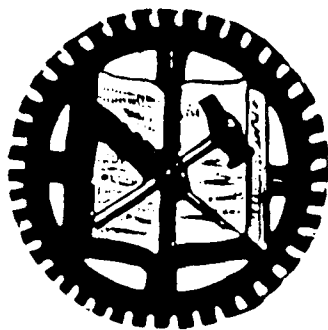
# STEAM INJECTORS: THEIR THEORY

AND

U S E.

TRANSLATED FROM THE FRENCH OF

M. LEON POCHET.



NEW YORK:  
D. VAN NOSTRAND COMPANY,  
23 MURRAY STREET AND 27 WARREN STREET.  
1890.

## P R E F A C E .

---

The following brief treatise was translated without abridgment from *Nouvelle Mécanique Industrielle*: M. LEON POCHET. It first appeared in its present form in *Van Nostrand's Magazine* for March and April, 1877.

The literature bearing on the subject of the Injector is not abundant, and to many engineers the philosophy of the action of the apparatus is obscure. In view of the fact that uses for the Injector have been devised other than the feeding of boilers, is judged to be a sufficient reason for the preparation of this little work.

# STEAM INJECTORS.

---

## GENERAL THEORY OF STEAM INJECTORS.

It is some years since M. Giffard introduced the injector apparatus which bears his name and which filled the scientific world with profound astonishment.

This ingenious apparatus, in which a jet of steam heading out of a boiler enters into the same boiler bringing with it a quantity of additional water, seems to proceed in accordance with a philosophical law contradictory to the ordinary laws of physics. It was in appearance a sort of perpetual motion. If the mechanical properties of heat had been better known, nothing would have appeared more simple.

M. Reech published, in 1858 (in the *Memorial du Genie Maritime*), a theory

founded upon laws of the old philosophy, which gives a good account of the functions of the Giffard injector.

The new theory which we proceed to give—of the Giffard injector in particular, and of steam injectors in general—rests upon the mechanical theory of heat. It seems the more important inasmuch as injectors are now applied to such a great variety of purposes.

We will describe first the action of an injector. A tube terminating in a conical pipe A, Fig. 1, discharges a jet of steam which comes from the boiler. This tube opens into a chamber B B, which communicates with a reservoir of cold water RR by a vertical tube CC. It is this water which is introduced into the boiler.

Under the action of the jet of steam the air in the chamber B is rarefied and the rarefaction results in the atmospheric pressure raising the water of the reservoir in the tube C. As soon as the cold water comes in contact with the steam in the chamber B a portion of the steam

is condensed and the apparatus is so regulated that this condensation is complete. Then we have, merely, a jet of liquid to pass on through the contracted

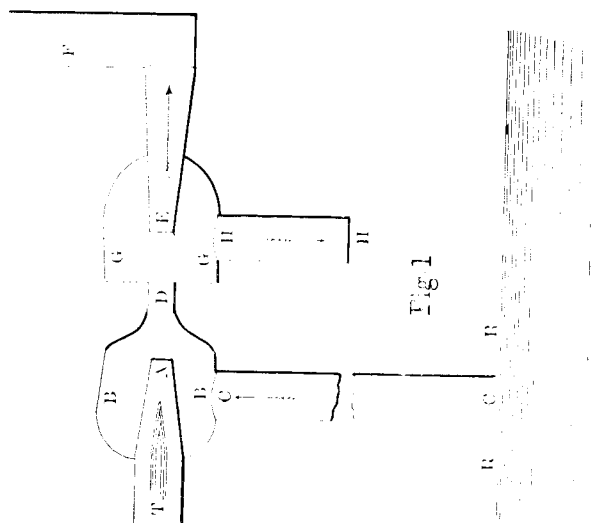


Fig 1

section D and be introduced into the conical diverging tube which communicates with the boiler. The tube EE is nothing more than a Venturi tube.

In such a tube, water introduced with

a certain velocity  $V$  would be able to overcome the pressure due to the height  $\frac{V^2}{2g}$ , provided that the liquid column be uninterrupted and the widening be progressive; or if we call  $\omega$  the section of the tube at its origin, and  $\omega'$  the section of the same tube at its entrance into the boiler,  $H$  the height of water corresponding to the effective pressure of the boiler, that is to say its absolute pressure diminished by one atmosphere, we shall have

$$\frac{V^2}{2g} \left( 1 - \frac{\omega^2}{\omega'^2} \right) = H.$$

In the Giffard injector we make

$$\frac{\omega^2}{\omega'} = 0,16,$$

whence

$$\frac{\omega^2}{\omega'^2} = 0,0256,$$

consequently

$$\frac{V^2}{2g} \times 0,9744 = H.$$

But we should be able to give to the

ratio  $\frac{\omega}{\omega'}$  greater value, and we can always assume approximately:

$$\frac{V^2}{2g} = H.$$

The condition that the liquid jet, through the tube  $EE$ , is uninterrupted, assumes that the jet is at too low a temperature to be transformed into steam at the atmospheric pressure in its passage through the chamber  $GG$ . Hence its temperature should be below  $100^\circ$ .

Should the temperature exceed  $100^\circ$  the working of the apparatus is imperfect. We are warned by a production of steam which fills up the chamber  $GG$  and which escapes by the discharge pipe  $HH$ .

Then we should remove the pipe  $A$  of the contracted orifice  $D$  in order to increase the useful section of this orifice, or, we should lessen the quantity of steam of the jet by diminishing the orifice  $A$  by the conical rod  $T$ . Thus the conditions of the proper working of the apparatus are:

1st. That all of the jet of steam A be condensed by affluent water;

2d. That the temperature of the mixture be lower than the temperature of corresponding saturation at the mean pressure of G.

In case that the chamber G communicates with the atmosphere, the temperature of corresponding saturation is  $100^{\circ}$ . But it might happen that there be any pressure in the chamber G. It may be higher or lower than the atmospheric pressure. We will make no special hypothesis upon its value.

Call  $t_0$  the temperature of the boiler;  $t$  the temperature of the jet of steam at the moment that it fills the chamber BB. This temperature will be the temperature of saturation corresponding to the mean pressure. It is easy to see that this pressure equals the atmospheric pressure diminished by the height of the column of water CC, if the feeding reservoir RR is lower, and augmented by this height if it is higher.

$\tau$ , the temperature of the liquid jet at

the moment that it enters the divergent tube EE. This temperature is lower than  $100^{\circ}$  when the chamber GG communicates with the atmosphere, which is the case in the Giffard injectors;

$\theta$ , the temperature of the water in the reservoir RR.

Suppose one kilogramme of saturated steam issuing from the pipe A and containing a proportion  $x$  of steam.

Let  $y$  be the weight of water which the kilogramme of steam raises and conveys from the reservoir RR.

Let  $w$  be the velocity of the steam jet in A;

$V$  the velocity of the mixture at the entrance of the tube E. To solve the problem we will write two equations.

1st. We assume that since there is no heat lost or gained by the material of the apparatus, the sum of internal heat augmented by the calorific equivalent of the living force has not changed during the phenomena; for this heat should always appear under the form of heat, or under the form of living force. This is

in accordance with the theorem of living force developed by the theory of heat.

2d The theorem of rational mechanics relating to momentum is here applicable, as it always is, whatever the exchange of heat may be, for in the equation of this theorem the interior forces disappear. The amount of internal heat above  $0^\circ$  in a kilogramme of steam of the jet **A** is:

$$\int_0^t l dt + (r - A p u) x.$$

\* The internal heat of any humid vapor, that is, part liquid and part vapor, is determined as follows:

Let  $x$  = the weight of the vapor in a kilogramme of the mixture.

Then  $1 - x$  the weight of the water in a kilogramme of the mixture.

Then the excess of internal heat of the vapor at  $t^\circ$  compared with water at  $0^\circ$  is,

$$(r + L - A p u) x.$$

In this expression,

$L$  is the quantity of heat required to raise a kilogramme of the liquid from  $0^\circ$  to  $t^\circ$  when in contact with its vapor.

The calorific equivalent of the living force has for value  $\frac{A v^2}{2g}$ .

The total quantity of heat is

$$\frac{A v^2}{2g} + \int_0^t l dt + (r - A p u) x.$$

The internal heat of the affluent water is

$$v \int_0^t l dt.$$

$A$  is the reciprocal of the Mechanical Equivalent of heat, or  $\frac{1}{424}$ .  
 $p$  is the pressure.

$r$  is the latent heat of the vapor.

$u$  is the excess of volume of the vapor over the liquid which yielded it.

$p u$  is therefore our expression for work;

And  $A p u$  is its heat equivalent.

Now, as the latent heat liquid in the vapor is

$L(1 - x)$ , the total internal heat,

$$Q = L(1 - x) + (r + L - A p u) x$$

$$= L + (r - A p u) x.$$

Or if  $l$  is the specific heat of the liquid at the temperature  $t^\circ$ , then

$$L = \int_0^t l dt$$

$$Q = \int_0^t l dt + (r - A p u) x.$$



The living force is almost nothing and may be neglected; the internal heat augmented by the calorific equivalent of the living force before the mixture, will be then

$$\frac{Av^2}{2g} + \int_0^t ldt + (r - Apv)x + y \int_0^\theta ldt.$$

The mixture forms, the steam is completely condensed, there is a diminution of volume and production of negative mechanical work. The total internal heat is augmented by the calorific equivalent of the work corresponding to the condensation, and which is

$$Apv\bar{x}.$$

When the mixture passes through the contracted section D, the sum of the living force and of the internal heat is

$$\frac{Av^2}{2g} + \int_0^t ldt + rx + y \int_0^\theta ldt \quad . \quad . \quad (A)$$

The introduction commences in the tube EE, the total weight of the mixture is  $(1 + y)$ , its internal heat, since it is entirely in a liquid state, is expressed by

$$(1 + y) \int_0^t ldt,$$

And its living force is,

$$(1 + y) \frac{AV^2}{2g},$$

since V is the common velocity.

The sum of internal heat above O, and of the calorific equivalent of the living force at the inlet of the tube EE, is therefore

$$(1 + y) \left( \int_0^t ldt + \frac{AV^2}{2g} \right)$$

This new expression of the total heat should be equal to the expression in (A). We have the equation

$$\frac{Av^2}{2g} + \int_0^t ldt + rx + y \int_0^\theta ldt = (1 + y)$$

$$\left( \int_0^t ldt + \frac{AV^2}{2g} \right) \quad . \quad . \quad (B)$$

Now in consequence of the fundamental formula for the cooling of vapors, we have

$$\frac{Av^2}{2g} = \int_t^t ldt + r_0 x_0 - r_0 x^*.$$

Substituting this value in the preced-

\*  $r_0$  and  $r$  designating the quantities of heat of vaporization at the temperatures  $t_0$  and  $t$ .

The living force is almost nothing and may be neglected; the internal heat augmented by the calorific equivalent of the living force before the mixture, will be then

$$\frac{Av^2}{2g} + \int_0^t ldt + (r - Apv)x + y \int_0^\theta ldt.$$

The mixture forms, the steam is completely condensed, there is a diminution of volume and production of negative mechanical work. The total internal heat is augmented by the calorific equivalent of the work corresponding to the condensation, and which is

$$Apv\bar{x}.$$

When the mixture passes through the contracted section D, the sum of the living force and of the internal heat is

$$\frac{Av^2}{2g} + \int_0^t ldt + rx + y \int_0^\theta ldt \quad . \quad . \quad (A)$$

The introduction commences in the tube EE, the total weight of the mixture is  $(1 + y)$ , its internal heat, since it is entirely in a liquid state, is expressed by

$$(1 + y) \int_0^t ldt,$$

ing equations it gives, after some transformations,

$$\int_0^t ldt + r_v c = (1+g) \left( \int_0^t ldt + \frac{AV^2}{2g} \right) (C)$$

This is the equation of living force. We will now establish the equations of momentum. We shall have them due to the contracted section D,

$$\omega V,$$

for this section is necessarily equal to that of the inlet of the tube EE and the weight of water has for its value

$$1000\omega V.$$

Its mass is

$$\frac{1000\omega V}{g}.$$

In short, the expression for momentum is

$$\frac{1000\omega V}{g} = \frac{1000\omega V^2}{g}$$

The amount of work of the affluent water from the reservoir RR may be neglected. As for the steam jet A, the amount delivered per second is evidently equal to that of the final mixture divided by  $(1+g)$ , and its velocity is  $v$  and its

quantity of work is therefore, before its passage into section D

$$\frac{1000\omega V}{g} \frac{v}{1+g}.$$

and we find also for the increase of the momentum during a second from one side to the other of the contracted section D

$$\frac{1000\omega V}{g} \left( V - \frac{v}{1+g} \right)$$

Let us call  $\pi$  the pressure per square meter in the chamber GG, which is equal to the atmospheric pressure in the Giffard injectors, and P the pressure in the chamber BB which is equal to the atmospheric pressure diminished or increased by the column of water CC according as the supply reservoir RR is below or above the apparatus.

The contracted section D separates the jet into two parts, that above being subjected to the pressure P, and that below to the pressure  $\pi$ . The impulse of exterior forces during the exchange of velocities will be, per second

$$(P-\pi)\omega,$$

We have then, in accordance with the principle of equality of moments

$$\frac{1000\omega}{g} V \left( V - \frac{w}{1+y} \right) = (P - \pi)\omega,$$

whence

$$V \left( V - \frac{w}{1+y} \right) = \frac{(P - \pi)g}{1000} \dots \dots (D)$$

The two equations (C) and (D) include the theory of steam injectors. I copy here:

$$\begin{aligned} \int_{\theta}^{\tau} l dt + r_0 x_0 &= (1+y) \left( \int_{\theta}^{\tau} l dt + \frac{AV^2}{2g} \right), \\ V \left( V - \frac{w}{1+y} \right) &= \frac{(P - \pi)g}{1000} \dots \dots (D) \end{aligned} \quad (C)$$

#### GIFFARD INJECTORS FOR FEEDING BOILERS.

In the Giffard injector (Fig. 1) the reservoir R R is ordinarily near the chamber B B, the pressure P is nearly equal to the atmospheric pressure, and as the chamber G G is in communication with the atmosphere,—we can take

$$P = \pi,$$

and we ought to have

$$\tau < 100^\circ.$$

Equation (D) of the moments reduces to

$$V - \frac{w}{1+y} = 0,$$

whence

$$V = \frac{w}{1+y}.$$

Take now the equation (C). In the second member of that equation we may neglect the term  $\frac{AV^2}{2g}$ .

In effect the range of temperature  $\tau$  and  $\theta$  is always large enough. The following table demonstrates that V varies almost precisely as the difference  $(\tau - \theta)$ :

The equation (C) gives then approximately,

$$1 + y = \frac{\int_{\theta}^{\tau} l dt + r_0 x_0 - \theta}{\tau - \theta} \dots \dots (E)$$

Under this form we observe that y diminishes as  $\tau$  increases. The mini-

WEIGHT OF WATER RAISED AND  
INJECTOR FOR

Press-  
5 ATMOSPHERES.  
(152, 22),  $m = 714m$ .

Value of $\theta$	Temper- ature of the Mixture.	Weight of Water raised per kilogr'm of steam suppos'd to be dry $y$	Velocity of the Mixture per second. $V$	Height to which the jet is raised. $\frac{V^2}{2g}$	$\frac{V^2}{y \frac{2g}{}}$
$\theta = 13$	100	6.35	97.29	482.3	m.
	80	8.55	74.87	285.7	m.
	60	12.61	52.54	140.7	m.
	40	22.70	30.17	46.4	m.
	20	90.42	7.82	3.12	m.
	13	$\infty$	0	0	m.
$\theta = 50$	100	11.06	59.29	179.2	m.
	80	19.10	35.57	64.5	m.
	60	59.50	11.85	7.17	m.
	50	$\infty$	0	0	m.

VELOCITY OF MIXTURE IN GIFFARD  
FEEDING BOILERS.

URE OF THE BOILER.

3 ATMOSPHERES.  
(133, 91),  $m = 596m$ .

Mechan- ical Work pro- duced. $\frac{V^2}{y \frac{2g}{}}$	Weight of Water raised per kilogr'm of steam suppos'd to be dry $y$	Velocity of the Mixture per second. $V$	Height to which the jet is raised. $\frac{V^2}{2g}$	Mechan- ical Work pro- duced. $\frac{V^2}{y \frac{2g}{}}$
km.	k.	m.	m.	km.
3063	6.29	81.73	340.5	2141
2443	8.47	62.94	201.9	1710
1774	12.50	44.15	99.4	1242
1053	22.50	25.36	32.8	737
282	89.63	6.57	2.21	197
0	$\infty$	0	0	0
1981	10.95	49.88	126.8	1389
1232	18.92	29.95	45.6	864
425	58.74	9.97	5.07	298
0	$\infty$	0	0	0

imum of  $y$  corresponds then with the maximum of  $\tau$ , that is to say, at  $100^\circ$ .

We see also that  $y$  increases when  $\theta$  increases: that is to say, in proportion to the heat of the feed water.

$y$  increases in the same proportion that the temperatures  $\tau$  and  $\theta$  approach each other in value. Consequently when  $\theta=100^\circ$   $y$  is infinite.

Experience demonstrates that the action of the injector ceases before reaching this limit, at about  $70^\circ$ .

We are able then to state the following propositions.

1st. The proportion of conveyed water increases, and, consequently the velocity of the mixture diminishes when the temperature of the water in the supply reservoir is raised.

2. The proportion of conveyed water increases when the temperature of the mixture diminishes. It is a minimum when the temperature of the mixture is of  $100^\circ$ . The velocity then attains its maximum.

3d. It diminishes, on the contrary,

when the steam is not dry and the proportion of water which it contains increases.

On pages 20 and 21 is a table of the values of  $y$  and of  $V$  for the boiler pressures of five and three atmospheres and the temperatures of  $13^\circ$  and  $50^\circ$  of the feeding water, the steam being dry.

The proportion of water raised increases rapidly as the temperature  $\tau$  of the mixture diminishes.

The velocity diminishes in nearly the same ratio.

The quantity of water raised corresponding to the boiler pressures five atmospheres and three atmospheres are nearly the same, but the velocities are widely different. If we would have the velocity, and, consequently the composition of the mixture corresponding to the pressure of the boiler, we must make

$$\frac{V^2}{2y} = 41,32 \text{ for five atmospheres,}$$

$$20,66 \text{ for three atmospheres.}$$

whence

$$V = 28^m,50 \text{ for five atmospheres,}$$

$$20^m,15 \text{ for three atmospheres.}$$

These numbers correspond to

$y = 24.06$  for five atmospheres,  
 $y = 31.02$  for three atmospheres.

The temperature of the mixture is nearly  $40^\circ$  if the temperature of the feed water is  $13^\circ$ .

#### ACTION OF THE GIFFARD INJECTOR.

There are two ways of considering the action of the Giffard injector. We measure the mechanical work performed without taking into account the heat carried away by the mixture; or, with taking this heat into account.

Following the last mode of operation, which is the only rational one, when employed in feeding the boiler the injector performs good service. It is clear that, since there is no loss of heat outside, and that the final living force is nothing, all the heat carried away by the steam jet is restored in the mixture, excepting that corresponding to the mechanical work accomplished,  $\frac{AV^2}{2g} y$ . Equation (C) is the mathematical expression of this fact.

It is not necessary to take into account the friction in the tubes, if we consider them impervious to heat, for the friction produces heat which is not lost by external radiation, but is found in the internal heat of the mixture.

The quantity of heat augmented by the living force in the mixture at the moment of its entrance into the convergent tube counted above, the temperature  $\theta$  (which is the exterior temperature, and which serves as the starting point for the temperature in the equation (C) is

$$(1+y) \left( \int_0^{\tau} dt + \frac{AV^2}{2g} \right).$$

The portion  $(1+y) \frac{AV^2}{2g}$  represents the heat equivalent of the living force of the mixture. This living force in part disappears in the work of introduction into the boiler. If things are so regulated that the height  $\frac{V^2}{2g}$  precisely correspond to the relative pressure of the boiler, the living force  $(1+y) \frac{V^2}{2g}$  is

effectually destroyed by the back pressure of the boiler; the introduction into the boiler will have no velocity, and the quantity of heat introduced will be definitely

$$(1+y) \int_0^{\tau} l \, dl,$$

or about

$$(1+y) (\tau - \theta).$$

If the velocity  $V$  of the mixture is greater than that which corresponds to the relative pressure  $H$ , of the boiler (measured by a column of water), the mixture will possess a certain living force

$$\frac{V^2}{2g} - H,$$

at its entrance into the boiler, but this living force becomes heat, in the motions which it occasions, so that no more heat can disappear than the quantity

$$AH (1+y).$$

Thus we know whatever the velocity  $V$  of the mixture, there will disappear only the quantity of heat corresponding to the work

$$(1+y) H,$$

of the introduction into the boiler. This work comprises two terms:

$$yH \text{ and } 1 \times H.$$

The first represents the useful work in feeding; the second corresponds in reality to a quantity of heat which ought to be found in the heat of the mixture; this is a loss which is balanced by a previous gain made by the steam at the moment of exit from the boiler.

Suppose, then, that the velocity  $V$  of the mixture be precisely that which gives

$$\frac{V^2}{2g} = H,$$

so that the introduction of the mixture into the boiler be made without velocity: determine, by experiment, the quantity of water raised  $y$ , its temperature  $\tau'$ , and calculate the same temperature by the formula (E). The heat which should be brought back to the boiler is, theoretically,

$$(1+y) (\tau - \theta).$$

The heat brought back is, in reality,

$$(1+y) (\tau' - \theta).$$

There is then, practically, a loss of heat

$$(1+y)(\tau-\tau').$$

Add to this loss the loss of heat resulting from work accomplished,

$$\frac{AV^2}{2g}y,$$

we have for total loss

$$(1+y)(\tau-\tau') + \frac{AV^2}{2g}y.$$

This waste of heat applied to the introduction of  $y$  kilogrammes of water into the boiler, gives for waste of heat per kilogramme:

$$i = \frac{1+y}{y}(\tau-\tau') + \frac{AV^2}{2g} \quad \text{. . . (F)}$$

Here is an experiment given by M. Reech. M. Giffard succeeded in feeding a boiler at five atmospheres, by conveying a weight of water equal to fifteen times that of the steam. The temperature of the mixture was  $48^\circ$ , the affluent water being  $13^\circ$ . We have then, in this experiment:

$$\begin{aligned} t &= 13^\circ \\ y &= 15. \end{aligned}$$

The formula (E) gives  
 $\tau = 53^\circ.01$ .

Now, then, the experiment indicates  
 $\tau = 48^\circ$ .

Consequently,

$$\tau - \tau' = 5^\circ.01.$$

Now the waste of heat per kilogramme of feed water is, (equation F):

$$i = \frac{16}{15} + 5.01 + \frac{41.32}{424}$$

$$= 5.34 + 0.097 = 5.44 \text{ heat units.}$$

This number represents  $\frac{15.5}{100}$  of the difference of temperature  $(\tau - t)$ .

This quantity of heat really disappears and is not found again. All other quantities of heat carried out of the boiler by the jet of steam  $y$  have been returned by the mixture.

Now, consider an ordinary supply pump, which introduces water into the boiler at the temperature of  $13^\circ$ . This pump is operated by the engine, and produces useful work,

AH



( $\tau - \theta$ ), but as the heating apparatus never uses but  $\frac{2}{3}$  of the heat developed by the combustion there will be  $\frac{1}{3}$  of the heat lost. The total consumption of heat will be then,

$$j=66, 6 \text{ AH} + \frac{1}{3} (\tau - \theta).$$

By feeding by means of an injector, we had found the loss of heat to be,

$$i=0, 155 (\tau - \theta).$$

It is easy to see that the first is the more important. Suppose, for example, a pressure of five atmospheres, we will have:

$$\begin{aligned} H &= 41.32, \\ \tau &= 48^{\circ}, \\ \theta &= 13^{\circ}, \end{aligned}$$

$$j=18 \text{ 20 heat units, } i=5.44 \text{ heat units.}$$

In this case, the cost of feeding by means of an injector is less than one-third of that of feeding by means of a pump.

These results would be somewhat modified if we had the use of a good condensing engine. Here the work of the engine is 10-100; that of the pump,

(H=height of water corresponding to the excess of the boiler-pressure over that of the condenser), per kilogramme of feeding water, but it utilizes only a fraction  $k$  of force by reason of the friction or resistances of various kinds.

Now this force is only that of the steam; and we know that ordinary non-condensing steam engines use scarcely three parts in 100 of the heat transmitted to the boiler; then the introduction of a kilogramme of water into the boiler, by means of a feed-pump, requires an expense of heat of

$$\frac{1 \text{ AH}}{0.03 \text{ } k}.$$

The co-efficient  $k$  of the ordinary pump is 0.50, consequently this quantity of heat has for its value

$$66, 6 \text{ AH.}$$

Observe that the water introduced is not of the temperature  $\theta$  of the supply reservoir. To raise the temperature of this water from  $\theta$  to  $\tau$  it will be necessary to consume a quantity of heat

if well established, 60 100, introducing water from the condenser at a temperature of  $50^{\circ}$ . The injector should work equally with the water of the condenser. We should always have  $y=15$ .

The value of  $\tau$  resulting from equation (E) would be

$$\tau=87^{\circ}, 70,$$

If we admit that the loss of heat by the injector will be more than 15.5-100 of the difference  $\tau-\theta$  we will have for this loss

$$i=0,155 \times 37,7=5 \text{ heat units, } 84.$$

The loss of heat from feeding by means of a pump, and of heating the water from  $50^{\circ}$  to  $87^{\circ}, 70$ , will have for value

$$j=\frac{1}{0.10} \frac{AH}{0.60} + \frac{1}{3} (87.70-50)=14.12 \text{ heat units.}$$

This is more than double the number 5.84 heat units. The economic advantage is always on the side of the Giffard injector; and this apparatus possesses also a great simplicity in adjustment and working, and an important economy of heat. The injector gains from nine to

thirteen *calories* per kilogramme (heat units) of water introduced into the boiler.

#### THE GIFFARD INJECTOR EMPLOYED AS A PUMP.

The Giffard injector is a suction and forcing pump, but its mechanical performance is weak, because the greater part of the heat is employed in raising the temperature of the water. The expression of the mechanical rendering per kilogramme of wasted steam is,

$$y \frac{V^2}{2g},$$

and its calorific equivalent

$$y \frac{AV}{2g}.$$

We have inserted in the table the values of the product  $y \frac{V^2}{2g}$  for the different cases (pages 20, 21).

We see, by an inspection of the table, that the velocity of the mixture varies from 0 to  $97^m, 29$ , that it corresponds to

the height of water from 0 to 482 metres. Consequently we are able to introduce water into a reservoir against a pressure of,

$$\frac{482}{10,33} = \text{about } 46 \text{ atmospheres.}$$

The mechanical work  $\frac{V^2}{2g}$  augments

with the velocity. At the temperature  $100^\circ$  of the mixture, there are 3,063 kilogrammes per kilogramme of wasted steam. If we compare this number with those of the preceding table, we see that it is only one-eighth of the theoretical work of steam in a non-condensing engine. The mechanical work would be one-third of that which would be performed by a pump placed in the same conditions for the same purpose.

If we take the numbers corresponding to the temperature of  $40^\circ$  of the mixture temperature for which  $\gamma = 22.70$ ,  $V = 30.17$ , the mechanical work produced is no more than 1,053 kilogrammes.

It is reduced to the third of that which it was for  $\tau = 100^\circ$ .

Considering, in a general manner, the Giffard injector as an exhausting pump, the problem ought to stand thus :

*The height to which it is necessary to raise the water being given, what will be the mechanical performance of the injector ?*

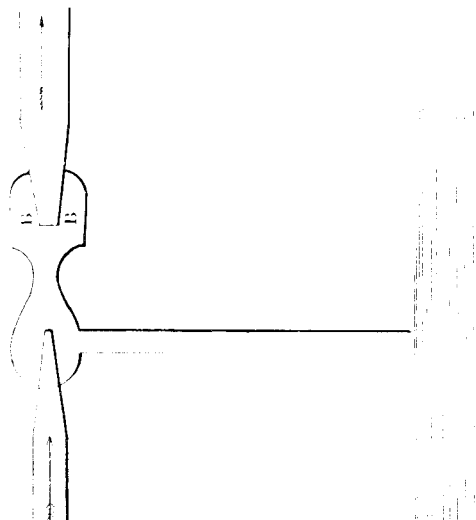


Fig 2

At first sight it is clear that we wish to place the apparatus at the greatest possible height above the reservoir to be drained. In doing this we diminish the

pressure in the chamber BB (Fig. 2). Consequently, we lower the temperature  $t$  of the steam jet, which is nothing more than the temperature of saturation corresponding to the pressure in the reservoir BB. The raising of the water into the chamber BB will be the same as raising it in a suction pump. We should be able then to raise it to the ordinary practical limits, that is to say, eight metres. Under these conditions, there will be the greatest possible fall of the temperature of the steam from the boiler to the orifice of the injector. We shall have the maximum of mechanical effect, and there will be, between an injector working thus, and an ordinary feeding injector, when the steam is at about  $100^{\circ}$ , the same difference as between a condensing, and a non-condensing steam engine.

The height being eight metres, the pressure in the chamber BB will be

$$10,33-8^m=2,33 \text{ of water}$$

or

$$176^{\text{mm}} \text{ of mercury.}$$

The temperature of corresponding saturation is about  $63^{\circ}$ . Going back to equations (D) (E), we will have for determining the minimum of the velocity of the mixture the equation

$$\frac{V^2}{2g} = h.$$

Equation (D) will give us

$$V\left(V - \frac{W}{(1+y)}\right) = -8g;$$

from these two equations we deduce

$$1+y = \frac{Vw}{V^2+8g} = \frac{\sqrt{hw}}{h+4}. \quad (\text{G})$$

The weight of water raised will be the greater as  $w$  will be greater. Now, the initial and final temperatures of the steam, during its flow, being determined,  $w$  depends only upon the moisture of the steam. The quantity of water raised will be greater in proportion as the steam is dry.

The mechanical work produced by the apparatus will be

$\tau=y(h+8)$ . (H)

Here is a table of quantities of water raised by an injector pump placed at eight metres above the exhausting reservoir, and fed by dry steam at five atmospheres:

INJECTION OF DRY STEAM AT 152,82. Velocity, $w=930^m$ .				
Total Height of Elevation.	Weight of Water raised per kilogram. of Steam used.	Mechani- cal Work obtained.	Temper- ature of Water raised.	$\tau$
$h+8$	$y$	$W$		
1+8=9	41.0	369	"	"
10+8=18	46.37	835	"	"
50+8=58	26.47	1535	"	"
100+8=108	19.18	2071	"	"
200+8=208	13.51	2810	"	"
500+8=508	8.30	4216	"	"
800+8=808	6.89	5163	100	

This table shows that the mechanical performance of the injector pump increases

rapidly with great heights, otherwise it is inferior to ordinary steam pumps. It is then for great elevations that the injector gives most satisfactory results. It would be little economy to employ it in common use, but it would be very useful for draining exceptional leaks in mines, when the ordinary pumps are not sufficient. The extreme simplicity of this kind of apparatus will often give it the preference over others that do more perfect work.

We ought again to remark the importance of placing the injector at the height of eight metres above the reservoir. Whereas, in the first table we have found a performance of 3,063 kilogrammetres for an elevation of 482<sup>m</sup>,3 the injector being at the level of the reservoir; the table above gives us a performance of 4,216 kilogrammetres for a height nearly equal to the former—that is to say, 508 metres.

Steam injectors are employed at the side of vessels for draining leaks in the hold. Under these circumstances the total height of lifting varies from five to ten metres, and each kilogranne of expended steam furnishes about 900 kilogranmetres. Now, in a ship's engine, one kilogranne of steam produces about 17,000 kilogranmetres, according to M. Freminville's treatise on Marine Engines. A pump in the hold would perform only one-fourth of this work, according to that, one kilogranne of steam would produce a useful work of 4,250 kilogranmetres.

Compare the number 900 kilogrammetres with this last, and we shall find the ratio of the work of the steam injector to that of the pump,

$$\frac{900}{4250} = 0,211.$$

According to M. Freninville, this number should, in practice, be diminished to 0.16.

We should consider two reservoirs of water  $R$  and  $R'$  (Fig. 3) placed at the heights, respectively  $H$  and  $h$ , above a

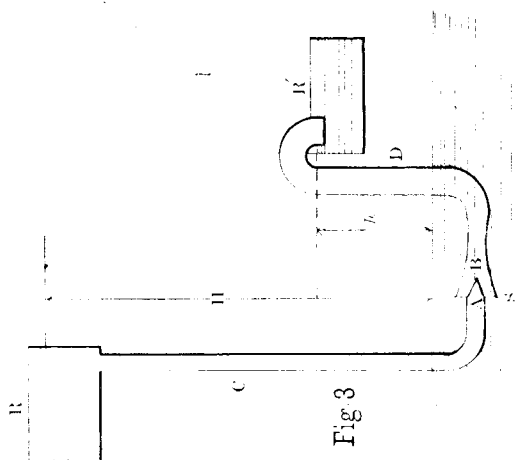


Fig. 3

reservoir S. R serves to raise the water from S, and discharge it into R'. Let us place below the reservoir R a vertical tube C, terminating in a nozzle A,

the interchange of quantities of motion will give us the equation

$$Pv = (P + P')u \quad \dots \quad (I)$$

Suppose that the water falls into the reservoir R' without appreciable velocity, then, all loss of living force will be avoided, consequently the velocity  $u$  will be determined by the condition

$$\frac{u^2}{2g} = h,$$

whence

$$u = \sqrt{2gh} \quad \dots \quad (J)$$

but

$$v = \sqrt{2gH} \quad \dots \quad (K)$$

To be sure we neglect the friction. Substitute these values of  $u$  and  $v$  in equation I, and we have

$$P\sqrt{2gH} = (P + P')\sqrt{2gh},$$

whence

$$\frac{P'}{P} = \frac{\sqrt{H} - \sqrt{h}}{\sqrt{h}} \quad \dots \quad (L)$$

To ascertain the modulus of such an engine, it will be necessary to divide the useful work

$$W_u = P'h,$$

entering into a funnel-shaped opening of a second vertical tube D, leading to the reservoir R'. If we open the stop-cock of the tube C, the water will run out by the nozzle A with great velocity, carrying a part of the surrounding liquid, and if the apparatus is well regulated it will be able to raise the water to the height of the tube D, and it would flow into the reservoir R'. The fluid vein proceeding from the upper reservoir R will, by communicating its motion to the water of the reservoir, carry it on to R'. We will consider the condition of the working of the apparatus.

Let P be the weight of water delivered at the nozzle A ;

P' the weight of water carried per second ;

$v$  the velocity of the water leaving the nozzle ;

$u$  the velocity of the water at its entrance into the tube B.

Suppose the velocity of the affluent water about the tube B to be neglected,

by the motor work or propelling force,  
 $W_m = P(H - h)$ .

This will give:

$$\rho = \frac{P'}{P} \cdot \frac{h}{H - h} = \frac{\sqrt{H} - \sqrt{h}}{\sqrt{h}} \cdot \frac{h}{H - h} = \frac{\sqrt{h}}{\sqrt{H} + \sqrt{h}};$$

or again,

$$\rho = \frac{1}{1 + \sqrt{\frac{H}{h}}} \dots (M)$$

The elevation  $H$  is necessarily higher than that of  $h$ . The minimum of ratio  $\frac{H}{h}$  is 1, hence the useful mechanical work will always be less than  $\frac{1}{2}$ .

We have supposed that the conveyed water comes to the nozzle  $A$  with no velocity. This is not so; and to make it more easily understood, we will take a very large funnel  $MN$  (Fig. 4).

If the suction of the tube at  $M$  differs but little from that at  $R$ , it is clear that the velocity of the water carried will be quite sensible.



Fig 4

Call this velocity  $v'$ . The equation (I) should be written in the following manner:

$$Pv + P'v' = (P + P')v \dots (N)$$

Since the apparatus is placed nearly at the surface of the water in the discharging reservoirs, the flow of water between the two points  $M$  and  $N$  can be produced only by difference of pressure. At  $M$  we have atmospheric pressure augmented by the slight height of water  $MP$ . At  $N$  we should have atmospheric pressure diminished by a small amount. If we call  $x$  this difference or *depression* expressed in head of water, we shall have

$$v'^2 = 2gx \dots (O)$$



The velocity  $v$  of discharge at the nozzle A will be given by the equation

$$v^2 = 2g(h+x) \quad \dots \quad (P)$$

and the common velocity of the water mixed in the tube R should satisfy the relation

$$u^2 = 2g(h+x) \quad \dots \quad (Q)$$

In short, if we call  $\omega$ ,  $\Omega$ ,  $O$ , the sections of the pipe and of the tube at M and at R, we shall have the relations :

$$\begin{aligned} P &= 1000 \omega v^2 & \dots & \dots & (Q) \\ P' &= 1000 \Omega v'^2 & \dots & \dots & (R) \\ P + P' &= 1000 O u^2 \end{aligned}$$

which gives the following :

$$O u^2 = \omega v^2 + \Omega v'^2.$$

The heights H,  $h$  and the weight P being given, the equations (N), (O), (P), (Q), (R), will allow us to calculate seven unknown quantities :

$$P', v, v', u, \omega, \Omega, O, x.$$

Here are eight unknown quantities. One of these is to be determined before

solving the problem. It is the value  $x$  of the difference of pressure, mentioned above, and which varies with the adjustment of the apparatus.

The formula expressing the work indicates in what way this value varies.

The useful work is

$$W_u = P'h,$$

and the motor work or propelling force

$$W_m = P(H-h).$$

The rendering of the system is then

$$\rho = \frac{W_u}{W_m} = \frac{P'}{P} \frac{h}{H-h}.$$

Now, from equations (N), (O), (P), (Q), we deduce :

$$\frac{P'}{P} = \frac{v-u}{u-v'} = \frac{\sqrt{H+x}}{\sqrt{h+x}} \frac{\sqrt{h+x}}{\sqrt{h+x}} \frac{h}{\sqrt{x}} \quad \dots \quad (S)$$

Substitute in the value of  $\rho$ , it becomes :

$$\begin{aligned} \rho &= \frac{\sqrt{H+x}}{\sqrt{h+x}} \frac{\sqrt{h+x}}{\sqrt{x}} \frac{h}{H-h} \\ &= \frac{\sqrt{h+x} + \sqrt{x}}{\sqrt{H+x} + \sqrt{h+x}}, \end{aligned}$$

or again,

$$\rho = \frac{1 + \sqrt{\frac{x}{h+x}}}{1 + \sqrt{\frac{H+x}{h+x}}} \quad (T)$$

If we compare this formula with (M), we discover that they are the same, when we make  $x=0$ . This supposes the velocity  $v'=0$ . It is easy to prove that the performance (T) increases with the difference  $x$ , and that it is always less than 1. We shall have the theoretical limit of its value in making  $x=10^m, 33$ . This difference may be artificially made by raising the injector above the reser-

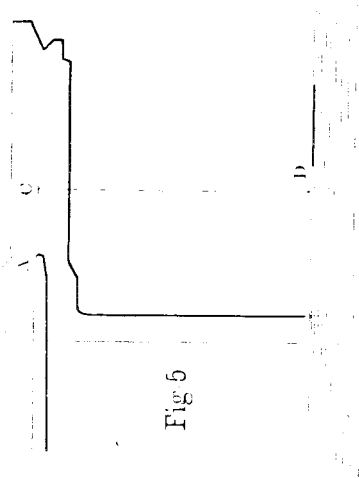


Fig 5

voir (Fig. 5), which will force the water to rise to the height C D.

Suppose

$$P=1, \quad H=500^m, \quad h=5^m.$$

If, at first, we suppose the depression to be nothing, the equations (L) and (M) give us :

$$P' = \frac{\sqrt{500} - \sqrt{5}}{\sqrt{5}} = 9,$$

$$\rho = \frac{1}{1 + \sqrt{100}} = 0.091.$$

To arrange the apparatus in a way to realize a depression of five metres, we make  $x=\rho$  in equations (S), (T), and we have :

$$P' = \frac{\sqrt{505} - \sqrt{10}}{\sqrt{10} - \sqrt{5}} = 20.85,$$

$$\rho = \frac{1 + \sqrt{\frac{5}{10}}}{1 + \sqrt{\frac{505}{10}}} = 0.211.$$

By this hypothesis the performance will have more than doubled. The

arrangement of the apparatus has then a great influence upon its action. It should be so that the water raised arrives with considerable velocity at the injector. For this object we direct currents of water by means of several successive funnels (Fig. 6).

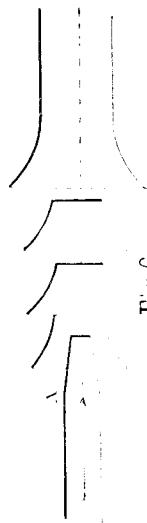


Fig. 6

This arrangement is found in several machines of English origin.

We readily understand that the jet of a steam injector may be used as a water injector.

A steam injector conveys, for example, fifteen kilogrammes of water per kilogramme of steam discharged, and communicates a velocity capable of surmounting a pressure of five atmospheres. In other words, the height to which the jet will be able to rise is 41<sup>m</sup>.32.

If we make this liquid jet pass through the nozzle A in Figs. (3), (4), (5), (6),

we will be able to carry a new quantity of water, which, it is true, is not raised so high. But if it is not necessary to raise the water above five meters to reach the 41<sup>m</sup>.32, it is clearly to our interest to adopt this arrangement.

The same considerations which we have recommended to place the injector above the supply reservoir are applicable here.

We will now give an account of the theoretical performance of the apparatus in (Fig. 7).

The proportion of water carried by the steam jet is reckoned from the height at which the injector is placed above the discharging reservoir, from the pressure of the boiler and from the amount of water practically raised. Equations (D) and (E) will furnish the proportion of the water carried and the velocity of the mixture. The reservoirs B and C being at the same pressure, that is to say, the atmospheric pressure diminished by the height A R, the equation (B) will give:

$$v = \frac{v''}{1 + g}$$

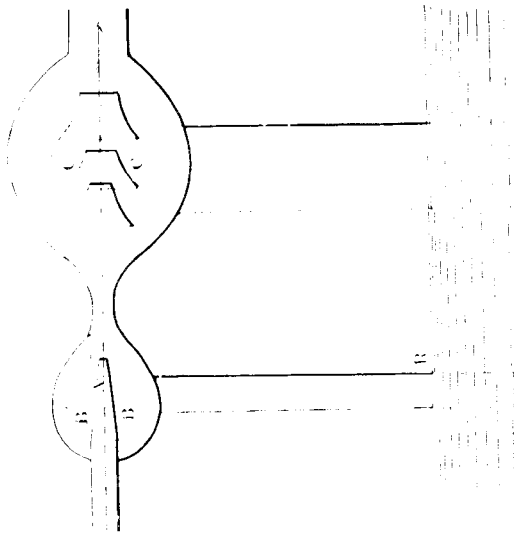


Fig 7

Knowing the velocity  $v$  of the liquid jet at its entrance into the chamber C, we calculate the weight of water carried by the jet by means of formula (S), in giving a start to the depressions  $x$ , and in calculating the dimensions of the suction apparatus by means of equation (R). We will remember in equation (O) that the velocity  $v'$  represents the projection upon the axis of the jet, of the real

velocity of the raised liquid streams. It will be necessary, then, to take into account the angle at which the funnels taper.

It is practice alone which can determine the best arrangement of this apparatus, whose theoretical principles only we have established.

We will show by an example how these theoretical calculations may be made.

*Example.*—To raise the water from the hold of a vessel, knowing the height of suction to be five meters; and the fall of the discharge, five meters. The pressure of the boiler is three atmospheres.

The table (3) gives us for the velocity of the flow of dry steam of three atmospheres at  $\frac{1}{2}$  atmosphere final pressure, 739 meters. It will be  $v=739$ . We will then have equation (D):

$$v = \frac{v'}{1+y}$$

If we make  $y=20$ , we will find:

$$v = \frac{739}{21} = 35^m 20.$$

UNDER DIFFERENT INITIAL AND FINAL PRESSURES.

water, containing  $x$  of steam and  $1-x$  of the numbers of the table below by  $1-x$

and Initial Temperatures.

5 at 152°,22	4 at. 144°,00	3 at. 133°,91	2 at. 120°,60	1½ at. 111°,74
499,13	545,02	512,22	521,70	527,99
meters.	meters.	meters.	meters.	meters.
..	..	..	..	..
..	..	..	..	..
..	..	..	..	..
283	349	..	..	..
421	420	279	..	..
501	485	372	..	..
555	519	417	190	..
584	553	460	276	..
613	588	504	347	..
645	625	549	463	274
678	666	596	477	366
714	688	621	498	409
734	710	647	543	451
755	735	676	578	494
777	763	706	615	539
802	792	739	655	585
830	826	770	699	636
861	866	821	751	694
899	918	877	814	765
947	993	958	906	865
1,017				

VELOCITY OF FLOW OF DRY STEAM PRESS-

The velocity of a mixture of steam and water may be obtained by multiplying

Pressures and Final Temperatures.		Pressures	
Press- ures.	Temper- ature.	8 at. 170°,81	7 at. 165°,54
			6 at. 159°,22
		485,79	489,71
			494,11
atmos.	degrees.	meters.	meters.
7	165,34	223	..
6	159,22	325	..
5	152,22	411	258
4	144,00	494	381
3	133,91	580	490
2,4	126,46	636	601
2	120,69	676	645
1,8	117,30	698	668
1,6	113,69	721	694
1,4	109,68	746	719
1,2	105,17	773	748
1,00	100,00	803	779
0,90	97,08	819	797
0,80	93,88	837	815
0,70	90,32	856	835
0,60	86,32	877	857
0,50	81,71	900	882
0,40	76,25	928	910
0,30	69,49	960	944
0,20	60,45	1,002	988
0,10	46,21	1,065	1,052
			1,037

The height designated by  $H$  is here :

$$\frac{v^2}{2g} = H = 63^m, 18.$$

Since the pressure which exists in chamber  $C$  about the funnels is only  $\frac{1}{2}$  atmosphere, we will be able to realize at the axis of the jet only a slight depression: we will suppose two meters. It will be, then,  $x=2$ , and we will have equation (S):

$$\frac{P'}{P} = \frac{\sqrt{63,18+2}-\sqrt{5+2}}{\sqrt{5+2}-\sqrt{2}} = 4,41.$$

The weight of water positively raised then will have been :

$$4,41 \times 20 = 88^k, 20,$$

per kilogramme of discharged steam. The mechanical work produced has for its value :

$$88^k, 20 \times 10^m = 882 \text{ kilogrammeters, per kilogramme of steam.}$$

The table (1), that for a weight of water raised to  $89^k, 63$ , which is nearly equal to  $88, 20$ ; the Giffard injector produces only **197** kilogrammeters. If we

keep the injector at five meters above the surface of the water to be raised and make use of this apparatus without the intervening injector of water, we should calculate the weight of water carried in the following manner. We should have for the necessary velocity to cause the jet to attain to five meters of height of discharge :

$$v = \sqrt{2g \times (5+5)} = 14 \text{ meters,}$$

$$1+y = \frac{739}{14} = 52,80,$$

whence

$$y = 51,80$$

The weight of water raised would be only  $51^k, 80$ , in place of  $88^k, 20$ , which we have found in employing the water injector.

The steam injector arranged with a water injector to serve as a pump has then a notable advantage over one used solely for steam. Several machines founded on these principles are used in England for draining mines. The preceding considerations demonstrate that

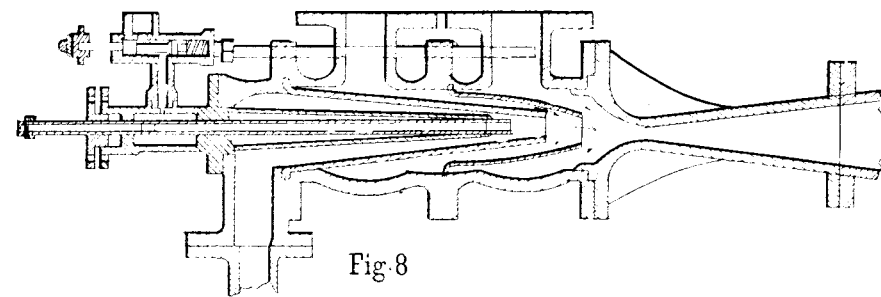


Fig. 8

the employment of these machines is not very convenient. Their use is justified only when it is necessary to accomplish rapid drainage with simple apparatus.

#### EJECTOR CONDENSERS.

Let us conceive that we put an injector on the escape pipe of a condensing engine. The apparatus will work as usual, that is to say, according as the escaped steam arrives it becomes condensed by the contact with the cold water furnished by the reservoir, will maintain a vacuum, and the mixture of water with the condensed steam imparting a great velocity will be capable of surmounting the excess of exterior atmospheric pressure over the pressure of escaping steam.

We shall thus be able, by the simple interposition of the injector apparatus, to supplant the air pump and all the accessories, and we shall economize the work absorbed by this pump, often very considerable.

Such is the principle of ejector con-

condensers, the employment of which tends, probably, to become general.

Professor Rankine has reported the experiments made in 1868, upon a condenser ejector of the Morton system. The apparatus (Fig. 8.) differs from ordinary steam injectors in that the cold water is drawn by the central tube; the escape of steam is distributed about the central jet by the very long and concentric funnels. In this way the living force of the cold water suffers no loss.

This living force is considerable, since the pressure which exists about the cold water, at the moment in which it mixes with the jet of steam, is necessarily less than the pressure at the escape, without which the steam would not flow out, so that the water possesses the velocity due to the excess of the atmospheric pressure over the pressure of the escape.

In the above named experiments Prof. Rankine has found the following results:

Per sq. centimeter.  
Absolute pressure at the boiler...3<sup>k</sup>, 427

Absolute pressure at commencement of escape..... 0<sup>k</sup>, 756  
Mean pressure maintained behind the pistons by the condenser ejector..... 0<sup>k</sup>, 299  
Pressure kept near the funnels. 0<sup>k</sup>, 210

Centigrade.  
Temperature of cold water... 8°, 4  
Temperature of water of condensation..... 30°, 3  
Weight of cold water employed per kilogramme of steam... 28<sup>k</sup>, 40

These results are, as we see, very satisfactory. They are not widely different from those which were obtained by the air pumps, but these latter require a notable expenditure of moving force.

In the machine experimented, Rankine valued the effective force at twenty-four horses, and the economy realized by the replacing one horse power air-pump at four per cent.

The theory of the condenser ejector does not differ from that of ordinary injectors, only there has been no account taken of the velocity at which the cold water arrives, that here has considerable



value, which is neglected in our general equation (C). To take account of it, we should add to the first member of this equation a term

$$\frac{AU^2}{2g} \rho,$$

representing the living force of the weight of water  $y$ .

In reality we will be able to neglect the term  $\frac{V^2}{2g}$ .

The determination of the velocity and the calculation of the dimensions of the apparatus are made, according to the method heretofore explained. This is a problem which presents no difficulties.

The Morton apparatus has one peculiarity which we ought to describe. To put the apparatus in motion we allow a priming of steam from the boiler to pass through a central tube. It may happen that the pressure falls below the proper limits for the working of the apparatus. Under these circumstances, the cold water flows into the escape-pipes, and

then into the cylinders. Every time that this inconvenience threatens the central steam jet is automatically opened by a spring piston, and its power communicates to the cold water jet a sufficient impulse to prevent its deviation towards the cylinders, and re-establishes the normal working of the machine.

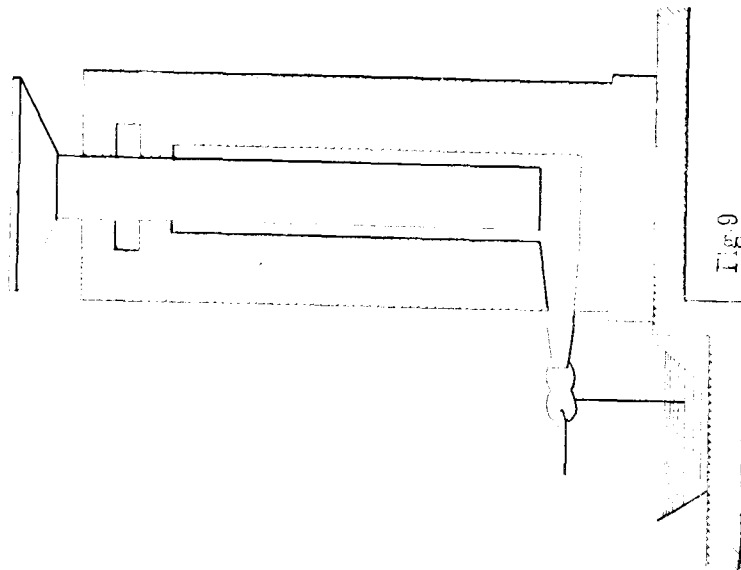
#### THE INJECTOR EMPLOYED IN A HYDRAULIC PRESS.

Suppose that we place an injector at the foot of a cylinder of a hydraulic press (Fig. 9). The jet of hot water may be introduced into the cylinder so that the pressure will be lower than that which corresponds to the velocity of flow. We should be able then to work a hydraulic press with a pressure

$$V^2 \\ 2g.$$

Suppose the pressure at the boiler be five atmospheres, the jet, according to table, pages 20 and 21, could rise to the height of 482 meters; this corresponds to

482,000 kilogrammeters per sq. meter,  
or to  
50 atmospheres.



The same table shows that the mechanical work realized in these conditions is only

3063 kilogrammeters, per kilogramme of steam used.

The work diminishes in the same proportion as the pressure diminishes. Consequently, it would be better to work with high pressure and so diminish the diameter of the hydraulic press.

This is a novel application of the injector, and may prove of service in situations where a hydraulic press is necessary, and where a pump of sufficient power is wanting.

Such an application has not yet been made, at least to our knowledge, and needs preliminary experiments.

#### PUMPING GAS BY STEAM — EXPLANATION OF THE FEEBLE WORKING OF FEEDING OR DRAINING INJECTORS.

That which causes the weakness of the performance of a steam injector employed as a draining pump is the disproportion between the height to which a liquid mixture may be raised, which is several hundred meters, and the height to which we in reality raise them. The apparatus

Now this circumstance will augment the performance, just as in the water injector.

Let  $W$  be the velocity of the steam,  $w$  that of affluent air,  $v$  that of the supposed mixture in the contracted section B B,  $y$  the weight of air drawn per kilogramme of steam.

The momentum of the steam will be

$$W \frac{W}{g},$$

that of affluent air,

$$\frac{w}{g}y,$$

that of the mixture,

$$(1+y) V.$$

Neglecting the difference of pressure in the sections A and B, we will have the following equation:

$$W + wy = (1+y) V,$$

whence we find

$$V = \frac{W + wy}{1+y}.$$

The living force of the steam was

$$\frac{W^2}{2g},$$

does not give its maximum of performance excepting for very great heights. The disproportion which exists between the specific gravity of the body raised, which is here water, and that which is carried along with it, that is to say, steam, is another source of loss.

In effect, the relative velocity of the water raised at the moment when it mixes with the condensed steam is so

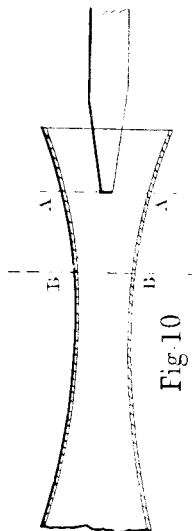


Fig 10

slight that is not worth taking into account. Let us suppose, on the contrary, that the steam escape in a gaseous medium which it will drag along by a sort of lateral friction (see Fig. 10), and as in a water injector. It may happen that the velocity of affluent air be considerable, consequently cannot be neglected.

that of affluent air,

$$\frac{w^2}{2gy},$$

that of air after the mixture,

$$\frac{V^2}{2gy}.$$

The performance of the apparatus will be then :

$$\rho = \frac{\frac{V^2}{2gy} y \left( 1 + \frac{w}{W} y \right)^2}{(1+y)^2}.$$

When we suppose the velocity of the material drawn to be nothing, as that in the Giffard injector for feeding boilers,  $w=0$ , and the formula of the performance is reduced to

$$\rho' = \frac{y}{(1+y)^2}.$$

We see at once how feeble this action is when  $y$  is not very small.

$$\begin{array}{ll} \text{When } y=1 & \rho' = \frac{1}{4} = 0,25 \\ \text{When } y=15 & \rho = 0,058. \end{array}$$

If, on the contrary, the ratio  $\frac{w}{W}$  be slightly increased, the term  $\left( 1 + \frac{w}{W} y \right)^2$  will increase very sensibly the value of the mechanical performance.

*For example.*—If we make  $y=15$  and  $\frac{w}{W} = \frac{1}{6}$  the ratio realizable in practice, the calculations give  $\rho=0,72$  in place of 0,058, which we have found in making  $w=0$ .

This simple discovery suffices to make us understand that steam injectors are more likely to give good results when employed as gas pumps than when used as water pumps.

#### LOCOMOTIVE EXHAUST.

The exhaust of a locomotive is only an application of preceding considerations. Only in these machines the steam jet is intermittent, notably augmenting the results which we should obtain with a continuous jet. People do not know

that the draught of the locomotive hearth is, if I may say so, due only to the escaping steam; this is, truly, the fundamental principle of the construction of these powerful machines.

Prof. Zeuner has demonstrated by calculation, and by experiment, that the weight of air drawn into the chimney of a locomotive is proportional to the weight of steam expended. So the combustion is more active when the engine works fastest.

It has been long known, in a general way, that the velocity of a locomotive engine ought to be pushed to its utmost limits when required to perform important work, as when ascending a slope.

Generally the proportion of the weight of air drawn to the weight of steam employed is between 2 and 3 to 1.

M. Pécelet reports the experiments made by M. Glépin upon the draught produced by the continuous steam jets opening into cylindrical tubes. The results are quite various, according to the diameter and the length of the tubes.

We have usually found that the performance increases with the length of the tubes. Its value has been a maximum with the tubes from 0<sup>m</sup>.50 to 0<sup>m</sup>.55 in diameter, and from 3 meters to 3<sup>m</sup>.50 in height. It was then raised to 0.1145. We here call performance the proportion of the living force of air drawn to the living force of the steam jet.

It seems demonstrated that the intermittent jets produce superior action, and according to MM. Flachet and Petiet the work produced by the intermittent injections of steam in the chimneys of locomotives varies from 0.5 to 0.16 of the work which the steam is able to produce.

Usually in this kind of apparatus it is necessary to multiply the surfaces of the contact of steam and air. Then annular jets are better adapted for such work than the compact cylindrical jets.

#### STEAM BLOWERS.

Several important processes are founded upon the conveying of air by a jet of

steam. This method has been applied to the ventilation of mines. It was also employed to ventilate the great machine gallery at the Paris Exposition, in 1867.

To conclude, M. Siemens has made a new application in the manufacture of steel. In his apparatus, the air is drawn by a double tube through an annular jet and a central conical jet. The air is introduced by an annular central orifice, and by orifices through the outside partition of the apparatus. The contacts of the fluid entering and the fluid escaping are thus greatly multiplied, and this circumstance is eminently favorable to the action.

The mixture of steam and air is introduced into a reservoir containing bits of coke crushed and washed by a current of cold water. The steam is condensed and the air escapes mostly free from steam.

As a means of forcing currents of air for purposes of ventilation this method of M. Siemens is worthy of consideration.

## KÜRTING'S LOCOMOTIVE INJECTOR.

Locomotive injectors as hitherto constructed labor under the disadvantage of feeding with cold water only, and they can hardly be relied upon if the temperature of the latter exceeds 104 deg. Fahr. Even then they require the most careful adjustment of the water supply. The reasons for this defect may be traced to the principles upon which the injectors are constructed.

With an injector of correct proportions the certainty of action depends upon the velocity with which the water enters the space where the steam and water combine. In locomotive injectors to which the water can flow with only a very small pressure, this velocity depends mainly upon the vacuum produced in the condensing nozzle. This vacuum must be kept as high as possible. With *constant* steam pressure and temperature

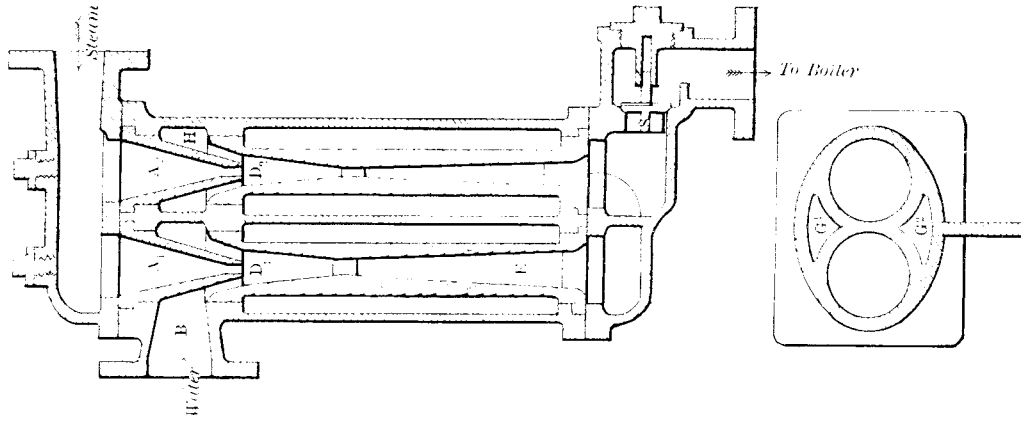
of water, the vacuum obtained is lower when the condensing nozzle is fed with too much or too little water; in the first case because the jet of steam has not sufficient power to impel the water which gives a back pressure; in the second case because the temperature of the mixture is not low enough, and consequently the vacuum is lessened. For these reasons the water supply requires to be very carefully regulated. With *variable* steam pressures and temperatures of the feed water, the vacuum becomes lower with increasing temperature of water and also with increasing steam pressure, as in both cases the temperature in the condensing space is raised, the maximum of which can be only 212 deg. Fabr. But at this point the certainty of action is *nil*; generally speaking, this temperature should not exceed 194 deg. Fabr. As the increase of temperature with high pressure steam is about 90 deg. Fabr., it follows that the feed water should not be hotter than 104 deg. Fabr. On this account many rail-

ways will not allow their drivers to warm the feed water in the tenders, as the reliability of the injectors increases with the coldness of the water, and certainty is of the first importance in railway management. This defect is almost entirely done away with in Körting's universal injector, which works with equal certainty at all pressures. This apparatus consists of two steam jet pumps combined. The second pump or real injector which forces the water into the boiler receives it from the primary or assistant injector under pressure, so that the second pump has only to overcome the difference in pressure existing between that of the boiler and that already overcome by the primary injector.

The required quantity of steam is therefore divided, and only a small portion of it used in the first part of the apparatus. Consequently the increase of temperature is much less than in ordinary injectors; the water entering it may therefore be much warmer without bring-

ing the temperature in the condensing space above 194 deg. Fahr., which is the maximum here as in ordinary injectors. The temperature of the feed water may safely be as high as 158 deg. Fahr. A special feature of this primary injector is that, with increased steam pressure, it delivers, without regulation, more water at increased pressure to the second part of the apparatus.

The second pump delivers into the boiler the water forced into it by the primary injector. The certainty of action of this second part of the apparatus depends upon the pressure with which it is fed by the assistant injector, and not upon any vacuum. As with increasing steam pressure the velocity of the water entering the second pump is also increased, it follows that with the same temperature of feed water, the reliability of this apparatus remains the same under all steam pressures, while with ordinary injectors it decreases as the steam pressure increases. On this account no water regulation is necessary. The tem-





perature in the condensing space does not come in question with the second part of the apparatus: it may, if required, exceed 212 deg. Fahr., and in fact does exceed it, for with feed water of 158 deg. Fahr., and 120 lbs. boiler pressure, the water fed into the boiler is actually 257 deg. Fahr. The apparatus therefore must not be provided with an overflow communicating with the atmosphere, as otherwise the high temperature would cause the formation of steam and an escape of water. The apparatus is started by opening a small cock behind the injector, similar to that with which other injectors are provided for letting the water out of the pressure pipe.

The foregoing illustration shows the Korting universal injector in longitudinal and cross sections. The working steam simultaneously enters the two steam nozzles  $A_1$  and  $A_2$  in the injector. The jet of steam from  $A_1$  draws the requisite water through the pipe  $B$ , and forces it through the cone  $D_1$  with corresponding velocity. This velocity is

transformed into pressure in the diverging tube  $E$  which communicates by means of the chambers  $G_1$  and  $G_2$  (see cross section) with the space  $H$  of the second pump. From here the water enters under pressure the condensing space  $D_2$ , whence it is forced by the steam issuing from the nozzle  $A_2$  into the boiler through the back pressure valve  $S$ . While starting the injector a cock communicating with space  $E_2$  is opened till water escapes from it, after which it is slowly closed.